GEOPHYSICAL MAPPING OF SUBSURFACE ARCHAEOLOGICAL FEATURES AT THE PORT ARTHUR HISTORIC SITE, TASMANIA, AUSTRALIA

BY

Fiona Links

B.Sc (Hons)

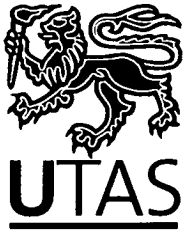

Submitted in fulfillment of the requirements
for the degree of Doctor of Philosophy (Geophysics)

University of Tasmania
Australia
February, 2008

STATEMENT AND AUTHORITY OF ACCESS

This thesis contains no material which has been accepted for a degree or diploma by the University or any other institution and, to the best of my knowledge and belief, no material previously published or written by another person except where due acknowledgement is made in the text of this thesis.

Date: 28th March 2008

Fiona Links Fiona Links

Authority of Access

This thesis may be made available for loan and limited copying in accordance with the Copyright Act 1968.

Fiona Links

10.6.08

Date

Abstract

The Port Arthur Historic Site, located in southeastern Tasmania, is a significant heritage-listed site which operated as a major convict settlement between 1830 and 1877. It was largely destroyed in the intervening years due to bushfires and demolition activities. Multi-disciplinary research over the past 30 years has generated a rich contextual framework of knowledge about the 19th century convict and post-penal periods, however information about buried physical evidence of the associated buildings, landscape features and cultural deposits that remain in the subsurface is very limited.

A range of geophysical techniques for mapping subsurface cultural features of archaeological value were assessed at three areas within the Port Arthur Historic Site: the Isle of the Dead, Settlement Hill and the Penitentiary Complex. Each of these areas is located within a distinct geological domain, and hosts different archaeological targets and near-surface stratigraphic conditions. Geophysical results were compared with historical documents, including maps and photographs, and oral sources. Archaeological ground-truthing was also employed to explore some features identified at Settlement Hill and the Penitentiary Complex.

Research on the Isle of the Dead cemetery aimed to map individual burials, former pathways and other cultural elements, and major stratigraphic interfaces. Prior knowledge of the cemetery layout on the 0.8 hectare island is limited to historic photographs, surface evidence (grave markers and depressions) and incomplete documentation – estimates of the total number of graves range from 1100 to over 1700. Magnetometry and frequency-domain electro-magnetics were effective in delineating near-surface ferrous cultural features such as former fence lines and paths but were ineffective for detecting burials. Resistivity imaging and seismic refraction tomography helped to resolve the stratigraphic context but were also ineffective for direct detection of burial sites. Ground penetrating radar (GPR) was the most effective technique for locating both individual burials and zones of stratigraphic disturbance. Radar data were very complex and the final interpretation product was a series of maps that depict the

density of subsurface ground disturbance rather than more conventional products that illustrate the distribution of hyperbolic responses or amplitude time-slice maps.

At Settlement Hill the main aim was to delineate subsurface structural remains in an area with multiple generations of convict era construction. Much of the site is characterised by a thin layer of demolition rubble. Magnetic data in this area is typified by high-amplitude, high-frequency anomalies attributable to natural variations in magnetic dolerite bedrock depth, as well as variations due to penal era cultural features such as terrace excavations, trenches and an aqueduct. Clear rectilinear anomalies in the 500MHz GPR timeslices and apparent resistivity variation map are attributed to very shallow well-preserved structural features, which correlate closely to the building layout available in several historic maps.

Surveys were conducted at two sites in the Penitentiary complex: the Sawpits - Tannery Complex and the Parade Ground area. Both sites are characterised by heterogeneous penal and post-penal fill material. At the Sawpits - Tannery Complex, 500 MHz GPR profiling and electrical resistivity tomography successfully map foundation walls, sawpit fill deposits, yard features and reclamation structures. The rubble fill stratigraphy apparent in the GPR data also provides indirect evidence of the Sawpits boundary. Resistivity tomography also clearly defines the interface between reclamation fill and underlying remnant Quaternary beach sands.

Integrated interpretation of multiple geophysical datasets from the Penitentiary Parade Ground area enabled the detection and characterisation of a diverse range of penal era archaeological targets, including sections of the parade ground wall, the parade ground gravel surface and remnants of the tramway. The most effective techniques in this complex environment are apparent resistivity and GPR, while the magnetic response is complicated by the presence of magnetic dolerite fill material.

A range of geophysical techniques have been successfully applied at the Port Arthur Historic Site for detection and characterisation of a diverse range of subsurface cultural heritage features. However, there is no single technique or recipe for future archaeo-geophysical activities that can be readily applied across the entire site. The choice of the optimal technique or combination of techniques for a particular site should be based on a prior assessment of the local geological conditions and likely target characteristics.

Acknowledgements

A big thankyou to my project supervisors Dr Michael Roach, Dr James Reid from UTas, and Greg Jackman from PAHSMA, whose guidance and input was invaluable. A second big thankyou to my wonderful family and close friends - particularly my parents and partner Andrew - for all their continued love, support and encouragement.

Financial and administrative support for this project was provided by a University of Tasmania Post-graduate Research Scholarship, along with sponsorship from PAHSMA. This study would not have been possible without the permission of PAHSMA to access historic documents and areas of the Port Arthur Historic Site. Thanks to the following PAHSMA staff and associated people for their essential input: Richard Tuffin, Jody Steele, Justin Welch, and Peter Roach and the crew of the *Marama (*for generously ferrying myself, field assistants and geophysical equipment to the Isle of the Dead and Point Puer). Thanks also to Susan Prior in the library, and the administrative staff for organising my on-site accommodation (usually a last minute request!) and answering office-related questions, PAHSMA guides and grounds staff for accommodating and assisting with the geophysical fieldwork, sometimes during the peak tourist season.

A big thankyou to the wonderful people in the UTas School of Earth Sciences: Christine Higgins, Di Steffens, Diane Madden, and Peter Cornish for helping me with administrative matters (and a home for my last months in Hobart). To Wally Herrmann and Garry Davidson for giving me advice on how best to cope with writing a PhD thesis - cheers. Thanks to my fellow corridor mates Cari Deyell, Anthony Harris, Andrew Rae, Steve Lewis, James Cannell and Wallace Mackay for injecting some humour into the working day and. Thanks to Karin Orth and Anna Johnston for providing encouragement outside the office hours.

Over the years I have also gratefully received technical assistance from a number of people including: Simon Williams, GBGeotechnics, Sydney; Neil Meadows, Cambium Technology; June Pongratz and Alistair Chilcott in the School of Earth Sciences.

Table of Contents

List of Figures

List of Tables

Abbreviations, Acronyms & Symbols

AGD	Australian Geodetic Datum
AMG	Australian map grid
AOT	Archives of Tasmania
CRM	Cultural resource management
DC	Direct current
E	Electric
EM	Electromagnetic
FEM	Frequency domain electro-magnetometry
GIS	Geographic information system
GPR	Ground penetrating radar
HCP	Horizontal co-planar
HM	Historic Map
IP	Induced polarisation
M	Magnetic
MS	Magnetic susceptibility
NP&WS	National Parks and Wildlife Service
PAHS	Port Arthur Historic Site
PAHSMA	Port Arthur Historic Site Management Authority
RMS	Root mean square
RX	Receiver
SI	International System of Units
TMI	Total magnetic intensity
TWTT	Two-way travel time (ground penetrating radar)
TX	Transmitter
UK	United Kingdom
US	United States (of America)
VCP	Vertical co-planar
cm	centimetre
km	kilometre
m	metre
mS/m	milliSiemens / metre
nm	nanometre
ns	nanosecond
nT	nanotesla
Ω	ohm
Ω.m	ohm.metre
kHz	kilohertz
MHz	megahertz
2D	Two dimensional
3D	Three dimensional

Chapter One: Introduction

1.1 PREAMBLE

Port Arthur, on the isolated Tasman Peninsula in Tasmania, is a significant heritage-listed site which operated as a major convict settlement between 1830 and 1877. During this period a series of major building programs were completed. After decommissioning as a penal station, the settlement was largely destroyed over time due to neglect, bushfires and sale of salvageable items. Today it comprises a 'vast material archive of standing structures, landscape elements and cultural deposits that contain evidence of, amongst other things, 19th century European colonisation processes, landscape perceptions and modifications, penal philosophies and strategies, convict responses, colonial and institutional economics, industrialisation, trade and consumer behaviour' (Davies and Buckley, 1987).

Comprehensive research by the Port Arthur Historic Site Management Authority (PAHSMA), previous management organisations, institutions and private individuals has created a rich contextual framework of historical, geographical and archaeological information on the site (PAHSMA internal reports; Lord, 1999; Bell, 1981; Brand, 1975). However, prior to this study, only a minor geophysical component existed within this framework. Limited investigations had been conducted at several areas on the main site (Ranson and Egloff, 1988; Dorn, 2002; Dorn *et al.*, 2002) and none at the Isle of the Dead offshore.

This chapter provides an overview of the Port Arthur Historic Site (PAHS) study area, including the geological, archaeological and historical contexts, and the contemporary setting. It briefly describes the outcomes of previous archaeo-geophysical surveys at the Site, and provides a rationale for this study. Project research objectives and investigation approach are followed by an overview of the thesis structure.

1.2 THE PORT ARTHUR HISTORIC SITE

1.2.1 General study area

The Port Arthur Historic Site is located on the Tasman Peninsula 114 km from Hobart, in Tasmania, Australia. Most of the site, which covers an area of approximately 40 ha, lies between the present-day Port Arthur Township, and the harbour of Mason Cove. The historic site also includes the Isle of the Dead, an island 1km offshore which was used as a cemetery, and Point Puer which lies at the end of an adjacent peninsula (Figure 1.1). Point Puer is not included within the scope of this project, as its terrain and archaeological potential are not deemed suitable for a multiple technique geophysical investigation. The main site is accessible by a network of intra-site roads, while a regular commercial tourist ferry services the Isle of the Dead year round.

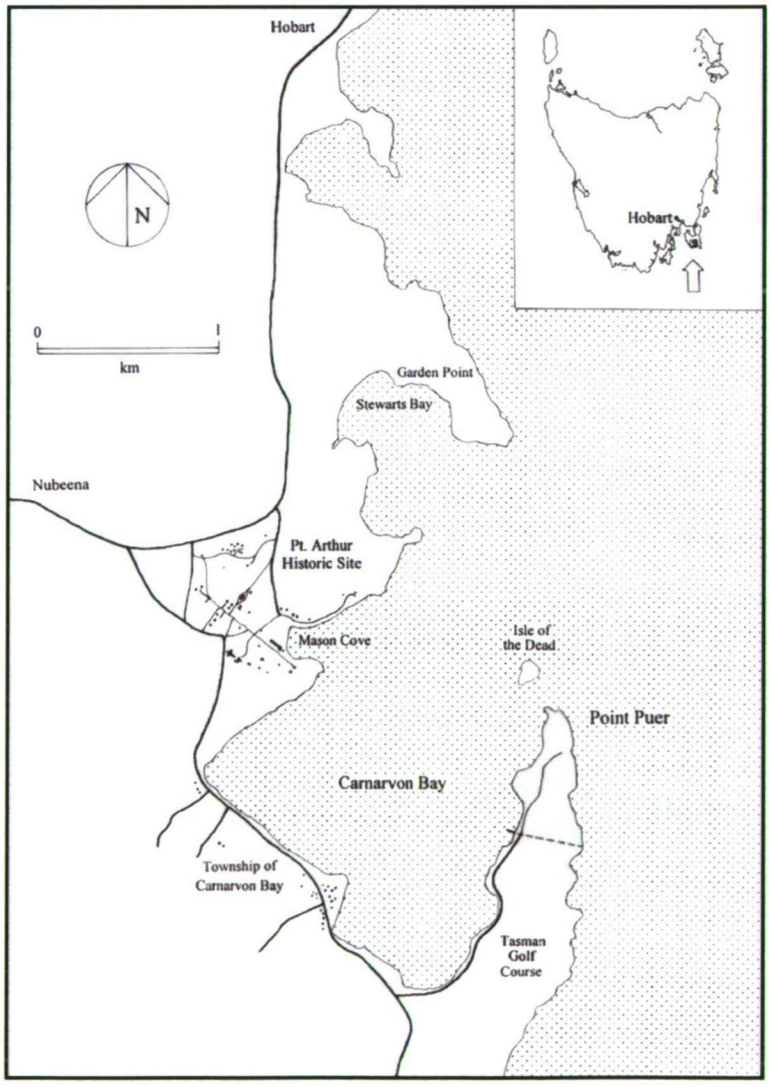

Figure 1.1: Map showing the Port Arthur Historic Site, with respect to the Tasman Peninsula and Hobart, Tasmania (courtesy of Austral Archaeology, 1997).

1.2.2 Geological context

The regional geology of Port Arthur is dominated by Permo-Triassic sedimentary rock types of the Parmeener Supergroup and intrusive Jurassic dolerite (Figure 1.2a-c). The Isle of the Dead, the Point Puer peninsula, and approximately half of Carnarvon Bay, are characterised by mid-Permian interbedded glacio-marine mudstones and siltstones of the Lower Parmeener Supergroup (Figure 1.3a). This formation is overlain by interbedded terrestrial mudstone and cross-bedded coarse-grained sandstone, which form part of the Upper Parmeener Supergroup deposited during the Triassic period (Figure 1.3b). The Upper Parmeener sandstones crop out on the flanks of Mt Arthur and Palmer's Lookout, and were used extensively in penal-period construction at Port Arthur (Greg Jackman, pers. comm. 2002).

The main Port Arthur Historic Site (excluding Point Puer and the Isle of the Dead) and Mason Cove lie within the Jurassic dolerite domain, which extends nearly 1 km westward from the Permo-Jurassic contact at Carnarvon Bay, northward to Stewart Bay. Low elevation areas of the site have a mantle of Quaternary beach sands and historic reclamation fill. Tasmanian dolerite intrusions are characterised by their remarkable thickness - forming sills up to 300 m thick - and overall extent (~ 200 x 300 km). They exhibit a range of grain/crystal sizes and textures from fine-grained chilled margins to coarse-grained granophyric segregations, and chemical compositions (Leaman, 2002).

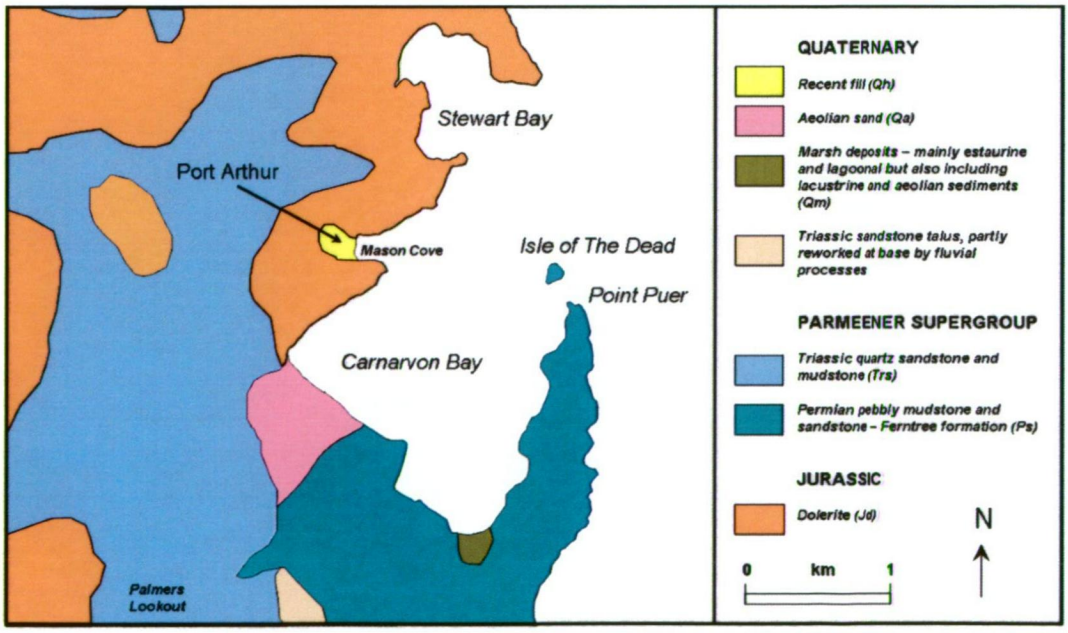

Figure 1.2: Geology of the Port Arthur District (modified after Dept of Mines, Tasmania, 1976).

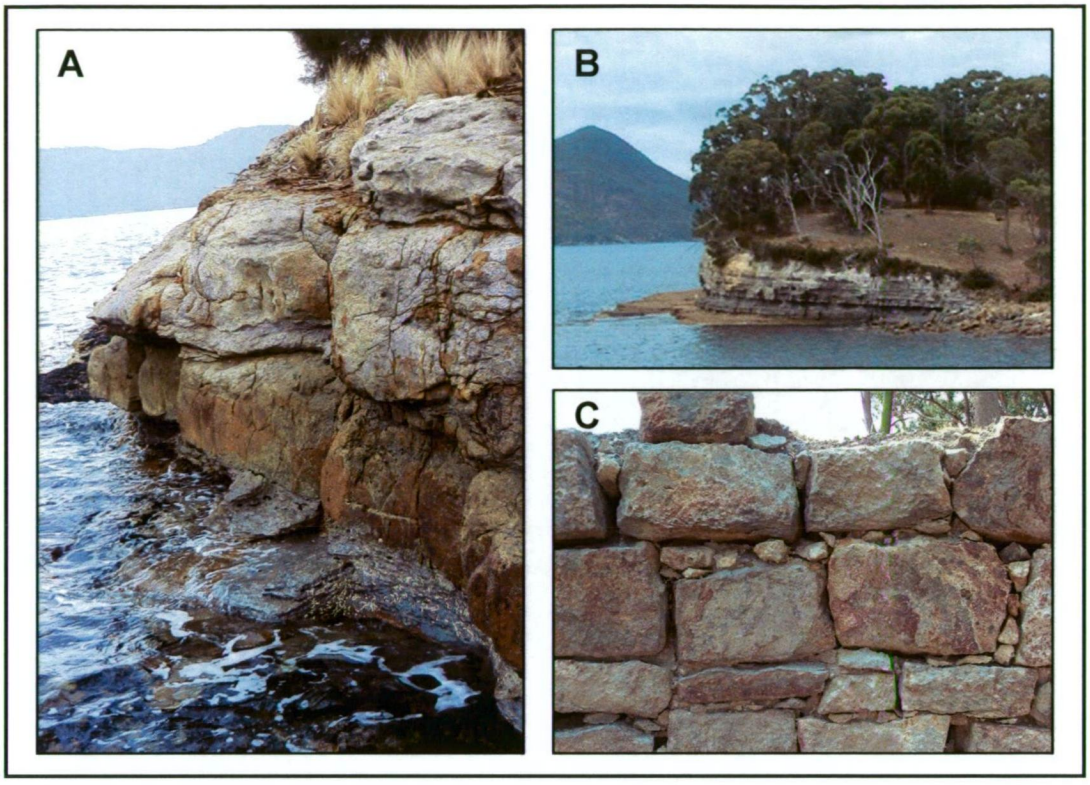

Figure 1.3: Examples of the mid-Permian interbedded mudstone-siltstones outcropping on the Isle of the Dead (**A**) and Point Puer (**B**), and a weathered mudstone masonry retaining wall on Point Puer (**C**) (photographs courtesy of David Roe, 2003).

Dolerite comprises two pyroxenes and plagioclase feldspar, with a number of accessory minerals including apatite, ilmenite, sphene, magnetite, and some sulphides (mainly pyrite). As a result of its compositional and textural variability, the dolerite presents a range of magnetic signatures. These represent the vector sum of thermo-remanent and induced magnetisation. Thermo-remanent magnetism may locally exceed the induced magnetisation by a factor of 25, but usually exceeds by a factor of 3 (Leaman, 2002). Because the remanence is approximately parallel to the induced field, anomalies derived from the former exhibit the same form, but higher than expected amplitudes than those due to induction. Where the rock is in piece form (i.e. building blocks) then the relationship between the induced and remanent vectors is random and the measured field may be quite erratic (Leaman, 2002).

The fine-grained intrusion margins typically exhibit lower bulk susceptibilities (MS) and stronger remanent magnetisation than the coarse intrusion interior (Dorn *et al.*, 2002). The susceptibility may vary from effectively zero for glasses, to 0.20 SI units for iron-rich granophyres (Leaman, 2002). Magnetic susceptibility measurements of dolerite blocks

(medium- to coarse-grained) used in wall construction at Port Arthur range from 0.038 to 0.14 SI units (Dorn *et al.*, 2002).

Chemical weathering of dolerite, primarily along joints and fractures and at the base of soils, degrades the magnetic character of the rock. Dolerite-derived soils typically contain conductive clays (calcium montmorillonite, kaolinite, metahalloysite and illite), carbonates of calcium and sodium, and hydrated iron oxides (Leaman, 2002).

Rock formations in the Parmeener Supergroup are effectively non-magnetic from the perspective of magnetic surveys, although the more feldspathic and micaceous younger units have slightly higher remanent magnetisation than other units. Magnetic susceptibility values measured from ten samples of penal period sandstone and mudstone masonry at Point Puer ranged from 0.03 to 0.14 x 10^{-3} SI units and from 0.02 to 0.11 x 10^{-3} SI units, respectively. This correlates closely to MS values of sandstone blocks at the main Port Arthur Historic Site (Dorn *et al.*, 2002).

1.2.3 Historical context

For the purposes of this project, the Port Arthur Historic Site historical context is divided temporally into three phases, according to functional transformations of the site fabric from 1830 to the present. The penal period, involving convict settlement at Port Arthur (1830 – 77), is followed by a post-penal phase (1877 – c1970) when Port Arthur emerged as a township and tourist destination. Phase three (c1970 – present) is a contemporary period of conservation management of the Site, associated with its further development as a tourist destination and the cultural resource. This section provides a brief overview of these phases - more detailed historical information for each of the survey areas is included in their respective chapters.

The following historical context has been largely derived from historical research by Richard Tuffin and Greg Jackman at PAHSMA. Additional contextual information is sourced from published secondary material, the Port Arthur Historic Site website (www.portarthur.org.au) and communications with PAHSMA staff.

1.2.3.1 Penal period: 1830 - 1877

The penal settlement of Port Arthur (1830 – 1877), in Van Diemen's Land (as Tasmania was then known), was initially established as a small timber-getting station in 1830, and quickly became a complex mix of penitentiary, town, industrial port and reformatory. A cemetery was sited on the Isle of the Dead, which would be continually used over the penal period as the final resting place of military officers and their families, convicts, invalids and paupers. The settlement was a place of secondary punishment for convicts, who were initially transported from other parts of the British Empire, such as England, Ireland, India or the Bahamas. Convicts who re-offended while still under the original transportation sentence could be sent to Port Arthur. While much of the early work involved ganged labour, as the settlement became more complex other maintenance and manufacturing industries came to prominence. Apart from those assigned to the timber, quarry and garden gangs, convicts could be directed to skilled tasks in ship building, shoemaking, smithing, brick making, carpentry, building and areas of value-adding. The 1840s witnessed a consolidation of the industrial and penal nature of the settlement as the convict population reached over 1100 (www.portarthur.org.au). Construction of workshops, a large flour mill, barracks, and a hospital (Figure 1.4) at this time was not only necessary but it also represented a commitment to the settlement's continued growth.

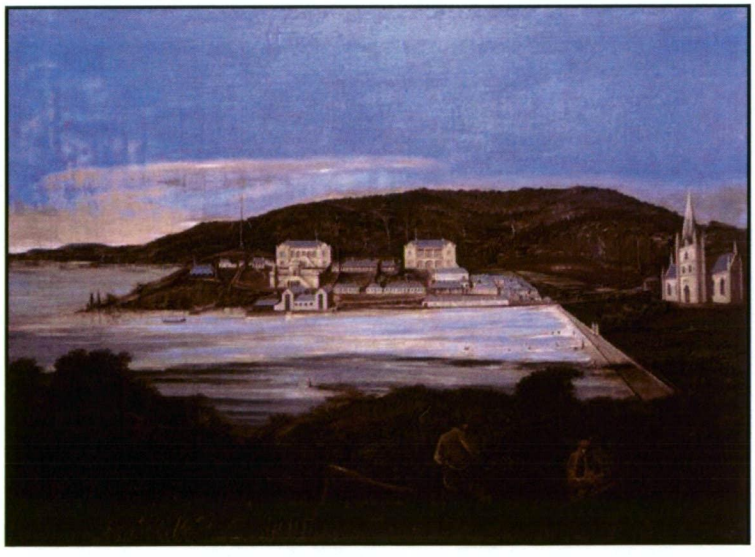

Figure 1.4: A Romantic-style oil painting titled 'Port Arthur' c1842, by an unknown artist. The modified southern shore of Mason Cove was the site of a wharf, stores and workshops, behind which stood military and civilian buildings, most notably the large barracks and hospital on Settlement Hill (courtesy of the Tasmanian Museum and Art Gallery, Ref AG2565).

The cessation of transportation in 1853 substantially slowed Port Arthur's convict population growth, although there were still a number of colonially sentenced men arriving from other stations. With an anticipated decline in transportees, activity during the 1850s and 1860s aimed to make the station economically sustainable, with 'expansive tracts of bush ... harvested to feed a burgeoning timber industry and large plots of ground ... turned over to cultivation' (www.portarthur.org.au). The flour mill and granary were converted into a convict penitentiary, and the adjacent workshops were remodeled to incorporate a steam-driven sawmill, blacksmith and forge, and carpentry workshop (Tuffin, 2003). Construction of a large lunatic asylum was started in 1864. It is estimated that over 250 buildings were clustered around Mason Cove during the peak of activity at Port Arthur, including accommodation for officials and their families, soldiers and prisoners (www.portarthur.org.au). However, without the influx of new convict labour the role of Port Arthur as a major penal settlement and notable industrial centre gradually diminished. Remaining invalids, paupers and insane convicts were transferred to Hobart Town by 1877.

1.2.3.2 Post-penal period: 1877 - c1970

Following decommissioning as a penal station, Port Arthur was surveyed and subdivided, and the Isle of the Dead cemetery ceased to be actively used. The Port Arthur Township was renamed Carnarvon, so that new residents might avoid the stigma associated with living in a former prison. Allotments of land were auctioned during the 1880s, and many convict structures were dismantled and removed. Two bushfires, in 1895 and 1898, gutted many of the larger institutional buildings, including the penitentiary, hospital, separate prison and destroyed much of what remained of the smaller structures (National Parks & Wildlife Service (NP&WS) brochure, c1980s). Despite all this, the free community of Carnarvon continued, further developing local timber industries and agriculture, and by constructing new infrastructure and buildings such as a post office, jetties and new cemetery (www.portarthur.org.au). The township was also the focus of tourism in the region, which started soon after the closure of Port Arthur; people being drawn to the buildings and ruins that remained as evidence of the harsh penal system. It was unaltered culturally until the 1930s when vegetation was cleared for a 'Garden of Remembrance'. Reports from that time indicate that the clearing

and establishment of a garden hastened wind erosion of the sandy soils, thereby reducing mound cover over the burials (AA 610/1 AOT, as cited in Lord, 1999). It is possible that some of the burial markers were rearranged during this period.

By the 1930s the Port Arthur area had three hotels, two museums, and guides, catering to tourism (www.portarthur.org.au). As recognition of its role as a key tourist attraction, Carnarvon was renamed Port Arthur in 1927. The State of Tasmania began to reacquire properties several decades after the establishment of Carnarvon, and by the late 1940s most of the site was again owned by the State. Initially the Tasman Council, subsequently the Scenery Preservation Board, and in 1972 the National Parks and Wildlife Service, were given the responsibility to not only manage and conserve the tangible remnants of the past but also to provide tourists visiting the historic site with modern services (Freeman Firth, 1998).

1.2.3.3 Contemporary period of Site Management: c1970 - present

By the early 1980s, many of the buildings erected at Port Arthur during the post-penal township phase had been demolished. With the Government's resumption of the Town Hall (the former Asylum) in 1974, the Municipal Council moved its offices to Nubeena and many of the other services followed suit. Port Arthur ceased to be a residential town in 1984, when the last of the private residents left the Historic Site (Freeman Firth, 1998). In 1987, the NP&WS site management was taken over by a newly established entity: the Port Arthur Historic Site Management Authority (PAHSMA).

Port Arthur's penal to post-penal history is represented by its structural fabric and landscape features, including cemetery markers on the Isle of the Dead. It has a legacy of structures ruined through neglect (purposeful and otherwise), salvaging of bricks and stone masonry, and bush fires. It is also characterised by a landscape of buried features, conserved ruins and re-used buildings from both the convict and post-penal township periods, which collectively constitute a unique historical and archaeological resource (Davies and Buckley, 1987).

1.2.4 Cultural significance of the Port Arthur Historic Site

For the past 30 years, Port Arthur's historical and archaeological record has provided archaeologists, historians, architects and other researchers with a rich source of information for the study of convictism and colonialism in Australia. The buildings, landscape features and cultural deposits that remain represent a significant material archive of '19th century European colonisation process, landscape perceptions and modifications, penal philosophies and strategies, convict responses, colonial and institutional economics, industrialisation, trade and consumer behaviour' (www.portarthur.org.au). Not only does the significance of the place reside in the inter-relationship of the remnant structures and sites (e.g. buildings, roads, cultivation areas, civil works, etc.) but also in its place within a national suite of convict sites (Freeman Firth, 1998).

As a formal acknowledgement of its significance, the Port Arthur Historic Site is listed on the Register of the National Estate, the National Heritage List and the Tasmanian Heritage Register. The PAHS officially includes the penal settlement and immediate surrounds, although archaeologists recognize that it extended further into the hinterland, where logging and other industrial operations took place during the penal period (Jackman, 2003).

1.2.5 Archaeology at the Port Arthur Historic Site

Initial excavations at the Prisoners' Barracks of the Port Arthur Historic Site in 1977, revealed evidence of a stratigraphy rich in historical structural and landscape features dating from the penal period to the present, and which indicated the archaeological potential of other areas of the site. From 1979 to 1986, the Site managers (Parks and Wildlife Service) involved a number of archaeologists in the Port Arthur Conservation and Development Project – a scheme of regional infrastructure upgrades and cultural heritage management programs (Egloff, 1987).

Conservation and research projects of this nature were continued by PAHSMA after 1987, aided by State Government funding. The annual summer archaeology and architecture programs (www.portarthur.org.au) are important educational tools which

add to the multi-disciplinary compendium of data and interpretations and aim to facilitate more comprehensive understanding of the site.

Archaeological excavation is a method of characterising subsurface cultural features within the confines of a trench or pit. It exposes physical evidence of a site's use, and provides complementary information to existing historical documentation, oral testimony and extant surface features. Although physical testing provides high detail in the selected test areas, it is difficult to assess what fraction of the record is represented by this point source sampling, and extrapolation is therefore limited. Excavation can easily fail to predict the presence of features or other important deposits outside the excavation area (Hargrave *et al.*, 2002).

Excavation (trenching) and test pitting typically requires significant expenditure of labour and time in order to generate this detailed information. Point sampling based on surface observations may be both inefficient and undesirable without a comprehensive site model (Hargrave *et al.*, 2002). While point sampling alone may be appropriate at small sites, it is more difficult at extensive sites such as Port Arthur. In order to make archaeology more efficient and effective, PAHSMA have supported a comprehensive program of geophysical surveys, the majority of which were undertaken as part of this doctoral research.

1.2.6 Archaeo-geophysics at the Port Arthur Historic Site

Geophysical surveys were first conducted at the site in 1986 – 87, during the Port Arthur Conservation and Development Project (Ranson and Egloff, 1988). These investigations were initiated as a response to a conservation plan that was prepared for the reconstruction of the foregrounds of the Junior Medical Officer's cottage. Elaborate landscape designs in surviving historical plans differed with respect to the physical representation of these features – all but a few surface vestiges of the original designs had been erased by contemporary site management practices. A soil resistivity profiling technique was applied in an attempt to identify any buried landscape features associated with known penal period garden paths and a carriageway. Archaeological excavations in areas of selected anomalous responses confirmed the position and characteristics of a pathway and circular carriageway indicated in historical sources. By

combining information from the archaeological excavations, documentary sources and the resistivity survey, the authors were able to establish a 'tentative' sequence of landscape development for the Medical Officer's residence.

Two factors were found to diminish the effectiveness of the survey. Firstly, the buildings were constructed on a terrace bench, which was cut into the hillside. Cutting spoil was used as fill to level part of the terrace, therefore creating an area of 'disturbed' soil, which tended to mask resistivity responses from overlying historical features. Secondly, an orchard was planted in the area, and was later grubbed out and smoothed. The authors believe that this process 'would have scattered the crushed rock or brick surfaces of the carriageways and paths' (Ranson and Egloff, 1998). With these factors under consideration, the fact that the resistivity survey did detect historical features indicated that the technique had wide range of application on the site.

It was to be another 14 years, however, until more archaeo-geophysical investigations were carried out at Port Arthur. Multiple technique surveys were conducted by the University of Tasmania (UTas) in the summers of 1999 - 2000 (Dorn, 2002) and 2000 – 2001 (Dorn *et al.*, 2002), to map the extent of structural and landscape features in six other areas (Figure 1.5). Investigations in 1999 – 2000 focused on three areas (geophysical targets in brackets):

- Separate Prison Keepers quarters (building foundations);
- Commandant's House rear (orchard walls and pathway); and
- a foreshore slipway (retaining wall, infill, seawater migration pathways).

Investigations in 2000 – 2001 were conducted at the following areas:

- Sawpit and Tannery Complex (walls, fill);
- Workshops (foundations, floor and yard surfaces); and
- Penitentiary Ablutions (walls, floor and yard surfaces).

Ground penetrating radar (1999 – 2000 season only), DC resistivity (Wenner α array), magnetometry (Overhauser), and frequency domain electro-magnetometry (EM-38 and EM-31) methods were applied at most sites. Induced polarisation (IP) was only used at the Sawpit and Tannery Complex, and Workshops. Outcomes for all areas will be summarised, to provide the geophysical basis upon which this project was developed.

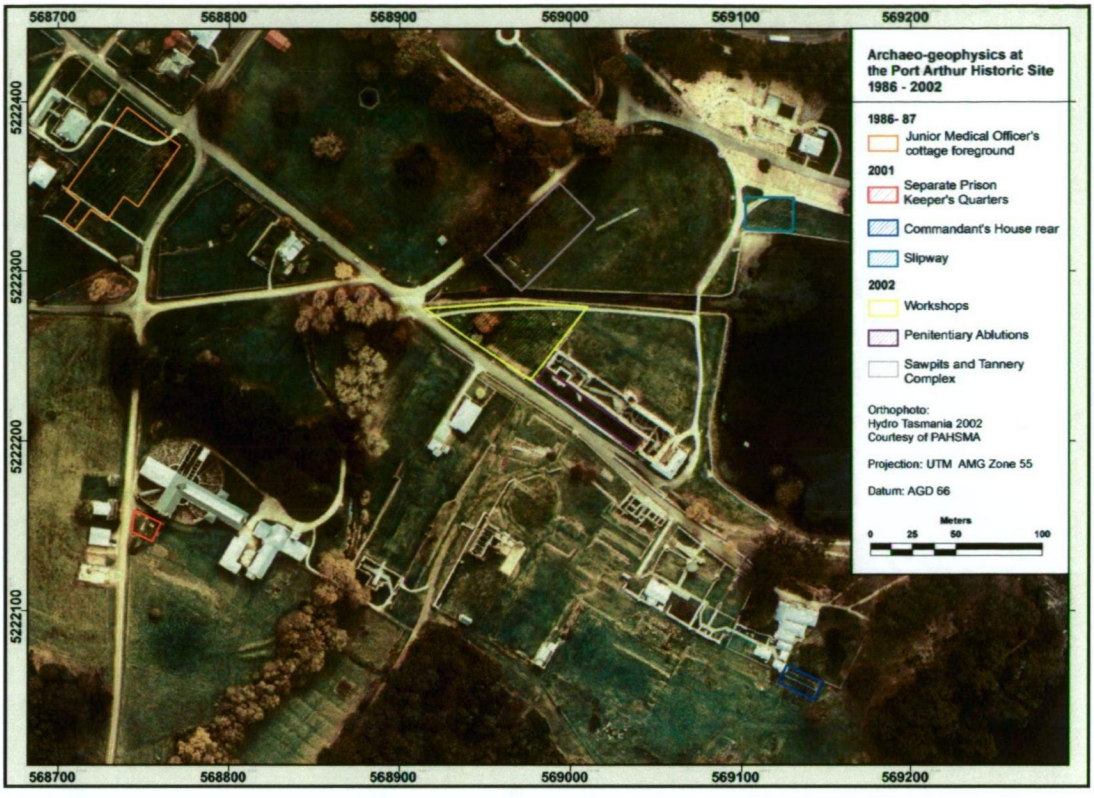

Figure 1.5: Previous archaeo-geophysics investigation areas at the Port Arthur Historic Site.

Surveys at the Separate Prison Keeper's quarters detected several strong resistive linear anomalies (inferred as contemporary pipes and wheel paths), and the dolerite bedrock. Penal period structural features were not clearly identified in the geophysical data, even though excavation subsequently revealed sandstone foundations within the top 0.3 m. The irregular distribution of responses was attributed to poor current flow in the dry summer soils and compacted dolerite road base deposits blanketing the area (Dorn, 2002).

Apparent resistivity and conductivity surveys of the Commandant's orchard area exhibited linear zones which correlated with the location of an inferred wall. Similar to the previous site, the magnetometer was strongly influenced by the irregular nature of the dolerite bedrock and no other cultural features of interest were detected.

At the slipway area, detection of any retaining wall remnants and seawater influx was compromised by strong responses from contemporary features, including bitumen and gravel road surface, garden beds, a steel grate, and the dolerite seawall. The magnetic survey measured an inferred structural break in the dolerite bedrock, which coincided with the slipway location anticipated by PAHSMA. This was interpreted as non-

magnetic masonry (probably sandstone) and/or fill material associated with the slipway. EM-31 and EM-38 data detected a sharp gradient coincident with the magnetic discontinuity, and also showed a gradual decrease in apparent conductivity with increased distance from the seawall, as was expected.

Trial ground penetrating radar surveys at the Separate Prison Keeper's quarters and slipway were poorly conducted and the least successful of all techniques used. Acquired data was presented with minimal processing and no comprehensive analyses were conducted. Preliminary analyses did not identify a slipway retaining wall in the radar profiles, an outcome the authors attributed to three factors: strong reflections from near-surface contemporary features, scattered signals from the rubble fill, and high wave attenuation at the conductive seawater interface (Dorn, 2002). Anomalous responses at the Separate Prison Keeper's quarters were unable to be correlated with anticipated wall locations. The geophysical grid and historical maps were later found to be misaligned, because the former had been incorrectly geo-referenced (Greg Jackman, pers. comm. 2002). The authors recommended further assessment of the effectiveness of this technique for detecting and characterising buried historic structural features.

Data collected during the 2000 – 2001 geophysical surveys was more comprehensively interpreted and better presented than that of the previous field season, although linear and areal trends were not as well resolved due to the 2 m line spacing.

At the Sawpit and Tannery Complex, foundation wall locations were not detected directly by the apparent resistivity, conductivity or magnetic techniques, but were inferred from mapping of the pit fill material. Two pits and/or several stages of infill were interpreted. Near-parallel linear features recorded between the Sawpit(s) and Radcliffe Canal, were interpreted as penal period retaining features constructed during foreshore reclamation. Well-defined lineaments alongside Tarleton Street were readily identified in all datasets as contemporary service pipes. Inverted IP sections and EM-31 variation maps provided an indication of salt water intrusion and the former shoreline, but not of the pit foundation walls (Dorn *et al.*, 2002).

Although the siting of several trenches in the 2001 – 2002 Summer Archaeology Program was based on the geophysical results, initial excavations to 0.6 m depth did not

uncover the sawpit foundation walls. Further trenches, located on the basis of lawn parch marks and infra-red aerial photographs, intersected the southern wall. In several areas, excavations found that the upper courses of sandstone masonry had been removed and replaced with sand (Steele, 2002). These findings suggested that the foundation walls were also incomplete in other unexcavated sections, which instigated a re-evaluation of the geophysical interpretation to remove unwarranted extrapolation of linear responses attributed to the walls.

Multi-technique surveys conducted at the Workshops were deemed successful in detecting and characterising near-surface remnants of foundations walls, floor horizons and other penal period features (Dorn *et al.*, 2002). Data interpretation was heavily influenced by historic maps and differential growth of the grass. Strong responses in the shallow EM-38 data apparently confirmed the location of lathe and boiler rooms (hypothetically associated with buried metal) shown on building plans. Both the EM-38 and deeper penetrating EM-31 instruments recorded linear trends subsequently attributed to modern buried pipes, and increased conductivity towards the Radcliffe Canal due to seawater influx. The magnetic survey clearly defined the dolerite canal wall, and a wall and rubble fill at the workshops rear. Scattered point anomalies were interpreted as buried metal objects and dolerite blocks.

The apparent resistivity data appeared to have mapped stone flagging or compacted surfaces in both floor and courtyard spaces, and isolated buried masonry blocks within 0.2 m depth (Dorn *et al.*, 2002). There was no data collected from a clay path intersecting the survey area. The apparent resistivity and conductivity techniques also measured variations in thickness of recent fill horizons, scree deposits upslope and the topsoil horizon. The two IP spreads confirmed the resistivity responses, including the location of inferred sandstone flagging, and several building foundations. They also showed a strong conductivity gradient associated with the tidal influx.

Data acquisition at the Penitentiary Ablutions was conducted at 1 m line intervals, which resulted in better resolution of anomalous responses than at the previous two areas. Interpretation was based on several penal-period building plans, although it was unknown how many of the planned structures were actually erected (Dorn *et al.*, 2002).

Primary resistivity anomalies corresponded to compacted stone floor surfaces and footings associated with three wooden sheds, as represented in one of the historic plans. Anticipated foundation walls of an adjacent masonry structure were not identified in the resistivity data, or the EM-38 conductivity survey. The latter technique did detect a strong linear feature, interpreted as buried drainage from the ablutions (Dorn *et al.*, 2002). The magnetic survey was essentially dominated by responses from the shallow dolerite bedrock, steel bars in the Penitentiary windows, and contemporary structural support beams overhead.

In summary, each site presented similar difficulties in terms of the data collection and detection of historic features. The dry summer conditions, for example, restricted current flow in the resistivity surveys, while responses from highly magnetic dolerite masonry blocks and inferred shallow bedrock effectively masked anomalies produced from magnetic targets, such as bricks. Contemporary site features, such as utility pipes and clay pathways were also considerable sources of undesirable signal in the data. Near-surface sandy loam deposits associated with 'incidental and culturally insignificant park management activities, namely the establishment of turf, and periodic patch filling, and top-dressing of localised potholes and rabbit burrows' (Jackman, 2005) were of minimal influence to the geophysics.

Post-penal demolition rubble leveling fill was a significant hindrance to detection of historic features. Archaeological excavations at the Workshops, Sawpit and Tannery Complex, Ablutions and Separate Prison Keeper's quarters revealed that this fill was typically composed of a heterogeneous mixture of dolerite, sandstone and brick fragments, within a sandy loam matrix. Clays, charcoal, artefactual material (including ferrous objects) and lime mortar were commonly also present (Steele, 2002; Jackman, 2005). There was often only a weak contrast between the physical properties of archaeological targets and the surrounding demolition fill, which further decreased the ability of geophysical techniques to detect features of interest. However the 2 m line spacing was the primary hindrance to resolving and characterising historic features in the 2000-01 field work.

1.3 STUDY OBJECTIVES, SCOPE AND RELEVANCE

This project aimed to determine the applicability of multiple geophysical techniques to discriminate a range of penal period archaeological targets hosted by contexts known to be, or suspected to be problematic. As demonstrated by historical evidence, previous archaeological and geophysical surveys, the Port Arthur Historic Site encompasses a range of environments suitable for this research. Most of the site (excluding the Isle of the Dead and Point Puer) is characterised by an unusually highly magnetic geological domain, culturally modified landscapes, and complicated near-surface stratigraphy defined by multiple phases of land use.

Three primary areas within the Port Arthur Historic Site were investigated: the Isle of the Dead, Settlement Hill, and the Penitentiary Complex (Figure 1.6). Each of these areas was chosen for its unique geological and historical land use characteristics, and a range of buried archaeo-geophysical targets. Typical penal period targets at the main site include structural features such as walls, wall foundations, floor and yard areas, drains and pits. Marked and unmarked burials (and potentially mass graves) are located on the Isle of the Dead. Features of interest were to be discriminated with some degree of certainty through appropriate data acquisition and processing methods, and by critical evaluation of the geophysical findings against historical and archaeological data. The author also aimed to achieve results and interpretations accessible to the non-technical or lay reader.

On the Isle of the Dead, a detached headland of Permian mudstone, an unknown number of people were buried during the Port Arthur penal period. Work at this site aimed to distinguish the geophysical signatures of graves from other anthropogenic elements (e.g. paths) and natural features such as tree roots and stratigraphic interfaces. The comprehensive suite of geophysical techniques included:

- frequency domain electro-magnetometry (FEM),
- apparent resistivity profiling,
- ground penetrating radar (GPR),
- seismic refraction, and
- magnetometry.

These are standard techniques used within archaeological practice both in Australia and world-wide (Clark, 1997; Clay, 2001; David, 2001), with the exception of seismic refraction which is commonly applied in environmental surveys (Sharma, 1996). Magnetic gradiometry, another standard technique used successfully at archaeological sites, would also have been applied if it had been available at the time. The use of specific hardware was largely dictated by equipment availability, the project budget and time constraints. While these parameters did not compromise the overall outcomes, they did occasionally limit the extent of surveying or density of data collected. The general principles of these geophysical methods and rationale for their use for this project are outlined in Chapter Two.

Investigations at Settlement Hill, a low ridge of Jurassic dolerite overlooking the Penitentiary and Mason Cove, aimed to detect and characterise buried structural features associated with residential and administrative buildings dating from the penal period. As no previous geophysical surveys had been conducted in the Settlement Hill area, multiple techniques were applied including ground penetrating radar, magnetometry, FEM and resistivity mapping.

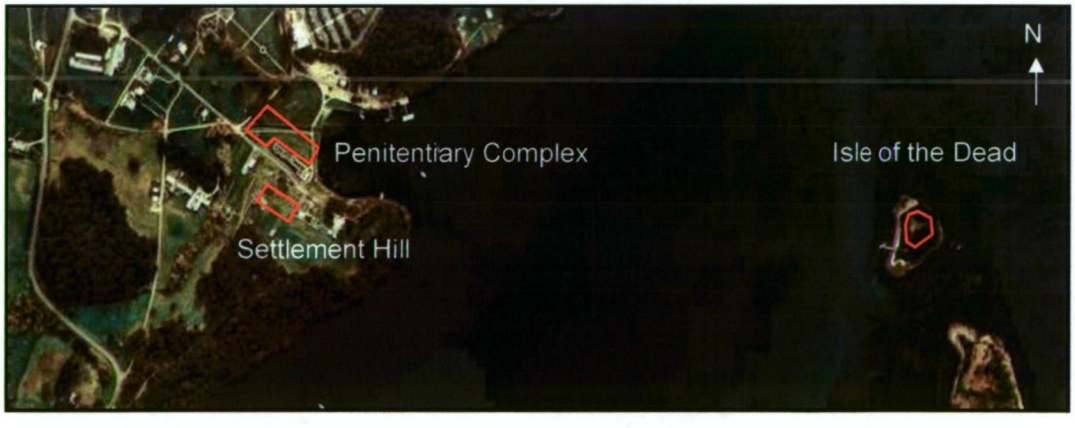

Figure 1.6: Aerial photo montage of the Port Arthur Historic Site survey areas, showing the relative locations of each geophysical survey area (courtesy of PAHSMA, 2002).

The Penitentiary Complex, located on 19th century reclaimed land around Mason Cove, comprises two survey areas: the Sawpits and Tannery, and Penitentiary parade ground. Structural features identified during previous archaeological excavations and geophysical investigations (2000 - 02) at the Sawpits and Tannery were mapped further using ground penetrating radar profiling and electrical resistivity. Archaeological

targets at the penal period parade ground, not yet studied, were surveyed using magnetometry, resistivity and ground penetrating radar.

Analysis of the geophysical datasets was 'integrated', involving processing (to 'smooth' and remove apparent recording anomalies), occasional inverse modelling, and then subjective ('qualitative') interpretation (Lines *et al.*, 1988). Interpretation encompassed the localization and classification of archaeological features of interest, the analysis of their spatial relationships, and effectively the creation of stratigraphic models (Neubauer, 2004). These site models acted as archaeological potential maps, which helped locate excavations over zones of high archaeological potential. Ground-truthing at Settlement Hill and the Penitentiary Complex by PAHSMA was then used to verify (or refute) the preliminary interpretations and refine the archaeological models.

To-date, no archaeological excavations have been carried out on the island, as had been originally planned in 2002. Unfortunately, statutory approval to undertake physical testing, during either the 2003 - 04 or 2004 – 05 field seasons, was not forthcoming due to the lack of appropriate guidelines for the statutory consent authority; the Tasmanian Heritage Office, to deal with such requests. A conservation management plan and revised assessment of scientific research values for the Isle of the Dead is currently in preparation.

1.4 GEO-REFERENCING AND DATA DISPLAY

Most of the geophysical results have been displayed graphically, within a standard geographic reference frame, because anomalies of cultural origin are generally recognised by their pattern, rather than by their numeric values alone (Scollar *et al.*, 1990). This presentation format also allows direct visual comparison between the data and interpretative maps, and other planimetric information sources in the geographic information system (GIS). The effects of topography are mostly very small and the geophysics reference frame is assumed to be a perfectly flat and rectangular system.

A six parameter affine transformation in ArcINFO® was used to co-register all local grid data to the Australian Map Grid Zone 55 (TM AMG 55) using Australian Geodetic Datum 66 (AGD 66). All AMG map co-ordinates in this thesis use a generalised notation

consisting of Eastings, followed by the Northings and separated with a comma (e.g. 568960, 5222460). Although all maps have been georeferenced, textual references to locations have usually been given in local (geophysical) grid co-ordinates. Co-registration of images was done in either the ERMapper® or ArcGIS® programs, using a linear polynomial transformation.

All geophysical information was eventually output into formats recognised by ArcGIS®, for compilation into a GIS database. The GIS provides a display platform for evaluation and interpretation of the geophysical data within a historical, archaeological and geological framework (Neubauer, 2004). This integrated approach has been applied successfully at other large-scale sites, such as the Wroxeter Hinterland Project (Gaffney *et al.*, 1998; Buteaux *et al.*, 2000; Nishimura and Goodman, 2000; Walker, 2000) and Fort Riley Army City site, Kansas (Hargrave *et al.*, 2002; Kvamme, 2006).

Gridding was used to produce image maps from the matrix of geophysical measurements, which were collected at regular intervals along parallel lines. Magnetic, conductivity and resistivity (Wenner array) datasets were gridded in Surfer® using a point kriging algorithm, unless stated otherwise. This method honours data points that coincide with the grid node and is therefore an exact interpolator (Bevan, 1998). The grid cell spacing was typically 0.2 of the survey line interval and search radius was 2.5 times line interval.

1.5 THESIS STRUCTURE

Chapter Two reviews the archaeo-geophysical literature relevant to the key themes of this project, Chapters Three to Five present geophysical survey results for three different survey areas. Chapter Three describes the geophysical survey methodology, findings and interpretation for the Isle of the Dead, and presents its historical and geological context. Settlement Hill and the Penitentiary Complex survey areas are described in Chapters Four and Five respectively, and include the results of archaeological ground-truthing. Chapter Six summarises the findings of each substantive chapter, and discusses these geophysical results in terms of overall site context and methodological issues in the use of geophysics in archaeological site assessment.

Chapter Two: Archaeo-geophysics

2.1 INTRODUCTION

This chapter comprises two parts: a technical overview of geophysical techniques used in this study, and a review of the geophysical literature relevant to research at the Port Arthur Historic Site.

Geophysical techniques are concerned with indirect measurements of the earth's physical properties, to map contrasts in 'mass-density relationships, ionic or electrical potentials, magnetic susceptibilities or elemental decay' (Heimmer, 1992). Geophysical techniques can be passive or active systems. Aerial photography and magnetometry are both examples of passive methods, where the sensor measures physical phenomena inherent in the archaeological target without altering the survey environment. Active methods, including electro-magnetometry and refraction seismic, transmit a local energy field which induces a measurable secondary field from subsurface material within the investigation area (Scollar *et al.*, 1990; Rapp, 1998). Although most geophysical techniques were originally developed for large-scale geological exploration, and military use (Sharma, 1996), high-resolution methods have been increasingly applied, since the 1950s, for investigation of near-surface features at archaeological sites (Aitkin, 1958; Atkinson, 1952; Clark, 1996).

The use of geophysics within an archaeological context is recognised as a discipline, widely termed *archaeo-geophysics*, which involves the 'process of pattern mapping for site prospection and/or intra-site characterisation of hitherto uninvestigated archaeological [features]' (Scollar *et al.*, 1990). This process is routinely applied in the UK (David, 1995; Clark, 1997), North America (Kvamme, 2001; Conyers, 2006), Japan (Conyers and Goodman, 1997; Nishimura, 2001) and Europe (Hasek, 1999; Neubauer, 2001; Neubauer *et al.*, 2002) as a relatively rapid means of undertaking a non-destructive, typically non-invasive reconnaissance survey of a site. In the US, for

example, geophysical information is routinely integrated into research and cultural resource management of a site, where it may be used as feature discovery tools for constraining follow-up excavations in areas of high archaeological potential (Heimmer, 1992; Kvamme *et al.*, 2001; Hargrave *et al.*, 2002). The geophysics may also be of benefit for sites where traditional archaeological approaches are not appropriate or not possible (Conyers and Goodman, 1997). Areas of great cultural or historic significance, cemeteries (such as the Isle of the Dead), and privately owned sites are typical examples.

2.2 OVERVIEW OF SELECTED GEOPHYSICAL TECHNIQUES

This section provides a descriptive overview of geophysical techniques applied at the Port Arthur Historic Site including magnetometry, ground penetrating radar, electrical resistivity, frequency domain electro-magnetics, and seismic refraction. It also presents the rationale behind a multi-technique approach for site assessment. For more detailed discussions on the technical specifications and applications of each geophysical method in archaeological prospection refer to Scollar *et al.* (1990), Heimmer (1992), Bevan (1998), and Nishimura (2001). Factors relevant to each of the survey areas are detailed in their corresponding chapters.

2.2.1 Magnetometry

Magnetic surveying is a passive potential field technique that measures anomalous conditions within the earth's magnetic field, the intensity of which ranges from ~ 70000 nanoteslas (nT) near the geomagnetic pole to ~ 25000 nT at the geomagnetic equator (Port Arthur has a nominal field strength of ~ 62000 nT). There are several types of magnetometers: the proton (or proton precession), fluxgate, Overhauser and alkali vapour (e.g. caesium). A technical discussion of the performance of each type is provided in the Geometrics Ltd report (2000).

The local field component of the measured total field intensity may be calculated by subtracting the diurnal variation recorded by a base station, collected by a stationary sensor distanced from the survey area, from the 'roving' magnetometer data. Collection

of diurnal-free data may also be achieved using a gradiometer, in which two sensors are mounted in vertical alignment (Llopis and Sharp, 1997). Usually, very little secondary processing of the data is required prior to gridding; only the removal or reduction of instrumental spikes, de-striping to equalise offsets resulting from surveying bi-directionally, and balancing to bring all the grids into the same data range (Heimmer, 1992; Sharma, 1997).

Anomalies are detected when a feature is in magnetic contrast with the surrounding medium, in terms of magnetic susceptibility (MS) and remanent magnetisation (Bevan, 1998). Magnetic susceptibility (the bulk magnetic property) is a measure of a material's ability to become magnetised in the presence of an external magnetic field. Remanent magnetisation is the natural or permanent magnetisation of a material, which characterises its composition and thermal or depositional history. Remnant magnetisation may include ferromagnetism, ferrimagnetism and superparamagnetism, with the dominant mode primarily dictated by the thermal history and the presence, volumetric abundance, and oxidation state of iron (Olhoeft, 1994).

Magnetometry is commonly applied at archaeological sites to detect ferrous metallic objects (20 - 2000 nT), structural materials such as brick walls, hearths and masonry, which are typically dominated by remanent magnetisation (Clark, 1997). The contrast in MS between the topsoil, subsoil, and rocks may permit the detection of ditches, pits and other excavated features backfilled with topsoil (Godio and Piro, 2005). Contrasts are often small relative to magnetic responses from other non-archaeological sources, which may obscure anomalies relevant to the investigation (Hasek, 1999). Undesirable magnetic signal may be due to recent debris associated with cultural activities, geologic conditions such as a shallow magnetic bedrock, and solar activity. A review of the practical aspects of magnetometer selection and survey design at historical archaeological sites is provided by Silliman *et al.* (2000), in which the authors compare alkali-vapour and proton precession sensors.

2.2.2 Ground penetrating radar

Ground penetrating radar is an active technique which propagates time-varying electromagnetic (EM) fields, comprised of coupled electric (E) and magnetic (M) fields, into the subsurface to map subsurface interfaces and discontinuities (Annan, 1999; Daniels, 2000). The system is typically comprised of two antennae, which are suspended just above the ground surface and sometimes shielded to eliminate interference from sources other than directly beneath the device (Clark, 1997). In the commonly-used reflection operational mode, the transmitter emits a series of high frequency radio waves (typically 100 to 1000 MHz) into the subsurface. A receiving antenna records energy reflected from material interfaces in terms of two-way travel time (in nanoseconds). Current research at the Port Arthur Historic Site utilised shielded fixed-offset antennae with centre frequencies of 250 MHz, 500 MHz and 800 MHz, to achieve a suitable resolution of features and depth of investigation.

Penetration depth depends on the electrical characteristics of a target or soil medium. This may be defined by the following macroscopic parameters: conductivity (σ), relative dielectric permittivity (ε), and relative magnetic permeability (μ) (Annan *et al.*, 1975). These parameters are determined by the molecular structure of the medium, and also vary with radar frequency (Young *et al.*, 1999). In most applications of GPR, electrical properties tend to be the dominant factor controlling responses while magnetic variations are usually weak in their effect (Annan, 1999). The relative dielectric permittivity (RDP) is a measure of the ability of a material within an electromagnetic field to become polarised and to propagate electromagnetic waves. It is influenced by the following parameters:

- Temperature;
- Moisture content;
- Dissolved salt ions;
- Pore structure; and
- Pulse frequency (Olhoeft, 1981).

The high variability in relative dielectric permittivity (RDP) of soil types and common building materials are shown in Table 2.1. In low loss non-magnetic materials, the velocity of propagation in the material is approximately equal to the speed of electromagnetic waves in a vacuum (C) divided by the square root of the relative dielectric permittivity:

$$v \approx c / \sqrt{\varepsilon_r}$$

where ε_r represents the permittivity relative to a vacuum (Olhoeft, http://www.g-p-r.com/velocity.htm).

Medium	Relative dielectric permittivity (K)	Typical velocity (m/ns)
Air	1	0.3
Fresh water	80	0.033
Sea water	81 - 88	0.033 - 0.032
Dry sand	3 - 5	0.173 - 0.134
Saturated sand	20 - 30	0.067 - 0.055
Dry silt	3 - 30	0.173 - 0.055
Saturated silt	10 - 40	0.095 - 0.047
Clay	5 - 40	0.134 - 0.047
Forested land	12	0.087
Rich agricultural land	15	0.077
Average sandy soil	12	0.087
Dry, sandy coastal land	10	0.095
Asphalt	3 - 5	0.173 - 0.134
Dry masonry	3 - 5	0.173 - 0.134
Moist masonry	5 - 26	0.134 - 0.059
Basalt	8	0.106

Table 2.1: Typical relative dielectric permittivity (RDP) and selected wave velocity of common media, using a 100 MHz antenna (modified after Davis and Annan, 1989; Conyers and Goodman, 1997; Annan, 1999; Maierhofer, 2003).

When the incident radar wave encounters an interface between two materials, some energy is reflected and some transmitted further into the subsurface. The strength of this reflection depends on the RDP of each material. When the radio wave encounters a medium of higher dielectric constant, wave velocity slows. Metallic features yield a very strong reflection as minimal energy can propagate further through the material (Kvamme, 2001). Radar penetration is optimal when the medium exhibits a high dielectric permittivity and a low electrical conductivity, and is therefore less in wet soils than in dry ones. The penetration depth thus is determined by the electrical conductivity due to ohmic losses, and is a function of moisture content, salt/ion content, number of reflection and scattering centres, frequency of the electromagnetic waves, and the effective angle of the antenna (Weymouth, 1986; Maierhofer, 2003).

GPR data is visualised as a two-dimensional vertical profile of distance versus two-way travel time (ns), known as a 'radargram' (David and Annan, 1989), which is comprised of a series of individual reflected waves digitised into traces. Radargrams may be horizontal stacked to produce a three-dimensional dataset - an amplitude volume - from which it is possible to extract 'timeslices' (Goodman and Nishimura, 1993). The vertical time axis may then be converted to depth values, by adjusting for electromagnetic propagation conditions, thereby enabling the estimation of target depth. The degree to which radar reflections can be 'seen' on profiles is related to the amplitude of the reflected waves - the higher the amplitude, the more visible the reflections. The reflection returned by a subsurface feature depends on its size relative to the wavelength or frequency employed - those smaller than the wavelength will yield weaker reflections (Conyers and Goodman, 1997).

The primary aim of most GPR investigations at archaeological sites is to differentiate subsurface interfaces associated with stratigraphic boundaries or physical discontinuities such as buried floor horizons or wall faces. This method has two advantages over most other non-invasive techniques: data can be used to locate and characterise targets in three-dimensions accurate to several centimetres, and both metallic and non-metallic objects are detected (Daniels, 2000; Young *et al.*, 1999).

2.2.3 Electrical resistivity

Galvanic electrical methods map the electrical resistivity of materials, by quantifying the difficulty of passing an electrical current through the subsurface. It involves the injection of current (I) into the ground through two electrodes (C_1 and C_2) and the measurement of voltage (V) across a second pair of electrodes (P_1 and P_2). Resistance (ohms) at each station is obtained using the equation $R = V/I$. Apparent resistivity values (in ohm-meters) are calculated by applying a geometric correction factor (k) appropriate for each array type, which is simply a function of the electrode geometry (Keller and Frischknecht, 1966). Apparent resistivity (ρ_a) values represent the weighted average of all ρ_a variations in the investigation area (Ellwood, 1990).

The apparent resistivity of a granular geological or archaeological material is primarily influenced by the moisture, clay and salt content. Dry sand, gravel, stone and very dry

soil exhibit high apparent resistivities while material saturated in salty water has the lowest. Approximate resistivity values for common materials are listed in Table 2.2.

There are many standard configurations of current and potential electrodes, including the Schlumberger, Wenner, pole-pole, pole-dipole, dipole-dipole, and square arrays. The layout and geometric factors for the Wenner alpha and dipole-dipole, symmetrical four-electrode collinear arrays used in the Port Arthur surveys, are shown in Figure 2.1.

Medium	Apparent resistivity (ohm.m)	Conductivity (mS/m)
Sand, gravel	1000 - 10, 000	0.1 - 1
Silty sand	200 - 1000	1 - 5
Loam	80 - 200	5 - 12.5
Clay	10 - 40	25 - 100
Saline soil	5 - 10	100 - 200

Table 2.2: Typical apparent resistivity and conductivity values for common media (after Bevan, 1991).

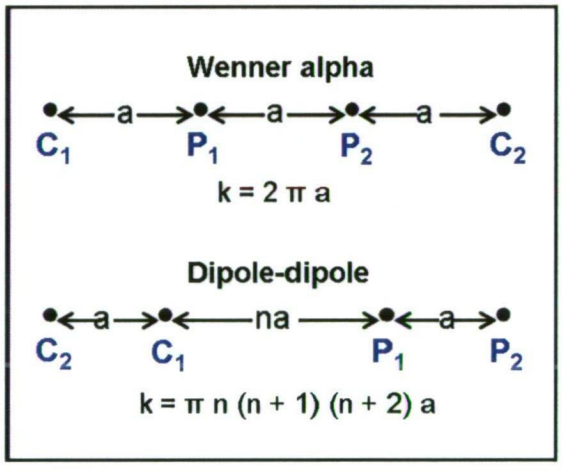

Figure 2.1: Schematic illustration of the Wenner α and dipole - dipole arrays and their associated geometric factors (k) (modified after Loke, 2002).

The effective depth of investigation is dependent on the array type, and subsurface layering, and is based on a homogenous isotropic half-space model (Barker, 1989). A low resistivity surface layer, for example, reduces the maximum investigation depth. For the Wenner array, this depth is approximately equal to the 'a' spacing (Bevan, 1998). Depth of investigation is one of many factors determining choice of array. Other parameters to consider relate to the target characteristics, sensitivity of the array to subsurface geometry and site geomorphology, as listed in Table 2.3.

- Signal-to-noise (S/N) ratio
- Electromagnetic coupling
- Resolution of steeply dipping structures
- Resolution of horizontal structures
- Depth of exploration
- Shielding by uniform conductive overburden
- Sensitivity to:
    - lateral location
    - depth of target
    - dip in strata
    - surficial inhomogeneity, sounding
    - surficial inhomogeneity, profiling
    - bedrock topography
    - lateral effects
    - topography

Table 2.3: Factors affecting selection of apparent resistivity arrays (after Ward, 1990).

The principal characteristics of these standard arrays have been well established through a variety of synthetic tests and comparisons of field data, and discussions are available in Ward (1990) and Telford *et al.* (1990). A summary of these results is provided here. The 'nesting' arrangement of the potential electrodes within the current electrodes means the Wenner and Schlumberger arrays have a higher voltage at the receiver compared to the dipole-dipole, and therefore has a higher signal/noise (S/N) ratio (Ward, 1990). The Wenner array is relatively more sensitive to vertical changes than to horizontal changes in subsurface resistivity, making it suitable for mapping horizontally layered structures such as archaeological floors and yard surfaces. It is, however, sensitive to surficial resistivity variations (Ward, 1990). Comparative studies by Sumner (1976) found that the dipole-dipole array presents steeper gradients of apparent resistivity and hence less uncertainty in lateral location. Griffiths and Barker (1993) note that data collected from dipole-dipole array are also easily affected by near-surface resistivity variations, and may therefore produce noisy data at sites with cultural debris. The pole-pole array provides the widest horizontal coverage and deepest penetration, but usually yields low-resolution information and low S/N data (Stummer, 2004).

There are two basic data collection methods: sounding and mapping, which map resistivity changes in the vertical and horizontal directions respectively. Soundings provide estimates of the thickness and resistivity of subsurface layers in an area, 'on the condition that lateral variations [in resistivity] are insignificant (Stummer, 2004). Once

the array centre is fixed in position, data is collected at every increase in the dipole spacing, to obtain resistivity information at incremental depths (Telford *et al.*, 1990). By comparing responses to established depth-curves, the depth and type of subsurface media may be predicted. Although not applied during these investigations at Port Arthur Historic Site, this method can be applied at archaeological sites to detect and characterise cultural horizons prior to excavation, such as compacted floors and bedrock (Bevan, 1998).

Mapping, or profiling, allows lateral changes in resistivity over narrow depth ranges to be delineated, ignoring the influence of vertical changes in resistivity (Stummer, 2004). Measurements are collected with fixed dipole separation, to achieve a particular effective depth of investigation, and the array is typically moved along parallel gridlines. This method may be applied at archaeological sites to produce a variation map in apparent resistivity, which allows the lateral location and shape of buried features to be estimated (Bevan, 1998). Profiling was conducted at Settlement Hill and the Penitentiary Complex at the Port Arthur Historic Site, to map the layout of shallow structural features.

The introduction of versatile multi-electrode acquisition systems (Griffiths and Turnbull, 1985; Griffiths *et al.*, 1990) and rapid versatile inversion schemes has allowed the production of two- and three-dimensional tomographic images of apparent resistivity variation where complex stratigraphy is expected (Griffiths and Barker, 1993; 1994; Loke and Barker, 1995). Vertical maps, or resistivity pseudosections, may be used to determine the depth and geometry of archaeological targets.

2.2.4 Frequency domain electro-magnetometry

Frequency domain electro-magnetometry (FEM) is used to measure differences in subsurface conductivity. Conduction in soils is (mostly) electrolytic, based on the displacement of ions in interstitial water. It is therefore aided by the presence of dissolved salts, water and increased porosity. Conductivity also increases with temperature because the quantity of dissolved salts rises with temperature and above all because the viscosity of water drops (Scollar *et al.*, 1990; Llopis and Sharp, 1997).

A FEM meter comprises transmitter (TX) and receiver (RX) coils set a fixed distance apart. The transmitter coil is energised with an alternating current at an audio frequency (kHz range) to produce a time-varying magnetic field, which in turn induces small eddy currents in the subsurface. Conductive bodies within the induction footprint generate secondary electromagnetic fields which are detected by the receiver coil. The quadrature or out-of-phase component of the induced magnetic field is recorded as a measure of the apparent conductivity, in milliSiemens per metre (mS/m) (Burger, 1992). The inphase component indicates the broad magnetic susceptibility of the investigation area, and is therefore useful for detecting large ferrous metal objects (Llopis and Sharp, 1997).

Optimal depth of investigation depends on the TX - RX coil orientation and spacing. The Geonics EM-31 and EM-38, instruments commonly used at archaeological sites, have maximum depths of 6 m and 1.5 m respectively (Bevan, 1991). Dual dipole instruments simultaneously measure in vertical (VCP) and horizontal (HCP) co-planar modes. In the VCP mode, the EM-38 instrument used at Port Arthur has maximum sensitivity at 0.4 - 0.5 m depth, above and below which it decreases markedly (Martin *et al.*, 1991). In the HCP orientation, it has a potential detection range of 1.5 m and highest sensitivity at ~ 0.5 m. These parameters are illustrated schematically in Figure 2.2.

At archaeological sites, the shallow penetration depth and narrow inductive footprint of the EM-38, and similar conductivity systems, are considered suitable for resolving small-scale targets, such as coffins, and soil contrasts (Wynn, 1986). As in the case of magnetic surveying, undesirable signal generated from near-surface clutter, which includes conductive soils, tree roots and surface debris, can easily overwhelm the useful signatures of more deeply buried targets. EM sensors are particularly sensitive to both ferrous and non-ferrous metals (Bevan, 1998).

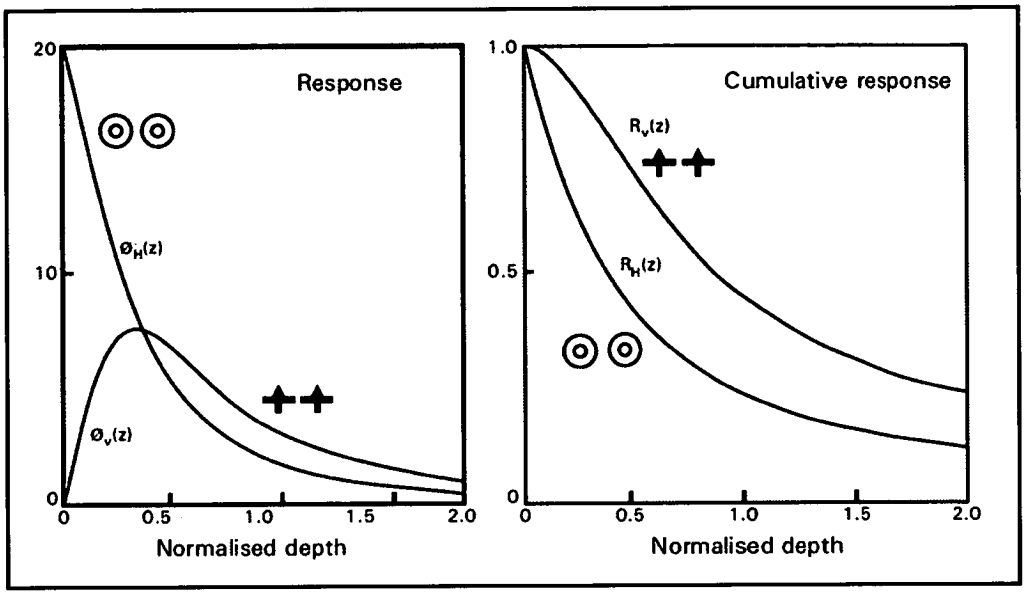

Figure 2.2: Variation of response (vertical axis) with depth for the EM-38. Left: a comparison of vertical dipole (φv) and horizontal dipole (φh) configurations. Right: cumulative relative contribution (response R), to various depths. RH = horizontal coils, RV = vertical coils. The horizontal axis on the graphs is the ratio of depth to inter-coil spacing (after McNeill, 1980).

2.2.5 Seismic refraction

Seismic refraction surveying measures the travel time of seismic waves refracted at the interfaces between subsurface layers of different transmission velocities (Telford *et al.*, 1990). Wave propagation depends on the elastic properties of the subsurface media: 'whenever a wave encounters an abrupt change in the elastic properties, as when it arrives at a surface separating two beds, part of the energy is reflected and remains in the same medium as the original energy; the balance of the energy is refracted into the other medium with an abrupt change in the direction of propagation occurring at the interface' (Palmer, 1980). This is similar to refraction of light waves at an air-water interface.

Data collection is time-consuming compared to the other techniques discussed here. After a spread of geophones is pushed into the ground, typically in a collinear or grid arrangement, seismic energy is generated at regular shot points via a hammer and plate on the surface, or detonation of a series of small explosives. From the shot point, some energy travels directly through the upper layer (to be recorded as direct arrivals), while some continues down to and then refracts laterally along interfaces with higher velocity layers, before returning to the surface. Beyond a certain distance from the shot point,

known as the cross-over distance, the refracted signal is observed as a first-arrival signal at the geophones (arriving before the direct arrival).

Observation of the travel-times of the direct and refracted signals provides information on the depth profile of the refractor. Depth profiles for each refractor are produced by numerical procedures, such as seismic tomography, based on consideration of shot and receiver geometry and the measured travel-times and calculated velocities. The final output comprises a depth profile of the refractor layers and a velocity model of the subsurface (Palmer, 1980). Any existing ground truth information such as soil augers may be overlain on the depth profile in order to help calibrate the seismic results and then provide an indication of the level of correlation along the survey line.

Seismic refraction is routinely used in environmental and engineering studies to map lithological interfaces, such as the regolith - bedrock boundary, and groundwater level (Telford *et al.*, 1990; Sheriff and Lloyd, 1995; Sharma, 1997). It has found only a few applications in archaeology, such as the prospection of underground tombs in sandy and limestone-rich environments (Papamarinopoulos *et al.*, 2003; Metwaly *et al.*, 2005). Difficulties may arise with shallow seismic refraction surveys, including coupling a sufficient amount of very high frequency energy to the ground - which is required for the detection of objects close to the surface (Carabelli, 1966; 1968). Near-surface interference may be severe and rapid attenuation of the higher frequencies with distance results in measurable pulse broadening.

Interpretation becomes very qualitative and difficult when there are velocity inversions representative of human cultural disturbance, or of archaeological features with complex geometry, such as burial sites or stone foundations (Ovenden, 1994). Refraction methods work best in mapping undisturbed layers that have velocities increasing with depth (Wynn, 1986). Thin layers or layers with a lower velocity cannot always be detected, which may result in a loss of archaeologically significant information (Ovenden, 1994).

Examples of seismic refraction at archaeological sites are thus limited, and include surveys conducted at Coombe Down, an Iron Age site with enclosure ditch, and Llantrisant Castle, an in-filled moat (Ovenden, 1994). Both yielded positive results, due

in part to the simple feature geometry, both results were confirmed by electrical resistivity profiling. Other notable seismic refraction surveys include Goulty *et al.* (1990), and Goulty and Hudson (1994) to locate the vallum at Vindobala, Hadrians Wall. In 1999, seismic experiments conducted on a linear earthen mound at Effigy Mounds National Monument, USA, identified anomalous values and stratigraphic variability in seismic velocities (Bevan, 1999).

2.2.6 The multi-technique approach to archaeological sites

The use of multiple geophysical techniques at archaeological sites is well documented (Brizzolari *et al.*, 1992; Heimmer, 1992; Clark, 1997; Bevan, 1998; Hesse, 1999; Dogan and Papamarinopoulos, 2006) and shown to have numerous advantages over a mono-technique survey. Utilising instruments which generally measure the same or similar properties, such as conductivity and resistivity, may give more reliable data when used in parallel. Using techniques that measure relatively different material properties, such as radar and magnetics, may also be advantageous. This approach theoretically increases the probability of finding mappable geophysical contrasts at sites where anomalies from archaeological targets are expressed ambiguously or minimally due to a low signal-to-noise ratio in individual datasets, or in cases of little variance between archaeological targets and surrounding material. It also allows for the potential detection of a greater variety of features (Clay, 2001; Piro *et al.*, 2000).

An evaluation of the concordance between data sets may enable a more comprehensive site interpretation, than would have been achieved through separate analysis of each data set (Scollar *et al.*, 1990; Kvamme, 2006). Nobes (1999) states that 'not only can one compare and contrast the anomalies, but some techniques are better suited to wide coverage in a short period of time, and others are better suited to detailed subsurface mapping'. Further, data obtained from different methods, may be imaged in parallel in three-dimensions - potentially providing a visually more digestible format for non-geophysicists (Cammarano *et al.*, 1998; Nishimura, 2001).

2.3 LITERATURE REVIEW

2.3.1 Review objectives and approach

For the purpose of this review, literature was selected according to two key themes pertinent to Port Arthur Historic Site archaeology: namely the intra-site geophysical mapping of (1) burials and (2) historic structural features and landscape elements associated with urban/industrial archaeological contexts. The shortcomings and successful outcomes of each study were assessed in terms of survey methodology (choice of techniques, data collection), data processing, presentation and interpretation. Due to the large number of primary studies available, the following sections will only highlight those of clear relevance to this project, with emphasis on the most recent texts.

Citations and brief reports for this review were found using several electronic bibliographic databases, such as Current Contents Connect, and the North American Database of Archaeological Geophysics projects (www.cast.uark.edu/nadag). Numerous unpublished reports were accessed through industry and Government departments, including the U.S. National Park Service bibliography (De Vore, 1999). The English Heritage Geophysical Survey on-line index of projects (www.english-heritage.org.uk) yielded little information relevant to this project, as most work in the UK focuses on Roman, Medieval and Early Historic archaeology.

2.3.2 Geophysical mapping of historic burial sites

Although geophysics has been used since the 1980s to locate burials at forensic sites (France *et al.*, 1992; Owsley, 1995), isolated and/or mass gravesites (Nelson, 1999; Davis *et al.*, 2000), this section will focus on mapping of individual burials in historic cemeteries - a subject relevant to research on the Isle of the Dead.

Geophysics is usually applied at burial sites where surface evidence is limited or non-existent and documentary records are lost or unreliable, and findings may augment information gained through visual assessment of surface features and aerial photography (Bevan, 1991; Conyers, 2006). The non-invasive and non-destructive approach is advantageous because it preserves the burial context at sites deemed

'sensitive' due to their religious or heritage nature (El-Behiry, 2000; Nobes, 1999). It is also less labour- and time- intensive than large-scale unfocused excavation (Wynn, 1986). Geophysical results may then be used to direct small-scale probing, test pitting and trench excavation, to ascertain the physical condition and/or to confirm/refute location of a burial (Hammon *et al.*, 2000). Both direct and indirect (geophysical) evidence can provide information on the mortuary behaviour among social classes (Bell, 1990). At several sites, the results of follow-up archaeological excavations were used to characterise the nature of health, morbidity and mortality among a range of social and economic groups (Parrington *et al.*, 1986; Wesolowsky, 1989; Brock and Schwartz, 2006).

Although customs of burial siting, orientation and depth vary across cultures, an individual grave is defined by several fundamental characteristics, including soil disturbance associated with trenching, a body with or without coffin, and possible artefactual material. These characteristics, and basic parameters for successful mapping of them, are succinctly defined by Bevan (1991), in what has become a widely cited seminal overview of the multi-technique approach, and Conyers (2006), in a discussion focusing on GPR for burial detection. In the former, Bevan introduces a range of geophysical instruments used in small-scale studies of historic U.S. cemeteries (17th century onwards), to highlight some of the limitations and advantages of each technique. He also proposes a limited number of unsuitable and suitable environmental conditions for the mapping of burials, although these are based on only a few of the sites.

The fundamental point to note from both articles is the variable, and therefore unpredictable, probability that geophysical techniques will detect burials. While ground penetrating radar is repeatedly proven to be the most successful technique for locating unmarked graves, results vary even where conditions are deemed favourable. At several sites studies by Bevan, profiles collected over marked graves were unable to establish totally reliable benchmark responses associated with burial material. Surface depressions were found to be unreliable indicators of burials. Archaeological ground-truthing of selected anomalies revealed only a moderate correlation between the physical evidence and radar results, as reflections were also attributable to complex stratigraphic conditions such as gravely soil. Bevan provides minimal discussion of how different frequencies, data collection and processing methodologies may aid in mapping

of graves. For example, either a 180 MHz or 315 MHz antenna are used, but no comparison is made between their corresponding responses at a single given site. Bevan also neglects to show how reflection characteristics may relate to the burial features outlined early in the article, except to say that closely spaced perpendicular profiles can define whether reflections are distinctly broader in one direction - as might be seen in a typical 2 x 1 m western historic burial shaft (Brock and Schwartz, 2006). These points are more comprehensively discussed by Conyers (2006).

With respect to conductivity techniques, Bevan notes that shallow excavations at one site demonstrated a strong correlation between high conductivity anomalies and burials, where the instrument came in close proximity to metal fittings on coffins. At another site, conductivity highs measured over marked graves were attributed to soil contrasts in the grave shafts.

Since these early case studies, the utility of geophysical techniques for the mapping of historic burials has been demonstrated repeatedly in North America (Mellet, 1992; Buck, 2003; Witten *et al.*, 2001; Kvamme, 1997 - 2002: in NADAG; Beem *et al.*, 2006) and Eurasia (El-Behiry, 2000; Ates, 2002; Papamarinopoulos *et al.*, 2003). Only a few published studies are from Australasia (Ranson and Egloff, 1988; Nobes, 1999; O'Neill, 2003), including a successful GPR survey of a 19th century Aboriginal prisoners' cemetery on Rottnest Island, Western Australia (Wilson *et al.*, 1994), and detection of an isolated 150 year old burial using resistivity tomography (Powell, 2004). The latter was verified through excavation.

An overview of these studies shows that the investigation approach to burials has been fairly consistent, with ground penetrating radar the most commonly used instrument - in conjunction with one or two other techniques. Magnetometry and EM are typically applied first, for large scale mapping, and detailed surveying achieved through GPR. Electrical resistivity profiling and profiling-soundings are least used, presumably as they are relatively time-consuming methods. There are, however, several successful examples which demonstrate the technique's potential for detecting graves (Ellwood 1994; Ahler *et al.*, 2000; Kvamme, 2000; Johnson *et al.*, 2001). Ellwood (1994) provides one of the most thorough assessments of the technique, in which he tests the Wenner array (0.5 m '*a*' spacing) at two historical cemeteries in Texas, by profiling known graves in

one cemetery and unmarked graves at another similar site. Excavations at the latter site confirmed that four of the eight low resistivity anomalies interpreted as potential burial shafts included human remains. These results show that the method can be effective, but unpredictable, for mapping areas of soil disturbance associated with individual interments, and therefore should be used in a multi-techniques approach.

The application of magnetometers to map burials at historic cemeteries is occasionally reported (Bevan, 1991; Rogers, 2001; Brock and Schwartz, 2006; Lockhart, n.d.). Studies at historic Californian cemeteries by Brock and Schwartz (2006) successfully used a proton magnetometer to detect ferrous objects buried with the body (e.g. metal cross), iron fittings on the coffin, and/or soil contrasts between the trench fill and surrounding relatively homogeneous stratigraphy. Surveys that have yielded poor results are marred by magnetic signal generated by ferrous material unrelated to the target(s), including metal flower pots, fences and power lines (Clark, 1997; Buck, 2003). Ellwood *et al.* (1994) recommends that the area be swept with a metal detector prior to survey, to locate near-surface metal wire, nails and other debris that can be removed before causing unnecessary large magnetic fluctuations in the data. The use of magnetic mapping in most circumstances, however, is questionable. English Heritage Guidelines recommend that this approach be used in conjunction with other geophysical techniques, to increase the probability of detecting the burial (David, 1995).

Until the mid-late 1990s, all radar data was presented and analysed in profile format (Bevan, 1991; King *et al.*, 1993; Clark, 1997). This involved the identification, categorisation and mapping of anomalous responses attributable to burial features (a somewhat subjective method), as symbols on a plan-view of the survey area. Response distribution patterns were then interpreted, to produce a map of the possible burial layout. Despite being a time-consuming and subjective approach, individual profile analysis continues to be applied (Johnson *et al.* 2001; De Vore, 2002), because the alternative of timeslice presentation and interpretation also has limitations (Conyers, 2006).

Three-dimensional data processing provides an objective visualisation of radar anomaly patterns in plan-view, without the requirement of prior qualitative interpretation. It has been applied at numerous burial sites (Ahler, 2000; Kvamme, 2000; Rogers, 2001; Briuer,

2002; O'Neill, 2003; Snader and Kozlowski, 2006; Beem *et al.*, 2006). Some limitations and advantages of this approach versus profile analysis are reported by Kvamme (2002), in a study at Fort Riley, Kansas. Timeslices were found to effectively display clusters of anomalies, attributed to possible mass graves, and numerous linear responses caused by historic paths through the cemetery. Variable amplitude hyperbolic responses and irregular diffractions from the trench edges, base and burial material, however, were not clearly defined in the amplitude maps, and appeared as 'indistinct and speckled'. A manual profile analysis method was therefore used to map the loci of hyperbolic responses interpreted as individual graves and sections of soil disturbance. By first selecting anomalies attributed to cultural sources, Kvamme produced an alternative image for interpretation, which was less cluttered and well-defined than the variation map of all recorded amplitudes.

A dual approach to data imaging was also applied by Davis *et al.* (2000), in a radar survey to locate 90 year old burials in permafrost. After amplitude variation maps poorly defined the responses from soil disturbance (potential indicators of a grave) due to scattered noise from natural geological phenomena, the authors conducted further profile analysis, to map near-surface dipping reflectors associated with trench sides in bedrock. This additional information helped to fine-tune the final interpretation of burial locations, which was then confirmed via ground-truthing excavations. This study shows that by comparing two different plan-views, researchers may more accurately discriminate between natural and man-made ground disturbances where graves are dug into shallow bedrock, or where responses do not fit the prescribed hyperbolic models seen with well-preserved coffin burials in homogeneous soils.

Other studies demonstrate that data migration enhances the definition of individual burials in the amplitude volumes, at sites with coffins and/or underground vaults (O'Neill, 2003) and without complex stratigraphy. In a comprehensive recent overview of the general use of radar for mapping graves, Conyers (2006) points out that amplitude analysis may be inappropriate at sites where subtle features, such as soil disturbance, may be the only detectable remnants of a burial. He therefore recommends that these features are 'visually identified in reflection profiles and manually plotted on maps'. Mapping the spatial distribution of responses enables better differentiation of

reflections caused by natural sources (e.g. linear tree roots) versus cultural features such as caskets, due to pattern recognition.

Once multiple datasets have been acquired, there are various ways of integrating data with different measurement units into a plan-view comprehensible to non-geophysicists (e.g. cultural resource managers). One presentation format, involving the simple layering of datasets, allows for the combination of information from disparate sources into interpretable displays. A good example is provided by Rogers (2001), in a study of a Native American burial ground dating from the 1850s, in which he overlays a magnetic gradiometry contour map onto a radar timeslice. Conyers (2006) points out, however, that this approach has 'relatively low dimensionality - only two or three data sources may be effectively represented', before the map becomes too complex. He further states that this method is purely descriptive - 'yielding only images, not new data that may subsequently be statistically analysed'.

A more objective approach to multi-technique, multi-dimensional data integration is provided by Nobes (1999), in a study of a Maori family burial ground in New Zealand using GPR, gradiometry and EM. Firstly, unmigrated radar hyperbolae were translated into one-dimensional standardised point data, then anomalies from all geophysical datasets were normalised and integrated into a composite anomaly map. Using a grading system, this was effectively transformed into an 'availability map', which indicated areas of the burial site most likely to be clear for use for future burials (no depth information was required). Unfortunately, due to the sensitive nature of this site, the geophysical data was not verified. Despite describing this neat process and presenting the final images, Nobes does not include visual examples of class '1' and '2' radar responses or variation maps of the EM and magnetic data.

In a (successful) search for a recent clandestine grave, Nobes (2000) addresses the challenges of surveying a site which has been irregularly disrupted and modified by tree harvesting and the partial removal of stumps. These factors resulted in numerous ambiguous anomalies, one of which was found to be the target upon excavation. The vegetation, sandy soils, and iron sands present at ~ 1 m depth encountered by Nobes (2000) are somewhat similar environmental conditions to those on the Isle of the Dead at Port Arthur. Based on the results, Nobes believes that conducting a reconnaissance

survey before detailed ground penetrating radar profiling 'should be standard procedure, since the EM survey can indicate potential problems and guide the choice of the GPR antenna frequency' - by characterising the background conductivity and potential for radar attenuation.

Finally, as only a small number of the studies reviewed here have been verified via ground-truthing, it is difficult to assess the reliability of techniques, data collection methodology, imaging and interpretation - although results suggest that a multi-technique approach increases the likelihood of detecting burial features.

2.3.3 Geophysical mapping of buried structural and landscape elements at historic sites

This section of the literature review concerns the geophysical mapping of structural features and landscape elements at historic archaeological sites. Archaeo-geophysical targets typically include rectilinear building foundations, internal floor layouts, hearths and yard structures, linear drains, paths/roads and ditches. By assessing the outcomes of selected case studies, this section provides insight into appropriate survey methodologies, data processing and imaging options appropriate to former urban/industrial areas at Port Arthur, such as Settlement Hill and the Penitentiary Complex.

General discussions on the topic are rare, with most literature concerned with the outcomes of site-specific studies. Bevan (2006) provides a notable exception, with his recent overview of the merits and limitations of archaeo-geophysics for the mapping of historic buildings. The most specific information about the use of archaeo-geophysics for mapping historical features derives from studies of large-scale historic sites in North America, where the approach is routinely used by government agencies, including the U.S. Army Corps Engineering Research Laboratories and the National Park Service, for cultural resource management (De Vore, 1999; Kvamme 2001, 2003; www.cast.uark.edu/nadag). Historic fort installations and trading posts such as Fort Riley, Fort Vancouver, Fort Clark, and Fort Bragg offer good analogues to Port Arthur, in terms of target types, survey environment and site scale.

The Army City Complex at Fort Riley, for example, is a 19th - early 20th century site largely destroyed by fire, where the remaining buildings were dismantled or moved in the mid-1920s, and 'the site now occupies a grassy field with little or no discernable evidence of the buildings and roads present there 75 years ago' (Larson *et al.*, 1999). Several associated farm sites are characterised by post-occupational disturbance, which presented additional sources of undesirable signal in the data. This was a problem experienced by previous geophysical studies of areas at Port Arthur (Dorn *et al.*, 2002; Dorn 2002). Clear descriptions and visual examples are provided of how various processing methods, such as non-linear high-pass filtering of resistivity data can compensate for this limitation, such as by enhancing both high- and low-contrast resistivity features (Somers, 1998; in Hargrave *et al.*, 2002). Overall, archaeological ground-truthing of geophysical results from extensive surveys demonstrated that resistivity, GPR, magnetic gradiometry and EM (both in-phase and quadrature phase modes) are effective techniques for mapping a variety of architectural features and associated infrastructure at Fort Riley (Larson *et al.*, 1999; Hargrave *et al.*, 2002; Kvamme, 2005).

Mankowski *et al.* (2000), in a study of a late 18th century sugar cane factory in the U.S. Virgin Islands, also demonstrate how the multi-technique approach and data processing can compensate for high ambient noise levels (due to soil inhomogeneity), and strong isolated sources of undesirable signal (highly magnetic firebrick foundations) which mask responses from more subtle structural features.

Few sites are characterised by dynamic change in the historical land use, where the original building configurations are overprinted stratigraphically by more recent developments - such as at the Port Arthur workshops area. Sylvester Manor, a major North American plantation/trade centre/residence dating from the 1600s to present, is one of the few exceptions. The 250 acre site includes a circa 1735 house, Quaker and African burial grounds, cottages, farm buildings, and a large two acre garden. On-going resistivity, gradiometry and ground penetrating radar investigations have been successfully applied to ascertain the nature and extent of buried cultural features associated with different building phases (Mrozowski, 2000-). Evidence of the site's stratigraphic complexity is particularly well-defined in radar timeslices, which show various structural patterns over a range of depths.

Numerous other studies have demonstrated the effectiveness of radar amplitude volumes in characterising structural features in three-dimensions (Malagodi *et al.*, 1996; Conyers and Goodman, 1997; Leckebusch, 2003) - particularly when comprised of perpendicular profiles (Pomfret, 2006). Electrical resistivity tomography has also been shown to be moderately successful in visualising wall configurations (Cammarano *et al.*, 1998; Cammarano *et al.*, 2000; Osella *et al.*, 2005), although with much less detail than the GPR.

Most sites are not directly comparable to Port Arthur in terms of geology and complexity of fill deposits. In the United Kingdom and Northern Europe, numerous studies have been conducted in geological domains dominated by chalk, limestone and chalk-gravel bedrock, (Scollar *et al.* 1990; Neubauer and Eder-Hinterleitner, 1997; Walker, 2000; Piro *et al.*, 2000) and therefore offer little insight into mapping in an environment dominated by highly magnetic near-surface dolerite and dolerite fill. Fort Riley, typical of many North American study areas, is characterised by deep alluvial soils and no near-surface bedrock (Larson *et al.*, 1999). Surveys of geophysically 'noisy' archaeological sites are relatively rare in the literature, compared to undisturbed sites buried by a fairly homogeneous overburden (e.g. Conyers, 1995; Pomfret, 2006). Studies of subsurface architectural features at these 'quiet' environments tend to produce readily interpretable maps because the targets often have clearly discernable and highly interpretable geometric response patterns unaffected by geophysical noise sources (Bevan, 1998; Kvamme, 2003).

Findings from the Army City, Fort Riley, are also presented using a novel method of integrating large-scale complex multi-dimensional datasets into plan-view displays, which involves fusing 'geophysical data (magnetometry, resistivity, conductivity, magnetic susceptibility and ground penetrating radar), aerial (thermal, panchromatic, multi-spectral) and space-based (panchromatic, multi-spectral) sensor data' into a single colour composite image (Ernenwein and Kvamme, 2002). Each data layer (band) is assigned a different colour and made partially translucent, for simultaneous display of robust and subtle anomalies.

This approach appears to be quicker, more objective and more effective than conventional imaging methods in providing a single informative map for interpretation

by non-geophysicists. Conventional methods typically involve the identification of anomalies in individual datasets for symbolising manually into a series of layered maps of the survey area (e.g. Buteux *et al.*, 2000; Gaffney *et al.*, 2000). Several of these options were introduced in Section 2.3.2. Ernenwein and Kvamme (2002) argue, for example, that they are 'manually intensive and subjectively driven processes', which rely on 'arbitrary thresholds to define significant anomalies, while more subtle ones must be ignored'. The output from either approach, however, still requires a degree of subjective qualitative visual interpretation to discriminate anomalies derived from archaeo-geophysical targets from those attributed to non-useful features.

Chapter Three: Isle of the Dead

3.1 INTRODUCTION

The Isle of the Dead served as the cemetery for the Port Arthur penal settlement during the period 1833 to 1877, and is a significant part of the Port Arthur Historic Site landscape. Knowledge of the cemetery layout is limited to historic photographs, surface evidence (grave markers and depressions) and incomplete documentation – estimates of the number of graves range from 1100 to over 1700. In addition to human impact, the cultural resource is also affected by the natural processes of deterioration. Site management by PAHSMA is an ongoing process of mitigating these impacts and includes monitoring of stone condition, grounds maintenance and management of tourists. Non-invasive geophysical investigations were conducted on the island to assist conservation and management of the island. Archaeological ground-truthing excavations that were initially planned by PAHSMA for 2003 - 04 had not proceeded at the time of writing.

The primary objectives of this investigation were to detect and characterise features associated with graves and to map major stratigraphic interfaces. These surveys were aimed at the production of a map of the "archaeological potential" of the surveyed area, and as a guide to future cultural resource and tourism management. Mapping of the subsurface remains and cultural modification of the soil was carried out using a number of geophysical techniques, including ground penetrating radar, magnetometry and frequency domain electro-magnetometry. Resistivity and seismic refraction tomography were also applied to locate the soil-regolith and regolith-bedrock boundaries, to maximise the information inventory.

This introductory section will define the site geology and geomorphology. It will detail the historical land use, the contemporary cultural resource management objectives, surface features of geophysical significance and anticipated archaeological targets. This chapter also provides a more complete description of acquisition processing methodologies that will be applied in Chapters 4 and 5.

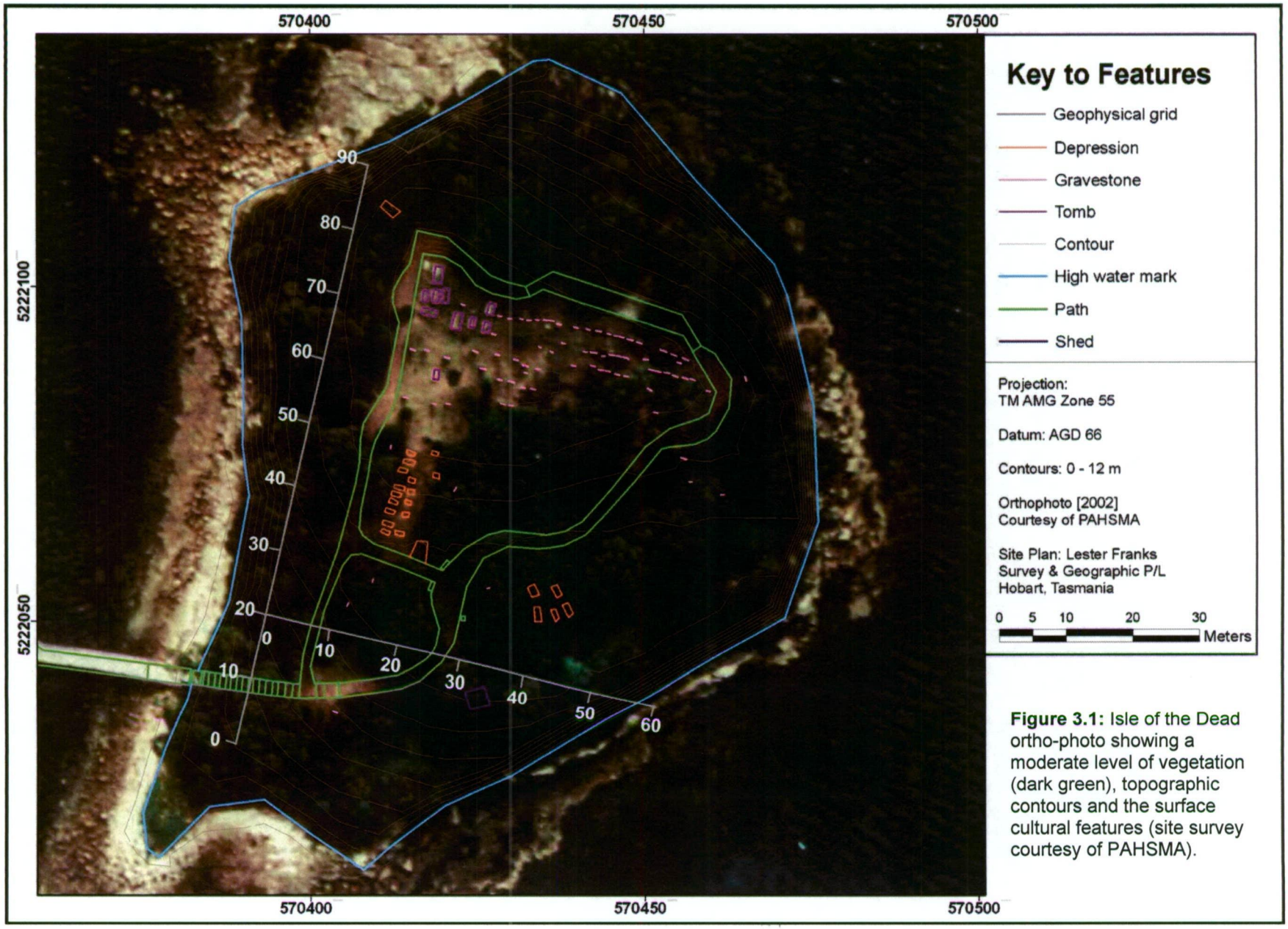

Figure 3.1: Isle of the Dead ortho-photo showing a moderate level of vegetation (dark green), topographic contours and the surface cultural features (site survey courtesy of PAHSMA).

3.1.1 Site geology and geomorphology

The Isle of the Dead is an isolated outcrop of Permian sandstone-mudstone that extends offshore from the adjacent Point Puer peninsula. The sedimentary lithology of the island produces sandy soils that differ significantly from the doleritic domain of the main Port Arthur site, and therefore provides a distinct set of geophysical conditions. An overview of the site geomorphology is shown in Figure 3.2, which is derived from a study conducted by Doyle and Cumming (2003). The island is defined by cliffs (<8m high) around most of the perimeter, which rise from stony beach ridges (western side only) and a marine platform. The northern end has moderate to steep slopes, with stony skeletal soils. A jetty and pathway are located on the low to moderate gradient of the southern slopes (Figure 3.1). The terrain is defined by two semi-level topographic benches, separated by moderately steep riser slopes. The sandstone – mudstone lithology has produced primarily sandy soils, which are augmented by aeolian sands of Pleistocene age.

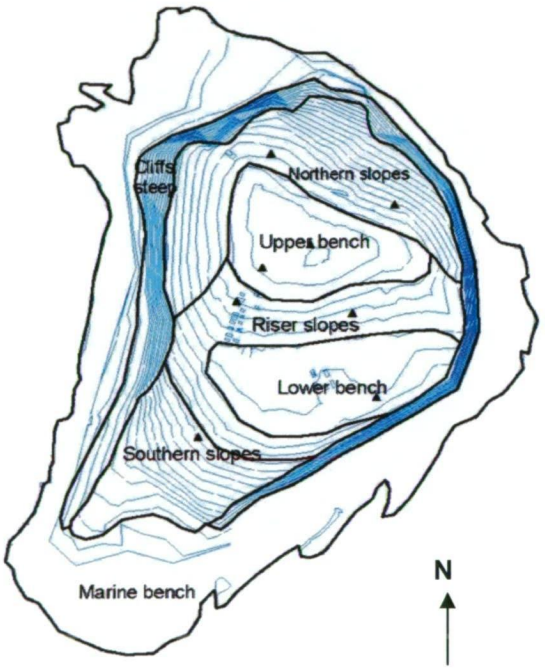

Figure 3.2: Isle of the Dead map showing broad morphological zones and auger sites symbolised as triangles (Doyle and Cumming, 2003).

Eight hand auger test sites (Figure 3.3a), located on the benches and slopes, provide detailed information on the soil profile (Doyle and Cumming, 2003). Profiles were classified largely in accordance with the defined morphological trends. All profiles classify as Humic Semi-aquic Podosols (McDonald *et al.*, 1996), with the exception of auger 4, which exemplified Shallow Rudosols. The soils are sandy, acidic, aerobic and highly permeable. Humic sandy topsoils overlie distinct bleached and leached horizons. In most profiles the latter caps a zone of humic enrichment, which in some cases changes to a dark reddish brown iron and humus accumulation. Underlying weathered, sandy regolith material derived from the Permian sandstone-mudstone bedrock caused auger refusal at every test site at depths ranging from 0.55 to 1.65 m. Results of the

auger tests were used to create an average soil stratigraphic profile, which is presented schematically in Figure 3.3b. The consolidated material forms a partial barrier to deep drainage, as evidenced by seepage near the base of the soil profile that is particularly visible on the eastern side of the island. Iron and humic material appear to be moving with the seepage water, typical in the podsol soil types that dominate the island (Doyle and Cumming, 2003).

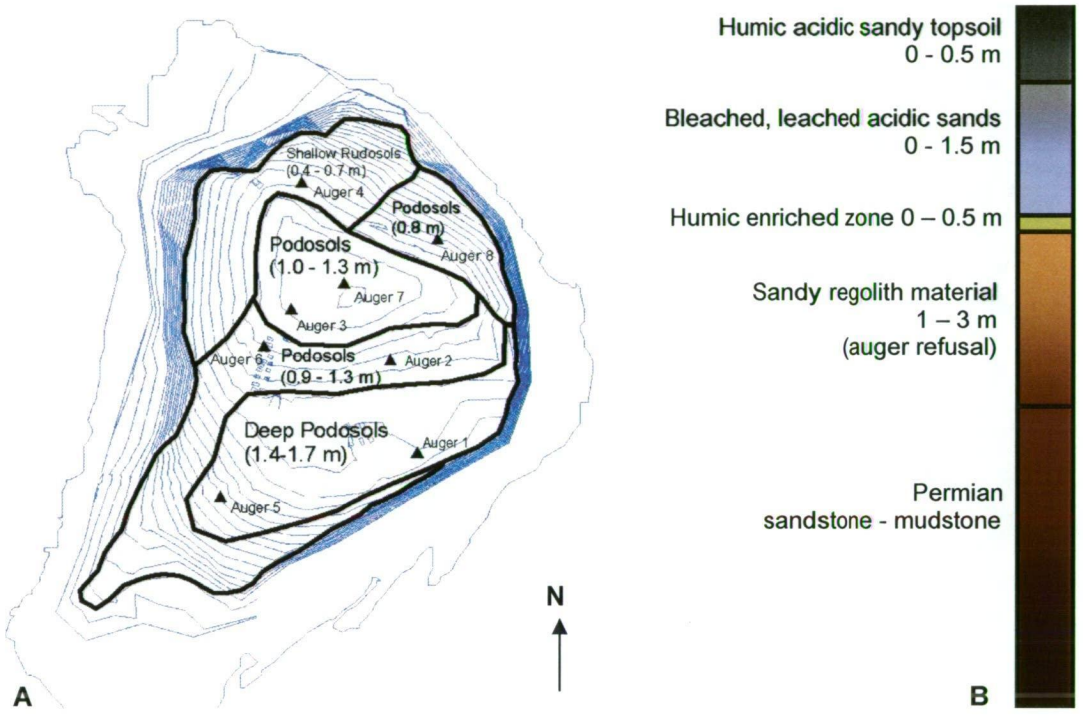

Figures 3.3a and 3.3b: An Isle of the Dead map, showing the zoning of soil types, and auger sites with the approximate depth to auger refusal (Doyle and Cumming, 2003). The image on right is a schematic soil profile, showing range of thickness for each horizon. Not to scale (modified after Doyle and Cumming, 2003).

3.1.2 Historical context

The Isle of the Dead was set aside as a cemetery for the Port Arthur settlement in 1833 at the instigation of the Wesleyan chaplain the Reverend John Manton. Manton considered that it would make a suitably peaceful resting place for the dead, after harsh life at the institution. In death however, as in life, the convicts, invalids and paupers were physically segregated from the Civil and Military officers and their families. This policy placed the latter at the elevated northern end, where their burials were able to be adorned with sandstone grave markers or chest tombs. Convict burials appear to have

been initially allocated to the southern, lower end of the island and marked with earth mounds with simple wooden crosses. No tombstone or other permanent mark was placed at convict graves until around 1854 (Lord, 1999), and only several of these remain on the island today.

After the closure of Port Arthur as a penal settlement in 1877, the island was no longer used as a cemetery. It was unaltered culturally until the 1930s when vegetation was cleared for a 'garden of remembrance'. Reports from that time indicate that the clearing and establishment of a garden hastened wind erosion of the sandy soils, thereby potentially reducing mound cover over the burials (AA 610/1 AOT, as cited in Lord, 1999). It is possible that some of the burial markers were rearranged during this period. Following the early abandonment of the garden, the island was allowed to revegetate, not being cleared of undergrowth again until the 1970s, by the NP&WS (Lord, 1999). The vegetation has since been maintained regularly by site management.

Today the Isle of the Dead is visited primarily by tourists to the Port Arthur Historic Site, relatives of those buried there, and people interested in its historic cultural value. Since the 1980s, the island has been managed to preserve the visible elements of the historic cemetery, which has included programs to mitigate deterioration of the grave markers and maintain vegetation in order to facilitate tourism.

Figure 3.4: Photograph (undated but likely c1890s) of the island cemetery looking southeast, showing unmarked burial mounts and the grave digger's hut. These burials were probably convicts, paupers and invalids (photograph courtesy of Lord, 1999).

Figure 3.5: Photograph taken from the northwest of the island, showing the arrangement of headstones, tombs and unmarked burial mounds in part of the military and civilian section of the cemetery c.1890s. Part of the original path is visible in the lower left corner. Over time, the markers and wooden borders of the graves were removed or destroyed, and the mounds gradually levelled. The present path runs over these former mounds, several metres in front of the headstones. The chest tomb on the image right is located at local grid (21x, 73y) in Figure 5.1 (photograph courtesy of Lord, 1999).

3.1.3 Geophysical survey area

In December 2002, a grid was set out by PAHSMA on the island, taking in the majority of the area thought to comprise the historic cemetery (Figure 3.1). The grid, which extended to a maximum of 92 m on the general N-S axis and to 65 m on the general E-W axis, was marked by wooden stakes placed at 10 m intervals. It was oriented (at 15 degrees from AMG grid north) so that the geophysical survey lines would transect the great majority of the marked graves normally (at 90 degrees to their length), to maximize the potential for detection. This layout was based on the assumption that the markers would remain in their original positions during the course of surveys (a several year period). A differential global positioning system (DGPS) recorded the location of selected grid points in AMG (datum AGD 66) coordinates for transformation of the geophysical grid. A reference point (AMG Zone 55, Datum AGD 66, 5222030E, 570390S) on the island's southwest corner was defined as the local origin (0, 0). Survey lines were located according to a rectangular coordinate system established with respect to the above origin. Spatial references to surveys are given in local grid coordinates, to enable easy visual location on the maps included in this chapter.

Access was the major constraint in achieving a full systematic survey of the entire study area. Many parts of the island had been cleared of low-lying vegetation during the preceding few years by the PAHSMA grounds crew, this activity was generally confined to areas immediately around the gravestones, paths and lower lightly wooded zones. Over the course of this project, more of the scrub was cleared, although the central area and perimeter remain inaccessible. Vegetation present on the island includes casuarinas, eucalypts and other dry forest/coastal scrub species, and remnants of the remembrance garden exotics. The northern slopes and upper bench were largely accessible except where interrupted by a raised timber walkway and established trees. The riser slopes and lower bench are lightly wooded and accessible south to the shed area where thick scrub prohibited surveying. The ground is covered in leaf litter in all vegetated areas. Sandstone headstones and footstones were minor obstacles to the surveying, which generally required no more than a temporary 30 cm deviation off-line.

The chest tomb area was not adequately sampled, although this was not a concern as they most likely remain in their original positions.

3.1.4 Surface features of geophysical influence

Prior to each survey, a visual inspection was made of the island to note surface features that would be sources of geophysical (magnetic and/or conductive) interference. When an anomaly did not correspond to any visible objects, the causative feature was presumed to be in the subsurface.

The primary contemporary cultural features of geophysical influence included the visitor access path and short timber walkway, rope fencing, timber benches, a metal bin and small colourbond steel garden shed. Several star picket posts (galvanised or plain steel spike) and occasional metallic debris were also visible on the surface.

Prior to the current network of paths being installed, the main group of headstones was protected from visitors by a chain fence, erected in 1974 and removed in 1985 (Lord, 1999). The pathway had been reconfigured several times since its inception, most recently in 1993. The present path surface is composed of a bark mulch layer (~ 0.1 m) that overlies a compacted loam base. Both the unconsolidated nature of the mulch and the base material hardness frequently prohibited adequate ground coupling of resistivity electrodes and seismic geophones. This was mostly overcome by clearing the bark to expose either soil or more consolidated material. The EM and magnetic surveys may also have detected remnants of a former gravel step pathway visible in Figure 3.6. Additional photographic evidence (Lord, 1999) suggests that this path probably followed a similar route to that taken presently, to encompass both lower and upper benches. In the 1990s, the gravel was replaced by a raised timber platform/walkway skirting the northernmost headstone row and bark mulch elsewhere.

Other contemporary features of potential geophysical influence include the subsurface remnants of several management initiatives: low tea tree brush fences on the upper bench, a small weather station (Figure 3.6) and metal dowels used in headstone repair. The fences (1984 – 1990s) were installed to protect the headstones by encouraging plant growth and reducing wind erosion (Thorn, 2002). Headstone condition assessment

reports from the 1990s detail the presence of iron, bronze and steel pins used to fix broken tombs and headstones. While some of these metal fixings have been removed in subsequent repairs, those remaining are a potential source of electromagnetic interference, particularly the ferrous metals. The penal period cultural features anticipated to cause undesirable geophysical signal were a cast iron railing fence bordering the grave of Eliza Caroline Aylett, at local grid 15x, 70y (Figure 3.7) and brick foundation platforms under the chest tombs (Figure 3.8).

Figure 3.6: Photograph c1985 showing the former gravel step path (**A**) between the rows of headstones, the protective low tea tree brush fences (B) and a small weather station. The chest tomb in the foreground, located at approximately (21x, 73y) on the local geophysical grid, is also pictured in Figure 3.5. Note that no mounds are visible (courtesy of Lord, 1999).

Figure 3.7: The elaborate grave of Eliza Caroline Aylett (13x, 70y) includes a headstone, footstone, sandstone border and metal railing fence. This is the only fenced grave on the island and proved a significant source of undesirable magnetic and conductivity signal (courtesy of James Cook University, 2003).

Figure 3.8: The chest tomb of Reverend George Eastman (13x, 77y) sits on a foundation platform of convict-made bricks accessible via sandstone steps from the path (see also Figure 3.7) (courtesy of James Cook University, 2003).

3.1.5 Archaeo-geophysical targets

The primary archaeological targets of the ground penetrating radar, conductivity and magnetic surveys were individual burials. Anticipated features associated with a burial include the trench, coffin or other material with the body, ceremonial artefacts such as personal belongings, or funerary architecture or hardware, such as buried markers or tomb platforms (Bevan, 1991; Conyers, 2006). In an ideal situation, all these causative features would be present and mappable. The geometry and depth of individual burials on the island is inferred from historic photographs (Figures 3.5 and 3.6), which show marked and unmarked lozenge-shaped burial mounds approximately 2 x 1m. These dimensions are similar to historic period Euroamerican burial trenches, with and without coffins, in which interments are placed horizontally (Conyers, 2006). Most burials on the island are assumed to be primary interments, although there is evidence to suggest that several are secondary burials (Lord, 1999). It has been suggested that there may have been multiple burials of convicts, invalids and paupers, which would produce a more complex geophysical signature than a single grave (Conyers, 2006). Depth of burials is unknown, and whether trenches were dug into the regolith is not recorded.

A partly decomposed coffin may be detectable by the GPR and EM system if the wood and contents (including voids) exhibited a measurable contrast in material properties to the sandy soil matrix. Coffin nails are usually undetectable, but some fittings could be larger metal objects (Bell, 1990). The latter could be potentially located with GPR, conductivity and magnetic surveys. Any convict-made associated with individual burials, such as buried chest tomb platforms, are expected to exhibit only low magnitude magnetic measurements from weak thermo-remanence, as they were typically underfired (Bell, 1981). Magnetic susceptibility values measured from eighteen convict-made bricks on Point Puer ranged from 0.06 to 2.05 x 10^{-3} SI units, averaging 0.57 x 10^{-3} SI units.

Soil auger tests indicated that the siliceous, permeable, sandy, acidic and leached soils, and moderate to high annual rainfall provide poor conditions for the preservation of human remains (Doyle and Cumming, 2003). In any case, direct geophysical detection of bones is highly unlikely (Bevan, 1991), although the presence of organic material

might increase soil conductivity (Dalan and Bevan, 2002) in the absence of a coffin (Bevan, 1991).

In the likelihood of poorly preserved burial remains and/or coffin, it is expected that the trench would be a more readily detected burial feature. A trench is defined by its interface or negative feature, the boundary between surrounding soil stratigraphy and the shaft fill. Dalan and Bevan (2002) suggest that fill may be mixed during redeposition, altering its consistency (the degree and kind of cohesion and adhesion) and structure. Greater stratigraphic complexity and higher porosity would mean that culturally emplaced material is more conductive than the soil surrounds, provided there is sufficient groundwater or rainfall.

The ridge (baulk) between burial trenches is also a potential archaeo-geophysical target. If not too narrow, it may be detected as a less conductive strip between two areas of disturbed stratigraphy. The ability of geophysical techniques to detect the shaft fill and baulk may be affected by soil development that has occurred since the burial, and the homogeneity of the natural soil column. Natural weathering processes such as intermixing and compaction, and biomechanical agents (burrows and tree roots) will also alter the physical contrast between culturally emplaced material and the soil host.

It was anticipated that the base of the weathered surface layer (regolith – bedrock interface) would provide a sharp geo-electrical contrast for depth profiling. It was further hoped that the boundary between the sandy soil column and unconsolidated regolith would provide a measurable material contrast for definition of subsurface topography. The weathered regolith surface was expected to be 1.0 - 1.5 m deep on average, as indicated by the soil tests and physical evidence on the sea cliff.

Surviving grave markers, several historic photographs and surface depressions provide some indication of the burial layout on the island. Most remaining headstones are located on the upper bench, and several chest tombs were clustered on the eastern upper bench (Figure 3.1). This configuration appears largely unaltered from the arrangement photographed in the 1890s (Figure 3.5), which suggests that geophysical responses coincident with extant markers could be used to provide benchmark 'burial signatures'. Historic photographic evidence of the upper and lower benches also shows

that the mounds of both marked and unmarked burials had their long axis roughly north-facing- which differs from the traditional Anglo-Christian tradition of east-west burial alignment with the feet to the east (Jordan, 1982; in Brock and Schwartz, 2006). Burial density appears to have been moderate to high based on historical photographs, and several graves had timber borders and standing markers (Figure 3.4). These have since gone, the mounds eroded, and several stone markers have been either removed for repair, or stolen (Greg Jackman, pers. comm. 2002).

While surviving grave markers demonstrate a consistent north-south orientation across the upper bench, and photographs suggest that mounds in the lower bench were also roughly aligned in this direction, surface depressions and a few headstones on the eastern riser slope are east-facing (Figure 3.1). Surface depressions not associated with markers may indicate subsidence of soil in the grave shaft due to collapsed burial material such as a coffin (Bevan, 1991). Documentary evidence of who was buried on the island is incomplete and the number of graves is therefore in dispute. For many years, the popular estimate was over 1700 (Lord, 1999), although a recent historical study of the available evidence by Ross (1995) calculated a figure closer to 1100. This number, and a nominal cemetery area of 3000 m^2, infers a burial density of one per 2.75 m^2 – an assessment broadly compatible with photographic evidence.

3.2 ARCHAEO-GEOPHYSICAL TECHNIQUES: METHODOLOGY, FINDINGS AND INTERPRETATION

3.2.1 Introduction

If archaeological deposits or features possess physical properties different from the surrounding subsurface, then they may offer a contrast against the natural background in terms of magnetic characteristics, resistance to an electrical current, or their ability to reflect radar energy (Kvamme, 2001). The first task of the archaeo-geophysicist is to assemble a matrix of measurements collected systematically across the site. This matrix is processed to create a map of a particular geophysical parameter(s), from which significant contrasts may be recognised for purposes of archaeological interpretation. Such contrasts are commonly referred to as 'anomalies', until their causes can be identified. Data recognition involves the assessment of individual anomalies relative to the background values, and distribution of responses across the whole site. Anomaly distribution patterns may help the geophysicist distinguish cultural from natural features (e.g. a burial shaft) (Scollar *et al.*, 1990).

Several geophysical techniques were applied in this study to map historic burials on the Isle of the Dead. These included ground penetrating radar, frequency domain electro-magnetometry (FEM), resistivity and magnetometry. The portable conductivity unit and magnetometer were used to survey the largest grid area, and a smaller area was covered using ground penetrating radar, due to time constraints and accessibility constraints. Refraction seismology and electrical resistivity tomography were used at selected locations to define major stratigraphic boundaries on the island.

The following sections describe the survey methodology and processing techniques used to create maps of different geophysical parameters on the Isle of the Dead. Primary geophysical images, data recognition maps and schematic interpretation images are included in the text, and additional information is presented in Appendix A. Findings from each survey are discussed broadly while significant anomalies and trends are characterised and interpreted in detail.

The processed data is presented here in two formats: as gridded maps or as distance by depth sections. Apparent conductivity and magnetic intensity variation maps are displayed in pseudo colour and artificially illuminated to highlight anomalous responses and directional trends. Selected profiles are also included to illustrate certain points in the discussion. Seismic refraction and resistivity transects are presented as tomographic depth models of velocity and apparent resistivity respectively. Ground penetrating radar data are shown primarily in section format, known as 'radargrams', with additional selected amplitude variation maps ('timeslices').

3.2.2 Apparent conductivity

Introduction

Electromagnetic investigations were conducted to map the apparent conductivity variation across the Isle of the Dead. Surveys were undertaken in February and April 2003, with the assistance of UTas geophysics students and PAHSMA archaeology volunteers. The following sections detail the data collection methodology and post-acquisition processing. Survey results will be presented and interpreted in Section 3.2.2.3.

3.2.2.1 Data acquisition

The initial survey period (six days) had high temperatures and no rainfall, so the permeable sandy soils were very dry. The long-term rainfall distribution chart shown in Figure 3.9 indicates that the local climate is typically moist and stable without excessive seasonal variations (Thorn, 2002). Due to these conditions, it was anticipated that there was possibly not enough variation in conductivities across the site to detect individual burials. A second survey was therefore conducted in the cooler, wetter autumn conditions. The initial data collection took six days, with the aid of an assistant, as access to the island was restricted by the ferry timetable to 5 ½ hours daily. The second survey was limited to five hours daily over four days, and so it included only the assumed main cemetery area. This provided enough data for comparison and minimised the effects of diurnal daily variations in apparent conductivity.

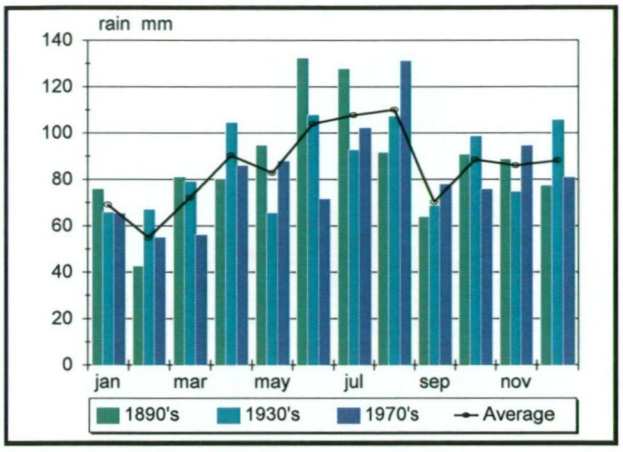

Figure 3.9: Rainfall charted from weather stations at Port Arthur (1890s) and nearby Palmers Lookout (1930s and 1970s) (courtesy of Thorn, 2002).

The EM-38 instrument was placed on the ground for sampling, to maximise the depth of investigation. Calibration was conducted in the same place every time and in accordance with instructions provided with the equipment. Fundamental survey data collection parameters are tabulated in Table 3.1.

Survey type	Low frequency electromagnetic induction		
Instrumentation	Geonics EM-38 dual dipole		
Area surveyed	~ 3575 m^2		
Method of coverage	Series of parallel traverses		
Orientation	Vertical and horizontal co-planar		
Station interval	0.5 m	**Operating frequency**	40 kHz
Output units	MilliSiemens/metre (mS/m)	**Traverse separation**	1.0 m
Phase	Quadrature	**Inter-coil spacing**	1.0 m
Comments	Profiling conducted with a ≤ 1.0 m offset from taped survey line. Dipole parallel to traverse direction. Calibration prior to survey and then every 30 - 40 minutes. Measurement recording delay time: 2 s. Digital meter accurate to whole number only. Removal of metallic objects on surveyor and obvious surface metallic debris on site prior to survey.		

Table 3.1: Tabulated apparent conductivity data collection parameters for the Isle of the Dead.

3.2.2.2 Post-acquisition data processing

Several forms of undesirable signal compromised the quality of the raw EM data, as shown in an unprocessed HCP apparent conductivity map from the summer survey (Figure 3.10). Artificial illumination highlights the most obvious noise: striations caused by instrumental and thermal drift. These stripes effectively distorted regional trends in apparent conductivity and masked isolated anomalous responses. Diurnal variations in

soil conditions and weather also influenced the results, causing block edge effects. Calibration every 30 - 40 minutes, as recommended, did not minimise instrumental drift of the EM-38 during the first survey. The drift values for this survey were unacceptably high, up to 40 mS/m over 60 m (30 minute period) as shown in gridline 67y, Figure 3.10. This error was greater than the range of conductivities across the Upper Bench.

The factors described above were lessened or removed by manual processing. De-striping removed the residual elongate along-line artefacts in the data. The data was also block shifted ± 2 - 4 mS/m to compensate for edge effects resulting from daily variation in local soil conditions.

3.2.2.3 Findings and interpretation

Introduction

This section presents the results from the four conductivity datasets: horizontal and vertical co-planar modes from both the summer and autumn 2003 site surveys. A discussion of the combined survey results for HCP and VCP modes will address the broad areal trends in apparent conductivity across the site, then isolated anomalous responses and linear trends in the data. Maps are displayed in pseudo colour images and filtered to highlight anomalous responses and directional trends.

Data recognition maps

Recognition maps are schematic representations of isolated anomalies, areal and linear trends in the gridded data. The methodology described here follows basic set criteria that may be applied to conductivity, resistivity and magnetic variation maps. Responses in which the anomalous values are confined to only one or two survey lines are termed 'isolated'. Broad classification of isolated anomalies was based on polarity - 'negative', 'positive' or 'dipolar'- and further subdivided according to amplitude. In some cases, 'negative' responses may actually be a central low surrounded by slightly higher values. This central low is caused by the inherent nonlinearity of the instrument near excellent conductors, such as metal. Metal that is closer than about 1 m can cause low or negative readings of apparent conductivity; at a somewhat greater distance, the readings can show high conductivity (Dalan and Bevan, 2002).

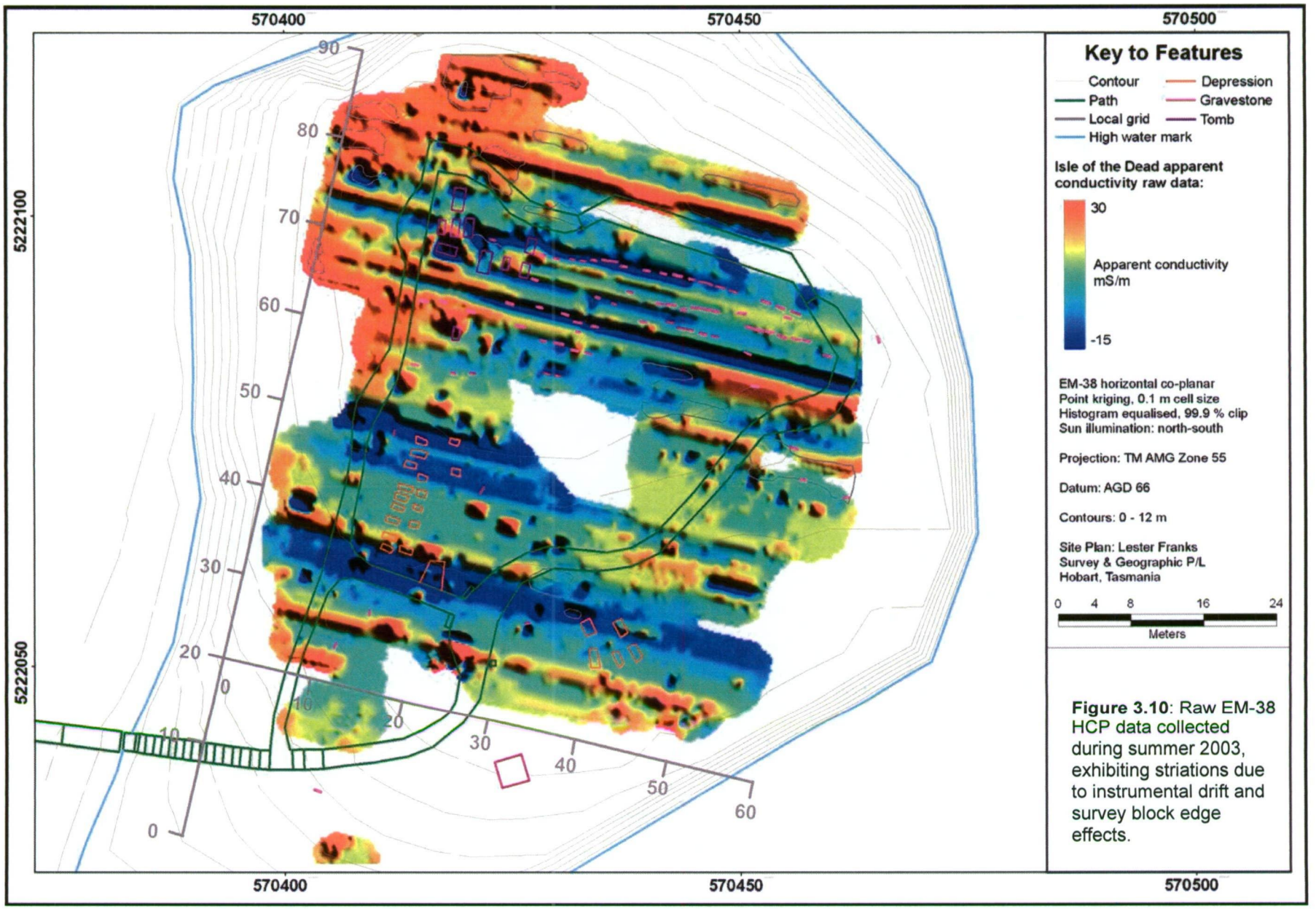

Figure 3.10: Raw EM-38 HCP data collected during summer 2003, exhibiting striations due to instrumental drift and survey block edge effects.

An isolated anomalous response is represented schematically on the data recognition map by a symbol such as a circle or cross. Symbol placement is based on preliminary qualitative interpretation of the location of the source centre. Linear trends are inferred when anomalous responses extend over more than two survey profiles and are represented schematically by a line along the source centre. The definition of areal features begins by estimating the local background values across the site, while excluding the effect of isolated anomalous responses and linear trends. These background values are then divided into subsets ranging from very low to very high.

Preliminary qualitative interpretation images

Geophysical anomalies are derived from causative features of known, inferred or unknown cultural origin. If the anomaly location and response type correlate closely with that anticipated from direct or indirect surface evidence, then this anomaly is attributed to the 'known' source. When the anomaly position and characteristics are consistent with known documentary or photographic evidence then it is attributed to the 'inferred' source. Remaining responses from 'unknown' sources are labelled as such.

Summer survey broad trends

The summer survey measurements range from -95 mS/m to 300 mS/m in the HCP mode, and from -53 mS/m to 115 mS/m in the VCP mode. These values are clipped for display purposes between -10 mS/m and 30 mS/m. The range is divided into four sub-ranges, to standardise the production of recognition maps. Values exceeding ± 15 mS/m above background are classified as very low ('negative') or very high ('positive'), ± 5 mS/m as moderate values and low where the amplitude is less than ± 5 mS/m. The background is characterised by a very narrow range of low readings (0 – 8 mS/m) in both the HCP and VCP datasets (Figures 3.13 and 3.14). The processed variation maps display similar lateral variation in apparent conductivity, with average values of 0 mS/m to 4 mS/m defining most of the survey area. Low measurements recorded on the exposed Upper Bench and Riser Slopes are interpreted as due to well-drained, sandy soils and dry conditions during the survey period. The Lower Bench and perimeter show higher apparent conductivities, due to moister, humic conditions. Greatest variability is exhibited in the vegetated areas, particularly in the HCP dataset (Figure 3.11). Very high conductivity readings (> 15 mS/m) are recorded in the northwest corner of the grid.

These are attributed to the shallow rudosols (0.4 m – 0.7 m deep) and perched water table interpreted from the auger testing (Doyle and Cumming, 2003).

Autumn survey broad trends

The autumn survey produced a range of values from -24 mS/m to 59 mS/m in the HCP mode, and from -53 mS/m to 115 mS/m in the VCP mode. Higher amplitude anomalies are clipped at –10 mS/m and 30 mS/m to be comparable to the summer results (Figure 3.13). Broad variations in autumn apparent conductivity are generally similar to the summer survey, for both the coil orientations, although the autumn data provide more detail because of a greater range of background readings (~ 40 mS/m).

Discrete anomalies and linear trends - combined summer and autumn results

Although the majority of isolated geophysical anomalies are present in both the summer and autumn datasets, the autumn survey detected additional sources due to the better survey conditions. It was therefore decided to combine both surveys, for the production of HCP and VCP mode data recognition maps (Appendix A, Figures A2 and A3).

Some point responses appear to lie on linear trends in a NW-SE direction across the midsection of the island, marked in Figure 3.11 as black lines. Very high amplitude anomalies along these lines are tentatively interpreted as remnants of former fence posts, of unknown origin. The lower amplitude responses are possible caused by post remnants in poor condition, or ones that lie offset from the survey area. Lesser trends are defined more easily when artificial illumination highlights the presence of lower amplitude responses.

A linear trend of elevated conductivity values running parallel to headstone rows in the Upper Bench (Figure 3.11 (**A**)) is attributed to the gravel pathway illustrated in Figure 3.6. Remnants of a former pathway are also inferred through a series of adjacent anomalies seen in the summer VCP mode results (Figure 3.12 (**B**)). Trends in the magnetic data indicate that these responses form part of the same feature. This will be discussed further in Section 3.2.3.3. Most lineaments in the data are due to unknown sources or tree root systems visible from the surface. Some of the 'unknown' lineaments

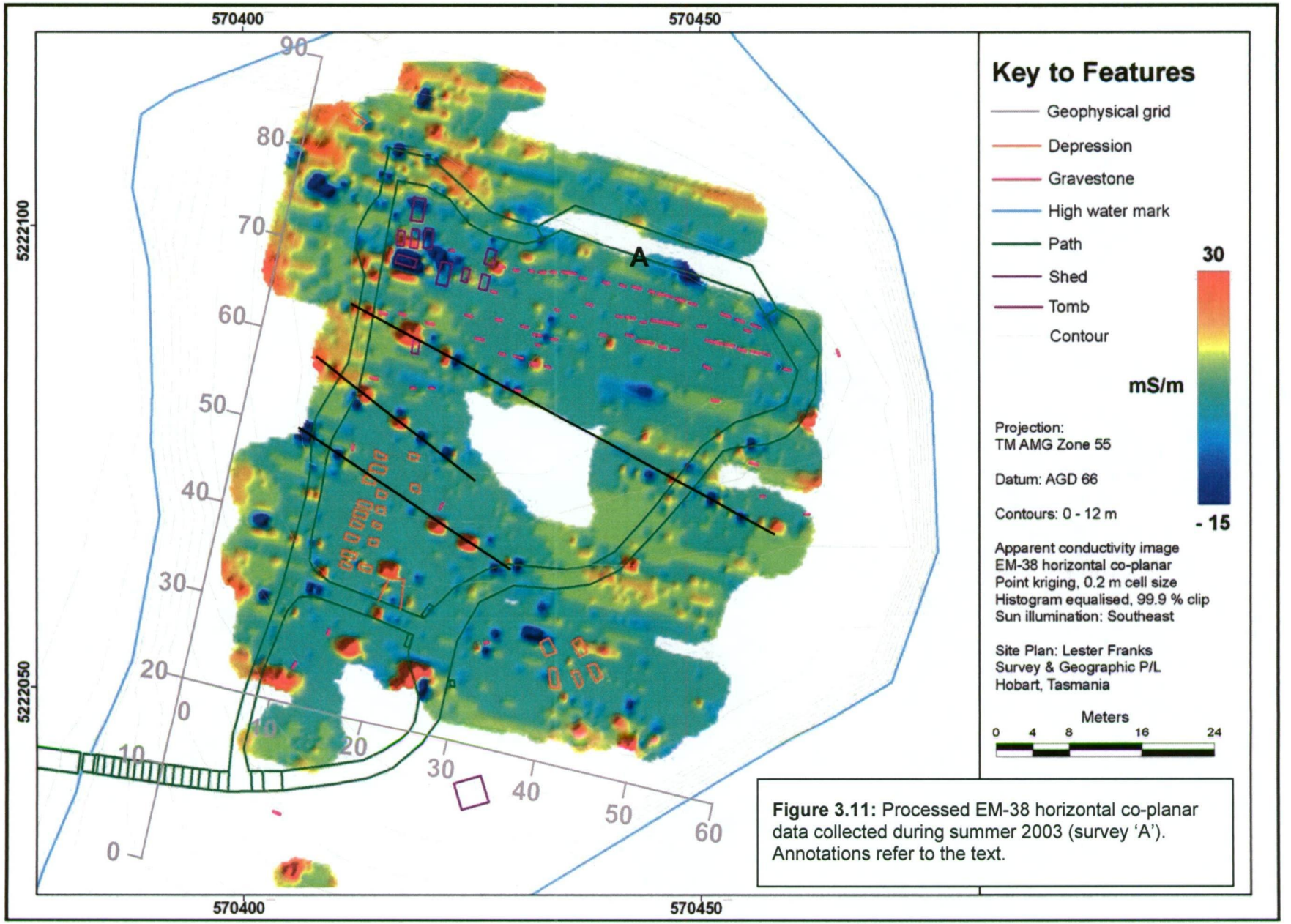

Figure 3.11: Processed EM-38 horizontal co-planar data collected during summer 2003 (survey 'A'). Annotations refer to the text.

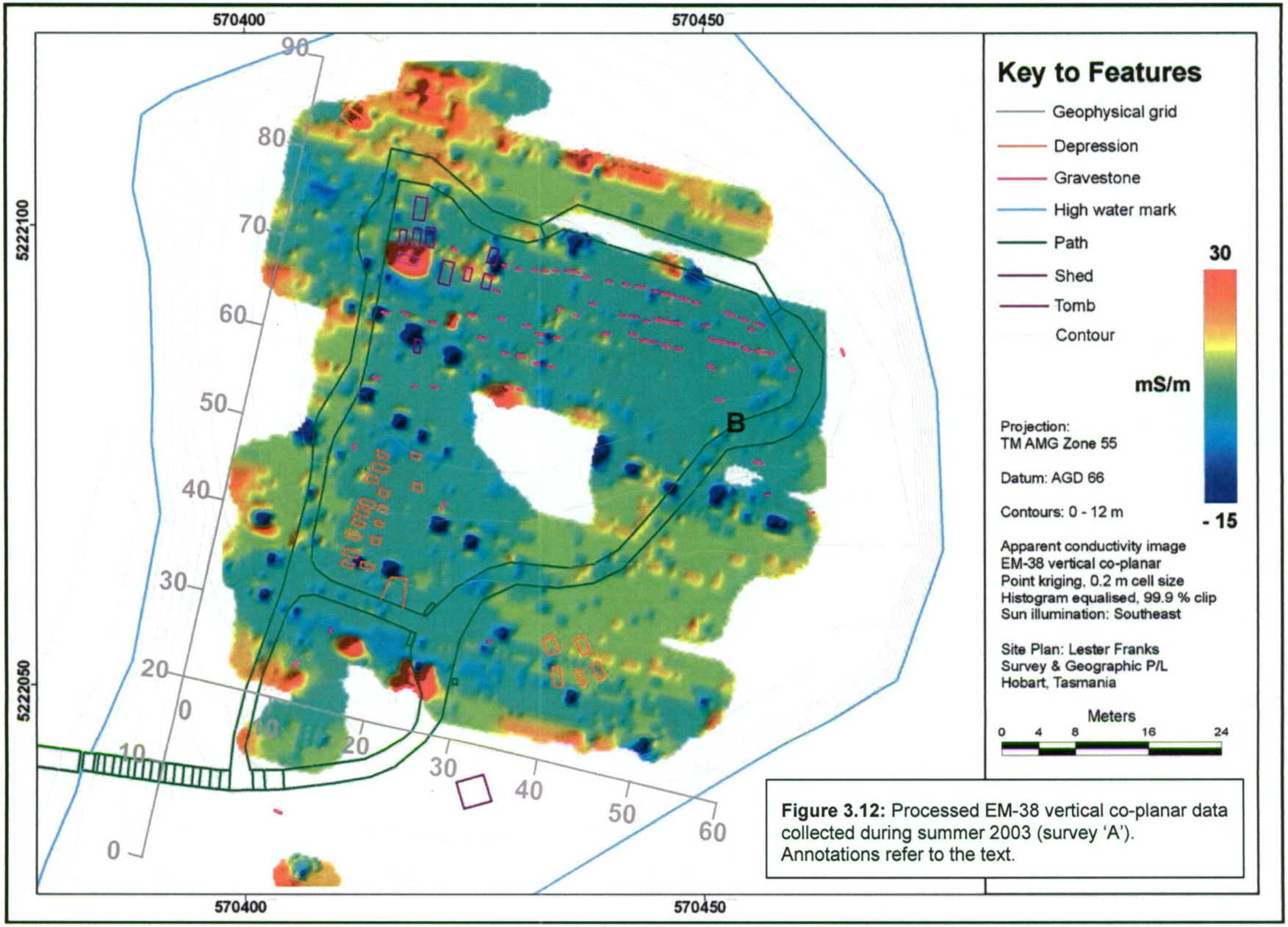

Figure 3.12: Processed EM-38 vertical co-planar data collected during summer 2003 (survey 'A'). Annotations refer to the text.

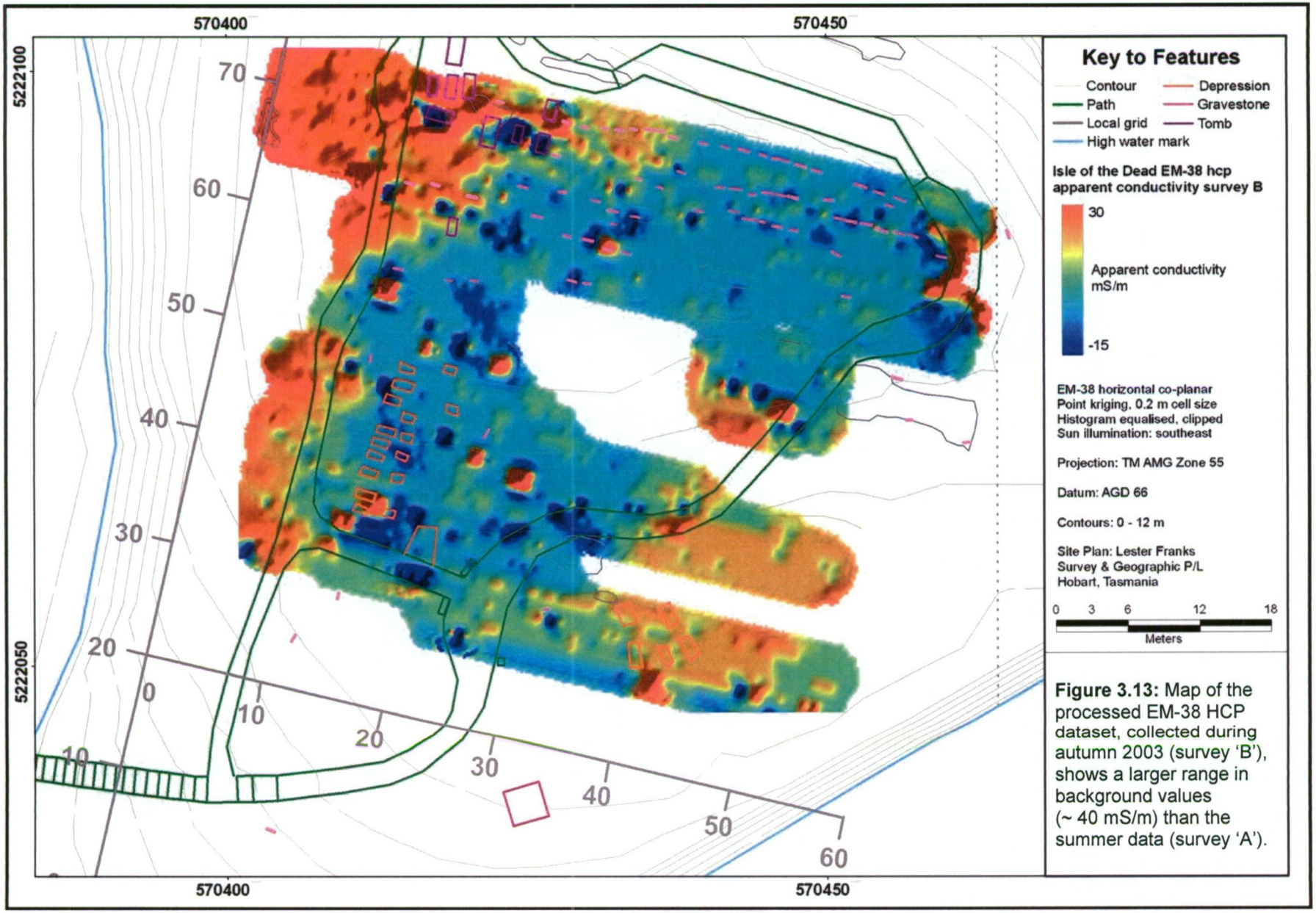

Figure 3.13: Map of the processed EM-38 HCP dataset, collected during autumn 2003 (survey 'B'), shows a larger range in background values (~ 40 mS/m) than the summer data (survey 'A').

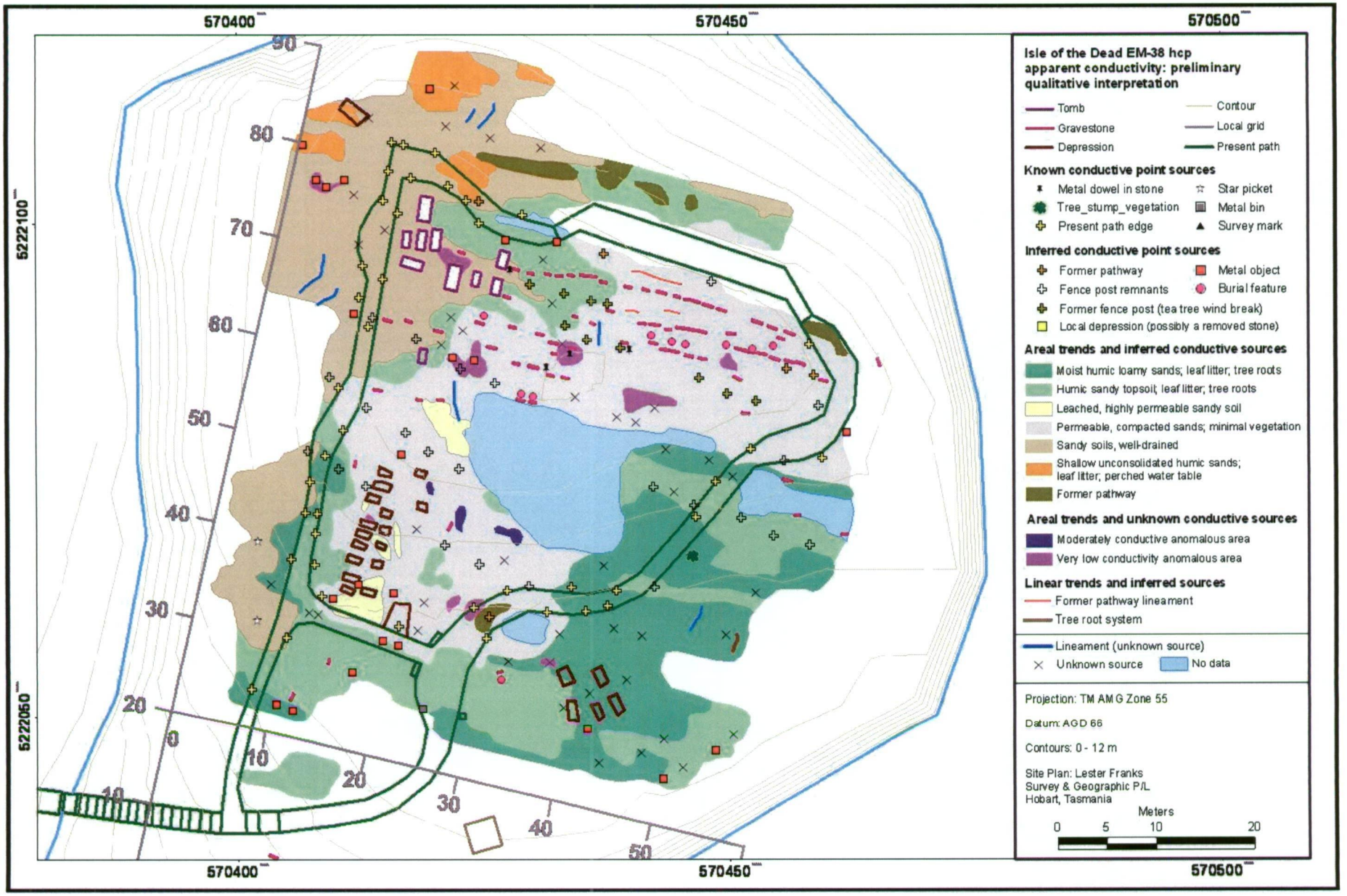

Figure 3.14: A schematic representation of point sources, linear trends and apparent conductivity variation, inferred from qualitative interpretation of HCP mode data. Annotations refer to the text.

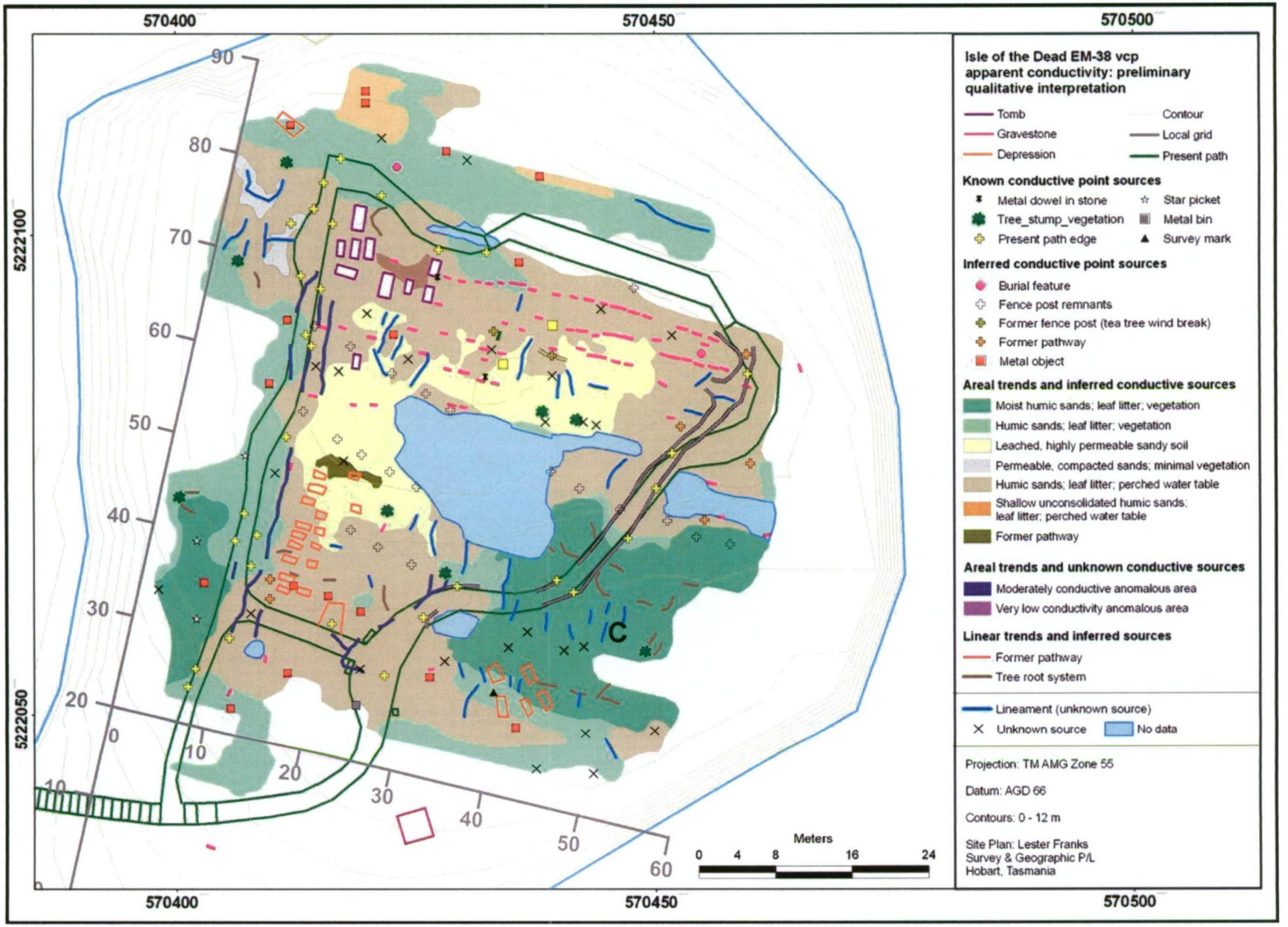

Figure 3.15: A schematic representation of point sources, linear trends and conductivity variation, inferred from qualitative interpretation of VCP data.

seen in the high to very high apparent conductivity zones of the Lower Bench (Figure 3.15, C) could be inferred as burial features. They are typically limited to several metres length, are spaced quite evenly and appear to be oriented NE - similar to the mounds photographed in Figure 3.4. The longer lineaments may be comprised of two shorter sections that were combined into one through gridding interpolation.

Figures 3.14 and 3.15 are qualitative interpretation maps that show the location of known, inferred and unknown point sources for the HCP and VCP survey modes respectively. Known causative sources of conductivity anomalies include contemporary cultural features such as the metal bin, star pickets, surveyors mark and nailing in the present pathway. Penal period features include metal pins used in stone repair, and metal railing around Caroline Aylett's grave (13x, 70y), shown in Figure 3.7. Large objects such as the railing are effectively sources of undesirable signal in the data, because they generate broad area very high amplitude responses that masked smaller nearby anomalies of lower value. Five cultural features are inferred as sources of geophysical anomalies, including the former fence post remnants mentioned above. Seventeen very high amplitude isolated anomalies, which do not correlate with known surface features, are interpreted as buried metal objects. Several of these anomalies may also be post remnants as they appear to align with the central NW – SE trends. A couple of low amplitude responses in the VCP data and ten in the HCP data are recorded adjacent to headstones and are interpreted as burial features. Numerous randomly distributed anomalies of various amplitude and width cannot be correlated to known or anticipated material, and are therefore attributed to unknown sources.

In summary, although the EM-38 is effective for mapping soil variations and for detecting some metallic objects, it does not systematically detect individual burials. The only inferred burial features are from the Upper Bench marked area, where coffins are most likely to have been used. Several contributing factors may have hindered the detection and characterisation of individual burials:

- the low geophysical contrast between burial material and surrounding soils,
- the masking effects of soil development in the permeable, porous sandy stratigraphy,
- a narrow dynamic range in apparent conductivities.

3.2.3 Magnetometry

Introduction

Mapping of magnetic field intensity across the Isle of the Dead aimed to locate any subsurface targets of a ferrous nature that are potentially associated with individual graves, including burial artefacts, coffin fixtures and chest tomb platforms of convict-made brick (King *et al.*, 1993). Magnetics has been successfully applied at several historic sites in North America, to map remnants of a cemetery enclosure, and detect buried metal artefacts (Kvamme, 2000; Witten *et al.*, 2001; Charles, 2003). It has also been used to detect interfaces of contrasting soil types associated with a trench (Brock and Schwartz, 2006; Lockhart, in press), although this is unlikely on the island because of its relatively non-magnetic homogeneous sandy stratigraphy.

3.2.3.1 Data acquisition

The survey was undertaken in October 2003, and in-filled in May 2004, during quiet geomagnetic conditions. Roving and base station measurements were collected using an Overhauser and proton precession magnetometer, respectively. The roving magnetometer sensor was attached to the end of a custom-built aluminium staff and held at a constant angle, 0.2 m - 0.25 m above ground. Positioning the sensor at this height avoided accessibility problems caused by low vegetation, helped to optimise depth sensitivity and reduced the effect of ferrous surface debris (Clarke, 1997). The base station sensor was mounted 1.6 m high on an aluminium tripod, and located at the Dockyards. Data acquisition parameters are presented in Table 3.2.

Table 3.2: Data collection parameters for the Isle of the Dead magnetic survey.

Survey type	Magnetic		
Instrumentation	GEM Systems GSM-19F Overhauser magnetometer Geometrics G-856 base station magnetometer		
Method of coverage	Bi-directional 'zigzag' surveying		
Traverse interval	1.0 m	**Distance trigger**	Time
Station interval	0.2 m	**Sensitivity**	0.1 nT
Comments	Profiling conducted with ≤ 1.0 m offset from parallel fibreglass measuring tape. Base station reading interval: 30 seconds.		

3.2.3.2 Post-acquisition data processing

The raw magnetic data (Appendix A, Figure A4) required several stages of processing to remove or reduce the effects of undesirable signal, and optimise visualisation for the detection and identification of archaeological features. Diurnal corrections were applied to both datasets, using a QuickBasic program written by Dr Michael Roach. Base station readings were subtracted from the mobile magnetometer data and the difference was added to a nominated reduction datum. No attempt was made to apply the reduction to the pole transformation to the data, since the inclination of the Earth's field at Port Arthur is steep (72 degrees) and also due to the predominance of small anomalies that were clearly caused by remanence. The May data was block shifted to match background values from the original survey.

Random dropouts and single point spikes in the data were visually identified in each profile and removed or attenuated by a spline interpolation between two correct measurements on either side of the error, using ChrisDBF® software. Nearly all types of magnetometer are subject to heading error - a subtle source of undesirable signal. Variation of sensor orientation from reading to reading or line to line will produce small deviations (~0.5nT) if uncompensated (Chapman and Bartels, 1962). Line effects in the raw magnetic data had an amplitude range of up to ~ 3 nT. Although these survey artefacts did not interfere with the interpretation, they were removed by manual micro levelling, to present a smoother map.

The raw magnetic data exhibited some parallax positional errors of 0.1 m – 0.2 m. These were mostly confined to the gravestone and tomb areas, where the presence of obstructions made it difficult to survey at a steady pace. The error was largely corrected by adjusting affected segments or whole lines by the lag value yielding to the best cross-correlation between the chosen section and its adjacent lines. Figure 3.16 shows the smoother TMI variation map after data processing.

3.2.3.3 Findings and interpretation

Introduction

A magnetic anomaly represents a local disturbance in the Earth's magnetic field that arises from a localised change in magnetisation or magnetisation contrast (Llopis and Sharp, 1997). An observed anomaly in processed data is an expression of the net effect of induced and remanent magnetisation. A discrete or linear magnetic anomaly is caused by point(s) source or linear features, such as a buried ferrous metallic object. An anomalous zone is an area of elevated values caused by an extended magnetic source, such as a gravel path. Geophysical anomalies are represented schematically on a data recognition map (Figure 3.17), and attributed to causative features of known, inferred or unknown cultural origin on a qualitative interpretation map (Figure 3.18).

A magnetic anomaly signature is affected by a number of factors, including the target characteristics, sampling rate, line spacing and gridding. If the target has permanent or thermo-remanent magnetism, then the anomaly tends to exhibit an irregular pattern (Nishimura, 2001). The issue of remanent magnetism is considered during the mathematical modelling process. High resolution was achieved in this survey only in the traverse direction, which has a 0.2 m sampling rate. All responses are therefore distorted laterally to some degree by the 1 m distance between profiles. Distortion has the potential to complicate interpretation, as exemplified by the 'zigzag' anomaly circled in black in Figure 3.16. This may represent one source, or two nearby sources interpolated into a single irregular shape during gridding. The gridding effect is also pronounced in the absence of measurements, such as at the grid edge, and is influenced by the 2.2 m search radius, as exemplified by the very low anomaly circled in white (Figure 3.16). Detection and identification of any linear features parallel and offset from the survey lines, or small point sources located between survey lines is limited by horizontal resolution in the north-south direction. Although narrower line spacing would have provided better longitudinal resolution, time constraints and equipment availability prohibited a more detailed survey.

The data recognition map and qualitative interpretation image show the inferred lateral position of magnetic source(s).

Broad areal trends in magnetic intensity

Background values for the island range from ~ 61900 nT to ~ 62050 nT, with the latter recorded in the exposed Upper Bench area enclosed by the walkway. There are a number of zones deemed 'anomalous' - where values deviated ± 50 nT from the local background – which are defined by relative amplitude in the data recognition map (Figure 3.17). The first zone (**A**), of moderately high magnitude, trends parallel to 28x and also follows the current pathway east up to the north-facing grave markers. There it joins to a very high amplitude (~ 62100 nT) area (**B**) and a high amplitude region (**C**) running parallel to the grave markers on the Upper Bench and partly following the path past the chest tombs. It then widens at the western side (**D**) into a very high magnitude zone (> 62300 nT).

The relatively high amplitude linear anomalies (**C**) that extend parallel to the burial markers and in the measurement traverse direction were initially interpreted as survey artefacts. In-line responses are typically caused by absolute errors such as instrumental drift or by a short abrupt change in the earth's magnetic field during the measurement of that line. When these anomalous zones are viewed collectively, the configuration and elevated magnetic values indicate that they are remnants of the late 20th century gravel step path (Figure 3.6), which is also visible in the EM-38 data. The short extension northeast at (**E**) is likely to be a section of the former pathway (Figure 3.5) that continued to the original landing place described by Lord (1999). The high magnitude zone (**D**) located in a clearing west of the chest tombs, may have been the site of the funeral party shelter also described by Lord (1999).

Responses from the brick chest tomb foundation platforms (Figure 3.8) are weak compared to the nearby high amplitude response from the wrought iron railing at Caroline Aylett's grave (Figure 3.7). Convict-made bricks used on Isle of the Dead likely only exhibit relatively weak thermo-remanence, due to under-firing (Bell, 1981).

Isolated anomalous responses and linear trends

The distribution and character of isolated anomalous responses is recorded on the magnetic data recognition map (Figure 3.17), and the interpretation map (Figure 3.18). Isolated anomalous responses on the data recognition map are marked as either

monopolar (dominant negative or positive) or bipolar - two basic categories from which most other more complicated anomalies with multiple peaks could be constructed. A monopolar anomaly as defined here consists of a group of measurements of magnitude 50 nT greater or lesser than the local background readings. A dipolar anomaly consists of two closely associated responses of higher and lower magnitude than the surrounding background values. Major anomalies interpreted at each site are discussed below.Two broad negative magnetic disturbances centred on (F) and (G), appear to be anomalous zones but are derived from known point sources: the Aylett grave cast iron railing (Figure 3.7) and a cluster of contemporary site features (metal bin, bench and shed). The responses at (H) corresponds to ferrous metal dowels used in 20th century stone repair, identified via physical evidence and/or the headstone condition assessment report compiled for PAHSMA by Thorn (2002).

There are numerous other anomalies attributed to contemporary features on the island. The visible remains of star pickets on the western side are apparent as very high amplitudes measured across several profiles. These anomalies are comparable in form and magnitude to a many others located between gridlines 40y and 65y. There also appear to be three pseudo-linear series of strong responses across the island - represented by black lines in Figure 3.17. These are similar to trends identified in the EM-38 data. The amplitudes of anomalies in these series range from low to very high. Some exhibit pronounced bilateral symmetry, which is a typical indicator of a source of uniform composition (Bevan, 1991), while others exhibit slightly symmetric to irregular shapes. Several broader anomalies have a low overall magnitude but exhibit a variety of localized magnetic peaks. It appears that these are probably relatively shallow sources.

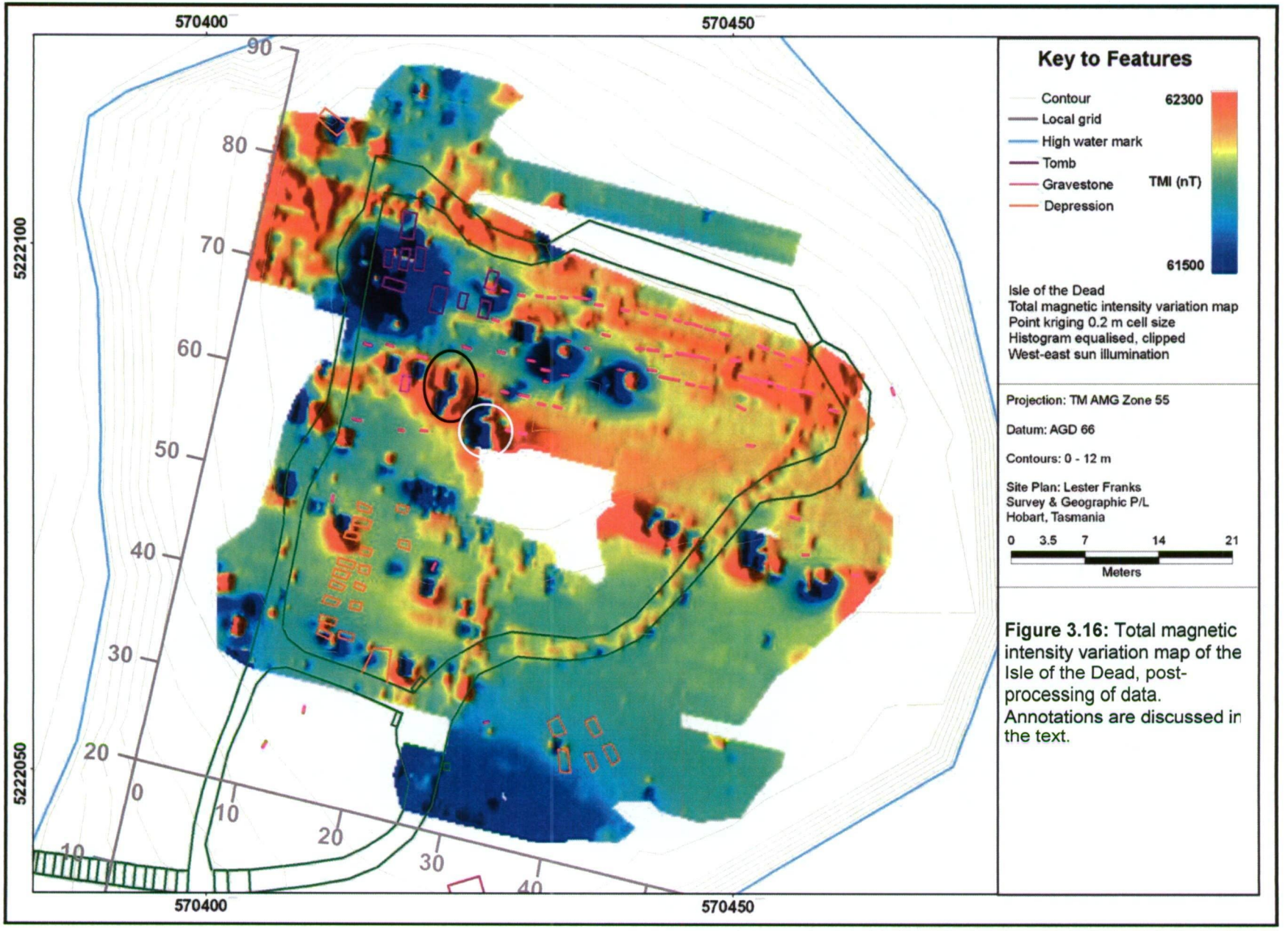

Figure 3.16: Total magnetic intensity variation map of the Isle of the Dead, post-processing of data. Annotations are discussed in the text.

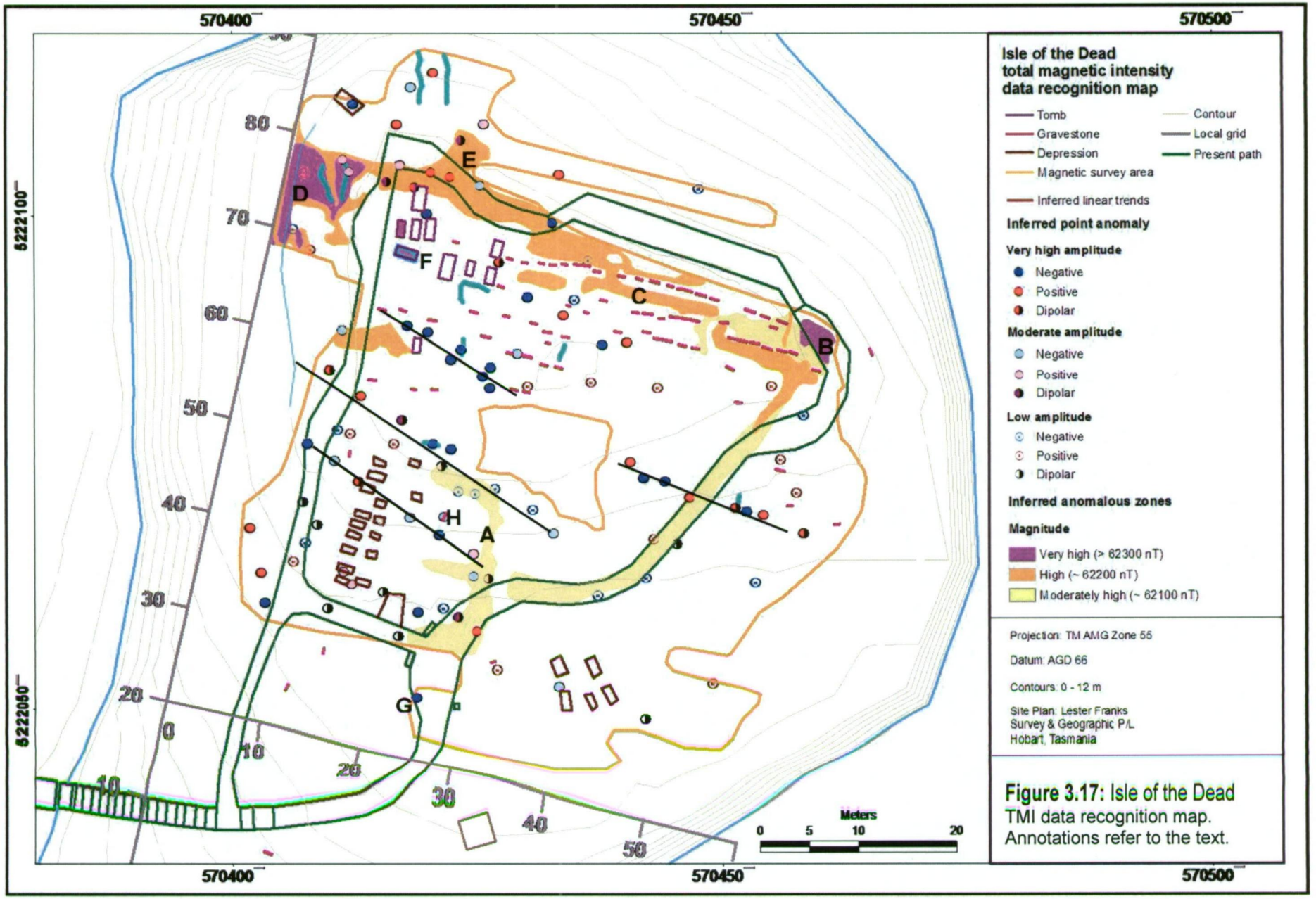

Figure 3.17: Isle of the Dead TMI data recognition map. Annotations refer to the text.

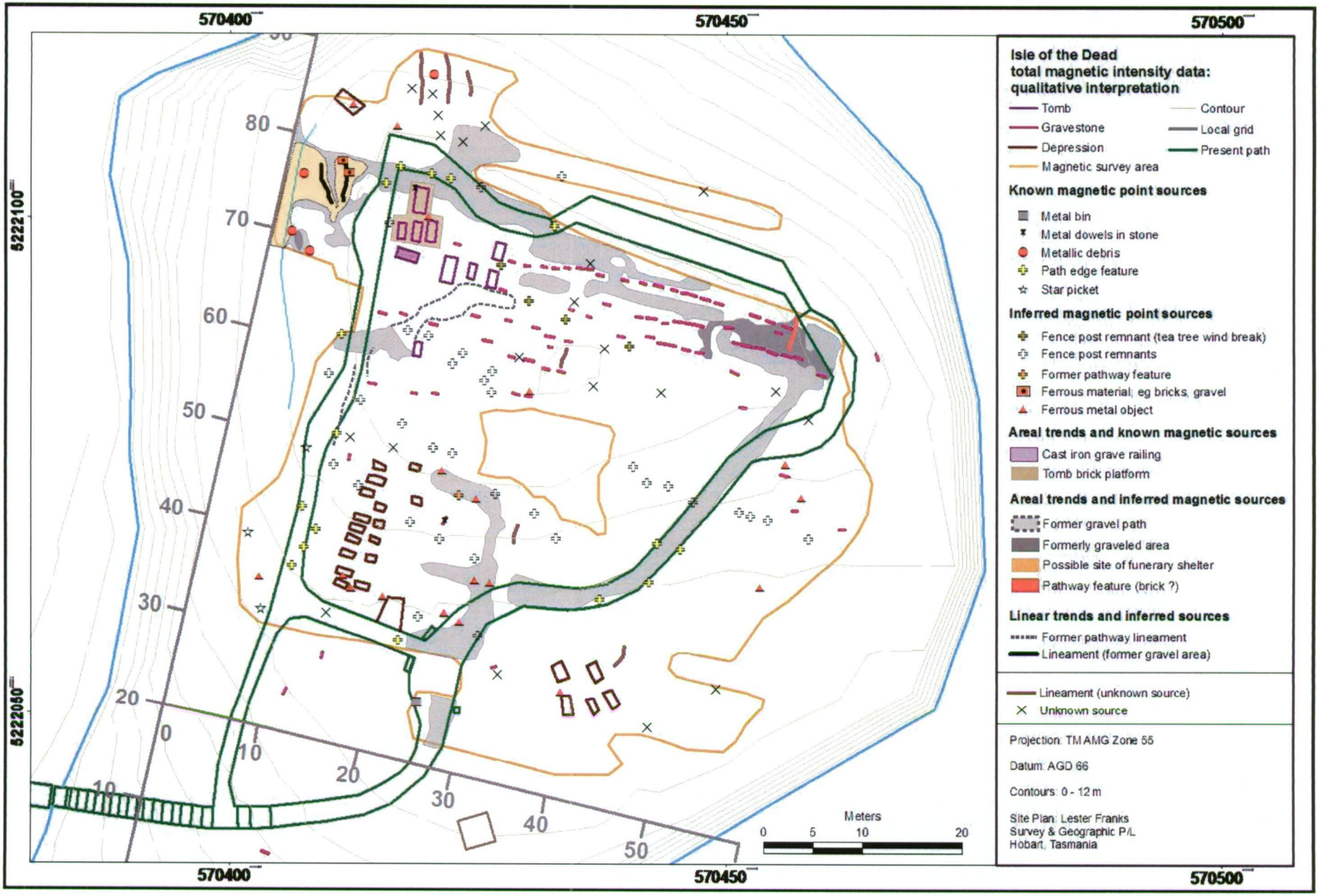

Figure 3.18: Isle of the Dead total magnetic intensity qualitative interpretation map.

The complex nature of the near field of any magnetic object tends to be emphasised by close proximity to the instrument (Bevan, 1998). High relative intensity also results from archaeological features with remanent magnetisation (Cammarano *et al.*, 1997).

The linear trends likely reflect a series of remnant fence posts and possible associated features such as brickwork. These features may date from the 1930s remembrance garden. This interpretation is supported by similar anomalies derived from the visible star pickets, which align with the linear trends in two out of three cases. Further, the orientation appears not to correlate with that of the burial markers - unless the markers have been moved from their original positions.

Other isolated symmetrical anomalies of low amplitude are attributed to features from the former gravel pathway and present bark chip pathway. Remnants of fence posts used in the former tea tree windbreak pictured in Figure 3.6 give very high magnitude signals over several profiles. This again probably indicates that they are at shallow depths, have remanent magnetism and low material deterioration - as might be expected from objects only ~ 20 years old.

Quantitative interpretation: estimation of source depth

Quantitative interpretation of anomalous magnetic responses in archaeological contexts usually includes estimating depth to top or centre of source and the lateral location. The breadth of the magnetic peak allows some estimation of the discrete source depth, as the amplitude decreases as a function of the inverse distance cubed (Telford *et al.*, 1990). The width of the anomaly also depends on its size - if the feature is of considerable width, then the shape of the anomaly changes to become flat-topped (Telford *et al.*, 1990). For the purposes of this investigation, the processed (unclipped) magnetic data was interpreted by estimating only the source locations and depths to centre, using data interpolated onto a regular grid.

Mathematical modelling and a basic standard method of manual quantitative interpretation were used to compare the depth estimations of four sources exhibiting different response signatures. Subset windows were chosen with reference to the automatic modelling method, so that they were small enough to minimize the effects of interfering sources and associated poor convergence, although large enough to

represent broad anomalies for reliable results. The use of gridded data enables simple and quick production of resulting images, which show regional structural patterns, and are easily overlain on other maps.

Subset 1 (22x, 72y) has a very high amplitude dipolar anomaly whose causative feature is inferred as a ferrous metal object. Subset 2 (12x, 56y) has a high frequency positive response over nine measurements, and subset 3 (14x, 47y) includes an equally strong dipolar anomaly. The latter two are interpreted as fence post remnants. Subset 4 (54x, 46y) is a narrow weak response, derived from a small ferrous metal object and/or buried bricks.

Mathematical modelling

The magnetic data presented numerous regular shaped isolated anomalies that were suitable for mathematical modelling to estimate source position and depth to centre. Subsets 1 to 4 were modelled as follows.

The inducing field for modelling was defined by a magnetic field 62000 nT, azimuth 14 degrees and inclination of –72 degrees. For each subset, a simple theoretical body (sphere) was created and used to model a corresponding magnetic anomaly. Sphere diameter was constrained during inversion. Inverted parameters included three - dimensional position, magnetic susceptibility K, and remanent magnetisation vectors. These include the inclination I, total geomagnetic intensity T and the projection of T into the x, y plane: the horizontal component H, situated in the direction of the local magnetic meridian. Two calculations were run for each subset, with the sphere diameter 0.5 m and 0.2 m, the results of which are shown in Tables 3.3 and 3.4 respectively. Depth is reported as distance between the sensor (0.2 m above ground) and source centre, and is at best only indicative since a spherical model will likely be a poor approximation for some features. Because both remanence and induction are inverted, the susceptibility and remanent magnetisation values are almost certainly poorly constrained and largely inconsequential, but the anticipated depths are probably little affected by the relative contributions from the two forms of magnetisation.

Subset	Local grid position (x, y)	Vertical distance to source centre from sensor (m)	Magnetic susceptibility K (SI Units)	Remanent magnetisation intensity (Amp m^{-1})
1	22, 72	0.68	0.18	20.15
2	12, 56	0.68	0.23	- 17.18
3	14, 47	0.67	- 0.37	- 7.95
4	54, 46	0.4	- 0.01	0.34

Table 3.3: Mathematical modelling results for a sphere of diameter 0.5 m.

Subset	Local grid position (x, y)	Vertical distance to source centre from sensor (m)	Magnetic susceptibility K (SI Units)	Remanent magnetisation intensity (Amp m^{-1})
1	22, 72	0.636	46	313
2	12, 56	0.64	70.19	- 294
3	14, 47	0.62	-2.06	- 120
4	54, 46	0.22	- 0.12	2.21

Table 3.4: Mathematical modelling results for a sphere diameter 0.2 m.

For subsets 1 to 3, the difference between the estimated depths calculated for a sphere of diameter 0.5 m and one of diameter 0.2 m is ~ 0.1 m. In each case, constraining the sphere diameter to 0.2 m resulted in unrealistically high compensatory values for the magnetic susceptibility and remanent magnetisation. Subset 4 shows minimal variation in the magnetic susceptibility and remanent magnetisation intensity vector. Based on these calculations, it is probable that isolated anomalies similar to subsets 1 to 3, i.e. very high frequency, would also lie within 0.5 m cover. A narrow low amplitude anomaly similar to subset 4 would be due to features on or just under the ground surface, most likely small metallic debris. The inversion process achieved good comparison between the calculated and measured responses, as seen in both the subset plans and section views (Figure 3.19). Calculated source locations concurred with those on the data recognition map that were manually estimated using the approach previously outlined by Telford *et al.* (1990).

Estimating the feature depth manually

The 'half-maximum rule' assumes that 'the vertical distance from the magnetic feature to magnetometer equals 1.3 times the lateral distance between the maximum measured value and one-half of this value' (Burger, 1992). Depth values estimated for the four subsets are listed in Table 3.5, adjacent to those modelled previously from spherical bodies. Comparison of the results shows that the manual method does not give consistently higher or lower estimates than the mathematical calculations. The maximum differences between the manual values and those modelled from 0.5 m and 0.2 m diameter spheres are 0.1 m and 0.17 m respectively.

Subset	Local grid position (x, y)	Half-maximum rule: estimated depth to source centre (m) from the sensor	Vertical distance (m) to source centre from sensor, modelled from a sphere of diameter:	
			0.5m	0.2m
1	22, 72	0.78	0.68	0.636
2	12, 56	0.65	0.68	0.64
3	14, 47	0.58	0.67	0.62
4	54, 46	0.39	0.4	0.22

Table 3.5: Depth to source centre from sensor height, estimated from manual qualitative interpretation methods, and the mathematical modelling.

Comparing magnetic and apparent conductivity data

Many inferred sources of discrete magnetic anomalies were coincident to responses shown in the EM-38 inphase interpretation maps. Close correlation indicates that these sources are ferrous and conductive – most likely iron objects. Point sources and linear trends recorded by both techniques have been synthesized into a combined interpretation map (Figure 3.20). The map also shows inferred broad area trends in magnetic intensity and schematic regional variation in apparent conductivity derived from both survey modes. The northern extension of the gravel path inferred from the magnetic data coincides with an area of high conductivity values, part of which was already interpreted as the pathway. A similar situation is apparent on the lower bench and eastern riser slope, where the gravel path detected by the magnetic survey confirmed the apparent conductivity lineaments interpretation.

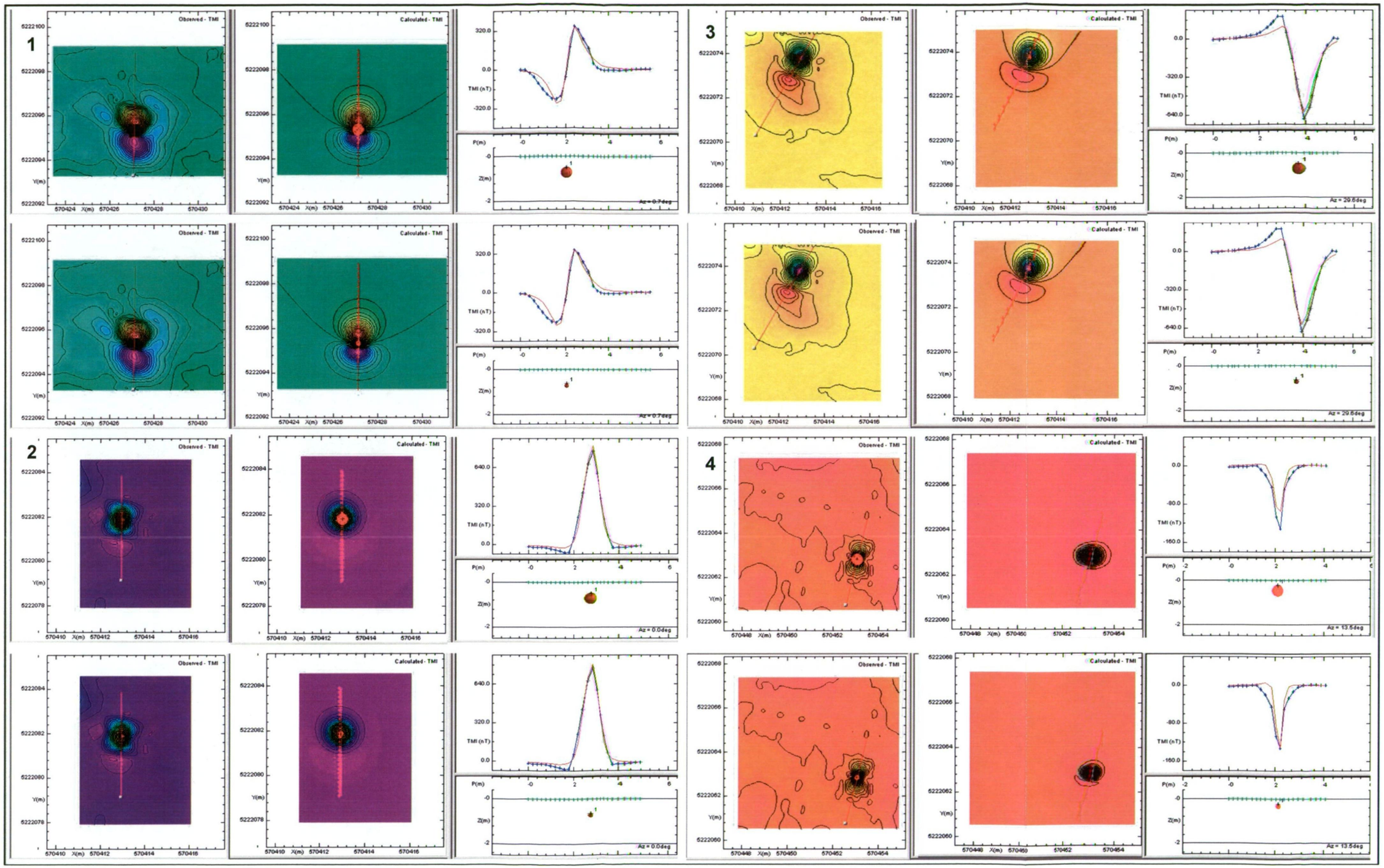

Figure 3.19: Observed (blue line) and calculated or 'modelled' (red line) responses for magnetic spherical bodies of diameter 0.5 m and 0.2 m, in both the subset plan and section format.

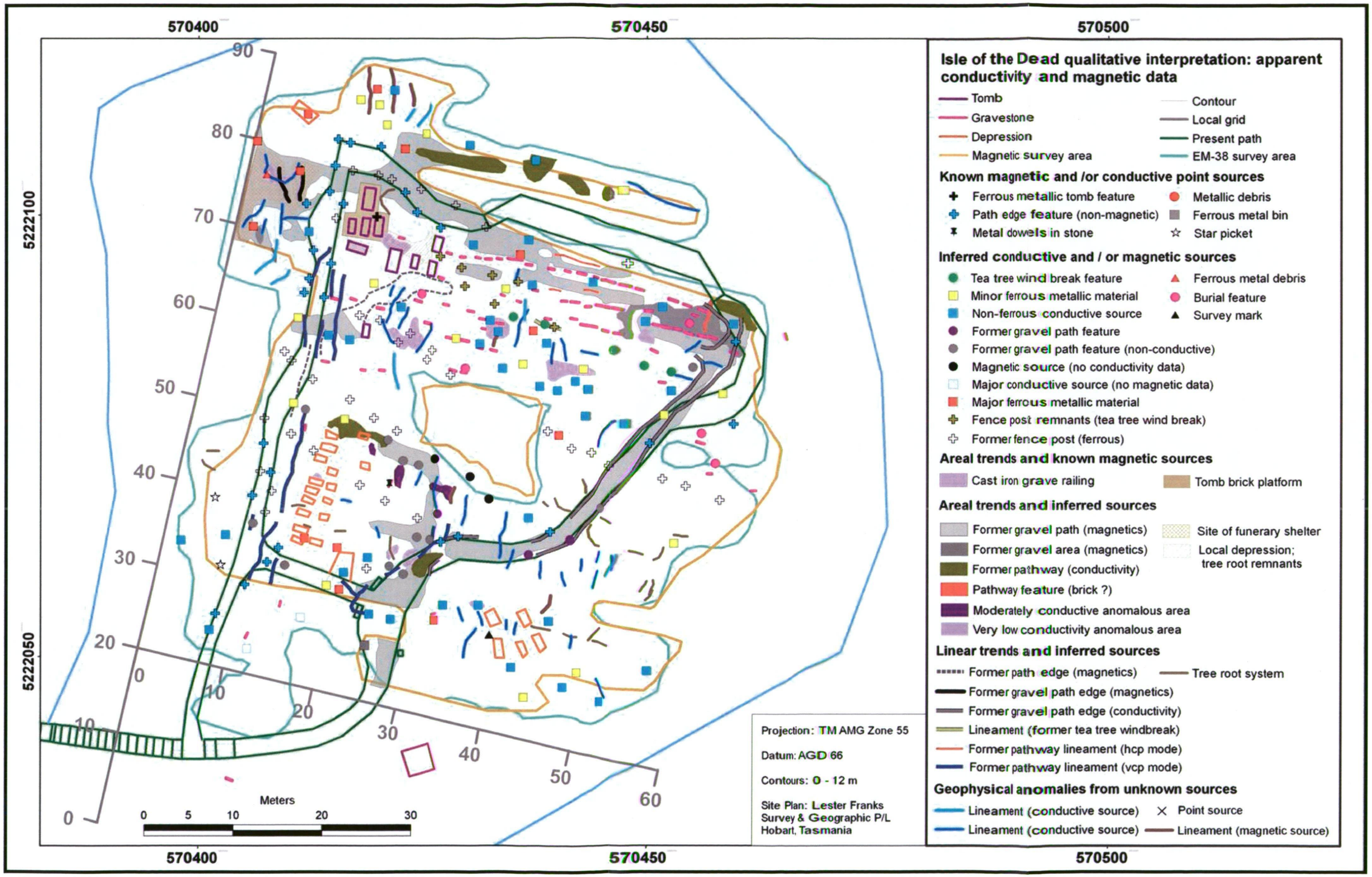

Figure 3.20: Isle of the Dead lateral distribution of known and inferred magnetic and/or conductive point sources and linear trends.

3.2.4 Seismic refraction

Introduction

A seismic refraction survey was conducted in October 2003. The Isle of the Dead presents a suitable site for this method, because of the relatively simple stratigraphy (compared to areas of the main site) and accessibility. It was anticipated that the base of the weathered surface layer (regolith – bedrock interface) would provide a sharp geo-mechanical contrast for depth profiling. It was also hoped that the more gradual boundary between the sandy soil column and unconsolidated regolith would provide a measurable velocity contrast. The soil column was expected to be at least 1.2 m deep, as indicated by the soil tests and physical evidence on the sea cliff. Hand auger refusal depths ranged from 0.45 m at the northern end to 1.65 m on the lower bench (Section 3.1.1), a conservative estimate of soil profile. The following sections describe the survey methodology and post-acquisition data processing. The results and interpretation for each transect will be discussed in terms of the site context, and illustrated by selected tomographic velocity models.

3.2.4.1 Data acquisition

Four transects were surveyed, along gridlines 15x, 66y, 32y and 45x, to span the northern and southern burial zones (Figure 3.21). Six of the eight hand auger sites were positioned coincident with these profiles, to provide stratigraphic information for calibration of the seismic data. Geophones and energy sources were located in a collinear arrangement parallel to survey line. An in-line spread was convenient for cable handling and ease of field data interpretation. The geophone spikes were positioned vertically and firmly into the soil, and 20 cm radius of vegetation cleared to minimise the influence of random noise produced by movement. For transects longer than 12 m (all except Line 45x) each spread of geophones was rolled along with twelve metres overlap. Shots were taken at 0.5 m offset from either end plus every 3 m along-line. Reversed profiles are generally needed to distinguish whether data indicate several refractors, refractor relief, or refractor velocity changes. The overlap and phone spacing created sufficient data redundancy in each spread to permit tomographic processing.

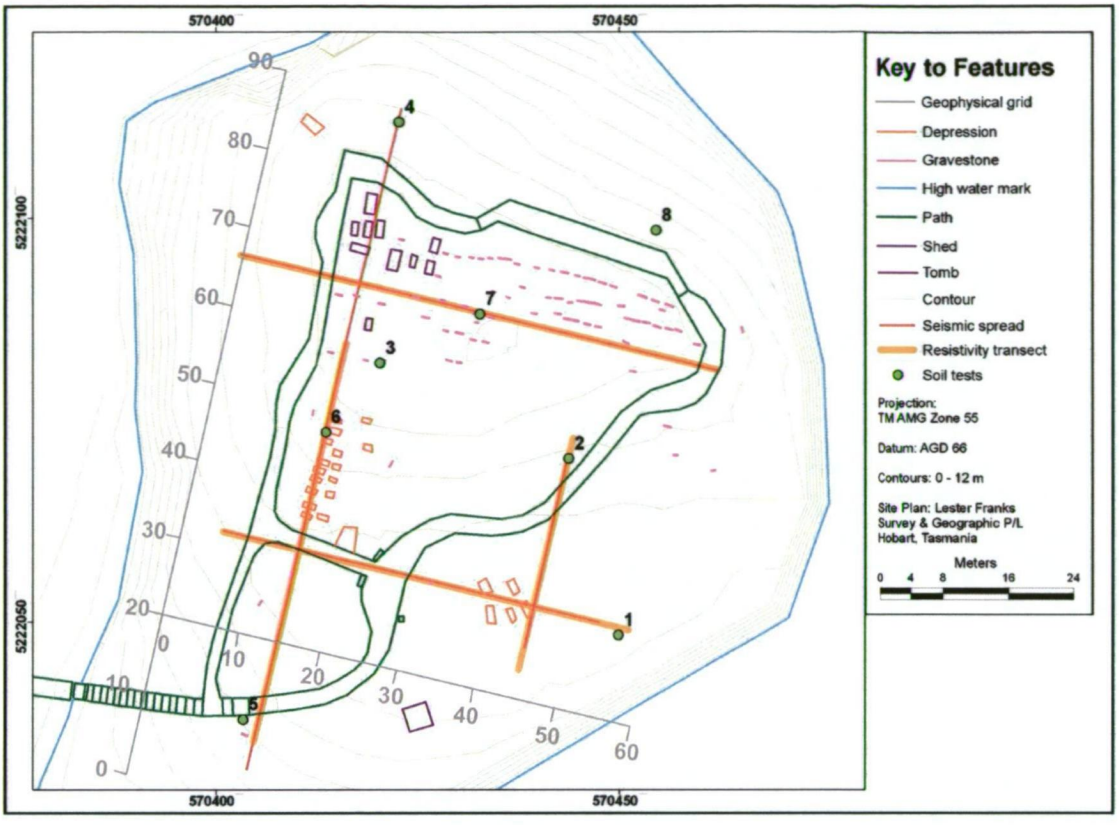

Figure 3.21: Seismic spread and resistivity transect locations, in relation to auger test sites.

Elastic waves were generated by striking a steel hammer against a steel plate, placed horizontally in small depressions excavated in all shot-point locations (Figure 3.22). The instant of impact was determined by a piezoelectric inertial switch on the hammer handle that was connected to the seismograph. Data were collected in periods of low wind and noise from island tours, both potential sources of non-repeatable random noise. After each shot, the data quality was assessed by making an initial calculation of overburden and refractor apparent velocities from the first breaks. If the signal-to-noise ratio (S/N) was too low, responses from successive shots were sometimes stacked or discarded and repeated to reduce both random and coherent noise. Data collection parameters are listed in Table 3.6.

Figure 3.22: Seismic refraction profiling along Line 15x, with the author and Dr Michael Roach (courtesy of PAHSMA, 2003).

Survey type	Seismic refraction		
Instrumentation	EG & G Geometrics Geode Seismograph (24 channel)		
Area surveyed	Four transects, total length 217 m		
Spread type	Collinear		
Shot position	End shots at 0.5 m offset and 3 m intervals along line		
Geophones	24	**Frequency**	28 Hz
Geophone interval	1 m	**Vertical stacks**	5
Comments	Occasional low frequency incoherent noise due to tour groups.		

Table 3.6: Tabulated seismic refraction survey parameters for the Isle of the Dead.

3.2.4.2 Post-acquisition data processing

Trace amplitudes were normalised and individually adjusted in the Seismodule Controller program shot window for optimum visualization of first breaks. The initial instance of both the direct wave and refractor head wave were manually picked in the shot window (Figure 3.23). Breaks that were too noisy for comfortable definition of the first arrival were not picked, thereby minimizing subjectivity. Occasionally, weakly refracted responses were too difficult to pick, where rapid attenuation resulted in small head wave amplitudes at large source-to-detector distances. Theoretical studies show that 'direct wave amplitudes attenuate as the inverse of the distance, and that head wave amplitudes attenuate approximately as the inverse square of the distance' (Palmer, 1980).

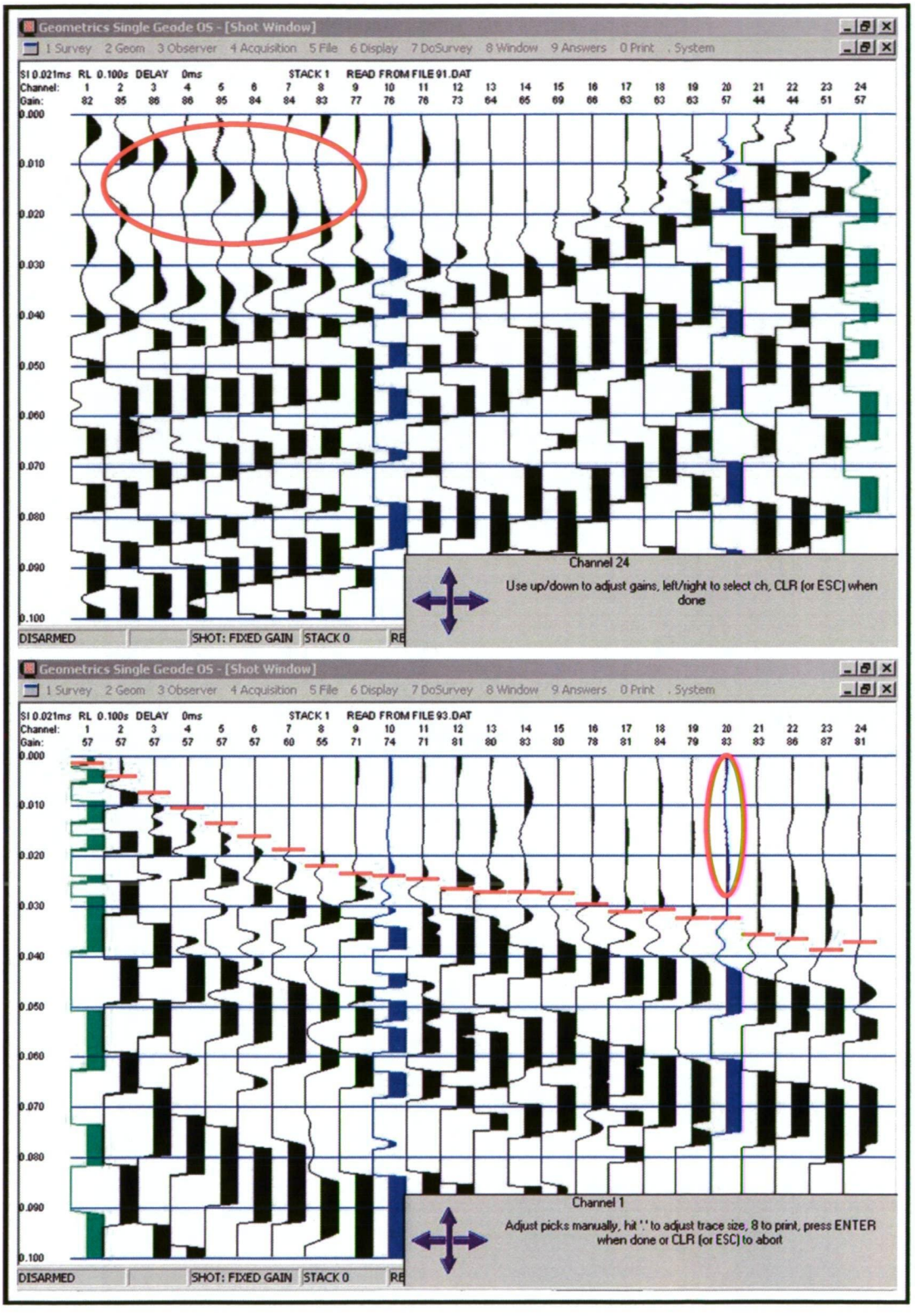

Figure 3.23: Seismograms from Line 66y with shots taken at 21.5 m (top) and 12.5 m (bottom). The top image exhibits coherent noise from traces 1 to 9 (circled), while the bottom image shows incoherent noise at trace 20.

First breaks recorded for each shot (e.g. Figures 3.23) were saved as 'break files' and imported into PlotRefa™ (version 2.66), a module of SeisImager™ (version 3.0), for analysis of each collection of nine shot records. The program was limited to processing nine appended files at one time. Observed results for all nine shots in a spread are displayed in a composite travel time plot as shown in Figure 3.24. The travel time data permits the calculation of the average seismic velocity of each layer and thickness to the top of each layer.

The travel time curves for each spread were processed in two stages comprised of forward modelling, followed by tomographic inversion. Two modelling options were trialled and the best results were used in the inversion. Tomographic inversion is a technique that can accommodate simple irregular interfaces and major variation in the seismic velocities, and is therefore suitable at this site. It uses a repeated forward modelling approach to produce depth profiles for each refractor, computed over a rectangular cell matrix. The analytical procedure considers the shot and receiver geometry and the measured traveltimes and calculated velocities. Elevation data collected by PAHSMA was also incorporated to correct for ground level. The velocity model was run through ten iterations, to optimise the travel-time error between the calculated and observed data. Although the model is displayed to the spread width and a nominated depth, interpretation was only valid for the region constrained by the ray paths.

The time-term inversion method involved manual definition of the crossover point to produce a two-layered model for tomographic inversion. Theoretical ray paths were executed and drawn on the model and calculated travel time curves displayed alongside the observed data. The alternative tomographic method produced a fifteen-layer model for inversion, with a velocity range of 300 m/s to 4000 m/s. The average error in convergence (RMSE) between the calculated and observed travel time curves for each shot was measured to determine which starting model (using either method) provided the best fit.

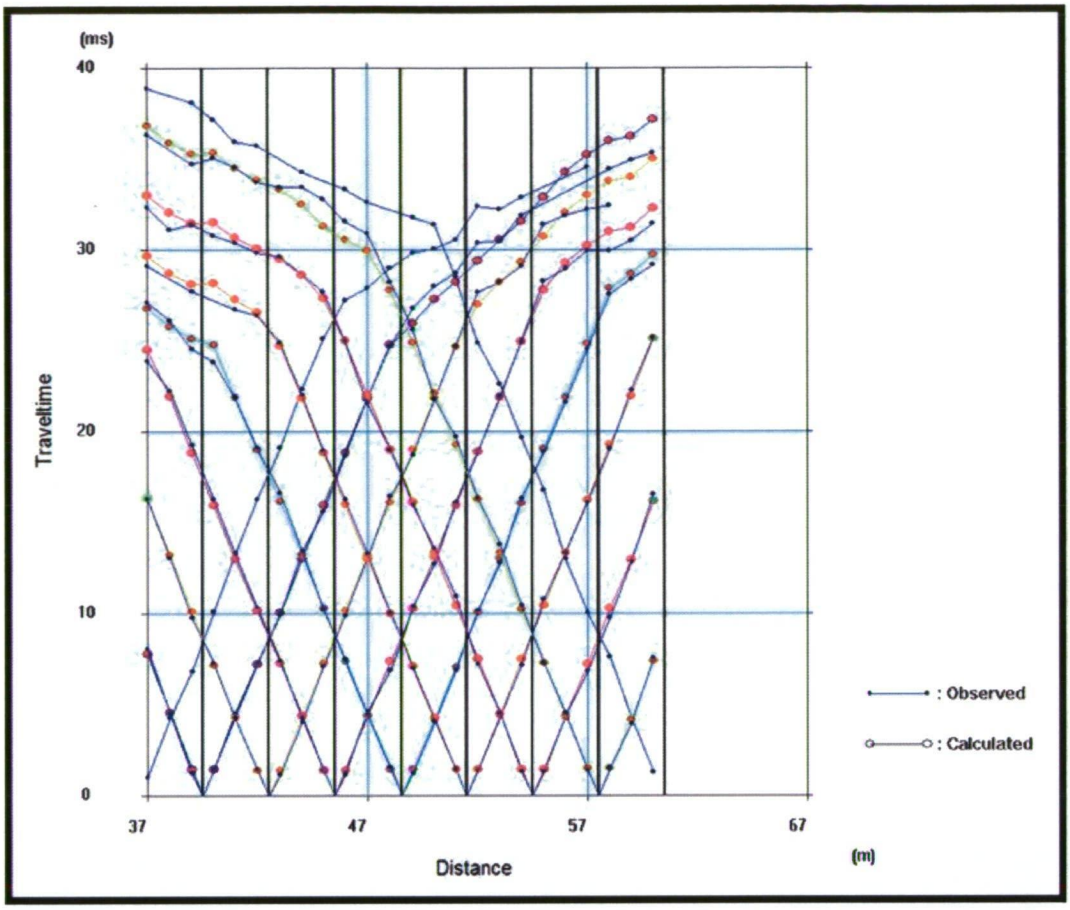

Figure 3.24: A typical example of travel time curves from the last spread of Line 66y. Calculated travel times are shown for all except the end shots, a common but inexplicable outcome of the tomographic inversion. The average error in convergence between the observed and calculated curves is 0.63 ms.

Multiple models were produced using the two methods, each based on an edited variation of the observed travel time curves. The initial version was processed from the original results and successive models were created from edited plots and/or occasionally with a redefined crossover point. Editing involved the deletion of outlying first break points that caused obvious 'kinks' in the travel time curve. Consistent rate of change in the travel time curves of the refraction line encouraged the inversion to converge to global rather than local minima, with the aim to reduce the RMSE to an acceptable level (< 0.8 ms). The preferred velocity model for each spread required a low RMSE and realistic assignment of layers and velocity values.

Final velocity models for each nine shot transect were saved in text format and amalgamated. The refraction data for an entire line was then re-gridded in Surfer® using point kriging (0.2 m cell size) to produce a final tomogram. Interpretation of the seismic results was based on this tomographic output and the site context.

3.2.4.3 Findings and interpretation

Introduction

This section presents the seismic refraction tomography results and interpretation and discusses them in the context of other geophysical profiling and soil testing conducted on the island. The data from Line 45x will be used to illustrate the process of converting the 2D tomographic velocity model to an interpretative section. Final velocity-depth models and associated interpretations for all transects are shown in Figure 3.25, with position and depth of hand auger refusal included as a comparative information source.

Data quality and curve matching

The reliability of seismic mapping is strongly dependent upon the quality of the records. The seismic profiles are occasionally affected by both coherent and incoherent noise. Coherent noise, such as the low frequency interference shown in Figure 3.23, can be followed across at least a few traces (phones 1 – 9 in top image). In this case, the noise was caused by a tour group standing just off the end of the spread. High frequency incoherent noise is evident in trace 20 in the bottom image.

The raw travel time curves were often quite irregular, but they typically did not have to be heavily edited to produce the preferred velocity model. Selected editing reduced the variation along refraction plots and the errors in convergence ranged from 0.44 ms to 0.98 ms, with the average at 0.73 ms - a satisfactory outcome. Redefining the crossover point did not have much effect on the resultant calculated curves. The time-term inversion proved more effective at producing a low RMSE than the initial tomographic forward model.

Two primary layers are apparent upon initial display of the Line 45x velocity model. Layer 1 has a velocity range from 300 m/s to 450 m/s and is separated by a sharp gradient from Layer 2, which has a faster wave speed of > 2000 m/s (Figure 3.25, image **A**). The latter is consistent with the values expected for consolidated but weathered sandstone. In image **B** the data is clipped from 300 m/s to 500 m/s to reveal that Layer 1 is actually comprised of two horizons, which are separated by an undulating interface. The position of this undulating boundary was manually interpolated. Image **D** presents

a schematic interpretation of the tomographic information, including the three strata and refusal depth for auger 2. The soil test result correlates well with the seismic refraction depth model, considering the different scales of investigation.

The stratigraphic trend identified in Line 45x is also exhibited in Lines 66y, 32y and 15x. Velocities are consistent across all tomographic models: Layer 1 (< 300 m/s), Layer 2 (~ 400 m/s) and Layer 3 (> 2000 m/s). Figure 3.28 shows the apparent velocity inversion results and corresponding interpretative depth models for each transect. Auger refusal depths are in very close agreement with the base of Layer 1, inferring that Layer 2 is most likely the highly weathered sandy regolith and Layer 3 the weathered but still consolidated Permian sandstone-siltstone bedrock.

Velocities lower than ~ 1200 m/s usually indicate that material is 'trenchable' (i.e. a ditch-digging machine can cut through it easily) in engineering parlance (Sharma, 1997). It is therefore possible that burial shafts could have been dug into the weathered sandstone regolith. Some undulations at the inferred soil regolith interface correspond with overlying surface depressions and disturbed subsurface (as interpreted from the GPR), such as in Line 15x between 30 y and 50y, although there is no consistent evidence of velocity changes between the culturally emplaced and undisturbed soils at the site. A relatively high velocity zone in Line 45x, Layer 2 (53 m – 55 m), coincides with several hyperbolic GPR responses recorded within a depth range of 0.5 – 1.5 m, and has been tentatively inferred as shallow regolith.

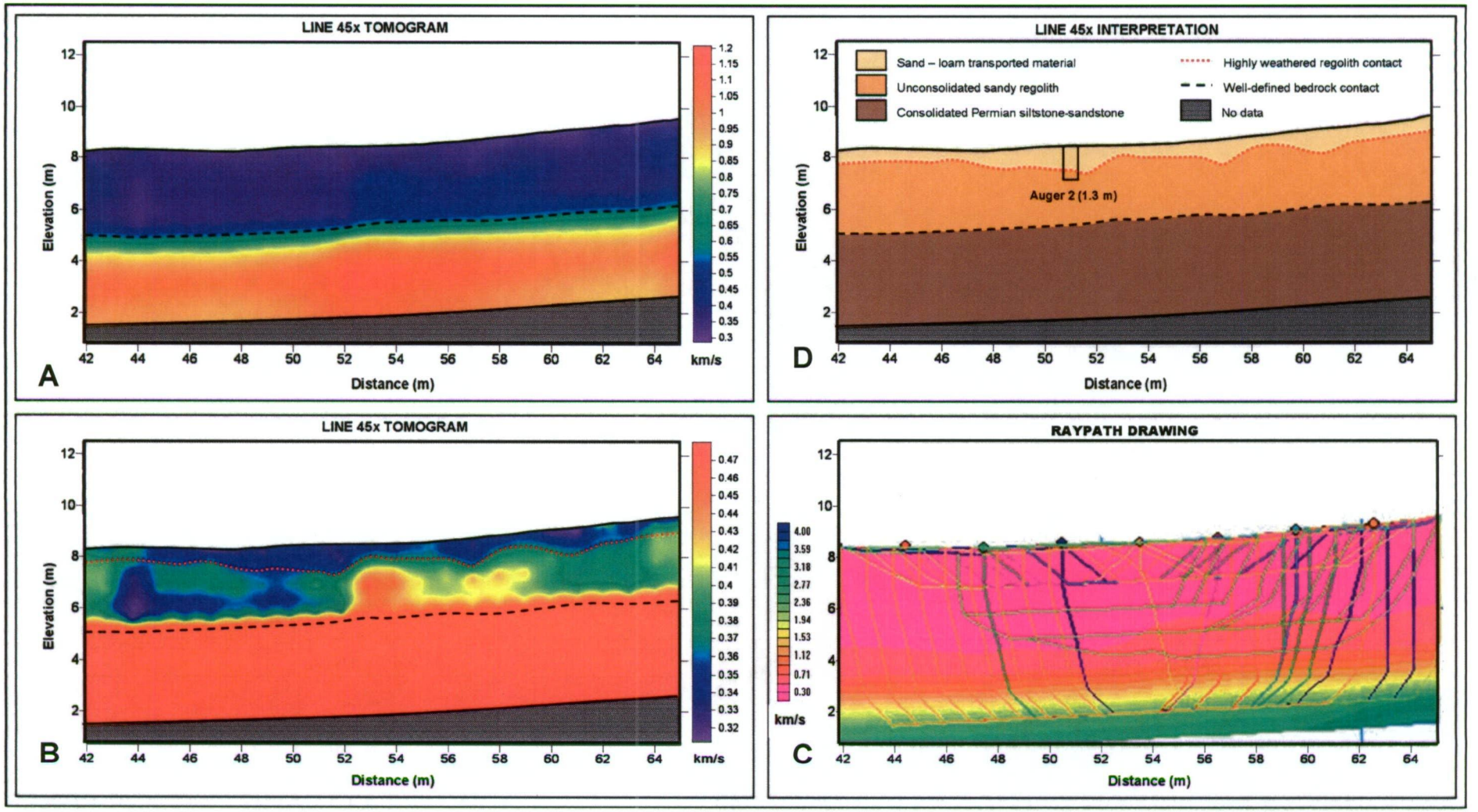

Figure 3.25: Interpretation approach for the Line 45x seismic refraction data. Tomogram **A** is a gridded cellular velocity model with the colour scale adjusted to show the primary velocity gradient. **B** is the same data with the colour adjusted to show a secondary gradient within the original Layer 1. Both of these images are derived from the raypath drawing and original layered model created in PlotRefa (**C**). The qualitative interpretation of Line 45x (**D**) is presented as a schematic section, which shows the two interfaces with respect to auger 2 refusal depth. The interpretation is only valid to the deepest ray path.

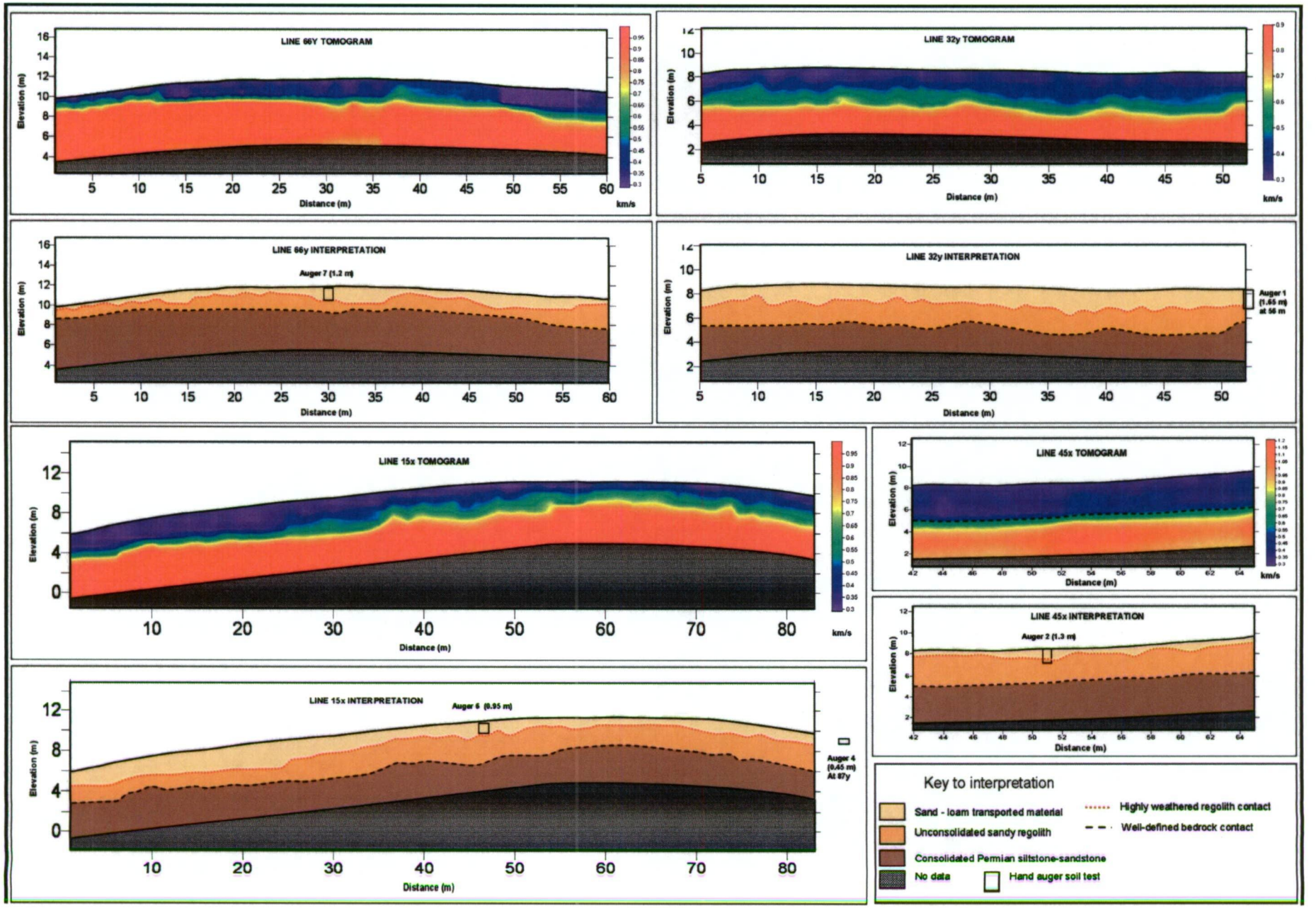

Figure 3.26: Isle of the Dead seismic refraction tomographic velocity profiles and schematic interpretation sections, overlain by the hand auger results.

Limitation of first arrival refraction data

The integrity of the tomograms was somewhat limited by the reciprocity of the travel time curves. Theoretically, switching the receiver and source will result in exactly the same travel time curve, but that is rarely the case (Palmer, 1980). The PlotRefa program had trouble processing the end shots of a spread, and often didn't calculate closely corresponding theoretical curves.

Accuracy of the first arrival travel time data also limits the calculation of velocity stratification, even in the absence of hidden layers. Palmer (1980) explains that because the 'travel times for each layer correspond to rays that only pass through the upper section of the layer. The velocity function, which is fitted to these data, is then extrapolated to the lower section of the layer. The errors in depth are caused by the errors of extrapolation. Since the average velocity is an artificial, but convenient replacement of the true layer velocities with a constant value, there will be errors in the depths calculated using this average'.

3.2.5 Electrical resistivity tomography

Introduction

Resistivity tomography allows the examination of vertical relationships between sediments, features, and stratigraphy (Kvamme, 2001). Electrical resistivity tomography (ERT) was used on the Isle of the Dead primarily to map stratigraphic interfaces, such as the regolith – bedrock boundary. The measured apparent resistivity is a volume-averaged value affected by the stratigraphy through which the induced current flows. The method is suitable for sites such as the Isle of the Dead that have minimal cultural debris, as near-surface resistivity variations typically produce poor quality data (Griffiths and Barker, 1993). The dipole-dipole array was chosen because it presents steeper gradients of apparent resistivity, and hence less uncertainty in lateral location, than other comparable techniques (Sumner, 1976).

3.2.5.1 Data acquisition

Four dipole-dipole array transects were surveyed on the island during September 2004. The spreads were positioned coincident with the seismic refraction transects, to allow comparison between the datasets (Figure 3.21). Data collection parameters are tabulated in Table 3.7, and a diagrammatical representation of the ERT data measurement sequence is shown in Figure 3.27. The dipole length 'a' and the dipole separation factor 'n' are constant for each traverse and increase with each successive traverse. Depth information increases, while resolution decreases, as the electrode separation widens (Zhou *et al.*, 2000).

The Lund multi-electrode system allows for automatic resistivity profiling, theoretically making the data acquisition process time and cost effective. Unfortunately, these factors were compromised due to practical and technical difficulties on-site. The highly resistive, well-drained sandy soils on the island often made it difficult to get adequate current flow between the electrode and ground. Surface dryness has been demonstrated to produce infinitely high probe contact resistances (Kvamme, 2003). In the sheltered survey areas of loamy sands, the stainless steel electrodes were inserted no more than 0.05 m into the soil where possible, and sea water (≤ 1 cup) was poured around the

probe to encourage current flow into the ground (Bevan, 1991). Dry sandy soils on the western riser slope proved most difficult, and viable data were only obtained here when electrode penetration exceeded 0.05 m and the surrounding soil was saturated with saltwater. Sufficient ground-coupling was achieved along the bark chip pathway and in leaf-littered areas, by clearing loose surface material and pushing the electrode into the path base or underlying soil. One section of the path (centred on gridline 25x) transacted by spread 32y had a concrete base and several readings were skipped so as not to produce erroneous results.

Survey type	Resistivity (2D)		
Instrumentation	ABEM Terrameter SAS 4000 with Lund resistivity imaging#		
Area surveyed	Four transects		
Array type	Dipole – dipole (collinear)		
Electrode spacing	1 m, (0.5 m for Line 45x)	**Output units**	Ω.m
Norm	Median	**Optimal output**	1000 mA*
Acquisition delay	0.3 sec	**Acquisition time**	2 sec
Stacking minimum	2	**Stacking maximum**	4
Comments	Electrode checks prior to data collection Non-magnetic surveyors tape used in grid layout # SAS (signal averaging system) is a method whereby consecutive readings are taken automatically and the results are averaged continuously. * Automatically stepped down to lower current if impossible to transmit selected current		

Table 3.7: Tabulated survey parameters for the Isle of the Dead dipole-dipole resistivity survey.

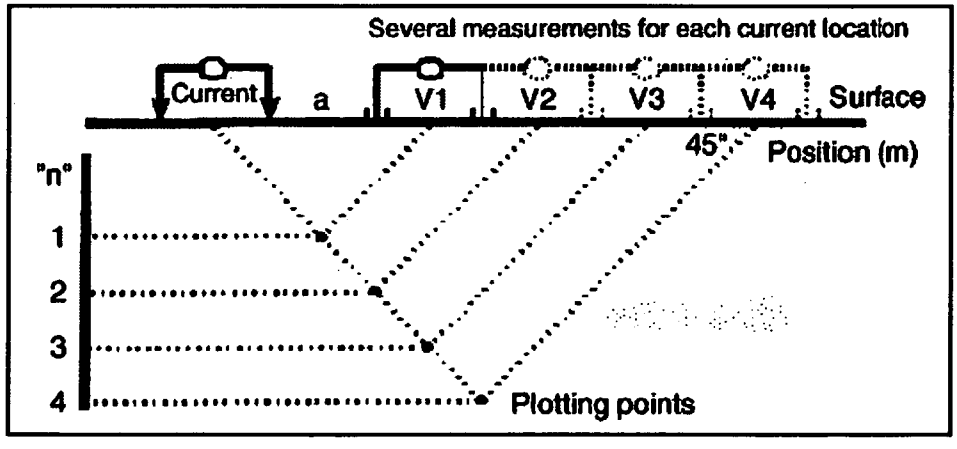

Figure 3.27: Electrical resistivity tomography data measurement sequence using the dipole-dipole array (modified after Zhou *et al.*, 2000).

3.2.5.2 Post-acquisition data processing

The inversion software RES2DINV version 3.4 (Loke, 1996) was used to edit and process the electrical resistivity data to generate a 2D tomographic image showing a distribution of true (modelled) resistivity values as a function of depth. This subsurface model is generated from a finite difference network (Dey and Morrison, 1979), in which a single element, defined by the initial resistivity value, coincides with each point on the pseudo-section. The 2D finite-difference forward response was applied using the robust constrained least-squares method algorithm (Claerbout and Muir, 1973; Sasaki, 1992; in Batayneh, 2001), to accommodate sharp boundaries and minimise absolute changes in the resistivity values (Diamanti *et al.*, 2005). An iterative process was used to refine the model, minimising the RMS values until there was a close correlation between the measured resistivity values and those calculated from the resistivity model. Elevation data was not integrated into these models but the gentle slopes and small elevation changes mean that the data interpretation should not be significantly compromised.

3.2.5.3 Findings and interpretation

This discussion will address the broad trends and isolated anomalies in each transect, followed by a comparative evaluation of the stratigraphic information provided by the auger tests and seismic refraction depth models. Measured apparent resistivity pseudo-sections are presented in Appendix A, Figures A5-8.

Gridline 66y

Measurements collected across the Upper Bench exhibited a very large range of values - 40 Ω.m - 1500 Ω.m (Figure 3.28c). Closely spaced contours in the tomogram indicate a horizontal boundary at ~ 1.3 m depth, which denotes the base of a high value (>750Ω.m) near-surface layer that is interpreted as transported sands and organic material. The resistivities here are consistent with those expected from a well-drained sandy soil with little vegetative groundcover. The gradient is most prominent from 30x to 58x, where it undulates between 1.0 m and 1.5 m depth, and it gradually thins toward the surface at 20x. This well-defined undulating section corresponds well with the zone of subsurface

disturbance interpreted from the GPR profile along gridline 66y. The soil-regolith interface is discontinuous from 0x to 20x, and is inferred at ~ 1 .0 m depth from a sharp gradient between 2x and 8x. The lateral variation in resistivity values within the top 1.5 m correlates closely with a shift from low to very high average apparent conductivities between 20x and 15x, as measured by the EM-38 in HCP mode (Figure 3.13). The soil-regolith interface depth estimate at 30.2x matches the 1.2 m obtained by hand auger refusal.

The boundary depth and undulation patterns also agree closely with those inferred from the seismic refraction velocity model for Line 66y (Figure 3.21), despite the fact that topographic corrections are not incorporated. This agreement may be seen at 12x - 13x, where a discrete high resistivity anomaly corresponds to a deepening of the soil profile determined from the seismic refraction. The correspondence suggests that the seismic irregularities are real features rather than artefacts of the first break picking or tomographic processing. This local depression in the soil-regolith topography is possibly related to a compacted burial feature associated with the headstone located <2m directly SSW. Similar responses are recorded less than 2 m in front of three other headstones, at 15x, 18x and 23.5x (Figure 3.28d) and are therefore inferred as burial features. The regolith-bedrock interface identified in the seismic refraction is only weakly defined in the resistivity tomogram, but the 2 - 3 m depth range correlates well.

Several discrete very high resistivity anomalies (> 2000 Ω.m) are observed within the near surface. The present and former (gravel) pathways, marked in orange and grey respectively in Figure 3.28d, are defined by shallow relatively high resistivity zones, which reflect the change in material composition and moisture content.

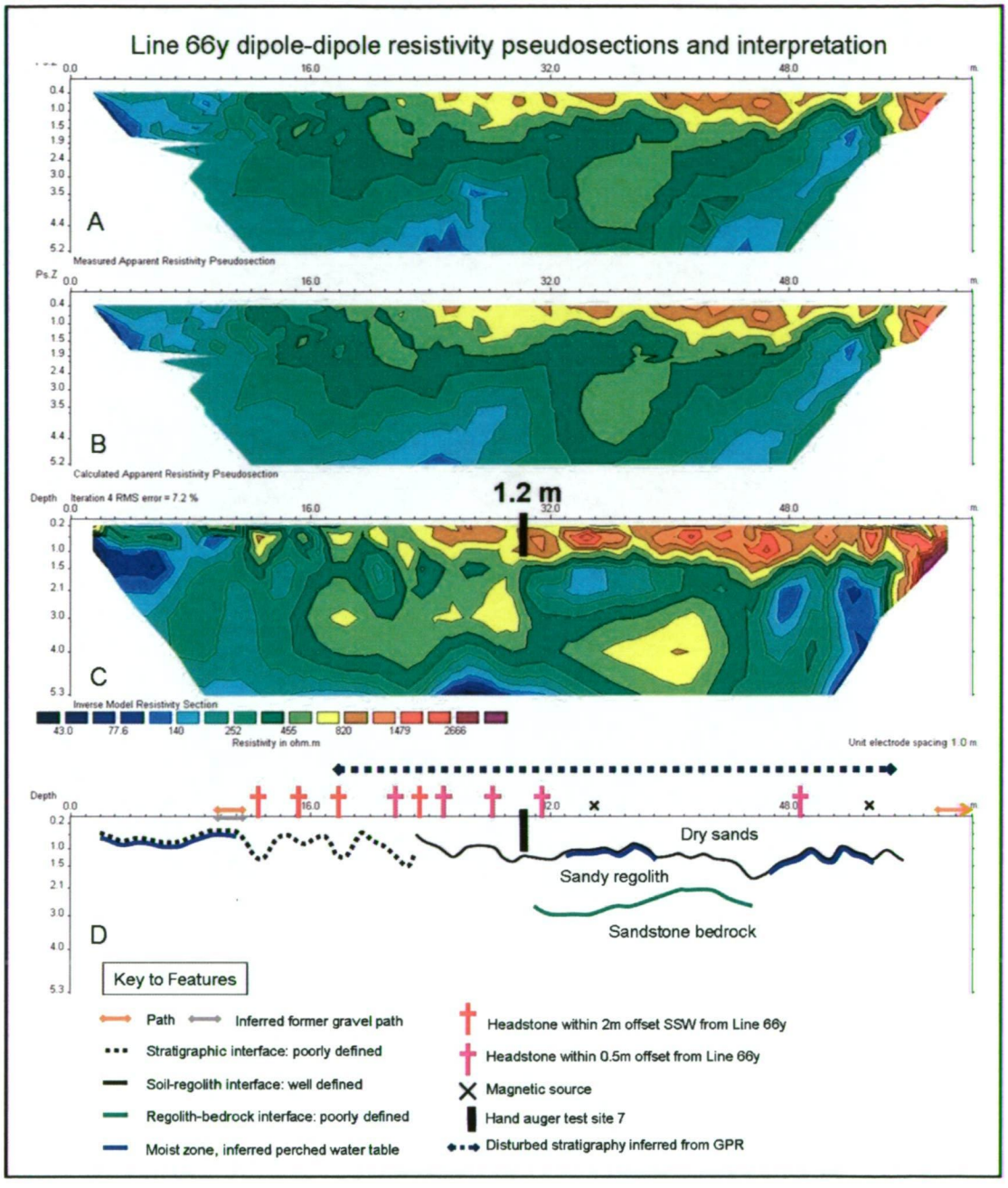

Figure 3.28: Gridline 66y observed (**A**) and calculated (**B**) resistivity pseudo-sections, tomographic model (**C**) and schematic interpretation (**D**).

Gridline 32y

Gridline 32y spans the sheltered Lower Bench of the Isle of the Dead, from 7x to 55x. The tomogram in Figure 3.29 shows a similar range of apparent resistivities to that of gridline 66y, and a corresponding near-surface layer (depth 1 - 1.5 m) of elevated values from 22x eastward. Numerous very high magnitude discrete anomalies of unknown source are present within this zone. The most prominent of these responses, located at

27.5x, corresponds with highly compacted material under the present pathway, which was also detected by the magnetic and seismic refraction surveys. Highly resistive point anomalies from 42 - 46x, and a distorted soil-regolith interface coincide with hyperbolic reflectors in the GPR data. These responses suggest, respectively, a moist local depression at the soil base and the presence of buried material of contrasting physical properties to the surrounding soil – both possible penal period burial features.

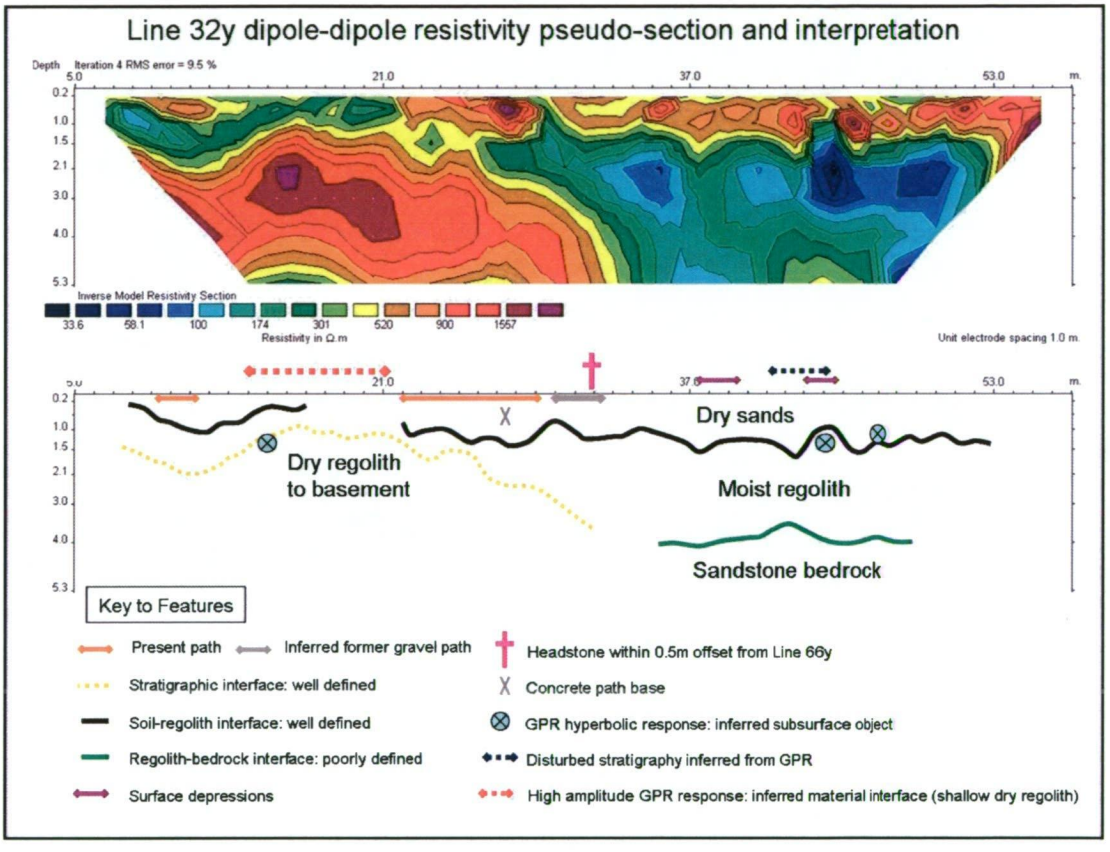

Figure 3.29: Gridline 32y tomographic model and schematic interpretation.

The most striking feature in gridline 32y is the lateral variation in apparent resistivities between 26x and 34x in the inferred regolith layer. The steep vertical gradient from very high (> 1500 Ω.m) to low (150 Ω.m) probably reflects a movement of water and weathering by-products from the western and northern parts of the island to the locally depressed Lower Bench. This interpretation is supported by the hand auger refusal measured at 56x, 31y, which was deep relative to soil cover at other test sites, and the seismic refraction schematic interpretation from the section 20x and 53x. The regolith-bedrock boundary is poorly defined from 35x to 48x, under the inferred moist regolith and possible perched water table (Doyle and Cumming, 2003).

The lateral variation does not appear to correlate well with the areal trends in background apparent conductivities in either the HCP or VCP survey modes. The exceptions include a relatively low conductivity zone in the HCP data centred on 15x, and high values west of the present pathway (both datasets). It is important to consider this apparent discrepancy in lateral trends from a quantitative perspective: although soil conductivity is the theoretical inverse of resistivity (1 mS/m = 1000 Ω.m), the EM meter and resistivity instrument employ fundamentally different sensing technologies that evaluate unequal earth volumes (Kvamme, 2001). In dry sandy topsoils, for example, it may be difficult to promote current flow through the steel electrodes whereas EM signals can sometimes penetrate to lower, moister layers (Frohlich and Lancaster, 1986; in Kvamme, 2001).

Gridline 15x

Survey complications along transect 15x, described in section 3.2.5.1, resulted in a poor quality dataset, as numerous measurements were skipped because of insufficient current flow. These gaps skew the inversion outcome, producing a tomogram with a false high (> 900 Ω.m) from 50x to 58x (Figure A7c, Appendix A). This anomalous zone does not correlate well with the closest corresponding results in transect 66y.

Gridline 45x

Gridline 45x differs from the other three transects, because it has a probe separation of 0.5 m instead of 1.0 m. This spacing gives better resolution of the soil horizons and weathered regolith material, and hence the depth of investigation (2.6 m) is approximately half that of the longer spreads. The tomographic model exhibits a similarly large range of apparent resistivity values to those of Lines 66y and 32y, with most measurements recorded between 100 Ω.m and 1000 Ω.m. Two dominant vertical resistivity gradients are visible at ~ 0.5 m and 1.5 m depths. Lower resistivity values in the layer recorded to ~ 0.5 m depth are attributed to moist, humic leaf litter. The other interface is represented by very close horizontal contours, which separate moderate-highly resistive well-drained loamy sands from the underlying weathered sandy regolith and possibly a perched water table (Figure 3.30). The inferred regolith topography agrees closely with that inferred from Line 32y and the hand auger refusal depth of 1.3 m at 45x, 51y. A relatively resistive zone centred at 47.5y is possibly caused by compacted material.

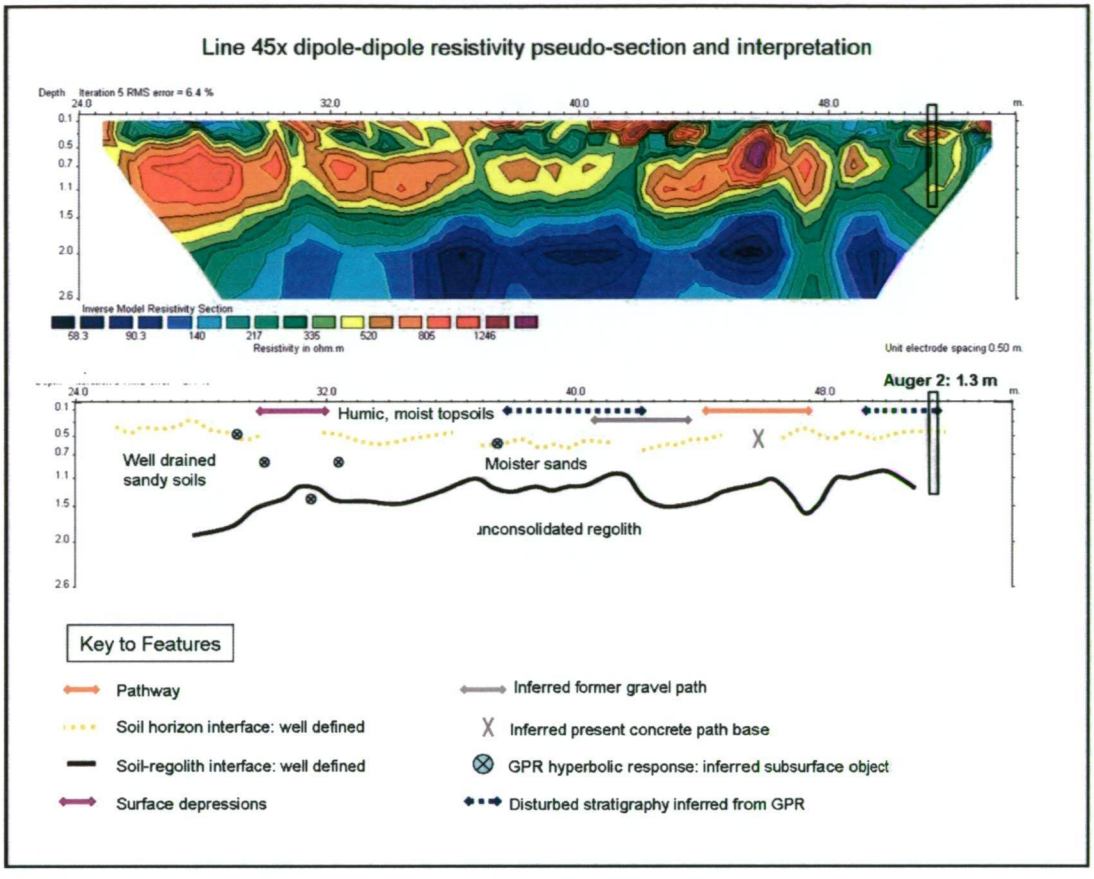

Figure 3.30: Line 45x tomographic model and schematic interpretation.

Lower resistivities recorded beneath a surface depression from 30 to 32 m, laterally coincident with four inferred GPR hyperbolae, is interpreted as a probably burial(s). Similarly, a relatively conductive section between 37 m and 41.5 m corresponds to subsurface disturbance and a possible buried object identified in the GPR, and is potentially another cemetery feature. The high value point anomaly at 45.5y (marked with a grey X in Figure 3.30) corresponds to highly compacted material beneath the present path, while the former gravel path manifests as very shallow high resistivities from 40.5 - 43.5 m. A moderately resistive lens at ~ 0.3 m depth, 50.5 m – 52 m, is coincident with loamy sands of loose consistency in the auger 2 results.

Limitations of electrical resistivity tomography

Interpretation of anomaly patterns in the apparent resistivity pseudo-sections are based on knowledge of the island's simple stratigraphy, as inferred from auger tests, physical evidence, and other geophysical datasets. Limitations to the qualitative interpretation process include the non-uniqueness of modelling results, the influence of complicated three-dimensional geology, and stratigraphic complexity due to archaeological material.

3.2.6 Ground penetrating radar

Introduction

Ground penetrating radar is a technique for evaluating the stratigraphic complexity of the subsurface. In suitable site conditions, it is applicable for mapping culturally emplaced soils and determining the approximate size, the general shape, and the depth of buried features (Clark, 1997; Miller, 1996; Conyers and Goodman, 1997; Bevan, 1998; Dalan and Bevan, 2002). Based on multi-technique case studies of historic cemeteries in North America, Bevan (1991) concluded that radar 'had the greatest success for locating unmarked graves. The best conditions for this instrument are sites where the radar detects few underground objects and either no apparent stratification or only weak, planar strata. The soil should be high in resistivity, possibly greater than 200 Ω.m.' As these conditions are applicable on the island - including highly resistive sandy loam soils, consistent stratigraphic patterns, uncomplicated historical site use, and a mixture of marked and unmarked graves for potential verification of results - it was considered an eminently suitable site for ground penetrating radar.

The primary objectives of this investigation were to detect and characterise features associated with graves and to ultimately produce a maps of 'archaeological potential' across the surveyed area. Targets of interest included coffins, buried objects and stratigraphic interruptions associated with trench geometry (edges and base) and fill material. Pre-survey knowledge of the burial layout was limited to historic photographs and surface evidence (markers and depressions). It was anticipated that trench dimensions were standard for a cemetery of this period and cultural context (Greg Jackman, pers. comm.), as noted in Section 3.1.5. The ability of the GPR technique to define major stratigraphic horizons on the island was also assessed, by comparing the findings with seismic refraction, resistivity tomograms and hand auger soil profiling. The merits of three-dimensional visualisation of GPR responses on the Isle of the Dead were assessed using a data volume derived from a small focus area on the western side, which included several marked graves and depressions.

Three-dimensional imaging of ground penetrating radar data has been shown to be an effective method of visualising buried coffins at historic cemeteries (Field *et al.*, 2001;

Davis *et al.*, 2000; Conyers, 2006). Kvamme (2002) writes that 'historic graves [with coffins] are often easy to recognize in radargrams, as evidenced by a pronounced hyperbola. When 3-D slices intersect these hyperbolae the graves are usually clearly evident in plan view. By slicing the radar data at various depths along the hyperbola, the aerial perspective can be refined for optimal viewing and recognition.' Conyers believes that this method is 'more precise and less time consuming than attempting to visually identify many reflectors of importance in each reflection profile in a grid, as there can often be tens or even hundreds of potentially important reflections' (2006).

The following sections describe the survey methodology and post-acquisition data processing. The findings from each survey will be considered as one dataset and discussed with the analysis in Section 3.2.6.3.

3.2.6.1 Data acquisition

Four series of GPR investigations were undertaken on the Isle of the Dead, in February and May 2003, July and November 2003 (Figure 3.32). The antenna frequency was based on investigation of the requirements for depth of penetration and vertical resolution of anticipated targets. The February 2003 survey primarily used a 500 MHz antenna, with several test lines conducted with a 250 MHz system. A comparison of the data collected using each frequency indicated that the latter provided better resolution and continuity of reflections, with a penetration depth of > 3 m. It yielded a less complicated image than the 500 MHz, without losing too much detail of features in the crucial first 2 m depth. The remaining three surveys used the 250 MHz to retest the original area and extend into other sections of the geophysical grid. Several other studies of historic burials have also used a moderate frequency antenna (200 MHz), to reduce excessive detail (Maijala, 1994; Nobes, 1999; Field *et al.*, 2001). Higher frequencies (≥ 500 MHz) have typically had success at forensic sites where burials are typically very shallow and there is good contrast between the disturbed trench soil and surrounding stratigraphy (Miller, 1996).

Data were collected with the assistance of Dr Michael Roach, UTas geophysics students, PAHSMA staff and Archaeological Summer Program volunteers. One surveyor carried

and operated the RAMAC radar control unit, laptop and battery pack while the other person towed the antenna (TX – RX) using an aluminium handle (Figure 3.33).

Data collection was maintained at a steady 0.5 m/s where possible and fiducial markers were added manually to the output file by the laptop operator as the TX - RX centre was drawn past a metre mark (accuracy of +/- 0.1 m). The antenna detoured around minor obstructions such as tree trunks and headstones, when the offset was less than 0.5 m. Survey was paused and re-established either side of larger objects such as stumps or tombs, a record of which was made in the comment file. Data collection parameters and equipment details are summarised in Table 3.8.

Survey type	Ground penetrating radar		
Instrumentation	Mala RAMAC X3M system, 250 MHz and 500 MHz antennae		
Area surveyed	500 MHz: 58 lines. 250 MHz: 226 lines. Total distance: 5146 m		
Method of coverage	Continuous data collection		
Traverse separation	0.5 m - 1.0 m	**Range**	100 ns
Tx - Rx separation	0.36 m (250 MHz) 0.18 m (500 MHz)	**Trace interval**	0.03 s, then converted to 0.05 m*
Stacking	16	**Samples**	256
Comments	Profiling conducted with ≤ 1.0 m offset from the measuring tape. * Post-acquisition trace interpolation using the fiduciary marks.		

Table 3.8: Tabulated survey parameters for Isle of the Dead GPR data collection.

The survey coverage was designed to provide a suitable network of measurements for achieving the investigation objectives within the given time frame. Theoretically, a profile spacing of 0.5 m would ensure adequate sampling of a generic individual burial trench (no greater than 1 m x 2 m) such as that defined in Section 3.1.5. This spacing has been successfully applied to locate historic burials in Maryland, USA (King *et al.*, 1993). Unfortunately, parts of the grid were not covered due to obstructions and other areas, such as the lower bench, were surveyed at 1.0 m line intervals. A 0.5 m traverse separation would cross the long axis of the trench up to 4 times (optimal situation), and only once along the short axis.

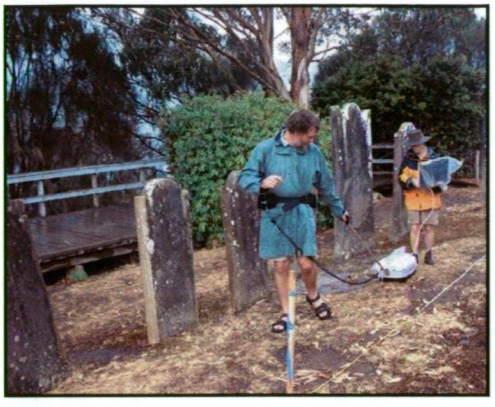

Figure 3.31: February 2003 500 MHz survey in the marked burial area of the Upper Bench, showing the raised wooden walkway in the middle ground. Pictured from left are Dr Michael Roach and the author (Photograph courtesy of James Cook University, 2003).

3.2.6.2 Post-acquisition data processing

The raw radar data required the following processing steps to correct for distance and three-dimensional location within the geophysical grid:

- reversal of profiles collected in the negative direction along line;
- trace interpolation to correct fiducial markers to distance;
- time to depth conversion of the vertical axis;
- ground surface reflection shifted to zero time/depth.

The ground surface response is expressed as a series of reflection bands in an interference zone near the top of each profile where no wave propagation occurs (Fletcher and Spicer, 1995). The maximum phase of the first band was used here for vertical correction of the ground surface. All radargrams were image enhanced for interpretation, using average trace subtraction and the application of an energy decay curve. Average trace subtraction suppresses strong horizontal responses, which may be multiples of the ground surface response, and enhances diffractions from soil disturbance, coffins and other point sources (Nobes, 1999; Witten, *et al.*, 2001). Energy decay curve is an exponential gain function which allows for better visualisation of weaker reflections caused by signal attenuation with depth. Each option highlighted certain aspects of the data while suppressing others, so it was necessary to create several versions for comparative purposes. Figure 3.33 shows the effects of image enhancement on a processed 250 MHz profile. Horizontal banding is reduced in versions B and D, through subtraction of average trace. Versions C and D have had an energy decay curve applied, which has increased visibility of reflections below 40 ns TWTT. Analysis of each profile on the island was conducted using these two versions, to maximise the information gleaned from the data.

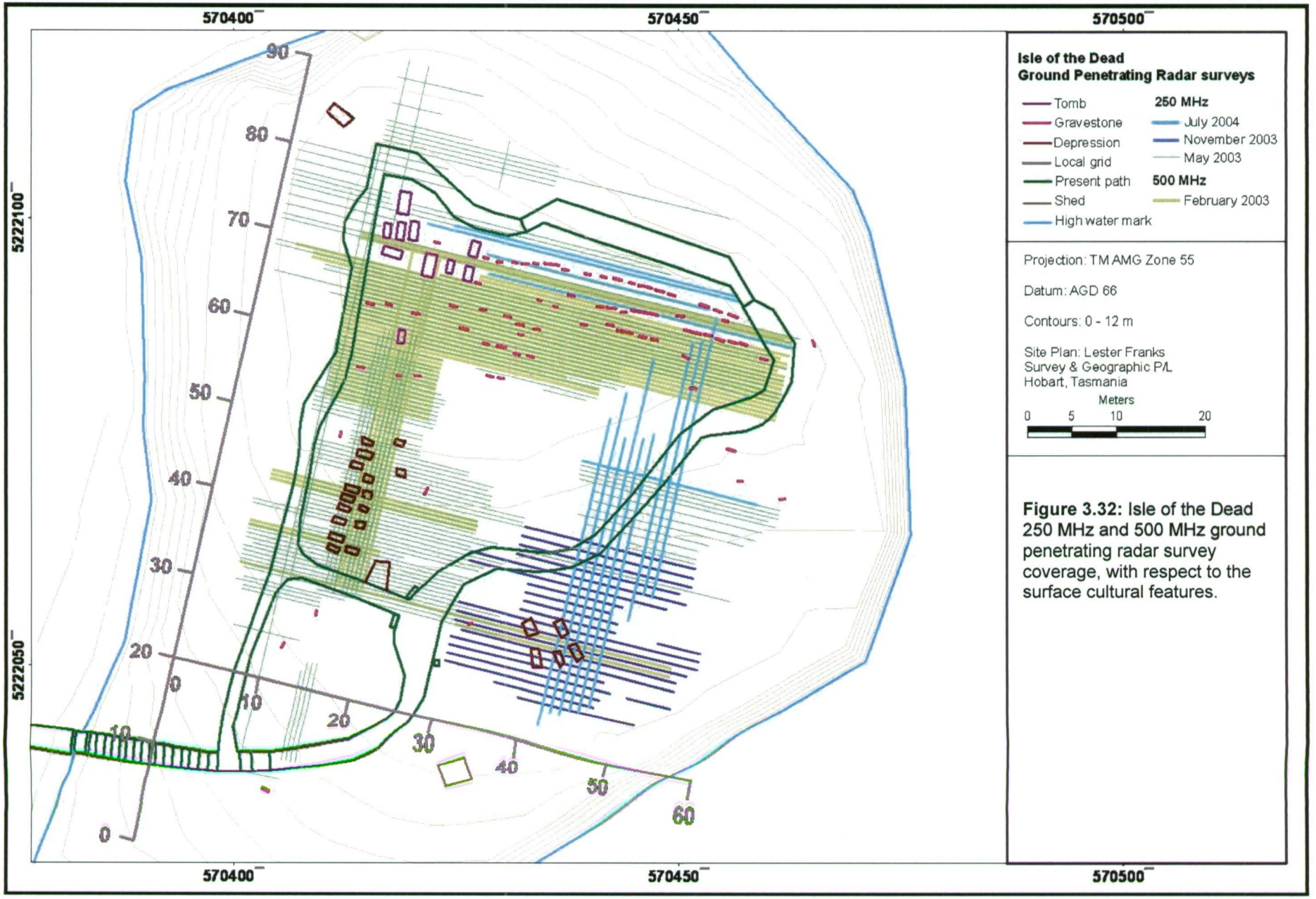

Figure 3.32: Isle of the Dead 250 MHz and 500 MHz ground penetrating radar survey coverage, with respect to the surface cultural features.

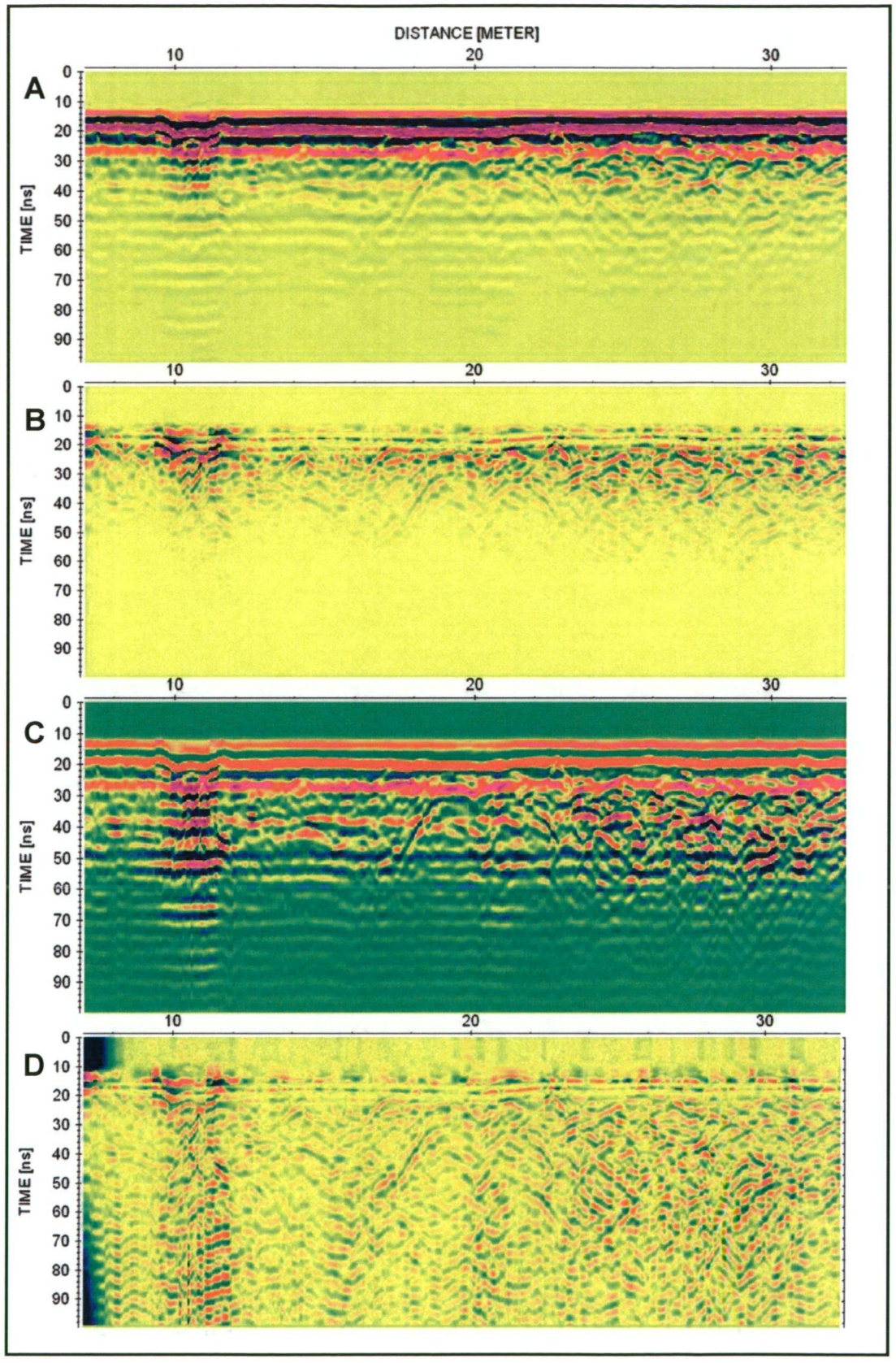

Figure 3.33: Processing a distance-corrected 250 MHz profile (**A**) with average trace subtraction (**B**). Images (**C**) and (**D**) show the effect of energy decay curve application to (**A**) and (**B**) respectively, to better visualise weaker reflections.

Time to depth conversion of the vertical axis

Calibration of the vertical axis from two-way travel time (TWTT) in nanoseconds to depth (metres) allows a calculation of target depth. As radar pulses are transmitted into the earth their velocity changes as a function of the electrical properties of the various materials through which they are travelling. When the subsurface is mostly homogenous, such as on the Isle of the Dead, one velocity is chosen which represents the 'average' of the true velocities. Excavation of an anomaly source is the most accurate method of calibrating actual depths (Conyers and Lucius, 1996) with travel times; however this was not possible on the island. The RAMAC system was also unsuitable for conducting common mid-point measurements to determine a site-specific velocity. Bevan and Kenyon (1975) reported a velocity of 0.19 m/ns in dry sand, 0.06 m/ns in wet sand, and ~ 0.074 cm/ns in wet clay, for example, at a frequency of 100 MHz. Diffraction curvature adaptations of selected well defined hyperbolae in the island data gave velocity estimates in the range of 0.085 to 0.11 m/ns. A theoretical wave velocity of 0.09m/ns was therefore used for the time-depth conversion, based on these outcomes and known dielectric properties of sandy loam soil types.

Three-dimensional data processing

Processed 250 MHz profiles (no image enhancement) within the focus area (gridlines 49y to 59y, and gridlines 13.5x to 18x) were compressed to a maximum of 512 traces, for horizontal stacking into data volumes in Reflex® (version 2.1.1). Compression resulted in 1 trace per 2.8 cm in the x-direction and 1 trace per 1.9 cm in the y-direction. Several test volumes were generated to determine which profile configurations and processing parameters produced the best visualisation of radar responses.

Test volume **A** comprised all profiles between gridlines 49y to 59y, stacked with no inter-profile interpolation. Volume **B** was created by interpolating amplitude values between the profiles, using a search rectangle of 0.2 m and 1.2 m - in the x- and y-directions respectively. Absolute amplitude values within the desired time range and search rectangle surrounding each data point were weighted according to their distance from the point, summed and the resultant value assigned to that point. Raster increments in both the x- and y- directions were equal to the trace increments. Test volume **C** interpolated across all profiles between gridlines 49y to 59y, and gridlines

13.5x to 18x (0.5 m intervals). The volumes were viewed at specific time values as two-dimensional raster images of contoured amplitude values ('timeslices') (Goodman *et al.*, 1995; Malagodi *et al.*, 1996). Gain values were consistent across all data volumes.

Test timeslices generated at approximate equivalent of 0.17 m depth in each data volume show the effect of inter-profile interpolation of amplitude values on anomaly edge definition (Figure 3.34). The most diffuse image was produced from volume **C**, generated from perpendicular profiles (Figure 3.34, **C**). The sharpest image was generated using parallel lines, with no interpolation (**A**), and was therefore adopted in all 3D processing at the site.

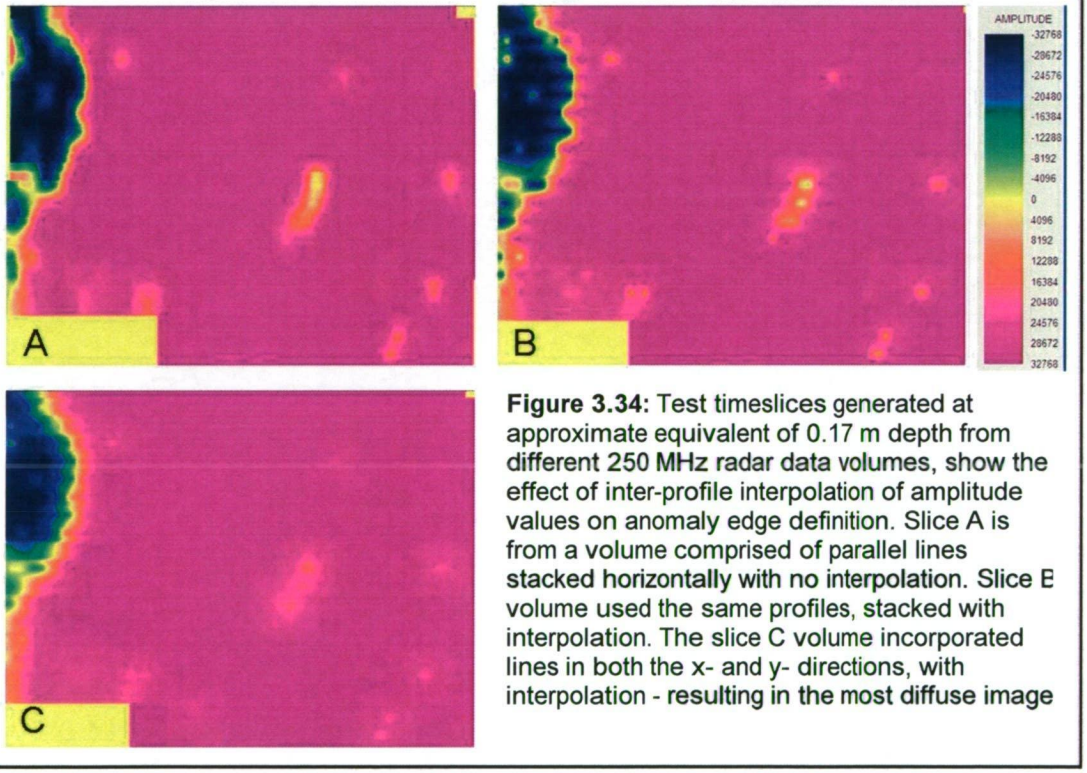

Figure 3.34: Test timeslices generated at approximate equivalent of 0.17 m depth from different 250 MHz radar data volumes, show the effect of inter-profile interpolation of amplitude values on anomaly edge definition. Slice A is from a volume comprised of parallel lines stacked horizontally with no interpolation. Slice B volume used the same profiles, stacked with interpolation. The slice C volume incorporated lines in both the x- and y- directions, with interpolation - resulting in the most diffuse image

3.2.6.3 Findings and interpretation

Introduction

Preliminary analysis involved the recognition of broad visual patterns in the ground penetrating radar profiles - the identification of background values, anomalous signals and depth of wave penetration to weak signals. Anomalous responses were classified and compared to anticipated radar signatures from ideal scenarios. Selected response types were abstracted and represented symbolically (King *et al.*, 1993) on plan views of the island. These were combined with interpreted source distribution patterns derived from the FEM and magnetic surveys, to provide archaeological potential maps of the site. By categorising and abstracting different response types, any 'ambiguity about group membership and anomaly limits' are removed and the data may be easily integrated and manipulated in the ArcGIS (Kvamme, 2006).

Stratigraphic information derived from profiles was compared with results from seven auger test sites, to assess the ability of GPR to determine primary soil horizons. The effectiveness of three-dimensional data processing was assessed, in relation to schematic plans derived from individual profile analysis, as a method for presentation of anomaly distribution.

Background response

The 'background response' is defined by relatively low-amplitude, near-continuous planar reflectors and is indicative of relatively undisturbed stratigraphy. Apart from an occasional shallow hyperbola, most likely associated with a tree root, the background response is homogeneous, with good resolution of features to ~ 2 m depth and ~ 3 m depth for the 500 MHz and 250 MHz frequency systems respectively. A clear example of how the background response contrasts with irregular, non-horizontal diffractions from inferred disturbed stratigraphy, and high amplitude reflections over the path, are shown in Figure 3.35.

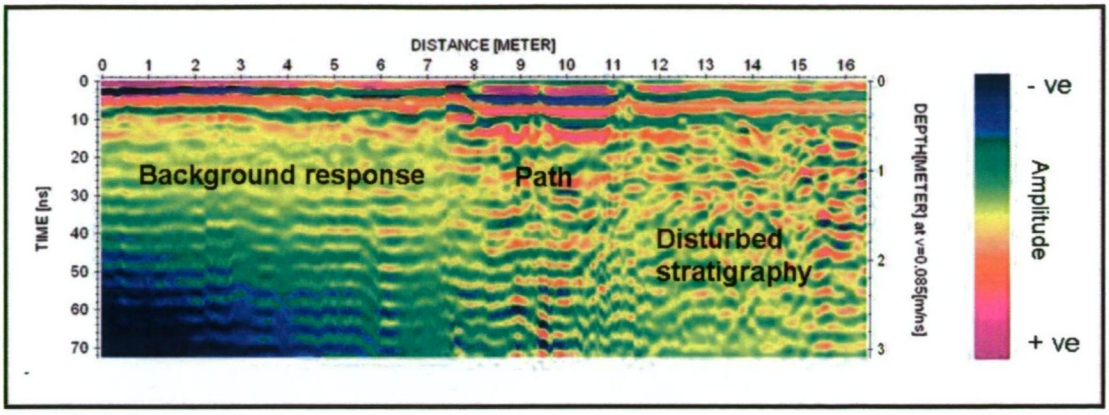

Figure 3.35: A 250 MHz profile along gridline 71.5 y, showing typical responses from stratigraphy inferred as undisturbed 'background' (0 –7m), high amplitude surface reflections from the path (8 – 11 m), and discontinuous, non-horizontal reflections from inferred disturbed stratigraphy (11 - 16.5 m).

Discrimination of anomalous responses

The discrimination of discrete hyperbolic responses and zones of overlapping diffractions of irregular form and amplitude is partly based on anticipated responses in the given conditions, reported patterns from similar geophysical targets at other sites (refer to Chapter 2), and modelled responses from various burial scenarios.

Simple models of radar patterns over hypothetical burial stratigraphy, generated by Conyers and Goodman (1997), produced three primary forms of response: the hyperbola, non-hyperbolic diffraction, and continuous planar anomaly. Two simple models in Figure 3.36 illustrate ideal radar signatures over 'V' shaped (**A**) or 'U' shaped (**B**) trenches filled with material with a higher relative dielectric permittivity. Trench (**B**) also contains a buried object, simulating a body/coffin. The relative dielectric permittivity of each medium is shown in each model. Although there are unlikely to be many model-like burials on the site, these scenarios provide an ideal visual reference for interpretation of more complicated responses as might be seen in the radargrams.

In scenario (**A**), primary diffractions derived from the shaft interface intersect to form a 'bow-tie' pattern, with the cross-over point indicating the trench base. Below the bow-tie, secondary reflections from the model baseline produce a hyperbola, which might be mistakenly attributed to a buried object.

In model (**B**), the simulated coffin/body is detected as a classic inverted 'U' shaped high amplitude anomaly above the bow-tie pattern. The hyperbolic shape that results from a discrete causative reflector is a consequence of the conical transmitted signal. In profile, the receiver senses echoes from a reflector for some distance before and after moving across it. The distance, and therefore time, the transmitted and reflected energy must travel is at a minimum when the receiver is vertically above the reflector (Goodman, 1994). Model (**C**) illustrates how radar signals from an undulating subsurface interface distort reflections from a deeper horizontal boundary, thereby making it difficult to accurately measure soil depth to the third layer. In reality, this effect may be observed if burial trench sides are eroded and overlying deposits have levelled the surface. On the Isle of the Dead, response (**B**) is expected from a coffin or other well-preserved burial material. Closely-spaced burials, such as indicated by headstones on the Upper Bench, would therefore produce a series of adjacent hyperbolae (**D**), due to the baulk between adjacent trenches. The response from this burial feature may be inadvertently attributed to a shallow buried object.

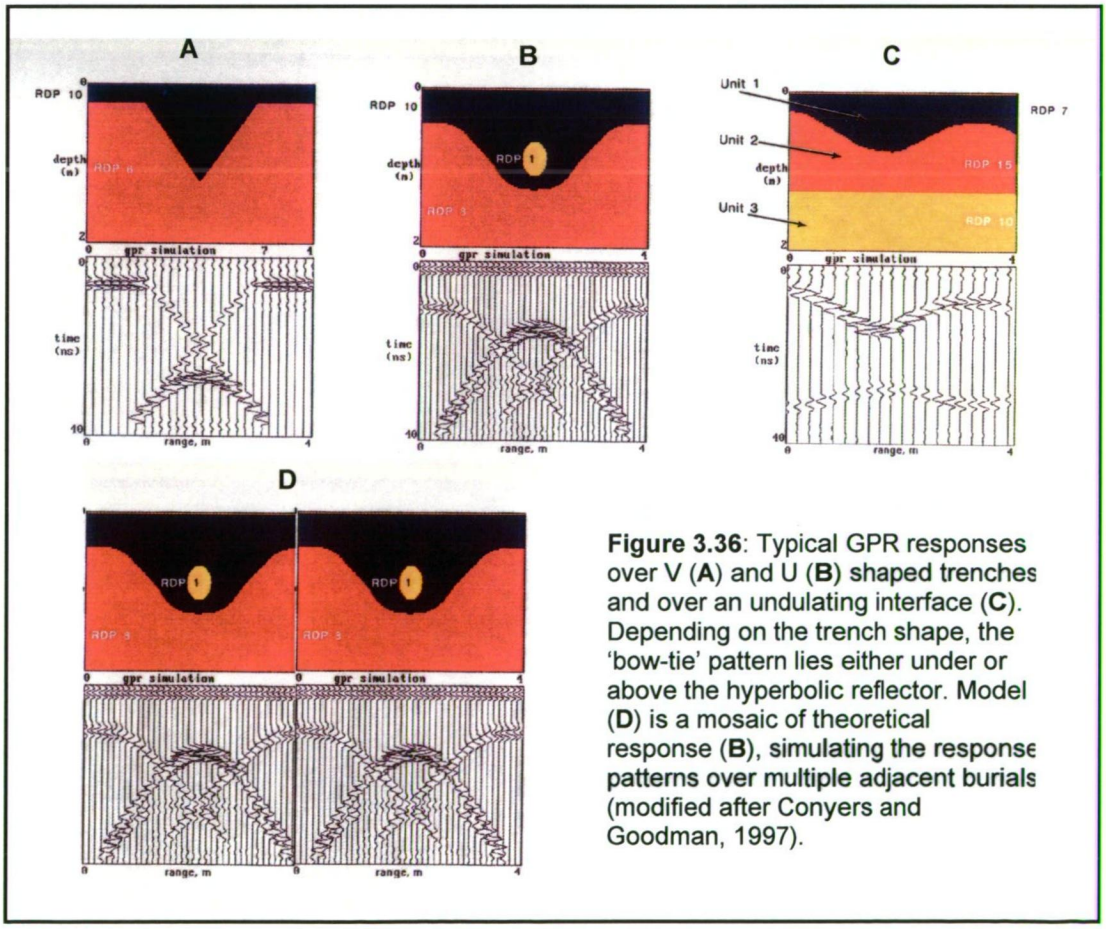

Figure 3.36: Typical GPR responses over V (**A**) and U (**B**) shaped trenches and over an undulating interface (**C**). Depending on the trench shape, the 'bow-tie' pattern lies either under or above the hyperbolic reflector. Model (**D**) is a mosaic of theoretical response (**B**), simulating the response patterns over multiple adjacent burials (modified after Conyers and Goodman, 1997).

As discussed in Section 3.1.5, numerous factors may contribute to deterioration of burial features. Soil intermixing, through leaching and bioturbation, may alter the trench interface, while decay can lead to collapse of a coffin/body, leaving little or no geophysical trace in the subsurface (Bevan, 1991; Conyers, 2006). In these instances, the radar may still detect soil contrasts such as those illustrated in Figure 3.37. Burial contrast (**A**) and subsidence strata (**B**), similar to Figure 3.36 (**C**), may manifest as a discontinuous undulating reflection; fill scattering (**C**) as narrow overlapping hyperbolae; strata break (**D**) and surficial subsoil (**E**) as diffractions.

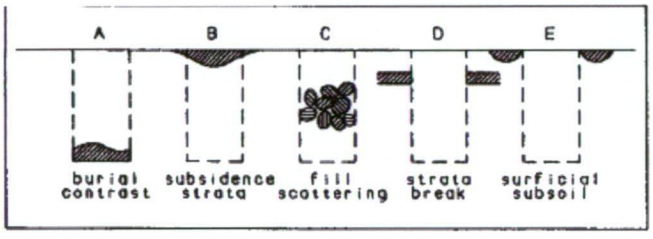

Figure 3.37: The hachured areas show soil contrasts that might suggest a grave on a radar profile. The broken lines indicate the cross-sections of the grave shafts (Bevan, 1991).

The three main response types produced by modelling were recorded for characterisation, to optimise the identification of individual burials and areas of archaeological potential on the island. The subjectivity of this process was minimised through line-by-line data analysis and correlation of adjacent lines to provide continuity in the picking of anomalies. Each profile was viewed simultaneously in the raw and processed formats to maximize information gleaned from the data.

The grid location and selected depth information was tabulated and imported into ArcGIS® for the production of maps showing the distribution of each responses type. The survey area was calculated by placing a buffer zone around every survey line. A buffer distance of 0.3 m was estimated from the 250 MHz GPR detection footprint radius at 1.5 m depth (Annan and Cosway, 1992). The elliptical cone of radar penetration is defined by the equation in Figure 3.38. This equation assumes a consistent RDP of the medium through which the energy passes. In reality, variations in soil properties result in changing RDP and therefore differing energy transmission patterns, so this equation provides only an estimate (Conyers and Goodman, 1997). The distance calculated here conveniently ensured a narrow footprint overlap of 0.05 m at depth 1.5m, where the survey line spacing was 0.5 m.

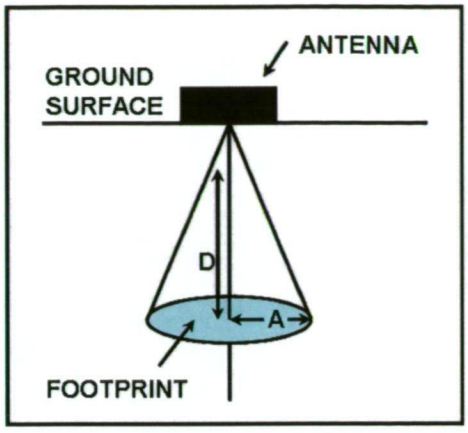

Figure 3.38: The elliptical cone of GPR penetration into the ground. The footprint is the shaded area on a horizontal surface (modified after Conyers and Goodman, 1997).

$$A = \lambda/4 + D/\sqrt{K+1}$$

A = approximate long dimension radius of footprint

λ = centre frequency wavelength of radar energy

D = depth from ground surface to reflection surface

K = average relative dielectric permittivity (RDP) of material from ground surface to depth (**D**)

Response Classes 1 and 2

Hyperbolic type responses are divided into two categories, based on reflection continuity and amplitude. Typical examples of both classes are presented in Figure 3.39 - vertical black lines indicate the hyperbolic axes. Class 1 anomalies exhibit well-defined hyperbolic form and high amplitude relative to local background values. Class 2 reflectors are less well defined and/or of lower amplitude. The high amplitude reflection of Class 1 indicates that the radar signal has detected an interface between materials of highly contrasting dielectric permittivity and/or magnetic permeability.

Anticipated archaeological features differing in physical properties to the loamy-sand matrix include wood (coffin, marker), stone, burial objects (corpse, artefacts) and voids. These features will also have the capacity to cause Class 2 anomalies - if the detectable contrast has lowered through structural and chemical deterioration, or void fill. Any arcing multiples generated from a trench base would likely be recorded as a Class 2 response, because of low contrast between shaft fill and the surrounding soils. Class 1 anomalies are therefore viewed as the best indicators of a burial.

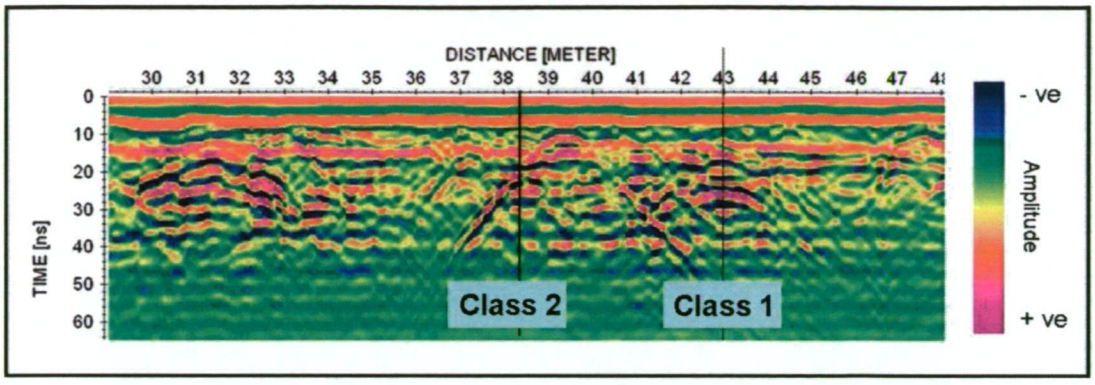

Figure 3.39: Typical examples of hyperbolic responses in a gain-adjusted 250 MHz radargram collected between rows of headstones on the Upper Bench. A black line delineates the central axis of each hyperbola and shows its distance along-line. The Class 1 response is centred on 43m, at ~25 ns TWTT, and Class 2 anomaly is recorded at 38.4 m and 22 ns TWTT.

Of the 718 hyperbolae recorded in the GPR survey of the Isle of the Dead, 499 are well-defined (Class 1). Both classes exhibit a range of gradients and configurations and are rarely as ideal as the models in Figure 3.36. Discrete responses are less common than hyperbolae which overlap to various degrees and manifest at different depths, as illustrated in Figure 3.40 from 16 - 19 m. Such anomaly groupings make interpretation of individual burials difficult.

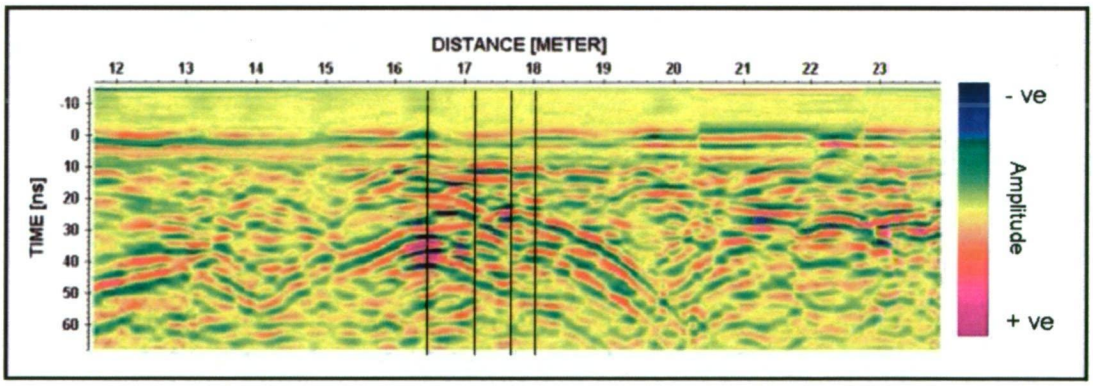

Figure 3.40: Multiple adjacent hyperbolic responses recorded in a processed profile from Line 72y. Black lines mark the central axis of anomalous responses between 16 m and 19 m.

Classes 1 and 2 are represented symbolically on the survey area map by a point, which records the hyperbolic apex position along-line, and estimated depth. Depth (m) is a product of the TWTT/2 (ns) and estimated average velocity (0.09 m/ns) of the radio wave through the subsurface. Class 1 and 2 point symbols are presented as scatter maps in Figures 3.41 and 3.42. This format allows the flexible display of selected parameters, to highlight different trends in the data. Figure 3.42 shows the distribution of all recorded hyperbolic apices at 0.5 m depth intervals. Each interval is represented by a

different colour, making it easy to determine that the majority of points lie within the top 1.0 m. Many responses within the same interval overlapped, indicating that the radar had detected a feature over several profiles, or closely-spaced sources. Other responses are laterally coincident but recorded at different depth. These distribution patterns may be caused by several geophysical sources within an individual burial, and/or closely spaced burials.

Within the area surveyed, the highest density of responses is recorded on the Upper Bench and western Riser Slope, where most of the sandstone markers and depressions are located. The eastern Riser Slope and Lower Bench are typified by isolated clusters of point anomalies. These findings suggest that coffins were probably used in conjunction with burial stones, to dignify primarily the graves of military officers and their families, rather then convicts, invalids and paupers (Lord, 1999; Greg Jackman, pers. comm.). The sparse distribution of hyperbolic responses on the Lower Bench and eastern Riser Slope may also be related to the terrain and soil properties. Topsoil erosion and movement of water down-slope have contributed to produce a relatively deep and moist humic soil column. Hand auger refusal reached 1.65 m at 56x, 31y and 1.3 m on the Riser Slope at 45x, 51y. These conditions may not be conducive to preservation of burial remains.

Response Classes 3 and 4

Some sections of the radargrams are characterised by clusters of overlapping non-horizontal diffractions, including both irregular and hyperbolic anomalies. These zones are defined as Class 3 responses and are suggestive of stratigraphic disturbance or possibly dense arrangements of burials (Figure 3.4). Identification of individual burials in Class 3 is very challenging. Class 4 zones are characterised by non-hyperbolic, high amplitude reflectors that indicate the radar has detected interfaces of strong material contrast, such as a soil-coffin boundary or a perched water table. Figure 3.43 shows good examples of Class 3 and 4 responses.

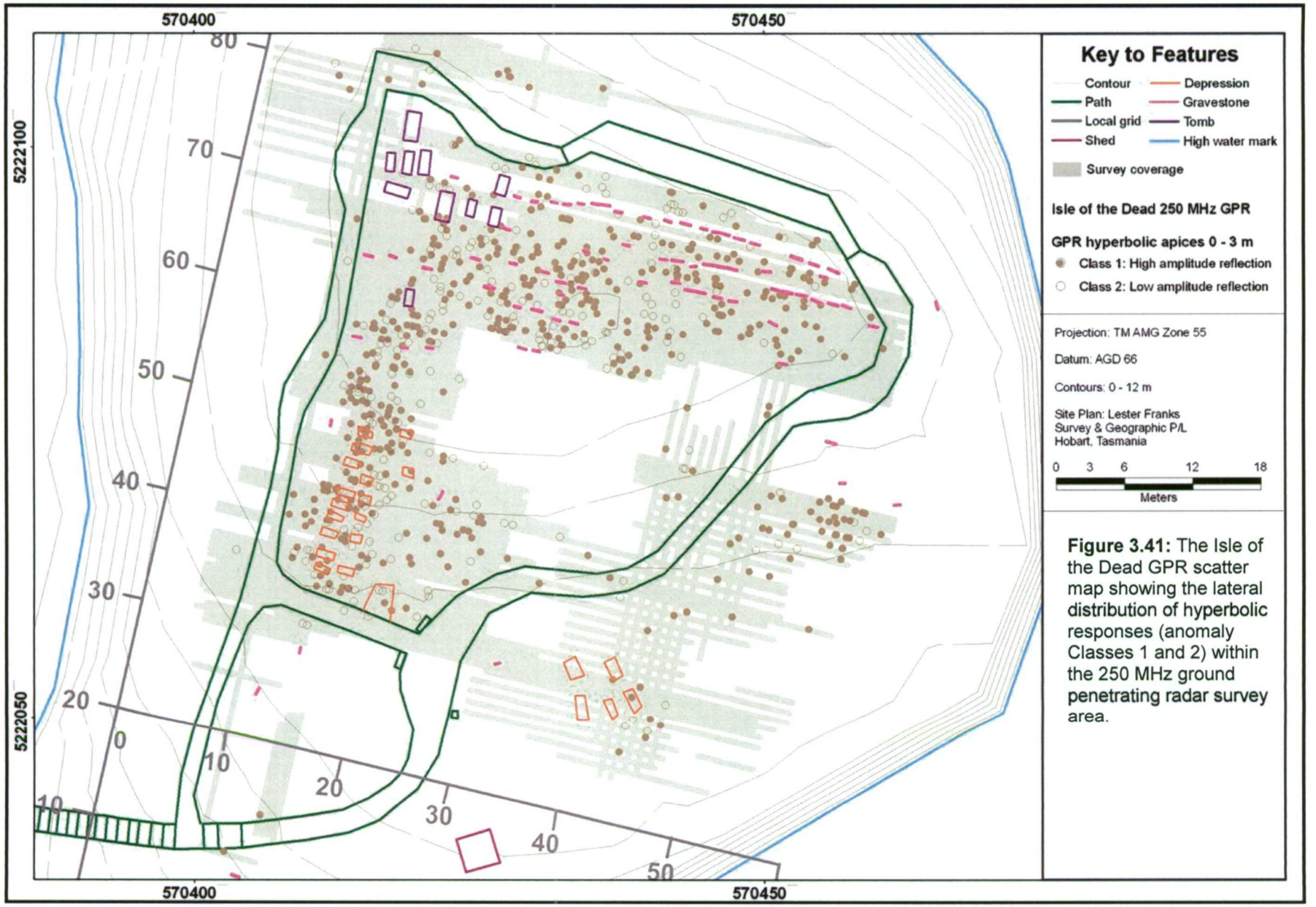

Figure 3.41: The Isle of the Dead GPR scatter map showing the lateral distribution of hyperbolic responses (anomaly Classes 1 and 2) within the 250 MHz ground penetrating radar survey area.

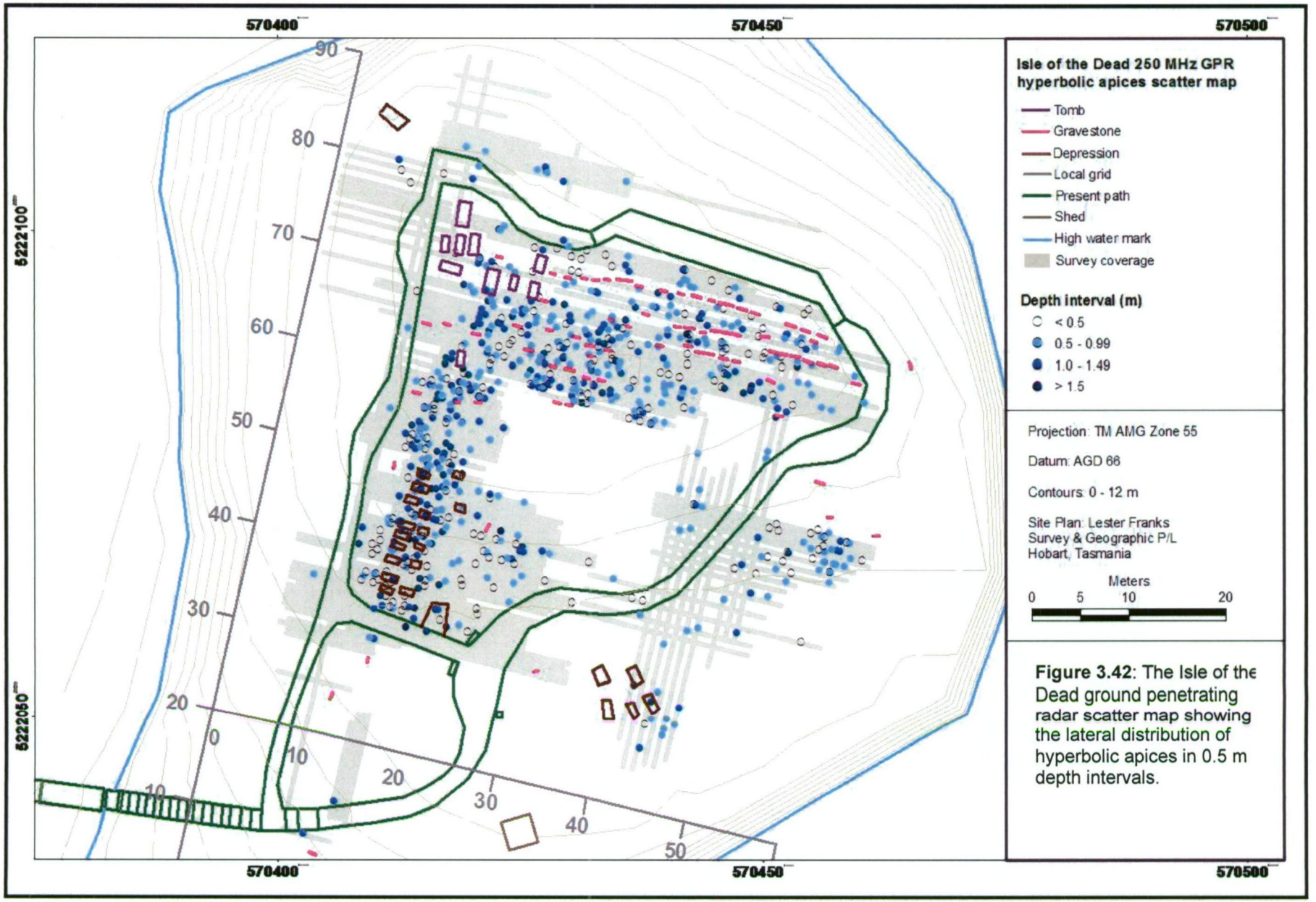

Figure 3.42: The Isle of the Dead ground penetrating radar scatter map showing the lateral distribution of hyperbolic apices in 0.5 m depth intervals.

The lateral extent of Classes 3 and 4 are represented schematically initially as a section along-line, and then translated to an area with a narrow (~ 0.3 m) buffer zone. Zones that correlate across adjacent profiles (0.5 m spacing) are interpolated into a cumulative anomalous area. Figure 3.44 presents the distribution of all recorded anomalous zones within the surveyed area. Similar to Figures 3.41 and 3.42, the map shows a high density of responses on the Upper Bench and western Riser Slope, with isolated zones in the southeast quadrant, such as at 58x, 50y. This close correlation suggests that Classes 3 and 4 are probably representative of cultural stratigraphic disturbance and/or burial features, rather than naturally-derived variation in the soil horizon.

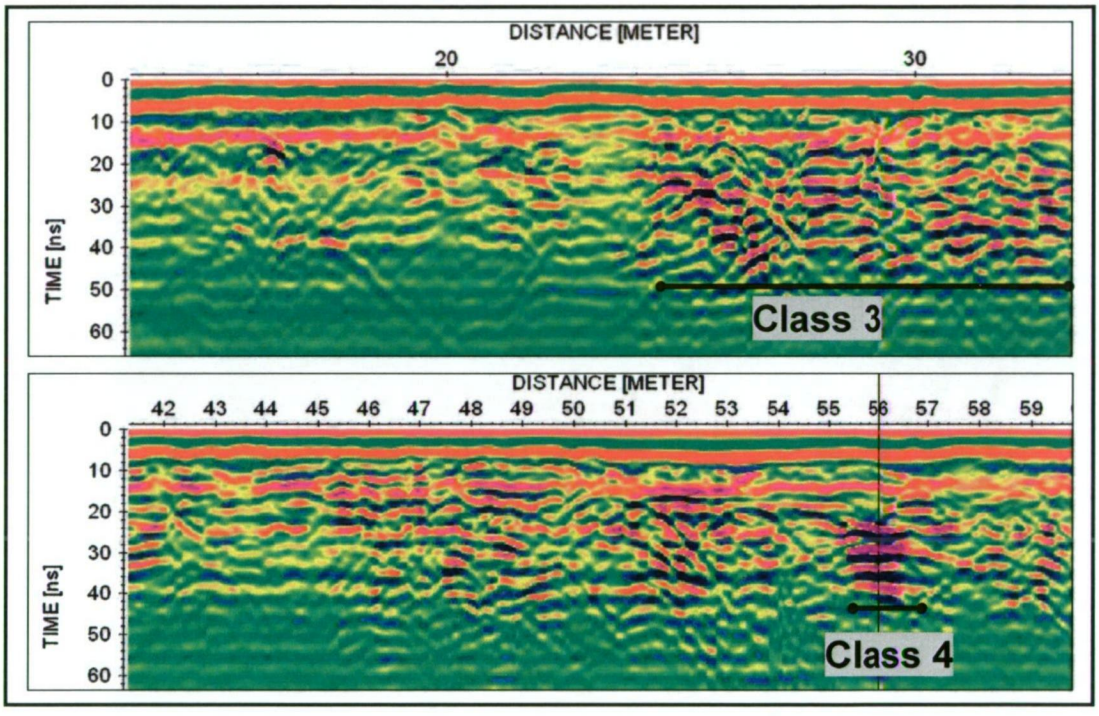

Figure 3.43: Typical examples of anomaly Classes 3 and 4 in gain-adjusted 250 MHz radargrams. A black line delineates either the lateral extent (Class 3) or central axis (class 4) of the response.

Density maps

To better visualise response distribution patterns for spatial analysis and interpretation, different response classes were integrated into a single dataset through the creation of density maps. This method uses a calculation of the density of point features around each output raster cell, within a given radius. A normalised density map of all hyperbolic reflectors is presented in Figure 3.45, where Class 1 and 2 responses are weighted at 0.65 and 0.35 respectively. This weighting is based on the presumption that stronger anomalies (form and amplitude) are more likely to represent burial features

than Class 2 responses. A radius of 1.0 m was used in the density calculation, to ensure responses potentially attributed to the one burial would be associated visually. This means that hyperbolae caused by graves spaced within 1.0 m of each other are also included in the calculated area. The most cluttered areas of Figures 3.41 and 3.42 are therefore translated into near continuous zones of varying densities. In areas of sparse point distribution, the density map tends to create short lineaments, such as those located at 30x, 75y (**A**) and 54x, 50y (**B**), circled in black in Figure 3.45. These are tentatively interpreted as individual burials. The net product of the density calculation is an archaeological potential map of the GPR survey area, in which the probability of detecting a burial increases from the blue to pink zones.

The inclusion of Class 3 and 4 anomalous zones enabled the assembly of a more detailed archaeological potential map. Initial map presentation comprised Class 3 responses as the base, overlaid by the density calculation (at 30 % transparency) of combined Classes 1 and 2, with Class 4 as hachured zones. This approach resulted in a visually complex image, as shown in Figure A9, Appendix A. It ineffectively presents areas of coincident stratigraphic disturbance and interfaces between materials of high geophysical contrast.

To better visualise all four radar classes in the same image, responses are integrated to form a single layer composite map (Figure 3.46). A binary representation is used for Class 3 and 4 anomalous zones, which are normalised to a value of 1 and then weighted relative to the point classes. Again, strong hyperbolic reflectors are given the highest weighting (0.4), followed by Class 2 (0.3) while the zones were rated equally as 0.15. The colour scheme is graded from green (low potential) to red (high potential) to allow the viewer to quickly determine subsurface areas most likely to contain archaeological material. Binary classification has been effectively applied in several other archaeo-geophysical case studies, where a '1' value was used to indicate the presence, and a '0' the absence, of an anomaly (Field *et al.*, 2001).

For a comprehensive overview of potential cultural features on the island, these density maps could be viewed in ArcGIS in conjunction with the EM-38 and magnetic qualitative interpretation images.

Figure 3.44: Isle of the Dead map showing areas of stratigraphic disturbance and high amplitude responses as inferred from the 250 MHz ground penetrating radar data.

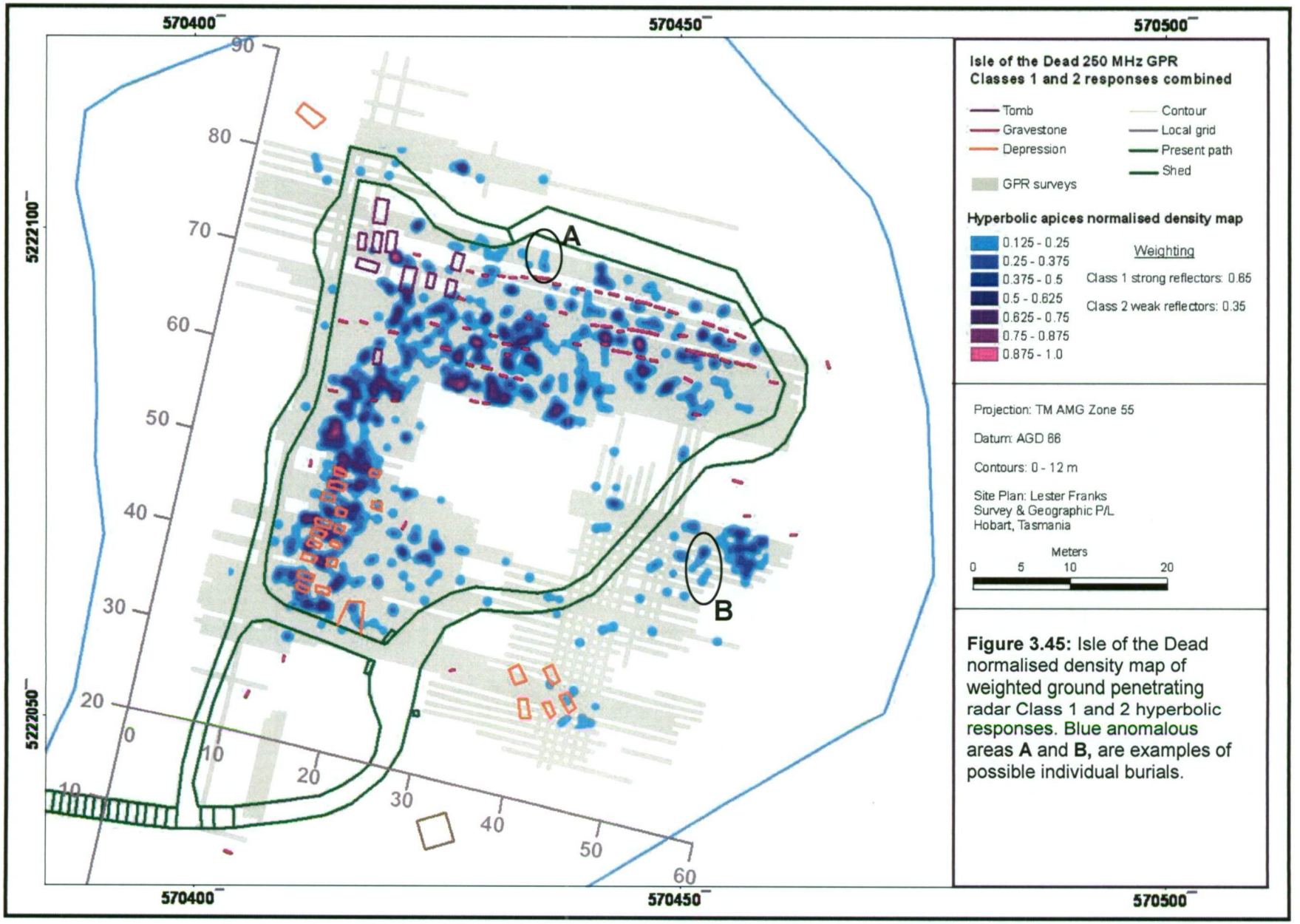

Figure 3.45: Isle of the Dead normalised density map of weighted ground penetrating radar Class 1 and 2 hyperbolic responses. Blue anomalous areas **A** and **B,** are examples of possible individual burials.

Figure 3.46: Normalised density map of all classified responses recognised from the Isle of the Dead 250 MHz ground penetrating radar survey.

Three-dimensional data visualisation

Three-dimensional visualisation was applied to data collected from a focus area on the Isle of the Dead, to assess its effectiveness for displaying hyperbolae identified through individual profile analysis. This was achieved by comparing amplitude variation maps generated at discrete two-way travel times with anomaly scatter maps and density maps. Profiles located within the focus area shown in Figure 3.47 were used to create a three-dimensional data volume for interpretation, using the method outlined in Section 3.2.6.2. This area was chosen because it has near-level topography, a known source of geo-electrical influence (present pathway) for reference, and several widely spaced surface depressions and headstones, which are possible indicators of burials. Previous analysis of individual profiles recorded many hyperbolic responses, primarily between 12 m and 18 m (Figure 3.47). One or two point anomalies are located in front of each north-facing headstone, suggesting a high probability of associated burials.

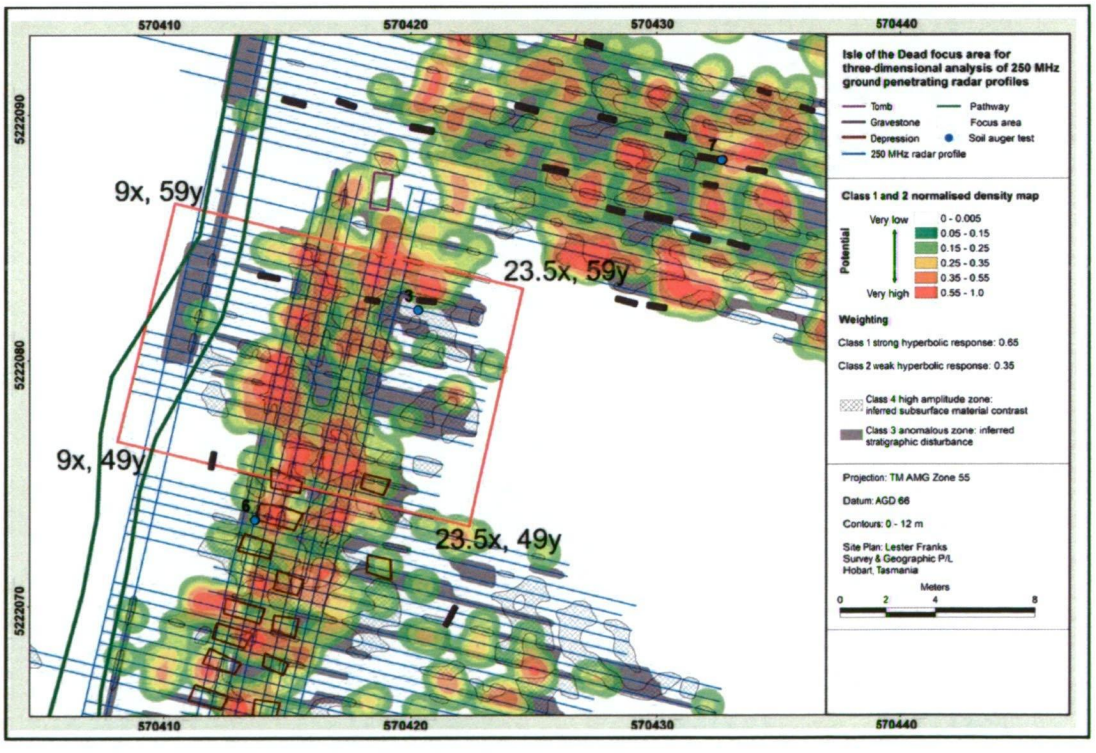

Figure 3.47: Map showing the profile density and anomaly distribution patterns within the 3D radar data focus area, as recorded from individual profiles.

Response distribution patterns in slices generated within the continuous surface reflections to 0.2 m depth correlate closely to topographic variations and material contrasts across the focus area. The raised path edge and a natural change in slope (dotted line) are clearly defined by a sharp amplitude gradient (Figure 3.48).

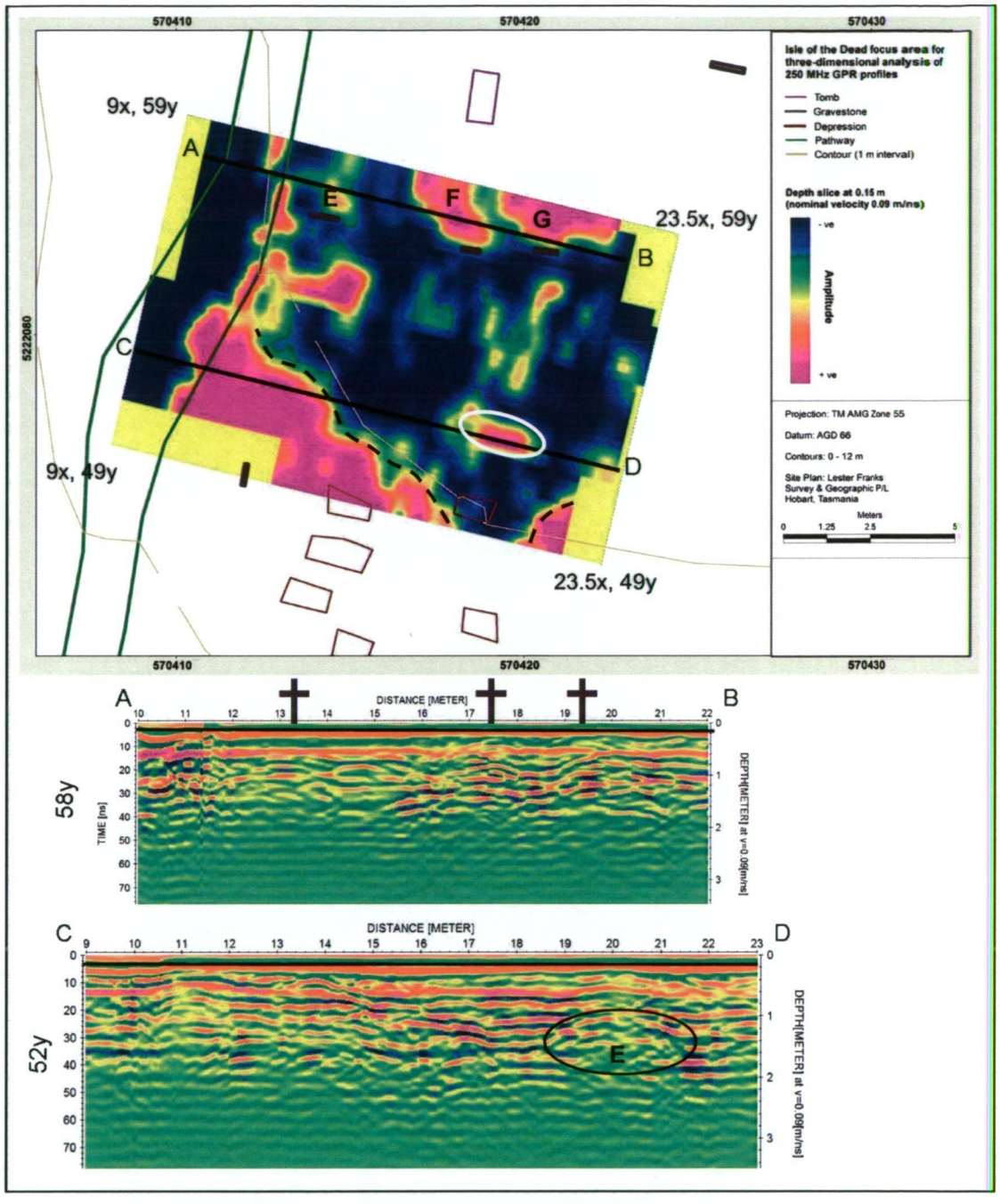

Figure 3.48: The map shows a depth slice generated at ~ 0.15 m from the preferred data volume (no image enhancement) and the location of two radargrams which provide vertical information. Profile **AB** intersects anomalous zones north of the headstones and **CD** crosses a high amplitude anomaly (**circled**) in similar orientation to the marked surface depressions. The slice depth and headstone locations are represented on the radargrams as black lines and crosses respectively.

Shallow depressions in front of north-facing headstones at 13.3x, 17.5x and 19.4x are also defined by a phase shift in the timeslice (Figure 3.48, **E- G**). These are attributed to settling of material in the burial trenches. This effect is illustrated in profile along transect **AB,** as a series of undulating reflections recorded below the headstones. None of the surveyed surface depressions corresponded to patterns in the amplitude map.

A high amplitude anomalous zone centred on 20x (**E**) and oriented parallel to the surveyed surface depressions is also coincident with a slight elevation in the surface band. In profile 52y, zone **E** in the timeslice correlates to a section of relatively low - moderate amplitude reflections between 18.5x and 21.2x (circled in black). This may indicate more conductive unconsolidated and/or more organic-rich material - possibly the former location of a large tree, or a burial site.

While this approach enables the mapping of any topographic variation associated with cultural features such as the path, or depressions manifesting from subsurface subsidence, it is also influenced by tree roots, burrows and other natural changes in gradient surface.

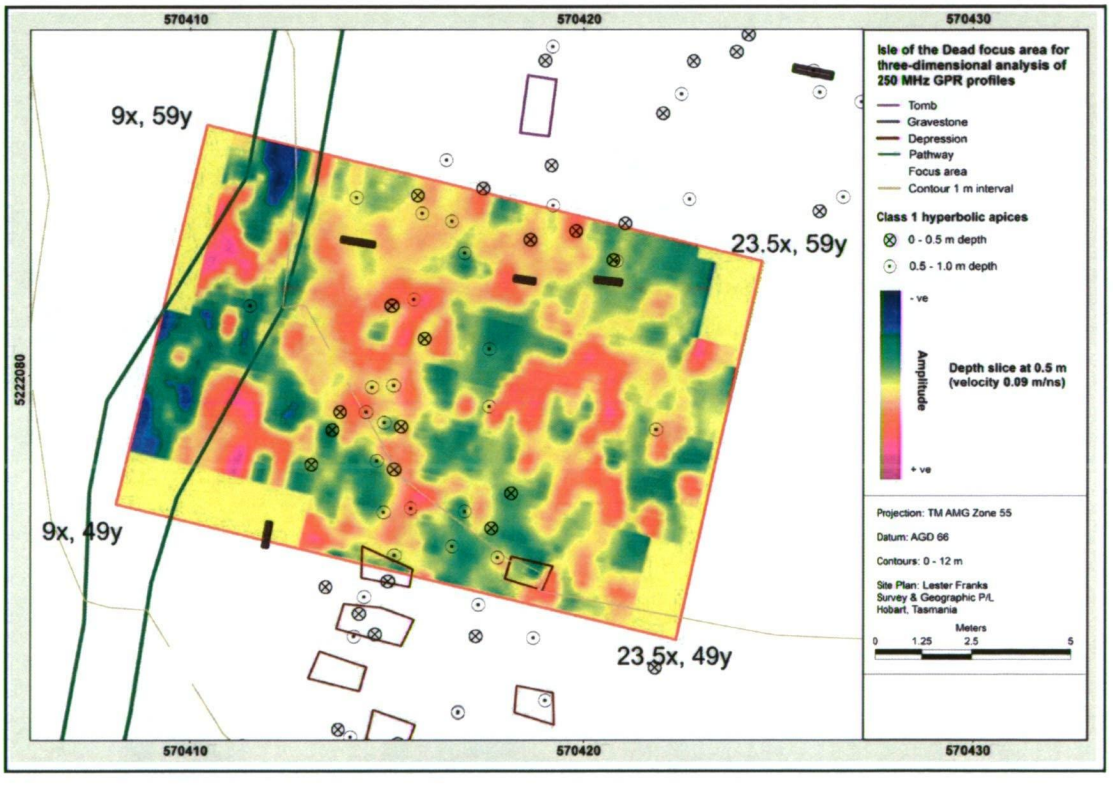

Figure 3.49: Map showing hyperbolic apices within 1.0 m depth range, as recorded from individual profile analysis, overlying a depth slice generated at ~ 50 cm from the preferred data volume (no image enhancement).

Defining the stratigraphy from radar data

The auger results were used as a correlative device for the definition of stratigraphic horizons in the radar data, as both datasets exhibit comparable scale of detail. Visual comparison between the soil profiling results and coincident GPR profile sections (surface corrected to time zero) is shown in Figure 3.47. The left radargram section in each case is a processed version of that on the right, with average trace subtracted and gain amplified. Overlying this data is the soil column to refusal depth, including horizon boundaries. Dark grey lines are drawn over moderate to high amplitude and/or near-continuous planar reflectors that may be attributed to mapped soil interfaces. Only one reflector was picked in the auger 5 radargram, due to the multiple adjacent overlapping responses typical of Class 3 stratigraphic disturbance. This roughly correlated (0.1 m error margin) to the boundary between sandy topsoil and underlying loamy sands. Radargrams at the other test sites also clearly recorded the topsoil-subsoil interface. The soil-regolith interface was picked with confidence at Augers 3 and 6, where it manifests as high amplitude reflectors laterally continuous over > 1.5 m. Without the soil columns as a guide, however, there is no method of confidently picking intra-soil horizons in the radar.

Viewing each radargram as a whole indicates that the picked horizons are mostly discontinuous. Response distribution patterns were therefore not mappable across profiles, or within each morphological zone. There are no distinctive reflections in the relatively undisturbed 'background' areas, which suggests that changes in RDP across soil horizons are too diffuse or graded for the radar to detect them. The strongest radar reflections usually occur at the interface of two horizons with greatly varying electrical properties (Conyers and Goodman, 1997). Picked reflectors not correlating closely to either the topsoil-subsoil or soil-regolith boundaries are therefore attributed to cultural material (e.g. coffin, buried headstone) and/or natural features such as major tree roots. In areas of stratigraphic disturbance, diffraction and hyperbolae distort, beyond identification, any reflections from the regolith surface. Hence it is difficult to detect and map responses from any burial trenches excavated into the substrate. This is illustrated by the simple synthetic model in Figure 3.37c, where the upper interface causes corresponding undulating responses from both it and the lower horizontal boundary.

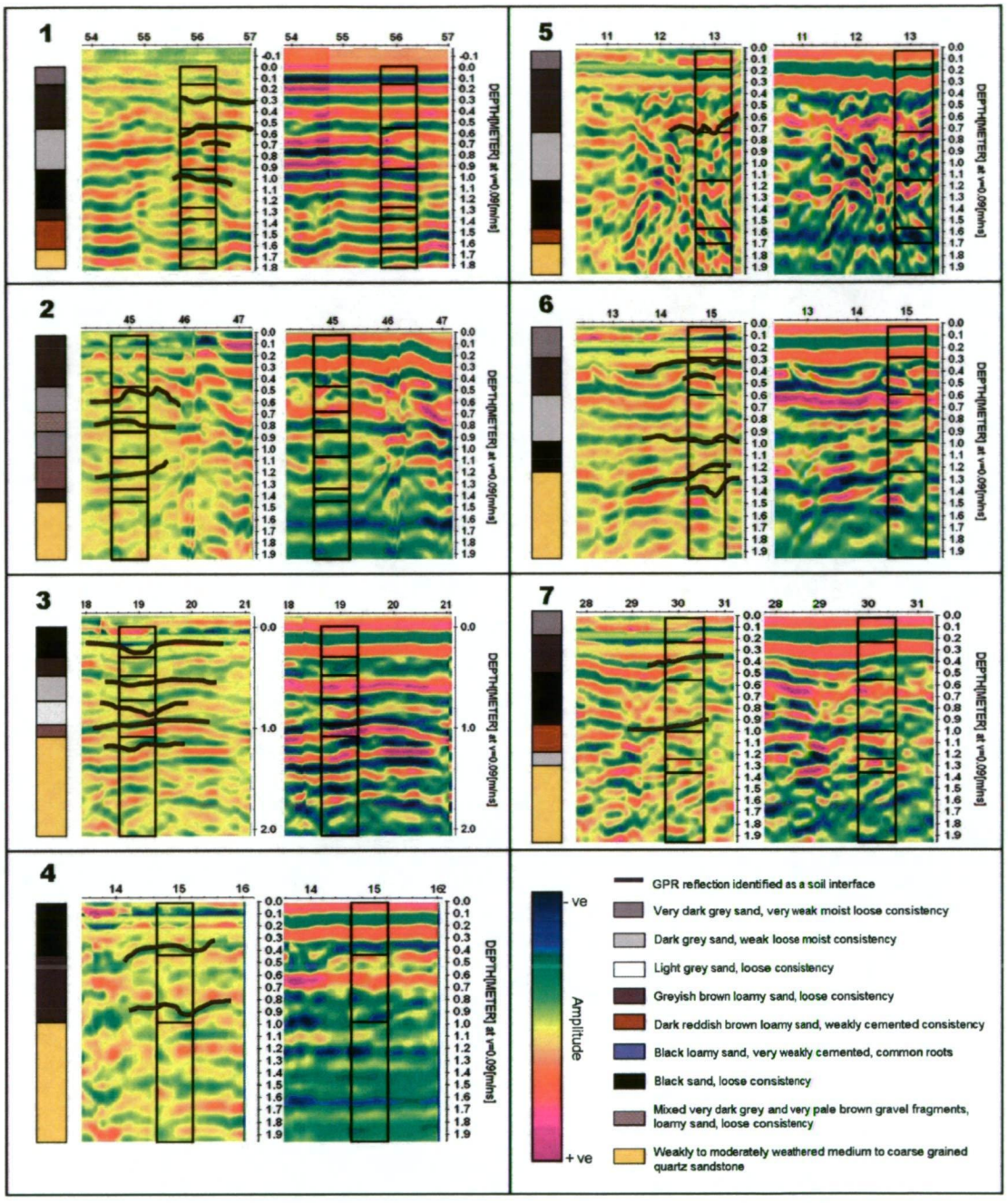

Figure 3.50: Comparison of average trace-subtracted (left) and raw (right) gain-amplified 250 MHz GPR radargrams to the corresponding soil auger profiles (courtesy of Doyle and Cumming, 2003). The negative polarity horizontal reflector visible at ~ 1.6 m in radargrams at sites 2, 4 and 5 is a multiple of the surface band.

Sources of undesirable signal in the radargrams

It is widely acknowledged that tree roots and forms of bioturbation (e.g. rabbit burrows) can have an adverse effect on the performance of ground penetrating radars (Conyers and Goodman, 1994). The primary effect of roots is to add a randomly distributed set of discrete clutter sources. Niltawach *et al.* (2004) found that any root-related loss in

performance could be partially offset by using frequencies lower than 500 MHz. Profiles collected in vegetated areas of the island exhibit evidence of root interference, in the form of multiple adjacent discontinuous reflectors less than 0.2 m in width. This effect is much more pronounced in the 500 MHz data than the 250 MHz, a result that further justifies widespread use of the 250 MHz frequency. It is unclear to what extent the 1930s clearing would have disturbed the present day upper soil horizons.

The pathway is a significant non-random source of interference in the radargrams. The bark mulch and base material are clearly defined by very high amplitude reflections and 'ringing' multiples at depth, while the path edges are marked by diffractions in the surface bands. The strength of these responses indicates that the path material has a high dielectric permittivity contrast relative to the surrounding sandy soils. Elevated magnetic intensity values associated with a former gravel pathway also suggest that the radar is detecting material of higher magnetic permeability. Both these factors cause rapid wave attenuation and therefore reduce the ability of the radar to detect underlying features.

3.3 SUMMARY

The primary objectives of this investigation were to define the penal period cemetery area, detect and characterise potential burial features. Geophysical targets included coffins, buried objects and stratigraphic interruptions associated with trench geometry (edges and base), and trench fill deposits. Because there was no archaeological ground-truthing, it was hoped that burials marked with both a headstone and footstone could be used to provide geophysical signatures of individual interments. This information could then be used as a benchmark for the identification of unmarked graves within the cemetery area. There are 6 double-marked graves on the Isle of the Dead. Cultural material associated with site use during the post-penal and contemporary phases were of secondary importance.

Several techniques were applied to map the graves, including ground penetrating radar profiling with a 250 MHz central frequency antenna, EM-38 frequency domain electro-magnetometry and total field magnetometry. Seismic refraction and dipole-dipole electrical resistivity profiling were used to identify primary stratigraphic interfaces across the island, including soil-regolith and regolith-bedrock transitions.

Two sessions of conductivity mapping on the Isle of the Dead, in both VCP and HCP modes, demonstrated that overall site conditions were highly resistive, with local background values restricted to a narrow range of low apparent conductivities. These results were consistent with those expected from dry soils derived from shallow sandstone-siltstone regolith (Bevan, 1998; Clarke, 1997). Broad trends in apparent conductivity across the survey area correlated closely with variation in surface vegetation, site topography and depth of the soil column as defined by Doyle and Cummings (2003). Moderate to high values were recorded on the lightly wooded Riser Slopes and Lower Bench, which were characterised by more humic topsoils and a deeper soil-regolith interface. The exposed, dry Upper Bench was typified by very low conductivities. Data from this area was also the most affected by instrumental drift, which was sometimes greater than the dynamic range of conductivities along-line. Despite calibration at regular intervals, this error was only lessened or removed through time-consuming manual processing.

The conductivity surveys did not systematically detect individual burials - neither through stratigraphic disturbance associated with burial trenches nor isolated ceremonial artefacts. Material contrasts were either not large enough to be measured or they did not illustrate clearly interpretable response distribution patterns. These results were probably due to a combination of the following factors:

- physical deterioration of burial material (e.g. coffin),
- soil development in the permeable, porous sandy stratigraphy,
- quantisation error, which is the difference between the apparent conductivity value and the approximated EM-38 digital value due to the 'rounding' that occurs while converting to the nearest mS/m.

The EM-38 surveys were most successful at detecting post-penal and contemporary cultural features, such as the pathway and metal debris from previous site surveys. Numerous high amplitude discrete dipolar responses, many of which were coincident with magnetic point anomalies, appeared to trend in three lines oriented NW-SE across the midsection of the island. These were attributed to iron-bearing remnants of former posts. There was no other evidence for these posts, in either historic documents or contemporary site photographs. It was thus postulated that they were installed during the post-penal period when the cemetery became a garden of remembrance, as they did not appear to be spatially related to the layout of original burial markers.

The magnetic survey primarily detected post-penal and contemporary cultural features in the subsurface, including former gravel pathways running between rows of headstones, as shown in site photographs from the 1980s. The cast-iron railing around one burial was the most prominent magnetic source from the penal period. There was no systematic identification of individual burials or cemetery layout within the surveyed area. This result is attributed to a lack of iron-bearing burial artefacts or caskets. Several aboveground features were prominent sources of undesirable signal in the data, including the bin, and benches, and responses from these sources effectively masked anomalies from any nearby smaller features.

Mathematical modelling and a basic standard method of manual quantitative interpretation (half-maximum rule) were used to compare the depth estimations of four sources exhibiting different response signatures. The maximum differences between the manual values and those modelled from 0.5 m and 0.2 m diameter spheres are 0.1 m and 0.17 m respectively, with sources typically located within 0.5 m cover. These results suggested that most similar-type responses are probably post-penal to contemporary iron-bearing debris, or objects such as the inferred fence posts, rather than convict-era burial artefacts.

Of all the techniques, ground penetrating radar was the most successful for delineating areas of ground disturbance, and subsurface features of interest. The background response was characterised by low-amplitude, near continuous planar reflectors and interpreted as undisturbed stratigraphy. Multiple-layered strong reflections over the present path obscured deeper responses and limited the amount of useful information in these areas.

Modelling of ideal burial scenarios and previous studies at historic burial sites provided the basis for identifying the anomaly types attributable to stratigraphic elements in an individual burial. Relevant responses were divided into four classes according to shape, amplitude and continuity. Class 1 anomalies were characterised by well-defined hyperbolic form and high amplitude relative to background values. Class 2 hyperbolic reflectors were less well-defined and/or of lower amplitude. Class 1 anomalies were therefore viewed as the best indicators of a burial. Clusters of overlapping non-horizontal diffractions, including both irregular and hyperbolic anomalies, were defined as Class 3 and were suggestive of stratigraphic disturbance or possibly dense arrangements of burials. Class 4 zones were characterised by non-hyperbolic, high amplitude reflectors that indicated interfaces of strong material contrast. All response classes were identified through profile analysis and presented symbolically on plan views of the survey area.

In the areas of ground disturbance, most responses were recorded within ~ 1 m of the surface, with only five responses at greater than 2 m depth. Resolution of features was achieved to ~ 2 m depth, with the 250 MHz antenna frequency, which theoretically included the soil-regolith interface (Doyle and Cumming, 2003). Of the 718 hyperbolae

recorded in the survey area, 499 were defined as Class 1, although they were rarely as ideal as the models. Discrete responses were less common than overlapping adjacent hyperbolae, the apices of which were recorded at various depths. It was therefore difficult to interpret individual burials. Point scatter maps of hyperbolic apices at 0.5 m depth intervals showed that the highest density of responses was recorded on the Upper Bench and western Riser Slope, where most of the sandstone markers and depressions are located.

There were no consistent anomaly patterns between sets of headstones and footstones, which made it unfeasible to characterise the geophysical signature of an individual burial with reliability. Without a benchmark response from marked burials, it was thus difficult to identify unmarked burials on the Isle of the Dead. The Lower Bench and eastern Riser Slope were typified by isolated clusters of point anomalies. A paucity of hyperbolic responses in the Lower Bench survey area belied the historic photographic evidence of densely arranged mounds. This either suggested that coffins were not used for the burial of convicts, paupers and invalids, and/or that soil conditions precipitated deterioration of any burial remains.

Point anomaly data were also synthesised into weighted and normalised density maps, in which Class 1 hyperbolae were given a higher weighting than Class 2. Then all positional data from response types were integrated into a single dataset as normalised density maps, with hyperbolae given a higher weighting relative to Classes 3 and 4. This was an effective way of presenting such a large amount of data. The net product of the density calculation is an archaeological potential map of the GPR survey area, in which the probability of detecting a burial may be inferred through the graded colour scheme. Zones of low density were possibly indicative of areas free of unmarked burials, or very poorly preserved burials.

The auger results were used to help identify stratigraphic horizons in the radar data, as both datasets exhibit comparable scale of detail. Radargrams at auger test sites typically recorded the topsoil base as a definable reflection, but did not consistently define the soil-regolith transition due to the masking effect of shallower diffractions. Without the soil columns as a guide, there was no method of confidently picking intra-soil horizons in the radar. Picked horizons were mostly discontinuous across the whole radargram.

The soil-regolith interface could therefore not be extrapolated between profiles, or across morphological zones. There were no distinctive reflections in the relatively undisturbed 'background' areas, which suggested that changes in RDP across soil horizons are too diffuse or graded for the radar to detect them. Thus it was difficult to detect and map responses from any burial trenches excavated into the substrate.

Three-dimensional radar processing was also assessed as an alternative approach to data visualisation. This was conducted at a small focus area which included several headstones and a surface depression, and the results were compared to those obtained using individual profile analysis. Timeslices generated at single TWTT indicated high variability in amplitude patterns throughout the data volume, even between slices separated by a few centimetres depth. Despite this variability, several trends were identified. Within 5 cm of the surface, well-defined high amplitude zones were recorded in the areas immediately north of the gravestones, and attributed to very shallow depressions associated with soil subsidence.

The pathway was clearly recorded due to a high material contrast to surrounding soil. However, there were no consistent patterns in time slices corresponding to intervals between 0.1 - 1.0 m. This is because the Class 1 hyperbolae, potentially definable in the slices, were juxtaposed with other irregular diffractions of varying amplitudes. These results showed that timeslicing is an unreliable method for visualising radar data on the Isle of the Dead, except where hyperbolae are recorded in the absence of other reflection types.

Electrical resistivity tomography was also applied to map stratigraphic boundaries on the Isle of the Dead, and determine whether burial trenches had been excavated into the substrate. Four dipole-dipole array transects were positioned to cross the two Riser Slopes, Upper and Lower Benches, coincident with the seismic refraction survey lines. Interpretation of anomaly patterns in the apparent resistivity pseudo-sections were based on knowledge of the island's simple stratigraphy, as inferred from auger tests, physical evidence, and other geophysical datasets.

Measurements collected across the Upper Bench exhibited a very large range of apparent resistivity values, from 40 - 1500 Ω.m. The soil column to ~ 1.3 m was

characterised by high values (> 750 Ω.m), which were consistent with those expected from a well-drained sandy soil with little vegetative groundcover. Undulation patterns at this interface also agree closely with those inferred from the seismic refraction velocity model for this line. Several local depressions in the soil-regolith topography were possibly related to a compacted burial features associated with nearby headstones. A near-surface layer (depth 1 - 1.5 m) of elevated values was also clearly visible in spreads collected across the Lower Bench and up the eastern Riser Slope. These findings also correlated closely to auger refusal depths at test sites coincident or offset < 2 m from the survey lines.

The Isle of the Dead was a suitable site for refraction surveying, due to its relatively simple profile (compared to areas of the main site), and a clear contrast between the soil-regolith and bedrock. The regular ground surface (low variation in ground level) and simple geology allowed for straightforward tomographic inversions. Complexities in the travel time curves were therefore attributed to changes in the first refractor interface - interpreted as a weakly defined soil – regolith boundary.

Interpreted stratigraphic trends and velocities were consistent across the four tomographic models. Layer 1 (< 300 m/s) corresponded to the sandy soil column, with auger refusal depths in very close agreement with the interpreted base of the layer. Layer 2 (~ 400 m/s) and Layer 3 (> 2000 m/s) were inferred respectively as the highly weathered sandy regolith and the weathered, but still consolidated, Permian sandstone-siltstone bedrock. Some undulations at the inferred soil regolith interface corresponded with overlying surface depressions and disturbed subsurface (as interpreted from the GPR), although there was no consistent evidence of velocity changes between the culturally emplaced and undisturbed soils at the site.

Chapter Four: Settlement Hill

4.1 INTRODUCTION

This chapter focuses on the terraced north-eastern slope of Settlement Hill, on which a number of administrative and residential structures and a subterranean aqueduct were erected during the penal period. Historical maps and building plans indicate that the original building layout underwent several modifications during the penal period, prior to widespread destruction through demolition and from bushfires in the 1890s. Unfortunately, a lack of suitable ground control points means that these documents cannot be accurately geo-referenced to a modern datum, and the position of some buildings remains uncertain. While surface evidence and parch marks inferred from aerial photographs indicate where very shallow structures existed, the location and condition of deeply buried features and ephemeral structures is unknown.

The primary objectives of this intra-site investigation were therefore to examine the surviving cultural fabric and assess the archaeological potential of Settlement Hill. Several questions were posed to direct this examination:

- Is the anticipated number and spatial patterning of historically documented buildings reflected in the geophysical data, particularly in the Hospital Precinct?
- Are there detectable differences in the geophysical data that would indicate the separate functions of building zones on Settlement Hill?
- If structural features are present, can they be functionally and/or spatially linked to other observable site features?
- Do geophysical signatures indicate occupational patterns that are not obvious in the historical documents

The approach adopted for this investigation is standard for archaeo-geophysical studies of historical sites, as discussed in Chapter 2. It involves the use of non-destructive multiple geophysical techniques and highly targeted 'ground truthing' excavations. Qualitative interpretation of the geophysical results has been based on numerous sources, including historic documentation (maps, photographs etc), surface evidence, previous experience at other similar sites and modelled outcomes. The primary results and preliminary qualitative interpretation of each technique have also been compared to those derived from other geophysical datasets and excavation. Ground truthed interpretation images, effectively archaeological potential maps, are a resource for the future conservation and management of the Settlement Hill area.

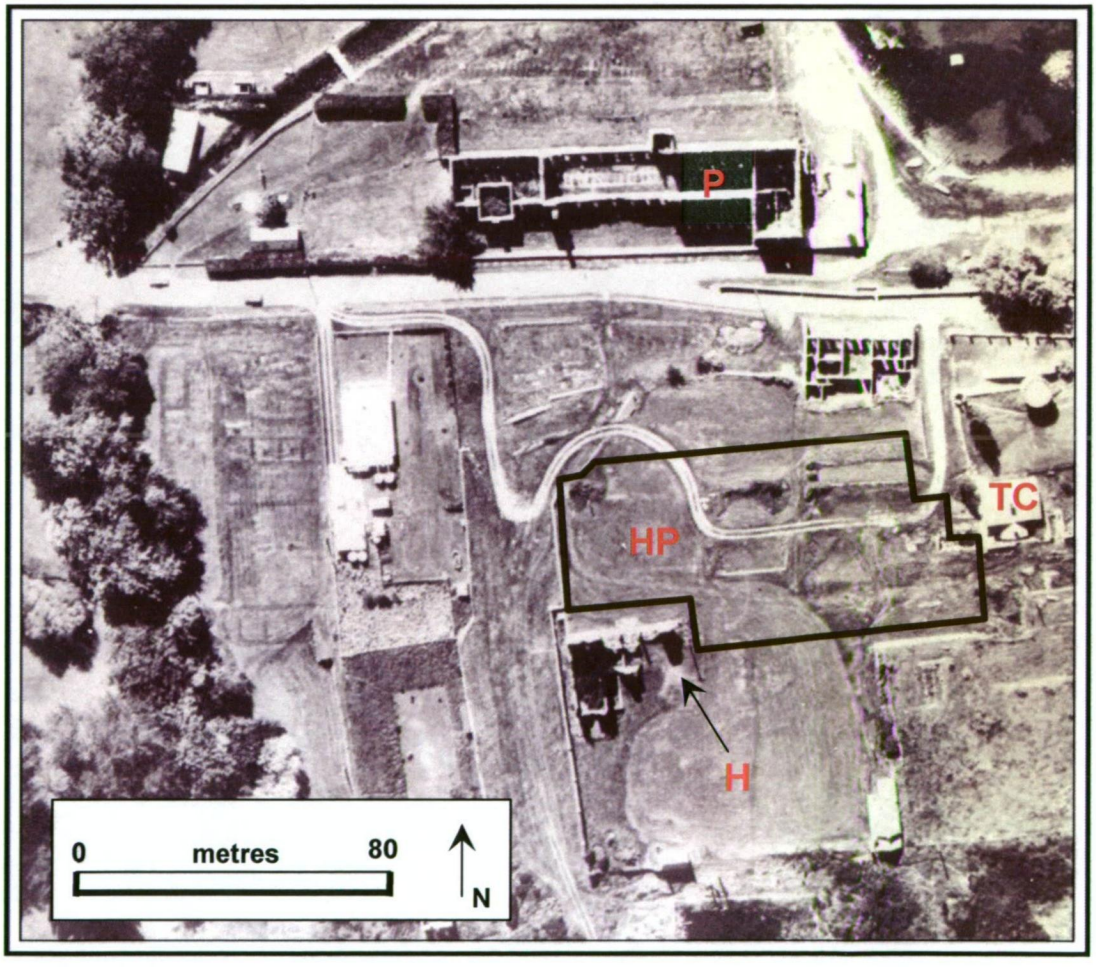

Figure 4.1: Aerial photograph of Port Arthur Historic Site c1970s, showing the Settlement Hill survey area (outlined in black) in relation to the hospital ruins (**H**), Tower Cottage (**TC**), and the Hospital Precinct (**HP**) focus area. The Penitentiary (**P**) ruins are located to the north (courtesy of Lord, 1999). Photograph is not rectified and oriented approximately north.

4.1.1 Site geology and topography

The natural terrain of Settlement Hill was extensively modified during the establishment period of the Port Arthur penal settlement to provide platforms for buildings and supporting infrastructure. Terrain at the site now ranges between 14 m and 20 m elevation above AHD. The shallow Jurassic dolerite bedrock, which characterises so much of the regional geologic domain, was cut to form large terraces parallel to Champ Street; the main settlement axis. Excavated rubble and transported loam was used to construct level benches and retaining walls. The physico-chemical qualities of dolerite, as described in Chapter 1, provide a markedly contrasting geophysical environment to the Permian sandstone-siltstone on the Isle of the Dead (Chapter 3) and to the anthropogenic fill deposits that characterise the Penitentiary site (Chapter 4).

4.1.2 Historical context

Evidence of site use was sourced from historical plans, photographs and other documentation from PAHSMA, and via personal communication with PAHSMA Archaeology staff Greg Jackman and Richard Tuffin. Unfortunately, due to scaling errors in the original maps and/or a lack of suitable correlating ground control points, rectification of these maps produced slightly warped images. As a result, they were viewed only as guides to the built landscape, rather than as definitive sources.

The hospital building that partially stands today was the third structure of such function erected at Port Arthur. The original and second hospitals were situated directly in front of this structure, an area referred to as the 'Hospital Precinct' (Steele, 2005). The second hospital was depicted in an 1833 Hughes plan as a basic 'C-shaped' structure, with prominent wings and two smaller outbuildings to the rear. An 1835 plan indicated it had taken a wingless rectangular shape and a rear 'Hospital Kitchen and Dead house' (morgue) erected (PAHSMA ref: HM 290/1459A). Internal divisions of this rectangular structure and its location relative to the outbuildings were recorded by Henry Laing in 1836 (Figure 4.2). The second hospital contained an assistant's room, store, dispensary and privies in rooms at its rear. The kitchen (of masonry construction) and morgue had northern entrances and fireplaces on their western sides. In his research on the Laing

drawings, Richard Tuffin notes that 'the main building was built on three main foundation lines, formed by a single row of ... sandstone, over four courses in height [while] the structure itself is weatherboard' (Tuffin, 2004). The front was skirted by a verandah (Figure 4.3). By 1845, the hospital buildings had been converted into 'Offices', augmented on the western end by newly constructed sandstone steps, while a third hospital was erected further up the hill (Figure 4.4). Stone Quarry Road, which originally ran past the second hospital, was diverted to below the west-facing terrace wall. A set of steps placed at the western edge of the former hospital precinct, enabled easy access to the third hospital (Steele, 2005).

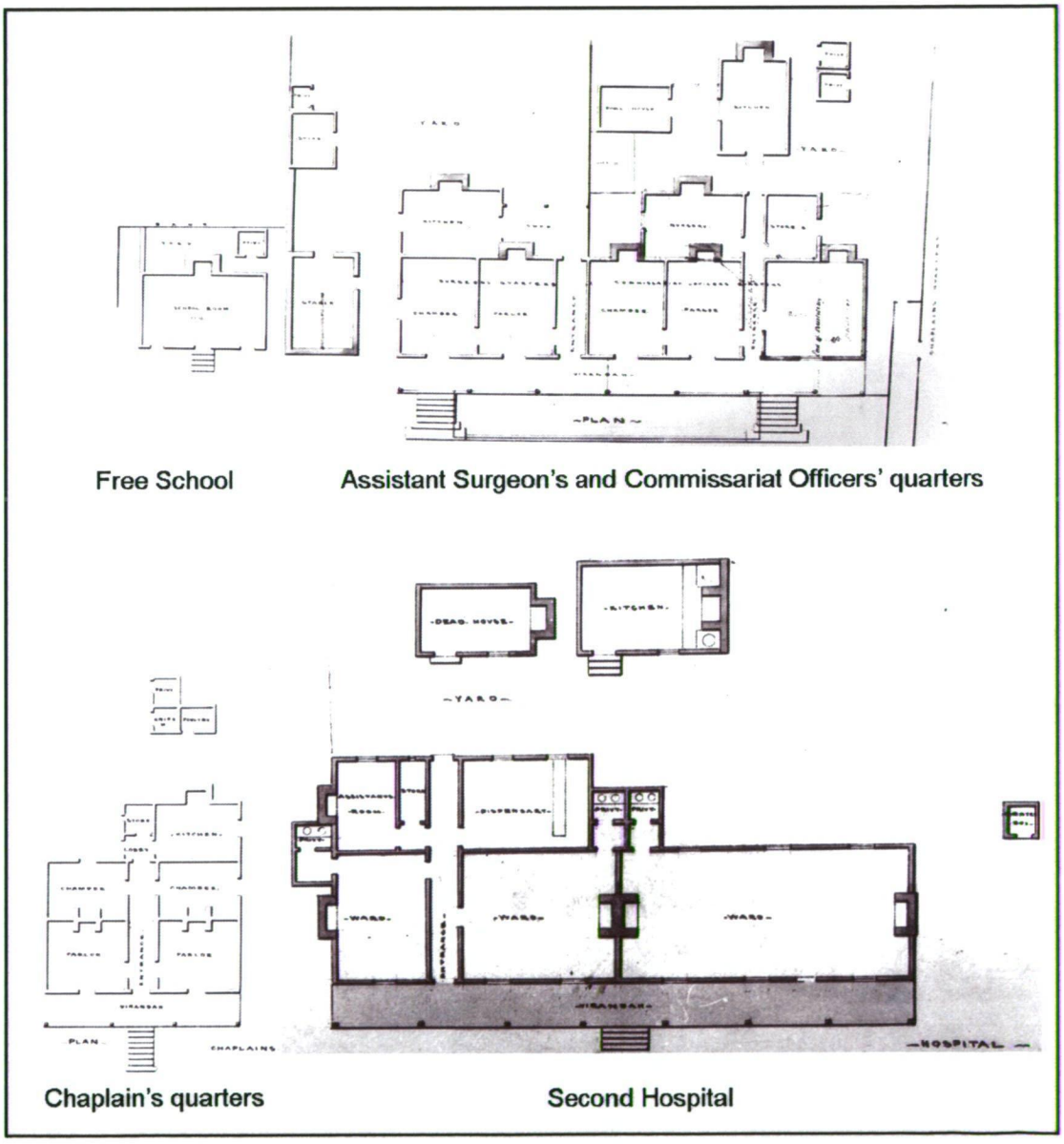

Figure 4.2: A montage of Laing plans c1836, depicting the internal configuration of rooms in the four primary buildings erected on the main terrace (courtesy of PAHSMA, AOT ref CON 87/#15, #18, #21, #26). Not to scale.

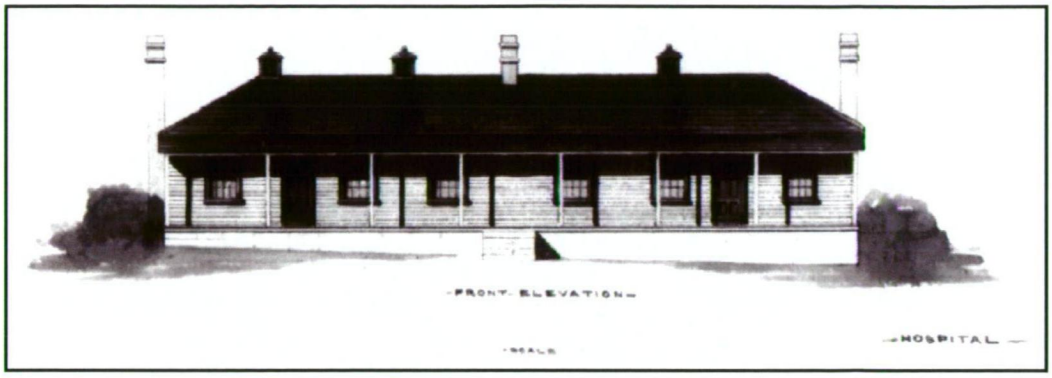

Figure 4.3: The first hospital front elevation, drawn by Laing c1833 (courtesy of Steele, 2005; AOT ref CON 87/#27).

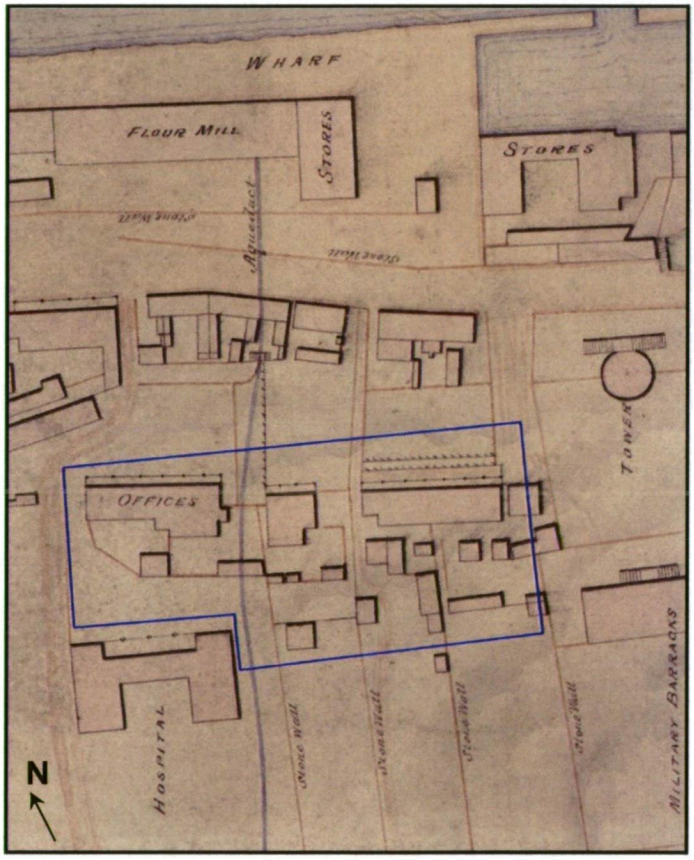

Figure 4.4: 1846 Hurst plan of Settlement Hill, showing the second hospital as 'Offices' and aqueduct (courtesy of PAHSMA, ref. HM 1846/1).

Along the same contour as the former second hospital stood a row of staff residences and associated outbuildings (Figure 4.5). To the west these included an 1833 bakehouse and carpentry shop, later to be civil accommodation; and to the east, and quarters for

the Chaplain, Commissariat Officer and Colonial Assistant Surgeon c1835, and a free school for officers' children (Tuffin, 2004).

By 1858, the former second hospital/offices had also been converted to 'Officers' Quarters' and the outbuilding was now a single elongate structure, as depicted in the alienation survey of 1877 (Blackwood C/19, Figure 4.6). A photograph c1865 – 68 (Figure 4.7) shows the high density of buildings that once stood between the bay-side Penitentiary and Military Barracks at the top of Settlement Hill. It is believed that the former second hospital building was demolished before the fires of 1895 and 1897 (Tuffin, 2004). At some stage, the other buildings standing in the same row were either removed or destroyed by the fires, with the exception of Tower Cottage, which although gutted in 1897 was rebuilt internally in the early 20th century. A small weatherboard house was erected on the site of the Commissariat Officers quarters during the 1930s, however it was short lived and today the landscape of Settlement Hill appears much as it did at the turn of the century.

Historic plans (Figure 4.4) also recorded the presence of an underground aqueduct, which led from a dam behind the third hospital, terminating in a pit covered by a timber trapdoor located at 35x, 35y on the local geophysical grid and continued southwest toward the dams. Built by 1845, it formed part of the infrastructure designed to supply water to the flourmill wheel. From the aqueduct pit the water was carried in an underground steel siphon to a riser, where it was lifted into an open flume leading to the top of an overshot waterwheel in the centre of the flourmill complex. The water supply for the mill ultimately proved to be too complicated and inefficient so the mill was gutted and converted into the penitentiary within a decade (www.portarthur.org.au). Although the millrace and overhead water race were dismantled, the underground aqueduct was left undisturbed. In 2003, Sinclair Knight Merz surveyed the aqueduct interior with a Leica Cyrax laser scanner, and located the central axis in three dimensions.

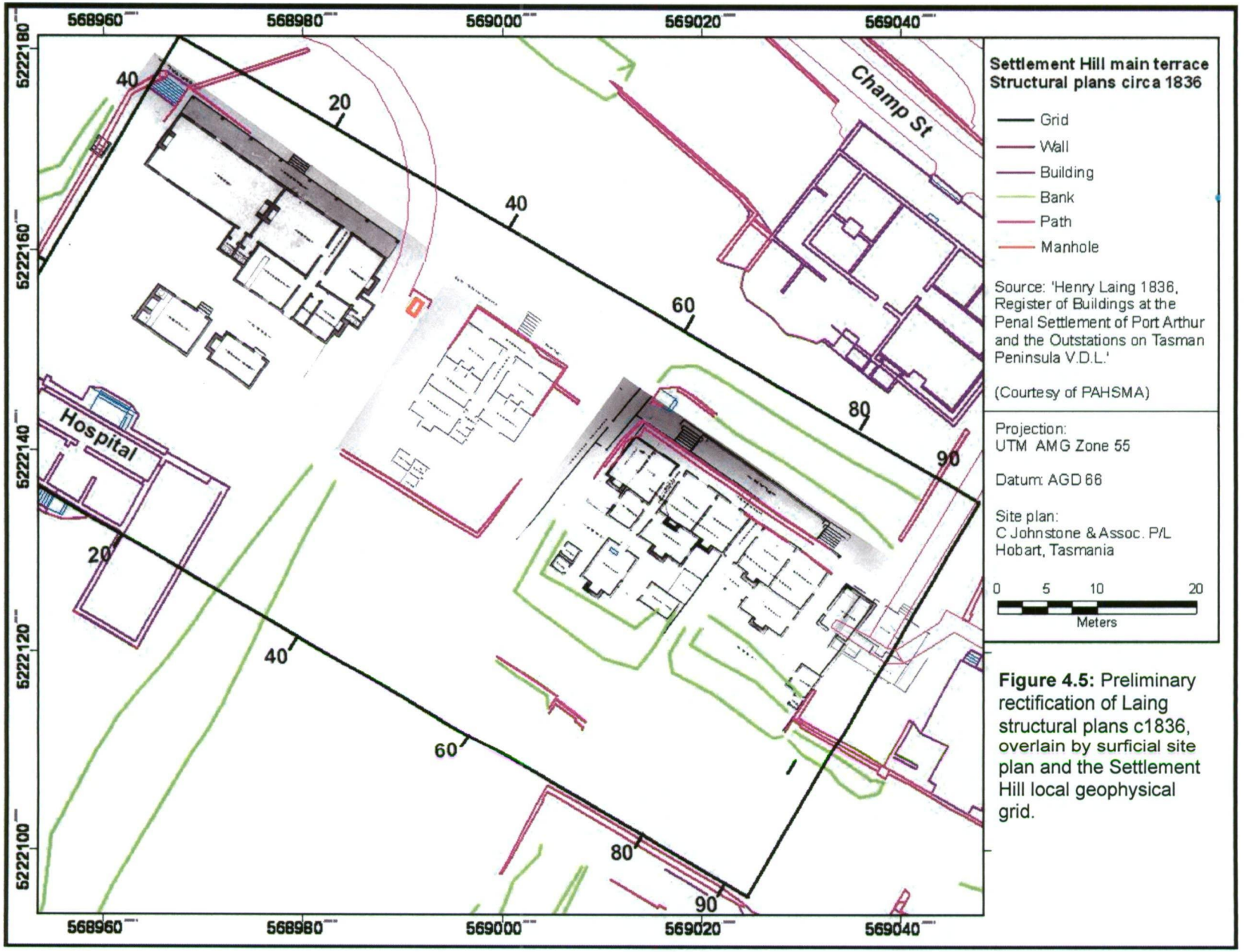

Figure 4.5: Preliminary rectification of Laing structural plans c1836, overlain by surficial site plan and the Settlement Hill local geophysical grid.

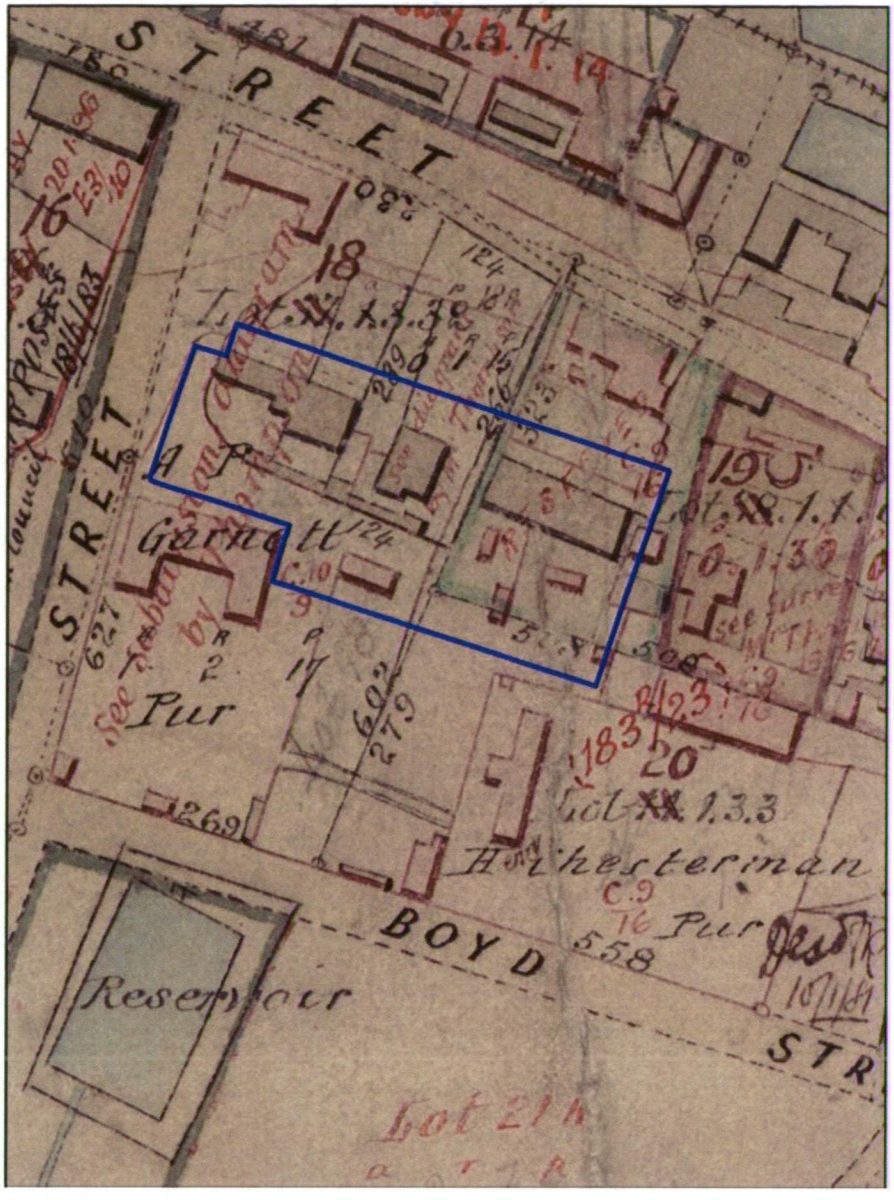

Figure 4.6: The 1877 Blackwood plan of Settlement Hill, showing fewer outbuildings behind the Assistant Surgeon's and Commissariat Officer's quarters and the consolidation of outbuildings behind the second hospital and Chaplain's quarters (courtesy of PAHSMA, ref. C/19).

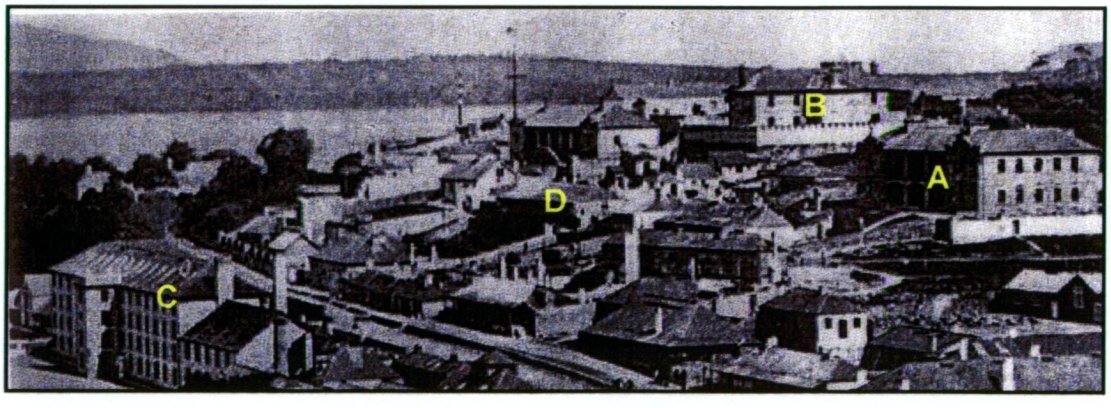

Figure 4.7: A portion of an historic photograph of Settlement Hill c1865-68, showing the third hospital on the far right (**A**), Military Barracks on the hill (**B**), and the Penitentiary to the lower left (**C**). The second hospital, by this stage civil officer accommodation, is shown at the centre right (**D**) (courtesy of PAHSMA, ref #1518).

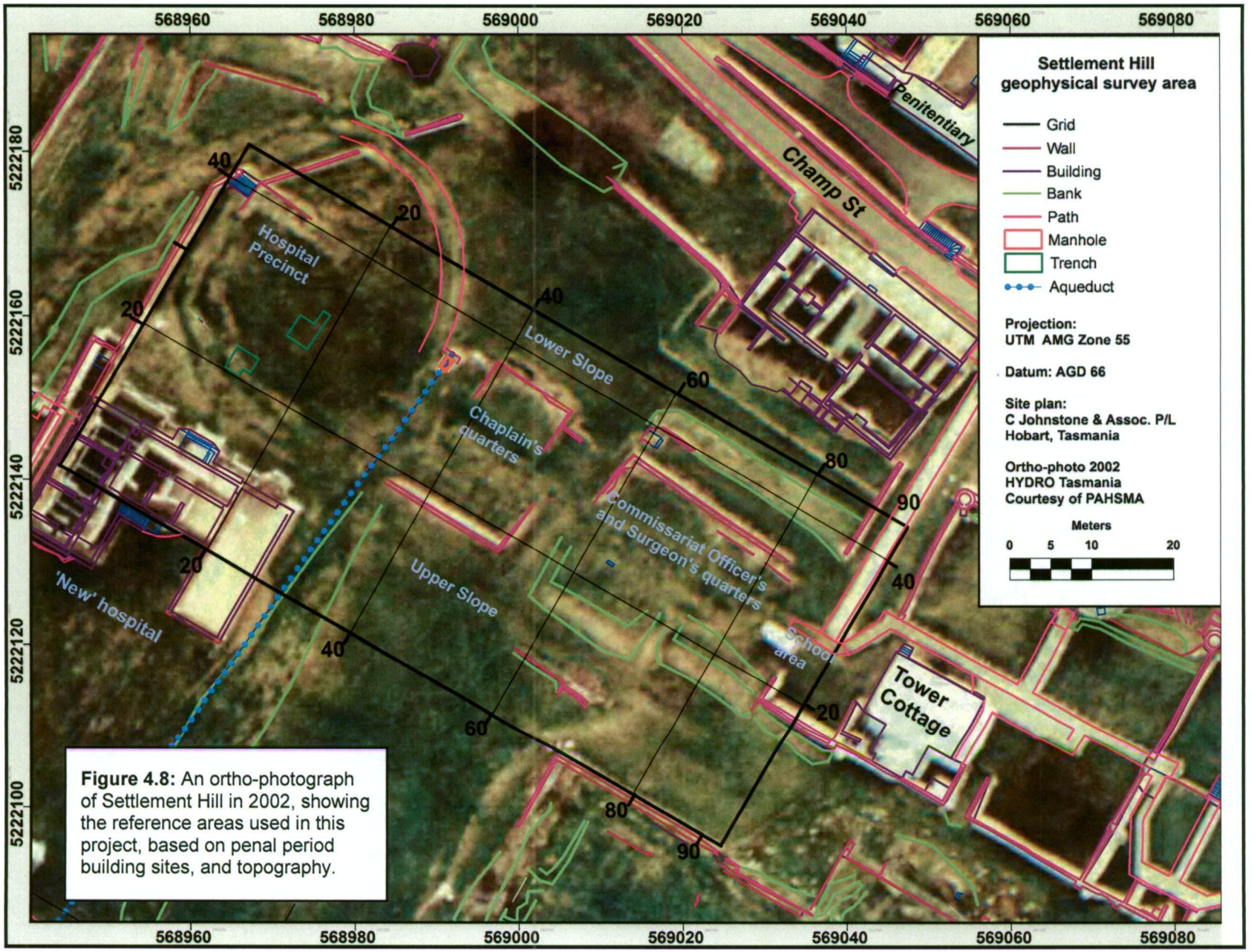

Figure 4.8: An ortho-photograph of Settlement Hill in 2002, showing the reference areas used in this project, based on penal period building sites, and topography.

4.1.3 Geophysical survey area

Settlement Hill terrain features, existing structures and other surficial cultural material were surveyed by C. Johnstone & Associates in 2002. PAHSMA staff marked out the geophysical survey grid (3570 m^2) using a Nikon total station. A local grid datum and eight additional reference points were positioned in a rectangular local coordinate system and recorded for affine transformation of the local grid into AMG coordinates. By using this approach, it was possible to relocate a historically mapped feature in the field to within a fraction of a metre. As indicated in Chapter 3, spatial references in this report will be given in local grid coordinates (x, y) to enable easy visual location of features within the maps.

The grid was oriented west to east to include five building sites on the main terrace: the Hospital Precinct (site of the first and second hospitals), the Chaplain's quarters, Commissariat Officer's and Assistant Surgeon's quarters, and the Free School adjacent to Tower Cottage (Figure 4.8). Up the hill (to the south), the grid incorporated the 'Upper Slope' bounded by the Military Barracks retaining wall, while to the north the 'Lower Slope' encompassed the former front yard of the Officers' quarters and hospital terrace. These two names were devised for the purposes of this report and the building zones were designated according to the Laing plans.

Obstructions to the geophysical surveys included terrace retaining walls, near-surface rubble, two sets of sandstone steps and the aqueduct pit hatch.

4.1.4 Archaeo-geophysical targets

Geophysical targets of the Settlement Hill investigation included subsurface elements associated with the first and second hospitals, and other buildings along the main terrace. Of primary interest were structural features within the hospital precinct, the focus area for the subsequence 2004-05 archaeological excavations. Also of interest was the hydro-engineering infrastructure associated with the flourmill; which included the channel-and-fill aqueduct and underground siphon. Remnants of numerous outbuildings located on the upper terrace, and landscaping features on the lower slopes were minor targets of interest.

The range of anticipated structural features was derived from historic plans, elevation drawings and photographs (Section 4.1.2), surface evidence and results from previous excavations within the Port Arthur Historic Site. It included the following:

- building foundations (trenches, footings, walls),
- yard walls,
- hearths and privies (toilets),
- internal and external occupational surfaces (floors, courtyards, yards),
- services (aqueduct, drains, pipes),
- landscape modifications (evidence of cut and fill).

Building layouts and the distribution of other elements within the survey area were inferred from historic maps, photographs and surface evidence. The Laing documents provided valuable information on the internal configuration of rooms, structural footings and hearths in buildings standing by 1836. Parch marks visible during dry periods and in aerial photographs (Figures 4.1 and 4.11) indicated the position of structural features within the near surface (< 0.2 m). The schematic section shown in Figure 4.9 presents the primary components of an ideal Settlement Hill stratigraphic context across the main terrace. These include the 'archaeological layer' (occupational deposits), resident soil profiles, and terrace construction features.

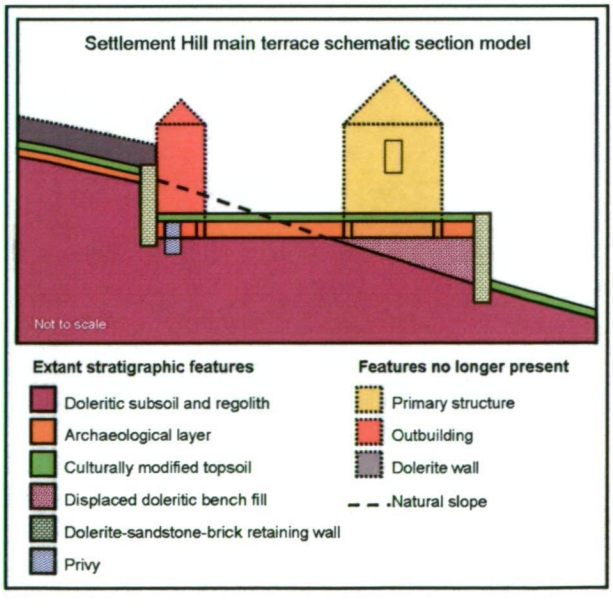

Figure 4.9: A model schematic section of the Settlement Hill main terrace, showing the basic stratigraphic units and features no longer present.

Information on the material characteristics of the archaeo-geophysical targets was gathered from historic sources and surface evidence. Drawings by Henry Laing, for example, showed that the second hospital's primary building was erected on three main foundation walls, formed by a single row of regular coursed sandstone, standing over four courses in height. Foundations of other principal structures along the terrace were constructed of various litho-types, including dolerite float (Chaplain's quarters), Point Puer mudstone (Commissariat and Assistant Surgeon's quarters) and sandstone for various extensions (pers. comm. Greg Jackman, 2007). External wall footings were likely comprised of sandstone, dolerite and/or brick, similar to remaining retaining walls (Figure 4.10). Most of the buildings along the main terrace were probably timber framed with brick nogging (pers. comm. Greg Jackman, 2007). The Hurst plan (c1846) showed three 'Stone Walls' running perpendicular to Champ Street, which indicated the use of sandstone and/or dolerite.

Courtyard surfaces were probably compacted earth or paved with sandstone flagging, similar to those visible in other areas of the Port Arthur site and uncovered during excavations. Convict period drains at Port Arthur are typically made from bricks or sandstone. The aqueduct is constructed of convict-made brick, ending at a sandstone headwall beneath the pit (Sinclair Knight Merz, 2004). Two iron pipes keyed into the headwall are presumed to continue toward Champ Street, in line with the aqueduct, as shown on the 1846 Hurst plan.

Figure 4.10: The third hospital ruins, retaining walls and steps. This photo was taken during a very dry summer (courtesy of James Cook University, 2003).

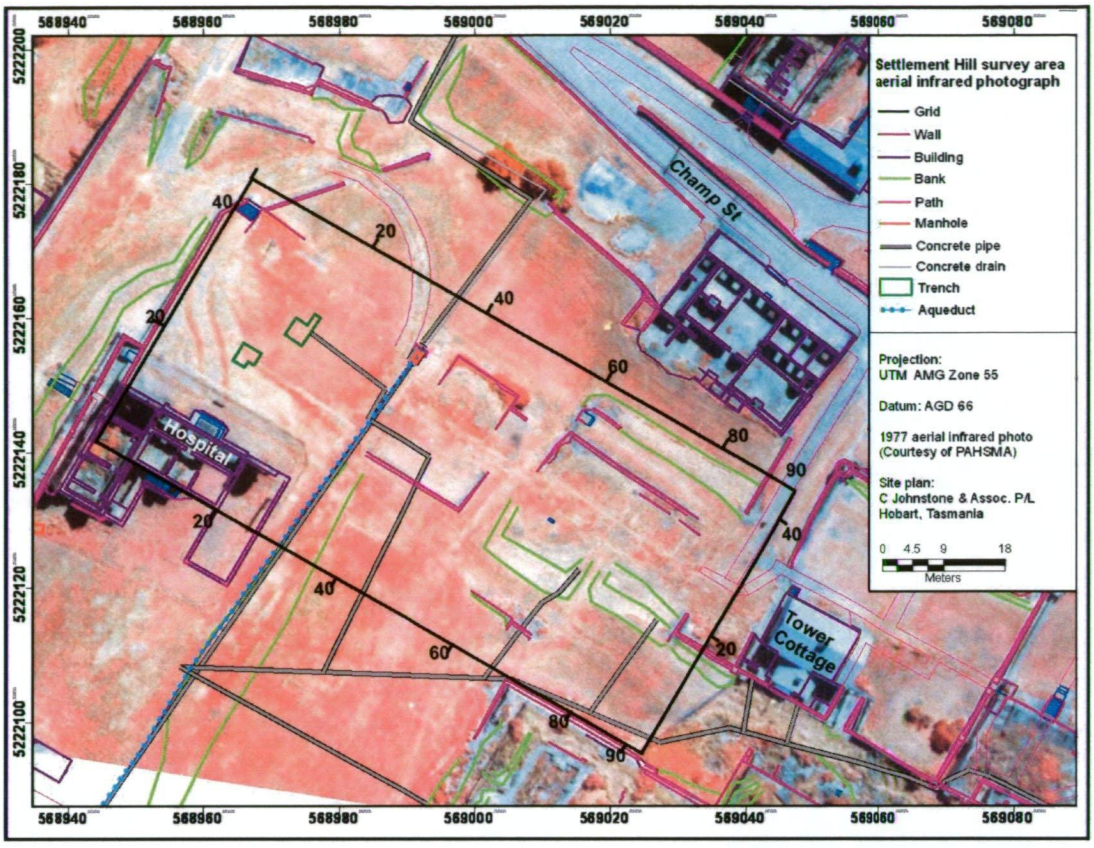

Figure 4.11: Infrared air photo of Settlement Hill 1977 overlain by the site plan, services and the aqueduct (courtesy of PAHSMA).

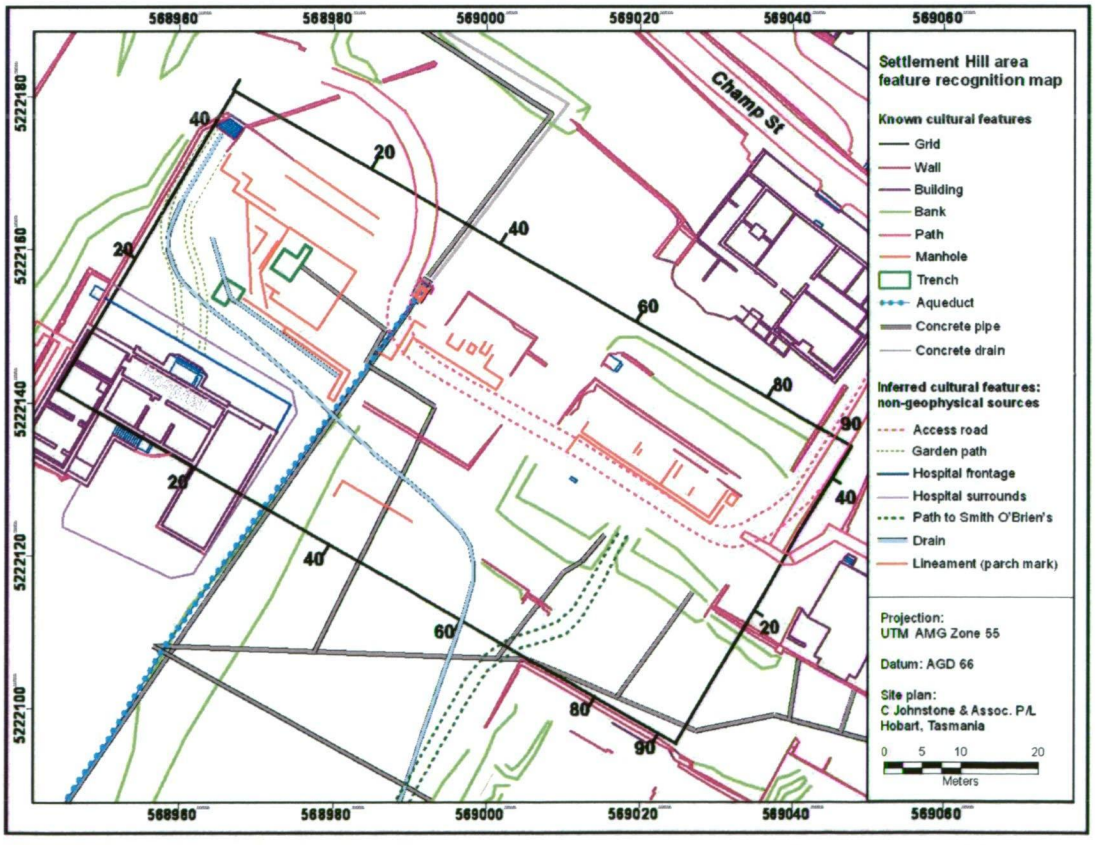

Figure 4.12: Known cultural features and those inferred by the author from photographic sources such as the 1977 infra-red aerial photograph.

4.1.5 Potential sources of undesirable signal in the data

This section identifies cultural and geological features, other than the targets, that may be potential sources of undesirable signal in the geophysical data. Forms of interference ('noise') originating from the instrument or survey methodology will be addressed separately in Section 4.2. The overburden of modified topsoil is estimated to be no thicker than 0.3 m on the terrace area, based on results from excavations at other sites at Port Arthur (Greg Jackman, pers. comm.), and is usually relatively structure-less compared with occupation layers. Nonetheless, all the parameters that characterised this overburden (inhomogeneity, water content, temperature, thickness, etc.) are likely to affect resistivity and EM measurements (Scollar *et al.*, 1990). This issue has been demonstrated many times in surveys of ploughed fields, which have produced striated geophysical variation maps (Clark, 1997).

Post-penal demolition rubble fill of heterogeneous composition and structure, located above and within the occupational layer, will probably contribute significant undesirable signal. Rubble fill associated with the original bench construction and collapsed retaining walls are another widespread potential source of interference for all surveys. Further, foundations may be obscured by rubble dating from time of construction (Bevan, 2006). The aqueduct trapdoor's iron hinges (Figure 4.13) and contemporary information signs are point sources of EM and magnetic influence. A visual survey of the site revealed no surface metal objects, however metallic debris, including fencing wire, architectural fastenings etc. are common containments of topsoils across the Historic Site. Topographic variation in the weathered dolerite substrate is likely to significantly affect the magnetic survey, be of interest to the GPR, and least relevant to the resistivity and EM. Contemporary pipes and a drain (Figure 4.12) are potentially features of geophysical interference for the EM and GPR. The accuracy of the Site services plan, however, is questionable (Greg Jackman, pers. comm. 2005).

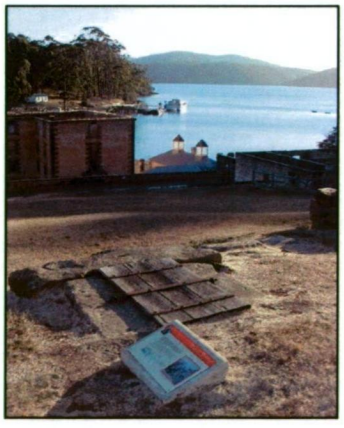

Figure 4.13: Aboveground access to the aqueduct, with sandstone blocking and metal-hinged trapdoor between the Hospital Precinct and Chaplain's quarters (courtesy of David Roe, 2003).

4.2 ARCHAEO-GEOPHYSICAL TECHNIQUES: METHODOLOGY, FINDINGS AND INTERPRETATION

4.2.1 Introduction

Four geophysical techniques were employed to study the archaeological landscape of Settlement Hill: frequency domain electromagnetic induction (FEM), magnetometry, ground-penetrating radar and electrical resistivity. The majority of fieldwork was carried out in May 2004, with the assistance of final year geophysics students from the University of Tasmania. Ground conditions were moist in the morning and dry during the day, and ionospheric magnetic conditions were stable.

Survey data for each technique were qualitatively assessed independent of other geophysical results and prior to archaeological excavation. No numerical interpretation has been conducted on these data. Recognition and interpretation maps were created according to the criteria established in Chapter 3. Responses in which the anomalous values are confined to only one or two survey lines are termed 'isolated'. Broad classification of isolated anomalies in the magnetic and EM data is based on polarity - 'negative', 'positive' or 'dipolar'- and further subdivided according to amplitude. An isolated anomalous response is represented schematically by a symbol such as a circle – located over the interpreted source centre. Linear trends in all datasets are inferred when anomalous responses extend over more than two survey profiles. They are represented schematically by a line along the source centre.

Geophysical anomalies in the data are attributed to either known, inferred or unknown sources, according to the correlation between anomaly position and characteristics and existing site information such as maps, photographs, surface evidence.

4.2.2 Apparent conductivity

Introduction

Electromagnetic induction surveys were conducted to map the apparent conductivity variation across Settlement Hill. The following sections detail the data collection methodology and post-acquisition processing. Survey results will be presented and interpreted in Section 4.2.2.3.

4.2.2.1 Data acquisition and processing

Data was acquired over two days using a Geonics EM-38, as the optimum penetration depths and narrow inductive footprint of the system were deemed suitable for resolving narrow structural features in the shallow subsurface. A 0.5 m sample spacing and 1.0 m line interval was expected to produce good resolution of features oriented north-south and adequate detection of targets parallel to the survey lines.

Due to the time and cost constraints on the survey, the EM-38 was only used in the Hospital Precinct - the focus area for 2004 – 05 archaeological excavations. Data collection methodology was the same as that used on the Isle of the Dead, as detailed in Chapter 3, Section 3.2.2.1. Fundamental data collection parameters are tabulated in Table 4.1. The EM-38 data underwent the same manual processing procedure as the Isle of the Dead data, to remove the stripes attributed to instrumental drift and to compensate for block edge effects. These factors were less obvious in the Settlement Hill data, for three reasons: firstly, calibration was conducted every 30 minutes instead of 45 minutes. Secondly, there was a greater dynamic range of readings, which meant that absolute error accounted for a smaller proportion of the total measurement. In addition, the smaller survey area only necessitated one block shift, compared to several in the Isle of the Dead data.

Survey type	Low frequency electromagnetic induction		
Instrumentation	Geonics EM-38 dual dipole		
Area surveyed	~ 800 m^2		
Method of coverage	Parallel traverses in longitudinal direction		
Orientation	Vertical (VCP) and horizontal co-planar (HCP)		
Station interval	0.5 m	**Operating frequency**	14.6 kHz
Output units	MilliSiemens/metre (mS/m)	**Traverse interval**	1.0 m
Phase	Quadrature	**TX-RX separation**	1.0 m
Comments	Profiling conducted with ≤ 1.0 m offset from parallel measuring tape. Calibration at 30 min intervals to minimize equipment drift. Removal of metallic objects on surveyor and surface metallic debris on site prior to survey. Digital meter accurate to whole number only. Measurement recording delay time 2 seconds. The dipole was positioned parallel to traverse direction.		

Table 4.1: Tabulated apparent conductivity data collection parameters for Settlement Hill.

4.2.2.2 Findings and interpretation

This section will firstly discuss the broad area variation in apparent conductivity across the Hospital Precinct, then isolated and linear anomalous responses relevant to the investigation objectives. Raw apparent conductivity background values ranged from -975 mS/m to 210 mS/m and -414 mS/m to 494 mS/m for VCP and HCP modes respectively, and varied considerably across the Settlement Hill survey area. Both datasets were clipped at - 40 mS/m and 40 mS/m to allow direct visual comparison of apparent conductivity variation (Figures 4.14 and 4.15). Artificial sun illumination was applied to emphasise low amplitude anomalies from background.

Anomalous zones in apparent conductivity

The HCP mode variation map (Figure 4.14) is characterised by several broad anomalous zones. Moderate average apparent conductivity values recorded from 14y to 18y (**A**) correspond to contemporary loam deposits which slope up to the hospital ruins. Penal period features within this area potentially included gardens and a path to the third hospital (Figure 4.13), although there is no obvious evidence for these.

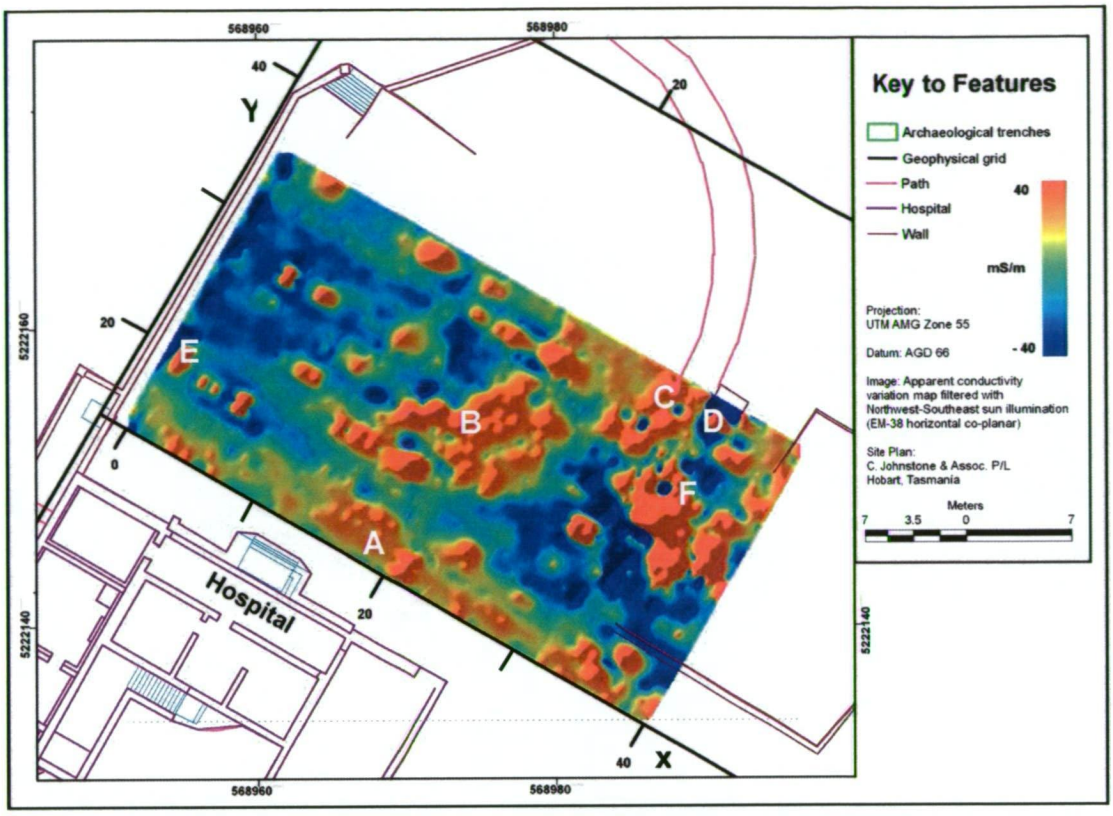

Figure 4.14: Hospital Precinct EM-38 HCP mode apparent conductivity variation map. Annotations are described in the text.

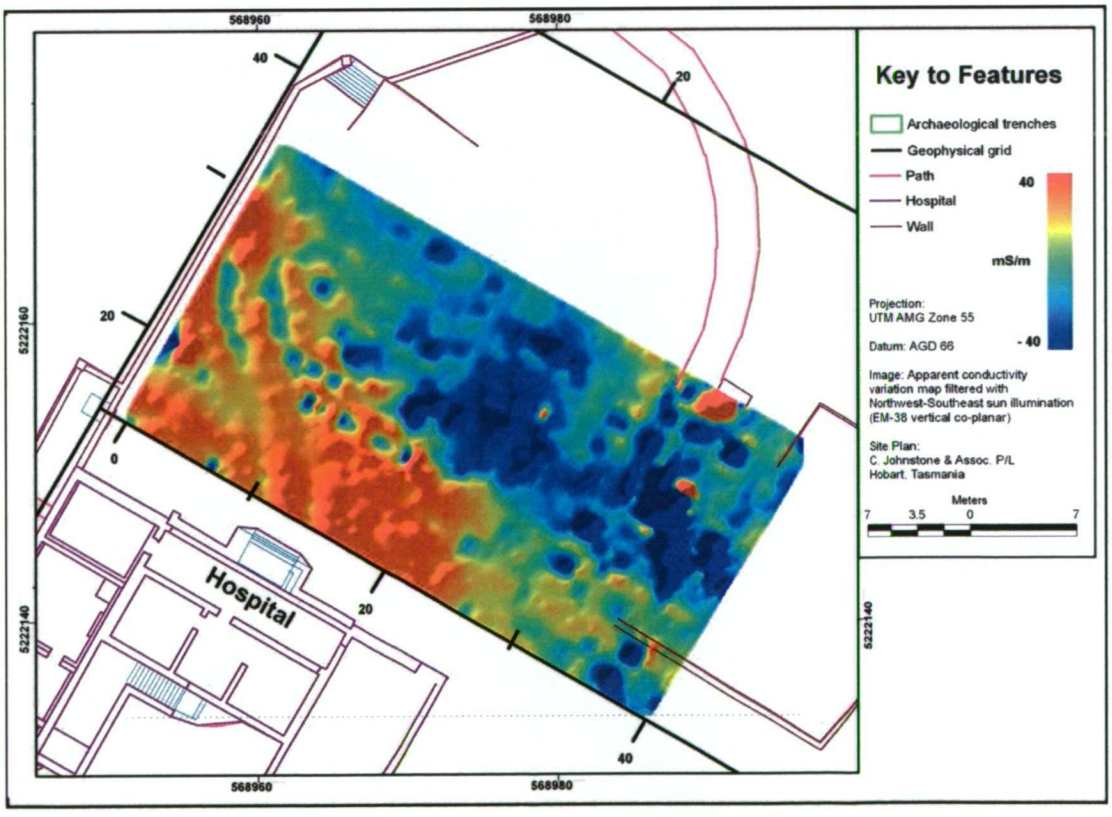

Figure 4.15: Hospital Precinct EM-38 VCP mode apparent conductivity variation map.

Further into the grid centre, the EM-38 map is dominated by a zone of closely spaced high amplitude anomalies (**B**), which are attributed to unconsolidated material of heterogeneous composition within the topsoil and occupational layer. According to aerial photographs and historic maps, this zone corresponds to a penal period yard area between the second hospital and its outbuildings. Very high amplitudes responses recorded near the access road at (**C**) are also probably due to more porous unconsolidated material within a clay-loam matrix, such as collapsed structural remnants from the second hospital's eastern end. A spatially coincident magnetic high indicates the presence of ferrous metal, possibly associated with the privy and hearth depicted in the Laing building plan (Figure 4.2).

Unlike the HCP data, the VCP mode apparent conductivity variation map is visibly divided into two well-defined zones, dominated by positive and negative values respectively (Figure 4.15). This division closely matches lineaments seen in aerial photographs, and the rectilinear boundary between the second hospital site and the yard/ third hospital site, as shown on historic maps. The broad area variation in VCP data is therefore likely to be culturally derived. Negative conductivities correlate with compacted yard surfaces and pathways, structural remnants and demolition rubble associated with the second hospital and Chaplain's quarters outbuildings, external walls and courtyard (Figure 4.12). Contrasting moderate to high values surrounding the third hospital indicates a lack of building remnants and demolition rubble within the occupational layer - confirming the historical documentary evidence which shows that no buildings were erected in this area.

Anomalies attributed to discrete and linear sources

Discrete responses visible in both the HCP and VCP datasets indicate the presence of causative features to a depth of ~ 0.75 m. Several of these isolated anomalies are derived from known sources identified from surface evidence and the laser survey by SKM. The metal-hinged aqueduct pit door (Figure 4.14, **D**) and tourist information sign (**E**), for example, cause significant dipolar anomalies in both datasets. Most causative features, however, are inferred from secondary sources such as aerial photography, historic maps and other geophysical data. Large very high amplitude dipolar anomalies are recorded in a local depression between the Hospital Precinct and Chaplain's quarters (Figure 4.14,

F). Out-of-range responses near the anomaly centres indicate that the source(s) are highly conductive and very shallow – an instrumental reaction explained previously in Chapter 3, Section 3.2.2.3. The services plan shows an intersection of concrete pipes in this region, offering one explanation for the geophysical anomaly. Corresponding very high amplitude dipolar responses in the magnetic data indicate the presence of shallow ferrous material, possibly objects associated with the pipes, such as a cover plate.

Qualitative interpretation maps in Figures 4.16 and 4.17 show the location of known and inferred point sources - classified according to amplitude and polarity. Spatially coincident conductivity and magnetic anomalies are attributed to ferrous metal features, and the remaining high amplitude responses are inferred as non-ferrous metal sources or conductive materials such as charcoal deposits.

Several linear trends are visible in Figures 4.16 and 4.17. High amplitude readings between gridlines 0x – 2x are attributed to a large brick retaining wall adjacent to the survey boundary (Figure 4.16). Rectilinear trends in the second hospital area correlate to the building elements depicted in historic plans, particularly in the VCP data which better resolves near-surface features. Lineaments between gridlines 23y and 35y are interpreted as either external or internal walls of the second hospital, or as associated structural elements (Figure 4.17). Oblique trending anomalies at 20x, 30y are due to unknown causes, while others recorded within the inferred courtyard are attributed to drains.

The third hospital yard area is dominated by two curved lineaments, detected by the VCP mode survey, which are visible in contemporary aerial photographs (Figure 4.11).. Based on this visual evidence and the anomaly configuration, the sources are interpreted as garden beds, characterised by relatively low conductivity material, bordering a path that formerly linked the sandstone steps to the third hospital's northern entrance. Spatially coincident linear discontinuities in the shallow apparent resistivity and ground penetrating radar datasets support this explanation.

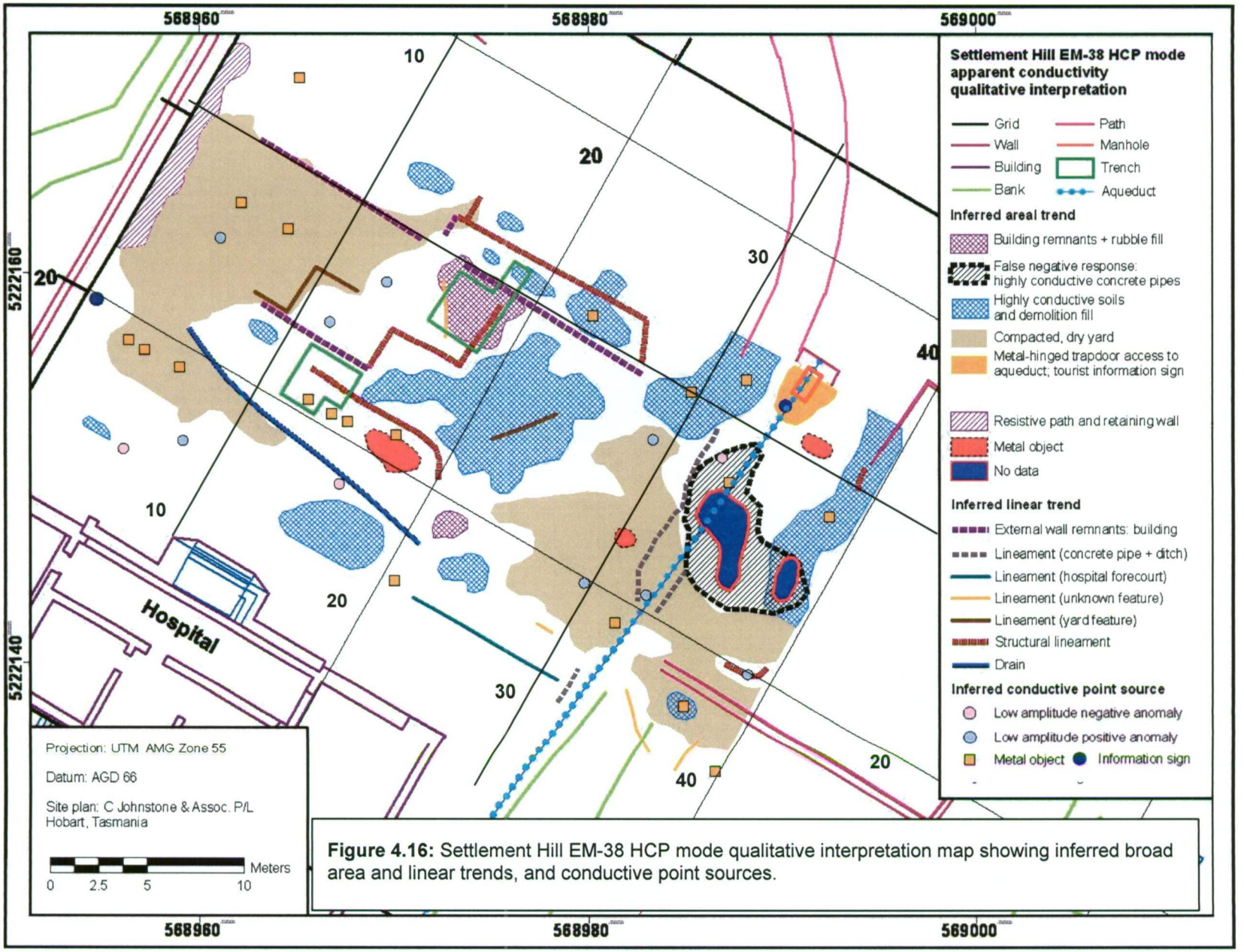

Figure 4.16: Settlement Hill EM-38 HCP mode qualitative interpretation map showing inferred broad area and linear trends, and conductive point sources.

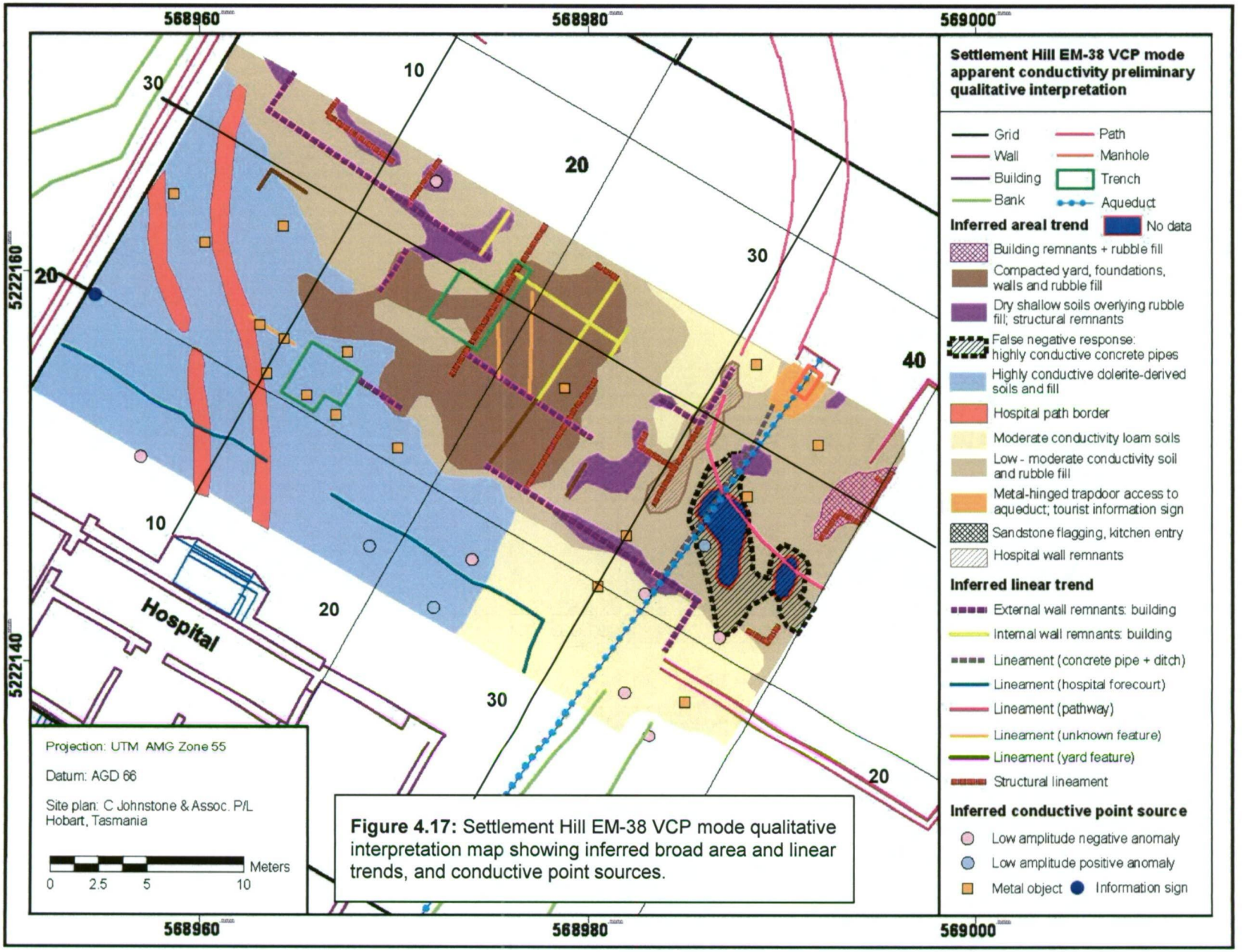

Figure 4.17: Settlement Hill EM-38 VCP mode qualitative interpretation map showing inferred broad area and linear trends, and conductive point sources.

4.2.3 Magnetometry

Introduction

A magnetic survey was conducted to identify materials of a ferrous nature and map variation in magnetic field intensity across Settlement Hill. The following section details the data collection methodology and post-acquisition processing. Survey results and qualitative interpretation are discussed in Section 4.2.3.2.

4.2.3.1 Data acquisition and processing

The magnetic survey was conducted over two days in May 2004, during quiet geomagnetic conditions. The magnetometer sensor was positioned on a wooden trolley that kept it constantly 0.15 m above the ground, to maximise detection of shallow small features. Total magnetic field data was also collected for diurnal correction, using a Geometrics G-856 proton precession magnetometer located further up Settlement Hill. Data acquisition parameters are tabulated in Table 4.2.

Survey type	Magnetic		
Instrumentation	GEM Systems GSM-19F Overhauser magnetometer		
Area surveyed	~ 4500 m^2		
Method of coverage	Continuous surveying along grid long axis		
Traverse interval	1.0 m	**Distance trigger**	Hip chain
Station interval	0.2 m	**Output units**	Nanotesla (nT)
Sensitivity	0.1 nT	**Sensor height**	0.15 m (sensor centre)
Comments	Profiling was conducted with ≤ 1.0 m offset from parallel measuring tape. Removal of metallic objects on surveyor and surface metallic debris on site prior to survey. Sensor was secured to a trolley. Base station: Geometrics G-856 proton precession magnetometer Reading interval: 30 seconds.		

Table 4.2: Tabulated apparent conductivity data collection parameters for Settlement Hill.

The raw magnetic data (Figure 4.18) required several stages of processing to remove or reduce the effects of undesirable signal and noise, and optimise visualisation for the detection and identification of archaeological features. Diurnal corrections were achieved using a modified version of the QuickBasic program used on the Isle of the Dead. Random dropouts and single point spikes in the data were visually identified in

each profile and removed or attenuated by a spline interpolation between two acceptable measurements on either side of the perceived error. The Settlement Hill data exhibited pronounced parallax positional errors of 0.5 – 3 m (Figure 4.18). This was primarily caused by the 'hip chain' distance trigger method, which consistently failed to produce profiles of the same length, particularly over irregular terrain where the data collection was discontinuous in sections. It was also amplified by the bi-directional survey mode. The editing method chosen to correct the displacement error was the same as that applied to the Isle of the Dead data (refer to Section 3.2.3.2, Chapter 3). Minor examples of residual herringbone effect remained in the data post-processing, although these artefacts did not unduly influence the interpretation.

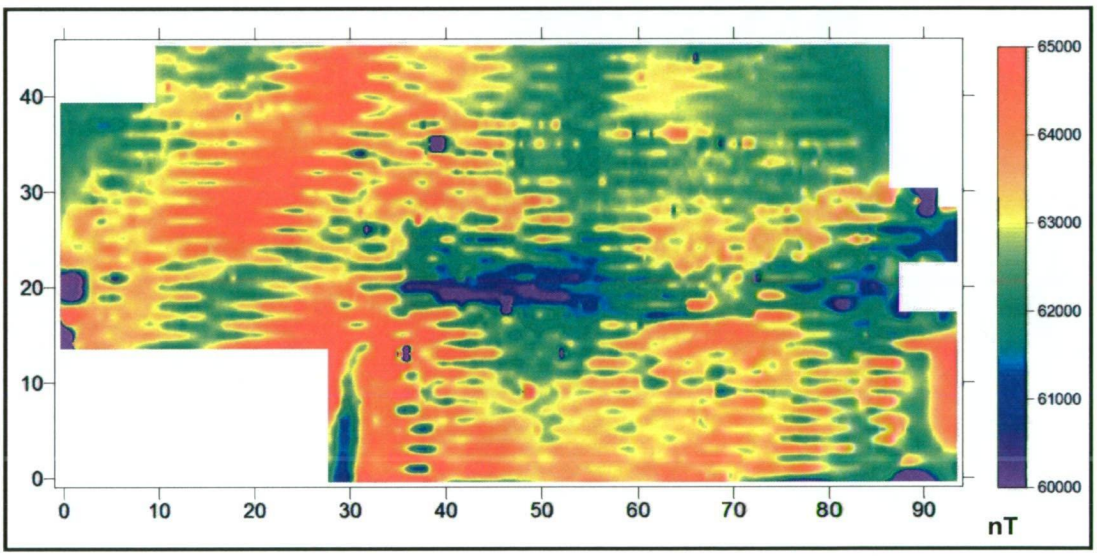

Figure 4.18: Settlement Hill total magnetic intensity variation map after diurnal correction, but prior to processing to correct for the pronounced parallax error.

4.2.3.2 Findings and interpretation

Background magnetic values across the Settlement Hill survey area average approximately 62000 nT, and the dataset has a large dynamic range: from less than 59000 nT to over 65000 nT. Figure 4.19 shows the processed TMI variation map in the context of Settlement Hill, with the data range clipped at 61500 nT and 63000 nT to emphasise sharp gradient boundaries. Figure 4.20 is presented as a comparative variation map, with clipping at 59000 nT and 65000 nT, to better delineate low amplitude anomalies. A qualitative interpretation map of the Settlement Hill magnetic data is illustrated in Figure 4.21.

Anomalous zones in magnetic intensity

Broad areal trends are attributed to a combination of cultural modification of, and natural variation in, the weathered dolerite topography of Settlement Hill. Natural variation in the dolerite surface was indicated by irregular and gradual changes in the TMI that did not conform to assumed culturally derived patterns. Broad positive TMI anomalies across the Hospital Precinct and upper slopes are interpreted as zones of near-surface, comparatively unweathered dolerite.

Large-scale cultural modification of the site topography, comprising the removal and redeposition of doleritic material, measurably influences the magnetic survey. This is particularly evident in a series of rectilinear anomaly distribution patterns along the main terrace between 18y and 30y (Figure 4.19), which suggest that they are derived from cultural, rather than natural sources. Distinctive high gradients, collinear with the Chaplain's quarters rear brick retaining wall (Figure 4.19, **A**) and similar features presently buried in the Assistant Surgeon's and Commissariat Officer's quarters embankments (**B** and **C**), suggest truncation of the magnetic dolerite substrate along the y-axis. Consistently low magnitude (< 60000 nT) anomalous zones north of these boundaries (**D** - **E**) may indicate where the substrate was deeply excavated during terrace construction, and filled with non-magnetic material. Such excavation may have been to accommodate foundations for the outbuildings, and privy trenches shown on historic maps, although this interpretation does not explain the geophysical low between the Chaplain's quarters and Commissariat Officer's quarters (Figure 4.19, **F**).

In the northeastern corner of the hospital precinct, the TMI data delineates another small rectangular zone of low magnetic intensity values (~ 62000 nT) bounded by steep gradients (Figure 4.19, **G**). This zone has similar characteristics to the region near the rear of the Chaplain's quarters (**D**), which suggests that the dolerite substrate may also have been previously removed from this area. This evidence therefore implies that the bench may originally have ended parallel to 8x and 33y, forming a 'corner' (**H**) supported by retaining walls similar to others visible on Settlement Hill. The second hospital building would therefore have been located between 8x and the aqueduct trench (**I**) – rather than in the position shown in historic maps. These retaining walls

were probably reconfigured when the sandstone steps were built in association with the third hospital, as discussed in Section 4.1.2.

Along the main terrace long axis (centred on 34y), east of the Hospital Precinct, high average intensity zones (> 62500 nT) are attributed to relatively undisturbed shallow dolerite substrate (Figure 4.19, **J - L**). Towards the terrace front, lower TMI probably reflects an increase in heterogeneous rubble overburden used to construct the benches. Other steep gradients, measured parallel to 11y (**M**) and 40x (**N**), correspond to minor retaining walls and benches on the upper slopes. There also appears to be evidence for excavation of the dolerite on the lower slopes, illustrated by moderately steep gradients parallel to 50x and 60x demarking the Assistant Surgeon and Commissariat Officer's quarters terrace front embankment.

Isolated responses and linear trends in magnetic intensity

In addition to deeper TMI perturbations, the magnetic image is characterised by zones of irregular, high frequency positive and dipolar anomalies from dolerite in the near-surface occupational layer, bench fill and demolition rubble. The regions of rubble are primarily located in the Hospital Precinct and along the terrace middle to front between 25y to 35y (e.g. Figure 4.20, **A**). There is a clear contrast between this 'noisy' tract and the zone of simpler stratigraphy of the upper and lower slopes. This contrast is particularly clear either side of the retaining walls in front of Chaplain's and Commissariat Officer's quarters (Figure 4.20, **B - C**).

The majority of high frequency dipolar responses visible in the Hospital Precinct are coincident with high amplitude isolated anomalies detected by the EM-38 and are therefore attributed to the magnetisation of shallow (< 0.75 m) iron-bearing metallic sources. As anticipated, several prominent anomalies are caused by tourist information signs (Figure 4.20, **D - E**) and metallic fixings on the aqueduct pit hatch (**F**). A high amplitude response at (**G**) corresponds with a strong dipolar and negative anomalies in the EM-38 HCP and VCP datasets respectively (Figures 4.14 and 4.15), the source of which was previously suggested to be very shallow metal object(s) associated with a contemporary concrete pipe network. Low amplitude responses in the magnetic

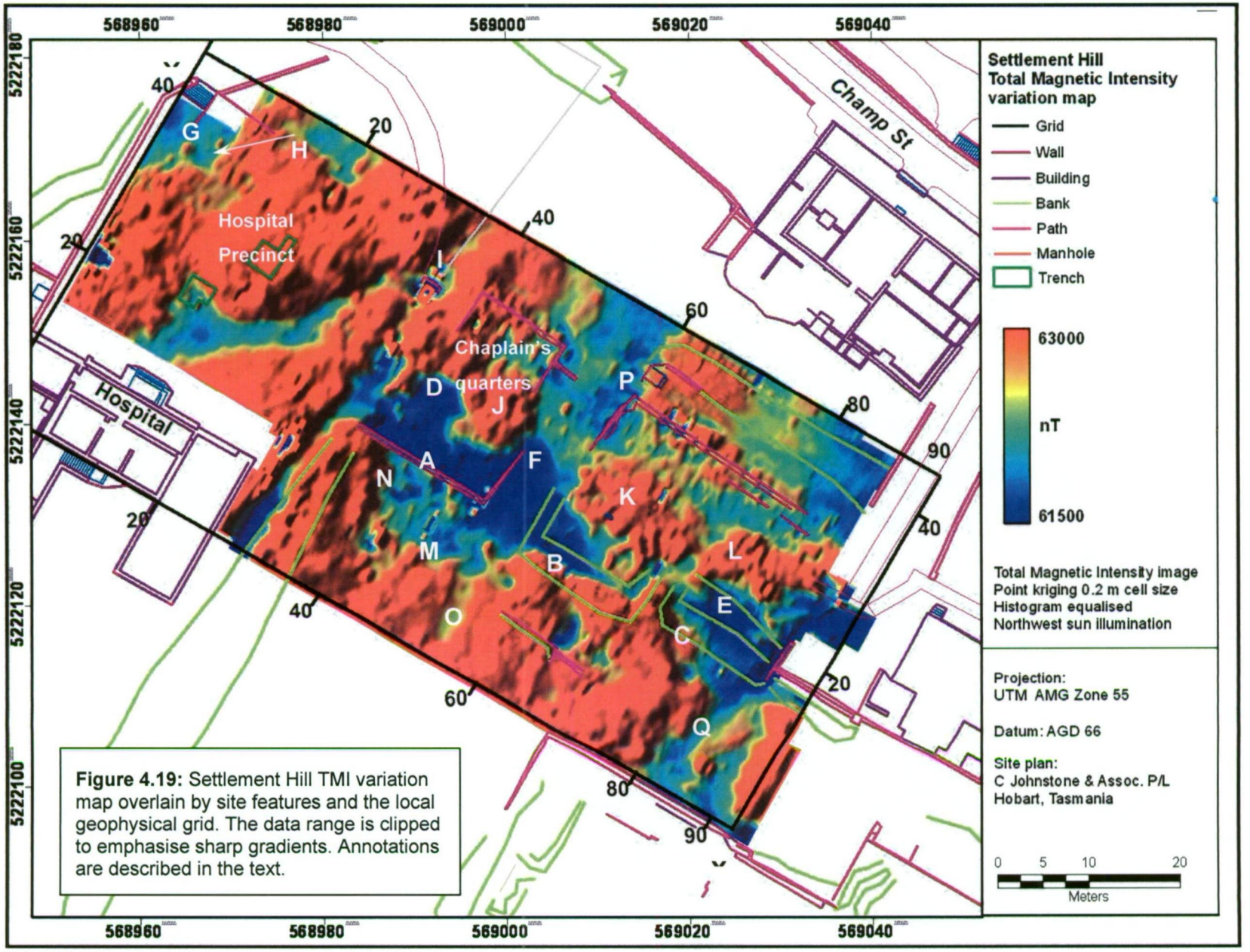

Figure 4.19: Settlement Hill TMI variation map overlain by site features and the local geophysical grid. The data range is clipped to emphasise sharp gradients. Annotations are described in the text.

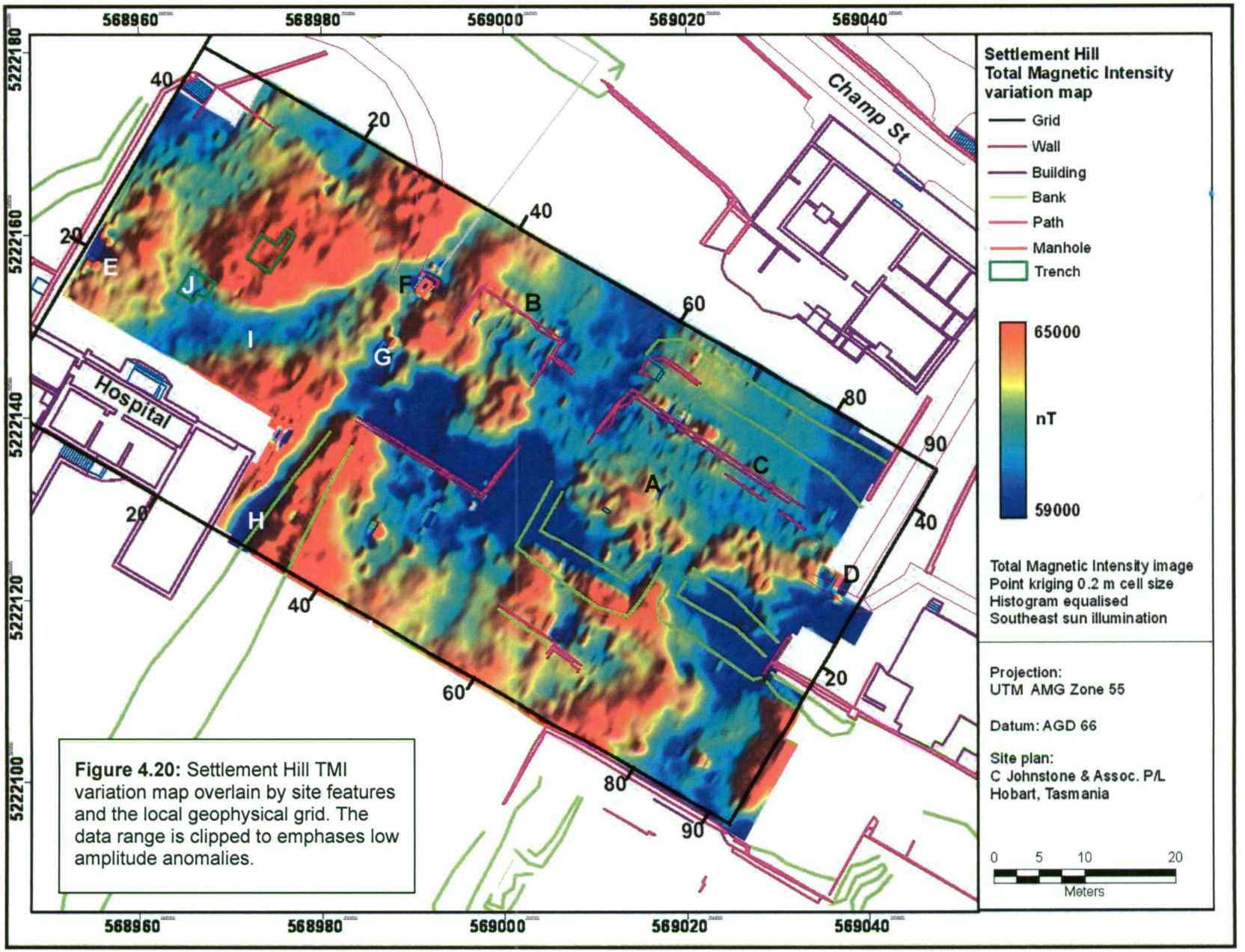

Figure 4.20: Settlement Hill TMI variation map overlain by site features and the local geophysical grid. The data range is clipped to emphases low amplitude anomalies.

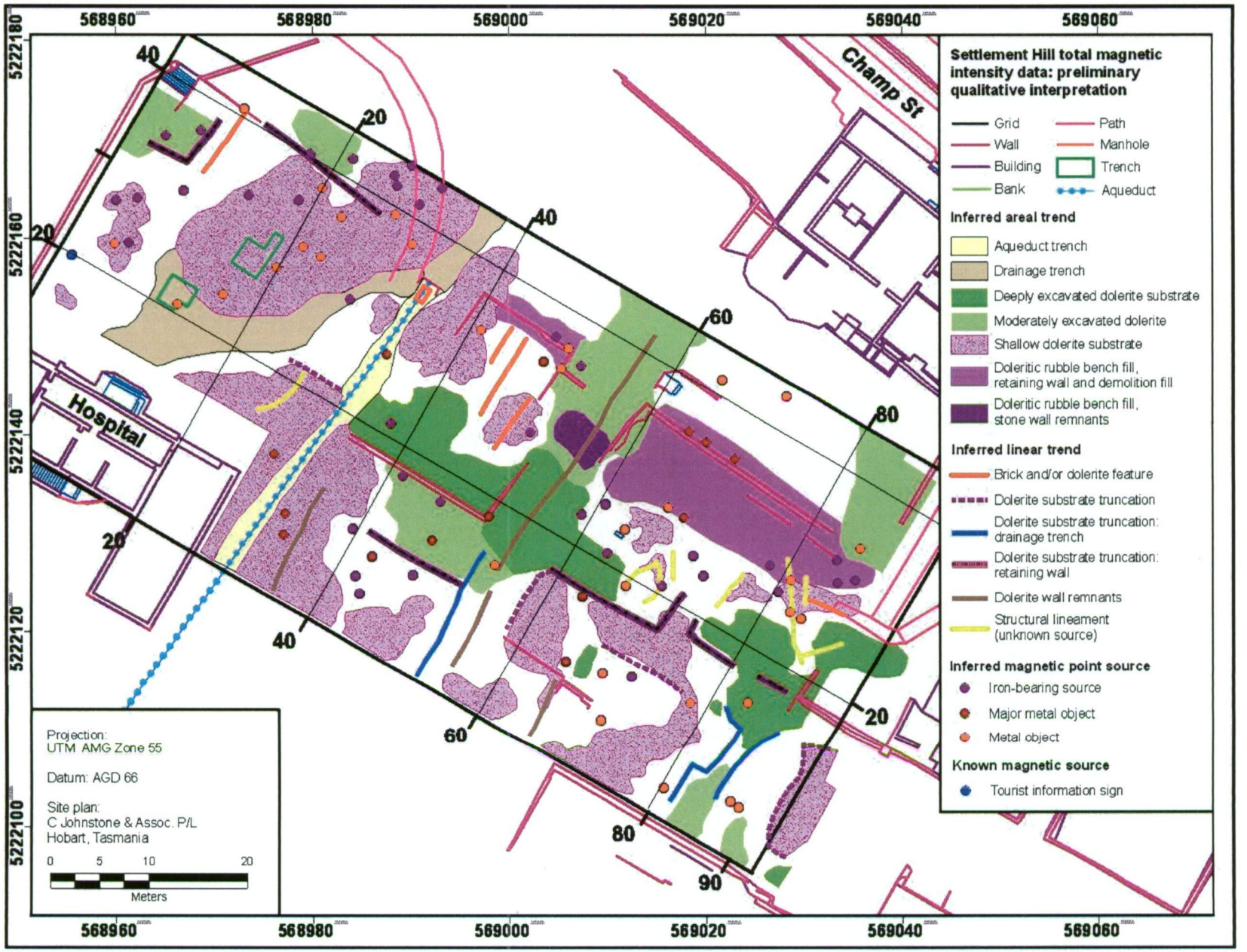

Figure 4.21: Settlement Hill TMI qualitative interpretation map showing inferred magnetic sources, site features and the geophysical grid.

image that correlate closely with anomalies in the apparent conductivity data are interpreted as minor buried ferrous metal objects within the topsoil or occupational layer. Other low amplitude magnetic responses within the shared survey area are attributed to brick or dolerite structural remnants or rubble.

Three major low TMI lineaments (< 60000 nT) are identified within, and adjacent to, the Hospital Precinct. The primary linear trend (Figure 4.20, **H**) extends from 30x, 0y to 37x, 45y and intersects the aqueduct pit located at (**F**). It is defined by a central low flanked by sharp field gradients 1 to 2 m apart, which suggest truncation of the dolerite substrate. These factors, combined with the close alignment with the aqueduct (as mapped by Hurst c1846 and surveyed in 2004 by SKM), indicates that the magnetic survey detected the deep trench constructed associated with the brick feature and iron pipes. A second, less well-defined and broader linear response (magnitude ~ 62000 nT) trends obliquely from the third hospital entrance to the aqueduct pit (Figure 4.20, **I**). This feature is characterised by a sharp gradient on the northern side comparable to that measured down slope of the access hatch. Both the anomaly signature and location suggest that the causative feature is another trench cut into the dolerite substrate, although probably not as deep as the aqueduct trench. Further, a north-south trending weakly defined moderate amplitude zone (**J**) adjoining the lineament at 15x, 20y is inferred as a third trench even shallower than the other two. Although there is no historic evidence for the second or third features, all three are interpreted as sections of a drainage system associated with the third hospital and aqueduct.

Elsewhere in the Settlement Hill survey area, there are several other magnetic lineaments of comparable magnitude and breadth to the secondary 'trenches' of the inferred hospital infrastructure. Two linear trending negative anomalies on the upper slope (Figure 4.19, **O**) and lower slope (**P**), closely correlate to the inferred position of a penal period external 'Stone Wall' dividing the Chaplain's and Commissariat Officer's quarters (Hurst plan Figure 4.4). Based on this correlation, and a lack of other documented structural features on the lower slope, it is feasible to attribute these anomalies to two sections of a relatively shallow drainage trench running alongside the wall (Figure 4.21). Southeast of the survey area, a narrow low amplitude zone perpendicular to the Military Barracks retaining wall (Figure 4.19, **Q**), runs parallel to

the inferred location of a wall c1877, is also interpreted as a drainage trench. Remnants of the trench and wall may lie under the present loam-rubble embankment.

Brick walls and hearths were difficult to define in the magnetic data, due to a combination of factors: a lack of contrast between the bricks and surrounding material, broad area responses from the dolerite basement, and displacement error in the survey procedure. In addition, the uneven terrain introduced positional errors during data collection that were difficult to remove completely by processing. As previously anticipated in Section 4.1.5 and described above, interference from demolition rubble within the occupational layer, and underlying material related to the bench construction, effectively masks responses from shallow, narrow targets. This interference is most obvious in the Hospital Precinct and between 30y and 40y along the main terrace.

4.2.4 Apparent resistivity profiling

Introduction

An electrical resistivity survey was undertaken to detect near-surface resistive targets on Settlement Hill, including brick and masonry features, demolition rubble and the compacted fill of trenches. Walls, in particular, constitute bodies that pose a significant barrier to the passage of current. The contrast with detrital material that results from their destruction or which led to their burial can be high (Scollar *et al.*, 1990). Compacted occupational layer(s), sandstone flagging or closely spaced linear/discrete sources would likely be recorded as a broad zone of elevated resistivity (Appel *et al.*, 1997). In general, metal objects would not be detected, although a large feature may produce a very low resistivity anomaly (Bevan, 1991).

4.2.4.1 Data acquisition and processing

The Wenner α electrode configuration was deemed a suitable array for the delineation of features such as walls, foundations and trenches/ditches (Clark, 1997; Bevan, 1991). Multiplex resistivity studies conducted over a buried Roman villa complex in Wroxeter, UK, demonstrated that a Wenner array with a 0.5 m '*a*' value emphasised the near

surface, cellular nature of the buildings and internal partitions (Walker, 2000). Griffiths and Turnbull (1985) showed that the sensitivity plot for the Wenner array has almost horizontal contours beneath the centre of the array. This makes it relatively more sensitive to vertical changes than to horizontal changes in subsurface resistivity than other arrays. The Wenner array was also convenient to use at the Port Arthur Historic Site, compared to other arrays such as the pole-pole or twin-pole configurations. While the latter require only two electrodes moved during the survey, these are connected via long cables to the other, widely spaced (e.g. 100 m), fixed electrodes. These wires would have potentially caused problems due to tourist foot traffic at the site.

For this investigation, the Wenner array was mounted onto a timber frame (Ehrenhard *et al.*, 1984) to abolish a potential source of error (parasitic anomaly) caused by incorrectly placed electrodes (Scollar *et al.*, 1990). The 0.33 m electrode spacing gives a corresponding ideal depth of investigation of between ~ 0.12 m (Roy and Apparao, 1971) and 0.165 m (Edwards, 1977), although the measurement will readily detect features both shallower and deeper than this optimum depth (Bevan, 1991).

The array was oriented parallel to the x-axis and the electrodes inserted no more than several centimetres into the ground, usually deep enough to reach moist soil. If rock, brick or concrete prevented insertion at the correct point, then the measurement was taken a short distance perpendicular to the line of the four electrodes (Bevan, 1998). Readings were typically collected at 1.0 m intervals along-line, except where the difference between adjacent readings exceeded 15 Ω. In this case, intermediate data was collected at the 0.5 m interval, to provide better resolution of features along-line. Other data acquisition parameters are shown in Table 4.3.

Statistical outliers (spikes) were not removed as they were often caused by coupling problems due to the near-surface hard layers and may have contained valuable information. Apparent resistivity values (Ω.m) were calculated by multiplying the resistance measurements provided by the Terrameter by the geometric factor $2\pi a$. Resistivity data were gridded to produce a map of values across the site (Figure 4.22). These values were then clipped at 15 Ω.m and 360 Ω.m, and the data filtered with artificial sun illumination, to highlight directional trends and low-contrast anomalies. High pass filtering (3 x 3 cells) was also conducted to enhance the visibility of subtle

features or more fully display the detail of internal structure within high resistivity anomalous zones.

Survey type	DC resistivity		
Instrumentation	12V Atlas-Copco ABEM Terrameter		
Area surveyed	~ 2250 m^2		
Method of coverage	Parallel traverses along longitudinal gridlines		
Traverse interval	1.0 m	**Array type**	Wenner α
Station interval	1.0 m*	**'a' spacing**	0.33 m
Cycle time	1.0 sec	**Output units**	Ohm (Ω) (resistance)
Electrodes	10 mm stainless steel probes were mounted on a wooden frame		
Comment	Profiling conducted with ≤ 1.0 m offset from measuring tape		

Table 4.3: Tabulated apparent resistivity data collection parameters for Settlement Hill.

4.2.4.2 Findings and interpretation

The Settlement Hill grid is marked by a wide range of apparent resistivity values (15 Ω.m to 729 Ω.m), which is clipped at 15 Ω.m and 360 Ω.m to enhance low amplitude anomalies and distribution patterns. The Hospital Precinct is characterised by broad areas of high average apparent resistivities intersected by small low apparent resistivity zones and linear trends. All other sections of the main terrace are typified by relatively narrow rectilinear positive features. True local background values are very difficult to estimate, as so much of the survey area had been levelled with demolition rubble or culturally modified through bench construction. On the 'quietest' sections of the Upper Slopes and Chaplain's quarters frontage, local background values average 20 - 50 Ω.m. These are typical for conductive loam-clay topsoils (Bevan, 1998).

The Hospital Precinct

The Hospital Precinct is dominated by broad areas of high average apparent resistivities (> 250 Ω.m) marked by numerous very high frequency peaks and linear trends (Figure 4.22). The most prominent zone (**A**) of elevated resistivities, which extends diagonally across the precinct, correlates closely with a very low conductivity area in the EM-38 VCP dataset, and is attributed to collapsed and in site structural features and demolition

rubble. The region corresponds closely to the second hospital's western end and courtyard/outbuilding area, as inferred from historic maps and aerial photograph parch marks.

Elevated apparent resistivity values (460 Ω.m) measured along 8x and 35y (**B**), coincident with a sharp linear gradient in the magnetic data, are interpreted as external walls of the second hospital. Low – moderate apparent resistivity values measured in this area are interpreted as regions with little or no demolition rubble fill.

Numerous low amplitude lineaments (< 150 Ω.m), in high contrast to the surrounding resistivity values, are mapped in the Hospital Precinct. The most prominent response zone (**C**), oriented oblique to the geophysical grid, is interpreted as a trench filled with more conductive material. This is most likely associated with the second hospital courtyard wall depicted in historic plans (Figures 4.4 and 4.6). Other low amplitude lineaments appear to crosscut the high resistivity zone, including a serpentine response (**D**) that originates at the sandstone steps (at 2x, 40y) and runs in front of the third hospital ruins. Aerial photographs from the 1960s show a coincident surface feature, presently grass covered, extending to the Upper Slopes towards Smith O'Brien's cottage (Figure 4.23). This feature likely post-dates the demolition and resurfacing of Settlement Hill and is identified as either a contemporary trench or narrow pathway. Several other non-linear areas of low apparent resistivity near the grid datum and the access road (**E**) are credited to increased topsoil conductivity within local depressions.

Minor point anomalies of moderate to high amplitude are most likely gridding artefacts originating from spurious readings, as the samples were not close enough together to discriminate discrete sources of undesirable signal, such as brick rubble, or masonry.

Chaplain's quarters, Assistant Surgeon's and Commissariat Officer's quarters

Remaining building zones along the main terrace are visually distinct from and less complex than the Hospital Precinct, exhibited numerous high resistivity features against a low value background. The rectilinear configuration of many of these features strongly suggests an assembly of buildings. Most lineaments are interpreted as external and internal building walls/foundations due to their close correlation with the historic plans,

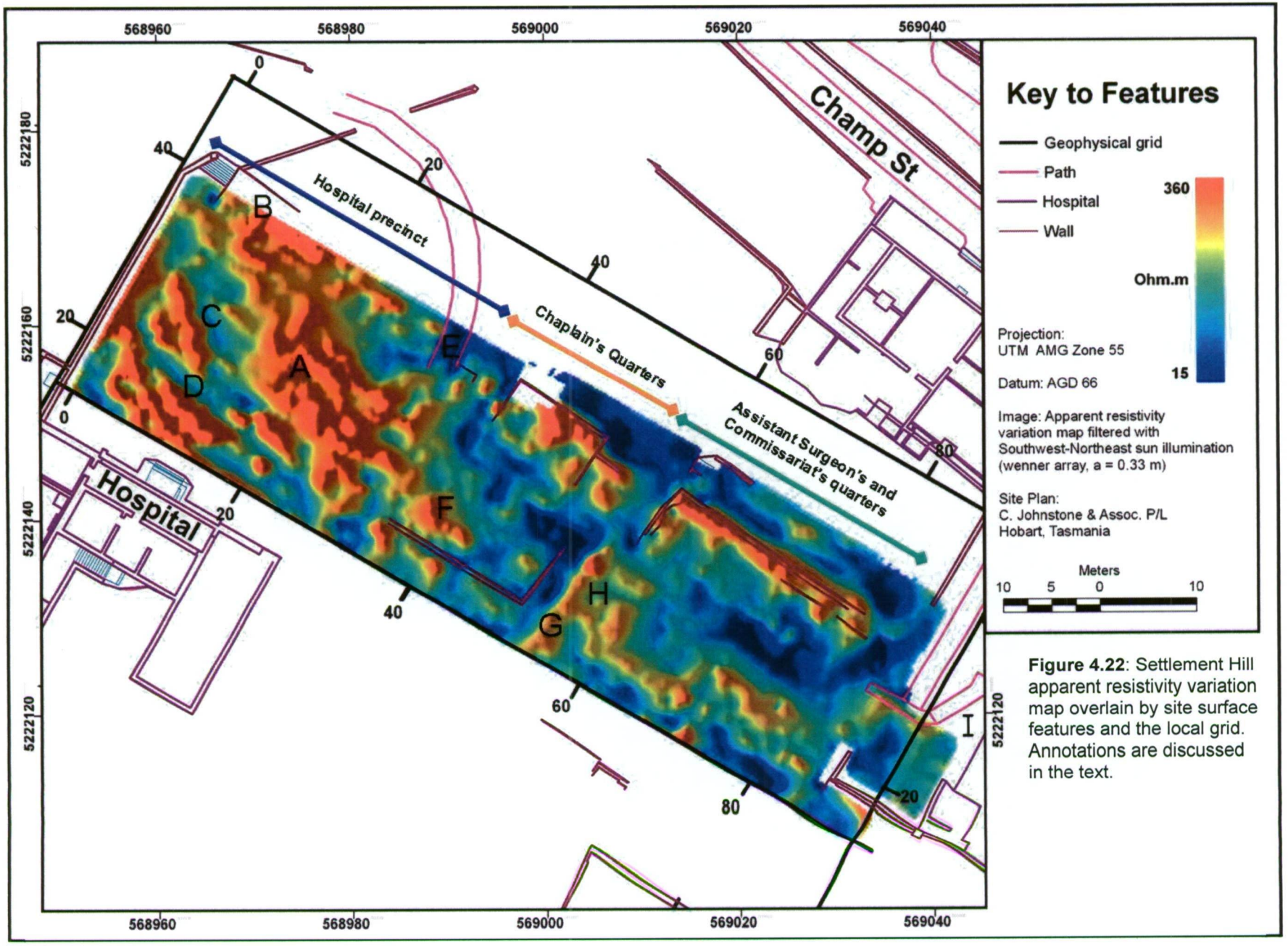

Figure 4.22: Settlement Hill apparent resistivity variation map overlain by site surface features and the local grid. Annotations are discussed in the text.

and parch marks (Figure 4.23). The inferred layout of external walls and internal divisions at the Chaplain's quarters, for example, is near-identical to that shown in the rectified Laing plan of 1836 (Figure 4.2). This relationship suggests that the original building footprint remains largely unaltered. High resistivity anomalies suggest that shallow remnants of yard walls on the south-eastern side are likely to be well preserved.

Outbuildings on the terrace are less well defined, especially behind the Assistant Surgeon's quarters where transported fill formed an overlying embankment. The locations of these features are mostly inferred from broad area anomalies, rather than linear trends. High resistivity values centred on (**F**) for example, are attributed to the Chaplain's quarters 'Knife House', 'Privy' and 'Poultry' sheds shown in the Laing plan c1836 (Figure 4.2) and Blackwood plan c1877 (Figure 4.6).

Very high values are recorded near the dolerite retaining walls on the terrace bench front, as expected (Figure 4.24). The resistivity survey appeared to locate buried retaining walls rear to the Assistant Surgeon's and Commissariat Officer's quarters, corresponding to the truncated dolerite surface apparent in the magnetic data. A penal period 'Stone Wall' (Figure 4.4), now grass covered, correlates closely to a high positive anomaly to 28y (Figure 4.22, **G**), beyond which it decreases rapidly in amplitude to end at ~ 30y. This attenuation is attributed to increasing topsoil cover, or removal of stone. A series of short lineaments that define a rectangular zone (**H**), with the stone wall forming the western side, probably reflect remnants of the privy block/larger outbuilding periphery depicted in Laing (1836) and Hurst (1846) plans respectively (Figure 4.24). The Blackwood plan (Figure 4.6) shows that this structure had been removed by 1877.

In contrast to these well defined features, there is minimal geophysical evidence of the more substantial 'Kitchen' and 'Fowl House' at the rear of the quarters, indicating either a lack of surviving features or deep overburden. Low to moderate resistivity lineaments adjacent to Tower Cottage (in the SE corner of the survey area) are inferred to mark remnants of the Free School House rear wall and outbuilding depicted in the Hurst and Blackwood plans (Figures 4.4 and 4.6 respectively).

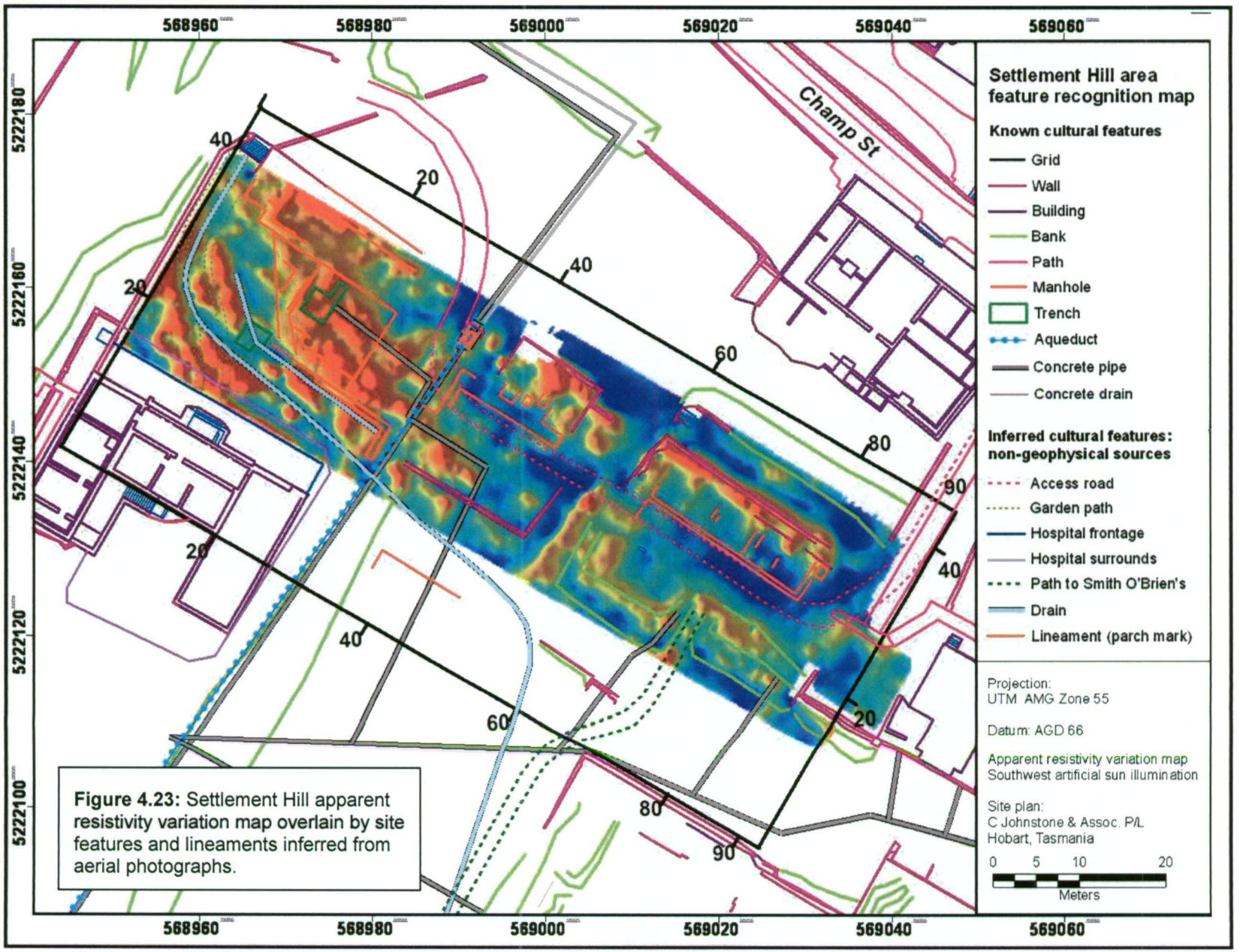

Figure 4.23: Settlement Hill apparent resistivity variation map overlain by site features and lineaments inferred from aerial photographs.

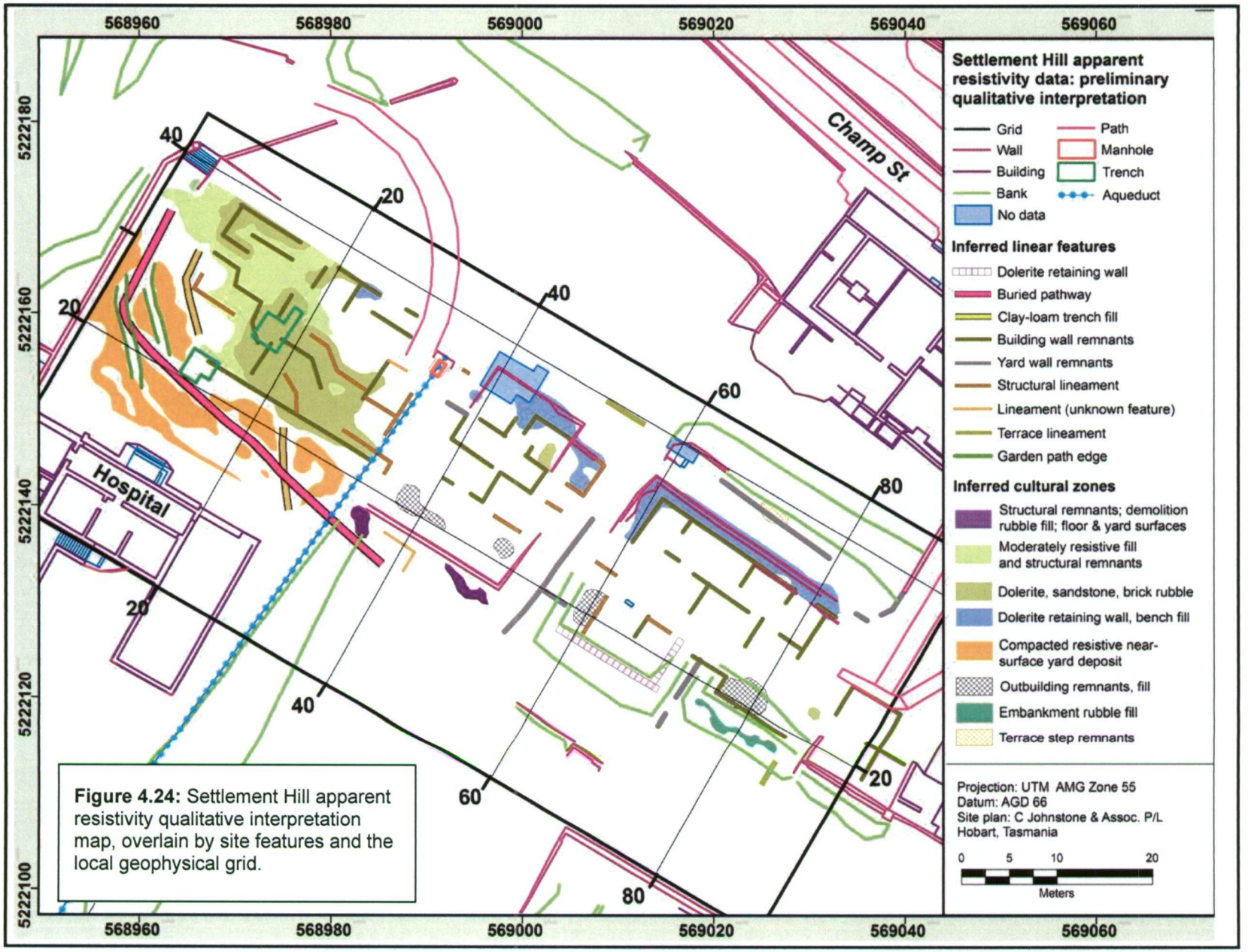

Figure 4.24: Settlement Hill apparent resistivity qualitative interpretation map, overlain by site features and the local geophysical grid.

4.2.5 Ground penetrating radar

Introduction

Ground penetrating radar profiling was conducted to detect and characterise surviving structural remnants of buildings and yard features at Settlement Hill. This technique has been used successfully to define shallow (< 1 m) masonry features such as foundations and limestone walls in other conductive environments with complex stratigraphy (Malagodi *et al.*, 1996; Appel *et al.*, 1997). Factors limiting identification of foundations are described by Bevan (2006), and include the masking effect of undesirable signal from construction rubble, and small cross-sectional target area, with an uneven top surface. Demolition rubble material within the occupational layer, dolerite bench fill and other sources of interference are expected to attenuate and complicate the radar signal and mask underlying structural anomalies. The following sections describe how processing and three-dimensional presentation were applied to compensate for these sources of undesirable signal, and enhance the data for qualitative interpretation.

4.2.5.1 Data acquisition

The two-part ground penetrating radar investigation was undertaken on Settlement Hill in May and July 2004 (Upper Slope). Pre-survey tests on site demonstrated that a 500MHz centre frequency with a 30 ns (two-way travel time) range provided ample penetration for target detection and suitable resolution. Wave penetration to noisy data was approximately 15 ns in the raw data and ~ 20 ns after application of an energy decay curve filter. Data collection was as described for the Isle of the Dead, with obstructions such as surface rubble and retaining walls, instead of vegetation. Radar traces were acquired without any kind of filtering or gain functions. Data collection parameters and equipment details are summarised in Table 4.4.

Survey type	Ground penetrating radar		
Instrumentation	Mala RAMAC X3M system with a 500 MHz shielded antenna		
Area surveyed	87 lines, within regular grid 43 x 93 m		
Method of coverage	East-West oriented lines, continuous data collection at 0.03 s intervals		
Traverse separation	0.5 m	**Stacking**	16
Trace interval	0.05 m*	**Tx - Rx separation**	0.18 m
Range	30 ns	**Samples**	192
Comments	Fiduciary marks added manually during data collection, estimated accuracy to +/- 0.1 m. Profiling conducted with ≤ 1.0 m offset from parallel measuring tape. Survey conducted at ~ 2 km/hr. * Calculated using fiduciary marks.		

Table 4.4: Tabulated survey parameters for Settlement Hill GPR data collection.

4.2.5.2 Post-acquisition data processing

Raw data collected on Settlement Hill required the following processing steps, similar to the Isle of the Dead GPR data:

- Reversal of profiles collected in the negative direction,
- Trace interpolation to correct fiduciary markers to distance,
- Ground surface reflection shifted to zero time/depth (static correction),
- Average trace subtraction (80-trace window) (Malagodi *et al.*, 1996),

  to minimise continuous horizontal reflections, and
- Application of an energy decay curve to amplify signals at depth.

Prior to data recognition mapping and interpretation, the vertical axis was also converted from two-way travel time (ns) to depth (m), using a nominal velocity of 0.09m/ns; typical for dry loamy soils (Conyers and Goodman, 1997). It was initially intended that this nominal velocity would be replaced by a more accurate site-specific value, calculated following the archaeological ground-truthing. However, excavations at the Hospital Precinct revealed a complicated near-surface stratigraphy comprising doleritic weathering products, structural remnants, demolition rubble fill of heterogeneous composition, and loamy topsoils. It therefore proved very difficult to reliably correlate excavated material interfaces to their corresponding radar reflections

(Conyers and Lucius, 1996). The relatively complex EM domain (compared to the Isle of the Dead) also meant that wave velocity would vary unpredictably across the survey area. For example, variation in the abundance of iron and iron-bearing minerals in the brick and dolerite rubble deposits would have measurably affect the velocity, with some energy loss due to ferromagnetic relaxation processes (Olhoeft, 1994). Findings were therefore referenced to two-way travel time (TWTT) in nanoseconds, although the nominal velocity was still used to provide broad depth estimates. Finally, because a realistic medium velocity could not be reliably estimated, migration or deconvolution was not applied to the radar data (Malagodi *et al.*, 1996).

Three-dimensional data imaging

Prior to three-dimensional processing, the Settlement Hill profiles were divided into five areas for practical data management. The May survey block (14 – 43y) was divided into three sections (0 – 40x, 40 - 70x and 70 – 93x), while the July block was halved (28 – 60x and 60 – 93x). File sizes were then compressed for imaging to a maximum of 512 traces in both x- and y- directions, resulting in 1 trace per 7.5 cm. Statically-corrected, unfiltered or gain-adjusted radargrams for each area were stacked horizontally to create a three-dimensional dataset, using the approach described in Chapter 3, section 3.2.6.3. Image enhancement was then performed on the whole dataset, rather than individual profiles. The volume was viewed at specific time values as two-dimensional contour maps of radar amplitudes or 'timeslices' (Malagodi et al, 1996). The amplitudes were gridded using search radii of 0.2 m and 1.2 m in the x- and y- directions respectively. Trials using several values demonstrated that these radii minimised the artificial enlargement of anomalies and provided good resolution.

4.2.5.3 Findings and interpretation

Preliminary profile assessment involves the recognition of broad visual patterns in the data, the identification of background values and anomalous response types. Timeslices derived from three-dimensional processing of these profiles provided a synoptic plan view of the surveyed area. Lateral patterning, in the form of linear trends and anomalous zones, are recorded in a data recognition map. This information is augmented with radargrams to illustrate selected features in the vertical plane. For the Hospital Precinct, a detailed recognition map and preliminary qualitative interpretation image were derived from profile-by-profile and timeslice data abstraction. Comprehensive qualitative interpretation gained by comparison with other geophysical datasets and archaeological ground-truthing is presented in Appendix B. Selected radargrams, data abstraction and qualitative interpretation maps are presented in the text.

Overview of profiles

Preliminary assessment of the radargrams indicated that sections of high amplitude and discontinuous anomalies, indicative of ground disturbance (Conyers and Goodman, 1997), correlated well with cultural modification of the Settlement Hill survey area. Unfiltered radargrams from Lines 20y, 25y, 30y, and 43.5y between 40x and 70x (Figure 4.25) illustrate the differences between former building sites and surrounding yard spaces. Line 43.5y, on the relatively undeveloped Lower Slope, is characterised by a sparse distribution of moderate-high amplitude discontinuous anomalous responses within a shallow depth range (8 ns). In the Chaplain's quarters front yard (**A**), these responses and the single interface immediately below the surface multiples likely signifies uncomplicated stratigraphy and thin occupational layer. Few isolated anomalies and lack of a clear subsurface interface in front of the Assistant Surgeon's and Commissariat Officer's quarters (**B**) confirmed that this area remained undeveloped, with the exception of a garden and later a paddock (Laing plan 1836, Figure 4.2; Blackwood plan 1877, Figure 4.6).

There is significant visual contrast between the radargram for Line 43.5y and those collected from the terrace bench. Lines 30y, 25y and 20y each contain a mosaic of predominantly high amplitude anomalous signals to ~ 20 ns depth, where the radar has detected interfaces between materials of contrasting dielectric permittivity, such as sandstone blocks and loam soils. These features include well defined hyperbolic forms (C), multiple adjacent non-hyperbolic diffractions (D) and continuous horizontal layers of reflections (E). Examination of radargrams collected from 0 – 93x suggests that remnants of primary structures and outbuildings are present the full length of the main terrace.

There is, however, no obvious correlation between the response distribution patterns and different building zones, probably due to buried yard elements such as external walls, drains and surfaces. Had the topography not been modified into building 'platforms' with retaining walls, and without the availability of historic maps, it would have been very difficult to determine the divisional layout within the main terrace from the radar only. Profiles collected from the Upper Slope exhibit a less complex stratigraphy than that of the main terrace.

Three-dimensional data presentation: timeslicing

Following initial analysis of profiles and characterisation of different response patterns across Settlement Hill, data recognition mapping was performed using three-dimensional amplitude maps. This technique has been found to be suitable at urban sites, when significant heterogeneity of the environment makes correlation of vertical profiles quite difficult (Godio *et al.*,2000; Conyers, 2006a). Interpretation of GPR data volumes is also much quicker and easier than individual profile assessment. Timeslicing presents non-subjective planimetric views of the survey area and is therefore a practical and convenient format for comparison with other geophysical images, site plans and photographs in ArcGIS®. This method of data visualisation has been routinely applied in archaeo-geophysical investigations for buried structural elements since the mid to late-1990s (Malagodi *et al.*, 1996; Goodman and Nishimura, 1995).

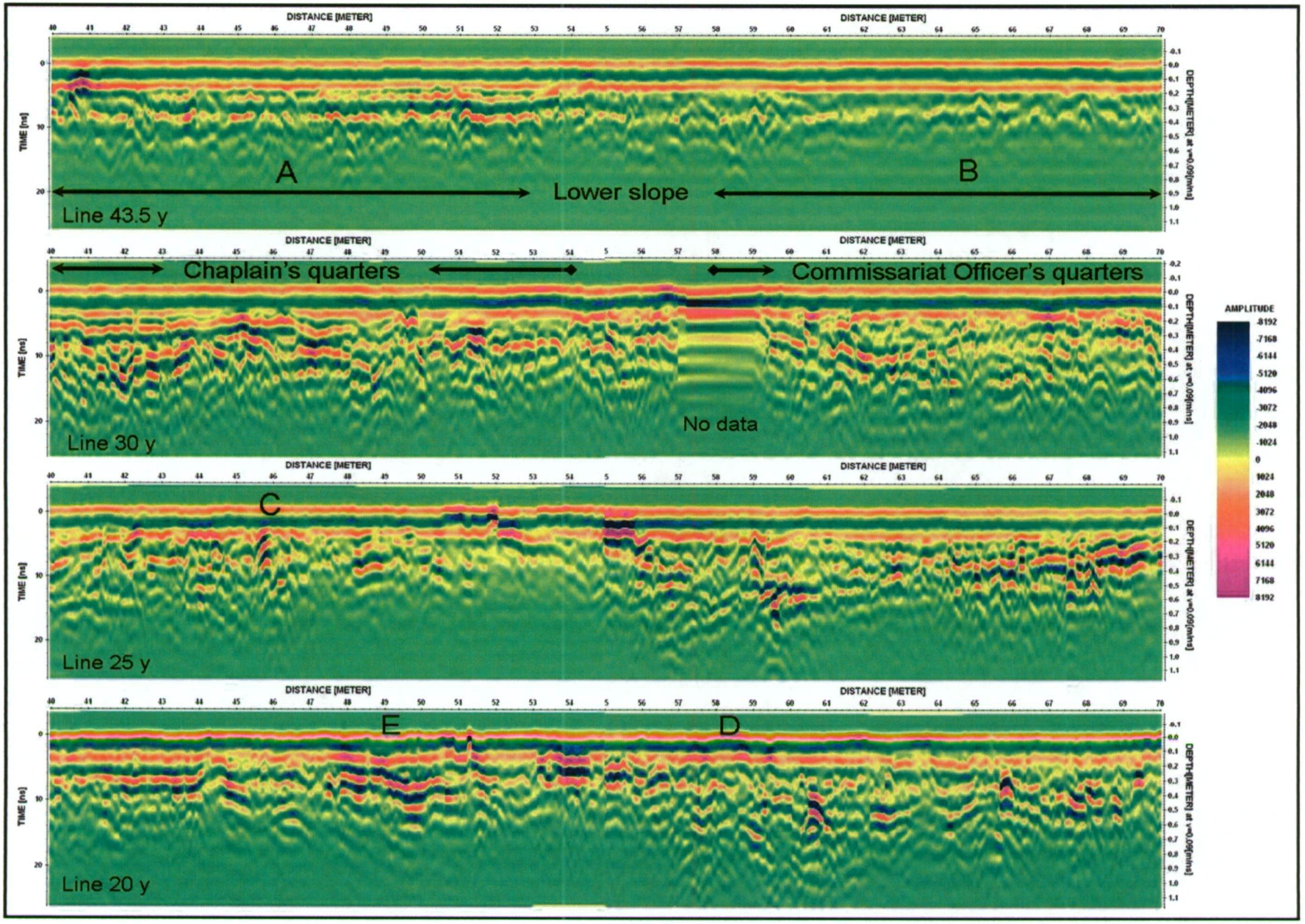

Figure 4.25: 500 MHz profiles (with energy decay curve) collected from the Chaplain's and Commissariat Officer's quarters. Annotations are discussed in the text.

Timeslices through the GPR data volume were analysed in increments of 0.4 ns, starting from the surface bands. Response patterns are clearly defined within the top 4 ns, where the timeslices include the high amplitude primary phase shift associated with initial detection of a material contrast. Three images from the Hospital Precinct (**A - C** in Figure 4.26) show good examples of these patterns. From 4 to 7 ns, the patterns in the timeslice are less well defined due to multiples of shallower responses and interference from overlapping diffractions. By 9 ns, the data exhibits a low signal-to-noise ratio and low amplitudes due to wave attenuation with depth, illustrated by a timeslice taken from the Hospital Precinct (Figure 4.26, image **D**). This correlates to an approximate depth of 0.6 m, assuming the nominal wave velocity of 0.09 m/ns.

Lineaments and anomalous zones are inferred from single time interval amplitude maps of each grid, conjoined to cover the Settlement Hill survey area. Two clear examples of these maps are provided in Figures 4.27 and 4.28, generated at 1.7 ns and 4.2 ns respectively. A cumulative map of inferred trends is presented in Figure 4.29, overlain on an infra-red aerial photograph of the site in 1977. Three distinctive response distribution patterns in the timeslice maps and data recognition map, which correspond to the Hospital Precinct, Lower and Upper Slopes, and remaining main terrace area.

The Hospital Precinct centre is dominated by a large (~ 180 m^2) rectilinear high amplitude zone (Figure 4.26, **X**) coincident with the supposed former courtyard of the second hospital, as shown in historic maps. The periphery of this zone also correlates closely to parch marks visible in the infra-red aerial photograph (Figure 4.29). Several oblique lineaments of unknown source are also evident in the timeslices. Two anomalies curving from the third hospital centre front to the sandstone steps are interpreted as geophysical evidence of garden beds bordering a path. These responses are well defined in Figure 4.26 (Image **C**). An inferred post-penal trench, with fill of contrasting material properties to the soil matrix, appears to crosscut these features and extend past the third hospital ruins to the Upper Slope (Figure 4.26, Image **A**; Figure 4.28, **A**). These interpretations are supported by evidence derived from the EM-38 VCP (Figure 4.17) and apparent resistivity surveys (Figure 4.24), and contemporary aerial photographs (Figure 4.1 and 4.29).

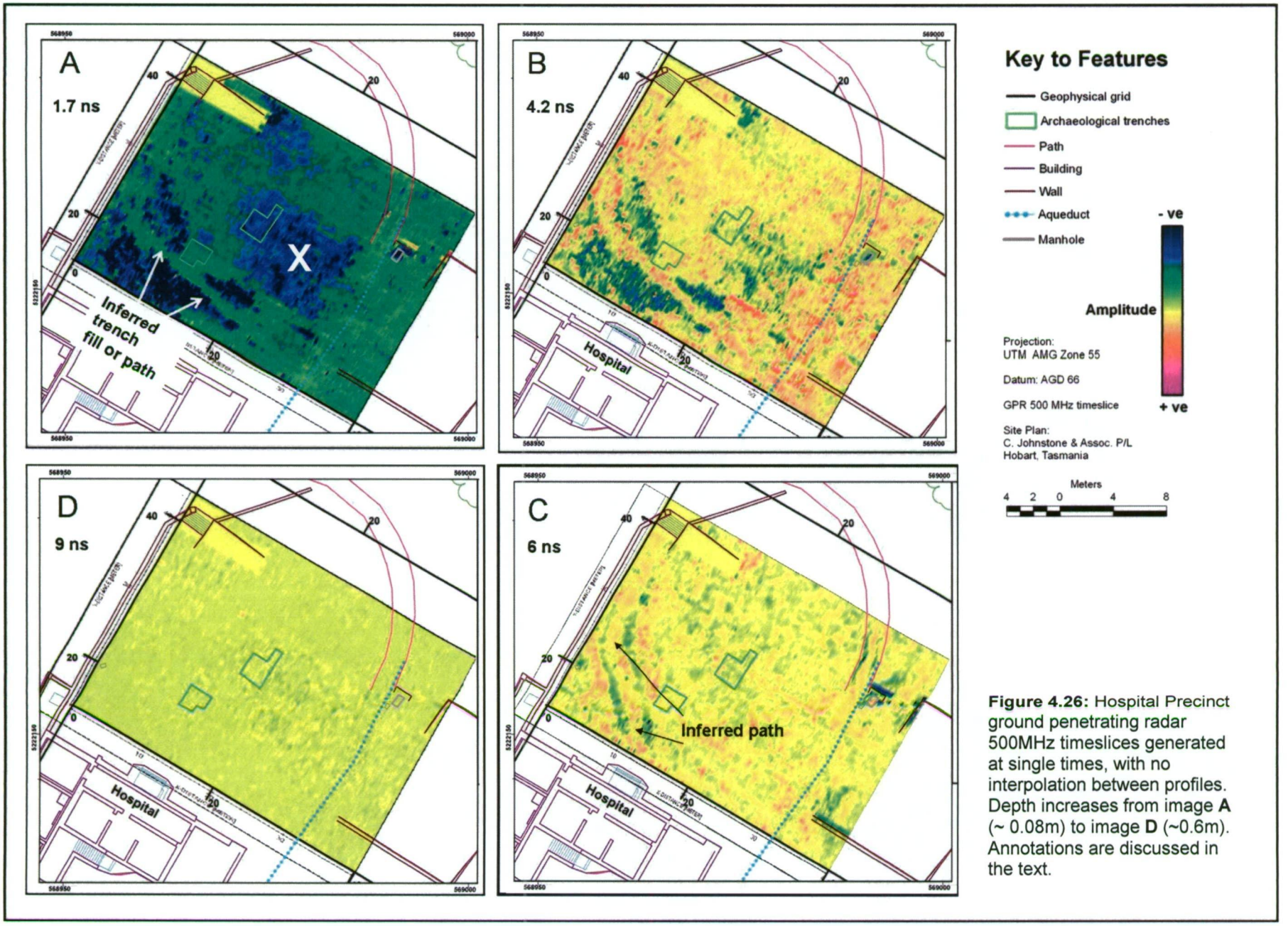

Figure 4.26: Hospital Precinct ground penetrating radar 500MHz timeslices generated at single times, with no interpolation between profiles. Depth increases from image **A** (~ 0.08m) to image **D** (~0.6m). Annotations are discussed in the text.

Structural targets in the Hospital Precinct were not defined in any detail from the amplitude maps. This lack of definition is probably due to very shallow high contrast heterogeneous demolition fill deposits, which reflect and disperse a large percentage of the transmitted energy and therefore masks underlying features. Good correspondence between high apparent resistivity measurements from these deposits, and the high radar amplitude zones, supports this interpretation.

Other building zones along the main bench are characterised by a detailed rectilinear arrangement of moderate to high amplitude linear anomalies within a low amplitude background. These responses were most clearly visible within the first 5 ns, indicating near-surface causative features (Figures 4.27 and 4.28). In contrast to the Hospital Precinct, the remaining section of terrace does not appear to be covered by a layer of resistive demolition fill and hence provides a less disturbed environment for the radar. This inference is also supported by parch marks in aerial photographs and well-defined anomaly patterns within the apparent resistivity data. Close correlation between the GPR timeslice recognition map and rectified historic plans implies that the lineaments are associated with near-surface structural features. The linear distribution of high amplitude discrete anomalies in Figure 4.29 (**B**), for example, is interpreted as buried remnants of a stone wall depicted in the Hurst plan (Figure 4.4). This feature is also manifest in the apparent resistivity data.

Similar patterns are visible on the Upper Slope, which was formerly the site of a few outbuildings and yard elements. Several zones of discrete high amplitude responses are attributed to collapsed retaining walls (Figure 4.28, **C - E**), and resistive compacted floor spaces and/or demolition rubble from small buildings depicted in the Hurst plan (Figure 4.4) and Blackwood plan (Figure 4.6). Additional evidence for these walls is provided by surface embankments and existing wall alignments, and truncated dolerite in the magnetic intensity variation map (as discussed in Section 4.2.3.2). Several timeslices show the linear anomaly attributed to a contemporary narrow trench (Figure 4.28, **D**) continues from the Hospital Precinct through the Upper Slope, passing through 60x, 0y. Had the survey extended further south, it is likely that this feature would have been recorded up to Smith O'Brien's cottage, as shown in the infrared photograph (Figure 4.29).

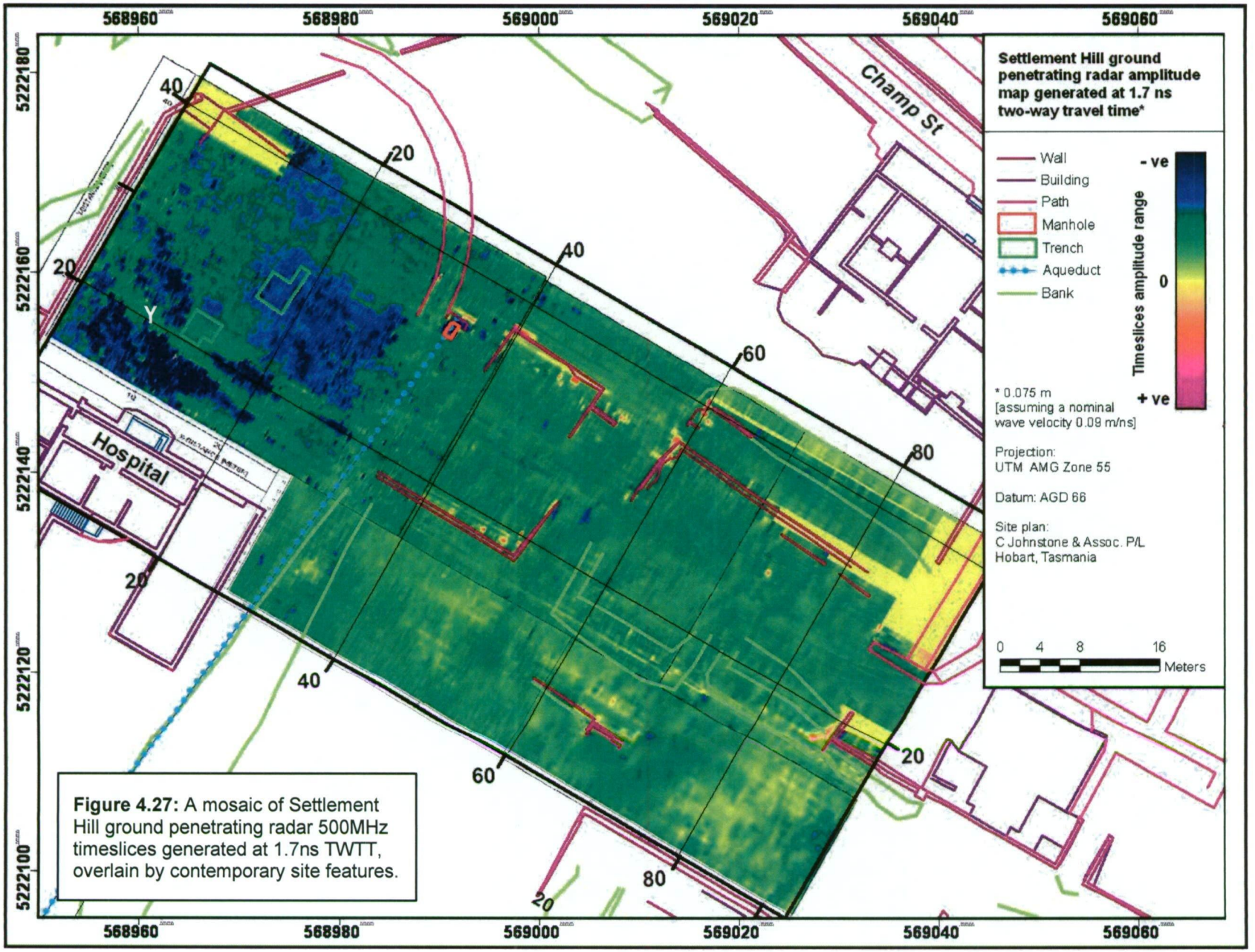

Figure 4.27: A mosaic of Settlement Hill ground penetrating radar 500MHz timeslices generated at 1.7ns TWTT, overlain by contemporary site features.

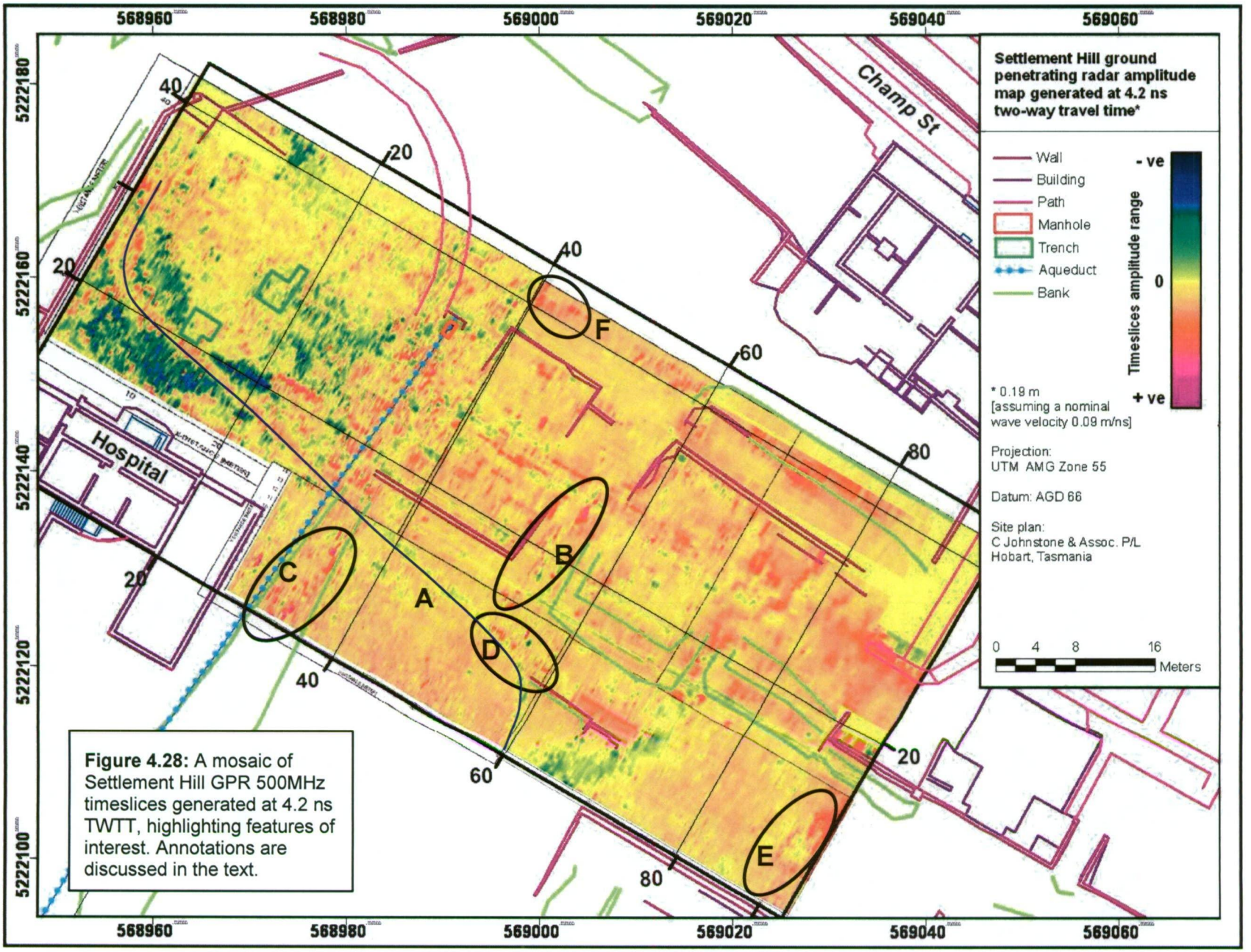

Figure 4.28: A mosaic of Settlement Hill GPR 500MHz timeslices generated at 4.2 ns TWTT, highlighting features of interest. Annotations are discussed in the text.

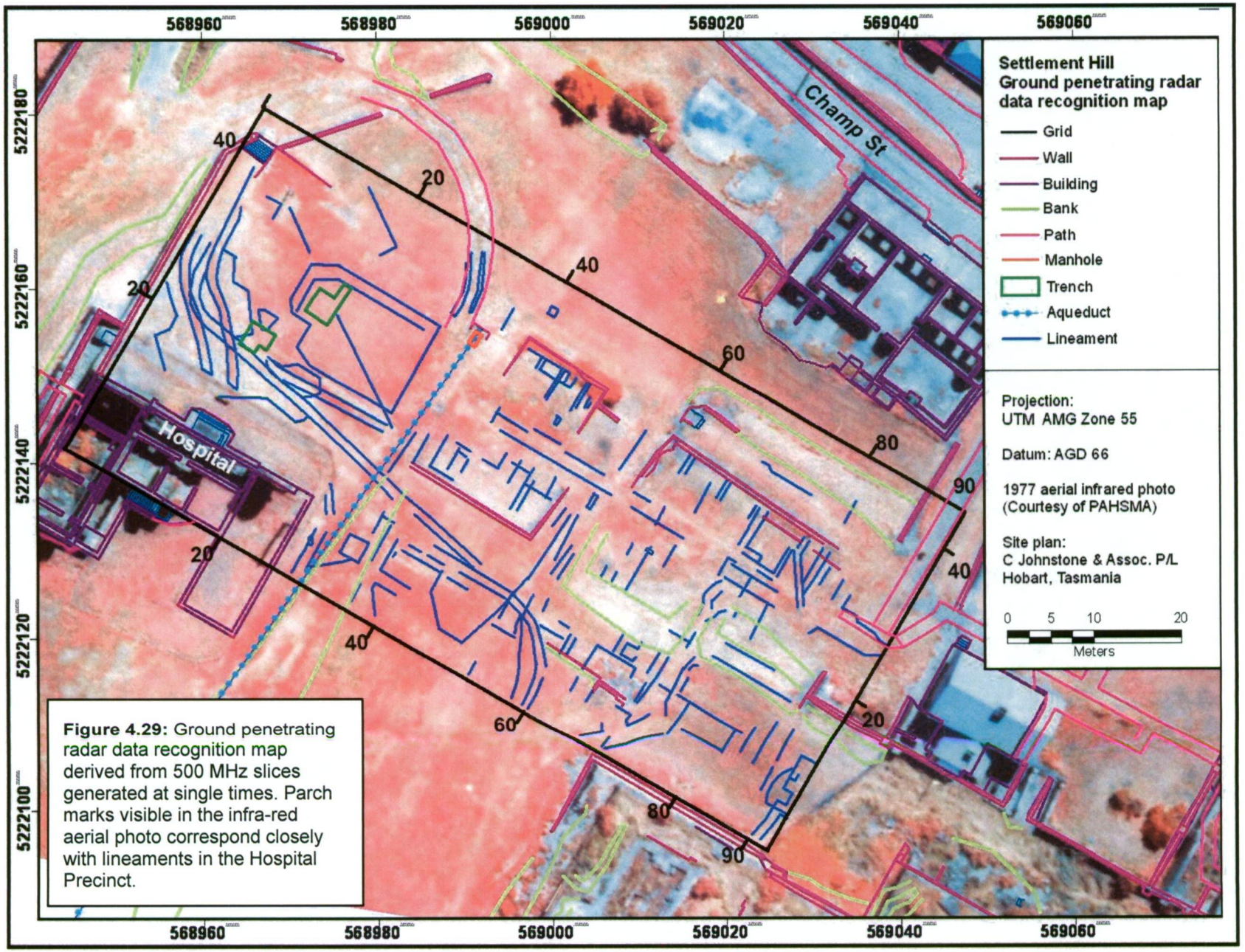

Figure 4.29: Ground penetrating radar data recognition map derived from 500 MHz slices generated at single times. Parch marks visible in the infra-red aerial photo correspond closely with lineaments in the Hospital Precinct.

In summary, the Upper Slope is characterised by comparatively uncomplicated anomalies attributed primarily to structural features, which indicate zones of high archaeological potential. Aerial photographs, apparent resistivity data and timeslices did not detect any extensive areas of near-surface rubble, such as visible in the Hospital Precinct.

The lack of geophysical anomalies in the Lower Slope is consistent with the historic plans, which show this area to have been undeveloped. A high amplitude response visible over several metres and centred on 41x, 42y (Figure 4.28, **F**), was possibly a garden or yard feature associated with the Chaplain's quarters. The Lower Slopes have low archaeological potential relative to the other survey areas on Settlement Hill.

The Hospital Precinct focus area

In order to recognise and characterise any structural targets beneath the demolition rubble fill in the Hospital Precinct, radar timeslices and individual profiles were assessed in more detail. Individual profile analysis was conducted using an approach similar to that adopted for the Isle of the Dead, involving abstracting the radar data into response classes and marking the results on a plan view of the site. This classification was based on responses modelled using ideal targets, and anomaly types recorded and verified at other sites with structural features. Four basic response types were deemed relevant to this investigation and classified according to amplitude, shape and reflection continuity as listed:

- high amplitude planar reflector,
- planar reflector with down-dipping edges,
- multiple adjacent reflections of irregular form,
- hyperbola.

The non-hyperbolic response types were recorded on the data recognition map (Figure 4.30) as a segment along-line, not incorporating any dipping edges. A discrete hyperbola was symbolised by a point coincident with its apex. Segments and points were coloured according to their vertical positions relative to 5 ns TWTT and 10 ns TWTT. This

classification was designed to distinguish anomalies attributable to causative features within or immediately below the surface, from those in the underlying stratigraphy.

Data in the recognition map was then interpolated into anomalous zones and lineaments, creating a more user-friendly presentation format for archaeologists, and an image suitable for preliminary qualitative interpretation (Figure 4.31). As described in Chapter 3 for Classes 3 and 4, segments that correlated between adjacent profiles were translated into anomalous zones. To reduce the subjectivity of this process, zones were primarily composed of segments of the same response type. Discrete areas were created from isolated segments. Interpolation along the x- and y-axes was dictated by a ~ 0.2 m buffer zone and the segment length respectively. Both parameters allowed for any positional error of the antenna during data collection, and the conical investigation footprint of the radar. In effect, the causative feature(s) were very highly likely to be located within this interpolated area.

Comparison of the information extracted from profiles to that derived from timeslice analysis (Figure 4.31) shows a close correlation between the high amplitude shallow (< 5 ns TWTT) anomalous zones and the inferred compacted resistive yard surface surrounding the garden path (**A**). Most of the central rectangular anomalous zone visible in the timeslices (**B**) coincided with an area of multiple discontinuous shallow non-hyperbolic reflectors. Several linear trends of point responses, such as along 17x (**C1**) and 24x (**C2**), align parallel to the anomalous zone perimeter and are interpreted as structural features. While low contrast lineaments recorded in the timeslices, such as (**D**), are typically not registered in the profile analysis, the latter method results in a much more detailed plan of the Hospital Precinct. The first main advantage of profile analysis is that it allows better recognition of discrete responses, such as short high amplitude planar reflections or hyperbolic anomalies. Because of the near-surface rubble, radar energy is randomly scattered along each profile. Rubble zones in the horizontal amplitude maps therefore exhibit a 'mottled' appearance where very shallow material heterogeneity exaggerates differences between profiles.

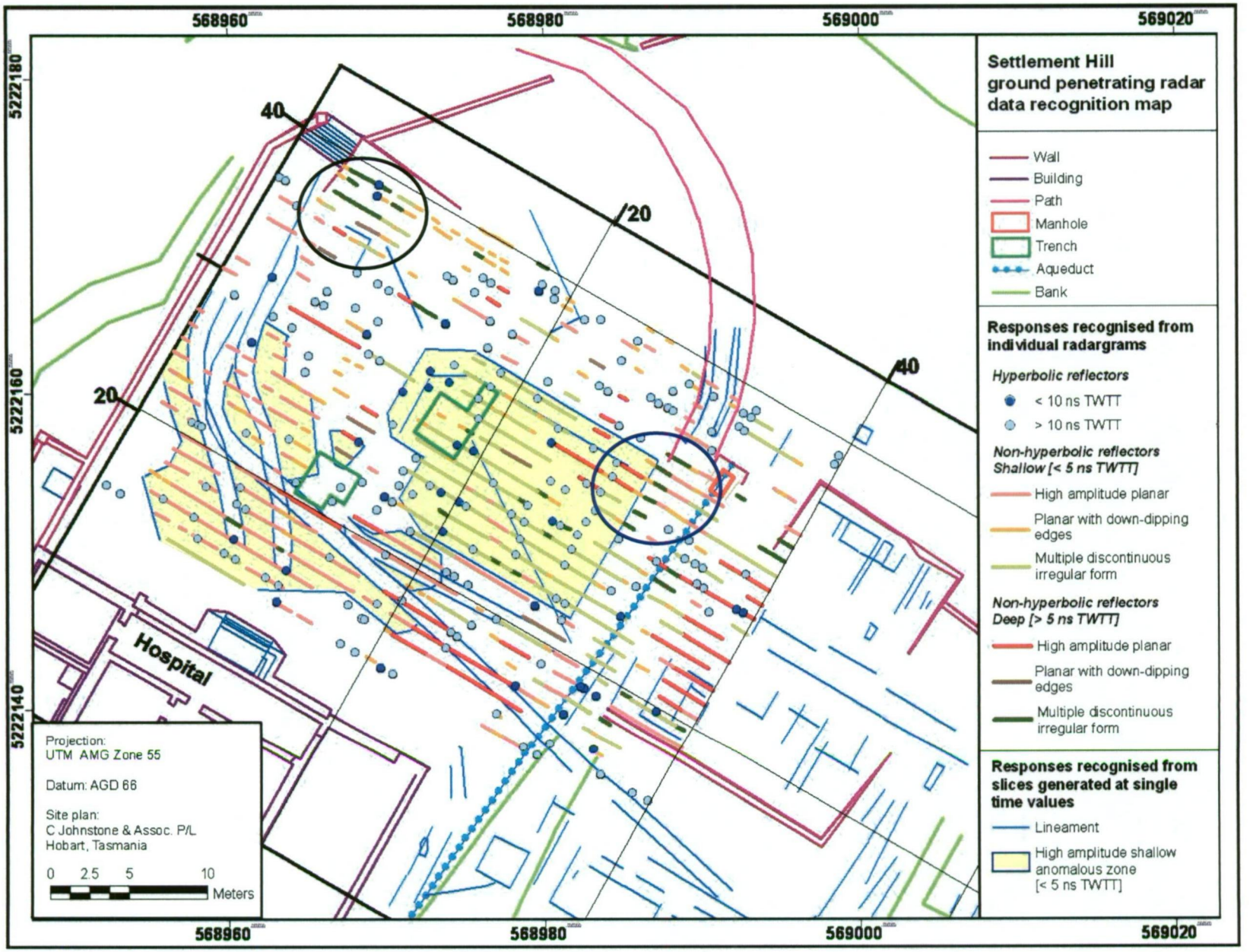

Figure 4.30: Hospital Precinct 500 MHz GPR data recognition map combining anomalies recorded from individual profiles and timeslices.

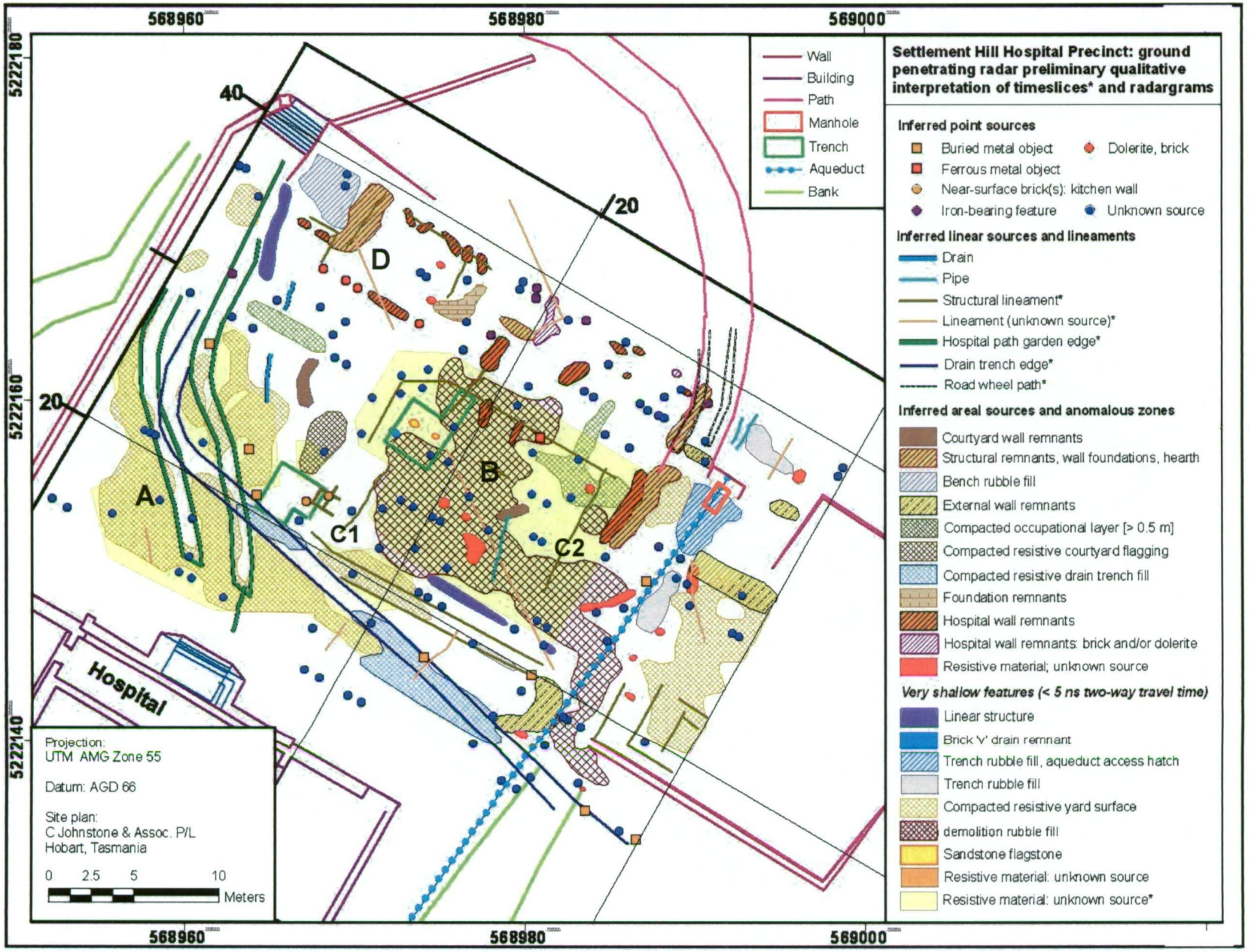

Figure 4.31: Hospital Precinct GPR qualitative interpretation map. Annotations are described in the text.

Individual profile analysis is a better method for the detection of anomalies below 5 ns TWTT – i.e. below the surface layers. Unlike the timeslice approach, this method does not rely on primary reflections or multiples derived from a material interface lying within a very narrow time window. In theory, reflections from a dipping or vertically irregular feature, such an uneven floor horizon, for example, may only show up partially in each time-slice as a lineament rather than the true areal anomaly. As a result, it is difficult to associate these responses with the appropriate causative feature.

In this case, Hospital Precinct timeslices generated using averages over 2 ns time ranges, instead of at individual values, offered some additional information (Figure 4.32). Discrete high amplitude responses at depth (> 5 ns TWTT), such as those circled, show improved definition and correlate closely to hyperbolic reflectors recorded through radargram analysis. Unfortunately, averaging responses over a time interval also results in smooth anomaly edges and decreases data resolution. Linear trends and the extent of anomalous zones are therefore often more difficult to identify from these images than in either the single timeslice or profile data recognition maps of the Hospital Precinct.

Preliminary interpretation of linear trends and anomalous zones in the Hospital Precinct (Figure 4.31) was based on historic documentation, surface evidence, anticipated responses from the archaeological targets and sources of undesirable signal. As it is not practical to describe or even list every feature, the following discussion will address principal features and areas of interest.

Small (< 4 m^2) areas of interpolated high amplitude responses are concentrated between 5x and 30x, 25y and 40y, and correlate closely with the predicted first and second hospital sites. These features are mostly planar type responses, or planar with down-dipping edges, and are interpreted as remnants of *in situ* masonry or brickwork. Regions of similar responses situated outside the anticipated architectural footprints of either the primary structures or numerous outbuildings, are classified as 'resistive material' of unknown source.

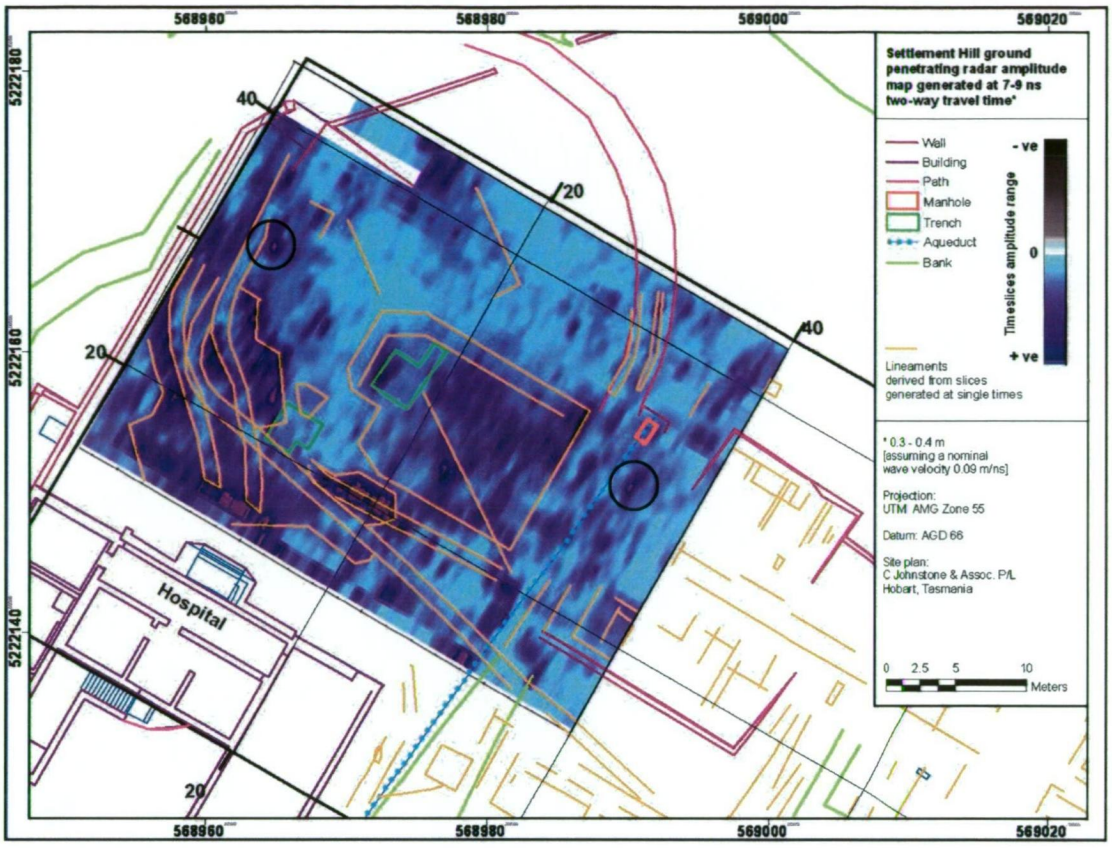

Figure 4.32: Hospital Precinct GPR timeslice of average amplitudes between 7 – 9 ns TWTT, overlain by lineaments recognized from timeslices generated at single time values (examples of newly identified anomalies are circled).

Several areas of the Hospital Precinct exhibit an unusual juxtaposition of very shallow and deeper response types - a relationship that implies a complicated stratigraphy and high archaeological potential. The northeastern corner of the area (circled in black, Figure 4.30), is characterised by a mix of deep and shallow multiple discontinuous irregular reflections and planar anomalies with down dipping edges adjacent to the sandstone steps. The deeper responses are attributed primarily to bench rubble fill and nearby sandstone/brick retaining walls, with the possibility of a deeper resistive horizon. Coincident low magnetic intensity values (~ 62200 nT) and steep linear gradients (Figure 4.19) suggest that the dolerite substrate had previously been removed from this area.

Inferred structural elements associated with the second hospital's western wall and hearth manifest in radargrams from Line 39y as hyperbolic responses of varying contrast – the apices of which are marked in Figure 4.33. Shallow moderate - high amplitude reflectors centred on 10.2x and 11.8x (circled) are also interpreted as

structural features. Linear parch marks in the infrared aerial photograph and apparent resistivity peaks (460 Ω.m) measured at 8x and 12x (Figure 4.33) also provide strong evidence for very shallow walls (< 5 ns TWTT). A sharp increase in average resistivity values (~ 400 Ω.m) at 8x defines a vertical change in fill material resistivity, which is considered to distinguish the yard from the second hospital's main building footprint.

Another juxtaposition of deep and shallow reflectors is also recorded immediately west of the aqueduct access hatch (Figure 4.30, circled; Figure 4.33, Line 31y). Radargrams from Line 31y (Figure 4.33) show near-surface linear planar reflections with down-dipping edges, (**A**) flanked by deeper high amplitude planar anomalies from 12 – 17 ns TWTT (**B**), with a narrow zone of multiple discontinuous irregular responses (**C**) to the west and east respectively. The central linear zone (**A**), which is coincident with a low amplitude apparent resistivity peak, correlates closely with the supposed end of the second hospital's main building. The geophysical source is therefore interpreted as a well-preserved near-surface *in situ* wall. Deeper responses to the east (C) are attributed to collapsed structural features, such as foundations, and the privy depicted in the 1836 Laing building plans (Figure 4.2). The picked high amplitude planar reflections (**B**) are associated with a compacted resistive interior occupational layer. A section of both strong near-surface radar responses and elevated resistivity values from 20.5x – 24x forms part of the anomalous zone mapped in Figure 4.31 which is interpreted as resistive demolition rubble fill. A discrete deeper high amplitude response at 23.2x is probably an internal feature of the second hospital, such as a foundation remnant. The stratigraphic proximity of this feature to the inferred occupational layer (**B**) suggests that the two units are functionally related.

A significant trough in the total magnetic intensity profile from 30x onwards illustrates the location of an inferred trench cut into the dolerite substrate to accommodate the aqueduct. There is no evidence of this feature in the radar data. Although the radar does not detect the aqueduct, it does locate the contemporary concrete pipe – represented by a hyperbolic response at 32.5 m (Figure 4.34). This is 1 m offset from pipe position on the services plan.

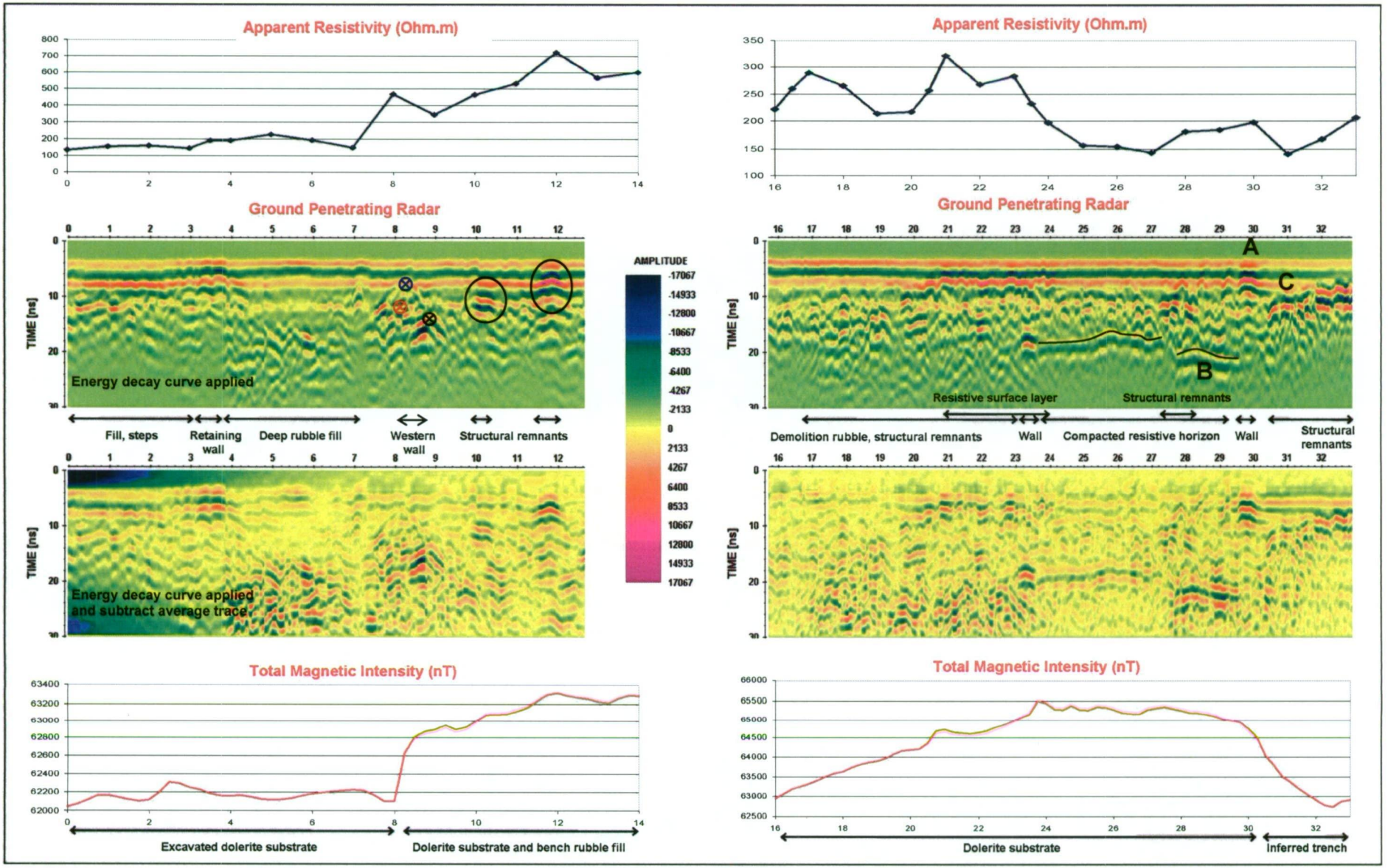

Figure 4.33: Interpreted 500 MHz GPR profiles collected from Line 39y (left image) and 31y (right image), shown in relation to coincident magnetic and resistivity data.

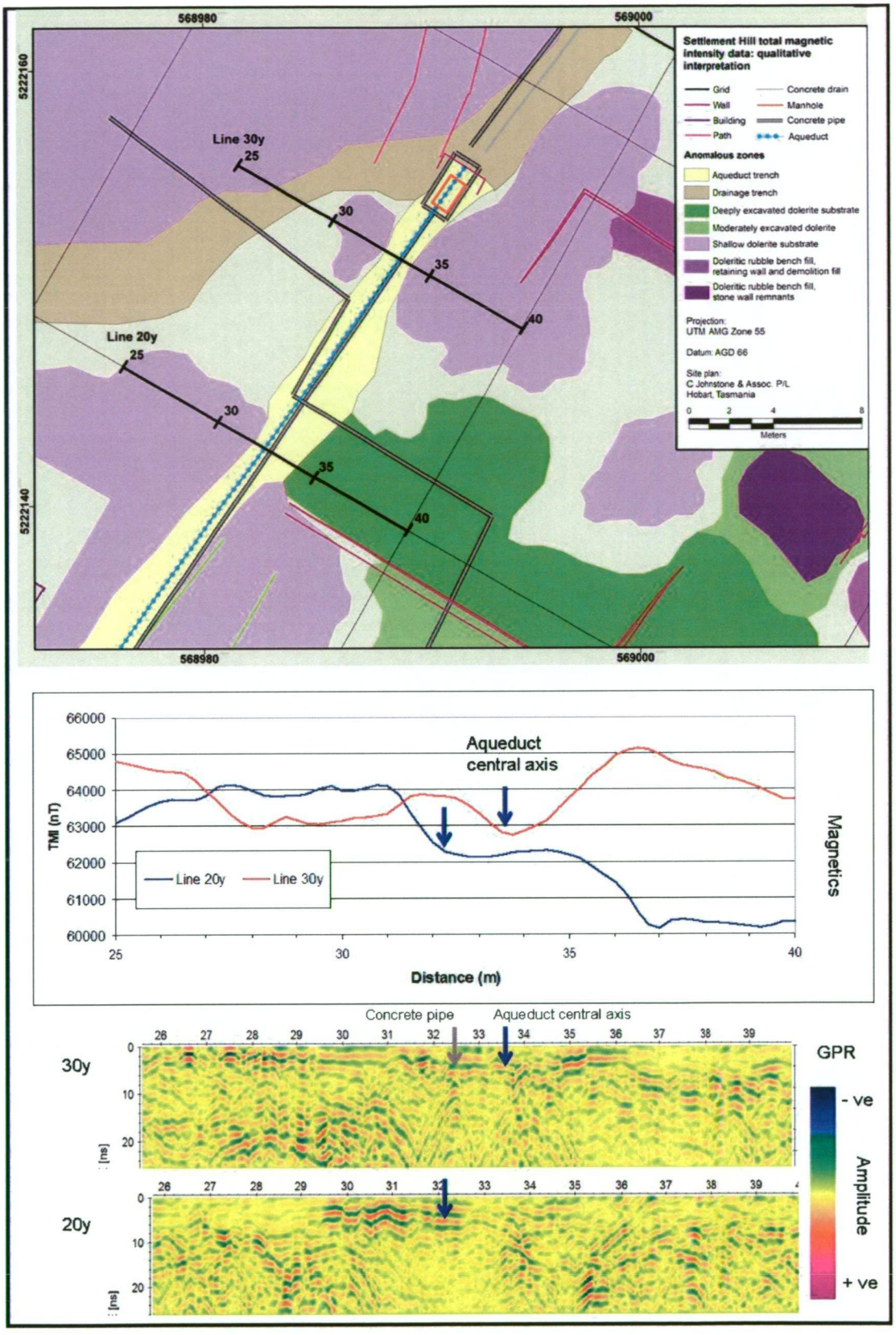

Figure 4.34: A map of the magnetic data qualitative interpretation, showing the location of two magnetic and GPR profiles across the aqueduct central axis. The GPR data is processed and image enhanced to accentuate non-horizontal reflections.

4.3 ARCHAEOLOGICAL GROUND-TRUTHING

4.3.1 Background

Following the geophysical investigations on Settlement Hill, excavations were conducted by PAHSMA during the Summer Archaeology Programme of 2005 (Figure 4.35). Two trenches were located within the Hospital Precinct, in an attempt to uncover part of the first and second hospital structures (Figures 4.36 and 4.37). The exact location of the first hospital building remained unknown since its demolition and subsequent burial during the second building phase.

Prior to excavation, the historic maps were rectified using ground control points, to indicate possible areas of high archaeological potential. The trenches were then sited with reference to the rectified historic plans, geophysical data, and features such as parch marks inferred from aerial photographs (Figures 4.1 and 4.11). According to Laing (1836) and Hurst (1846) maps of the second hospital, anticipated archaeological targets within the bounds of Trench 1 (11 m^2) included exterior and interior wall foundations, courtyard surfaces, and floors of the dispensary and privy areas. Trench 2 (8 m^2) potentially encompassed the inner and outer structural features of a kitchen outbuilding and yard spaces. Rubble fill was expected within the cultural layer immediately below the topsoil horizon, as the site had been largely undisturbed since demolition and resurfacing. The following sections summarise the excavation results relevant to this project's objectives, and assess their implications for geophysical surveying. Trench photographs were taken facing towards the northeast, unless specified otherwise. All information presented was derived from the Settlement Hill archaeological report (Steele, 2005).

Figure 4.35: Excavation of Trench 1 by Jody Steele, with the third hospital ruins in the background (courtesy of Steele, 2005).

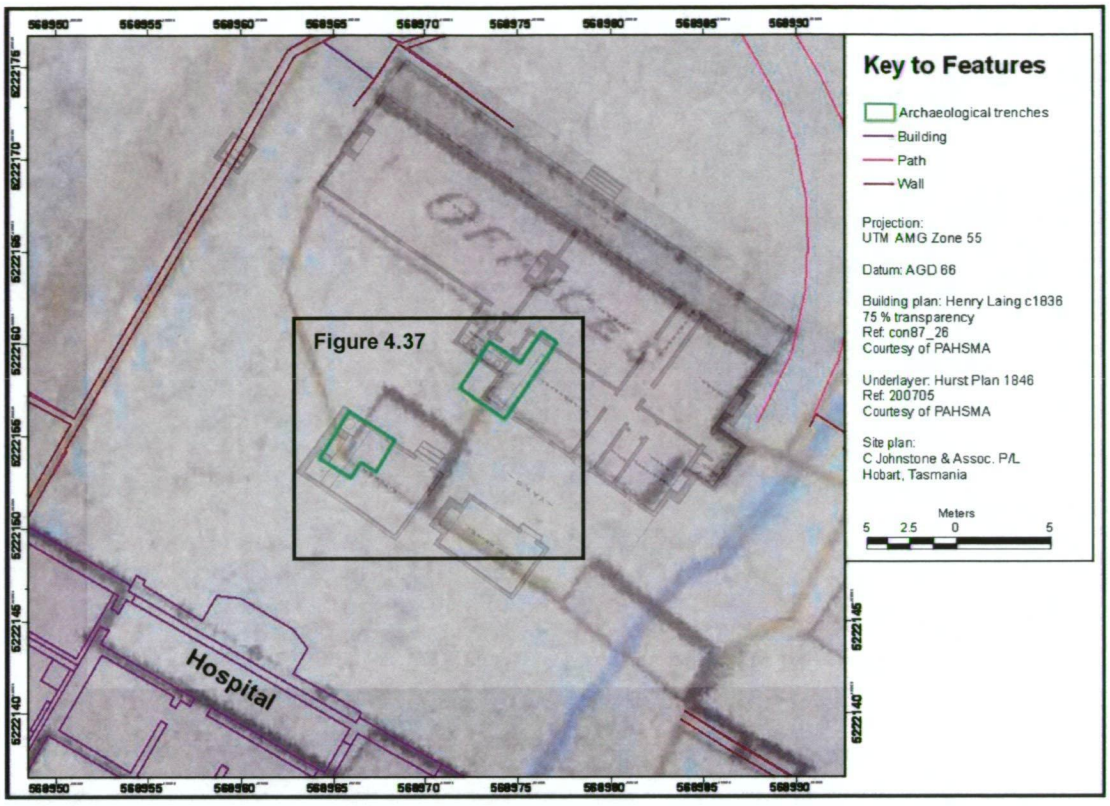

Figure 4.36: Map of the hospital precinct and trenches for the 2004-5 Summer Archaeology Program, underlain by a rectified Laing building plan (1836) and Hurst site plan (1846). The selected area is enlarged in Figure 4.37 (below).

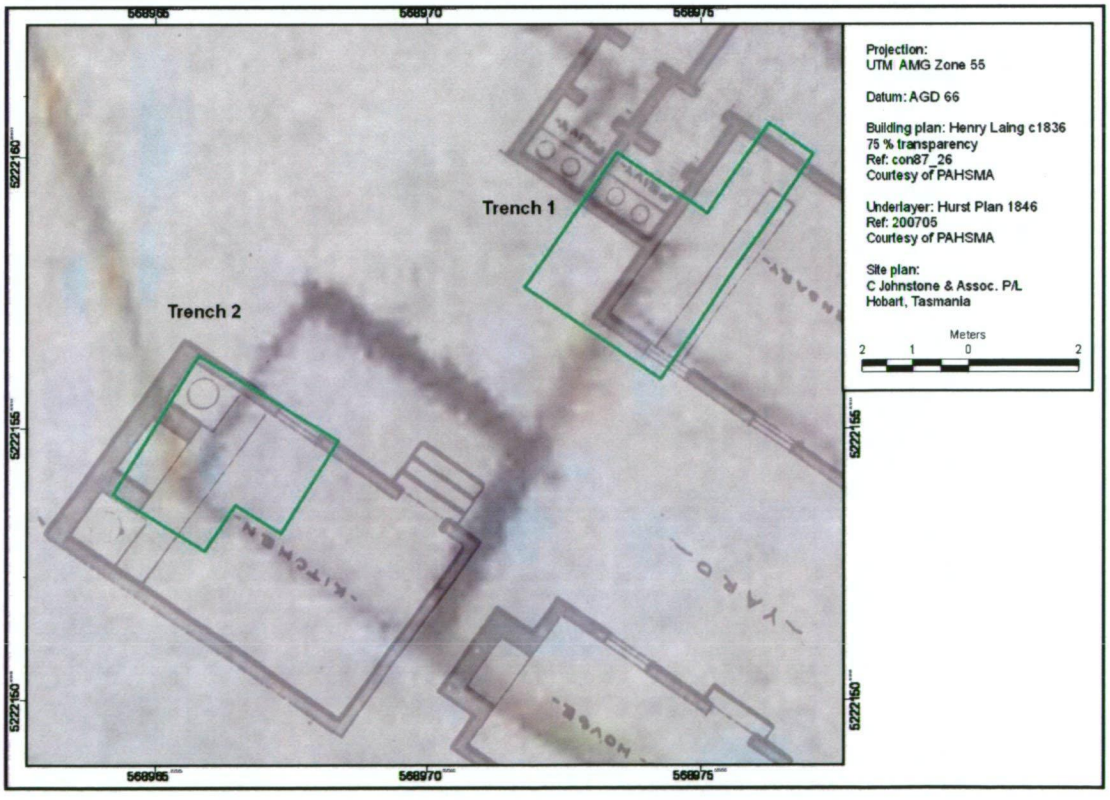

Figure 4.37: A detailed view of the Hospital Precinct archaeological trenches in relation to rectified historic plans of the second hospital. Rectification was conducted prior to excavation or geophysical survey results were analysed, using ground control points at the third hospital and aqueduct pit.

4.3.2 Trench 1

The first stratigraphic layer below the grassed surface consisted of a grey loam topsoil with minor amounts of brick fragments, dolerite pebbles and mortar debris. The maximum thickness of this layer was approximately 0.35 m (Figure 4.38). Further layers were characterised by brick rubble, building debris and a dark brown loam, in the centre of which was an accumulation of lime/shell mortar containing brick and sandstone fragments, and shell components. Removal of the smaller brick fragments and loam left a moderate concentration of artefacts such as nails, mostly associated with structural demolition. Further excavation of the loam on the western side of the mortar deposit revealed solid sandstone flagging juxtaposed with brown clay soil and a brick spoon drain with silty drain wash (Figure 4.39). Several of the moulded spoon-drain bricks were no longer present, only their mortar base. The alignment of the drain and pavers indicated that these features were related (Figure 4.40).

Figure 4.38: Trench 1 section showing building rubble within a grey loam matrix, to 0.35 m depth (courtesy of Steele, 2005).

Figure 4.39: Trench 1 after removal of the topsoil and part of the demolition rubble. The central mortar-rich deposit separated two compositionally different zones: a solid occupational level of sandstone flagging and a drain to the left, and more debris to the right (courtesy of Steele, 2005).

Figure 4.40: Trench 1 western corner, showing the flagging, remnants of a moulded brick 'spoon' drain and underlying shell mortar (courtesy of Steele, 2005).

In contrast, the eastern corner yielded more rubble debris with increasing depth (Figure 4.39). The excavated material contained many partial bricks and a large number of artefacts, including nails, structural fittings (small amounts of lead) and piping (Figure 4.41). Removal of the central mortar-rich deposit showed that the flagging extended towards the eastern corner, ending at a sandstone slab shelf. Bedding for the stone consisted primarily of fine crushed sandstone, with few artefacts. The eastern corner was characterised by a deposit (< 0.2 m thick) of near-complete brick fragments and a high concentration of artefacts, including ferrous metal, bone and a tin food pan. The brown clay soil matrix was loosely consolidated and sandy fines had resettled to form a thin lens (< 0.04 m) at the deposit base. The trench was then extended another 2 x 1 m northeast from the eastern corner (Figure 4.43), in order to further investigate the exposed heavily compacted surface.

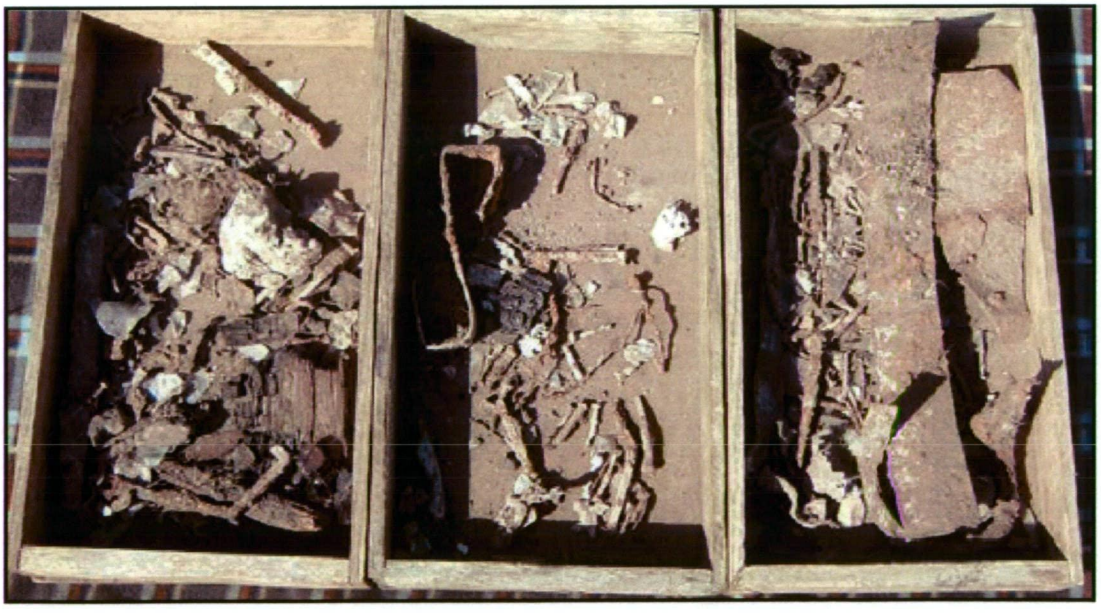

Figure 4.41: Sample of artefactual material from the brick rubble and loam demolition fill layers, including nails, structural fittings and window glass fragments, small amounts of lead fittings and piping (courtesy of Steele, 2005).

Figure 4.42: Trench 1 extension showing the 'v' drain and brick foundations (courtesy of Steele, 2005).

The extension showed similar shallow loam topsoil to the first trench, and underlying brick rubble like that of the original eastern corner. No sandstone features, mortar or loamy deposits were present. Further excavation revealed a T-junction of bricks within the brown/grey loamy soil matrix. These were interpreted as foundation lines for the second hospital privy shown in the Laing building plans. Three bricks *in-situ* above the inferred foundations may have been bearers for the privy floor (Steele, 2005). Removal of irregularly arranged bricks and soil between the T-junction and flagstone shelf edge exposed a brick 'v' drain and a solid mortar-like deposit (Figure 4.42). The primary features of Trench 1 after final excavation are shown in Figures 4.43 and 4.44. In summary, the excavation 'exposed a small section of brick foundations and a substantial portion of the second hospital's rear flagstone yard' (Steele, 2005).

Figure 4.43: Final excavation of Trench 1 with extension, photographed from the northeast. Sandstone flagging occupies most of the original area, forming part of the courtyard located between the main structure and its outbuildings. A brick spoon drain is located in the top right corner, and the change in level with brick foundations and 'v' drain is visible in the bottom left (courtesy of Steele, 2005).

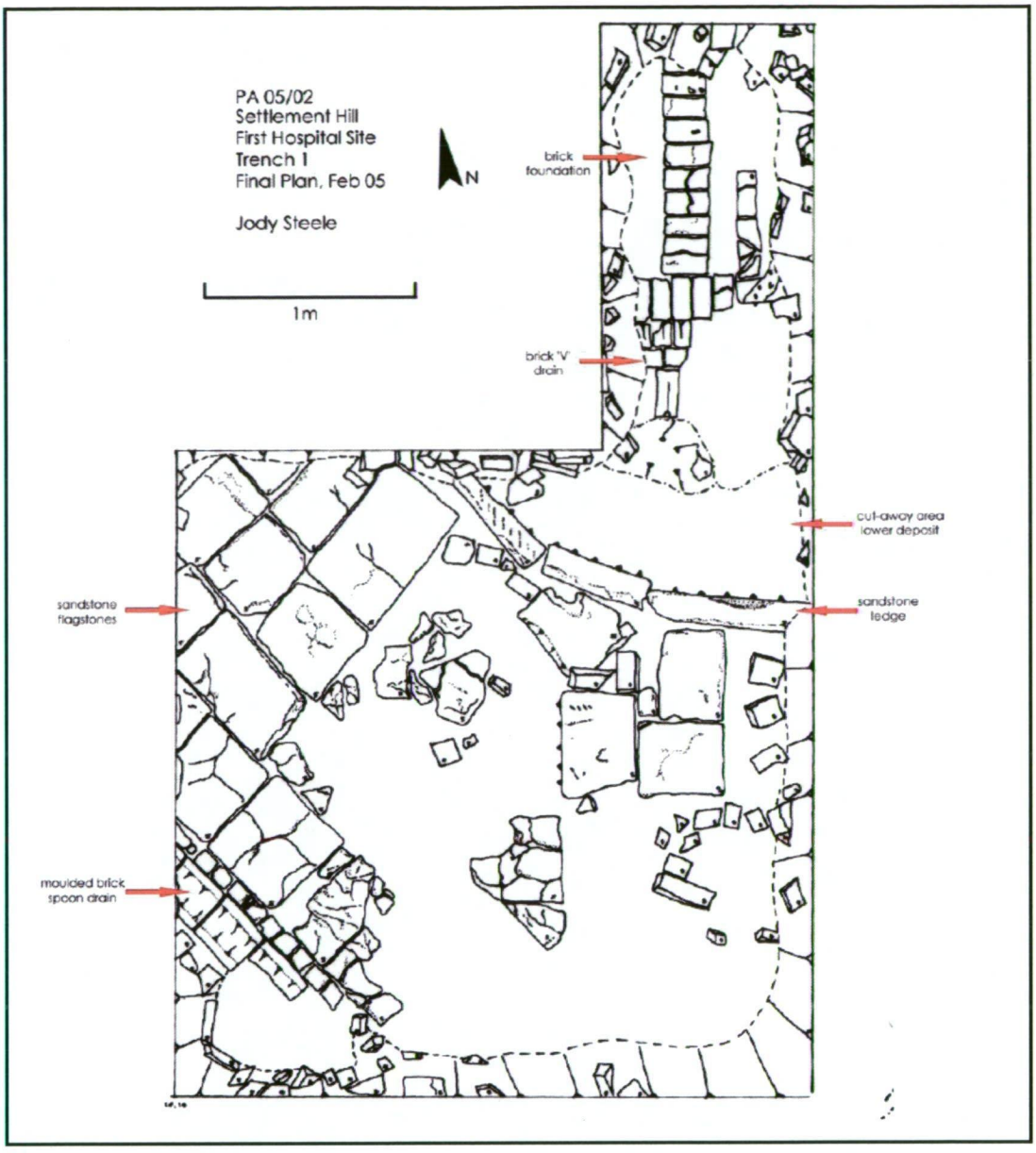

Figure 4.44: Trench 1 final plan of the second hospital site, Settlement Hill (February 2005) showing primary cultural features (courtesy of Steele, 2005).

4.3.3 Trench 2

Trench 2 was initially laid out over a 3 x 2 m area suspected to include the kitchen outbuilding of the hospital, as depicted by Laing in 1836 (Figure 4.2) . Excavation of the sandy loam topsoil in Trench 2 revealed it to be shallower than in Trench 1, with a penal-period occupation layer evident within 0.12 m depth. Material in the western half comprised clay soil, crushed brick, dolerite fragments and embedded artefacts, and was interpreted by Steele as a compacted yard or path surface. Removal of soil, brick rubble and a mortar deposit from the eastern half exposed more gravel (Figure 4.45).

Figure 4.45: Trench 2 deposits immediately underlying the topsoil include clay, crushed brick, dolerite fragments and embedded artefacts (courtesy of Steele, 2005).

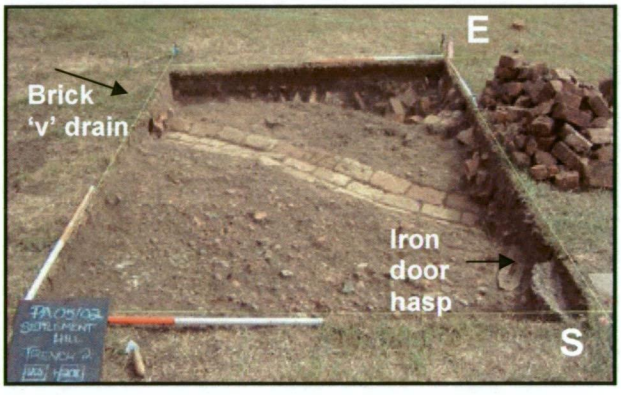

Figure 4.46: Trench 2 showing the penal period oblique trending brick 'v' drain, yard surface, and iron hasp, a contemporary post feature and building remnants (courtesy of Steele, 2005).

A contemporary concrete post base and an adjacent penal-period corroded iron door hasp were uncovered in the southern corner (Figure 4.46). Very fine crushed brick deposits present only in the western corner were attributed to a post-penal or contemporary period path surface (Steele, 2005).

Excavation of the demolition rubble in the eastern corner revealed a near-intact brick 'v' drain trending obliquely to the trench (Figure 4.46). A small section of brick 'wall' and a shallow foundation trench with collapsed wall bricks were also uncovered in the eastern corner.

At this stage, Trench 2 was extended eastward by 2 x 1 m, to gain more insight into these structural features. Photographs in Figure 4.47 illustrate the excavation progress of this extension, through the topsoil and demolition rubble similar to that seen in the adjacent section. The lower right image shows that the compacted yard material continues between the drain and structural features. The small brick wall remnants are keyed into a thicker brick 'C' shaped wall interpreted as a corner of the hospital kitchen. Mortar deposits and charred brickwork inside the corner were correlated with the hearth depicted in the Laing plans (Steele, 2005). Excavation of brick rubble associated with the small brick wall revealed clay bedding and some very dark brown soil with broken brick fragments. 'Neither of these was fully dug, as the results were conclusive enough to confirm that the wall had been robbed from its foundation trench, not simply deteriorated' (Steele, 2005). In summary, Trench 2 located a small section of the hospital kitchen, the adjoining boundary wall and an external brick 'v'

drain that ran along the north side of an exterior path or road, directing surface water away from the second hospital compound (Figure 4.48).

Figure 4.47: Trench 2 extension stages of excavation revealing the kitchen corner and diagonal wall junction (courtesy of Steele, 2005).

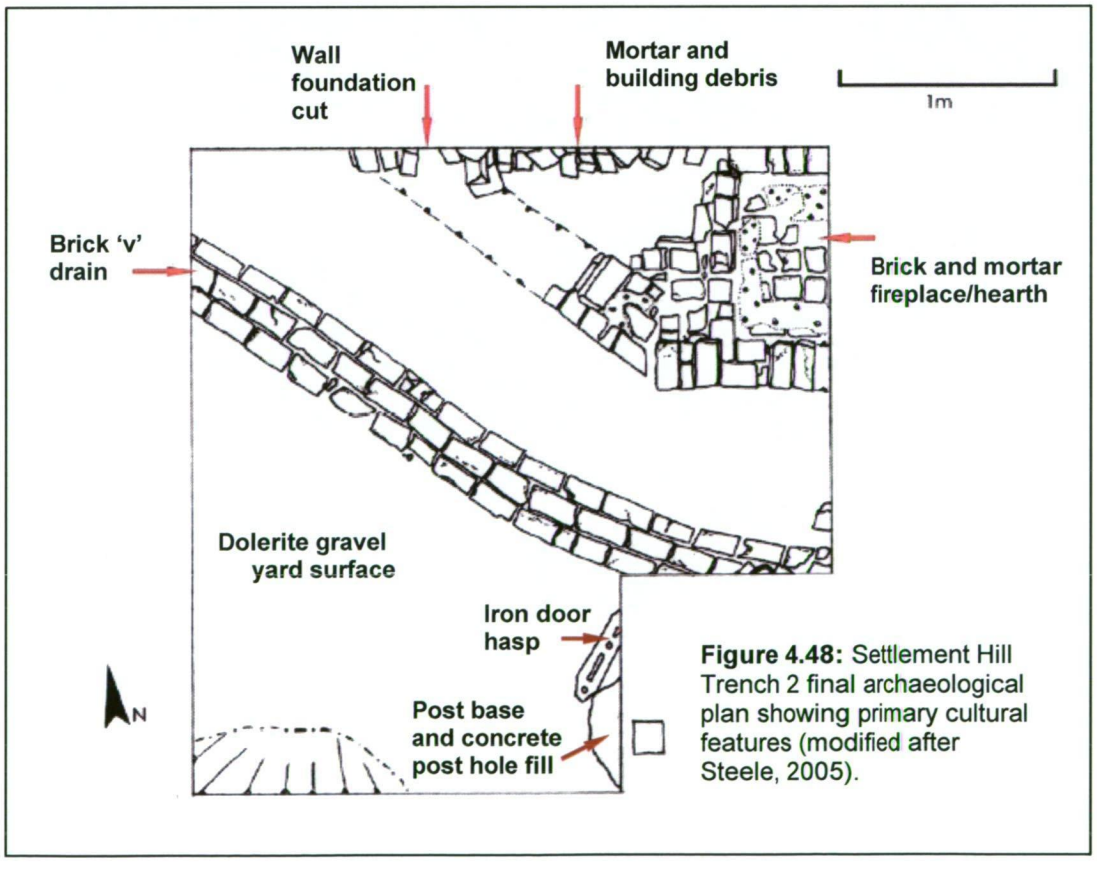

Figure 4.48: Settlement Hill Trench 2 final archaeological plan showing primary cultural features (modified after Steele, 2005).

4.3.4 Implications

Elements of the structural features located through excavation were used as ground control points for new registration of historic plans. These included the wall intersection interpreted as the kitchen south western corner / courtyard wall junction, and the second hospital privy brick wall foundations. This method was significantly more reliable than using surface features such as the terrace retaining wall / sandstone steps intersection. Re-registration of the Laing plan (c1836) shifted the second hospital and its outbuildings ~ 1.5 m northeast from the position previously calculated using unreliable ground control points. Due to original scaling errors, rectification of the 1846 Hurst plan was not accurate, although the new, skewed fit did provide a better guide to feature layout than the previous one. Spatial discrepancies are clearly evidence in Figure 4.49, which presented the re-rectified historic documents, the final archaeological excavation plans, and contemporary site map.

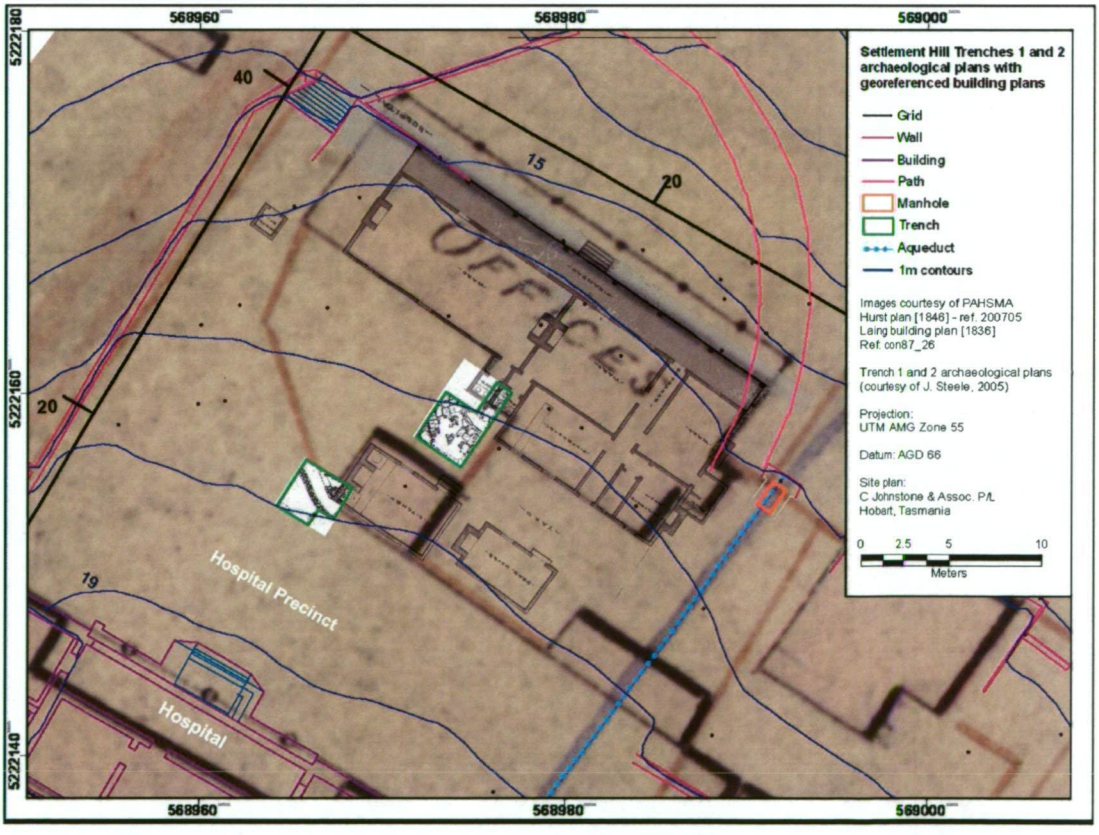

Figure 4.49: Map of the Hospital Precinct showing the re-rectified Hurst map c1846 and Laing building plan c1836, and contemporary site survey in relation to the final archaeological plans. Note that there are still spatial discrepancies between the two historic documents, due to scaling errors in the Hurst map and a lack of reliable ground control points.

4.3.5 Comparison of trench findings to geophysical data

This section will compare each geophysical dataset and the preliminary qualitative interpretation with the ground-truthing findings and repositioned Laing building plan of the second hospital. Refined qualitative interpretation images derived from this feedback are presented in Appendix B, Figures B1 - 4.

4.3.5.1 Apparent conductivity

Most of the original Trench 1 area was positioned within a relatively low apparent conductivity zone (< - 20 mS/m), as measured by the EM-38 in HCP mode (Figure 4.50). This was attributed to compacted resistive material, possibly including foundations, external wall remnants, and rubble fill. Excavations confirmed the presence of resistive material - shallow brick rubble, building debris and a dark brown loam, underlain by sandstone flagging– although no external wall remnants. A brick spoon drain and mortar base in the western corner correlated with an oblique-trending linear boundary, which was interpreted as a lineament of unknown source.

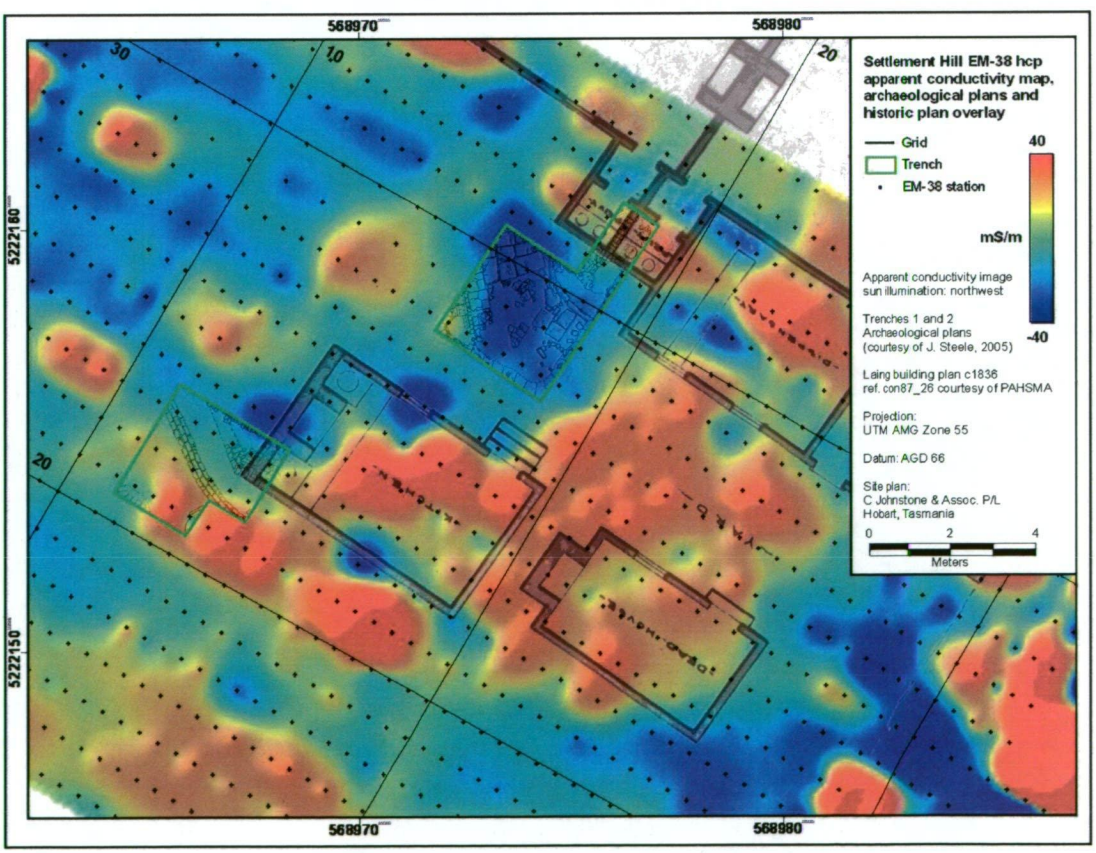

Figure 4.50: Hospital Precinct map of the final archaeological plan, re-rectified Laing building plan, apparent conductivity horizontal mode variation map and the sampling grid.

High conductivity values in the Trench 1 extension were initially attributed to clays, charcoal, metallic debris and lime mortar. Excavation revealed that they actually corresponded to a poorly consolidated, artefact-rich brick and clay rubble fill deposit associated with the privy. An inferred external building wall along 31y was closely aligned with excavated brick foundations. A lineament recorded along gridline 18.5x was not matched by an excavated structural feature. The VCP mode measured low to moderate conductivities for all of Trench 1 - there was no differentiation of the extension such as seen in the HCP data (Figure 4.51). These values are probably caused by the extensive near-surface resistive rubble fill.

Trench 2 was characterised by a thinner rubble layer than Trench 1, and no stone flagging. All but the eastern corner was outside the hospital courtyard. These findings are reflected in the overall higher apparent conductivity values measured by the EM-38 in both survey modes (Figures 4.50 and 4.51). The EM-38 did not detect the diagonal courtyard wall remnants, second hospital kitchen SW corner or shallow brick 'v' drain, probably because the relatively conductive soil matrix provided preferred current pathways. A couple of point anomalies recorded along gridline 21y are coincident with the iron hasp and concrete base of a metal post located within 0.2 m depth (Steele, 2005).

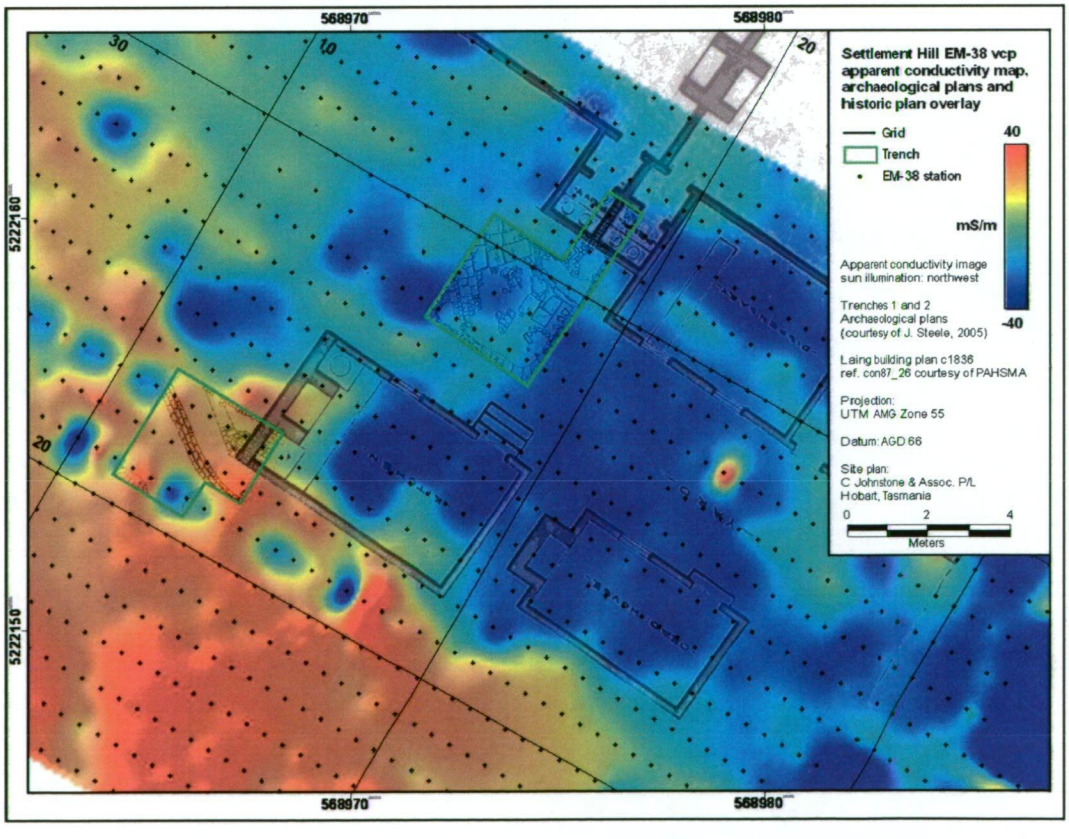

Figure 4.51: Hospital Precinct map of the final archaeological plan, re-rectified Laing building plan, apparent conductivity vertical mode variation map and the sampling grid.

4.3.5.2 Magnetics

The magnetic survey did not detect any of the brick features (foundations, drains) excavated in Trench 1, due to undesirable high frequency signal derived from brick and dolerite pieces in the demolition fill and the highly magnetic dolerite substrate. Most of Trench 2 was positioned over an inferred trench in the dolerite. The strong magnetic gradient was roughly aligned with the courtyard perimeter, as demarked by the diagonal wall remnants. This suggested that the trench was constructed concurrently or after the second hospital was built. The magnetic survey produced a discrete dipolar anomaly over the iron hasp.

4.3.5.3 Apparent resistivity

Sixteen data points were sampled in Trench 1 and apparent resistivity values averaged over 300 Ω.m (Figure 4.52). These consistently high values were primarily attributed to dolerite, sandstone and brick demolition rubble fill. Several high resistivity lineaments surrounding the trench were interpreted as remnants of walls, foundations associated with the second hospital's main building. Excavations confirmed the presence of near-surface rubble fill beneath the shallow topsoil, and also revealed evidence of courtyard flagging in the original trench area. The extension was characterised by resistive brick foundations and more rubble fill. Due to a lack of resistivity contrast between the paved area and the change in level to the second hospital's privies, and the geophysical noise contributed by the surrounding rubble, it is impossible to infer how far the sandstone flagging extends either side of the trench. The lineaments initially interpreted as structural features are possibly indicative of well-preserved sections of stone pathways that skirted the second hospital's main building and also linked it to the kitchen and mortuary.

Trench 2 was characterised by low average values relative to Trench 1, which suggested that the resistive near-surface rubble fill and courtyard surface was present as a thin layer and/or was nonexistent in parts. Excavations confirmed a lack of sandstone flagging, and the presence of a compacted occupational layer within 0.12 m depth which was comprised of gravel (crushed brick and dolerite) within a conductive clay soil matrix. There was no noticeable increase in resistivity in the eastern half of the trench,

even though excavations revealed a thicker demolition rubble (brick pieces) near-surface deposit in this area (Figure 4.46).

The oblique trending low resistivity lineament (Figure 4.52, **A**), interpreted as a drainage trench, was found to align with a courtyard foundation trench (at least five courses deep) filled with unconsolidated demolition material. The brick 'v' drain was offset slightly to this lineament and did not cause a measurable anomaly in the data, probably because it is too narrow (three bricks) and thin (single brick) to be resolved by the 1 x 1 m sampling density. Only one measurement was collected over the feature. There appears to be little contrast in resistivity between the bricks and surrounding compacted gravel yard surface.

A very fine crushed brick deposit in the SW corner intersected with a low resistivity linear anomaly running from the Hospital Precinct to the Upper Slope (Figure 4.52, **B**). The archaeological findings strongly suggested that this feature was a pathway, rather than a filled-in trench as originally proposed. The resistivity response patterns enabled the pathway layout to be extrapolated beyond the trench boundary, which showed that the feature is superimposed over the third hospital's garden path and is thus younger.

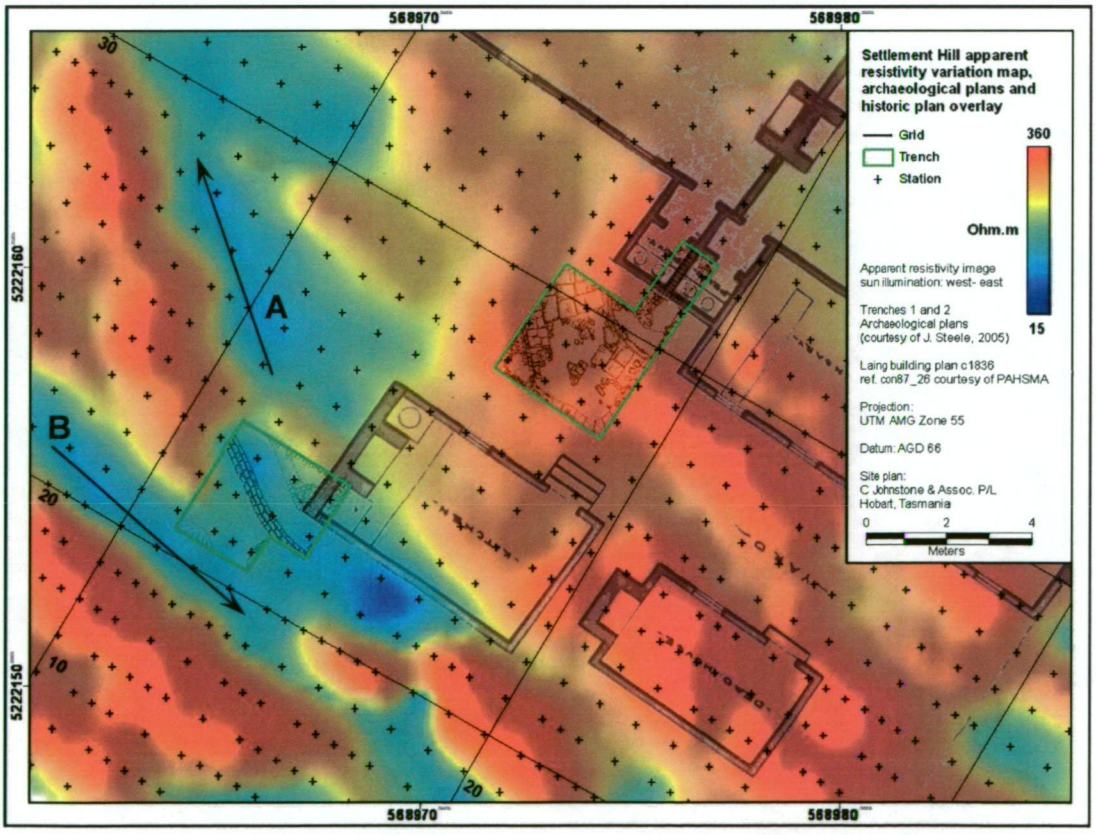

Figure 4.52: Hospital Precinct map combining the final archaeological excavation plans, re-rectified Laing building plan of the second hospital, apparent resistivity variation map and sampling grid.

4.3.5.4 Ground penetrating radar

Excavations at both trenches confirmed that weak and discontinuous near-surface reflections were caused by near-surface rubble fill of heterogeneous composition. Because responses from underlying features were distorted or masked by scattering of the reflected signal, it was very difficult to accurately define horizontal strata of cultural relevance, such as the courtyard stone flagging. The radar was therefore most effective at detecting and characterising very shallow targets such as the tops of foundations or walls that lay just under the topsoil. Unfortunately, the anticipated targets appeared to elicit similar responses to the rubble matrix, both in form and amplitude.

4.3.6 Discussion

Excavations at two trenches within the Hospital Precinct uncovered several planar and linear archaeo-geophysical targets within the shallow subsurface (< 0.35 m), including:

- sandstone courtyard flagging and edging;
- brick foundations;
- brick drains; and
- a compacted dolerite gravel yard surface.

The primary obstruction to detecting these features using geophysics was the demolition rubble fill, with its heterogeneous composition of brick, dolerite and sandstone remnants, and ferrous metal artefacts - particularly in Trench 1. Interpretation of the geophysical data in the Hospital Precinct was thus only moderately assisted by archaeological ground-truthing. It did prove that point anomalies in the magnetic, EM and GPR data were derived from the iron brace and contemporary post and concrete base. Further, it also demonstrated why the brick 'v' drain was not identified in the resistivity, conductivity or the GPR (due to the masking effects of overlying demolition rubble).

Geophysical resolution of linear features was also limited by the sample spacing and line interval, which varied between techniques, and the smoothing effects of gridding. In contrast to the highly detailed (sub-centimetre) resolution of stratigraphy achieved through archaeological excavation, geophysical surveys yielded relatively low

measurement density. Ground penetrating radar profiling provided the best horizontal and vertical resolution of features, with 3 - 5 cm trace increment, continuous sampling along-line and 0.5 m line spacing. While the presented variation maps of each dataset appear continuous due to interpolation, the density of actual measurements varied according to trench position relative to the local geophysical grid. The density of original observations in a magnetic survey was 4 - 12 per square metre, while the EM-38 and Wenner array varied between 2 and 6. Further, each measurement has an investigation footprint, with different footprints corresponding to each method.

Gridding is a filtering operation and also affects the apparent continuity of the final geophysical image. Kriging, which was the most commonly used interpolation technique in this project, consistently replicates data at the observation locations, but the resulting surface has greater continuity than reality because of the smoothing effect of the process (David *et al.*, 1994). Despite the discrepancy in resolution between geophysical data and archaeological findings, useful information derived from the geophysical-archaeological correlations was extrapolated to other parts of the survey area with a moderate to high degree of confidence (Conyers and Cameron, 1998).

4.4 SUMMARY

The built environment of Settlement Hill during the penal period comprised a complex of buildings, yards and other infrastructure sited on a series of terraces excavated into the shallow dolerite bedrock. These buildings included military officers' quarters, Military Barracks and most notably the Port Arthur hospital, which was remodeled several times during the 1800s. Some of the complex was destroyed by fire in the 1890s, after which all remaining structures, except for the third hospital, were dismantled or plundered, and the site was leveled with demolition rubble and topsoil. Today, parch marks visible in aerial photographs, the terraced topography, several retaining walls, and the ruins of the third hospital provide the only surface evidence of this former built environment. Limited information is available on the material composition, dimensions, and possible depth of any subsurface archaeological features, via historic documents. The actual layout of structures is inferred, with low confidence, from maps and plans, due to a lack of suitable ground control points.

To better define these parameters and assess the archaeological potential of Settlement Hill, the site was surveyed with a magnetometer, a Wenner array resistivity configuration, and 500 MHz ground penetrating radar, and partially surveyed using an EM-38 conductivity meter. Following the geophysical study, trench excavations were conducted at the Hospital Precinct. These revealed remnants of the second hospital privies, kitchen outbuilding, a courtyard wall and brick drains. Several occupational horizons were uncovered within 0.2 m depth, including a compacted gravel yard surface, and courtyard stone paving. Material surrounding the archaeo-geophysical targets was predominately gravel-rubble fill derived from post-penal building demolition and contemporary surface levelling. This physical evidence provided ground control points for more accurate registration of the historic plans, which demonstrated that the relative building layout in the Hospital Precinct was largely intact. Both the archaeological findings and newly geo-referenced maps were then used, where feasible, to fine-tune preliminary qualitative interpretation of the geophysical data.

The Settlement Hill magnetic data was dominated by variation in response from the highly magnetic shallow dolerite bedrock, which was systematically excavated and deposited to form terrace benches for building platforms. Truncated dolerite along the terrace retaining walls were defined by steep magnetic gradients and rectilinear zones of high magnetic values, while the benches of deposited dolerite rubble were characterised by high average values superimposed by irregularly distributed high frequency, high amplitude magnetic intensities. The penal-period aqueduct trench was detected as a well-defined linear zone of very low magnetic intensities, which indicated that the dolerite substrate had been deeply excavated. Its position, from the Upper Slope, through the main terrace between the Hospital Precinct and Chaplain's quarters, toward the Penitentiary, correlated closely with the historic plans. Two other low magnitude linear zones in the Hospital Precinct were attributed to previously undocumented trenches, and interpreted as penal period drainage features.

Brick and dolerite architectural targets on Settlement Hill were difficult to map due to a low magnetic contrast with the surrounding fill material, broad area undesirable signal from the dolerite basement, and displacement error derived from the data collection methodology. Closely spaced high frequency point responses derived from the bench fill and demolition rubble tended to mask discrete or linear anomalies caused by brick structural features such as hearths and foundations.

With respect to the other geophysical techniques, responses from the demolition rubble and dolerite bench fill proved to be both sources of desirable and undesirable signal. In GPR, apparent resistivity and conductivity data from the Hospital Precinct, the distribution patterns of responses from demolition rubble deposits clearly discriminated the generally resistive second hospital and courtyard areas from the more conductive third hospital yard. This was particularly well-defined in the VCP mode conductivity variation map and in GPR timeslices generated > 2 ns TWTT.

Undesirable signal from the complicated near-surface stratigraphy also made it difficult to establish benchmark responses from well-preserved architectural targets within the trenches. This limitation was compounded by a significant difference in data resolution between the highly detailed archaeological excavation and the relatively sparsely

sampled geophysics - especially the conductivity and resistivity surveys. Despite this limitation, numerous linear trends and zones of interest were identified in data from within the second hospital building and courtyard, which appeared to correlate closely with the excavated privy foundations (conductivity), courtyard stone paving (resistivity and GPR) and oblique-trending boundary wall (resistivity), and hearths (GPR).

Sources of randomly-distributed resistivity and GPR point anomalies were typically uninterpretable, due to the ambiguity between responses from *in situ* masonry in poor condition, demolition rubble and dolerite bench fill. This uncertainty was demonstrated through comparison between the ground-truthing findings and geophysical data collected within the trench area. Discrete coincident conductive and magnetic point sources that did not correspond directly to surface features (e.g. metal-hinged aqueduct access hatch) or indirectly to targets inferred from maps and photographs were attributed to ferrous objects of unknown origin. Occasional close correlation between an apparent conductivity anomaly and high amplitude GPR diffractions suggested the presence of buried metal.

The third hospital's yard area was characterised by three prominent curved lineaments, mapped by the VCP mode conductivity survey, Wenner array and GPR profiling. Two of the lineaments, coincident with parch marks in contemporary aerial photographs, were attributed to garden beds bordering a path that formerly ran between the sandstone steps and third hospital northern (front) entrance. Adjacent zones of very high apparent resistivities, also recorded as high amplitude planar reflections in the GPR, were derived from a thin layer of demolition rubble, inferred via extrapolation of the ground-truthing results. The third lineament, which also originated at the steps, crossed the inferred pathway and wound onto the Upper Slope towards the south. This was clearly defined in the GPR timeslices and resistivity variation map as a relatively low resistivity anomaly. Excavations over a small portion of this feature showed it to be a very fine crushed brick deposit overlying the inferred penal period gravel surface. These findings strongly suggested that this feature was a post-penal or contemporary pathway, rather than a filled-in trench as originally interpreted from the geophysics.

Response patterns in the remaining areas of Settlement Hill were considerably less complicated than at the Hospital Precinct, which allowed for better detection and characterisation of *in situ* architectural elements. Moderately high amplitude rectilinear anomalies in the GPR timeslices were clearly defined against relatively neutral background values along the main terrace. These correlated closely to the layout of building foundations, yard and terrace retaining walls depicted in historic maps, which indicated a high archaeological potential in this area. Coincident lineaments in the apparent resistivity variation map, further suggested that these features were well-preserved, very shallow, and covered by a relatively thin layer of fill material.

A paucity of non-random anomaly patterns in geophysical data collected from the Upper and Lower Slopes indicated that little remained of the few structures erected here. Strong responses in the magnetic, resistivity and GPR data were primarily due to collapsed and/or *in situ* remnants of the terrace retaining walls, and previously unmapped linear features such as a drainage trenches. The brick-lined aqueduct was not successfully detected by the GPR.

Chapter Five: Penitentiary Complex

5.1 INTRODUCTION

The 'Penitentiary Complex' incorporates two survey areas: the Penitentiary Parade Ground, and Sawpit and Tannery Complex, located either side of Radcliffe Canal (Figure 5.1). Together with the adjacent workshops, the Penitentiary Complex infrastructure and yard spaces formed the heart of the Port Arthur settlement - supporting a hub of activity into the late 1800s. During the penal period, the two areas were linked by a tramway which ran from the Sawpits southern end, through the Parade Ground area, and eastward to the Commissariat Stores. Unfortunately, there is no remaining surface evidence of this tramway, or the Sawpits and Tannery Complex, and few of the Parade Ground structural features except for the ruined Penitentiary and a section of the western enclosure wall. While the sequence of land use and development detailed by the PAHSMA portfolio of maps and plans are clear in general terms, there are some discrepancies between documents. This is exacerbated by a lack of suitable ground control points, which means that maps may not be geo-referenced accurately.

In contrast to the Isle of the Dead and Settlement Hill survey areas, archaeological and geophysical research had been conducted at the Penitentiary Complex prior to this study. Multi-technique surveys were undertaken at the Sawpits in 2001 - 02, using FEM, magnetometry and Wenner array apparent resistivity mapping (Dorn, 2002; Dorn *et al.*, 2002). Data from these surveys exhibited anomalous response patterns that correlated to the pit area, foundation walls and fill deposits, as inferred from historic plans and photographs, and parch marks defined from infra-red aerial photography. Subsequent archaeological ground-truthing of selected anomalies (Owen and Steele, 2002) exposed some of the primary structural targets - although not always in the locations identified through the geophysical interpretation.

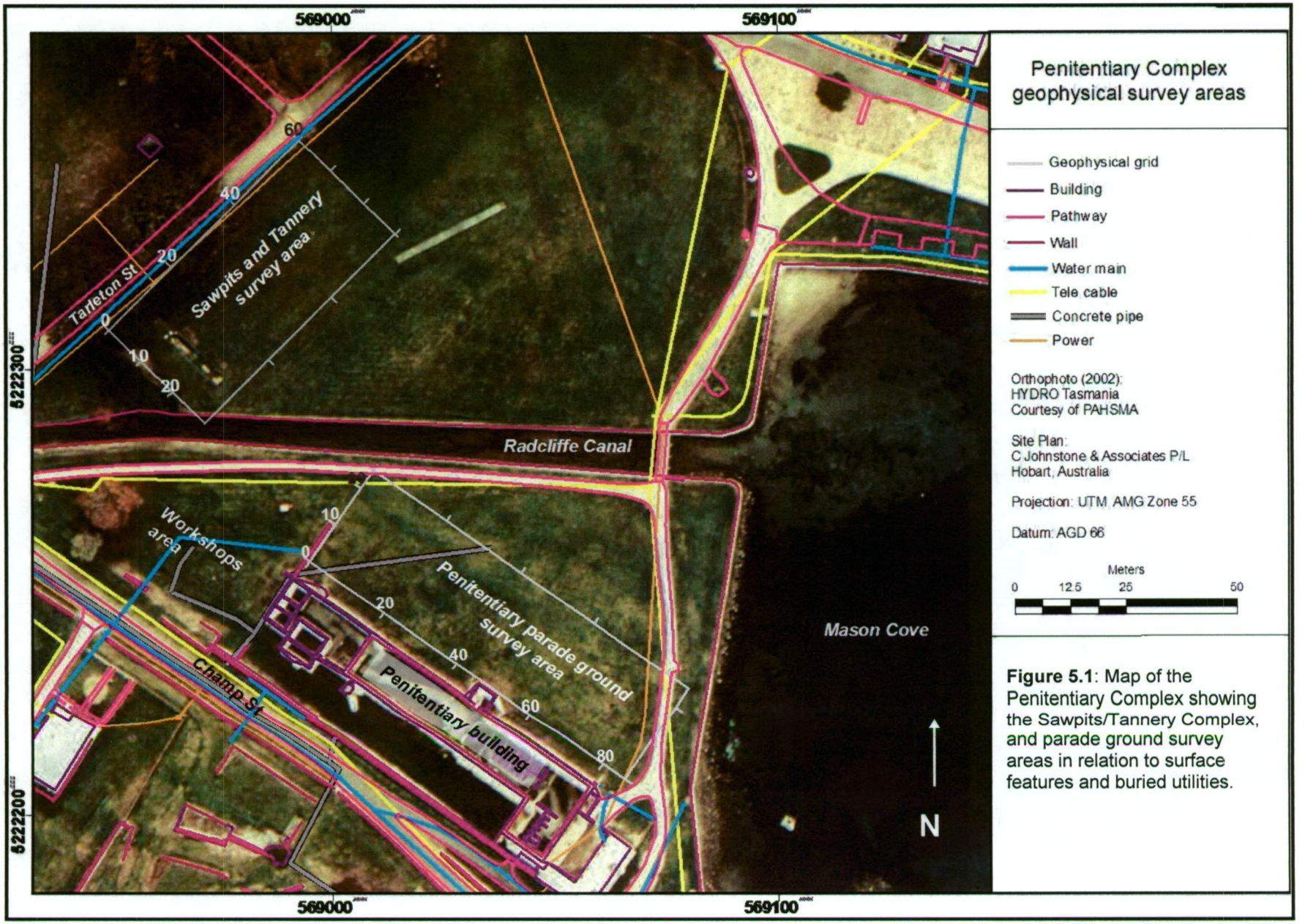

Figure 5.1: Map of the Penitentiary Complex showing the Sawpits/Tannery Complex, and parade ground survey areas in relation to surface features and buried utilities.

Limited archaeological excavations at the Penitentiary foreground yielded some evidence of the penal period enclosure wall and the Parade Ground gravel surface, buried within a multi-layered stratigraphy of shallow contemporary levelling deposits and the deeper reclamation rubble fill (Steele, 2004).

Geophysical surveys conducted at the Penitentiary Parade Ground and Sawpits area aimed to assess the effectiveness of multiple techniques for the detection and characterisation of features associated with the reclamation of Mason Cove and site use during the penal period. At the Sawpits area, ground penetrating radar profiling and electrical resistivity tomography were applied to provide information in the vertical plane, to complement the planimetric views derived from other geophysical techniques (Dorn *et al.*, 2002). A multi-technique approach was applied at the parade ground area, comprising GPR, magnetometry, and apparent resistivity mapping. Data interpretations will be presented in a format accessible to non-geophysicists, via 'archaeological potential maps' of the Penitentiary Complex. It is hoped that these may be used for the targeted cultural resource management strategies of PAHSMA.

This section will first define the site context in terms of geology, physiology, and historical land use, and summarise the excavation findings. Surface features of geophysical significance and anticipated archaeological targets will then be discussed. The chapter body will describe the survey methodology and processing techniques used to create maps of different geophysical parameters at the Penitentiary Complex. Findings from each survey are discussed broadly while significant anomalies and trends are characterised and interpreted in detail. Data maps from previous studies at the Sawpits area are presented in Appendix C (Dorn *et al.* 2002).

5.1.1 SITE GEOLOGY AND PHYSIOLOGY

The Penitentiary Complex local geology is defined by shallow Quaternary remnant beach sands and transported fines, and deeper Jurassic dolerite bedrock (Figure 1.2). This lithology provides a markedly contrasting geophysical environment to the shallow doleritic domain at Settlement Hill and the Permian sandstone-siltstone on the Isle of the Dead.

Both the Sawpits and Parade Ground grids are located on land reclaimed from Mason Cove. Progressive modification of the natural foreshore during the penal period created a near-level platform 1 - 2 m above mean sea level, on which buildings and yard spaces were constructed. Local archaeological excavations have demonstrated that, following decommissioning of the site in the 1870s, this platform was raised slightly through the deposition of demolition rubble fill and contemporary levelling material. These deposits are typically comprised of varying ratios of dolerite and sandstone ranging from fine fragments to coarse rubble, intermixed with loam, sand and/or clay (Owen and Steele, 2002; Steele, 2004a; Steele, 2004b).

5.1.2 GEOPHYSICAL SURVEY AREAS

Two local geophysical grids were measured out by PAHSMA, using conventional optical surveying techniques. The Sawpits and Tannery complex grid (60 m x 30 m) was positioned coincident with the 2001 – 02 trial geophysical survey area, with the datum (0x, 0y) located in the southwest corner and long axis parallel to Tarleton Street (Figure 5.1). The Penitentiary Parade Ground grid (25 m x 86 m) was positioned to encompass the parade ground and tramway, anticipated enclosure wall locations and a perimeter several metres wider than the features of interest. Local grid co-ordinates were transformed to the AMG reference system for planimetric data presentation. The Penitentiary Complex provides excellent conditions for geophysical surveying, due to near-level topography, and no obstructions or vegetation apart from the grass surface.

5.1.3 POTENTIAL SOURCES OF GEOPHYSICAL NOISE

Anticipated sources of geophysical noise and problems at the Parade Ground are primarily cultural and located above-ground or in the near-surface. These may include a contemporary buried concrete pipe, power and telephone cables, the approximate locations of which are shown in Figure 5.1. A dry compacted clay path was also known to restrict resistivity measurements in the grid's north-eastern corner, by not allowing sufficient contact between the electrode and ground (Dorn *et al.*, 2002).

Demolition rubble fill of heterogeneous composition, such as used for site levelling at the Workshops (Jackman, 2005) is also a potential source of noise in the GPR and

magnetic surveys. Penal-period reclamation material and the weathered dolerite substrate may hamper detection of the Parade Ground gravel surface by the magnetometer. Surface metallic debris, and iron fixtures associated with the penitentiary structure are also sources of magnetic noise. The modern clay path and natural tidal influx of conductive seawater also have the potential to attenuate ground penetrating radar radio waves - potentially inhibiting the detection of historic reclamation features at depth.

5.1.4 A NOTE ON THE HISTORICAL CONTEXT

Most of the information provided here derives from historical documents compiled by PAHSMA. Archival materials, such as photographs from the penal period, provide textural and pictorial accounts of development at each survey area within the Penitentiary Complex. Rectified historic maps of Port Arthur, including the schematic Hurst (1846) and Blackwood (1877) plans were used as guides to the built landscape. Unfortunately, the accuracy and reliability of this information is compromised by original scaling errors, distortions produced by scanning/copying (probably minor) and errors from a lack of accurate ground control points during rectification.

5.2 Penitentiary Parade Ground

5.2.1 Historical context

The development of the Parade Ground area is intrinsically linked to land use of the Mason Cove waterfront during the penal period. The southern foreshore of Mason Cove was reclaimed early in the penal period for construction of a wharf, which became a focal point for the transportation of goods and persons. By 1846, a flour mill and granary had been constructed on the waterfront, east of the workshops (Figure 5.2).

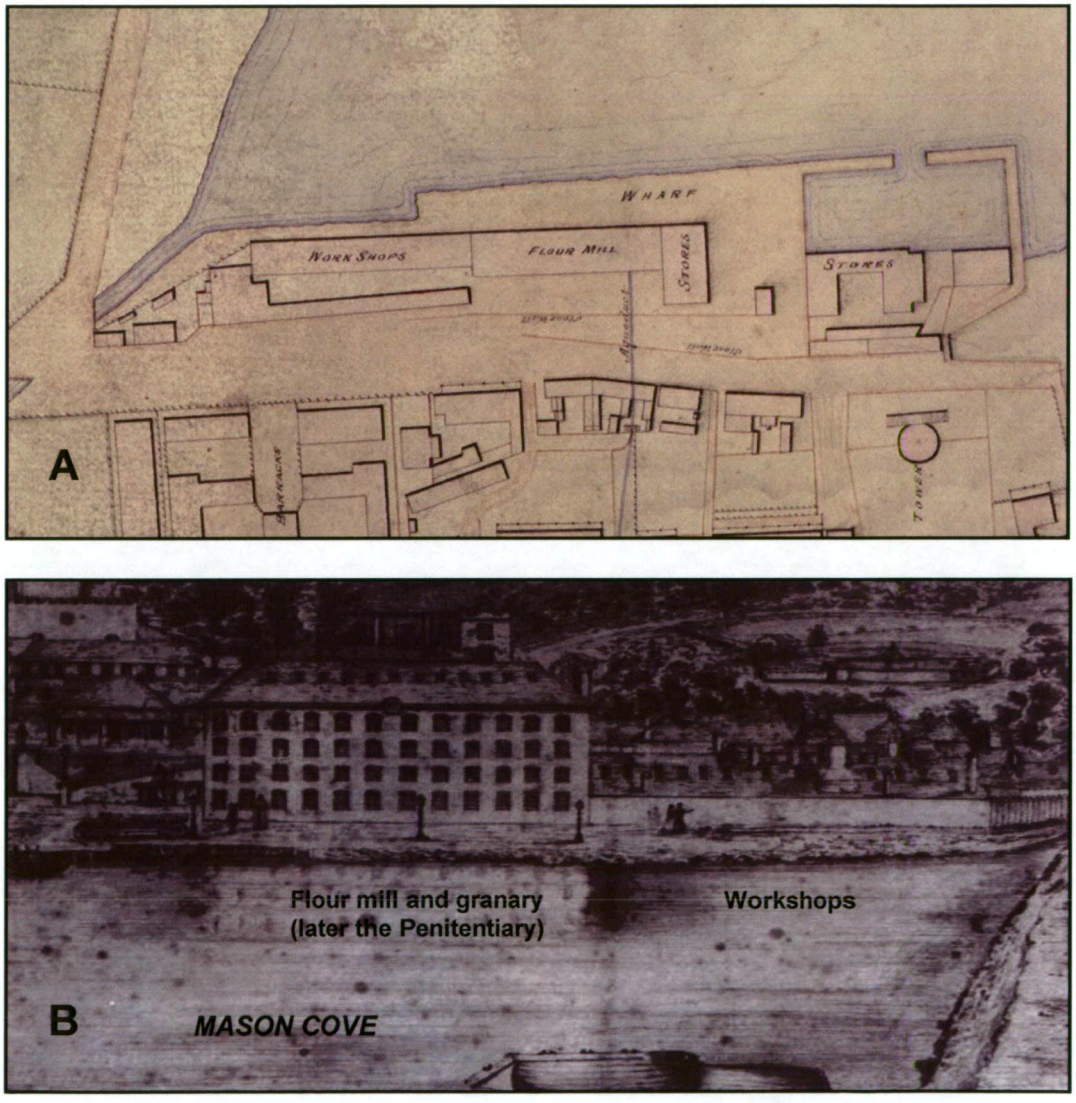

Figure 5.2A and B: Detail of the Hurst plan c1846 (**A**) and sketch (**B**) of the flour mill and workshops northern façade on the partly reclaimed southern shore of Mason Cove. The Parade Ground and Radcliffe Canal were not yet constructed (courtesy of PAHSMA, ref. 1352 (**A**); ref. HM 1846/1 (**B**)).

Conversion of these buildings into the convict Penitentiary in 1852 - 55 necessitated further reclamation of the cove in 1854 – 55, to provide more structural stability and a space for military use as a Parade Ground. The reclaimed area further north was used as an overflow area for storing timber awaiting trans-shipment (Richard Tuffin, pers. comm. 2005). By 1860, the Parade Ground comprised a large gravelled square bisected by a tramway which ran from the saw mill to the Commissariat Stores, and a low masonry wall skirting the northern side. By 1863, eastern and western enclosure walls had been constructed, each with an opening (Figures 5.3 and 5.4). A gateway and a square-platform sandstone drinking fountain were erected in the northern wall during the late 1860s (Steele, 2004).

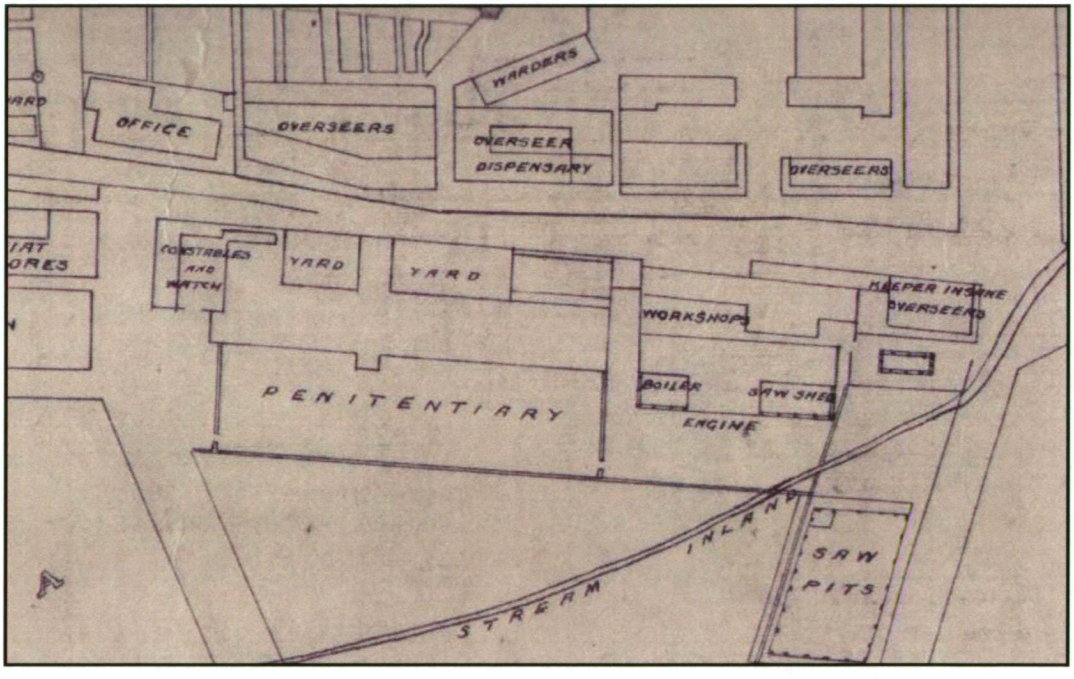

Figure 5.3: Schematic map of the Penitentiary, Workshops, Sawpits and final reclamation of Mason Cove (c1863). At this stage the Parade Ground (misleadingly labeled the 'Penitentiary') had only western and eastern entrances (courtesy of PAHSMA, ref. HM_PWD #6154).

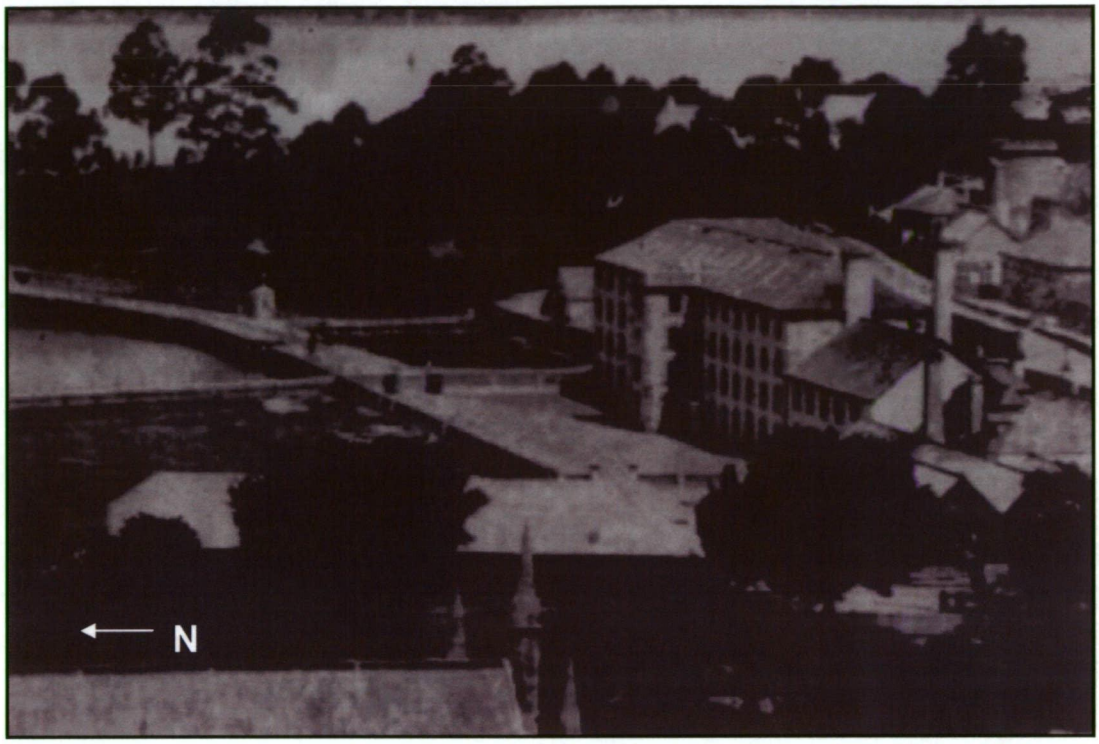

Figure 5.4: Portion of a photograph showing the Penitentiary and enclosed Parade Ground c1865– 68 prior to the installation of the northern gateway (courtesy of PAHSMA, ref: #2381).

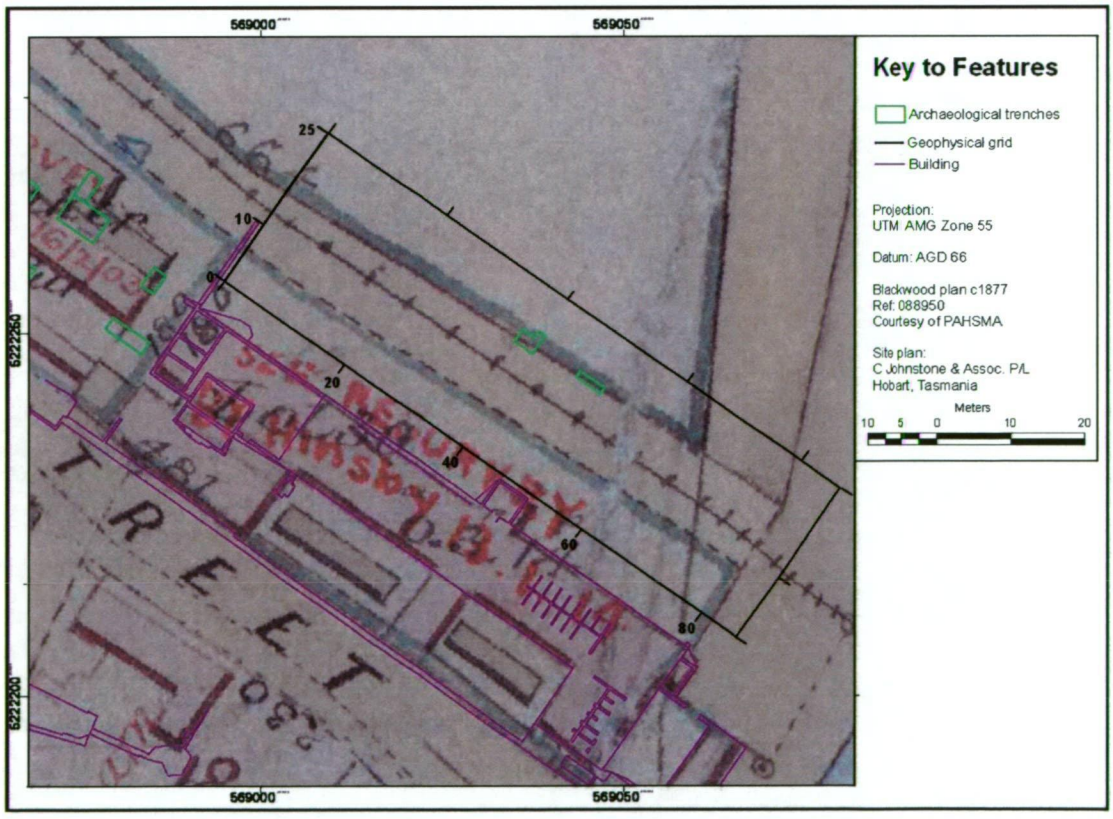

Figure 5.5: The Penitentiary Parade Ground geophysical survey area, trench locations and the Blackwood plan c1877 (courtesy of PAHSMA, ref: HM C/19A).

Following site decommissioning, the area deteriorated and the enclosure walls were dismantled and sold or plundered. The fountain was relocated to another part of the Port Arthur site and the grounds were used for a variety of other functions relating to the post-penal period. Tennis courts and a shed were erected to the northeast of the Penitentiary in the early 20th century, and in the 1960s – 80s a caravan park was located in the former parade area (Tuffin, 2003). Today the site is simply grassed (Figure 5.6).

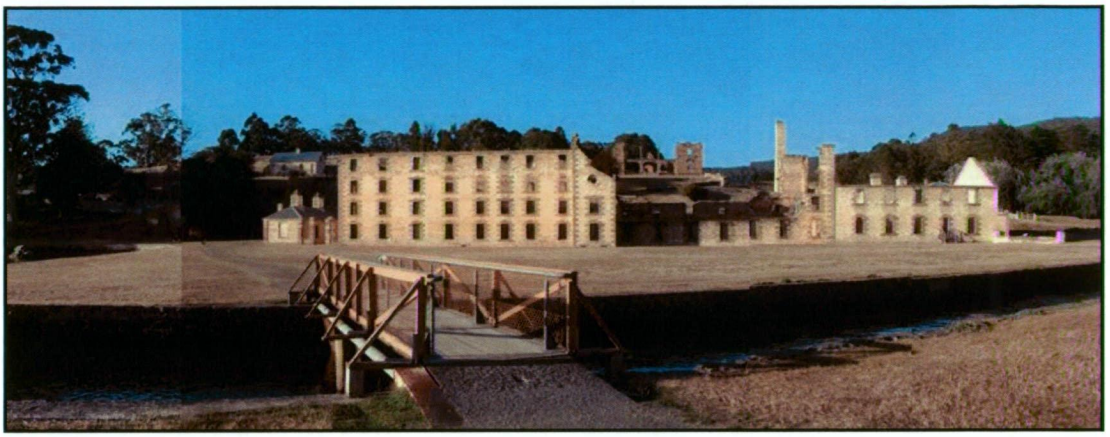

Figure 5.6: Panoramic photographic montage of the Penitentiary Parade Ground from the northern side of Radcliffe Creek canal. The Penitentiary ruins clearly dominate the built environment. The ruins of the third hospital may be seen in the background, on Settlement Hill (photographs courtesy of David Roe, 2003).

5.2.2 ARCHAEOLOGICAL CONTEXT

5.2.2.1 Background

Just prior to the geophysical survey, excavations were conducted at the Penitentiary Parade Ground by PAHSMA during the Summer Archaeology Program of 2003 - 04, with the aim to 're-establish the location of the boundary wall to the parade ground and identify the original location of the water fountain' (Steele, 2004). Historic maps, panoramic photographs, and aerial photographs (historic and contemporary) were used to infer feature locations and therefore guide the placement of two trenches for optimal target detection. Figure 5.7 presents the trench siting with reference to the local geophysical grid, rectified schematic Blackwood map c1877, and the Penitentiary as it stands today.

The excavation results were used to guide qualitative interpretation of magnetic, resistivity and ground penetrating radar data collected at the Penitentiary parade ground. The following section provides a summary of those archaeological findings and interpretations relevant to the geophysical investigation objectives. All information is derived from the archaeological report compiled by Steele (2004). Figures from the report have been modified by the author to illustrate the archaeological context relevant to the geophysical study. The author did not assist in these excavations.

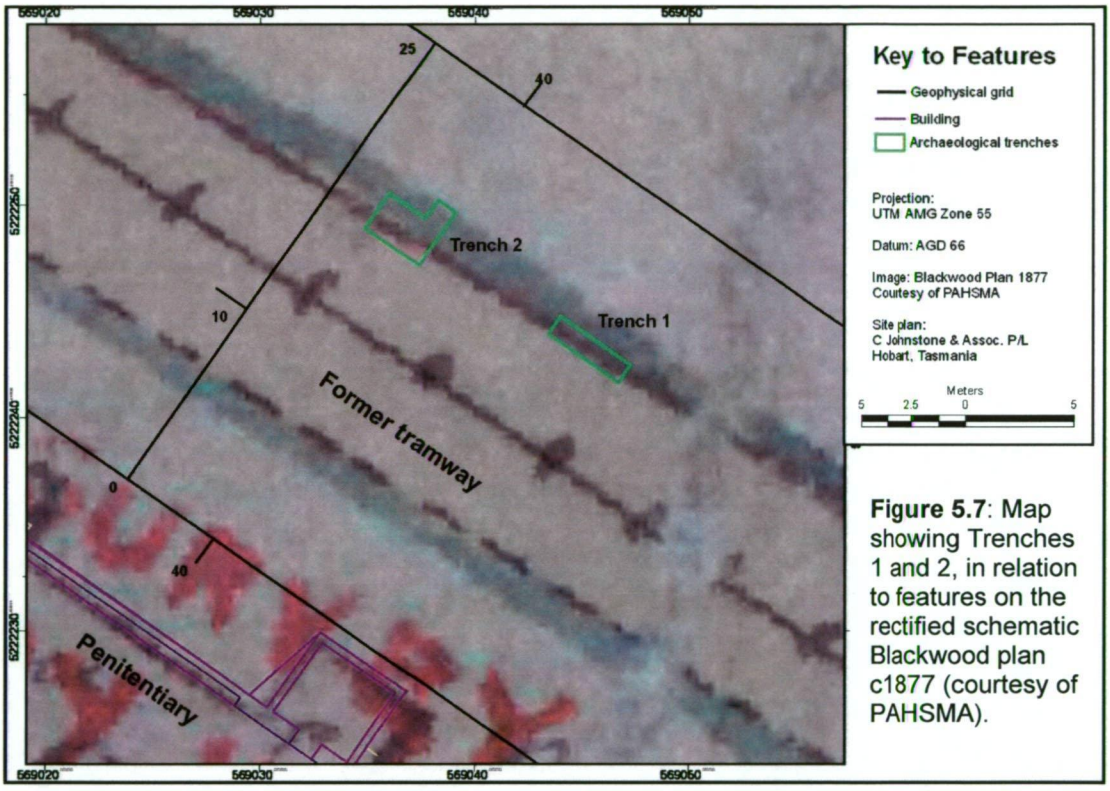

Figure 5.7: Map showing Trenches 1 and 2, in relation to features on the rectified schematic Blackwood plan c1877 (courtesy of PAHSMA).

5.2.2.2 Excavation findings and interpretation

Trench 1

Trench 1 (4 x 1 m) was sited over the inferred location of a gateway in the parade ground northern wall (Figure 5.7). Removal of the turf and fine sandy loam subsoil revealed a layer of sand used in the 1980s to level localised subsidence (Steele, 2004). Excavation then uncovered a loam horizon and two gravel layers with dolerite and brick fragments, which increased in coarseness and compaction with depth (Figure 5.8, **A**). Both gravel layers were attributed to the post-penal to contemporary periods, when the Parade Ground was used for tennis and later, a camping area (Steele, 2004).

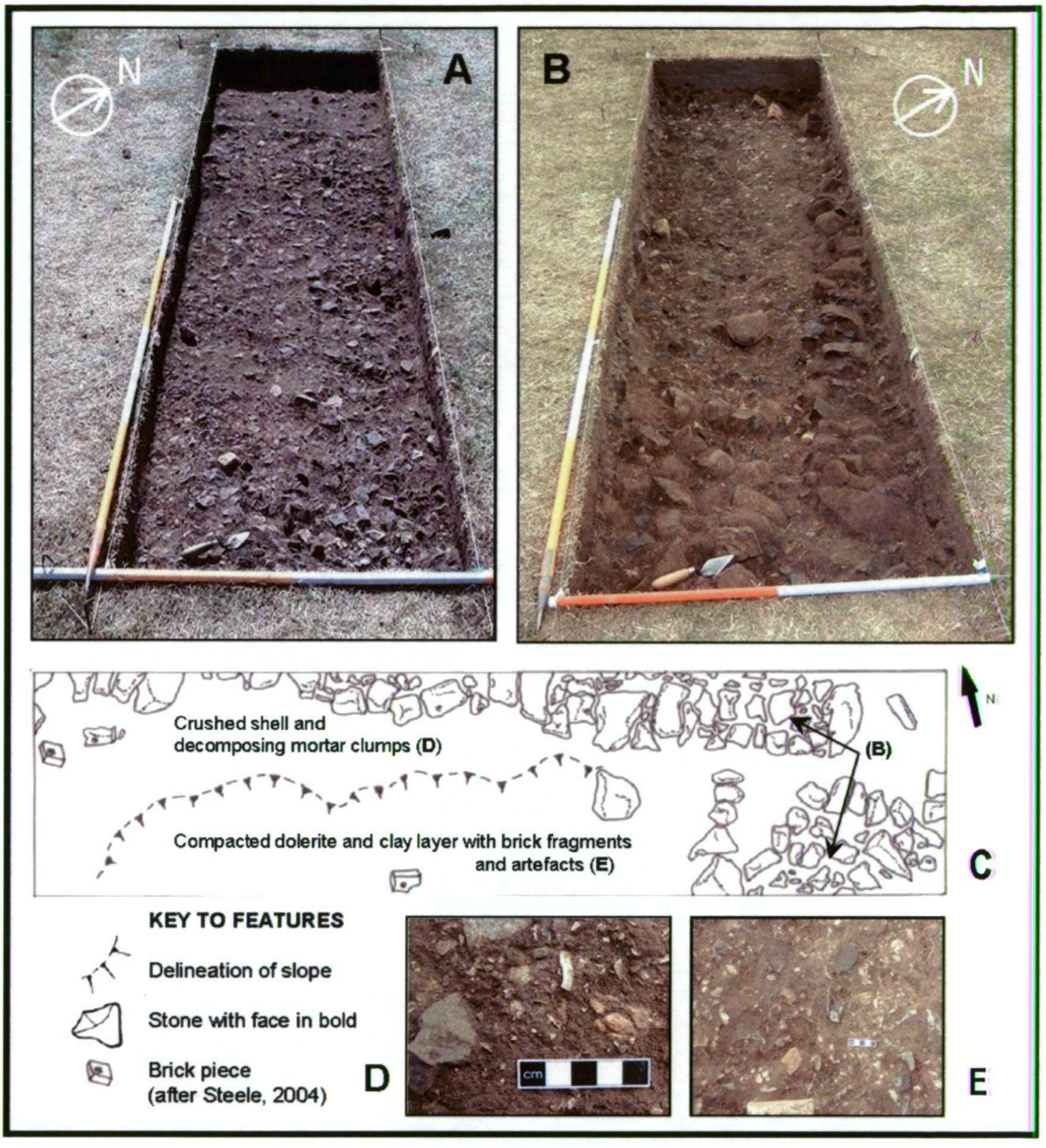

Figure 5.8: Trench 1 photographs and archaeological plan, showing shallow fill deposits dominated by doleritic rubble. Annotated details of this figure are discussed in the text (after Steele, 2004).

Deposits in the northern half of the trench, exhibited varied composition and distribution patterns. A 0.3 – 0.4 m wide lens of crushed shell, decomposing mortar clumps and artefacts (Figure 5.8, **D)** was associated with the enclosure wall construction. Scattered dolerite pieces measuring 0.15 - 0.18 m in diameter (Figure 5.8, **B**) were also revealed, and interpreted as post-penal fill material. In the southern section, a compacted artefact-rich clay layer with dolerite and brick fragments (Figure 5.8, **E**) was exposed and inferred as the convict period yard surface. The spatial relationships between these contexts are illustrated in plan view in Figure 5.8, **C**.

Removal of these varied deposits uncovered silt-sand soils and direct evidence of the northern enclosure wall - a primary archaeo-geophysical target. Five sandstone foundation blocks (with the mortar on top) were located under the dolerite rubble fill in the western end (Figure 5.9, **A**). These were abutted by sandy clay deposits (0.05 - 0.1 m thick) with varying concentrations of sandstone fragments, some of which suggested a working surface for cutting and refining of the foundation stones (Steele, 2004). A basic dolerite and clay fill was recorded under the inferred wall, indicating that the stones were probably part of the base course. Partial removal of these contexts from the trench's western end (via a sondage - a deeper excavation within the original trench area) revealed a moist clay deposit, with dolerite and sandstone fragments, that archaeologists linked to the original Mason Cove reclamation process (Figure 5.9, **A**). The final excavation plan is presented in Figure 5.9.

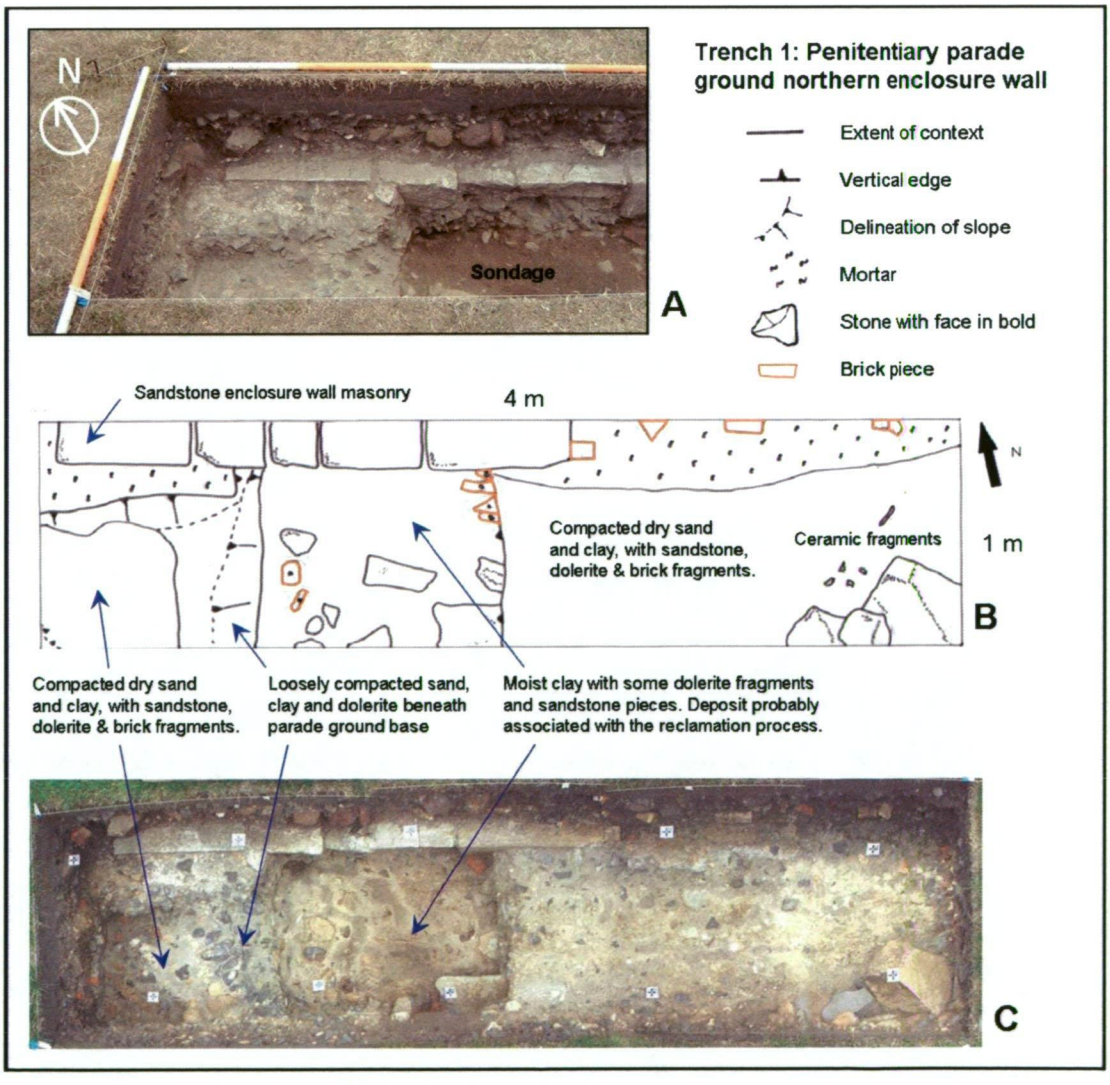

Figure 5.9: Trench 1 final excavation plan and photographs. Annotated details of this figure are discussed in the text (modified after Steele, 2004).

Trench 2

Trench 2, initially measuring 3 x 2 m, was sited to uncover the former location of the late penal period sandstone fountain located in the parade ground northern enclosure wall (Figures 5.7 and 5.12). The shallow stratigraphy of trench 2 was similar to trench 1, comprising a sandy loam turf subsoil (~ 0.1 m thickness) which increased in compaction with depth, deposits of levelling sand and compact loamy soil with dolerite, brick and sandstone fragments (Figure 5.10, **A**). At this stage, sandstone masonry was exposed in the western end, which was attributed to the penal period drinking fountain platform base (Steele, 2004).

Removal of the sandy loam and levelling sand horizons exposed a deeper deposit inferred as the penal period yard surface (Figure 5.10, **B**). This compacted horizon was composed of dolerite, brick and friable sandstone gravel (~ 50 mm average diameter) in a fine soil matrix. In the northern half of trench 2, the compacted loamy fill also included dolerite, brick and friable sandstone fragments, although they were much smaller in average diameter. The gradual thickening of levelling sand to the northeast (Figure 5.10, **B**), indicates subsidence of deeper reclamation material (Steele, 2004). Fill layer thicknesses are shown in section in Figure 5.10, **C**.

Excavation of a 2 x 1 m sondage in the original trench centre revealed new deposit types and stratigraphic relationships along the trench's long axis. The inferred yard surface (Figure 5.10, **B**; Figure 5.11, **b**) was abutted by a highly compacted shell-rich deposit (Figure 5.11, **d**) interpreted as a mortar surface for the enclosure wall (Steele, 2004). Partial removal of this mortar exposed some compacted rubble fill (Figure 5.11, **c**) - believed to extend throughout the southern half (i.e. inside the parade ground) - and a soil layer with some artefactual material. No physical evidence of the enclosure wall was found, although the mortar deposits and fountain base indicated its likely position. A trench extension was therefore added to ascertain whether any wall structure remained to the north. As expected, the extension contained similar stratigraphy to the main trench. It also had a decaying shell mortar deposit similar to (**d**), which was underlain by the clay and crushed sandstone rubble fill (**c**) - interpreted as a possible building or working layer (Steele, 2004). Excavation ceased at this point, when it became obvious that no wall structure remained in this section.

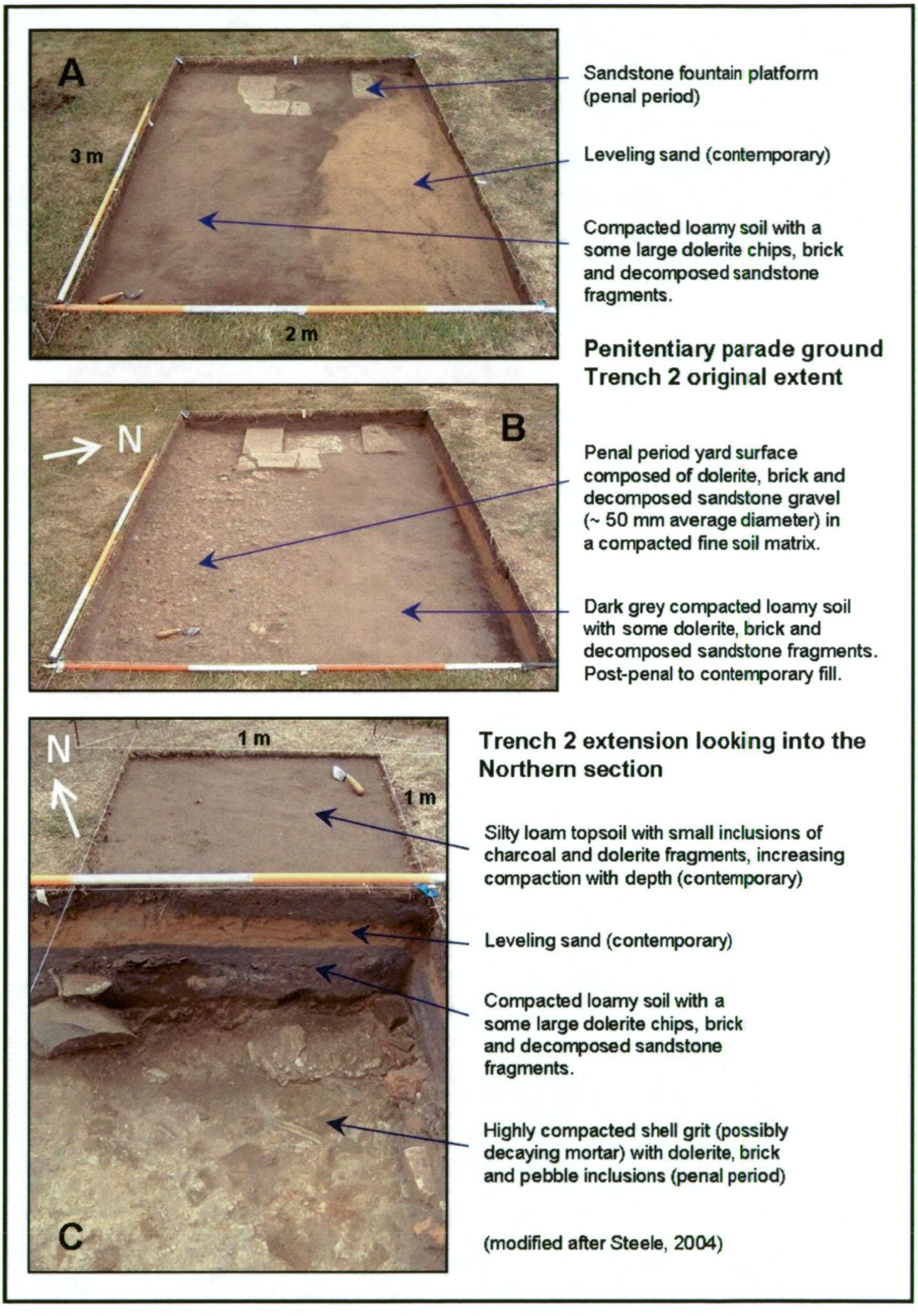

Figure 5.10: Photographs of Trench 2 showing the near-surface contemporary fill material and evidence of the sandstone drinking fountain platform (**A**), underlain by a penal period yard surface and further levelling soils (**B**). An extension in the NE corner shows the relative thickness of these horizons, and final excavation down to the top surface of penal period compacted mortar deposits (**C**) (modified after Steele, 2004).

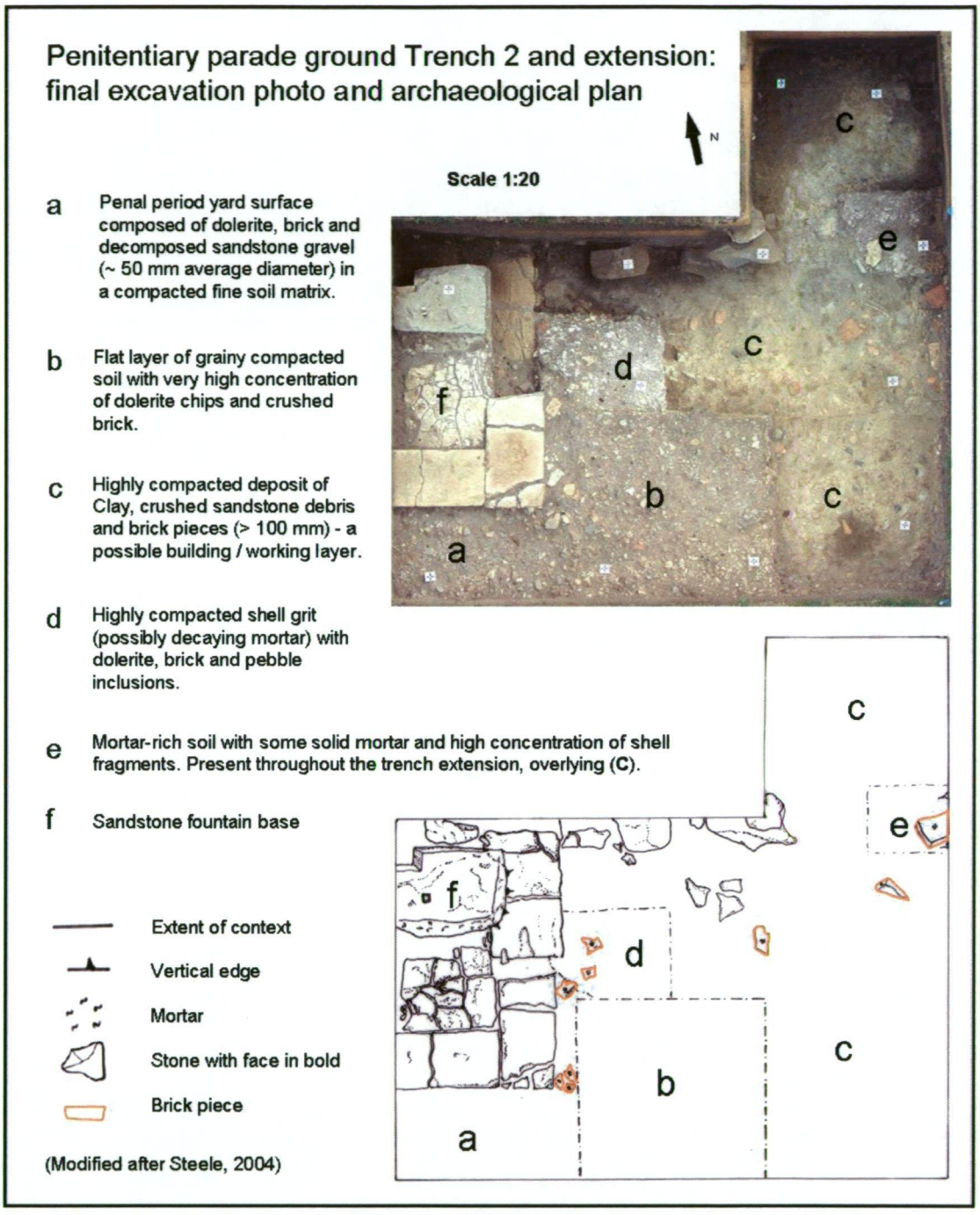

Figure 5.11: Final excavation photograph and archaeological plan of Trench 2 with extension, showing penal period contextual information (modified after Steele, 2004).

5.2.2.3 Summary

Excavations at two trench sites positioned over the parade ground northern boundary revealed limited physical evidence of the penal period enclosure wall. Five sandstone foundation masonry blocks in Trench 1, and mortar deposits in both trenches were indicative of the intra- and inter-trench wall alignment. Highly compacted dolerite, brick and sandstone gravel material south of the wall provided clear evidence of the parade ground yard surface. Selective excavations to 0.4 - 0.5 m depth in the trench centre uncovered moist clay containing relatively few artefacts, which was interpreted as evidence of the reclamation fill.

From a geophysical perspective, the near-surface Penitentiary Complex stratigraphy was very similar to the Settlement Hill hospital precinct, which proved to be a challenging environment for the mapping of archaeological targets. Excavated features of interest were either non-existent or exhibited variable material condition. Further, they were located within multiple layers of fill of heterogeneous composition, some of which were highly compacted. Responses from the parade ground gravel yard surface were expected to be dominated by noise from the dolerite fragments and rubble pieces. Highly compacted sandy horizons may produce similar apparent resistivity values and GPR amplitudes to sandstone masonry, while deposits with a clay matrix will most likely affect the optimal investigation depth of both techniques.

5.2.3 ARCHAEO-GEOPHYSICAL TARGETS

Primary geophysical targets at the Penitentiary foreground include cultural elements associated with the penal period Parade Ground, and the reclamation of Mason Cove. These are inferred from the archaeological findings, historic plans, photographs and surface evidence, and are listed below:

- Parade Ground enclosure walls (sandstone),
- tramway (iron rails, wooden sleepers),
- southern boundary of tramway (refer to Blackwood plan c1877),
- Parade Ground surface (dolerite gravel),
- drinking fountain (sandstone), and
- reclamation features and former shoreline.

Buried remnants of cultural elements associated with post-penal and contemporary site use, such as paths and tennis courts, are archaeo-geophysical features of secondary importance. Target locations, as inferred from historic plans, photographs, and surface evidence (including Figures 5.12 to 5.14), are shown in Figure 5.15. Spatial and contextual discrepancies between inferred feature locations are due to numerous factors, including the accuracy of each source and error margins associated with rectification (refer to Chapter 4, Section 4.1). The schematic 1877 Blackwood map (Figure 5.5), for example, shows the approximate location of a single tram line, while parch marks visible in a contemporary aerial photograph (Figure 5.15) suggest that two tramways ran through the parade ground - possibly not active at the same time.

The (possibly main) tramline location is inferred, with a high degree of confidence, from historic photographs of the Parade Ground return walls and their gateways. Originally positioned between the 4th and 5th pillars when the area functioned as a 'General Parade and Exercise Ground' during the 1860s (Figure 5.12), the side entrances were relocated towards the Penitentiary to accommodate the tramway in the early 1870s (Figure 5.13).

Material characteristics of the archaeo-geophysical targets were also gathered from surface evidence and historic sources (e.g. Figure 5.12). Owen and Steele (2002) report that the tramway had iron rails, which were presumably fixed to wooden sleepers. While the exact method used to reclaim part of Mason Cove is unknown, it is thought that a series of timber pens were built during low tides and progressively filled with doleritic stone rubble and sandy loam (Greg Jackman, pers. comm. 2005).

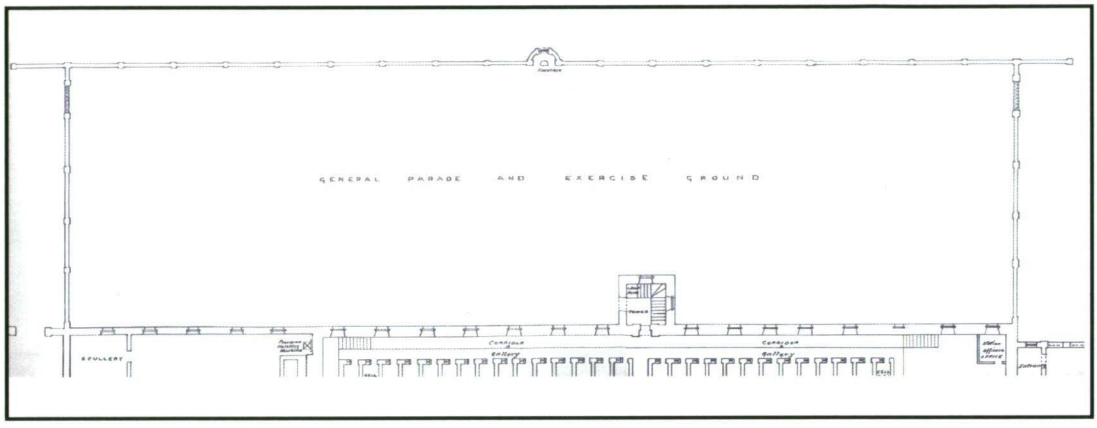

Figure 5.12: Survey of the completed modified 'GENERAL PARADE AND EXERCISE GROUND' in the Penitentiary foreground c1867, with the sandstone drinking fountain and closure of the northern gateway, and openings in the return walls (courtesy of PAHSMA, ref: PWD #6137).

Figure 5.13: A cropped photograph of the Penitentiary eastern façade and (largely intact) eastern Parade Ground enclosure wall taken from the former Commissariat Stores site during the post-penal period (courtesy of PAHSMA, ref. #66 – 1044).

Figure 5.14: The Parade Ground sandstone drinking fountain and sandstone platform, now located at another part of Port Arthur (photograph courtesy of Steele, 2004).

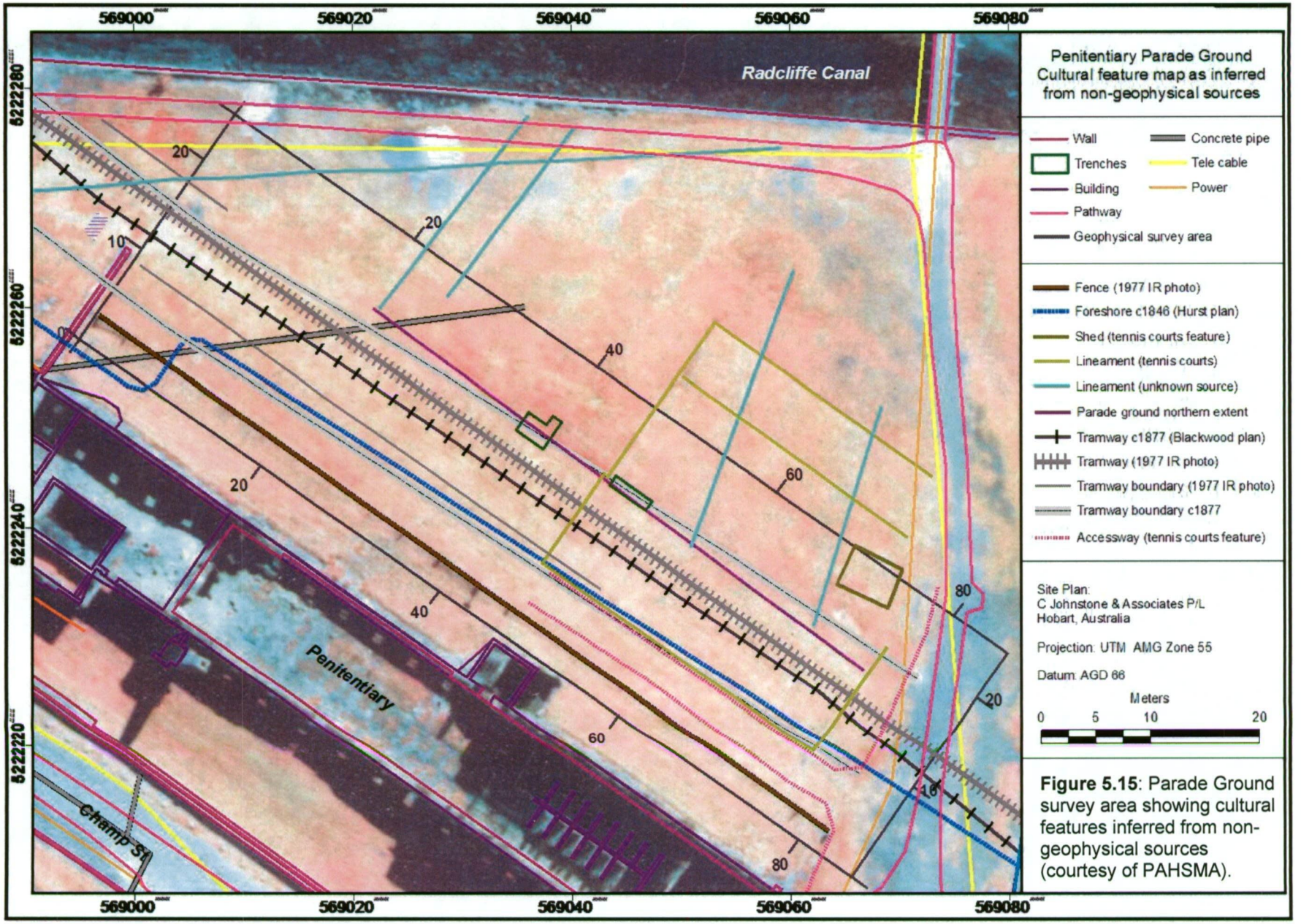

Figure 5.15: Parade Ground survey area showing cultural features inferred from non-geophysical sources (courtesy of PAHSMA).

5.2.3 GEOPHYSICAL SURVEY, FINDINGS AND INTERPRETATION

5.2.3.1 Introduction

Three geophysical techniques were employed to study the archaeological landscape of the Penitentiary parade ground survey area: magnetometry, ground-penetrating radar and electrical resistivity. Survey data for each technique were initially qualitatively assessed independent of other geophysical results and archaeological findings. The archaeological data were not available during geophysical data acquisition, processing and preliminary interpretation. No numerical (quantitative) interpretation has been conducted on these data. Recognition and interpretation maps were created according to the criteria established in Chapter 3. When the archaeological reports became available, all geophysical datasets were comprehensively re-assessed and final interpretation maps produced.

This section describes the survey methodology, data processing and analysis, and discusses the findings and final comprehensive interpretation. Selected geophysical imagery and interpretation maps are included in the text.

5.2.3.2 Magnetometry

The variation in magnetic field intensity across the Penitentiary parade ground was mapped in an attempt to detect any surviving remnants of the tramway iron rails, the muster yard gravel surface, and evidence of foreshore reclamation. Anomalies due to buried ferrous objects attributable to unknown sources were also mapped.

Data acquisition and processing

The survey was conducted over two days in June 2004, during a period of stable ionospheric magnetic conditions. The magnetometer sensor was secured to a wooden trolley to maintain a constant height of 0.15 m above the ground (Figure 5.9), thereby maximising detection of shallow small features (Clark, 1997). Data acquisition parameters are shown in Table 5.1.

Survey type	Magnetic		
Instrumentation	GEM systems GSM-19F Overhauser magnetometer		
Area surveyed	93 x 25 m (2325 m^2)		
Method of coverage	Continuous surveying along transverse gridlines		
Traverse interval	1.0 m	**Sensor height**	0.15 m (sensor centre)
Station interval	0.2 m	**Output units**	Nanotesla (nT)
Distance trigger	Time	**Sensitivity**	0.1 nT
Comments	Removal of metallic objects on surveyor and surface metallic debris on site prior to survey. Base station data for Hobart provided by Australian Government IPS Space and Radio Services www.ips.gov.au. Reading interval 1 sec.		

Table 5.1: Tabulated magnetic data collection parameters for the Penitentiary parade ground.

Figure 5.16: Photograph of the author conducting the Penitentiary Parade Ground magnetic survey, with the sensor mounted to a wooden trolley (Links, 2004).

The raw magnetic data required several stages of processing to remove or reduce the effects of noise, and image enhancement to optimise the detection and identification of archaeological features. Diurnal corrections were achieved using a modified version of the QuickBasic program used on the Isle of the Dead. Random dropouts and single point spikes in the data were visually identified in each profile and removed or attenuated by a spline interpolation between two correct measurements on either side of the error. Parallax positional errors of were minimal (0.2 – 0.5 m), compared to the

Settlement Hill data, due to the level topography at the parade ground. The editing method chosen to correct the displacement error was the same as that applied to the Isle of the Dead data (refer to Section 3.2.3.2, Chapter 3). Minor examples of residual herringbone effect remained in the data post-processing, although these artefacts did not unduly influence the interpretation.

Findings and interpretation

Processed magnetic data at the parade ground exhibits a narrower dynamic range and lower average (by 638 nT) than the Settlement Hill data, as shown in de-quantised histograms (Figure 5.17). These differences are primarily attributed to the presence of very shallow dolerite basement topography at Settlement Hill and a buffer of non-magnetic Quaternary deposits at the Penitentiary Complex.

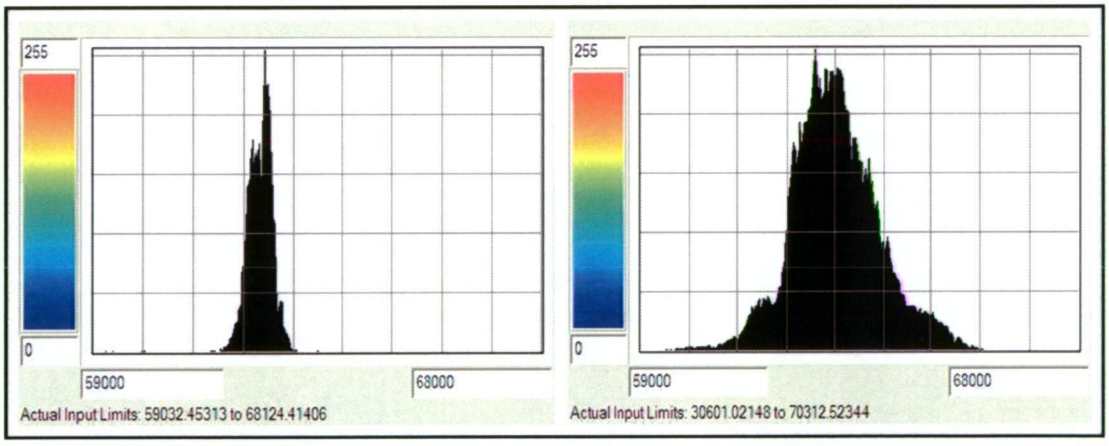

Figure 5.17: Histograms of the Penitentiary Parade Ground (left) and Settlement Hill (right) magnetic data, clipped to 59000 and 68000 nT. Actual input limits are displayed below the histograms.

While dolerite rubble in the Mason Cove reclamation material contributes to variation in background magnetic intensities across the grid, prominent anomalous zones are primarily attributed to known and/or inferred near-surface (< 1 m) or surface features. High magnitude dipolar and negative zones located on the southern grid boundary (Figure 5.18, **A - D**) are caused by iron structural features in the Penitentiary building, including penal period window bars, and contemporary I-beams supports in the clock tower (**C**) (Greg Jackman, pers. comm. 2006).

High to very high magnetic intensities near the Radcliffe canal (**E**) are due to the dolerite masonry wall and rubble backfill. The broad high magnitude zone centred on (**F**) and

point anomalies encircling (**G**) probably represent remnants of the Parade Ground gravel surface, and more recent shallow dolerite rubble. This interpretation is based on archaeological excavation findings and the enclosure wall locations inferred from historic sources.

The magnetic variation map is also characterised by a scattering of moderate to high amplitude point responses, as illustrated by the clipped and sun-shaded image in Figure 5.18. These are enhanced in Figure 5.19, through use of a highpass 5 x 5 cell filter and an alternative colour scale. Known sources of strong dipolar anomalies include the information sign (Figure 5.19, **A**) and Mason Cove seawall features (**B**). Prominent responses along the eastern pathway (**C**) may be caused by buried ferrous metal associated with the post-penal to contemporary site use, as they do not correlate to any known penal period elements. Other high and moderate amplitude anomalies are attributed to buried ferrous metallic objects and other sources, such as near-surface dolerite (Figure 5.20). Although some of these sources may be tramway remnants, the irregular distribution of point responses suggests that the rails structures have mostly been removed. There is also no direct evidence for the different phases of Mason Cove reclamation.

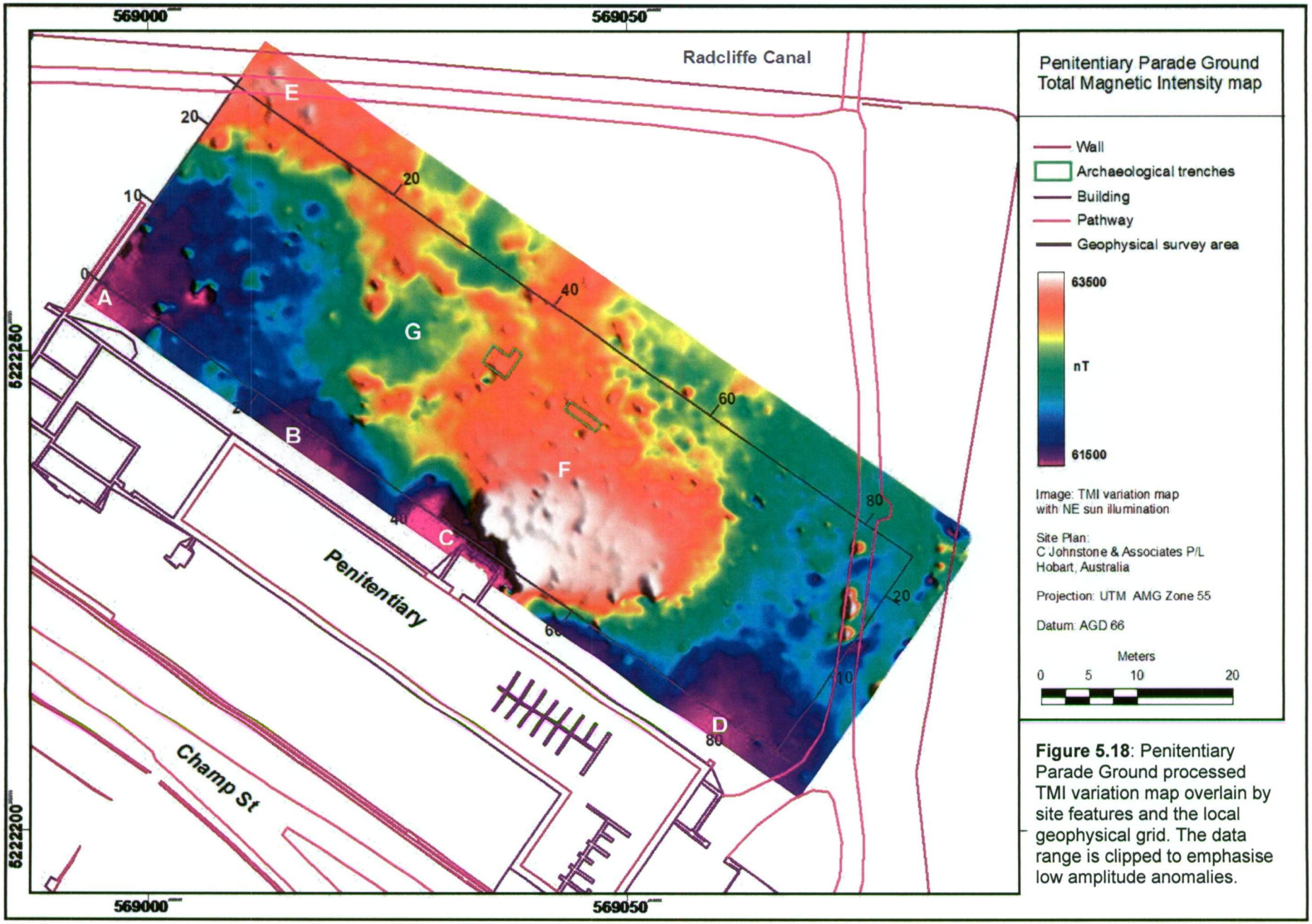

Figure 5.18: Penitentiary Parade Ground processed TMI variation map overlain by site features and the local geophysical grid. The data range is clipped to emphasise low amplitude anomalies.

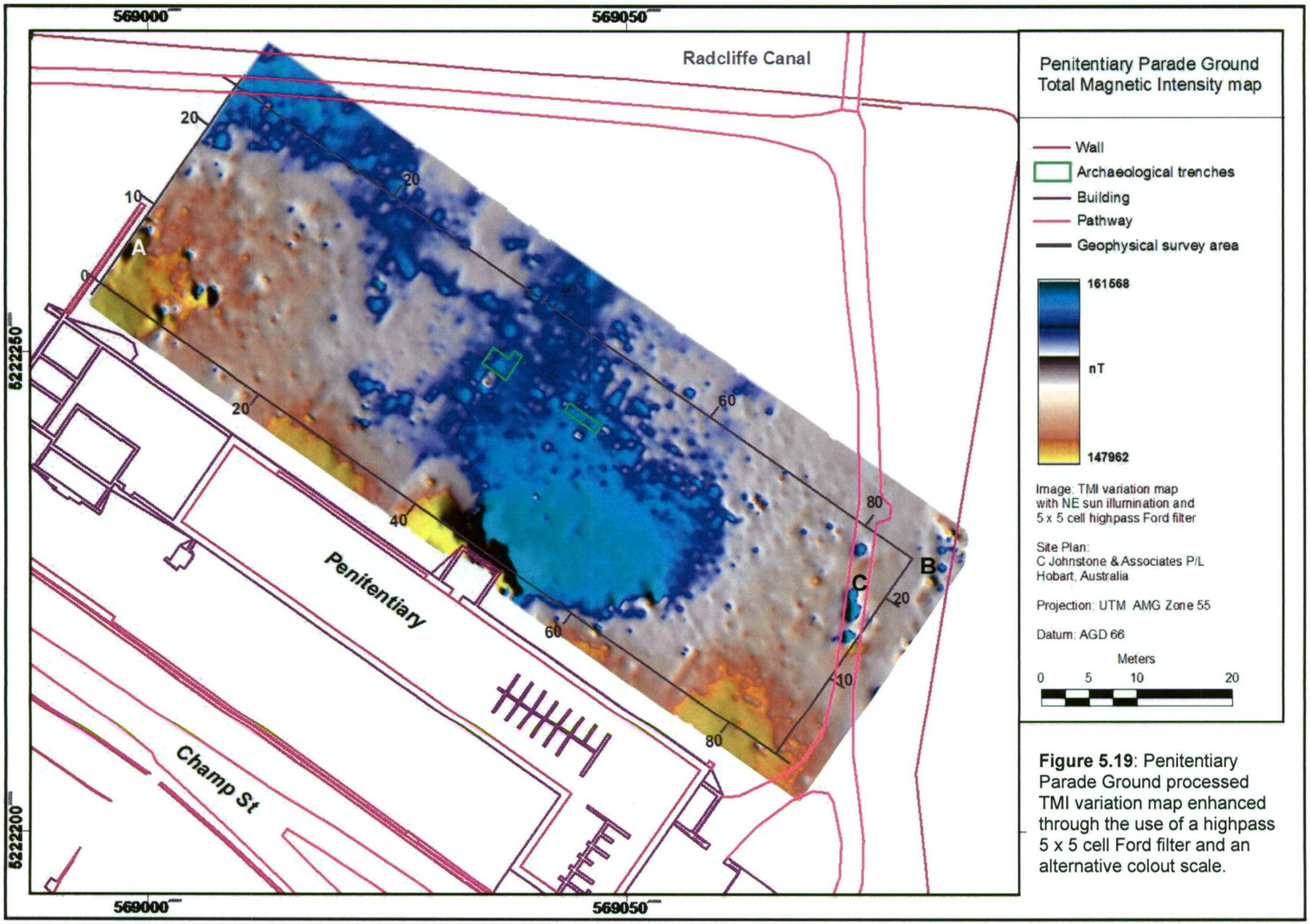

Figure 5.19: Penitentiary Parade Ground processed TMI variation map enhanced through the use of a highpass 5 x 5 cell Ford filter and an alternative colout scale.

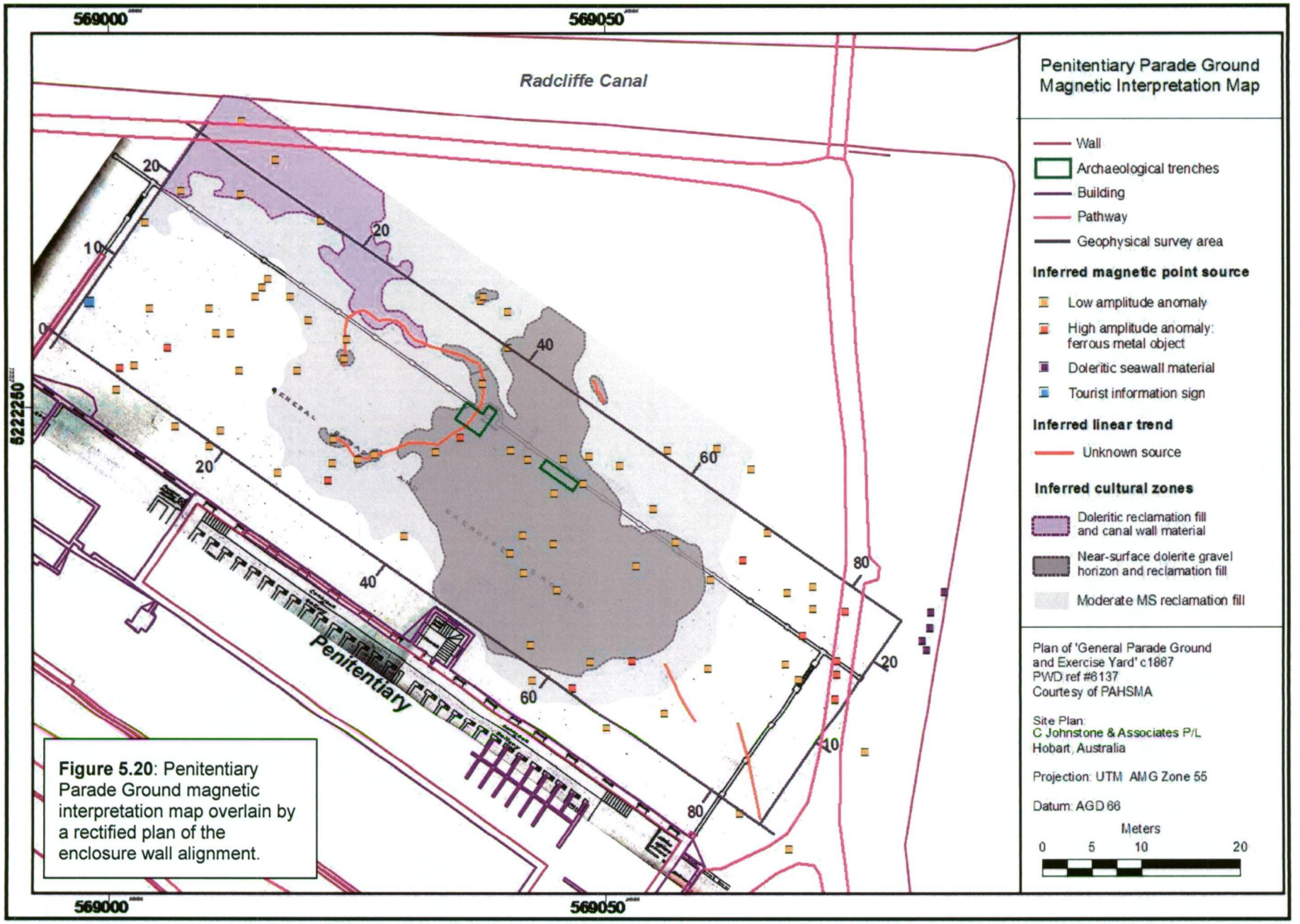

Figure 5.20: Penitentiary Parade Ground magnetic interpretation map overlain by a rectified plan of the enclosure wall alignment.

5.2.3.3 Apparent resistivity profiling

Wenner array apparent resistivity profiling was conducted at the Penitentiary Parade Ground primarily for the delineation of any remnant enclosure wall foundations, tramway features and the Parade Ground gravel surface. Post-penal and contemporary elements associated with the tennis courts and camping ground are secondary archaeo-geophysical targets. The Wenner array was chosen as it theoretically provides good vertical resolution and generally high S/N data. This may increase the probability of detecting any foundation wall remnants under the coarse gravel deposits, and offsets its moderate lateral resolution capabilities (Stummer *et al.*, 2004).The following section details the data collection and processing methodology, survey findings and their qualitative interpretation.

Data acquisition and processing

Data were collected over four consecutive days in May 2004. Data acquisition parameters for the Parade Ground area are the same as for the Settlement Hill site. A Wenner α electrode configuration with 0.33 m spacing was mounted to a wooden frame and oriented parallel to the local grid x-axis. The electrodes were inserted no more than several centimetres into the ground, which was usually deep enough to reach moist soil. When gravel, clay or rock prevented insertion at the correct points, the frame was moved a short distance perpendicular to the survey line (Bevan, 1998). Any statistical outliers (spikes) caused by limited coupling between the electrodes and near-surface hard layers were removed from the data. Readings were typically collected at 1.0 m intervals along-line, except where contact between the electrode and ground precluded sufficient current flow. Other data acquisition parameters are shown in Table 5.2.

Apparent resistivity values were calculated by multiplying the resistance measurements provided by the Terrameter by the geometric factor $2\pi a$. Resistivity data were gridded into a variation map of the Parade Ground survey area (Figure 5.21), using the kriging method with a 0.2 m cell size and 2.1 m search radius.

Survey type	DC resistivity		
Instrumentation	12V Atlas-Copco ABEM Terrameter		
Area surveyed	86 x 25 m		
Method of coverage	Continuous surveying along transverse gridlines		
Traverse interval	1.0 m	**Array type**	Wenner α
Station interval	1.0 m*	**'a' spacing**	0.33 m
Stacking	4	**Output units**	Ohm (Ω)
Electrodes	10 mm stainless steel probes mounted in a wooden frame		
Comments	0.2 mA current typically sufficient to provide non-noisy data *Station interval changed to 0.5 m where the difference between two adjacent readings was > 15 Ω.m.		

Table 5.2: Tabulated resistivity profiling survey parameters for the Penitentiary Parade Ground.

Findings and interpretation

The Parade Ground grid is characterised by a very wide range of apparent resistivity values (12 Ω.m to 2834 Ω.m), which suggests deposits and features of diverse material contrast. A variation map of clipped values (15 - 1500 Ω.m), with gradient enhancement to highlight directional trends, is presented in Figure 5.21. Identification of anomaly sources is based on comparison between this dataset, magnetometry and GPR findings, and archaeological ground-truthing. Results of the qualitative interpretation are presented in Figure 5.22.

The only direct evidence for the Parade Ground enclosure wall is recorded parallel to 81x as a moderate amplitude lineament from 0 - 6y (Figure 5.21, **A**) and a low amplitude anomaly from 14y - 16y. The first trend coincides with a very shallow, well-preserved section of eastern wall visible on the surface as a hump, while the second response corresponds to a deeper or less well-preserved section near the north-east corner, as inferred from historic plans respectively. Excavation findings suggest that other sections of the wall have been either totally removed, lie below the investigation depth and/or are poorly preserved, and therefore exhibit low resistivity contrast with the surrounding materials. Measurements collected over the fountain feature (**B**) did not produce an anomaly, probably due to a low contrast between the sandstone blocks and surrounding sands.

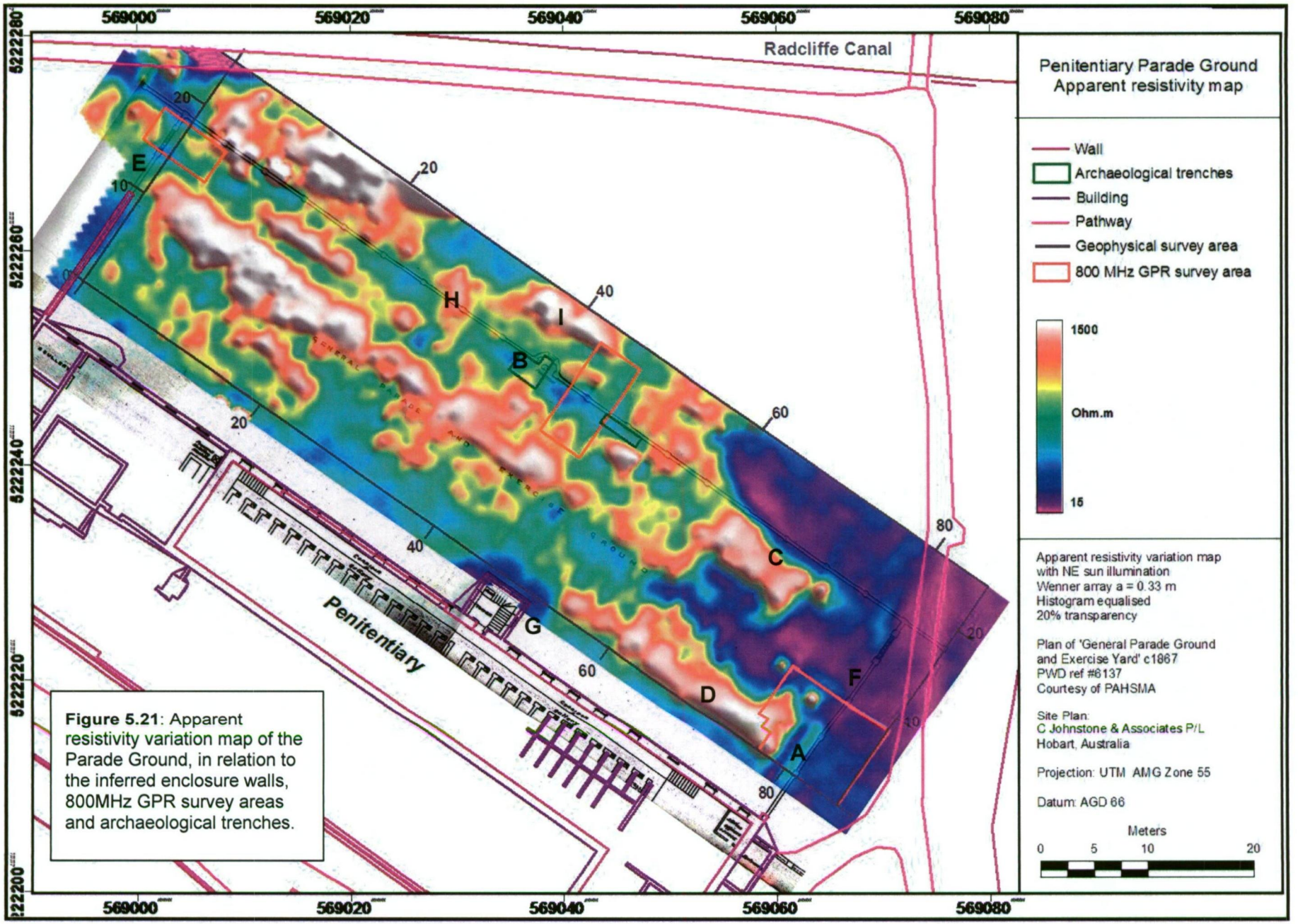

Figure 5.21: Apparent resistivity variation map of the Parade Ground, in relation to the inferred enclosure walls, 800MHz GPR survey areas and archaeological trenches.

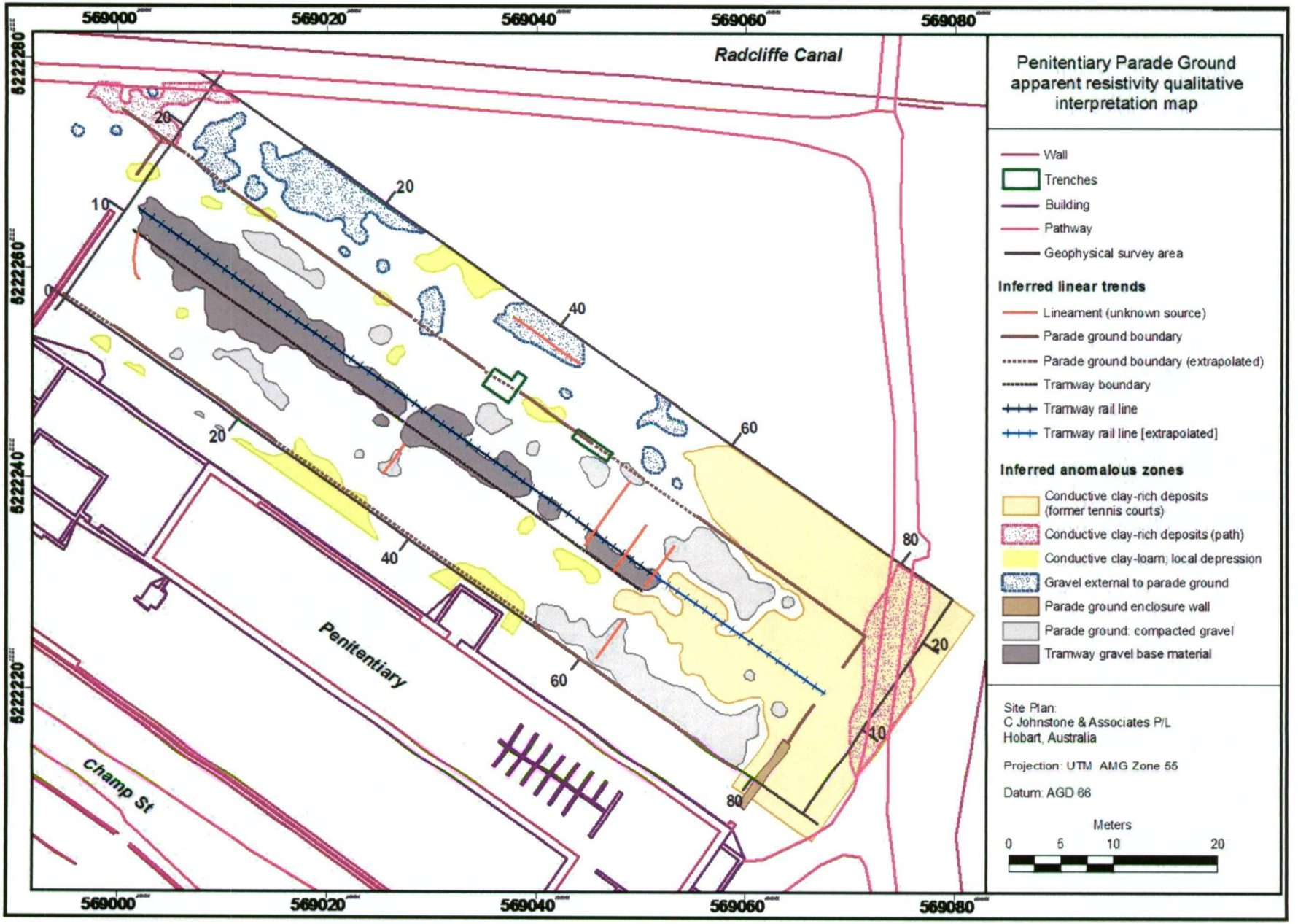

Figure 5.22: Apparent resistivity variation map of the Parade Ground area, in relation to the inferred enclosure walls location and archaeological trenches.

One section of the northern Parade Ground boundary correlated well with a steep resistivity gradient at (C) in Figure 5.21. This relationship suggests that the adjacent high resistivity zone is caused by material deposited prior to removal of the enclosure wall - possibly the Parade Ground yard surface. Another high value zone located at (D) may be further evidence of this surface. If so, then the steep resistivity gradient parallel to gridline 1y may correspond to the Parade Ground southern boundary (Figure 5.22). Broad areas of very low apparent resistivity (15 - 50 Ω.m) around these two high zones probably indicate where the inferred gravel deposits were replaced by conductive clay-rich material for the tennis courts and pathways.

The remaining Parade Ground area is characterised by a prominent broad high to very high apparent resistivity zone (> 1250 Ω.m) between gridlines 8y and 14y, which correlates closely to part of the inferred tramway. Contemporary infra-red photography and the 1877 Blackwood plan (Figure 5.5) indicate that this feature extended laterally to the northern enclosure wall, while probably demarked by a fence roughly aligned with gridline 10 y. Historic photographs indicate that the rail lines entered and exited the Parade Ground through inter-pillar openings (E) and (F), which are not shown in the 1867 map (Figure 5.21). It is likely, therefore, that this prominent anomaly is caused by remnants of tramway gravel material (Figure 5.22).

Other high to very high resistivity zones within the inferred Parade Ground are also interpreted as remnants of the 'General Parade and Exercise Ground' gravel surface (Figure 5.21). Very low measurements at (G) are attributed to conductive clay fill used during the 1980s after I-beam supports were added to the Penitentiary clock tower (Greg Jackman, pers. comm. 2006).

The area north of the Parade Ground (gridlines 18y to 25y) is characterised by zones of very high apparent resistivities, some of which coincide with rubble fill (H, I) - as interpreted from shallow irregular GPR reflections. Comparison between resistivity values around the trenches, and archaeological excavation results, show that contemporary deposits of levelling sand generate moderately high resistivity values (up to 1000 Ω.m). Similar values distributed along most of the northern Parade Ground area are probably also associated with these near-surface sandy horizons. Higher apparent resistivities are attributed to a combination of gravel and sand material.

5.2.3.4 Ground penetrating radar

Ground penetrating radar was applied at the Penitentiary Parade Ground to provide geophysical information in both the horizontal and vertical planes, to augment the two-dimensional interpretation plans derived from the magnetometry and apparent resistivity surveys. Primary objectives were to identify and characterise responses attributed to known and inferred archaeological targets associated with the penal period, using individual profile and timeslice analysis.

Data acquisition and processing

Surveying of the Parade Ground geophysical grid was conducted in spring 2004, using a 500 MHz shielded antenna. Tests on-site demonstrated that this frequency provided ample penetration for target detection and suitable resolution, as excavations indicated that most important features are probably located within 0.5 m depth. The investigation range was set to 30 ns two-way travel time (TWTT), which corresponds to a depth of investigation of ~ 1.15 m when assuming a nominal velocity of 0.09 m/ns - typical for dry loamy soils (Conyers and Goodman, 1997). Profiles were collected in both transverse and longitudinal directions at 0.5 m line spacing, to maximize detection of rectilinear targets aligned with the geophysical grid, such as the enclosure walls. This is because the electro-magnetic field orientation from the transmitting antennae 'will usually reflect more readily from features orientated perpendicular to the profile direction' (Annan and Cosway, 1992). Data were acquired over consecutive days to minimise the effect of varying soil conditions, and there were no surface obstructions.

Three areas (A, B & C) were also selected for detailed investigation of near-surface structural targets, based on historical documents, surface evidence and archaeological excavation. An 800 MHz antenna was used to acquire data at 0.5 m line intervals, to allow direct comparison with the 500 MHz survey results. Maximum depth of investigation was approximately 0.6 m with a 16 ns TWTT range, although wave penetration to noisy data was only ~ 0.45 m. This was deemed sufficient to detect and characterise the features of interest, based on excavation results (Section 5.2.2). Area **A** was positioned to encompass material both interior and exterior to the Parade Ground, part of the western return wall and its gateway c1867. After the tramway was installed

during the early 1870s (Blackwood plan c1877, Figure 5.5), this opening appears to have been relocated one set of pillars further towards the penitentiary (Greg Jackman, pers. comm. 2006). It was hoped that the radar might detect physical evidence of the first gateway, even though it was bricked in during the wall restructuring. Area **B** was sited to detect and characterise any remnants of the northern enclosure wall between Trenches 1 and 2, while the eastern return wall was the focus of Area **C** (Figure 5.23). A portion of the return wall is visible from the surface, where it is manifest as a linear mound extending several metres out from the Penitentiary. Profiles in each area were collected perpendicular to the inferred feature alignment, to optimise the detection of the wall. Fundamental parameters and equipment details for both the 500 MHz and 800MHz surveys are summarised in Tables 5.3 and 5.4 respectively.

Raw data collected at the Parade Ground was processed using the steps described in Chapters 3 and 4, to correct the bi-directional profiles for three-dimensional data presentation and analysis. These included the reversal of negative direction profiles, trace interpolation to correct fiduciary markers to distance, static correction and time/depth conversion (using the nominal velocity of 0.09 m/ns). Horizontal high pass filtering and/or an energy decay gain function were then applied to increase the S/N ratio for anomaly recognition and qualitative interpretation.

Three-dimensional data imaging

Prior to three-dimensional processing, the Parade Ground profiles were divided into three 20 x 25 m blocks and one 26 x 25 m block for practical data management. The files were then compressed to a maximum of 512 traces in both x- and y- directions, due to software limitations (512 x 512 pixels) - resulting in 1 trace per 4.8 cm and 4 cm respectively. Statically-corrected, unfiltered unmigrated radargrams for each block were stacked horizontally to create longitudinal and transverse three-dimensional datasets, using the approach described in Chapter 3, section 3.2.6.3. Image enhancement was then performed on the whole dataset, rather than individual profiles, using gain adjustments and/or the application of an energy decay gain function.

Survey type	Ground penetrating radar		
Instrumentation	Mala RAMAC X3M system with a 500 MHz shielded antenna		
Area surveyed	86 x 25 m	**Stacking**	8
Method of coverage	Continuous data collection at 0.03 s intervals		
Traverse interval	0.5 m along transverse and longitudinal gridlines		
Trace interval	0.01 m*	**Tx – Rx separation**	0.18 m
Range	30 ns	**Time samples**	192
Comments	Fiducial marks added manually during data collection, estimated accuracy to +/- 0.1 m. Profiling conducted with ≤ 1.0 m offset from parallel measuring tape. Survey conducted at ~ 2 km/hr. * Calculated using fiducial marks, with maximum 512 traces per profile for three-dimensional data visualisation.		

Table 5.3: Ground penetrating radar 500 MHz survey parameters for the Parade Ground.

Survey type	Ground penetrating radar		
Instrumentation	Mala RAMAC X3M system with a 800 MHz shielded antenna		
Area surveyed	Area **A**: 11 x 8.5 m; Area **B**: 4.5 x 10 m; Area **C**: 7 x 3.5 m		
Method of coverage	Continuous data collection at 0.03 s intervals		
Trace interval	0.0137 - 0.02 m*	**Tx – Rx separation**	0.14 m
Range	16 ns	**Time samples**	154
Stacking	8	**Traverse interval**	0.5 m
Comments	Fiducial marks added manually during data collection, estimated accuracy to +/- 0.1 m. Profiling conducted with ≤ 0.5 m offset from parallel measuring tape. Survey conducted at ~ 2 km/hr. * calculated using fiducial marks, with maximum 512 traces per profile for three-dimensional data visualisation.		

Table 5.4: Ground penetrating radar 800 MHz survey parameters for the Parade Ground.

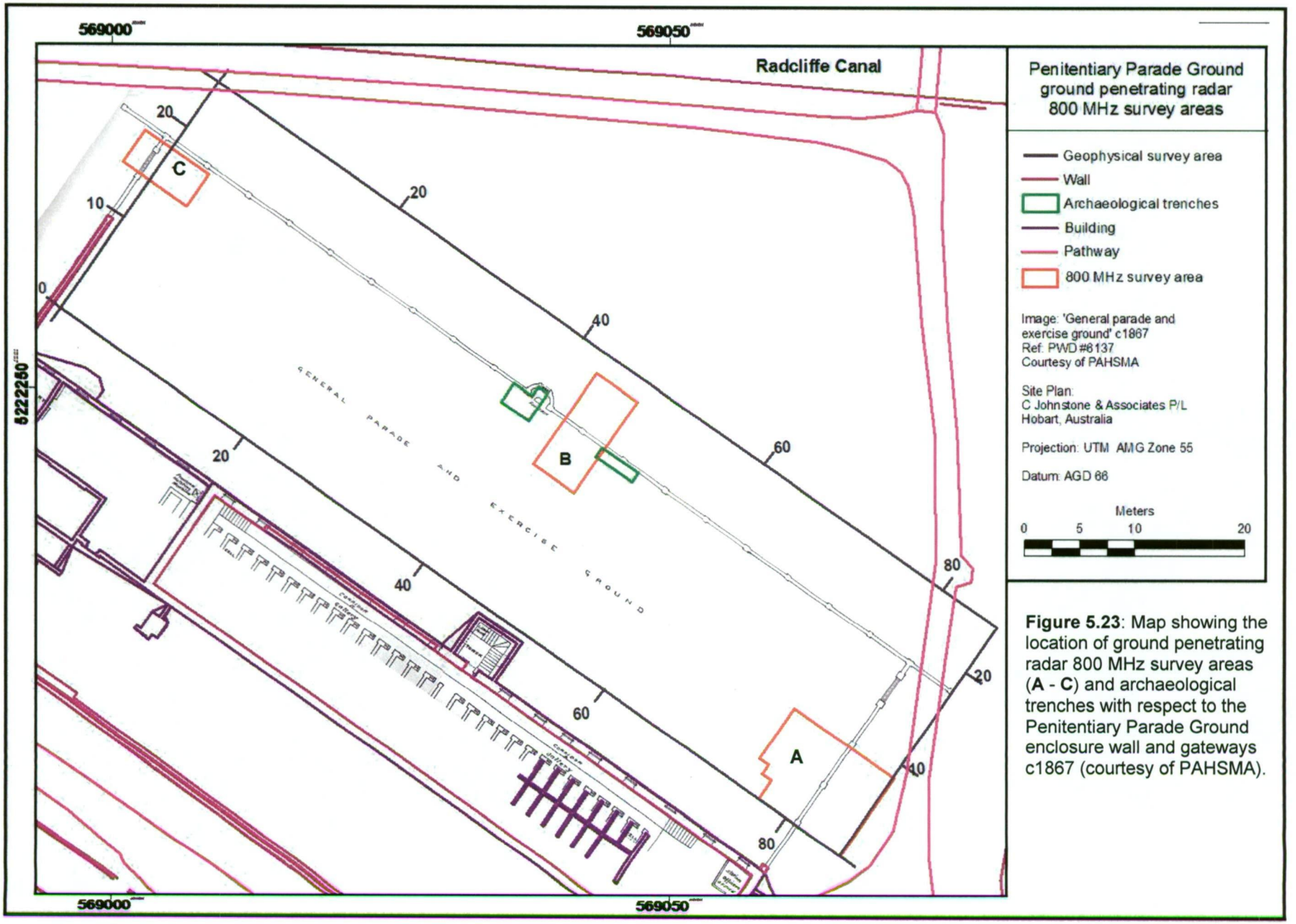

Figure 5.23: Map showing the location of ground penetrating radar 800 MHz survey areas (**A** - **C**) and archaeological trenches with respect to the Penitentiary Parade Ground enclosure wall and gateways c1867 (courtesy of PAHSMA).

Findings and interpretation

Transverse profiles (parallel to the y-axis) were assessed visually to identify broad anomaly patterns in the vertical plane and categorise response types. The data were viewed after initial processing (correction of axes), after gain enhancement and following average trace subtraction. Synoptic plan views of the Parade Ground are provided by timeslices derived from separate three-dimensional processing of transverse and longitudinal profiles. Lineaments, anomalous zones and point responses recognised in the timeslice and profile analysis are symbolised in a data abstraction map - according to the approach described in Chapters 3 and 4. Qualitative interpretation images were created by comparing the abstraction map to the resistivity and magnetometry datasets and archaeological ground-truthing results, as described in Section 5.2.2.

Individual profile analysis

Preliminary profile assessment identified three main anomaly types for data abstraction: hyperbolae, planar reflectors and multiple adjacent diffractions. The first two types are exemplified in Figure 5.24, which shows radargrams derived from gridlines 4x and 53x with filtering and gain adjustment to increase the S/N ratio and enhance responses at depth. Anomalous responses are categorised according to their vertical position, amplitude and continuity, which enables abstraction and systematic interpretation of the data. Any reflection which extends more than 1 m laterally is defined as 'continuous' and attributed to a stratigraphic horizon (e.g. floor surface), the depth of which is estimated using the maximum amplitude. Any reflection confined to 1 m laterally which exhibits tapered edge diffractions is termed 'discrete'. These responses typically indicate that the radar has traversed over a relatively flat-topped isolated feature, such as a flagstone, rather than a continuous stratigraphic horizon (Conyers and Goodman, 1997). Results of the transverse profile analysis and data abstraction process are presented in Figure 5.25, which provides a plan view of anomaly distribution with inter-line interpolation to assist pattern recognition.

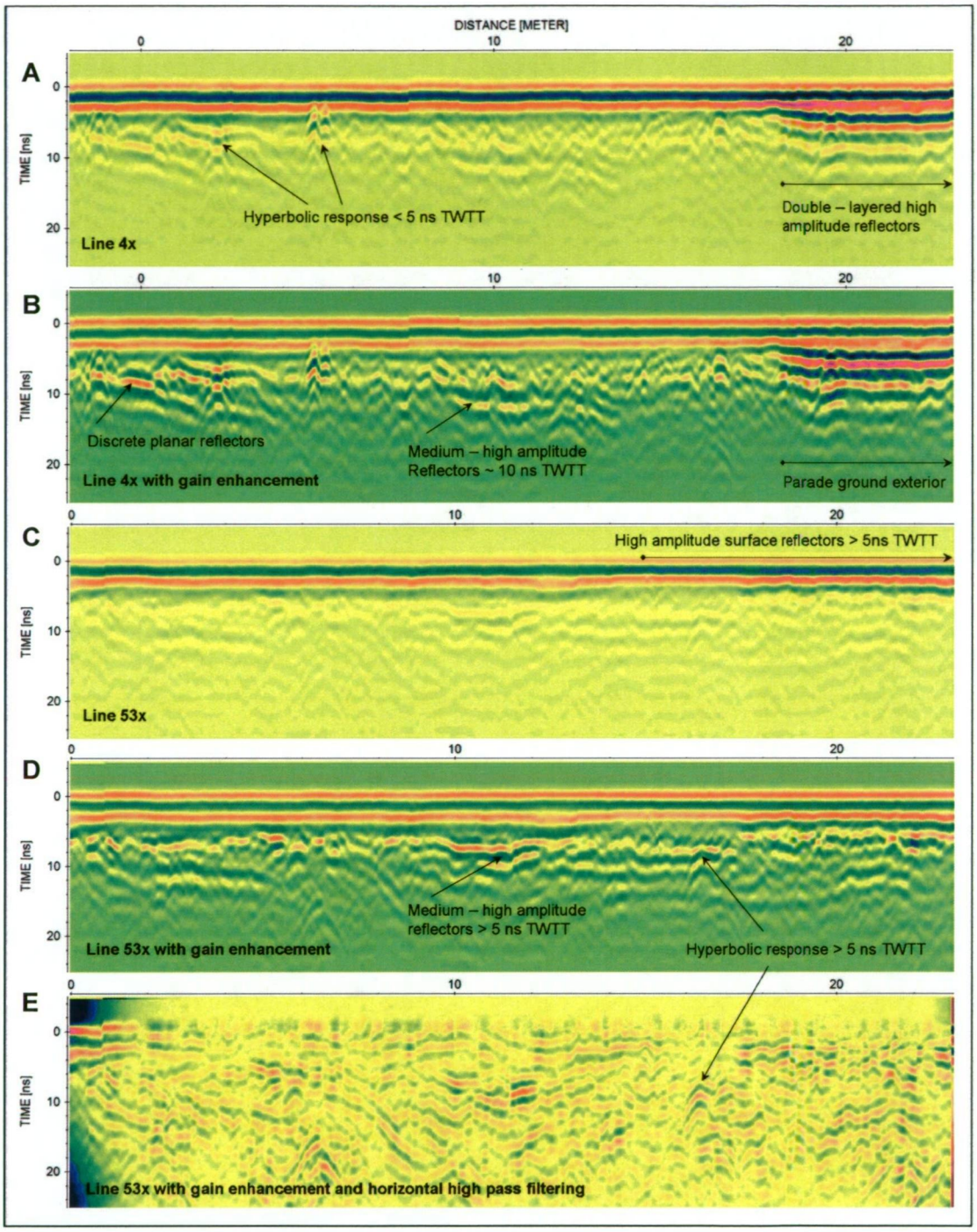

Figure 5.24: Processed GPR 500 MHz radargrams from gridlines 4x (**A**) and 53x (**C**) are dominated by strong surface reflections and low contrast anomalies from ~5 ns down. Images (**B**) and (**D**) illustrate how gain enhancement can accentuate signals in the subsurface. Image (**E**) is also highpass filtered to enhance non-horizontal reflections and effectively increase the signal-noise ratio. Primary response types identified here include hyperbolae, continuous and discrete planar reflectors.

Several gross anomaly distribution patterns evident in the data recognition map are attributed to known and inferred cultural features. The most striking of these is a single to triple layered zone of high amplitude planar responses, visible between gridlines 18y and 23y (Figure 5.25, **A**) - an example of which is shown in gridline 4x, Figure 5.24.

Excavation findings from Trench 2 suggest that these anomalies are caused by the radio wave reflecting off interfaces between the topsoil and layered deposits of resistive levelling sand and gravely loam, located at 0.1 - 0.2 m depth. Deeper responses (not illustrated in the data recognition map) are characterised by relatively weak multiple diffractions, which are attributed to less resistive coarse gravely reclamation fill underlying the levelling material.

Comparison between these high amplitude anomalous zones and the 1867 plan (Figure 5.23) shows that the levelling material covers most of the Parade Ground exterior between gridlines 0 - 55x, and therefore provides indirect evidence for the northern enclosure wall alignment. The prominent rectilinear zone around (**B**) (Figure 5.25) may be caused by in-filled foundation trenches of a former outbuilding or platform relating to contemporary site use. Smaller anomalous areas recorded proximal to the Penitentiary are also attributed to fill deposits, because they show similar response characteristics to those at (**A**). Remnants of the sandstone fountain platform excavated in Trench 2 (Figure 5.10) are characterised by medium to high amplitude reflectors at < 5ns TWTT (Figure 5.26 - red square). This corresponds to a depth of < 0.22 m, which agrees with the excavation results. Similar responses across Trench 1 correlate to the loamy subsoil / levelling sand interface. A linear zone of multiple adjacent diffractions, shown in green (**C**), are attributed to rubble material used to fill a contemporary pipe trench within the main subsidence zone (**A**).

The former Parade Ground area near-surface (< 5 ns TWTT) is primarily characterised by irregularly distributed zones of medium - high amplitude surface reflectors, which show poor correlation with variations in the apparent resistivities. Hence, the reflections probably indicate localised variations in soil moisture at time of surveying, rather than variation in composition. Three zones of medium-high amplitude planar reflectors recorded between 8 - 10 ns TWTT (e.g. Figure 5.25, **D**) are coincident with the former tramway and may therefore be remnant base material (Figure 5.27). Clusters of discrete planar reflectors, shown as brown areas in the data recognition map, are attributed to buried features such as stone flagging or brick pieces. The linear zone at (**E**) (Figure 5.25) is possibly caused by an *in situ* section of penal period drain, or a contemporary feature related to the camping ground. Isolated planar anomalies, and other point reflectors

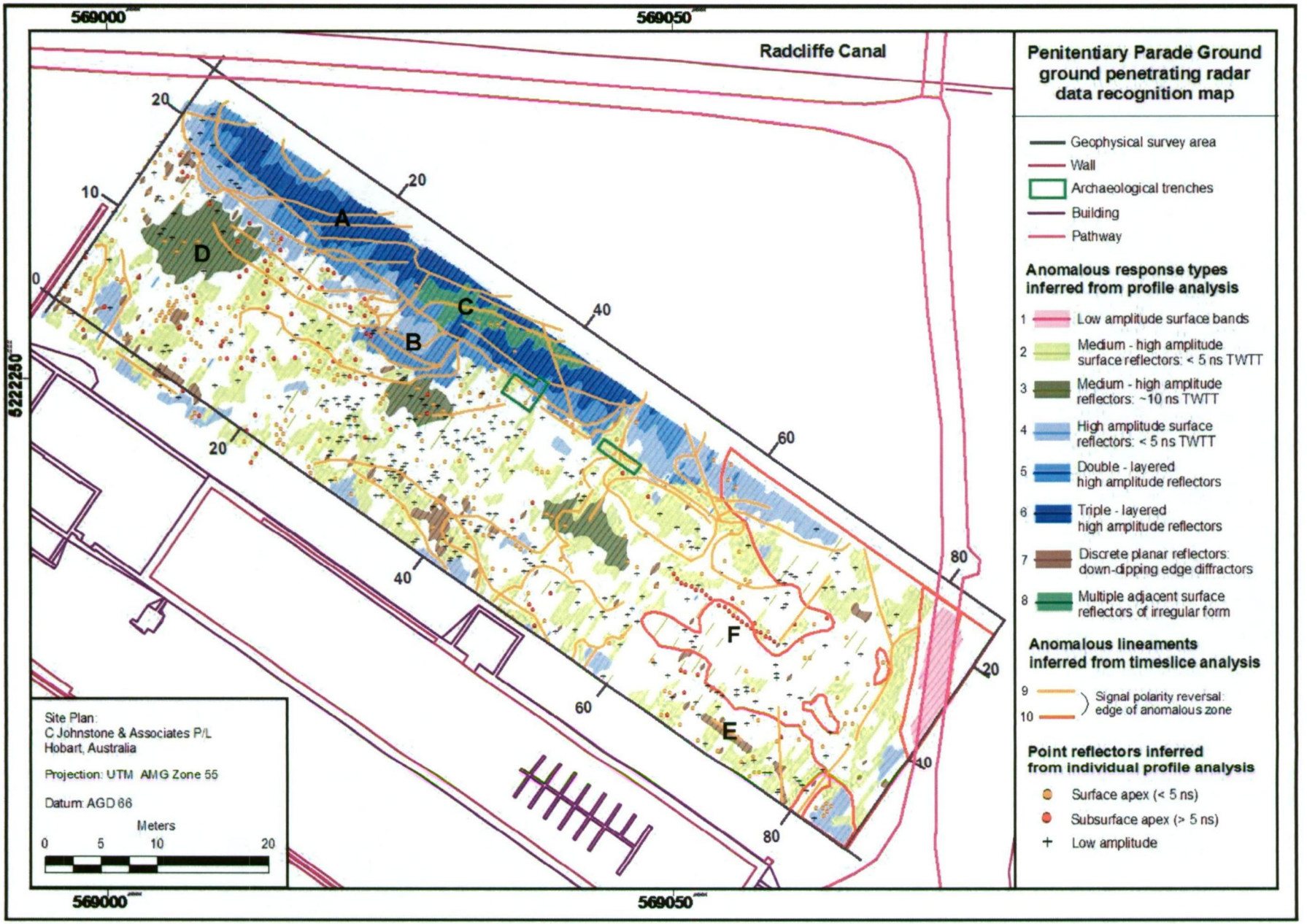

Figure 5.25: Parade Ground 500 MHz GPR data recognition map showing anomalous zones and point responses derived from profile and timeslice analyses.

Anomalous response types inferred from profile analysis

1 Low amplitude surface bands
2 Medium - high amplitude surface reflectors: < 5 ns TWTT
3 Medium - high amplitude reflectors: ~10 ns TWTT
4 High amplitude surface reflectors: < 5 ns TWTT
5 Double - layered high amplitude reflectors
6 Triple - layered high amplitude reflectors
7 Discrete planar reflectors: down-dipping edge diffractors
8 Multiple adjacent surface reflectors of irregular form

Anomalous lineaments inferred from timeslice analysis

9 / 10 Signal polarity reversal: edge of anomalous zone

Point reflectors inferred from individual profile analysis

Surface apex (< 5 ns)
Subsurface apex (> 5 ns)
\+ Low amplitude

0 Metres 10

Figure 5.26: Detailed view of the Parade Ground 500 MHz GPR anomalous zones and point responses derived from individual profile analysis and timeslice data recognition. The sandstone fountain base is delineated by a red polygon as inferred from excavation of Trench 2 (T2).

located along this linear trend may be associated remnants. Other lineaments inferred from the point response distribution (Figure 5.27) are derived from unknown sources, except for a line of hyperbolic apices recorded parallel to gridline 12y between 60x - 70x. The depth (> 5 ns TWTT) and position of these anomalies strongly suggest that they relate to the tramway.

Most isolated point responses appear to be randomly distributed throughout the inferred Parade Ground area. Few are recorded in the subsidence zone or grid SE, suggesting that the source material (probably isolated rubble or metallic debris) is associated with the penal period site use, and/or that reflections from the levelling sand rubble are masking responses from underlying rubble fill material. Although the scattered distribution makes it difficult to determine if any anomalies are caused by *in situ* archaeological targets, comparison between radar anomalies and other geophysical results enables several unknown sources to be characterised. A cluster of shallow hyperbolic responses at locus 10x, 5y (circled in black, Figure 5.27), for example, coincides with a localised apparent resistivity low and very high magnetic peak - suggesting buried ferrous metallic material and surrounding clay-rich rubble fill.

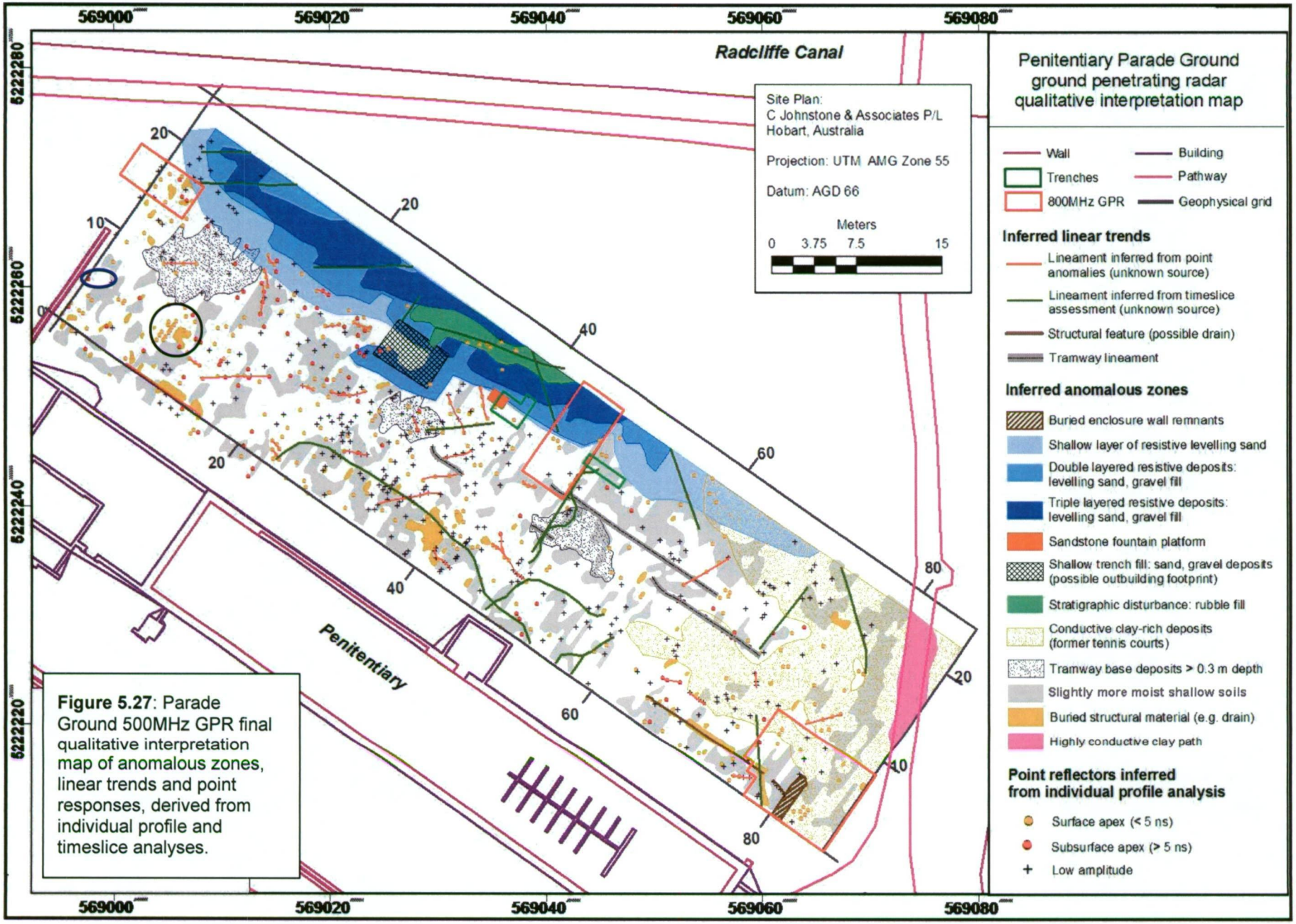

Figure 5.27: Parade Ground 500MHz GPR final qualitative interpretation map of anomalous zones, linear trends and point responses, derived from individual profile and timeslice analyses.

Three-dimensional data visualisation: timeslicing

Following the profile analyses and characterisation of different response types across the Parade Ground, data recognition mapping was performed using three-dimensional amplitude maps. Lineaments and anomalous zones are inferred from single time interval amplitude maps of each grid, conjoined to cover the whole survey area. Response patterns are clearly defined within the top 5 ns, but by 10 ns (~ 0.45 m) the data exhibits a low signal-to-noise ratio and low amplitudes - due to wave attenuation with depth. The timeslices in Figure 5.28 typify such patterns.

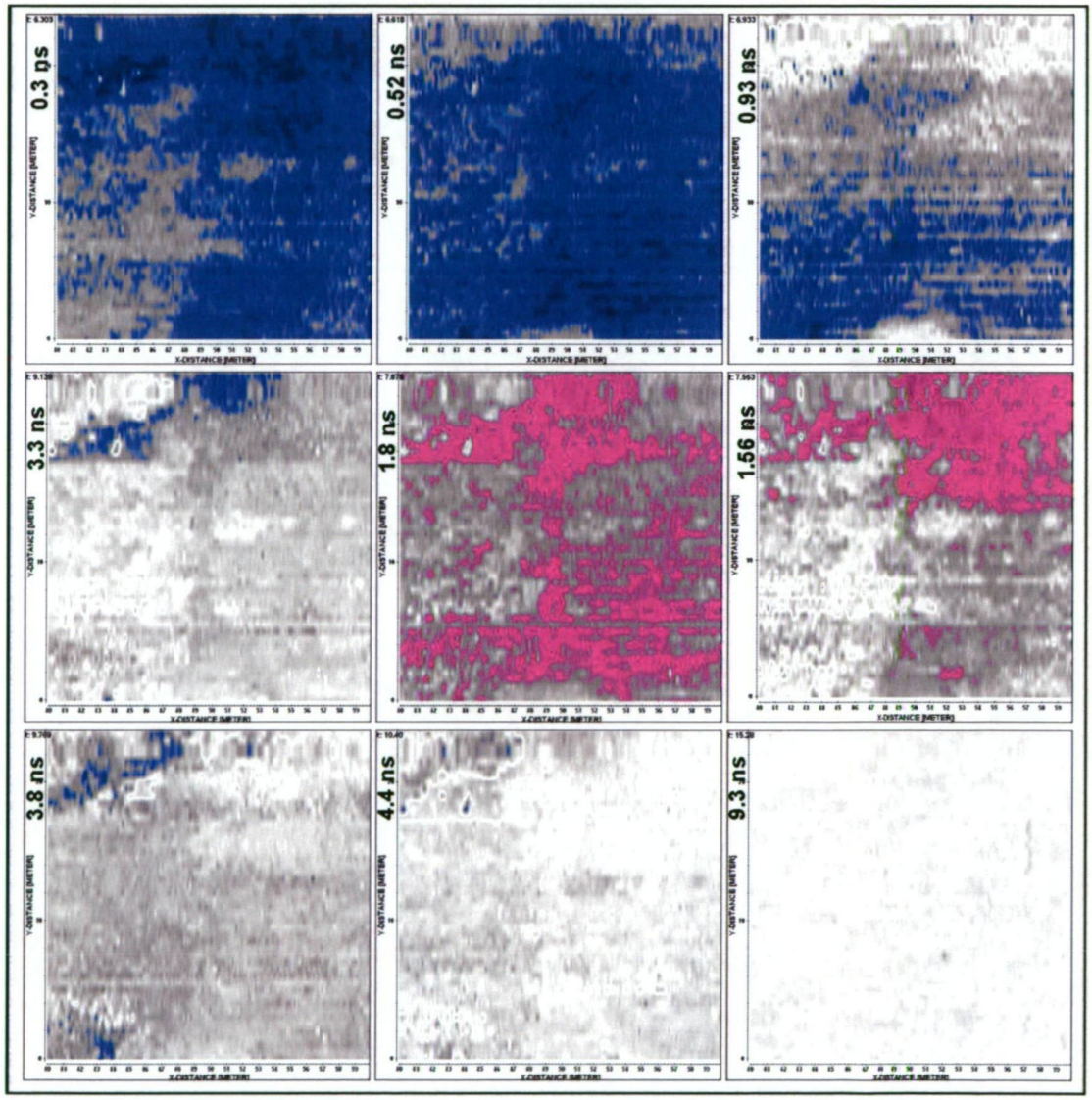

Figure 5.28: A mosaic of unfiltered 500 MHz timeslices from the 40x - 60x grid section of the Parade Ground area, showing the variation in high amplitude zones with increasing penetration, to an effective maximum of ~ 10.0 ns TWTT.

A synoptic plan view of the parade ground survey area is provided in Figure 5.29. This image shows a series of adjacent timeslices generated between 3 - 4 ns, overlain by the cumulative record of linear trends and anomalous zones inferred from all timeslices. Several gross anomaly patterns are clearly visible - some of which are not obvious in the profile data recognition map.

Strong lineaments resulting from highly contrasting amplitudes between layers of levelling sands (**a** - **c**) correlate closely to anomalous zones **A** - **C** inferred from individual profile assessment (Figure 5.25). A large section of the SE half of the grid is characterised by moderate to high amplitude reflections (e.g. **d**), the distribution of which partly align with parch marks associated with the tennis courts (as inferred from aerial photographs). A zone of moderately low amplitudes outlined in pale green (Figure 5.29, **e**), that correlates closely to very low apparent resistivities, is attributed to remnants of the tennis court clay surface. This relationship is clearly illustrated in Figure 5.30, which presents a timeslice overlain by the apparent resistivity data recognition map. The strong amplitude gradient in Figure 5.29 along gridlines 80 - 81x (**f**), between gridlines 0 - 5y, coincides with the Parade Ground eastern boundary, which suggests that there are *in situ* remnants of the original gravel surface. The effect is not visible along the inferred northern enclosure wall, indicating that the tennis court(s) clay surface extended further than this boundary - an interpretation supported by photographic evidence.

Direct geophysical detection of the enclosure wall is limited to a section visible in slices generated around 6 - 7 ns TWTT, manifesting as a line of point responses parallel to gridline 81x (Figure 5.30, **A**). This trend coincides with physical evidence from the surface, and a high amplitude anomaly in the apparent resistivity data. A more detailed view of this archaeological target, and other stratigraphic features, is provided by profiles collected using the 800 MHz antenna (Figure 5.31).

Limited detection of the enclosure wall by the 500 MHz GPR is due to a range of possible factors, as inferred from the archaeological excavations. These include a low material contrast between the sandstone and its surrounding stratigraphy, poor target condition (Trench 1), too few *in situ* remnants to produce a visual trend, and masking responses from overlying rubble and sand deposits.

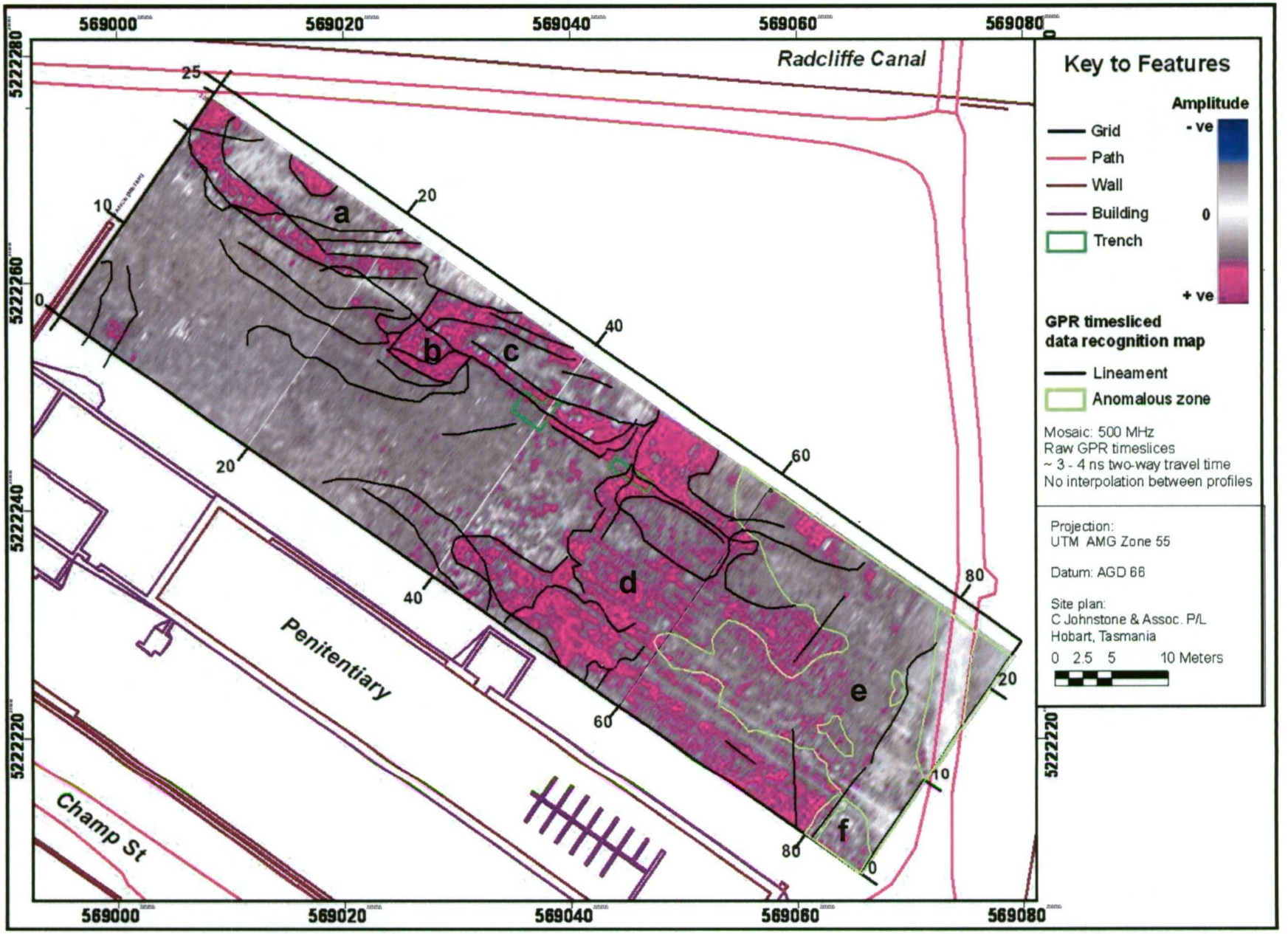

Figure 5.29: A mosaic of Parade Ground 500 MHz GPR raw timeslices generated between 3 - 4 ns TWTT, overlain by lineaments derived from preliminary qualitative interpretation of all timeslices.

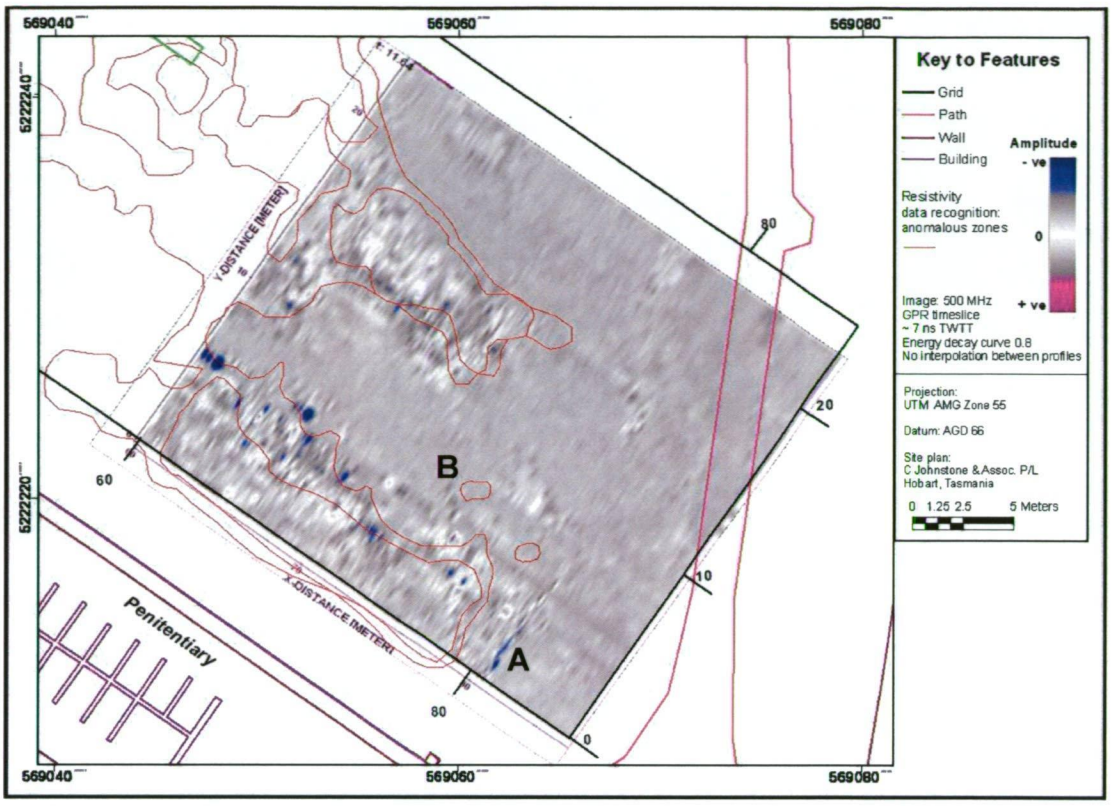

Figure 5.30: Map showing the close correlation between a 500 MHz GPR timeslice generated at ~ 7 ns TWTT and anomalous zones inferred from the apparent resistivity variation map. Annotations are described in the text.

800 MHz data visualisation

Area A

A series of closely-spaced 800 MHz profiles provide high resolution images of stratigraphic features within focal area A (Figure 5.23). These are presented in section format and as horizontal amplitude maps. The eastern parade ground wall is detected in gridlines 0y - 5.5y, where it manifests as shallow diffractions between gridlines 80x - 81x (Figure 5.31). Signal intensity, form and vertical position enable the wall's structural integrity to be inferred. Well-defined, high amplitude responses within 0.1 m depth (e.g. gridlines 0y and 4.5y) are attributed to well-preserved sections, while irregular, low amplitude anomalies below 0.1 m (e.g. gridline 2.5y) indicate where the wall is probably deteriorated or partly removed (Figure 5.31). A lack of geophysical evidence between gridlines ~ 5.5y - 8.5y suggests that little or no wall remains in this section - as also suggested by interpretations of the 500 MHz and apparent resistivity data.

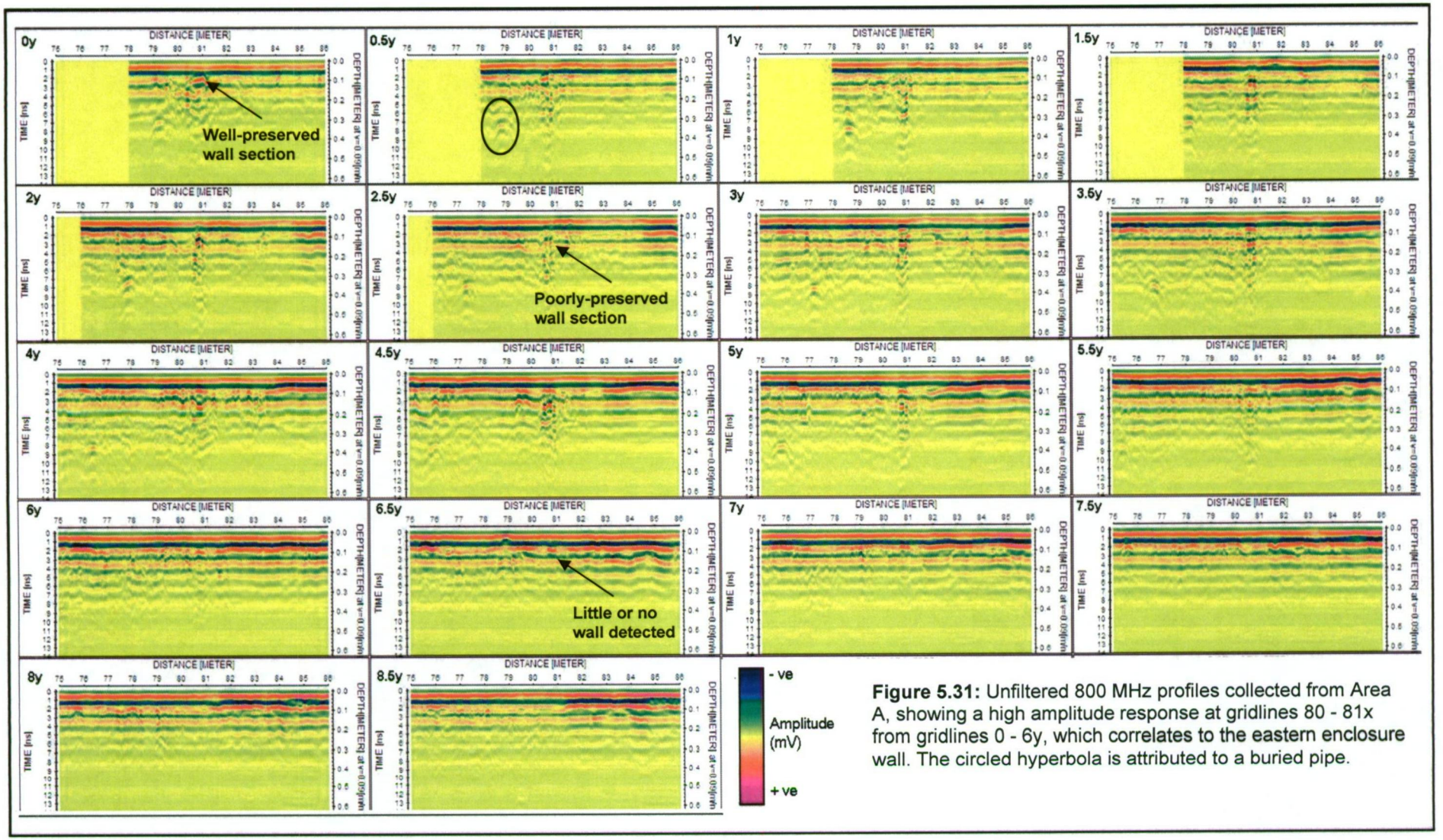

Figure 5.31: Unfiltered 800 MHz profiles collected from Area A, showing a high amplitude response at gridlines 80 - 81x from gridlines 0 - 6y, which correlates to the eastern enclosure wall. The circled hyperbola is attributed to a buried pipe.

A series of hyperbolae visible in the radargrams at 6 - 7 ns TWTT (~ 0.3 m depth) (Figure 5.32) are trending linearly from 79x, 0y to 75x, 6y in the timeslices in Figure 5.33. These are attributed to a pipe originating from the enclosure wall/penitentiary junction, which may be a penal period drainage feature as it does not correlate to any known element in the contemporary services plan. Timeslices of the 500 MHz amplitude volume show that this feature appears to stop at 74x, 8y (Figure 5.30, **A**), so perhaps it is associated with the post-penal tennis courts.

Near-surface point anomalies are probably derived from buried brick and sandstone rubble (Figure 5.32). Continuous high amplitude reflectors to ~ 4 ns TWTT in the Parade Ground exterior are caused by relatively resistive material such as a compacted yard surface.

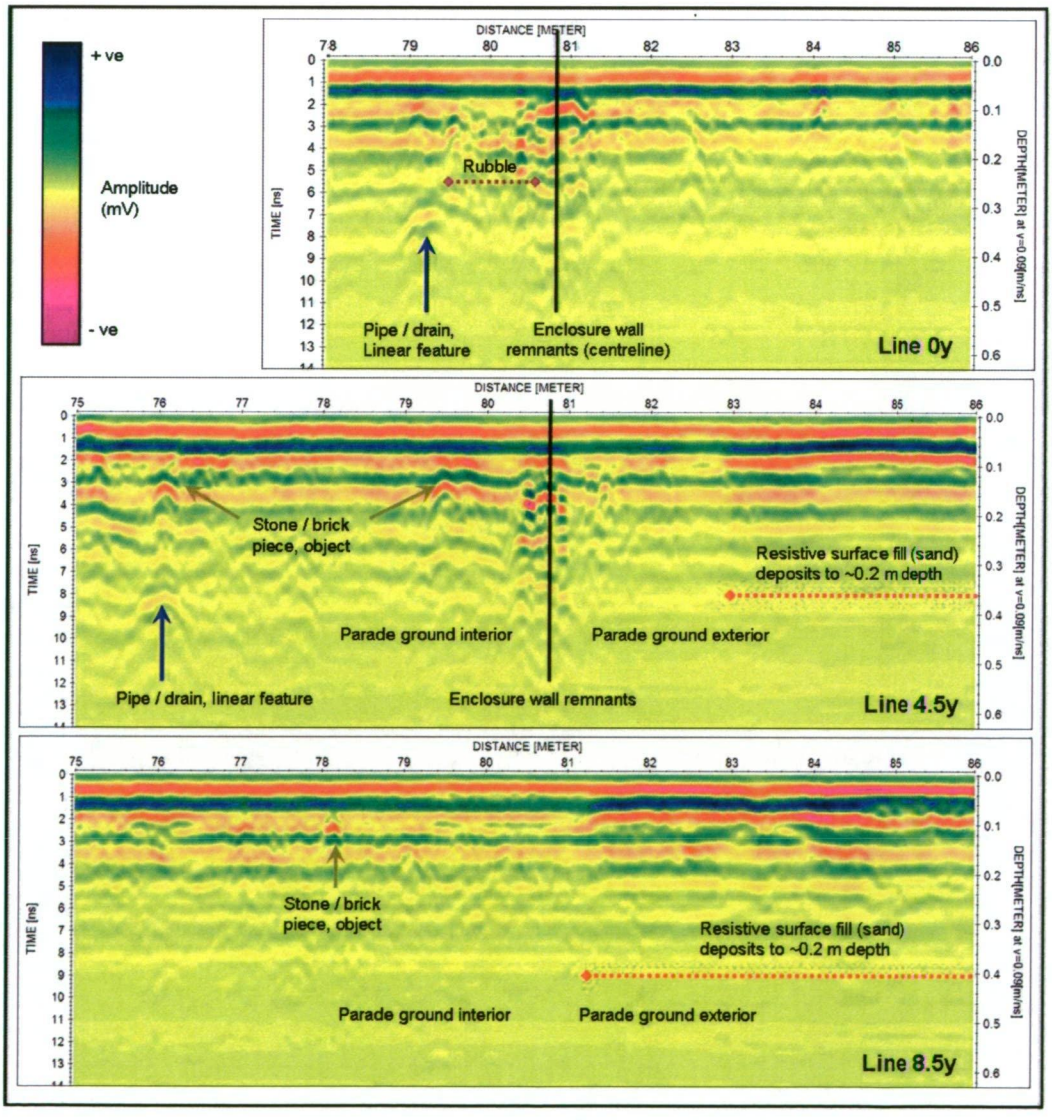

Figure 5.32: Unfiltered 800 MHz radargrams from Area A with interpretative annotation of anomalous responses attributed to features of interest, including a pipe tracking at an angle to the profiles as evidenced by the shift in distance in successive lines.

Amplitude maps generated at individual times from horizontally-stacked profiles provide plan views of Area A, some of which are presented in Figure 5.33. Due to variations in response amplitude, form and vertical position, the enclosure wall feature is not visualised as consistently as the pipe feature and resistive zone. Diffractions from well-preserved remnants in the immediate subsurface, for example, are often masked by continuous horizontal reflectors. The remaining wall portion is better delineated by summing all amplitudes recorded below the surface reflectors (> 30 samples) and setting amplitude thresholds to filter out low intensity signals from the surrounding media. Results using two sample ranges (depths 0.14 m and 0.16 m) and threshold values 3000mV and 3550 mV are shown in Figure 5.34.

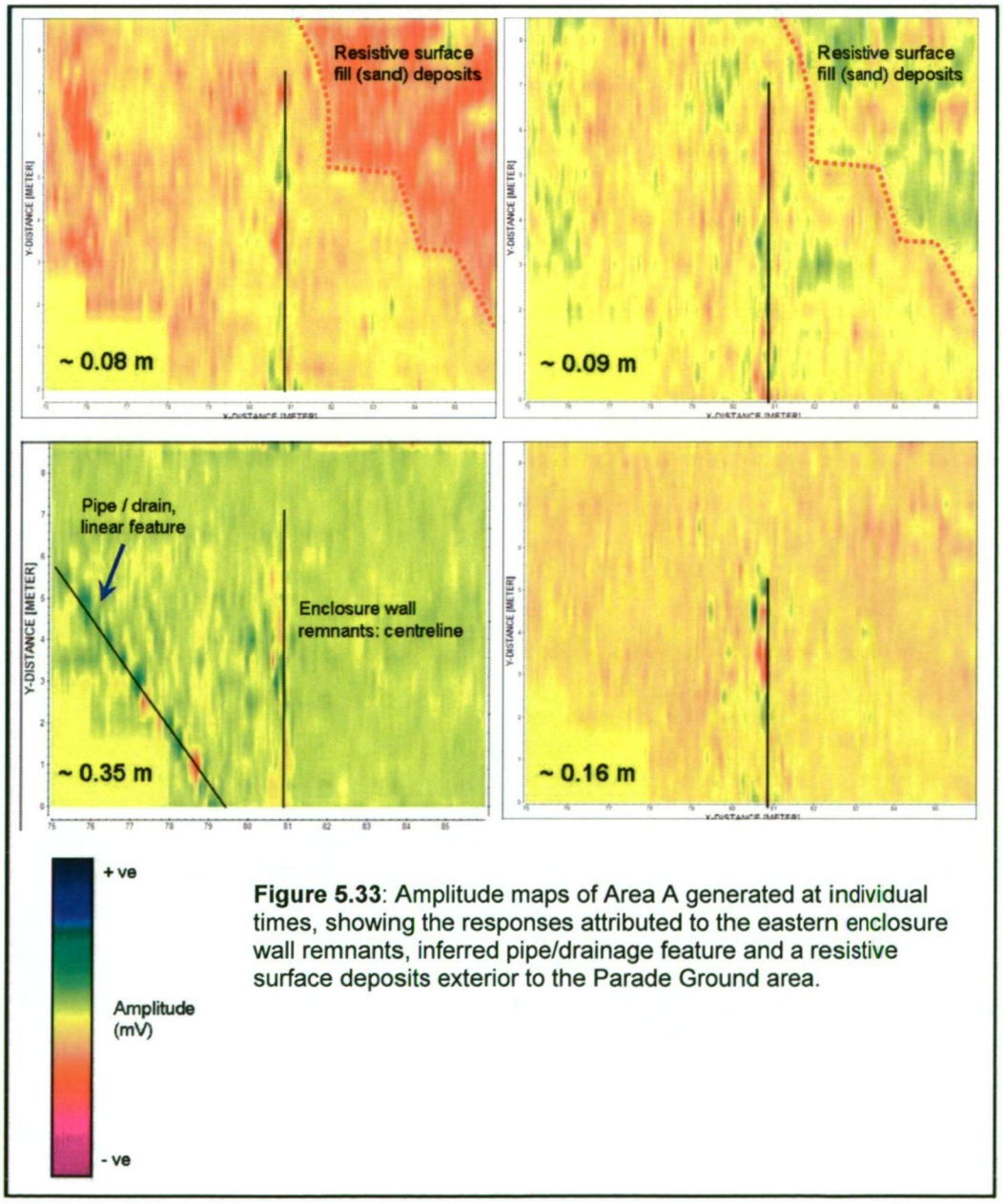

Figure 5.33: Amplitude maps of Area A generated at individual times, showing the responses attributed to the eastern enclosure wall remnants, inferred pipe/drainage feature and a resistive surface deposits exterior to the Parade Ground area.

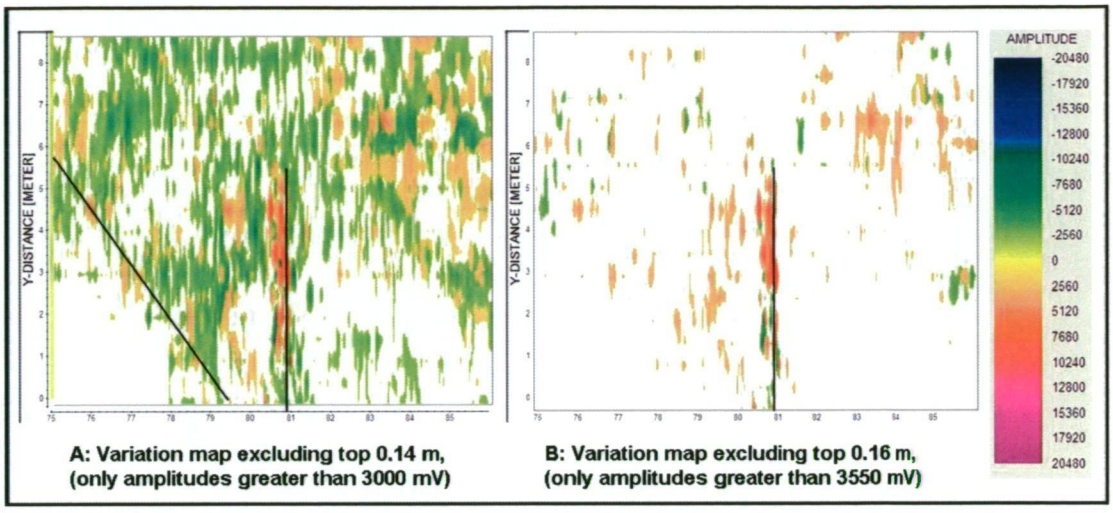

Figure 5.34: 800 MHz timeslices from Area A generated by absolute summing of amplitudes values below 0.14m (A) and 0.16 m (B) and clipping to 3000 mV and 3550 mV respectively. The black lines mark the eastern enclosure wall centreline and inferred pipe location.

Area B

Profiles collected parallel to the y-axis in Area B provide detailed information about material contexts to 0.5 m depth. A distinct geophysical contrast is measured between the inferred interior and exterior Parade Ground areas, although no apparent evidence of the northern enclosure wall. Responses inside the parade ground are characterised by continuous low amplitude reflections to ~ 0.15 m depth and minor hyperbolae primarily located within 0.15 - 0.2 m depth (Figure 5.35). These anomalies are attributed to contemporary loam deposits and remnants of the penal period reclamation fill respectively - as inferred from archaeological results. Moderately strong discrete diffractions between gridlines 13y and 14y (gridlines 44x - 45.5x) coincide with shallow point reflectors in the 500 MHz data, whose causative features are possibly associated with the tramway.

From 17 - 18y onwards, the profiles record multiple layers of high amplitude responses, including dipping planar reflectors and multiple adjacent point anomalies (Figure 5.35). Source materials for the planar types include contemporary sandy fill horizons, loam and gravel deposits, while rubble fill (dolerite, brick and sandstone pieces) probable cause the irregular signals. The average layer thickness (~ 0.1 m) and average depth of 0.3 m to the deepest responses correlates closely to excavation results.

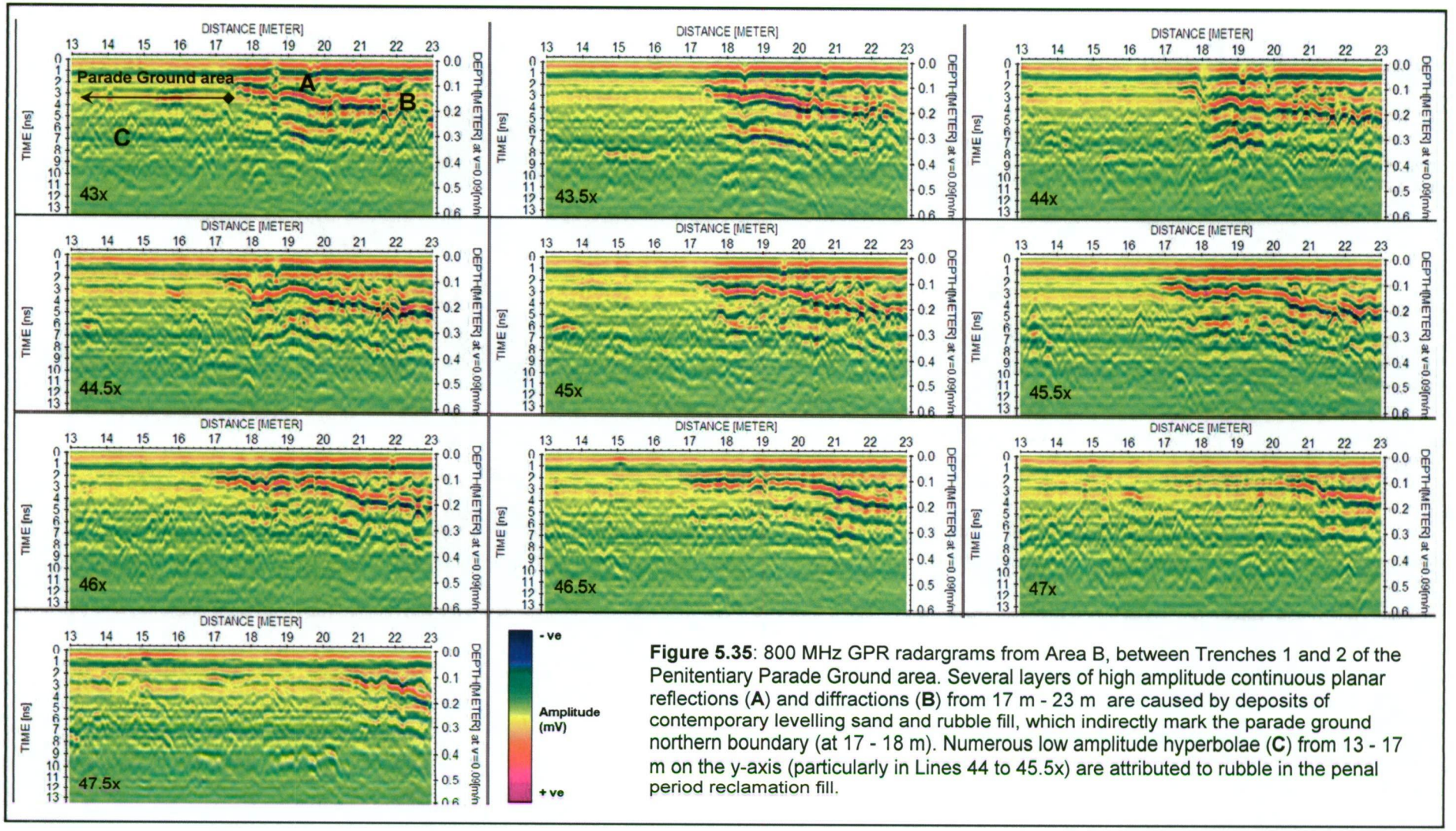

Figure 5.35: 800 MHz GPR radargrams from Area B, between Trenches 1 and 2 of the Penitentiary Parade Ground area. Several layers of high amplitude continuous planar reflections (**A**) and diffractions (**B**) from 17 m - 23 m are caused by deposits of contemporary levelling sand and rubble fill, which indirectly mark the parade ground northern boundary (at 17 - 18 m). Numerous low amplitude hyperbolae (**C**) from 13 - 17 m on the y-axis (particularly in Lines 44 to 45.5x) are attributed to rubble in the penal period reclamation fill.

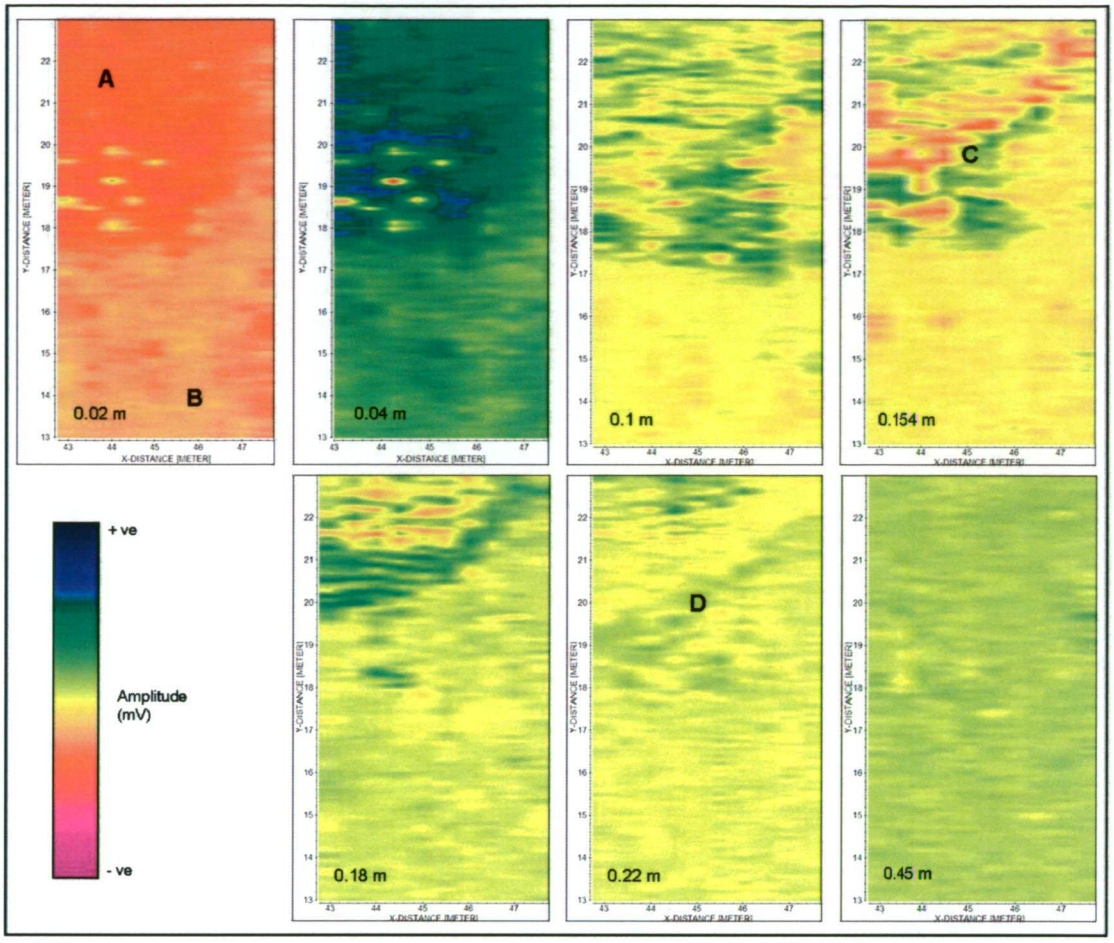

Figure 5.36: GPR 800 MHz amplitude maps of Area B, generated at individual times, showing variation in response patterns with increasing depth.

Amplitude maps generated at individual times effectively illustrate the distinct anomaly distribution in Area B (Figure 5.36). Strongest responses are visible in slices to 0.05, which correspond to the top interface of subsoil deposits (**A**). Multiples of the surface reflections and new signals from underlying material (**C**) appear as curved lineaments in plan view - indicating that layers are dipping gently. By 0.45 m, depth the timeslice is dominated by background noise.

Area C

The objective of surveying Area C was to detect and characterise any remnants of the western enclosure wall and Parade Ground interior surface. Profiles were collected perpendicular to the expected structural feature, at 0.5 m intervals, and are presented as radargrams in Figure 5.37. The top 3 - 4 ns are dominated by low-moderate amplitude continuous horizontal reflectors (**A**), with numerous discrete anomalies recorded to

~10ns TWTT. This is similar to the data from the Parade Ground interior in Area B. The only geophysical evidence which may possibly be attributed to the wall at the inferred location of -1.5 m appears in gridlines 15.5y (**B1**) and 17.5y (**B2**). Discrete planar reflectors and narrow hyperbolae recorded between -3x and -2x (**C**) across all lines except gridline 15.5y and may be caused by rubble associated with wall collapse, or a separate structural feature of unknown provenance. Continuous planar responses which dominate gridline 17.5y, from 1 - 4 m (**D**), exhibit similar amplitude and vertical position to anomalies mapped in Area B. They also coincide with the edge of an anomalous zone in the 500 MHz data, and a high apparent resistivity zone which extends NE from the Parade Ground wall - both of which are attributed to contemporary deposits of levelling sand.

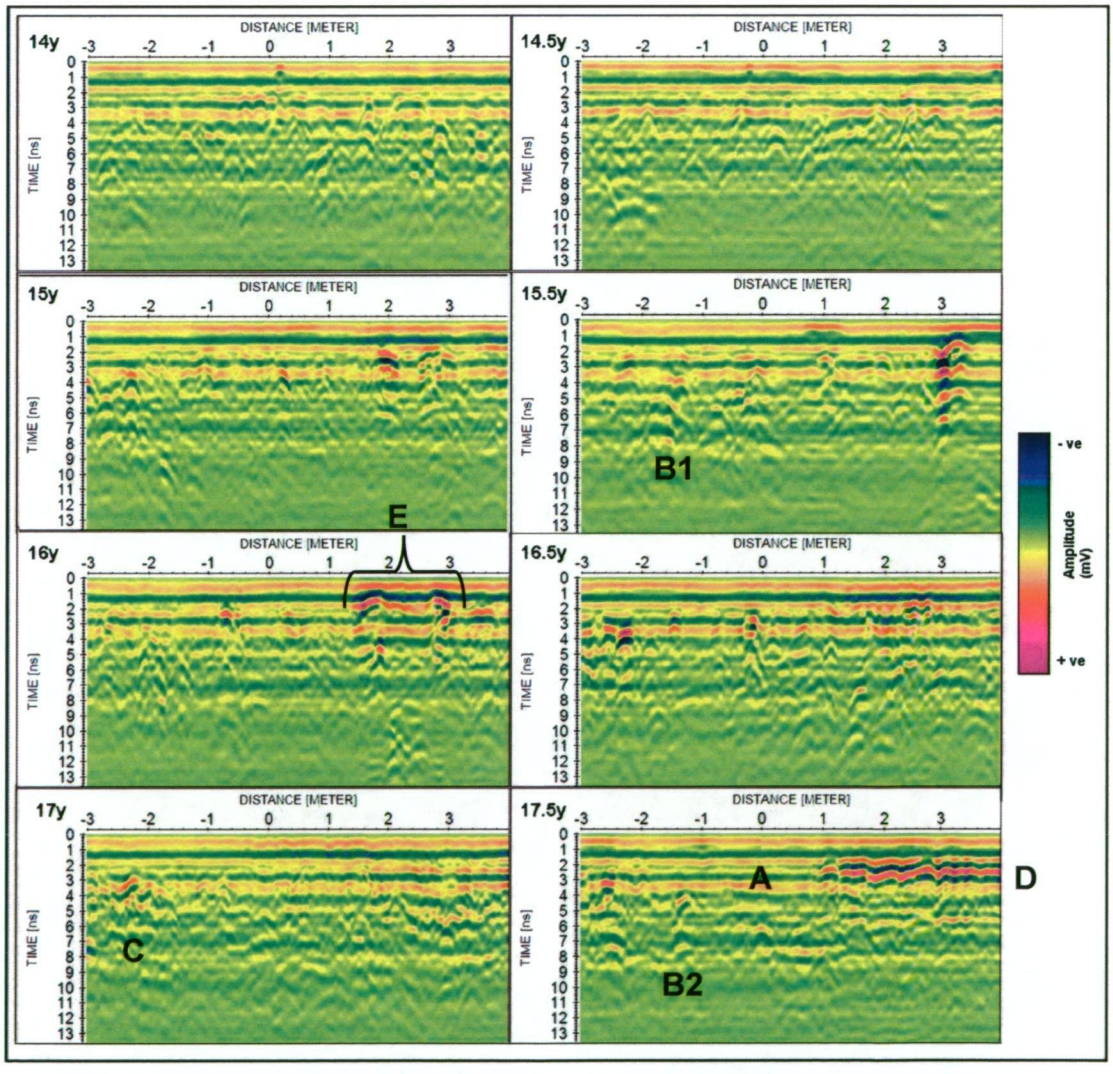

Figure 5.37: 800 MHz GPR profiles collected from Area C, across the western Penitentiary Parade Ground enclosure wall. Annotated responses are discussed in the text.

Unexpected high intensity responses are recorded between 1.5 - 3.0 m in gridlines 15y to 16.5y (Figure 5.37, **E**), and in the timeslices as a series of strong point anomalies to ~0.15m depth (Figure 5.38). While not attributable to any known feature(s), they do correlate to a zone of elevated apparent resistivity and hyperbolae in the 500 MHz data. This coincidence suggests that the GPR has detected shallow structural material, such as sandstone, which may be *in situ* remnants of a single feature. Neither the radargrams nor amplitude maps show any response patterns that define the Parade Ground interior and exterior areas. Aside from isolated anomalies, background intensities across Area C exhibit a very narrow dynamic range. These findings suggest that there is minimal lateral variation in material contexts in terms of composition and compaction, except for the shallow layer of levelling sand along 17.5y.

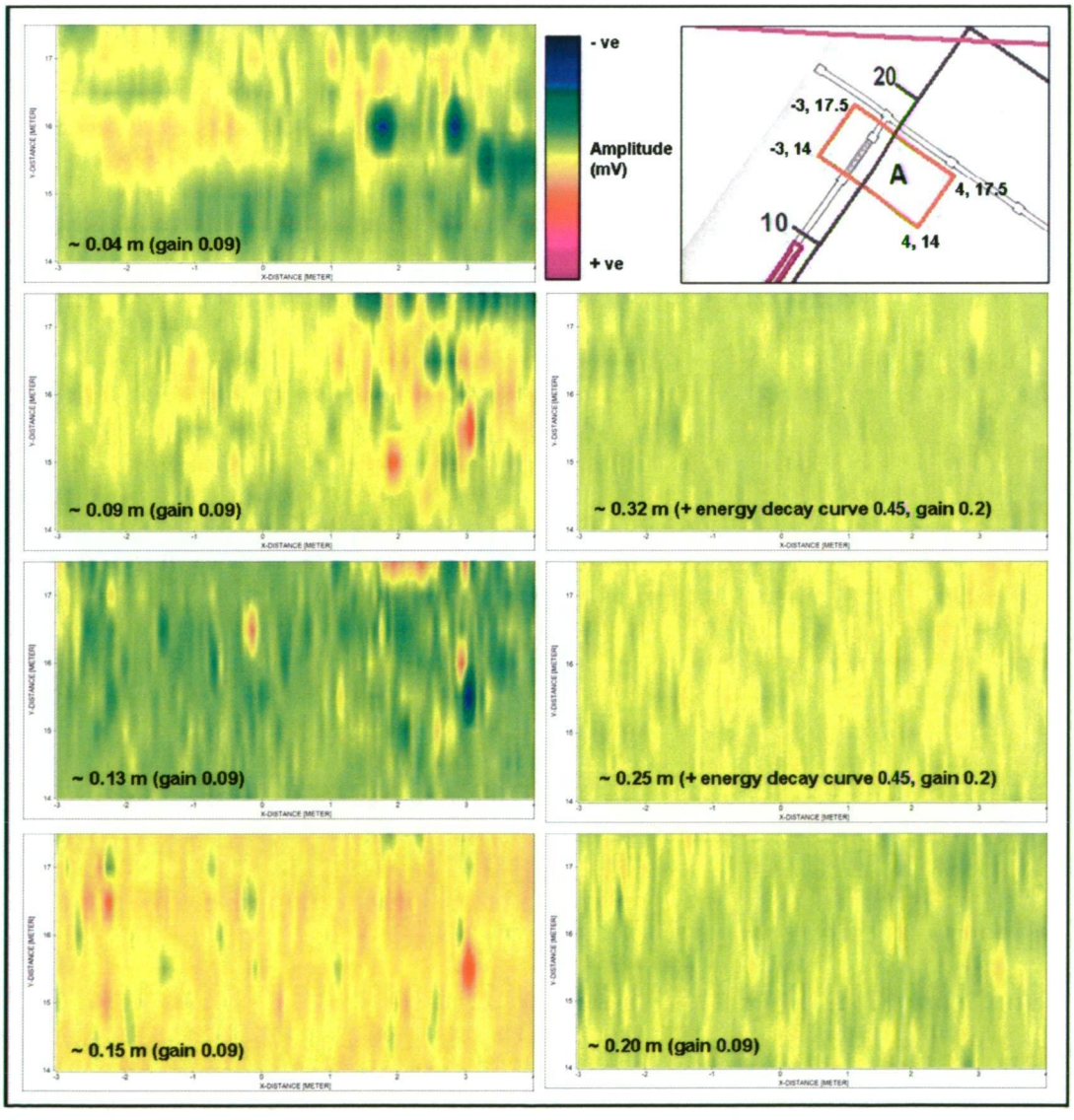

Figure 5.38: 800 MHz amplitude maps generated at increasing depths, showing that causative features are located within 0.15 m of the surface.

5.3 SAWPITS AND TANNERY COMPLEX

5.3.1 HISTORICAL CONTEXT

The Sawpits and Tannery Complex were constructed in 1856, following the closure of Cascades probation station – the main source of cut timber on the Tasman Peninsula, and in response to increased industrial activity at Port Arthur (Owen and Steele, 2002). Located on reclaimed land immediately north of the workshops and Radcliffe Creek (Figure 5.39), it formed the heart of the timber processing undertaken on site, in conjunction with 'the steam sawmill housed in the penitentiary workshops (Tuffin, 2003). Reclamation of the western and southern shores of Mason Cove took approximately two years, using convict labour, and was probably a multi-stage process. While the exact method is unknown, it is thought that a series of timber pens were built during low tides and progressively filled with stone rubble (Greg Jackman, pers. comm. 2005).

Figure 5.39: Portion of an ink drawing c1863 showing the Penitentiary, workshops (right side) and sawpits complex (far right). Radcliffe Canal was covered during this period (courtesy of Steele, 2004; PAHSMA ref. #1356).

Timber was supplied to the sawpits via three methods: 1) an iron-railed tramway, 2) floated into Mason Cove on flat bottomed barges, or 3) brought by convict labour gangs (Owen and Steele, 2002). The sawpits were decommissioned in 1872, when a lack of available convict labour forced their closure. Bushfires in the 1890s severely damaged the timber sheds, and it is believed that structural remnants, and other rubbish from the Carnarvon Township, were deposited into the pits (Owen and Steele, 2002). By the 1940s, the rubble-filled pits were levelled, dressed with topsoil and grassed over for use as a football field, cricket ground, car park and other purposes (Dorn *et al.*, 2002).

5.3.2 ARCHAEOLOGICAL CONTEXT

5.3.2.1 Background

Initial excavations at the Sawpits and Tannery Complex were conducted by PAHSMA during the Summer Archaeology Program of 2001. A small trench (2 x 1 m) was positioned over a grass parch mark which indicated the likely location of the southern sawpits external wall. The discovery of two faced stones, interpreted as part of the wall, inspired further archaeological excavations (Owen and Steele, 2002) and trial geophysical investigations in the summer of 2001 - 02 (Dorn *et al.*, 2002).

A local grid measuring 40 x 60 m was established to encompass the sawpits and surrounds (Figure 5.1). The following geophysical techniques were used: magnetics (Figure 5.40), frequency domain electro-magnetics (EM-38 and EM-31), electrical resistivity profiling (Wenner array) and Induced Polarisation. For a summary of these results, please refer to Section 5.4.5. All related geophysical images and interpretation maps are presented in Appendix C.

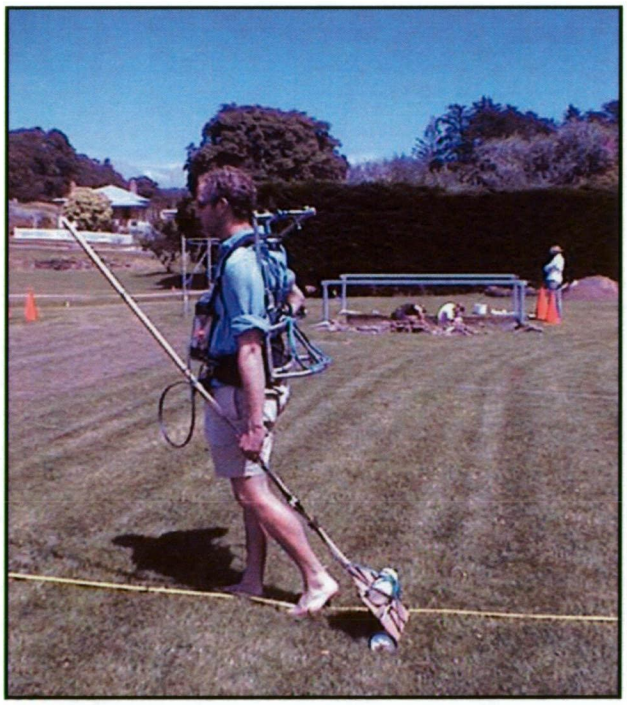

Figure 5.40: Magnetic surveying and excavations at the Sawpits and Tannery Complex during summer 2001 – 02 (photograph courtesy of Dorn *et al.*, 2002).

Archaeological investigations were conducted during the summers of 2001 – 02 and 2002 – 03. The first program involved extending the 2001 test trench by 3 m to the southeast and siting three others in alignment with the expected southern wall location. Later excavations were then conducted to locate the Sawpit western and northern external walls. These, and other known and inferred cultural features at the site, are shown in Figure 5.41.

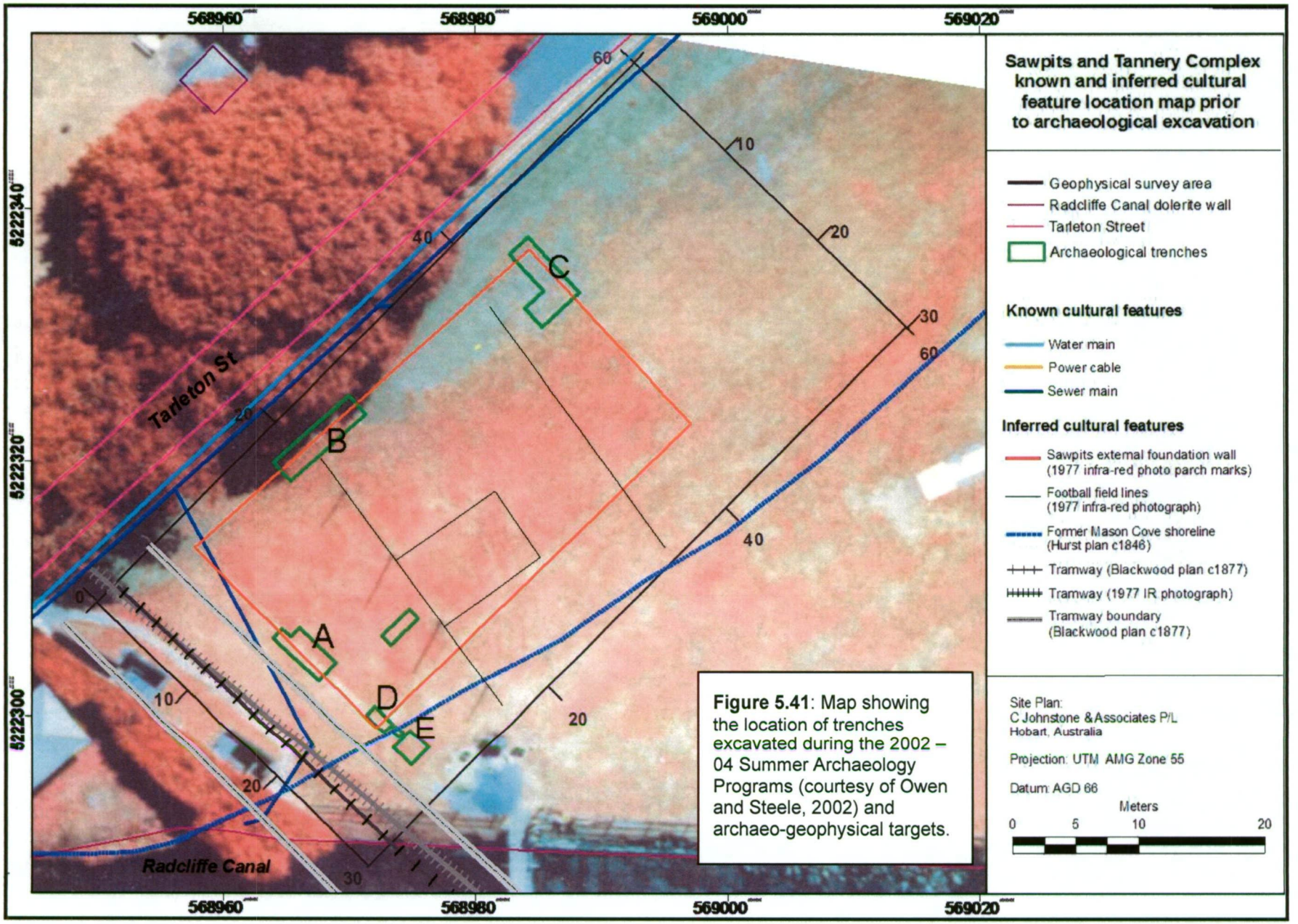

Figure 5.41: Map showing the location of trenches excavated during the 2002 – 04 Summer Archaeology Programs (courtesy of Owen and Steele, 2002) and archaeo-geophysical targets.

5.3.2.2 Excavation findings and interpretation

The following section provides a brief summary of the archaeological findings that are relevant to this project's objectives. All stratigraphic information presented is derived from the Sawpits and Tannery Complex Archaeological Report by Owen and Steele (2002), with the exception of several photographs.

Excavations conducted at Trench **A** allowed the partial characterisation of key cultural features, by providing insight into their geometry, composition and function. Surficial deposits, to ~ 0.15 m depth, comprise of a layer of turf, black silty loam topsoil and sand fill. Immediately underlying these contemporary deposits, the dominant structural feature in Trench A is a wall running NW – SE (Figure 5.42). This is identified by archaeologists to be the southern external foundation wall of the Sawpits. Constructed primarily of faced dolerite and sandstone masonry, it measures ~ 0.6 m (2 ft) wide and descends to the original beach sand deposits at 1.43 m. Brick, dolerite and sandstone fragments in a soil matrix (rather than mortar) fill the wall core (Owen and Steele, 2002). Some sections of the wall are missing, as shown in the scaled section drawing in Figure 5.42, possibly as a result of site levelling following the 1890s bushfires.

In the NE end of Trench A, excavations also uncovered a penal period red clay brick lined drain which transects the foundation wall at an oblique angle (Figure 5.42). Capped with dolerite masonry blocks, it 'interfaces with the wall just below modern surface level' and likely drained from the sawpit or tannery (Owen and Steele, 2002).

Soils on the southern side of Trench A are typically more compact and dry than those on the northern side. A shallow deposit of dolerite gravel in a yellow clay matrix present is interpreted as a possible walkway around the Sawpit perimeter. This is juxtaposed with the coarse rubble material originally used to support the foundation wall (Owen and Steele, 2002).

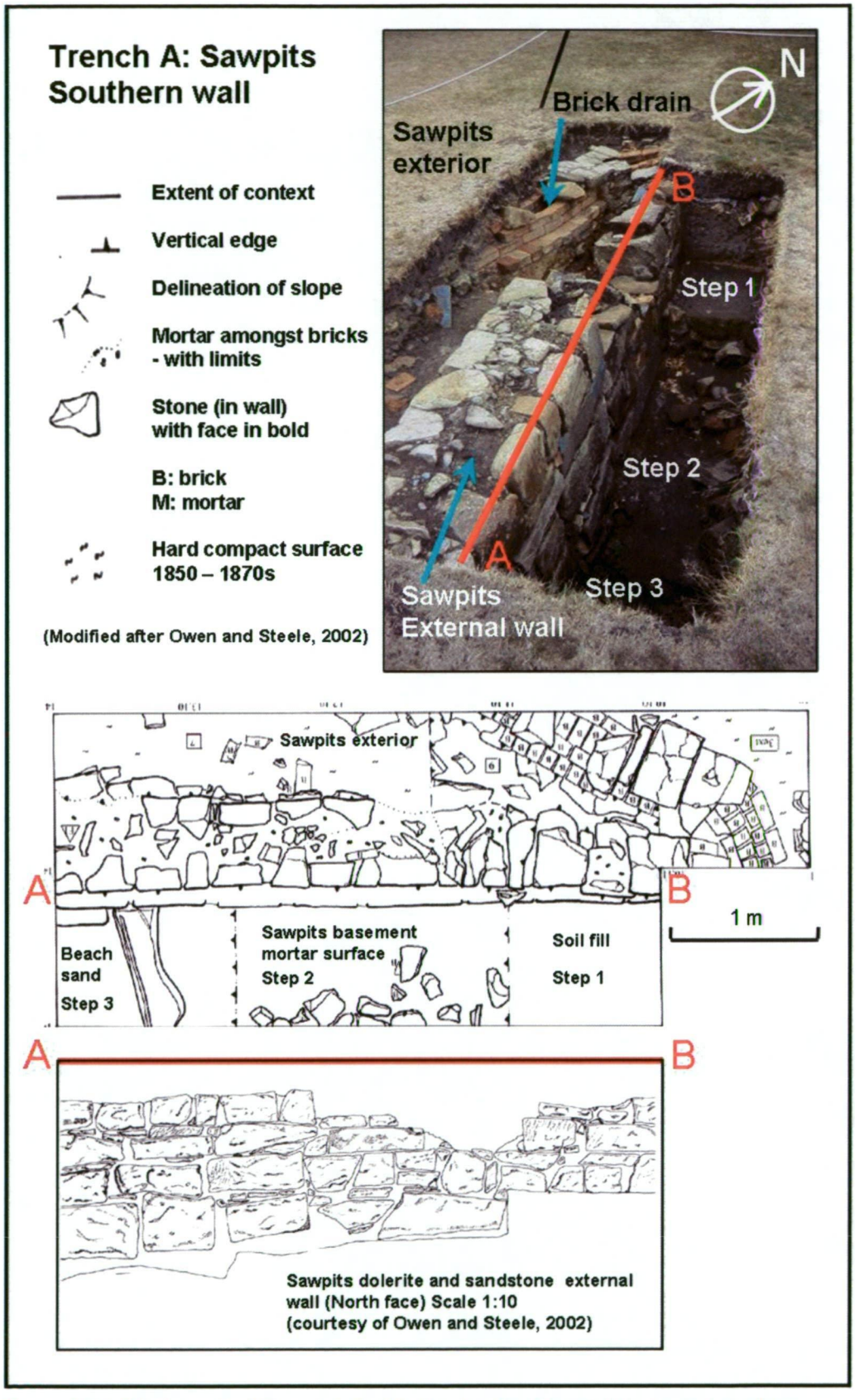

Figure 5.42: Photograph of Trench A (right) showing the Sawpit dolerite and sandstone external wall and contemporaneous brick drain with dolerite capping blocks. The Sawpit mortar floor deposit was uncovered at 1.43 m depth, as seen here with some of the rubble pit fill (photograph courtesy of the J.Johnston, 2002). Trench A final excavation plan (centre) and section drawing (bottom) along **AB** are both to scale (courtesy of Owen and Steele, 2002).

North of the foundation wall, inside the Sawpit perimeter, a series of stepped excavations (1 - 3) reveal the stratigraphy to 0.76 m, 1.2 m and 1.43 m (Figure 5.42 photograph). Deposits immediately underneath topsoil predominantly comprise of bricks, with charcoal, ash and other artefactual material, such as glass, ceramic ware and metallic objects (Step 1, Figure 5.42). The latter were mainly of iron composition (e.g. nails), but there was also some tin, copper and lead. Most penal period artefacts and the surrounding rubble deposits are believed to have been dumped in the sawpits between 1873 and 1920, particularly following destruction of the timber Sawpit and Tannery Complex by the 1890s bushfires (Owen and Steele, 2002).

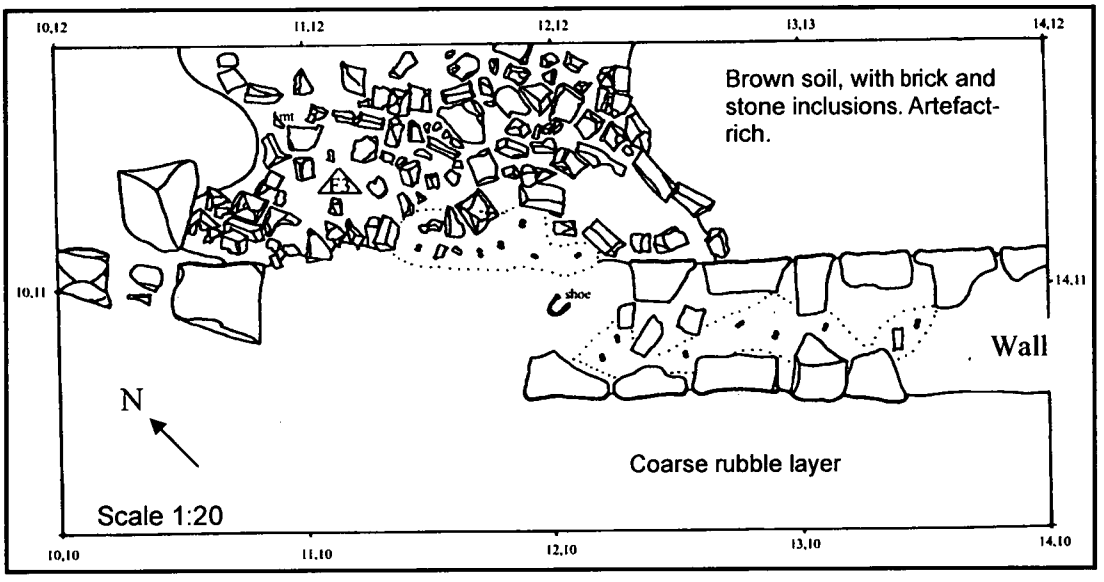

Figure 5.43: Trench A prior to the 1 x 1 m NE extension, showing the top of the Sawpits exterior foundation wall, compacted pathway horizon and brick rubble Sawpit fill. For legend see Figure 5.40 (courtesy of Owen and Steele, 2002).

To a depth of 1.2 m, the excavation encountered brown-black soil and clay horizons, dolerite rubble fill and a thick layer of highly disintegrated mortar. The latter is believed to have formerly provided a solid and level sawpits floor surface (Owen and Steele, 2002). Below the mortar, archaeologists revealed beach sand and sandstone blocks, attributed to the original Mason Cove shore, and the deepest course of dolerite masonry associated with the foundation wall (Figure 5.42). These features provide evidence that the reclamation depth was approximately 1.43 m at this location (Owen and Steele, 2002).

Trench B was excavated to < 0.5 m depth and revealed a stratigraphy dominated by the western external foundation wall (Figure 5.44). The structural integrity of this feature is well-preserved and the top width is comparable to the southern wall. Compacted gravel deposits exposed outside the sawpits perimeter are interpreted as a continuation of the penal period pathway recorded in Trench A. Darker clay-loam and rubble fill material in the Sawpits interior was also similar to that of Trench A, and is characterised by large dolerite blocks, brick pieces, artefacts, ash and charcoal.

Excavations at Trenches C and D were successful in locating the northern wall return and southern wall continuation (northern edge only) respectively. Feature dimensions and surrounding deposit types were similar to those uncovered in Trenches A and B. A 2 x 2 m Trench (E) was placed over the proposed southern-eastern sawpit foundation wall intersection (Figure 5.41). Underlying the turf and topsoil contexts, three quarters of the trench was excavated to a compacted layer of dolerite gravel and beach pebbles. Further digging in the northern quarter revealed a compacted clay deposit at ~ 0.6 m depth, the right-angled boundary of which provided indirect evidence of the wall position (Owen and Steele, 2002). This layer is assumed by archaeologists to be the same penal period ground level uncovered in Trench A. The known and interpolated positions of these perimeter walls are presented schematically in Figure 5.45.

Figure 5.44: Trench **B** (left) and **C** (above) showing the Sawpit external wall, exterior and interior rubble fill material (photographs courtesy of Johnston, 2002; Steele, 2003 respectively). Trench **D** photograph (below left) and final excavation plan (below) confirming the southern foundation wall location (courtesy of Owen and Steele, 2002).

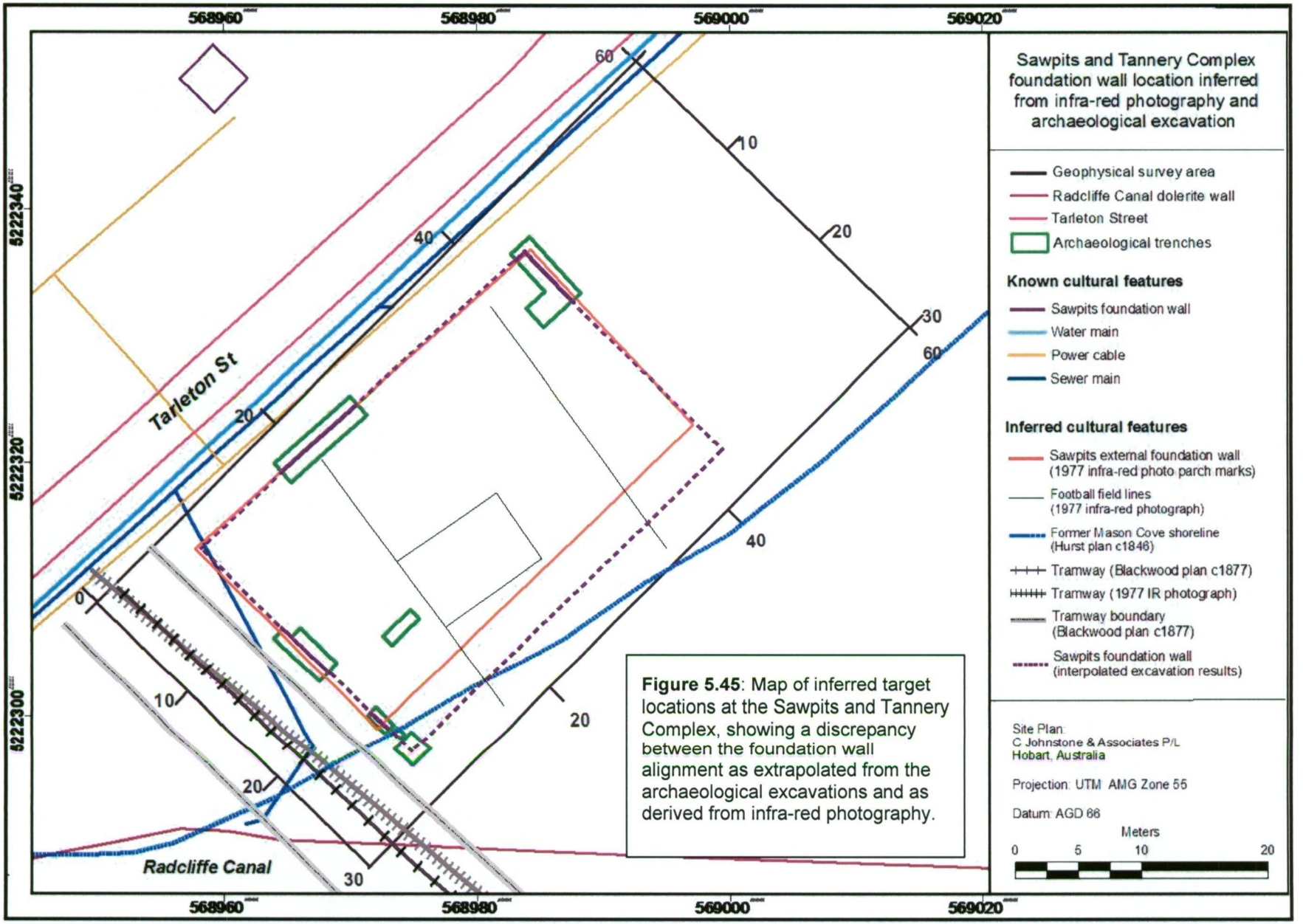

Figure 5.45: Map of inferred target locations at the Sawpits and Tannery Complex, showing a discrepancy between the foundation wall alignment as extrapolated from the archaeological excavations and as derived from infra-red photography.

5.3.3 ARCHAEO-GEOPHYSICAL TARGETS

For this study, archaeo-geophysical targets at the Sawpits and Tannery Complex include penal period structural elements associated with the industrial complex, reclamation features and deposits, post-penal and contemporary fill deposits, as listed below:

- sawpit external foundation walls,
- penal period yard surface(s),
- sawpits interior floor surface(s),
- post-penal to contemporary Sawpits interior fill material(s),
- reclamation features, former shoreline.

No historical evidence exists for the construction or design details of the sawpit building, floor depth or internal layout (Owen and Steele, 2002). Target locations, outside the archaeological trenches, are inferred from a few historic plans, photographs, and surface evidence, and are illustrated in Figure 5.45. Spatial discrepancies between inferred feature locations are partly due to the accuracy of each source and error margins associated with rectification.

Target dimensions and composition, were also derived from the archaeological excavation results (Section 5.3.2). The Sawpit foundation wall in Trench A, for example, measured 0.6 m wide at the top and was estimated to be 1.0 m wide at the base (Owen and Steele, 2002). Similar findings at Trenches B - D suggested that the dimensions may be consistent along the entire sawpit perimeter, although some of the dolerite and sandstone masonry may be removed. It was expected that any drains dating from the penal period were constructed of brick, sandstone and mortar, such as the one excavated in Trench A. The ability to detect these structural features using GPR and dipole-dipole techniques primarily depends on the comparative resistivity of surrounding fill material.

5.3.4 GEOPHYSICAL SURVEY, FINDINGS AND INTERPRETATION

5.3.4.1 Introduction

Ground penetrating radar and dipole-dipole electrical resistivity surveying was conducted at the Sawpits and Tannery Complex, to augment previous geophysical investigations of the site by PAHSMA and UTas in 2001 and 2002. As described in Chapter One, these techniques included magnetometry, FEM (EM-31 and EM-38), apparent resistivity (Wenner array) and several GPR transects (Dorn, 2002). Data from this earlier work was re-gridded as part of this project, giving the author greater understanding of the archaeo-geophysical context at the site. Variation maps and new interpretation images are presented in Appendix D.

5.3.4.2 Ground penetrating radar

Ground penetrating radar profiling was conducted to detect and characterise primary archaeological targets associated with the penal period Sawpit and Tannery Complex. Assessment of individual profiles and horizontal amplitude maps aimed to identify broad anomaly patterns in three dimensions and to characterise responses attributable to known and inferred features. Lineaments and anomalous zones were symbolised in a data abstraction map and interpreted qualitatively to provide a synoptic plan view of the Sawpits area. This process was primarily achieved by comparing the GPR response distribution patterns to the archaeological ground-truthing results.

Data acquisition and processing

Surveying of the Sawpit and Tannery geophysical grid was conducted in May 2004, over consecutive days to minimise the effect of varying soil conditions. Maximum wave penetration of the 500 MHz system was set to 30 ns TWTT, which corresponds to a depth of investigation of ~ 1.45 m when assuming a nominal velocity of 0.11 m/ns - typical for dry rubble and loamy soils (Conyers and Goodman, 1997). Profiles were collected in both transverse (x) and longitudinal (y) directions, at 0.5 m and 2.0 m line

spacing respectively. Fundamental survey parameters are summarised in Table 5.5. Data was processed using the approach adopted for the parade ground area.

Survey type	Ground penetrating radar		
Instrumentation	Mala RAMAC X3M system		
Area surveyed	129 lines, within a regular grid measuring 56 x 30 m		
Method of coverage	Continuous data collection at 0.03 s intervals		
Traverse interval	0.5 m along transverse gridlines (0 - 30m) 2.0 m along longitudinal gridlines (4 - 60m)		
Trace interval	0.01 m*	**Tx- Rx separation**	0.18 m
Range	30 ns	**Samples**	192
Stacking	8	**Antenna frequency**	500 MHz (centre frequency)
Comments	Fiduciary marks added manually during data collection, estimated accuracy to +/- 0.1 m. Profiling conducted with ≤ 1.0 m offset from parallel measuring tape. Survey conducted at an even pace of ~2km/hr * distance interpolation calculated using fiducial marks		

Table 5.5: Ground penetrating radar 500 MHz survey parameters for the Sawpits and Tannery.

Findings and interpretation

Individual profile analysis

Broad anomaly patterns and discrete responses recognised through individual profile analysis were used to infer and characterise primary archaeological targets. Benchmark responses were established for known features, such as the foundation walls, by comparing excavation results to anomaly patterns in profiles collected near the trenches. This information was used as a primary reference for qualitative interpretation of similar responses across the surveyed area. GPR interpretation was also guided by the feature location map, derived from infra-red photography and extrapolation of ground-truthing results.

Responses attributed to the foundation wall exhibit a range of amplitudes and forms, which provide geophysical evidence for differences in feature construction and condition. Primary reflections from the wall's top surface are recorded between 0.3 - 0.5m depth and extend less than 1.0 m laterally. These values correlate closely to the depth and width (~ 0.6 m) of excavated sections. A good example is provided in the

boxed section from gridline 28y, outlined responses derive from the western perimeter wall (Figure 5.46). Two sets of adjacent high amplitude diffractions centred on 3.5 m (circled in **a**) suggest that the wall's top surface is two blocks wide and located at ~ 0.4 m depth (7 - 8 ns TWTT). These findings are consistent with the excavation results from Trench B. Reflections from the wall exterior surface (**b**) extend deeper (~ 1.2 m) relative to those from the interior wall face. This is probably because reclamation fill around the Sawpits is more homogeneous, and therefore less obstructive to the radar signal, than the coarse interior rubble fill.

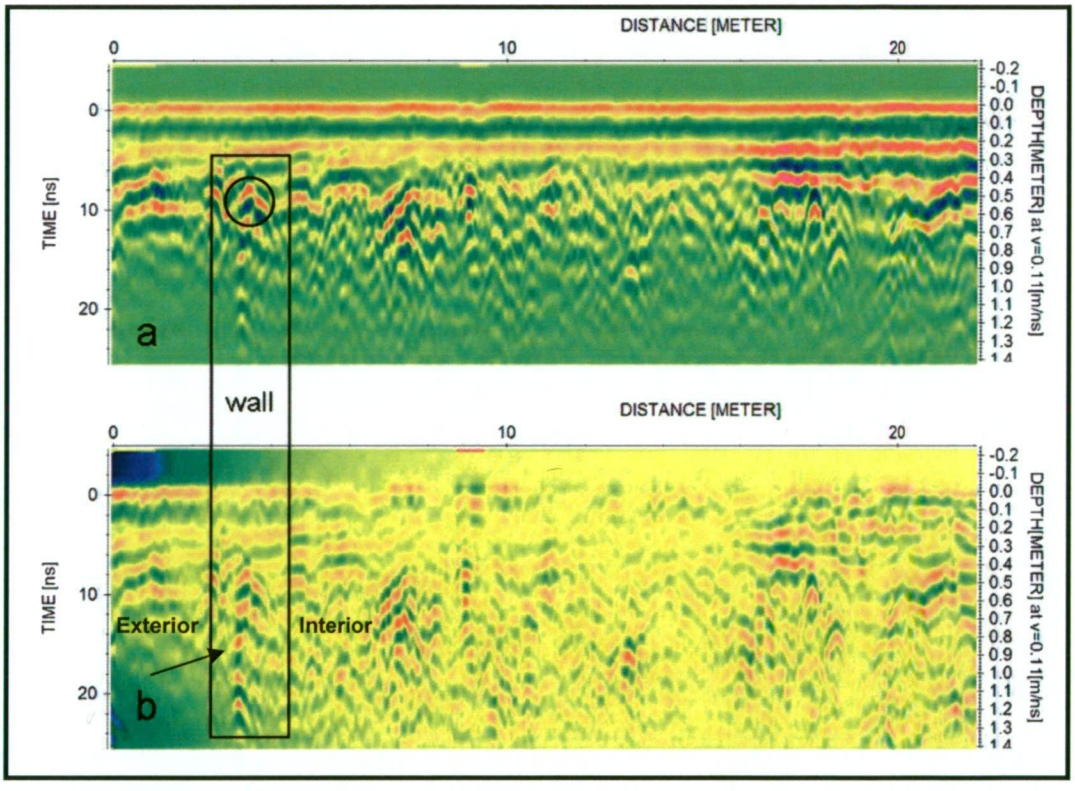

Figure 5.46: 500 MHz data from gridline 16.5y, highlighting anomalous responses attributed to the Sawpits perimeter wall. Both radargrams are distance and depth corrected, with a gain function applied to compensate for signal attenuation. Image **b** has had the average trace subtracted to enhance high amplitude signals.

Several anomalies coincident with inferred wall locations exhibit weak amplitude contrasts with surrounding responses, and are therefore identified primarily by their diffraction form - such as the anomaly highlighted at 3 m distance in Figure 5.47a. A high amplitude hyperbolic response at 22 m correlates to a parch mark in the infra-red photograph and is interpreted as originating from the eastern Sawpit perimeter wall. Adjacent point anomalies recorded at 26.5 m (Figure 5.47a) are attributed to a second masonry feature which trends parallel to the perimeter wall. A coincident zone of very

high apparent resistivities exhibited in the dipole-dipole tomogram for gridline 29y (Figure 5.51) supports this interpretation. Further analysis of transverse radar profiles indicated that the linear structure abuts the southern Sawpit perimeter wall at Trench E. Indirect evidence of this intersection is provided by Owen and Steele (2002), who uncovered a shallow right-angled lateral interface between compacted clay deposits adjoining a layer of dolerite gravel and beach pebbles (interpreted as the penal period yard surface) external to the Sawpit (Owen and Steele, 2002). These deposits manifest in GPR profile as weak responses overlying the wall anomaly, and adjacent high amplitude planar reflections respectively (Figure 5.47a).

The boxed response at 42 - 43 m in gridline 10x (Figure 5.47b) is derived from the Sawpits northern perimeter wall, as inferred from the infra-red photography and archaeological excavation of Trench C. It is characterised by high amplitudes, which reflect a strong contrast in material properties between the masonry and overlying loamy topsoil, and therefore indicates that this section of wall has a level top surface.

Gross changes in stratigraphy are also effectively illustrated in profile by broad variations in response amplitude, form and position. The Sawpits interior is characterised by narrow diffractions over a large range of intensities, typical of responses derived from coarse rubble material (Figure 5.47b). High amplitude hyperbolic reflections are attributed to isolated objects, such as dolerite pieces and metallic debris, which exhibit contrasting dielectric permittivity to the fill matrix (clay, loam, sand) (Figure 5.47b, 22x). Diffractions derived from the Sawpits rubble fill are visible from ~ 0.3 m depth underlying continuous planar reflectors from the sandy loam topsoil and continue to maximum penetration of ~ 1.4 m depth. This range correlates closely to archaeological findings from Trench A, where excavation uncovered the inferred compacted floor deposits at 1.43 m (Owen and Steele, 2002). The lateral distribution of Sawpits rubble fill and the known and interpolated positions of all Sawpit walls are presented schematically in Figure 5.51.

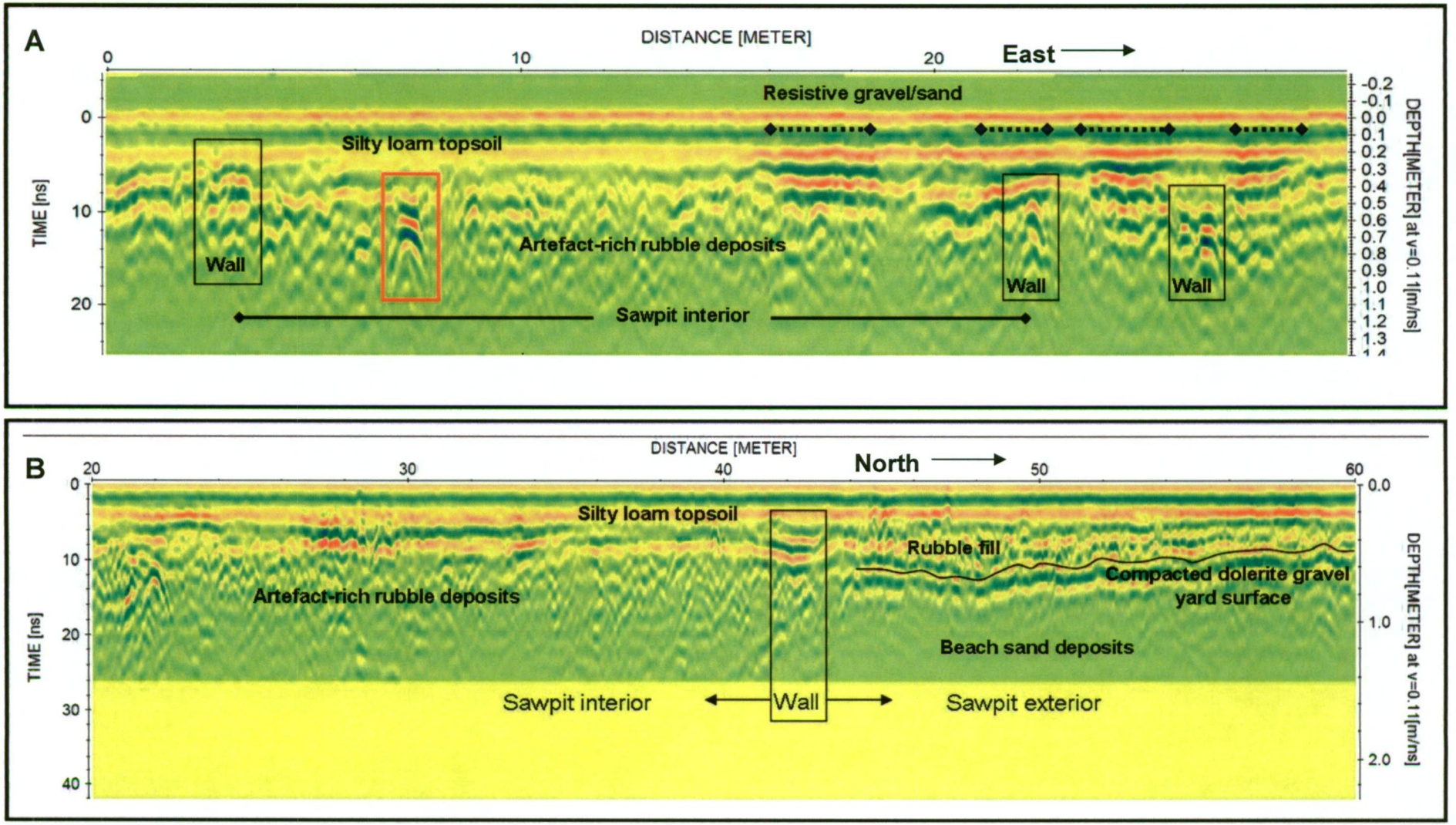

Figure 5.47: Processed and gain-adjusted 500 MHz GPR profiles along gridlines 16y (**A**) and 10x (**B**) at the Sawpits and Tannery Complex, showing response distribution patterns and interpretion of key stratigraphic features.

Response patterns north of the Sawpits are in sharp contrast to those recorded inside the perimeter wall, as shown in a radargram from Line 10x (Figure 5.47b). Exterior to the Sawpits, discontinuous diffractions of irregular shape and amplitude, between 0.3 m and 0.7 m depth, are attributed to post-penal fill material underlying the contemporary levelling topsoil. High amplitude continuous reflectors external to the northern Sawpits wall, from 44 m to 60 m at 0.5 - 0.6m depth (marked by the black line), are possibly derived from compacted dolerite gravel yard surface deposits similar to those excavated in Trenches A and B (Owen and Steele, 2002). A deeper zone of relatively weak amplitude responses in this area is associated with homogeneous beach sand deposits of Mason Cove.

Timeslice analysis

The timeslice in Figure 5.48, generated at 17.57 ns TWTT (~ 0.91 m depth) clearly defines the Sawpits interior as a rectilinear zone of irregular high frequency amplitude variations typical of multiple diffractions in section. Surrounding material from the former Mason Cove foreshore are characterised by consistently weaker signal intensities, as discussed previously, which suggests that it is more homogeneous and with little rubble. High amplitude hyperbolae derived from contemporary service pipes are visible as a linear trend with an offshoot at 50 m, which is not marked on the Port Arthur Historic Site service plan.

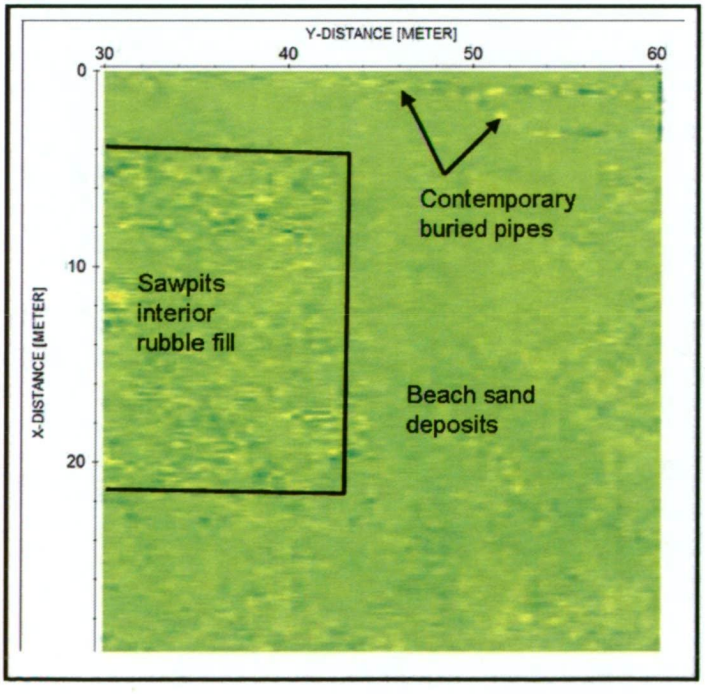

Figure 5.48: A 500 MHz GPR timeslice from the Sawpits northern end, generated at 17.57 ns TWTT (~ 0.91 m depth), which shows the difference in response distribution patterns between the Sawpits interior and surrounding Mason Cove remnant beach deposits.

Anomalous zones and linear trends within the topsoil fill are discernable in selected amplitude maps in Figure 5.49. Lineaments circled in slice **A**, generated at 1.85 ns, are caused by surface indentations from a former football field - as inferred from infra-red photography (Figure 5.41). Other shallow features include a pathway marked with arrows, and deposits in the eastern corner (**X**) which correlate to a zone of very high apparent resistivities (Dorn *et al.*, 2002; Appendix D).

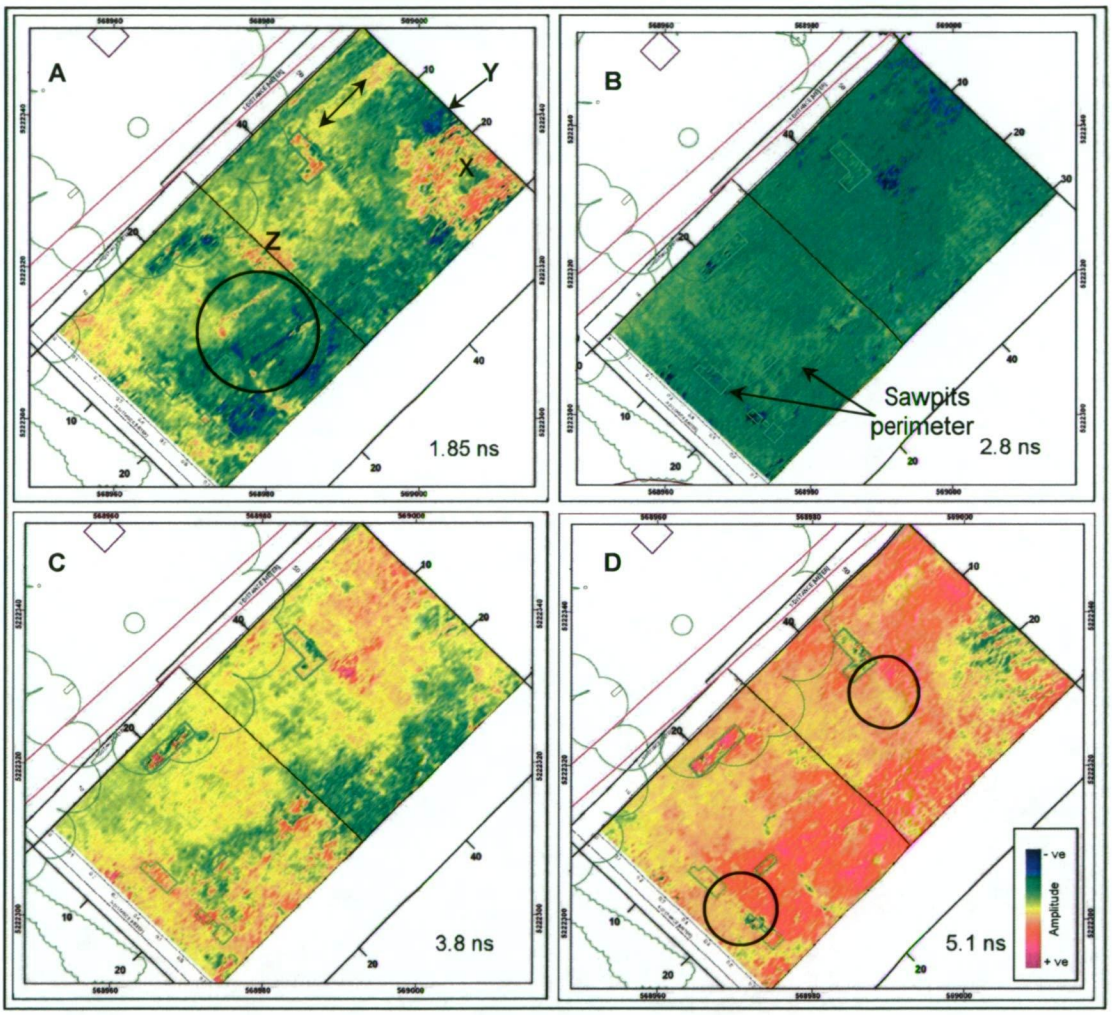

Figure 5.49: 500 MHz amplitude maps of the Sawpit and Tannery Complex, generated at individual TWTT time intervals as shown.

The latter may be levelling sand similar to fill deposits at the Penitentiary Parade Ground that were used to level the compacted central area of the former football field. Small zones of very high signal intensities (**Y**) are attributed to patches of sand or gravel - an interpretation supported by coincident anomalous highs in the apparent resistivity survey results from 2002 (Dorn *et al.*, 2002). A cluster of positive anomalies at (**Z**) may be associated with remnants of a structural feature within the Sawpits, an explanation

proposed by Dorn *et al.* (2002). Analysis of individual radar profiles identified a series of high amplitude primary reflectors at ~ 0.3 m depth, and secondary diffractions to ~ 0.9m - possible evidence of an interior wall separating two pit areas.

The timeslices in Figure 5.49 also provide indirect geophysical evidence of the Sawpits perimeter wall. For example, the eastern and southern wall alignment is inferred from relatively high amplitude rectilinear responses which intersect at Trench E in slice **(B)**. Matching parch marks identified in the infra-red photography, due to dry soils (i.e. more resistive) overlying the shallow masonry, support this interpretation. Slice **D**, generated at 5.1 ns TWTT, clearly defines the Sawpits northern and southern wall alignments, via lateral interfaces between anomalous zones attributed to shallow gravel/sand deposits (circled). Lineaments and anomalous zones inferred from these four timeslices are recorded schematically in the Sawpits and Tannery Complex data abstraction map (Figure 5.50). Qualitative interpretation of key responses derived from both timeslice and individual profile analyses is presented in Figure 5.51.

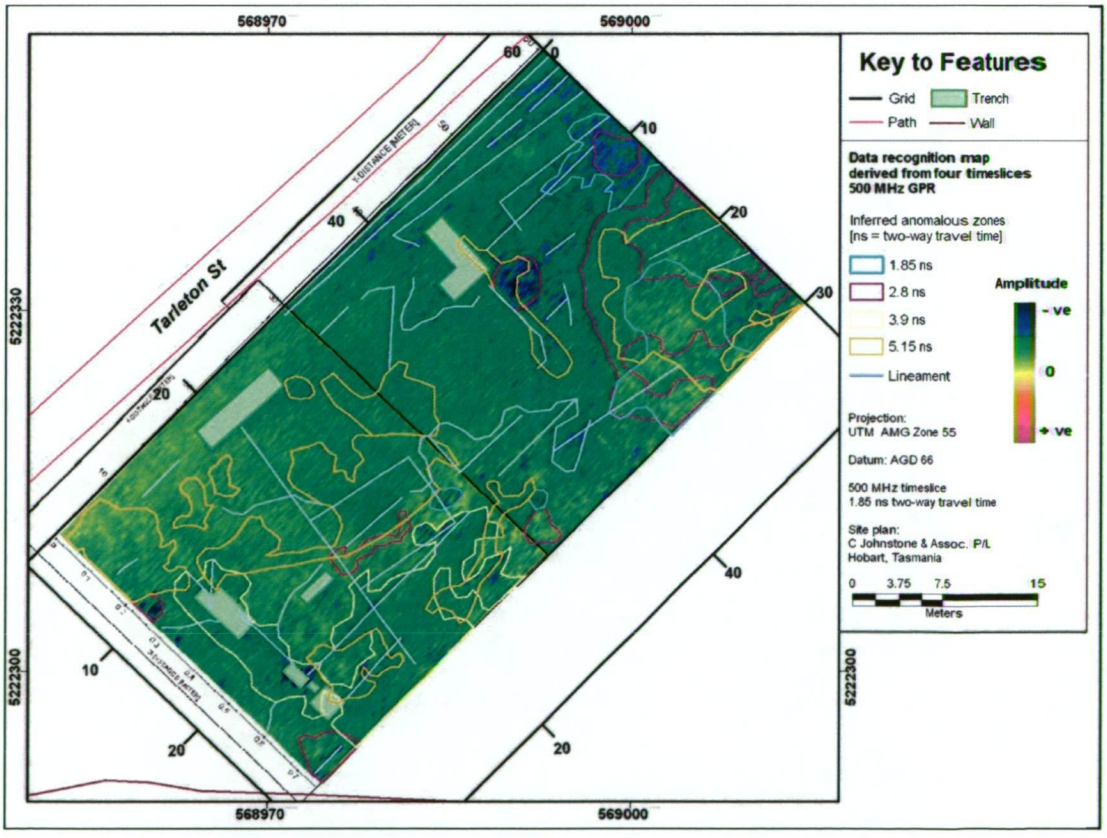

Figure 5.50: Sawpits and Tannery Complex ground penetrating radar amplitude map at 2.8 ns TWTT, overlain by inferred linear trends and anomalous zones from data recognition of four timeslices. Interpretation of these anomalies is shown in Figure 5.51.

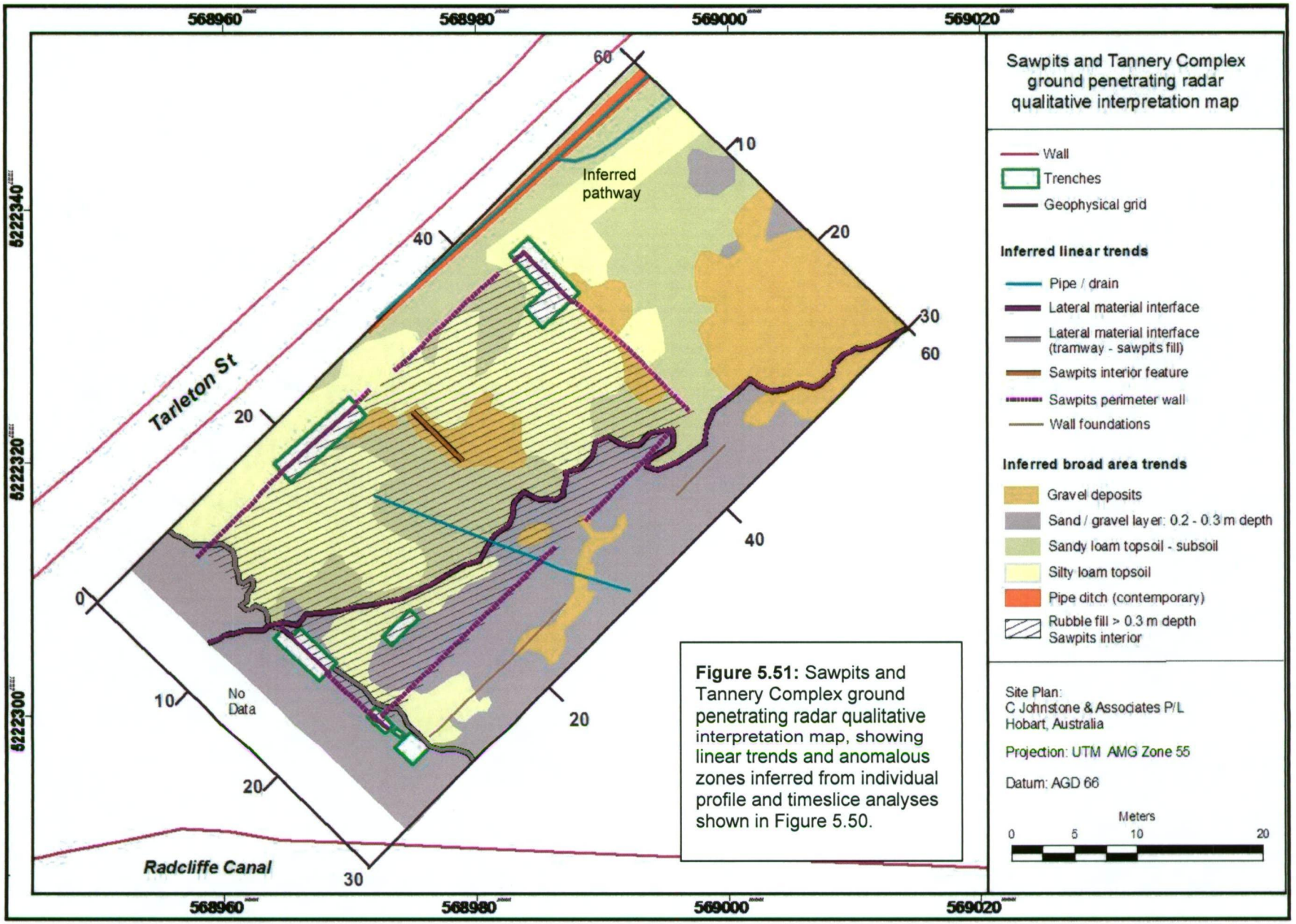

Figure 5.51: Sawpits and Tannery Complex ground penetrating radar qualitative interpretation map, showing linear trends and anomalous zones inferred from individual profile and timeslice analyses shown in Figure 5.50.

5.3.4.3 Electrical resistivity tomography

Introduction

Electrical resistivity tomography (ERT) survey at the Sawpit and Tannery Complex primarily aimed to detect and characterise any remnants of the foundation walls and pit fill. Secondary objectives were to identify fill deposit patterns and features that may be associated with the reclamation process of Mason Cove.

Data acquisition and processing

Data from a single dipole-dipole transect was acquired at the Sawpit over one day in September 2004. The spread was positioned perpendicular to the east and west walls, to transect the Sawpit exterior and interior (Figure 5.52). Data collection parameters are presented in Table 5.6.

The electrical resistivity data was manually de-spiked and processed using the inversion software RES2DINV version 3.4 (Loke, 1996). A 2D tomographic image was generated from the matrix of apparent resistivity data, to show the distribution of true (modelled) resistivity values as a function of depth.

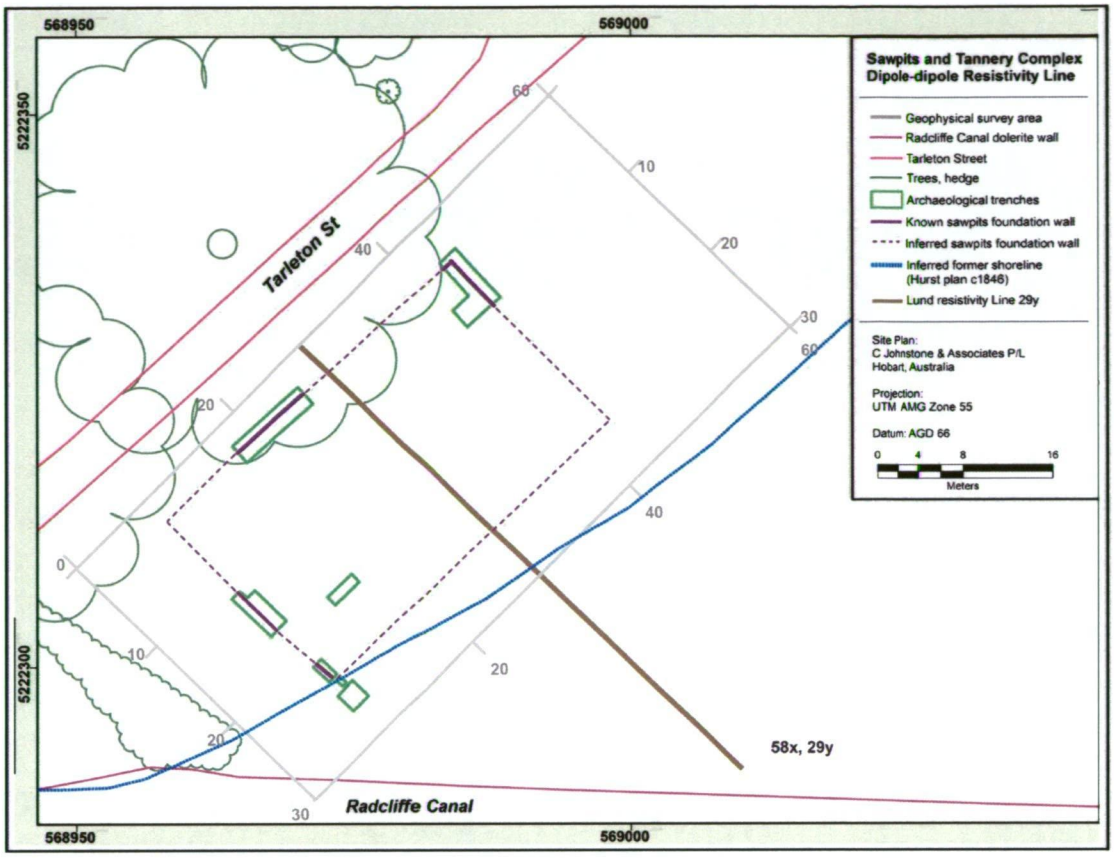

Figure 5.52: Map showing the location of dipole-dipole resistivity transect across the Sawpit and Tannery Complex local geophysical grid.

Survey type	Resistivity		
Instrumentation	ABEM Terrameter SAS 4000 with Lund resistivity imaging#		
Area surveyed	One transect (0x, 29y) to (58.5x, 29y)		
Array type	Dipole – dipole (collinear)		
'a' spacing	1.0 m - 6.0 m	**Output units**	Ω.m
Norm	Median	**Optimal output**	1000 mA*
Acquisition delay	0.3 sec	**Acquisition time**	2 sec
Stacking minimum	2	**Stacking maximum**	4
Comments	Electrode checks prior to data collection. 'a' spacing increment = 1m. Fibreglass surveyors tape used in grid layout. # SAS (signal averaging system) is a method whereby consecutive readings are taken automatically and the results are averaged continuously. *Automatically stepped down to lower current if impossible to transmit selected current		

Table 5.6: Dipole-dipole resistivity survey parameters for the Sawpits and Tannery Complex.

Findings and interpretation

The observed and calculated resistivity pseudo-sections for gridline 29y dipole-dipole transect are presented in Figure 5.53, accompanied by a tomographic model and schematic interpretations of key features. Calculated apparent resistivities range from 1Ω.m to ~ 750 Ω.m, less than half of the range measured on the Isle of the Dead, presumably due to a more moist, loamy subsurface and the influx of conductive seawater at depth.

Two stratigraphic zones dominate the tomographic model: a shallow layer of relatively high apparent resistivities (> 80 Ω.m) and deeper conductive material, which are separated by a horizontal boundary of closely spaced contours. From 0 - 40 m, the interface undulates between 1.0 - 1.75 m depth, which agrees with the Sawpits basement depth derived from archaeological excavation of Trench A (Owen and Steele, 2002). Eastward of 40 m the interface gradually rises to 0.5 m depth (Figure 5.53**c**). Low resistivity values measured below this interface are attributed to remnant beach sands saturated by conductive seawater, the influence of which increases towards Radcliffe Canal. This trend is clearly visible in the EM-31 apparent conductivity data collected by Dorn *et al.* (2002), presented in Figure 5.54.

Values in the near-surface layer are consistent with those expected from silt-sand loam deposits (Bevan, 1998), of which the contemporary topsoil, and Sawpits interior and exterior fill matrices are comprised (Owen and Steele, 2002). Very high apparent resistivity zones measured between 10 - 32 m correlate closely to anomalous response patterns in the ground penetrating radar timeslices, and high values in the Wenner array variation map (Dorn *et al.*, 2002), suggesting that they are not artefacts of poor electrode contact.

Several of the deeper resistive zones coincide with structural features, as inferred from the GPR, infra-red photography, and archaeological excavation results. The western and eastern Sawpits perimeter walls are visible as a small area high at 3.6 m and a broader, deeper, very high resistivity zone at 23 m, respectively (Figure 5.53**d**). The inferred Sawpits yard wall at 26 m also manifests as a deeper anomaly (~ 1.5 m). Troughs in the fill/beach deposits interface at 34.75 m and 38 m are attributed to reclamation

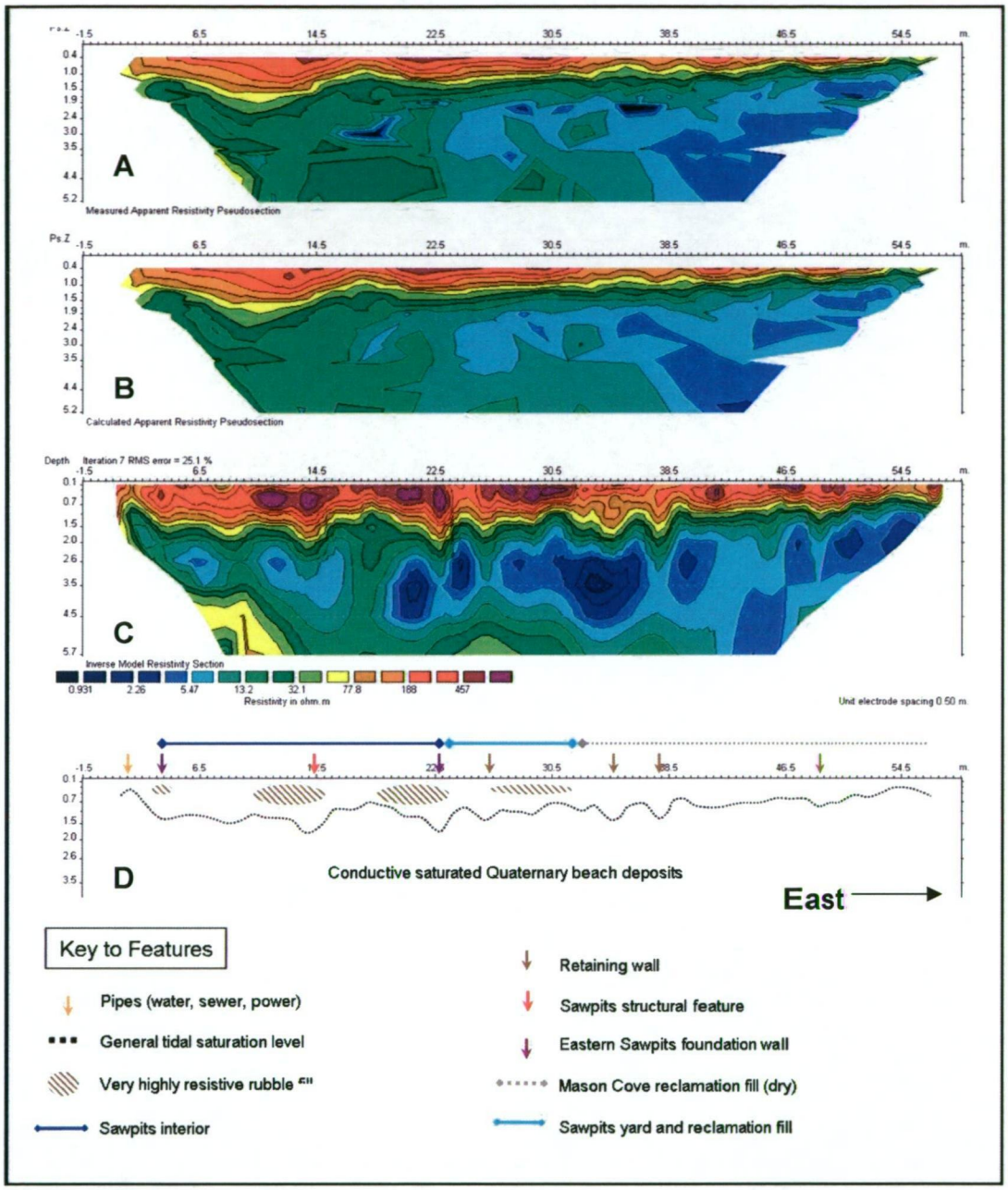

Figure 5.53: Sawpit and Tannery Complex dipole-dipole Line 29y observed (**A**) and calculated (**B**) resistivity pseudo-sections, tomographic model (**C**) and schematic interpretation (**D**).

structures external to the Sawpits. Very high apparent resistivities between 26 m and 32m may be caused by a penal period compacted gravel yard surface and underlying rubble used to fill reclamation pens. Coincident planar responses recorded at ~ 0.4 m depth in the GPR profile for gridline 29y, support this analysis. The inverse model resistivity section, radargram and schematic interpretation of key features are presented in Figure 5.55. Elevated values centred on 11 m and 14 m, and corresponding high amplitude reflections in the GPR, are possibly due to a coarse rubble fill and remnants of a masonry structure dividing the Sawpits area.

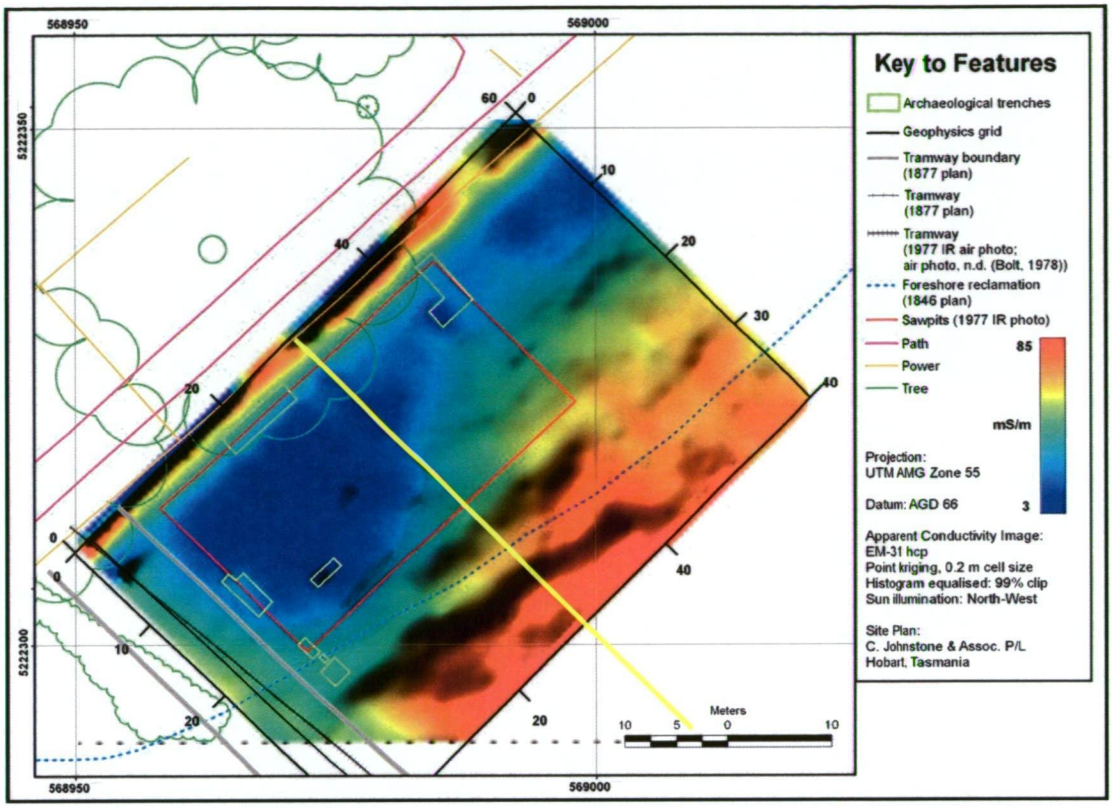

Figure 5.54: EM-31 apparent conductivity variation map of the Sawpits and Tannery Complex, overlain by the Sawpits perimeter (inferred from parch marks), archaeological trench layout and the dipole-dipole resistivity spread in yellow. Demolition rubble fill in the Sawpits area contribute to the very low conductivity values. Values increase towards Radcliffe Canal, primarily due to the influence of tidal flow (Geophysical data courtesy of Dorn *et al.*, 2002; site plan and trench locations courtesy of PAHSMA).

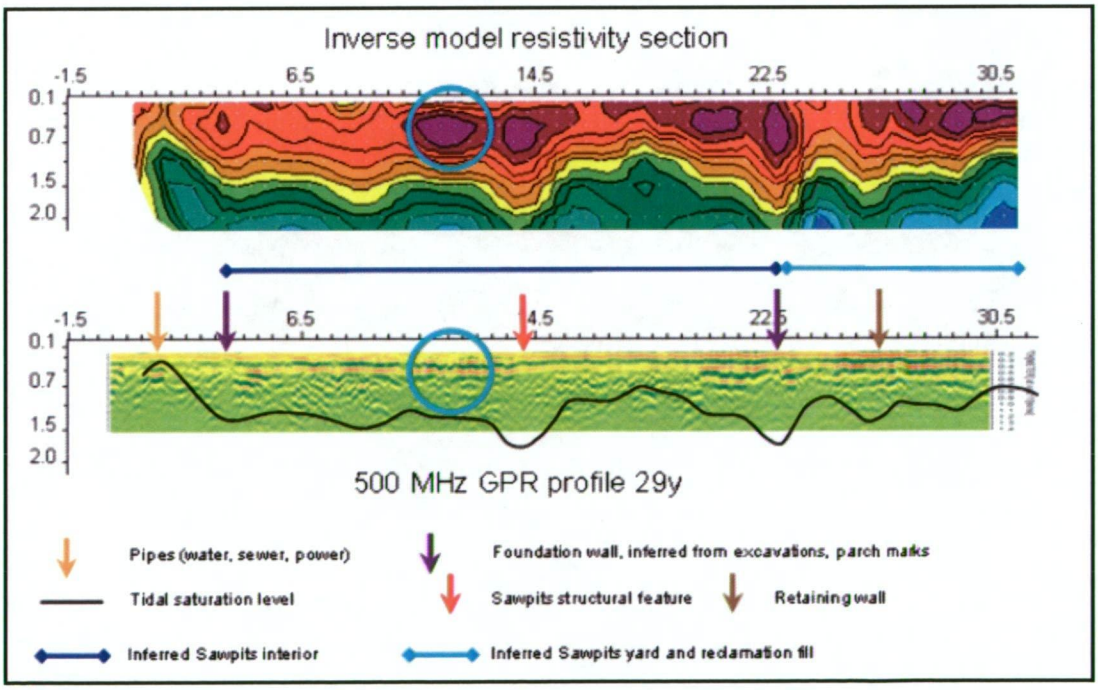

Figure 5.55: Sawpits and Tannery Complex dipole-dipole inverse model resistivity section and 500 MHz ground penetrating radar profile from Line 29y, overlain by schematic interpretation of key stratigraphic features. High resistivity zones in the top 0.8 m depth correspond closely to high amplitude reflections in the ground penetrating radar profile.

5.4 SUMMARY

Both the Sawpits and Tannery Complex and Penitentiary Parade Ground survey areas are essentially characterised by six known stratigraphic elements, which vary in scale and material composition between the sites. These included a walled rectangular enclosure, deposits associated with the interior and exterior spaces, surficial levelling material and reclamation fill/structures overlying and underlying the enclosure features, respectively. Physical evidence of all elements, except the tramway, has been provided through limited archaeological excavations in each area.

Ground penetrating radar profiling (500 MHz) and electrical resistivity tomography was conducted at the Sawpits and Tannery Complex, to provide information in the vertical plane and complement the planimetric datasets derived from previous geophysical studies at the site (Dorn *et al.*, 2002). Three techniques were applied at the Parade Ground: GPR (500 MHz and 800 MHz), magnetometry, and apparent resistivity mapping. The following section summarises the findings of geophysical surveys conducted at each area, and discusses the effectiveness of each technique for the detection and characterisation of these key features.

5.4.1 Penitentiary Parade Ground

Archaeological excavations at the Penitentiary foreground revealed a complex stratigraphy within 0.4 m depth. Two trench sites positioned over the Parade Ground northern boundary revealed limited physical evidence of the penal period enclosure wall. Five sandstone foundation masonry blocks in Trench 1, and mortar deposits in both trenches were indicative of the intra- and inter-trench wall alignment. Highly compacted dolerite, brick and sandstone gravel material south of the wall provided clear evidence of the Parade Ground yard surface. Selective excavations to 0.4 - 0.5 m depth in the trench centre uncovered moist clay containing relatively few artefacts, which was interpreted as evidence of the reclamation fill.

Multi-layered near-surface stratigraphy in the trenches made it difficult to establish benchmark anomalies for the sandstone fountain base, foundation wall and Parade Ground gravel surface, as responses from the fill deposits of similar composition

typically dominated each dataset. This situation was exacerbated by the variable material condition or non-existence (i.e. missing sections of wall) of the archaeo-geophysical targets. However, the ground truthing findings were effectively correlated to GPR reflections from sandy levelling fill horizons, which were primarily deposited north of the original parade ground. These interpretations were extrapolated from profiles and timeslices across the survey area, and the resultant response distribution patterns provided indirect evidence of the northern enclosure wall position.

Direct mapping of the enclosure wall by the Wenner array and GPR profiling was only achieved clearly at one location, where a very shallow, well-preserved section extended several metres from the Penitentiary north-eastern corner. Remaining sections of the eastern wall and northern wall return appear to have been removed to accommodate clay tennis courts and pathways, which were detected as high conductivity zones. Anomalies from any remnants of the northern wall, west of the former tennis court area, were obscured by responses from compacted, dry sand and gravel fill material.

Remnants of the Parade Ground gravel surface were inferred from the geophysical datasets with a low degree of confidence, as it was impossible to establish a reliable benchmark anomaly signature. Response distribution patterns from the target horizon were ambiguous with, or obscured by, noise patterns from historically unrelated fill deposits. This outcome is one example of how the multi-technique approach did not increase the probability of detecting a feature of interest.

However, the multi-technique approach was advantageous for the interpretation of some other features of interest. For example, a broad high resistivity zone located at the eastern end of the former muster yard was confidently attributed to a linear structure (e.g. drain segments), rather than a resistive deposit, because it correlated closely to a series of high amplitude diffractions mapped by the 500 MHz GPR profiling. Aerial photographic evidence suggested that the structure was coincident with a former fence line parallel to the Penitentiary northern façade, which may have replaced an original parade ground boundary line.

There was no discernable magnetic evidence for the two phases of reclamation, which suggested that the fill deposits comprise similar ratios of dolerite to soil. The 500 MHz GPR data did not exhibit clearly definable response distribution patterns that could be attributed to reclamation material. This is due to high signal attenuation in the conductive clay-rich horizons below the near-surface stratigraphy (~ 0.5 m depth). Total magnetic intensity values increased substantially near the dolerite canal wall, seawall, and iron fittings in the Penitentiary fabric, as expected. The irregular distribution of discrete magnetic highs recorded across the site was indicative of buried ferrous metal debris, and shallow dolerite rubble similar to that excavated in Trench 1 (Steele, 2004).

Well-defined highly resistive anomalous zones and areas of coincident sub-surface planar reflections in the 500MHz GPR profiles provided strong evidence for the penal period tramway position parallel to the Penitentiary northern façade. These findings correlated closely to the tramway shown in historic maps and photographs. The magnetic survey did not detect any regular anomaly patterns attributable to buried rails and fittings, which indicated that they had been removed.

5.4.2 Sawpits and Tannery Complex

Extensive archaeological excavations at the Sawpits and Tannery Complex provided physical evidence of the construction, material composition and preservation state of the primary targets at several trench sites. The dolerite and sandstone Sawpits perimeter wall top surface measured ~ 0.6 m wide, and widened to ~ 1.0 m at a depth of ~1.4 m (only shown in one trench). Rubble fill in the Sawpits interior was heterogeneous in composition and included dolerite, brick, sandstone and artefactual pieces in a sandy loam matrix. The Sawpits exterior was characterised by compacted gravel and clay yard surfaces. Surficial deposits of sandy loam topsoil averaged 0.15 m thick. Feature composition and geometry were consistent between trenches, although the perimeter wall exhibited variable material condition as some masonry was missing. Sections of the northern, western and southern walls had been exposed, while the eastern Sawpit boundary remained elusive.

Sections of each Sawpit perimeter wall were identified in the ground penetrating radar profiles with moderate confidence, with the invaluable aid of parch marks in infra-red

aerial photography and the excavation results. The fill stratigraphy was useful in providing indirect evidence of the Sawpits boundary. In profile, there was a visible difference in anomaly patterns between the demolition rubble and reclamation fill deposits, associated with the Sawpit interior and exterior, respectively. This effect was also exhibited in deep horizontal slices of the data volume, which characterised the pit area as a distinctive rectilinear zone of mottled amplitudes.

Timeslices from the surface layers provided additional indirect geophysical evidence of the Sawpits layout, in the form of sharp linear contrast in amplitudes across the survey area. These response patterns were attributed to variation in topsoil moisture content over different fill deposits and very shallow structural remnants. Anomalies from the walls were less well-defined in the timeslices, due to numerous shallow diffractions from rubble fill and high amplitude reflections from overlying resistive material.

The ground penetrating radar also detected remnants of another wall parallel to and offset 3 - 4m from the eastern pit boundary. This structure was also inferred from the previous resistivity mapping by Dorn et al. (2002), and the electrical resistivity tomography, and was interpreted as either another wall in the Sawpits, or a reclamation support feature. The extrapolated position of the external wall/southern perimeter wall intersection correlated closely to a right-angled stratigraphic interface in Trench E. Anomalous responses in the Sawpits interior were attributed to a structure dividing the area into two square-shaped work zones. This interpretation was initially put forward by Dorn *et al.*, (2002), based on the FEM and apparent resistivity survey results. Several other reclamation support structures were inferred from the dipole-dipole resistivity transect, east of the GPR survey area. These correlated closely to linear anomalies in the Wenner array resistivity data (Dorn *et al.*, 2002) and parch marks.

The Sawpits basement appeared to be defined by the ERT, as a sharp undulating interface between 1 - 1.5 m depth, although this may be indicative of seawater saturated sediment. ERT also mapped the interface between the reclamation fill and remnant Quaternary beach sands. These results showed that the technique is useful for defining primary stratigraphic interfaces associated with uncomplicated structural features and large fill deposits. Limitations to the technique include time-consuming data collection and reduced current penetration in material subject to conductive salt water influx. GPR

did not effectively map the reclamation fill basement, due to scattering of the signal by the rubble fill, high absorption of energy in deposits saturated by seawater, and conductive clays in the fill matrix at depth. Responses from contemporary service pipes, levelling sands and deposits associated with site use as a car park and football field were readily identified in the GPR timeslices.

In summary, multi-technique geophysical investigations at the Penitentiary Complex were moderately successful in mapping penal period cultural features. Paradoxically, the detection and characterisation of archaeological targets were both limited and aided by prominent responses from post-penal to contemporary stratigraphic deposits.

Chapter Six: Conclusions

6.1 INTRODUCTION

This project assessed the applicability of different geophysical techniques for mapping a range of buried penal period cultural features within three areas of the Port Arthur Historic Site: the Isle of the Dead, Settlement Hill, and the Penitentiary Complex. Each of these areas was chosen for its unique geological and historical land use characteristics, and a range of buried archaeo-geophysical targets. The following sections summarises the main outcomes of each survey, and critically evaluates the effect of different factors on the degree of certainty to which targets were discriminated, including data acquisition and processing methods, comparison between the geophysical findings and historical sources and archaeological data, site geology and geomorphology.

6.2 ISLE OF THE DEAD

Research on the Isle of the Dead focused on the detection and characterisation of graves, including individual and mass burials, other anthropogenic features (such as former pathways) and major stratigraphic interfaces within a resistive, non-magnetic geological environment. Mapping of the subsurface remains and cultural modification of the soil matrix was carried out using ground penetrating radar, magnetometry and frequency domain electro-magnetometry. This multi-technique approach is based on the outcomes of previous geophysical studies at historic cemeteries (Bevan, 1991; Ellwood 1994; Ahler *et al.*, 2000; Kvamme, 2000; Johnson *et al.*, 2001; Rogers, 2001; Brock and Schwartz, 2006) and recommendations from fieldwork guidelines (David, 1995). Resistivity and seismic refraction tomography were also applied to locate the soil-regolith and regolith-bedrock boundaries (Palmer, 1980; Telford *et al.*, 1990; Sheriff and Lloyd, 1995; Sharma, 1997), and to attempt to determine whether burial shafts were dug into consolidated substrate.

The Isle of the Dead lithology provided a suitable environment for resistivity, ground penetrating radar and magnetic surveying, with its non-magnetic, low conductivity loamy sandy soils and sandstone-siltstone bedrock (Bevan, 1991; Rogers, 2001; Conyers, 2006; Brock and Schwartz, 2006). Consequently and not unexpectedly, the high background resistivity limited the FEM data to a narrow range of low average apparent conductivity values across the island. The broad variation in conductivity correlated closely to the vegetation distribution, and also the depth to the soil-regolith interface.

The conductivity surveys did not systematically detect individual burials - neither through stratigraphic disturbance associated with burial trenches nor isolated ceremonial artefacts. Geophysical contrasts were either not large enough to be identified or they did not illustrate clear interpretable response distribution patterns. These results may also be partly due to a paucity of burial artefacts and the masking effects of soil development over time. Similar results have been reported by Bevan (1991) and Nobes (2000). Despite these results, the FEM was effectual in mapping numerous known surface and inferred near-surface conductive features, many of which were coincident with small magnetic point anomalies. These correlations show that the conductive sources are iron-bearing (remnant fence posts and metal bin), and illustrate one advantage of applying multiple geophysical techniques to measure contrasting material properties for better interpretation (Scollar *et al.*, 1990; Kvamme, 2006).

The magnetic survey also did not systematically detect individual burials or define the cemetery layout within the surveyed area. This was due to a lack of ferrous burial artefacts, and because the original substrate was almost completely non-magnetic it was not possible to map zones of substrate disturbance. However, the magnetometer did clearly define contemporary cultural features, including a buried gravel pathway and shallow ferrous objects attributed to three previously unmapped fence lines transecting the island. As expected, several surface features were prominent sources of noise in the data, including a metal bin, and a penal period grave railing. Responses from these sources effectively masked anomalies from any nearby smaller features. Such site conditions are not uncommon and difficult to avoid at historic cemeteries (Clark, 1997; Witten *et al.*, 2001; Buck, 2003).

In contrast to the FEM and magnetometry, the 250 MHz ground penetrating radar surveys yielded a significant amount of potentially useful information pertaining to burials on the Isle of the Dead. After pre-survey tests, the 250 MHz antenna was chosen over the 500 MHz antenna, as it provided a less complicated image and was less prone to interference from shallow tree roots. Several other studies of historic burials have also used a similar centre frequency (200 MHz), to reduce excessive detail (Maijala, 1994; Nobes, 1999; Field *et al.*, 2001).

Initial analysis of the radar data was a straightforward process, involving the discrimination between 'background' and 'busy' sections in the profiles, which were interpreted and mapped as areas of undisturbed and disturbed soil stratigraphy, respectively. Response patterns within these disturbed areas exhibited moderate to high complexity, and proved to be labour-intensive and time-consuming to interpret. Due to this complexity, all profiles from the Isle of the Dead were processed and assessed individually, using a variation of a method commonly applied to data from historic cemeteries (Nobes, 1999; Johnson *et al.*, 2001; De Vore, 2002; Conyers, 2006). This involved the visual identification, categorisation and mapping of anomalous responses attributable to burial features, based on the results of ground-truthing at other burial sites and modelling of GPR reflection patterns at various hypothetical burial scenarios (Conyers and Goodman, 1997).

Four different anomaly classes were identified according to amplitude, form and depth, and symbolised on a plan-view of the island (King *et al.*, 1993; Davis *et al.*, 2000). Responses such as the distribution of hyperbolic apices were displayed in separate ArcGIS® map layers for flexible viewing. Anomaly patterns recorded between matching headstones and footstones and over surface depressions appeared to be inconsistent. Other authors have also found it difficult to reliably establish a benchmark response associated with an individual burial (Bevan, 1991; Rogers, 2001; Conyers, 2006).

Despite the complex nature of the responses and the difficulties of interpretation, several broad trends were identified in the composite maps. The highest density of responses was recorded on the Upper Bench and western Riser Slope, where most of the sandstone markers and depressions are located. The eastern Riser Slope and Lower Bench were characterised by isolated clusters of point anomalies. These findings

suggested that the radar was mainly directly detecting remnants of coffins, which were used in conjunction with burial stones, to dignify primarily the graves of military officers and their families, rather then convicts, invalids and paupers (Lord, 1999; Greg Jackman, pers. comm.). The sparse distribution of hyperbolic responses on the Lower Bench and eastern Riser Slope may also be related to the terrain and soil properties. The identification of individual burials in the scatter maps was difficult in areas where anomalies were densely clustered, such as on the Upper Bench and western Riser Slope. Only the isolated clusters of hyperbolae confined to less than 2 m^2 may be interpreted as individual burials with a high degree of confidence.

It was not possible to identify with certainty any mass graves in the unmarked sections of the cemetery. While responses on the Lower Slopes were relatively sparse, several areas extending beyond 2 m^2 were possible sites of mass burial on the Riser Slopes. However, these areas showed similar medium-high density responses to those recorded in the marked Upper Bench, and thus may suggest closely-spaced single interments, rather than mass graves. These findings were supported by historic photographic evidence of closely-spaced burial mounds on the island (Lord, 1999).

The difficulty in producing clear, consistent interpretations of individual burials in the layered data recognition maps was not only due to complex anomaly distribution patterns across the surveyed area. It was also influenced by the composite presentation format, which proved suitable for displaying one or two of the four map layers but became too visually complicated when all data was included. This effect has been previously noted by Conyers (2006), who criticised the approach for having 'relatively low dimensionality' and for being purely descriptive - 'yielding only images, not new data that may subsequently be statistically analysed'.

To compensate for this limitation and minimise subjectivity, all radar response classes were weighted and normalised for integration into density maps - a process which detoured from the conventional manual production of interpretation maps (King *et al.*, 1993; Johnson *et al.* 2001; De Vore, 2002). This novel approach was adapted from Nobes (1999) and Field *et al.* (2001), in which multi-dimensional GPR, EM and magnetometry data was processed to yield dimensionless single composite anomaly 'probability' and 'availability' maps, respectively. In this project, density maps were clear and simple

indicators of the variation in archaeological potential across the surveyed area, and were therefore a suitable basic resource for non-geophysicists. For comprehensive understanding of the site, these density maps should be viewed in conjunction with the scatter maps, to provide anomaly depth and class information.

Four tomographic sections were produced from dipole-dipole electrical resistivity surveying across the primary morphological zones on the Isle of the Dead. Prominent resistivity interfaces were readily identifiable and closely correlated to auger test results, and seismic refraction depth information. Depth to the weathered regolith estimated from the resistivity inversions averaged ~ 1.2 m in the Upper Bench and 1.5 m in the Lower Bench. These depths correlated closely to the auger test results, which suggested that burial shafts may have been dug into the regolith in the Upper Bench and Riser Slopes.

Primary stratigraphic interfaces were not consistently defined in the ground penetrating radar data. Picked reflections correlating to the topsoil base and soil-regolith interface were mostly discontinuous and indistinct and distribution patterns were therefore not mappable across profiles, or within each morphological zone, even in the relatively undisturbed 'background' areas. These findings suggested that changes in relative dielectric permittivity across soil horizons were too diffuse or graded for the radar to detect them. Further, diffractions in areas of soil disturbance distorted, beyond identification, many reflections attributable to the regolith surface. Hence it was difficult to detect and map responses from any burial trenches excavated into the regolith substrate, using the ground penetrating radar.

In summary, despite some interpretational difficulties, ground penetrating radar nonetheless appeared to be the most promising technique for locating unmarked graves on the Isle of the Dead, compared with the limitations of the other techniques (Bevan, 1991; Conyers, 2006). FEM was a reliable technique for the detection and characterisation of metal, which also made it prone to interference from noise sources such as surface debris. It was less useful as a method of mapping stratigraphic disturbance, due to the highly resistive sandy soils and rapid soil development (Doyle and Cummings, 2003). For future surveys at historic cemeteries, both FEM and magnetometry should be applied in conjunction with other geophysical techniques, to

increase the probability of detecting burials with iron-bearing burial artefacts or caskets (David, 1995; Brock and Schwartz, 2006) where there are few or no sources of noise from ferrous material unrelated to the target(s) (Ellwood *et al.*, 1994; Clark, 1997; Buck, 2003).

6.3 SETTLEMENT HILL

Multi-technique geophysical investigations were conducted at Settlement Hill to detect and characterise cultural deposits and architectural remains in the near-surface, including building foundations and yard features, and a deeper brick-lined aqueduct. The site was surveyed with a magnetometer, an EM-38 frequency domain conductivity meter, Wenner array resistivity, and 500 MHz ground penetrating radar. Archaeological excavations were conducted by PAHSMA at two sites in the Hospital Precinct, and the results were used to confirm and/or refute the geophysical interpretation. A summary of the geophysical findings is provided below.

Results from the Settlement Hill magnetic survey offered insight into mapping in an environment dominated by highly magnetic near-surface dolerite and dolerite rubble fill, a relatively rare scenario in the literature compared to sites characterised by a fairly homogeneous overburden and non-magnetic substrate (e.g. Conyers, 1995; Pomfret, 2006). As expected, the magnetic survey did not effectively map the sandstone and brick structural features due to interference from the surrounding demolition rubble fill and underlying shallow magnetic substrate. Large-scale cultural modifications to the dolerite substrate, associated with cut-and-fill terracing and trenches were clearly discernable and result in readily interpretable linear response patterns.

While the brick lining of the penal-period subsurface aqueduct was not detected by the magnetometer due to the overwhelming signal from the dolerite, the feature was successfully defined by a linear zone of relatively low magnetic intensities, caused by trench excavations into the bedrock. Its position correlated closely with historic plans, without which the anomaly would have been attributed to a possible drainage trench. Two similar lineaments in the Hospital Precinct were attributed to previously undocumented trenches, and interpreted as penal period drainage features. These findings illustrated one benefit of the productive relationship between the historical

sources and geophysical data, in which each source informs the other to enable a more confident and comprehensive understanding of the site.

Preliminary qualitative interpretation of the geophysical analyses was also refined following feedback from the results of archaeological excavations in the Hospital Precinct. This was most clearly exemplified where a small compacted gravel deposit coincided with part of a long narrow curved lineament in the GPR timeslices and apparent resistivity map. These findings appeared to confirm the preliminary qualitative interpretation, which inferred the anomaly source as a pathway. By extrapolating from these results, the path was then mapped from the geophysical data with a high degree of confidence.

In several other cases, excavations showed that inferred source locations of magnetic and apparent conductivity point anomalies coincided with buried metal objects, thereby reinforcing the reliability of each technique to accurately map shallow geophysical targets, and the validity of the data interpretation. However, most point sources were difficult to interpret, unless they formed part of a definable (non-random) response pattern that extended outside the trench area (Scollar *et al.*, 1990). It is therefore recommended that any further archaeological ground-truthing be conducted primarily to characterise non-random (regular) anomaly distribution patterns rather than discrete responses, to maximise the potential for useful extrapolation of the geophysical data beyond the trench boundary.

Ground-truthing was also useful in identifying some of the sources of geophysical interference in the Hospital Precinct. The discovery of near-surface heterogeneous rubble fill deposits, associated with post-penal demolition processes, confirmed why the radar profiles from this area were characterised by complicated high amplitude diffraction patterns. In unprocessed data, these patterns tended to mask the useful signals from any of the well-preserved (and therefore potentially mappable) structural features and yard surfaces uncovered through excavation, including several *in situ* well-preserved brick drains, and highly compacted gravel deposits. GPR data processing applications (exponential gain adjustment, subtract average trace) were moderately successful in enhancing the signal-to-noise ratio for the discrimination of continuous planar reflectors from target horizons such as the compacted yard surface. They were

less successful for the delineation of linear features oriented obliquely to the radar profile, such as drains, because the resulting narrow anomaly was similar in form and amplitude to responses from brick debris. Heterogeneous demolition fill within the Hospital Precinct also compromised interpretation of the radar data because it precluded a reliable estimation of the average wave velocity, and therefore only enabled a reliable calculation of relative feature depths in individual profile analysis.

Excavated features in poor condition (e.g. incomplete) typically produced anomaly patterns that were indistinguishable from responses from the surrounding rubble fill (Pipan *et al.*, 1999; Hargrave *et al.*, 2002). Such targets included isolated remnants of the courtyard sandstone flagging, and partially demolished brick foundations. This effect was visible in the GPR data (both in profile and amplitude maps), apparent resistivity and FEM variation maps across much of the central Hospital Precinct, where a multitude of point anomalies and short linear trends appeared to be randomly distributed. It was thus very difficult to infer the building layout in this part of the site with a great degree of confidence. Processing of the radar data failed to improve the low S/N ratio in these areas.

In contrast to the Hospital Precinct building zone, other sections of the Settlement Hill main terrace were characterised by clearly discernible and readily interpretable geophysical expressions. This was primarily due to a relatively thin layer of rubble fill, as revealed by excavations in the yard space between the second and third hospitals (Steele, 2005). Several well-defined curved lineaments in this area were attributed to penal period cultural features not shown in historic maps, including an inferred garden path between the sandstone steps and third hospital. Rectilinear anomalies in the apparent resistivity variation map and GPR timeslices were readily interpretable as the well-preserved near-surface architectural remnants of other structures along the main terrace. This inference was reinforced by a close correlation between the geophysical patterns and building layout available in several historic maps. These clear results confirmed that GPR, operated at a centre frequency of 500 MHz, and Wenner array resistivity techniques were suitable for mapping shallow architectural features within an environment subject to limited post-occupational disturbance (Larson *et al.*, 1999; Hargrave *et al.*, 2002; Kvamme, 2005; Mrozowski, 2000-). They also indicated that this section of Settlement Hill has high archaeological potential.

6.4 PENITENTIARY COMPLEX

Surveys were conducted at two sites in the Penitentiary complex, the Sawpits/Tannery complex and the Parade Ground area, which provided a contrasting substrate to the Settlement Hill and Isle of the Dead. Previous archaeological excavations by PAHSMA showed that the near-surface stratigraphy is culturally-derived, comprising a relatively thin surface layer of contemporary fill, and a thicker layer of reclamation rubble material overlying natural beach sands from Mason Cove. Primary investigation objectives were to assess the effectiveness of geophysical techniques for the detection and characterisation of features associated with the reclamation of Mason Cove and site use during the penal period. Ground penetrating radar profiling and electrical resistivity tomography at the Sawpits and Tannery Complex were applied to provide information in the vertical plane, to complement the planimetric views derived from other geophysical techniques (Dorn *et al.*, 2002). A multi-faceted approach was applied at the Parade Ground, comprising GPR, magnetometry, and apparent resistivity mapping. Survey findings were used to create qualitative interpretation maps for guiding further archaeological excavations at each area.

The results of previous investigations at the Sawpits, Workshops and Penitentiary ablutions (Dorn, 2002; Dorn *et al.*, 2002) influenced the survey methodology at the Penitentiary complex. Magnetic data were collected at 1.0 m line spacing and 0.2 m station intervals instead of 2.0 m and 0.25 m respectively, and the density of apparent resistivity data points was also increased by reducing the line and station spacing to 1 m and 0.5 - 1.0 m respectively. These adjustments resulted in better resolution of linear and areal trends and therefore more confident interpretation of anomaly patterns.

6.4.1 Sawpits and Tannery Complex

Geophysical features at the Sawpits area were successfully detected using a ground penetrating radar 500 MHz antenna. Features included remnants of the penal period foundation walls and reclamation structures, multiple-period fill deposits, and shallow contemporary cultural features. These were inferred, with varying degrees of confidence, with the invaluable aid of previous geophysical maps (Dorn *et al.*, 2002),

infra-red aerial photography and archaeological results (Owen and Steele, 2002). Data were analysed in both profile and timeslice formats.

In profile, GPR responses attributable to the foundation walls were located at depths between 0.3 m and 0.5 m and exhibited a range of amplitudes and forms, which provided geophysical evidence for material condition and feature geometry. Profiles located adjacent to archaeological trenches demonstrated that a series of stacked moderately high amplitude (relative to reflections from other sections of the wall), short planar diffractions with down-dipping edges correlated to the top surface of sections of well-preserved wall. These benchmark responses were used to interpret similar anomaly patterns across the survey area, with a high degree of confidence. The top surface of masonry in poor condition was characterised by irregular responses of weaker amplitude recorded at various two-way travel times. Identification of masonry in such condition was less reliable due to a similarity between reflections from the wall's top surface and those from surrounding rubble fill. This ambiguity is a previously acknowledged limitation to geophysical studies at the Port Arthur Historic Site, in areas where structural features are buried in stratigraphy dominated by post-occupational demolition rubble deposits (Dorn, 2002; Dorn *et al.*, 2002).

Despite this limitation, fill stratigraphy within the top metre proved useful in providing indirect evidence of the Sawpits boundary. For example, along the Western side close to Tarleton Street, high amplitude near-horizontal reflectors at 10 - 12 ns TWTT (0.5 m - 0.6 m depth) interpreted as remnants of a compacted dolerite gravel yard surface abruptly discontinued at the Sawpits wall, as inferred from infra-red photographs and other geophysical sources. There was also a visible difference in anomaly form and amplitude patterns between the demolition rubble associated with the Sawpit interior, which extended to at least 25 ns TWTT (~ 1.4 m), and the surrounding relatively weak amplitude responses associated with homogeneous beach sand deposits of Mason Cove.

Timeslices from the surface layers provided additional indirect geophysical evidence of the Sawpits layout, in the form of sharp linear contrasts in amplitudes across the survey area. Such response patterns were attributed to variation in soil moisture content in the topsoil over different fill deposits and very shallow structural remnants. These interpretations are supported by the close correlation between geophysical anomalies

and parch marks in infra-red aerial photography. Responses from contemporary service pipes, levelling sands and deposits associated with site use as a car park and football field were also readily identified in the timeslices.

In summary, the Sawpit layout was successfully mapped using the ground penetrating radar data, and its position was found to correlate closely to that inferred from other sources (Dorn, 2002; Dorn *et al.*, 2002; Owen and Steele, 2002). These results demonstrate the advantages of analyzing data from three dimensions, for the mapping of simple structural features in stratigraphy dominated by fill material of heterogeneous composition (Malagodi *et al.*, 1996; Conyers and Goodman, 1997; Leckebusch, 2003).

A single dipole-dipole resistivity spread also successfully defined known and inferred pit foundation walls, and the previously unknown structures interpreted as reclamation supporting walls. It also mapped the interface between the reclamation fill and remnant Quaternary beach sands. These results showed that the technique is useful for defining primary stratigraphic interfaces associated with uncomplicated structural features and large-scale fill deposits. Limitations to the technique include reduced current penetration in material subject to conductive salt water influx (Dorn *et al.*, 2002). Further work at the Sawpits site could include collection of a grid of perpendicular transects, for three-dimensional tomographic imaging of the foundation walls, internal structural divisions and reclamation features (Cammarano *et al.*, 1998; Cammarano *et al.*, 2000; Osella *et al.*, 2005).

6.4.2 Penitentiary Parade Ground

Integration of multiple geophysical techniques was moderately successful in detecting and characterising archaeological targets at the Parade Ground. The parade ground enclosure wall was directly detected by the Wenner array apparent resistivity mapping and GPR in only one area, where a very shallow section (just below the topsoil) extended ~ 6 m from the Penitentiary eastern corner. It was postulated that missing sections were either in too poor a condition for detection, positioned below the Wenner array's investigation depth, or exhibited low geophysical contrast with the surrounding fill deposits.

All of these possible explanations were subsequently confirmed through archaeological excavations of two trenches on the Parade Ground northern boundary. Ground-truthing revealed a complex stratigraphy to 0.4 m depth, dominated by dry compacted resistive materials associated with post-penal and contemporary period activities. These included loamy topsoil, levelling sands and underlying deposits of coarse dolerite gravel, brick rubble, and loam soils. The parade ground gravel horizon, remnants of the sandstone foundation wall and mortar deposits were located within 0.3 m of the surface (Steele, 2004).

Despite not directly detecting these archaeological targets, the different near-surface fill deposits associated with the Parade Ground interior and exterior produced radar and resistivity anomaly distribution patterns that correlated closely to the Parade Ground northern wall alignment. The distribution of these deposits, while contributing significant undesirable signal to the survey data, also acted indirectly as sources of useful information.

Remnants of the inferred parade ground gravel surface appeared to be mapped by all three techniques, although the GPR and resistivity anomaly patterns might also be attributed to surfacing materials from later site use as a tennis court area and caravan park. Sources of broad area magnetic noise, including near-surface post-penal to contemporary gravel levelling fill and dolerite rubble, also masked the magnetic response from the Parade Ground gravel surface. There was no evidence in the magnetic dataset for the different phases of Mason Cove reclamation, which suggested that the different fill deposits are similar in composition.

Anomaly patterns in the resistivity data provided evidence of the tramway boundaries, while deeper reflections in the GPR were attributed to tramway base material. The magnetic survey did not detect any regular anomaly patterns coincident with the penal period tramway. This result was probably due to removal of rails and fittings, as well as geophysical interference from near-surface dolerite pieces in the rubble fill, and buried metallic debris. An important conclusion from this work is that magnetic surveys are best conducted in areas of the Port Arthur Historic Site not characterised by extensive reclamation and/or site levelling.

Ground penetrating radar surveys using the 800 MHz frequency antenna provided high resolution stratigraphic information on very shallow features in three focus areas. Responses from linear features were easier to identify and interpret than discrete anomalies caused by point sources, because the patterns were more obvious to the eye and less ambiguous (Scollar *et al.*, 1990). Analyses of both profiles and timeslices showed the Parade Ground foundation wall, in variable material condition and with missing sections, different fill horizons, and in addition several previously unmapped linear features. These findings correlated closely to, and augmented, the 500 MHz GPR and apparent resistivity interpretations. Due to time-consuming data collection and the detail obtained at this frequency, the 800 MHz surveying is only recommended for small areas where there is extensive *a priori* knowledge of target characteristics, either through previous geophysical surveys, archaeological excavation and/or historic resources. This will enable more confident interpretation of the data.

In summary, multi-technique geophysical investigations at the Penitentiary area were moderately successful in mapping penal period cultural features. Paradoxically, the detection and characterisation of archaeological targets were both limited and aided by prominent responses from post-penal to contemporary stratigraphic deposits. There was enough geophysical evidence to delineate primary targets such as the Parade Ground enclosure wall and tramway, and to demonstrate the variability in material condition of *in situ* remnants, from well-preserved to missing sections/horizons.

As a result of this variability, and the multitude of other geophysical sources, each dataset was too visually complex for integration into a single composite image (Ernenwein and Kvamme, 2002). Further, interpretation maps of each technique were also too complicated to be combined into one comprehensive archaeological potential image. The output was therefore presented as individual map layers, for use within a GIS database (Larson *et al.*, 1999; Buteux *et al.*, 2000; Gaffney *et al.*, 2000; Hargrave *et al.*, 2002). This approach is recommended for other sites at Port Arthur Historic Site where features are inconsistently defined across the survey area. Ground-truthing results were very useful for interpretation of the ground penetrating radar, but proved to be less relevant to the magnetic and resistivity analyses.

6.5 ARCHAEOLOGICAL GROUND-TRUTHING

Interpretation of the geophysical data at the Port Arthur main site was assisted by the excavation results. Archaeological excavation of trenches at Settlement Hill and the Penitentiary Complex provided a highly detailed view of stratigraphy within each of the test areas. In contrast, relatively low measurement density was achieved through geophysical surveys over the same areas. Ground penetrating radar profiling, particularly with the 800 MHz antenna, provided the best horizontal and vertical resolution of features, with 3 - 5 cm trace increment, continuous sampling along-line and 0.5 m line spacing. While the presented variation maps of each dataset appear continuous due to interpolation, the density of actual measurements varied according to trench position relative to the local geophysical grid. The density of original observations in a magnetic survey was 4 - 12 per square metre, while the EM-38 and Wenner array varied between 2 and 6. Further, each measurement has an investigation footprint, with different footprints corresponding to each method.

Gridding is a filtering operation and also affects the apparent continuity of the final geophysical image. Kriging, which was the most commonly used interpolation technique in this project, consistently replicates data at the observation locations, but the resulting surface has greater continuity than reality because of the smoothing effect of the process (David *et al.*, 1994). Despite the discrepancy in resolution between geophysical data and archaeological findings, overall the ground-truthing proved to be a useful feedback mechanism for refining qualitative interpretation of the stratigraphy at the Port Arthur Historic Site (Larson *et al.*, 1999; Mrozowski, 2000-; Hargrave *et al.*, 2002; Kvamme, 2005). At both the Settlement Hill and Penitentiary complex, information derived from the geophysical-archaeological correlations was extrapolated to other parts of the survey area with a moderate to high degree of confidence (Conyers and Cameron, 1998). Further, these interpretations were used to evaluate the reliability of original site maps and increase the accuracy of image rectification by providing additional ground control points.

6.6 SUMMARY

The Port Arthur Historic Site provided a range of geophysical survey environments, in terms of the local geology, soil profiles, type of geophysical target (e.g. wall foundations, burial, and floor horizon), construction materials and post-occupational processes. Consequently, each type of cultural feature expressed a range of geophysical signatures both within and between survey areas. Individual methods and techniques experienced variable success at feature detection and characterisation, due to challenging conditions such as a weak physical contrast between the archaeological targets and surrounding media, but overall the multi-technique geophysics at Port Arthur yielded very worthwhile outcomes. Qualitative interpretation maps generated from multi-dimensional datasets provided a synoptic perspective on the archaeological potential at the Penitentiary Complex, Settlement Hill, and the Isle of the Dead. They also indicated, to varying degrees, differences between the present and original layout of features, as depicted in historic documents.

The process of identifying culturally relevant patterns in geophysical data at Port Arthur may also be applied to explore specific archaeological questions at other areas of this or other accessible historic sites in Tasmania, for which there is limited or no knowledge of remnant cultural features in the near-surface. Following is a list of salient points to consider when planning future field studies:

- A mixed discipline strategy is highly recommended, starting with cost effective, rapidly executed and non-destructive multi-technique reconnaissance surveys (FEM, magnetometry - except in doleritic domains), and to be followed by focused detailed studies using high resolution methods (GPR, ERT) and selective archaeological excavations.
- Ground penetrating radar is highly suitable for mapping for the areal extent of a cemetery, and/or defining individual burials within a known burial area. It is also useful for detecting burials that are not too closely-spaced, although it has difficulty discriminating mass graves from closely-spaced individual burial trenches when there are no caskets and the trench base is poorly defined.

- FEM and magnetometry is recommended only as a means to identify caskets or other metallic/ferrous burial artefacts were used, not as a method of detecting burial trenches in non-magnetic soils.
- Tightly-spaced three-dimensional ERT is potentially highly useful for visualising randomly-oriented burials with caskets if they are well-separated, or individual burials spaced at regular intervals.
- Vegetation (especially trees) in a cemetery limits the survey methodology, restricting consistent access to site and density of survey lines. It can also produce undesirable signal in FEM, and less so GPR, data. It is therefore recommended that the survey grid is located in open area where possible.
- To ensure adequate coverage of the grave, it is advisable to use a survey line interval of ≤ 0.5 m for GPR, and ≤ 1.0 m for other techniques - particularly if the site has unmarked and closely-spaced graves of inconsistent orientation.
- Rubble material, derived from reclamation, slope cut-and-fill for terracing, construction or demolition, will impact to varying degrees on the success of geophysical mapping of structural targets at other areas of the Port Arthur Historic Site. Doleritic reclamation rubble underlying archaeological deposits may negatively influence the outcome of a magnetic survey if the target has low magnetic contrast to the surrounding material. A gradiometer may provide better resolution of iron-bearing features within the near surface than a magnetometer.
- Reclamation fill may be a source of undesirable signal in FEM and resistivity mapping if it lies within the detection footprint; but not in GPR profiling. Pre-survey knowledge of nominal depth to reclamation fill and general fill composition would assist in the choice of best geophysical technique and survey parameters (such as probe spacing). This information may be obtained from selective test pitting, probing and/or geophysical transects (e.g. resistivity profiling) across the proposed survey area.
- Rubble derived from the initial building construction, and later demolition phases is likely to be of similar composition to the targets, and thereby prove to be a major source of undesirable signal in the data (Bevan, 2006).

- In areas of rubble overburden, rather than looking for remnants of the walls and foundations, it may be easier to define the structural footprint from enclosed floor spaces and yard areas, as it is very difficult to remove the effect of the rubble from the data.
- Surveys at the Sawpits demonstrated that a pit, or trench, or privy, may be effectively mapped where fill material exhibits a measurable geophysical contrast with the surrounding stratigraphy. This is advantageous where trench/pit sides were not originally supported by a wall or lining, or are poorly preserved due to collapse, demolition etc, or if the pit lining is of low geophysical contrast (e.g. wood).
- Linear features such as walls, foundations and drains were most easily definable when they were continuous across more than three survey lines.
- EM-38 is useful for defining well-preserved linear features of high conductivity contrast with surrounding material. It is poorly suited to narrow targets (< 0.5 m width) such as foundations, drains, postholes, especially in an environment dominated by rubble material.
- In areas of the site underlain by highly magnetic dolerite, or characterised by doleritic rubble, it is very difficult to discriminate in situ linear brick structures or isolated brick features in magnetic data. Brick targets may be effectively mapped at sites characterised by non-magnetic geology, such as on Point Puer.
- The negative effects of near-surface rubble may be partially mitigated by using multiple techniques.
- In a site with complicated stratigraphy, focus on mapping linear features that would extend over three survey lines, and areal features such as floors, yard spaces, rather than isolated elements such as pit holes.
- Magnetic surveys are best conducted in areas of the Port Arthur Historic Site not characterised by extensive reclamation and/or site levelling with highly magnetic doleritic fill material.

References

Ahler, S., K. L. Kvamme, J.C. Kvamme (2000). Summary Report on 2000 Field Investigations at Fort Clark State Historic Site, 32ME2, Mercer County, North Dakota, ArcheoImaging Lab, Department of Anthropology and Center for Advanced Spatial Technologies, University of Arkansas, Arkansas.

Aitken, M. J., G. Webster, A. Rees (1958). "Magnetic Prospecting." *Antiquity* **32**: 270-271.

Annan, A. and S. Cosway (1992). Ground penetrating radar survey design. Symposium on the Applications of Geophysics to Engineering and Environmental Problems, Oakbrook, IL., USA, SAGEEP.

Annan, A., W. M. Waller, D. W. Strangway, J. R. Rossiter, J. D. Redman, R. D. Watts (1975). "The electromagnetic response of a low-loss, 2-layer, dielectric earth for horizontal electric dipole excitation." *Geophysics* **40**: 285-298.

Annan, A. P. (1999). Ground penetrating radar workshop notes. Ontario, Canada, Sensors & Software Inc.

Appel, E., J. Wilhelm, M. Waldhor (1997). "Archaeological Prospection of Wall Remains using Geoelectrical methods and GPR." *Archaeological Prospection* **4(4)**: 219-229.

ATES, A. (2002). "Archaeomagnetic surveys of the anonymous graves in Khosho Tsaidam, Mongolia." *Archaeological prospection* **9**(4): 197-205.

Atkinson, R. J. C. (1952). Methodes electriques de prospection en archeologie. La Decovert de Passe. A. Laming. Paris, Picard: 59-70.

Barker, R. D. (1989). "Depth of investigation of collinear symmetrical four-electrode arrays." *Geophysics* **54**: 1031 - 1037.

Batayneh, A., A. Al-Zoubi, U. Tobasi, G. Haddadin (2001). "Evaluation of archaeological site potential on the Tall al- Kharrar area (Jordan) using magnetic and resistivity methods." *Environmental Geology* **41**(1-2): 54-61.

Beem, K., A. Dippold, J. Horner, T. Snader, A. Kozlowski (2006). "A multi-method geophysical approach to locate unmarked graves in Milton, Pennsylvania." Geological Society of America Abstracts with Programs for Northeastern Section 41st Annual Meeting **38**(2): 71.

Bell, A. (1981). "Why Port Arthur Crumbled." *ECOS* 27: 32.

Bell, E. L. (1990). "The historical archaeology of mortuary behaviour: Coffin hardware from Uxbridge, Massachusetts." *Historical Archaeology* **24**: 54-78.

Bevan, B. W. (1991). "The Search For Graves." *Geophysics* **56** (9): 1310-1319.

Bevan, B. W. (1998). Geophysical exploration for archaeology: an introduction to geophysical exploration. Lincoln, Nebraska, United States Department of the Interior National Park Service.

Bevan, B. W. (1999). Some Geophysical Experiments at Effigy Mounds. Weems, Virginia, Geosight.

Bevan, B. W. (2006). "Geophysical exploration for buried buildings." *Historical Archaeology* **40** (4): 27-50.

Bevan, B. W., J. Kenyon (1975). "Ground-penetrating Radar for Historical Archaeology. *MASCA Newsletter* **11**(2):2-7

Brand, I. (1975). Port Arthur, 1830-1877. Hobart, Jason Publications.

Briuer, F. (2002). Ground Penetrating Radar Survey and Interpretation Ft. Eustis, Virginia, US Army Fort Eustis Directorate of Public Works.

Buck, S. C. (2003). "Searching for graves using geophysical technology: Field tests with ground penetrating radar, magnetometry, and electrical resistivity." *Journal of Forensic Sciences* **48**(1): 5-11.

Burger (1992). Exploration geophysics of the shallow subsurface, Prentice Hall.

Brizzolari, E., F. Ermolli, L. Orlando, S. Piro, L. Versino (1992). "Integrated Geophysical Methods in Archaeological Surveys." *Journal of Applied Geophysics* **29**(1): 47-55.

Brock, J. and S. Schwartz (1991). "A little slice of heaven: Investigations at Rincon Cemetery, Prado Basin, California." *Historical Archaeology* **25**(3): 78-90.

Buteux, S., V. Gaffney, R. White, M. Van Leusen (2000). "Wroxeter Hinterland project and geophysical survey at Wroxeter." *Archaeological Prospection* 7(2): 69-80.

Cammarano, F., P. Mauriello, D. Patella, S. Piro, F. Rosso, L . Versino (1998). "Integration of high resolution geophysical methods. Detection of shallow depth bodies of archaeological interest." *Annali Di Geofisica* **41**(3): 359-368.

Carabelli, E. (1966). "A new tool for archaeological prospecting: the sonic spectroscope for the detection of cavities." *Prospezioni Archaeologiche* **1**: 25 - 36.

Carabelli, E. (1968). "Ricerca delle cavita superficiali con l'impiego di vibratori primi esperimenti." *Prospezioni Archaeologiche* **3**: 37-44.

Chapman, S. and J. Bartels (1962). Geomagnetism. Oxford, The Clarendon Press.

Charles, M. (2003). Report on the Geophysical Survey of the Fort Crawford Cemetery, Montrose County, Colorado. Durango, CO, Fort Lewis College.

Claerbout, J., and Muir, F. (1973). "Robust modelling with erratic data." *Geophysics* **38**: 836-844.

Clark, A. (1997). Seeing Beneath the Soil. London, B. T. Batsford Ltd.

Clark, D. (1968). Analytical Archaeology. London, Methuen.

Clay, R. (2001). "Complementary Geophysical Survey Techniques: Why Two Ways are Always Better Than One." *Southeastern Archaeology* **20**: 30-43.

Conyers, L. (1995). "The Use of Ground-Penetrating Radar to map the buried structures and landscape of the Ceren Site, El Salvador." *Geoarchaeology-An International Journal* **10** (4): 275-299.

Conyers, L. (2006)a. "Innovative Ground-penetrating Radar Methods for Archaeological Mapping." *Archaeological Prospection* **13**: 139-141.

Conyers, L. (2006)b. "Ground-penetrating Radar techniques to discover and map historic graves." *Historical Archaeology* **40 (3)**: 64-73.

Conyers, L. and C. Cameron (1998). "Finding buried archaeological features in the American Southwest: new ground-penetrating radar techniques and three-dimensional mapping." *Journal of Field Archaeology* **25**(4): 417-430.

Conyers, L. and D. Goodman (1997). Ground Penetrating Radar: An Introduction for Archaeologists, Altimira.

Conyers, L. B. and J. E. Lucius (1996). "Velocity Analysis in Archaeological Ground-Penetrating Radar Studies." *Archaeological Prospection* **3**(1): 25-38.

Coskun, N. and J. E. Szymanski (2000). "A discussion on the resolution of two-dimensional resistivity modelling." *Archaeological Prospection* **6**(4): 179-186.

Dalan, R. A. and B. W. Bevan (2002). "Geophysical indicators of culturally emplaced soils and sediments." *Geoarchaeology-an International Journal* **17**(8): 779-810.

Daniels, J. (2000). Ground penetrating radar fundamentals, The Ohio State University.

David, A. E. U. (1995). Geophysical Survey in archaeological Field Evaluation. London, English Heritage.

Davies, M. and K. Buckley (1987). Archaeological Procedures Manual: Port Arthur Conservation and Development Project. Hobart, Department of Lands, Parks and Wildlife.

Davis, J. and A. Annan (1989). "Ground Penetrating Radar for high resolution mapping of soil and rock stratigraphy." *Geophysical Prospection* **37**: 531-51.

Davis, J., J. Heginbottom, A. Annan, R. Daniels, B. Berdal, T. Bergan, K. Duncan, P. Lewin, J. Oxford, N. Roberts, J. Skehel, C. Smith (2000). "Ground penetrating radar surveys to locate 1918 Spanish Flu victims in permafrost." *Journal of Forensic Sciences* **45**(1): 68-76.

De Vore, S. (1999). Selected Bibliography for Remote Sensing/Geophysical Techniques for Cultural Resource Management. FY1999 Recent Advances in Archeological Prospection Techniques Workshop, Lincoln, NE, Midwest Archeological Center.

De Vore, S. (2002). Geophysical Investigations at the Kane Cemetery (48BH3104), Bighorn Canyon National Recreation Area. Wyoming, Midwest Archeological Center, Lincoln, Nebraska.

Dey, A., and Morrison, H. (1979). "Resistivity modelling for arbitrarily shaped two-dimensional structures." *Geophysical Prospecting* **27**(106-136).

Diamanti, N., G. Tsokas, P. Tsourlos, A. Vafidis (2005). "Integrated interpretation of geophysical data in the archaeological site of Europos (northern Greece)." *Archaeological Prospection* **12**(2): 79-91.

Dogan, M. and S. Papamarinopoulos (2006). "Exploration of the Hellenistic Fortification Complex at Asea Using a Multigeophysical Prospection Approach." *Archaeological Prospection* **13**: 1-9.

Dorn, N. (2002). Geophysical responses at Port Arthur Historic Site, Tasmania, as part of the 2001 Summer Archaeology Programme: Final Report. Hobart, University of Tasmania.

Dorn, N., D. Gibbons, L. D'Andrea, J. Legg (2002). Port Arthur 2002 Summer Geophysics Programme as part of the annual Summer Archaeology Programme for Port Arthur Historic Site Management Authority. Hobart, University of Tasmania.

Doyle, R. and J. Cumming (2003). Isle of the Dead Soil Types. Hobart, University of Tasmania.

Edwards, L. S. (1977). "A modified pseudosection for resistivity and IP." *Geophysics* **42**: 1020-1036.

Egloff, B. J. (1987). Archaeology in the Port Arthur Project. Archaeological procedures manual. M. Davies and K. Buckley. Hobart, Department of Lands, Parks and Wildlife.

Ehrenhard, J., W. Athens, R. Johnson (1984). "A practical deployment array for the Geohm 3 soil resistivity meter." *CRM Bulletin* **7**(3): 3-6.

El-Behiry, M. G. (2000). Nondestructive Geophysical Surveys for Delineating Buried Tombs and Identifying their Environmental Status. Symposiun on the Application of Geophysics to Engineering and Environmental Problems, Arlington, VA, Environmental and Engineering Geophysical Society.

Ellwood, B. B. (1990). "Electrical resistivity surveys in two historical cemeteries in northeast Texas: a method for delineating unidentified burial shafts." *Historical Archaeology* **24**: 91-98.

Ellwood, B. B., D. Owsley, S. Ellwood, P. Mercado-Allinger (1994). "Search for the Grave of the Hanged Texas Gunfighter William Preston Longley." *Historical Archaeology* **28**(3): 94-112.

Ernenwein, E. and K. Kvamme (2002). Multi-dimensional Remote Sensing at Army City Kansas: A SERDP Project Fusing Ground Air, and Satellite Data. Plains Anthropological Conference, Oklahoma City.

Field, G., G. Leonard, D. Nobes (2001). Where is Percy Rutherford's Grave? Australasian Connection and New Directions: Proceedings of the 7th Australasian Archaeometry Conference, Auckland, Department of Anthropology, University of Auckland.

Fletcher, M., D. Spicer (1995). "Simulation of ground penetrating radar". In *Computer Applications and Quantitative Methods in Archaeology.* J. Wilcock and K. Lockyear. editors. BAR International Series No. 598. Oxford: 45-49

Freeman Firth and Austral Archaeology (1998). Point Puer, Port Arthur Historic Site. Archaeological Heritage Assessment.

France, D., T. Griffin, J. Swanburg, G. Lindemann, C. Davenport, V. Trammell, C. Armbrust, B. Kondratieff, A. Nelson, K. Castellano, D. Hopkins (1992). "A Multidisciplinary Approach to the Detection of Clandestine Graves." *Journal of Forensic Sciences* **37**: 1445-1458.

Gaffney, V., C. Gaffney, M. Corney (1998). Changing the Roman Landscape: the role of geophysics and remote sensing. *Science in Archaeology: an Agenda for the Future.* J. Bayley. London, English Heritage: 145 - 156.

Geometrics (2000). Total Field Magnetometer Performance, Published Specifications and What They Mean: 13.

Godio, A., L. Sambuelli, L. Socco (2000). "Electromagnetic survey for detection of archaeological remains in urban sites." *The Leading Edge* **19**(8): 850-54.

Godio, A. and Piro, S. (2005). "Integrated data processing for archeological magnetic surveys." *The Leading Edge* **24**(11): 1138-1144.

Goodman, D. and Y. Nishimura (1993). "A ground radar view of Japanese burial mounds." *Antiquity* **67**: 349-54.

Goodman, D., Y. Nishimura, J. Rogers (1995). "GPR time slices in archaeological prospection." *Archaeological Prospection* **2**: 85-89.

Goulty, N. R., J. S. Thatcher, M. J. Findlay, J. E. Kragh, P. D. Jackson (1990). "Experimental investigation of crosshole seismic techniques for shallow coal exploration." *Quarterly Journal of Engineering Geology* **23:** 217-228

Goulty, N. R., A. L. Hudson (1994). "Completion of the seismic refraction survey to locate the vallum at Vindobala, Hadrian's Wall." *Archaeometry* **36:** 327-335.

Griffiths, D., and Turnbull, J. (1985). "A multi-electrode array for resistivity surveying." *First Break* **3**: 16-20.

Griffiths, D., Turnbull, J., and Olayinka, A.I. (1990). "Two-dimensional resistivity mapping with a computer controlled array." *First Break* **8**(4): 121-129.

Griffiths, D. and Barker, R.D. (1993). "Two-dimensional resistivity imaging and modelling in areas of complex geology." *Journal of Applied Geophysics* **29**: 211-226.

Griffiths, D. and Barker, R.D. (1994). "Electrical Imaging in Archaeology." *Journal of Archaeological Science* **21**: 153-158.

Hammon, W. S., G. A. McMechan, X. X. Zeng (2000). "Forensic GPR: finite-difference simulations of responses from buried human remains." *Journal of Applied Geophysics* **45**(3): 171-186.

Hargrave, M. S., LE; Larson, TK; Shields, R; Dendy, J (2002). "The role of resistivity survey in historic site assessment and management: An example from Fort Riley, Kansas." *Historical Archaeology* **36**(4): 89-110.

Hasek, V. (1999). Methodology of Geophysical Research in Archaeology. BAR International Series 769. Oxford, Archaeopress: 127.

Heimmer, D. H. (1992). Near-Surface, High Resolution Geophysical Methods for Cultural Resource Management and Archaeological Investigation. Denver, National Parks Service Interagency Archaeological Services, Rocky Mountains Regional Office.

Hesse, A. (1999). "Multi-parametric survey for archaeology: how and why, or how and why not?" *Journal of Applied Geophysics* **41**(2-3): 157-168.

Jackman, G. (2003). Port Arthur Historic Site Archaeology Plan, Port Arthur Historic Site Management Authority.

Jackman, G. (2005). Penitentiary Workshops Archaeological Site Report, Port Arthur Historic Site Management Authority.

Johnson, W., G. Johnson, G. Gozdzik (2001). Merritt Cemetery, Barboursville, West Virginia. Geophysics Comes of Age in North American Archeology; Society of American Archaeology, 66th Annual Meeting, New Orleans, Louisiana, Society of American Archaeology.

Keller, G. and F. Frischknecht (1966). Electrical Methods in Geophysical Prospecting. New York, Pergamon Press.

King, J., B. W. Bevan, R. Hurry (1993). "The Reliability of Geophysical Surveys at Historic-Period Cemeteries: An Example from the Plains Cemetery, Mechanicsville, Maryland." *Historical Archaeology* **27**(3): 4-16.

Kvamme, J. C. (2002). Fort Riley Post Cemetery, NADAG: http://www.cast.uark.edu/~kkvamme/geop/ft-riley-cem.htm.

Kvamme, K. L. (2000). Bozeman Cemetery Survey (work in progress), ArcheoImaging Lab, Department of Anthropology, Arkansas.

Kvamme, K. L. (2001). Current Practices in Archaeogeophysics: Magnetics, Resistivity, Conductivity, and Ground-Penetrating Radar. *Earth Sciences and Archaeology.* V. H. P. Goldberg, and R. Ferring. New York, Kluwer Academic/Plenum Publishers: 353-384.

Kvamme, K. L. (2001). An Electrical Resistivity Study of Waraju Distillery, New Ulm, Minnesota. Fayetteville, ArcheoImaging Lab, Department of Anthropology and Center for Advanced Spatial Technologies, University of Arkansas.

Kvamme, K. L. (2006). "Integrating Multidimensional Geophysical Data." *Archaeological Prospection* **13**: 57-72.

Laing, Henry (1836). *Register of Buildings at the Penal Settlement of Port Arthur and the Outstations on Tasman Peninsula V.D.L.* AOT Reference CON 87.

Larson, T., Lewis E. Somers, Dori M. Penny, Michael L. Hargrave (1999). Geophysical and Archaeological Investigations of Historic Sites at Fort Riley, Kansas. CERL Technical Report, US Army Corps of Engineers.

Leaman, D. (2002). The Rock which makes Tasmania. Hobart, Leaman Geophysics.

Leckebusch, J. (2003) "Ground-penetrating Radar: A Modern Three-dimensional Prospection Method." *Archaeological Prospection* **10**(4): 213-240.

Lines, L. R., Schultz, S. Treitel (1988). Cooperative inversion of geophysical data. Geophysical inversion and applications, Memorial University of Newfoundland.

Llopis, J. L. and M. K. Sharp (1997). "Geophysical Investigation for the Location of a Historic Heiau, Kawaihae, Hawaii." *Geoarchaeology: An International Journal* **12**(7): 751-764.

Lockhart, J. (n.d.). Archaeo-geophysical Prospection and Mapping. Two Historic Cemeteries in Crawford County, Arkansas. R. C. J. Mainfort and J. M. Davidson, Arkansas Archeological Society.

Loke, M. H. (2002). Rapid 2D resistivity forward modelling using the finite-difference and finite element methods: M. H. Loke, 29p

Loke, M. H. and R. D. Barker (1995). "Least squares deconvolution of apparent resistivity pseudosections." *Geophysics* **60**: 1682-1690.

Lord, R. (1999). The Isle of The Dead: Port Arthur. Hobart, Richard Long & Partners.

Maierhofer, C. (2003). "Nondestructive evaluation of concrete infrastructure with ground penetrating radar." *Journal of Materials in Civil Engineering* **15**(3): 287-297.

Maijala, P. (1994). Ground penetrating radar and related data processing techniques. Department of Geophysics, University of Oulu, Finland.

Malagodi, S., L. Orlando, S. Piro, F. Rosso (1996). "Location of Archaeological Structures using GPR method: Three-dimensional Data Acquisition and Radar Signal Processing." *Archaeological Prospection* **3**(1): 13-23.

Mankowski, L., S. Lemke, S. Martin, D. Hayes, P. Martin, C. Young, J. Diehl (2000). A geophysical investigation of a sugar cane plantation, St. Croix, U. S. Virgin Islands: Using multiple techniques to assess a complex industrial site. Symposium on the Application of Geophysics to Engineering and Environmental Problems: SAGEEP 2000, Arlington, VA, Environmental and Engineering Geophysical Society.

Martin, W. A., J. E. Bruseth, R. Huggins (1991). "Assessing Feature Function and Spatial Patterning of Artifacts with Geophysical Remote-Sensing Data." *American Antiquity* **56**: 701-720.

McDonald R., J. Speight, J. Walker, and M. Hopkins (1996). Australian Soil and Land Survey - Field Handbook, Goanna Print.

McNeill, J. (1980). Electromagnetic terrain conductivity measurements at low induction numbers. Mississuaga (Ontario), Geonics Ltd.

Mellet, J. (1992). Location of human remains with ground-penetrating radar. Fourth International Conference on Ground Penetrating Radar, Rovaniemi, Finland, Geological Society of Finland.

Metwaly, M., A. Green, H. Horstmeyer, H. Maurer, A. Abbas, A. Hassaneen (2005). "Combined Seismic Tomographic and Ultrashallow Seismic Reflection Study of an Early Dynastic Mastaba, Saqqara, Egypt." *Archaeological Prospection* **12**: 245-256.

Miller, P. (1996). "Disturbances in the soil: finding buried bodies and other evidence using ground penetrating radar." *Journal of Forensic Sciences* **41**: 648 - 52.

Mrozowski, S. (2000 -) http://www.shelter-island.org/sylvester_dig/index.html.

National Parks and Wildlife Service, T. (n.d.). Port Arthur Historic Site. information brochure. Hobart, National Parks and Wildlife Service, Tasmania.

Nelson, A. (1998). "Wandering Bones: Archaeology, Forensic Science, and Moche Burial Practices." *International Journal of Osteoarchaeology*. **8**: 192-212.

Neubauer, W. (2001). "Images of the invisible-prospection methods for the documentation of threatened archaeological sites." *Naturwissenschaften* **88**(1): 13-24.

Neubauer, W. and A. Eder-Hinterleitner (1997). "3D-interpretation of postprocessed archaeological magnetic prospection data." *Archaeological Prospection* **4**: 191-206.

Neubauer, W., S. Eder-Hinterleitner, S. Seren, P. Melichar (2002). "Georadar in the Roman civil town Carnuntum, Austria: an approach for archaeological interpretation of GPR data." *Archaeological Prospection* **9**(3): 135-156.

Neubauer, W. (2004). "GIS in Archaeology - the Interface between Prospection and Excavation." *Archaeological Prospection* **11**: 159-166.

Nishimura, Y. (2001). Geophysical Prospection in Archaeology. Handbook of Archaeological Sciences. D. R. Brothwell and A. M. Pollard, John Wiley & Sons, Ltd.

Nishimura, Y. and D. Goodman (2000). "Ground-penetrating Radar survey at Wroxeter." *Archaeological Prospection* **7**(2): 101-105.

Nobes, D. (1999). "Geophysical surveys of burial sites: A case study of the Oaro urupa." *Geophysics* **64**(2): 357-367.

Nobes, D. (2000). "The search for "Yvonne": A case example of the delineation of a grave using near-surface geophysical methods." *Journal of Forensic Sciences* **45**(3): 715-721.

Olhoeft, G. (1981). "Electrical properties of rocks." In *Physical properties of rocks and minerals*. S. Touloukian and C. Ho (ed.). McGraw-Hill, New York: 298-329.

Olhoeft, G. (1994). Modeling out-of-plane scattering effects. Fifth International Conference on Ground Penetrating Radar, Kitchener, Ontario.

O'Neill, A. (2003). GPR Applications in Western Australia. Perth, UWA Geology and Geophysics.

Osella, A., M. de la Vega, E. Lascano (2005). "3D electrical imaging of an archaeological site using electrical and electromagnetic methods." *Geophysics* **70**(4): 101-107.

Overdon, S. (1994). "Application of Seismic Refraction to Archaeological Prospecting." *Archaeological Prospection* **1**: 53-64.

Owen, T. and J. Steele (2002). Sawpit and Tannery Complex Excavation Report, Port Arthur, (PA 04/02) Port Arthur Historic Site Management Authority.

Owsley, D. (1995). "Techniques For Locating Burials, With Emphasis On the Probe." *Journal of Forensic Sciences* **40**(5): 735-740.

PAHSMA (1998). Pat Jones' Cottage Conservation Plan. Port Arthur, Port Arthur Historic Site Management Authority.

Palmer, D., Ed. (1980). The generalized reciprocal method of seismic refraction interpretation. USA, Society of Exploration Geophysicists.

Papamarinopoulos, S., A. Liosis, L. Polymenakos, P. Limnaeou-Papakosta (2003). "In Search of the Royal Ptolemaic Cemetery in Central Alexandria, Egypt - the First Contact." *Archaeological Prospection* **10**: 193-211.

Parrington, M. (1986). Occupations and Health Among Nineteenth-Century Black Philadelphians. Philadelhia, Museum Applied Science Center for Archaeology, University Museum, University of Pennsylvania. *MASCA Journal* **4**: 37-41.

Piro, S., P. Mauriello, F. Cammarano (2000). "Quantitative Integration of Geophysical Methods for Archaeological Prospection." *Archaeological Prospection* **7**: 203-213.

Pomfret, J. (2006). "Ground-penetrating Radar Profile Spacing and Orientation for Subsurface Resolution of Linear Features." *Archaeological Prospection* **13**: 151-153.

Powell, K. (2004). "Detecting buried human remains using near-surface geophysical instruments." *Exploration Geophysics* **35**: 88-92.

Ranson, D. and B. Egloff (1988). "The Application of Earth-Resistivity Surveys to Australian Archaeological Sites." *Australian Historical Archaeology* **6**: 57-73.

Rapp, G. and C. Hill (1998). Geoarchaeology: The earth science approach to archaeological interpretation. London, Yale University Press.

Rogers, M. (2001). Detection of Burials at the Confederated Tribes of Siletz Indians Historic Period Cemetery, Oregon: A Comparison of Ground-Based Remote Sensing Methods; *Unpublished Master's Thesis*. Oregon, Oregon State University.

Ross, L. (1995). Death and Burial at Port Arthur: 1830 - 1877. History. Hobart, University of Tasmania.

Roy, A. and A. Apparao (1971). "Depth of investigation in direct current methods." *Geophysics* **36**: 943-959.

Sasaki, Y. (1992). "Resolution of resistivity tomography inferred from numerical simulation." *Geophysical Prospecting* **40**: 453-464.

Scollar, I., A. Tabbagh, A. Hesse, I. Herzog (1990). Archaeological Prospecting and Remote Sensing. Cambridge, Cambridge University Press.

Sharma, P. (1997). Environmental and Engineering Geophysics. Cambridge, Cambridge University Press.

Sheriff, R. and P. Lloyd (1995). Exploration Seismology, Cambridge University Press.

Silliman, S., P. Farnsworth, K. Lightfoot (2000). "Magnetometer prospecting in historical archaeology: Evaluating survey options at a 19th-century rancho site in California." *Historical Archaeology* **34**(2): 89-109.

Snader, T. and A. Kozlowski (2006). "A breath of life to the dead: Applications of three-dimensional impulse ground penetrating radar for the delineation of late 19th- early 20th century unmarked graves in Milton, PA." Geological Society of America: Abstracts with Programs for Northeastern Section 41st Annual Meeting 38(2): 71.

Steele, J. (2004)a. Port Arthur Parade Ground Archaeological Excavation Draft Report, (PA 04/02) Port Arthur Historic Site Management Authority.

Steele, J. (2004)b. Port Arthur Commissariat Stores Archaeological Excavation Draft Report, (PA 04/06) Port Arthur Historic Site Management Authority.

Steele, J. (2005). Port Arthur First Hospital Site Archaeological Excavation Draft Report, (PA 05/02) Port Arthur Historic Site Management Authority.

Stummer, P., H. Maurer, A. Green (2004). "Experimental design: Electrical resistivity data sets that provide optimum subsurface information." *Geophysics* **69**(1): 120-139.

Sumner, J. (1976). Principles of induced polarization for geophysical exploration, Elsevier Scientific Publishing Company.

Telford, W., L. Geldart, R. Sheriff, D. Keys (1990). Applied Geophysics. Cambridge, Cambridge University Press.

Thorn, A. (2001). The Isle of the Dead, Port Arthur: Condition Survey and Assessment of Treatments. Prepared for the *Port Arthur Historic Site Management Authority* by ARTCARE, North Melbourne. 19 March 2001.

Tuffin, R. (2002). Assorted historical notes on the Port Arthur Historic Site, courtesy of the Port Arthur Historic Site Management Authority.

Walker, A. (2000). "Multiplexed Resistivity Survey at the Roman Town of Wroxeter." *Archaeological Prospection* **7**(2): 119-132.

Ward, S. (1990). Resistivity and Induced Polarisation Methods. Geotechnical and Environmental Geophysics. S. H. Ward, Society of Exploration Geophysicists. Investigations in Geophysics 5.

Wesolowsky, A. (1989). The Osteology of the Uxbridge Paupers. Archaeological Excavations at the Uxbridge Almshouse Burial Ground in Uxbridge, Massachusetts. R. Elia and A. Wesolowsky. Boston, Office of Public Archaeology, Boston University: 303-336.

Weymouth, J. (1986). Geophysical Methods of Archaeological Site Surveying. In *Advances in Archaeological Method and Theory*. Schiffer, B. M. (ed). Academic Press, New York City. **9:** 311-395.

Wilson, V., C. Frampton, P. Randolph (1994). Location of burial sites using ground-penetrating radar surveys on Rottnest Island, Western Australia. 64th Annual International Meeting, Society of Exploration Geophysicists.

Witten, A., R. Brooks, T. Fenner (2001). "The Tulsa Race Riot of 1921: A geophysical study to locate a mass grave." *The Leading Edge* June: 655-660.

Wynn, J. (1986). "A Review of Geophysical Methods used in Archaeology." *Geoarchaeology* **1**: 245-257.

Young, J., J. Peters, C. Chen (1999). Characteristic resonance identification techniques for buried targets seen by ground penetrating radar. Detection and identification of visually obscured targets. C. Baum, Taylor & Francis.

Zhou, W., B. Beck, J. Stephenson (2000). "Reliability of dipole-dipole electrical resistivity tomography for defining depth to bedrock in covered karst terranes." *Environmental Geology* **39**(7): 760-766.

Appendix A: Isle of the Dead

Additional geophysical images

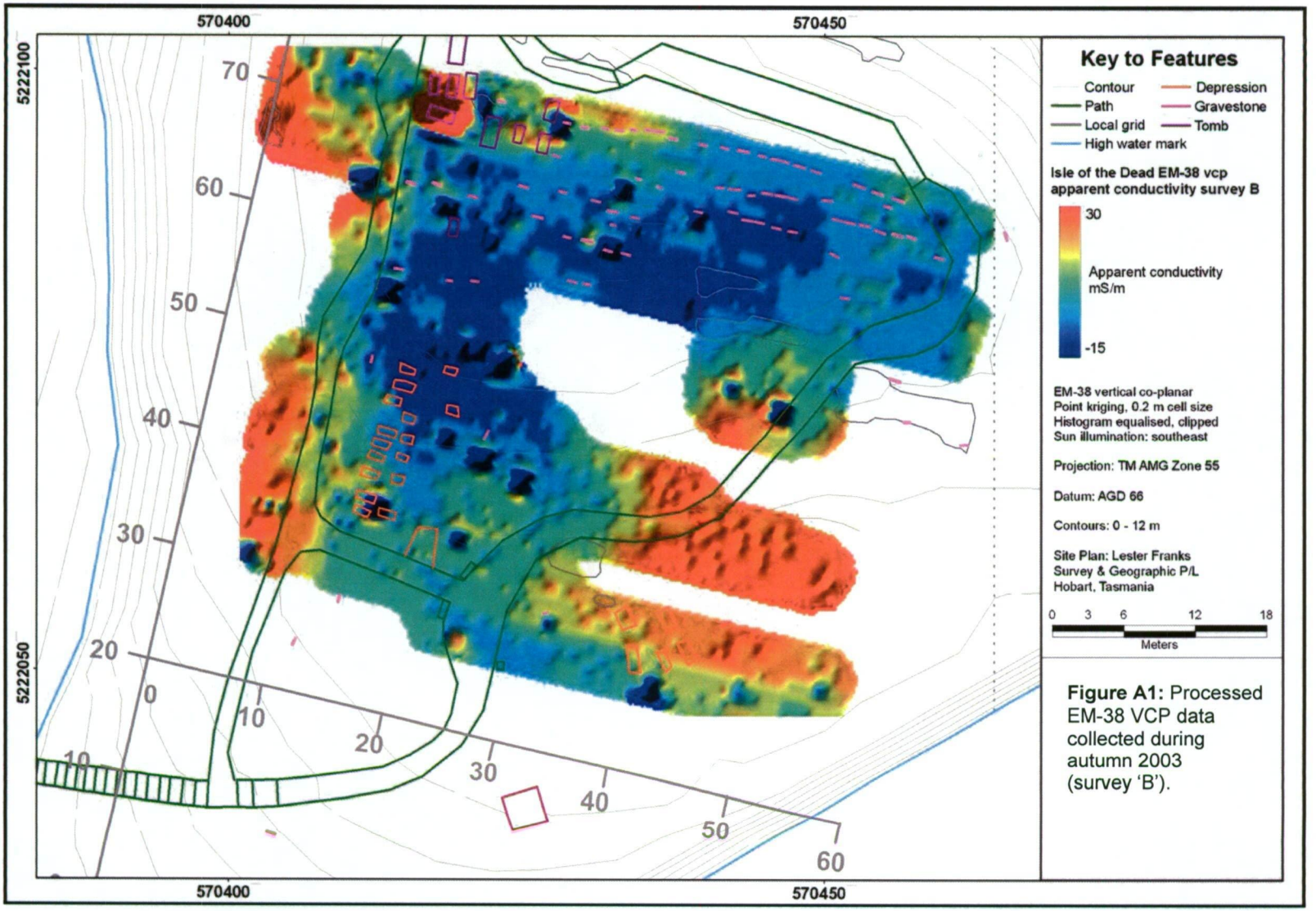

Figure A1: Processed EM-38 VCP data collected during autumn 2003 (survey 'B').

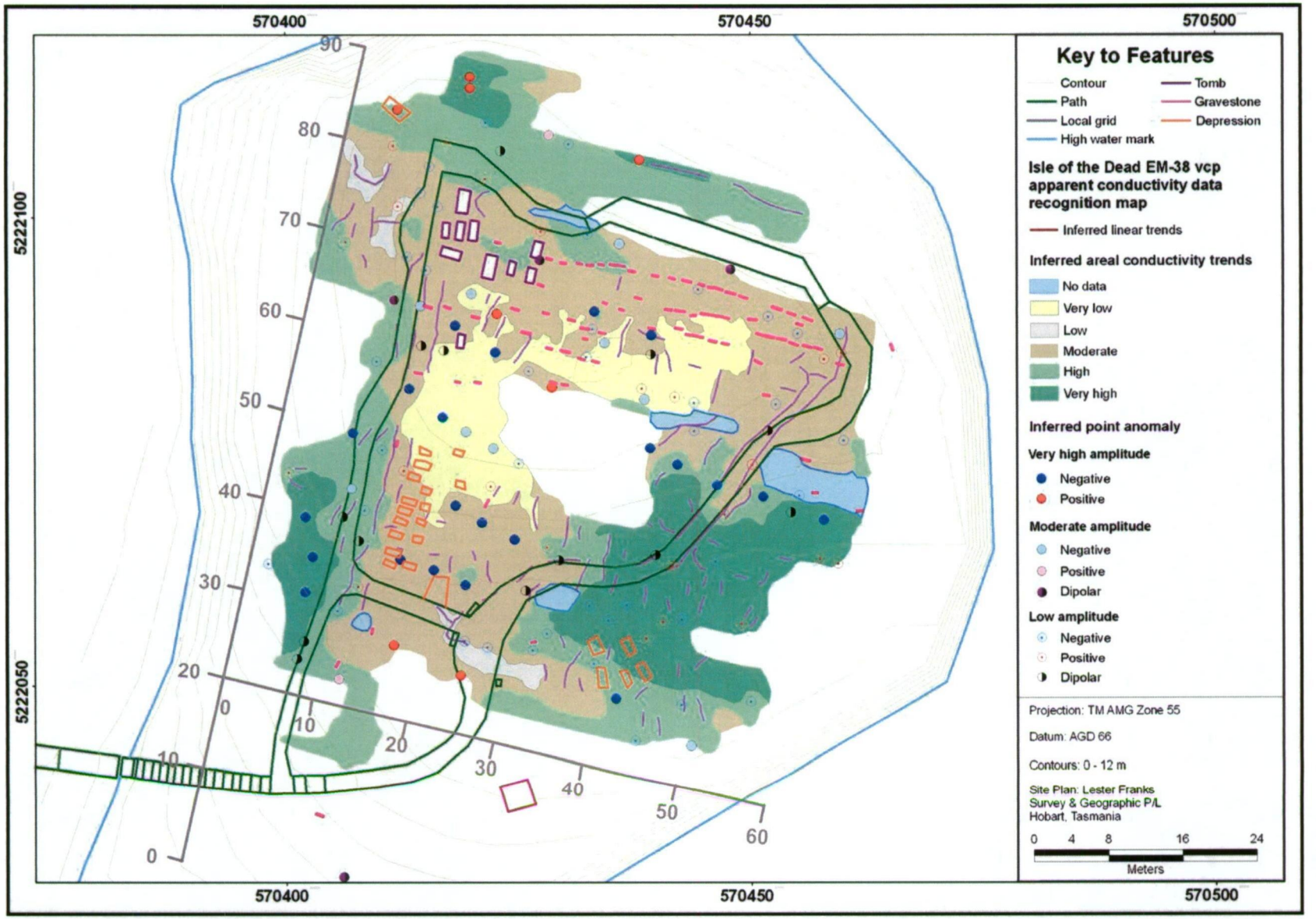

Figure A2: Isle of the Dead EM-38 VCP data recognition map, combining Survey A and B. This shows the lateral variation in apparent conductivity, point anomalies and linear trends. Amplitude of the point anomalies is with respect to average background values within a 2.5 m radius.

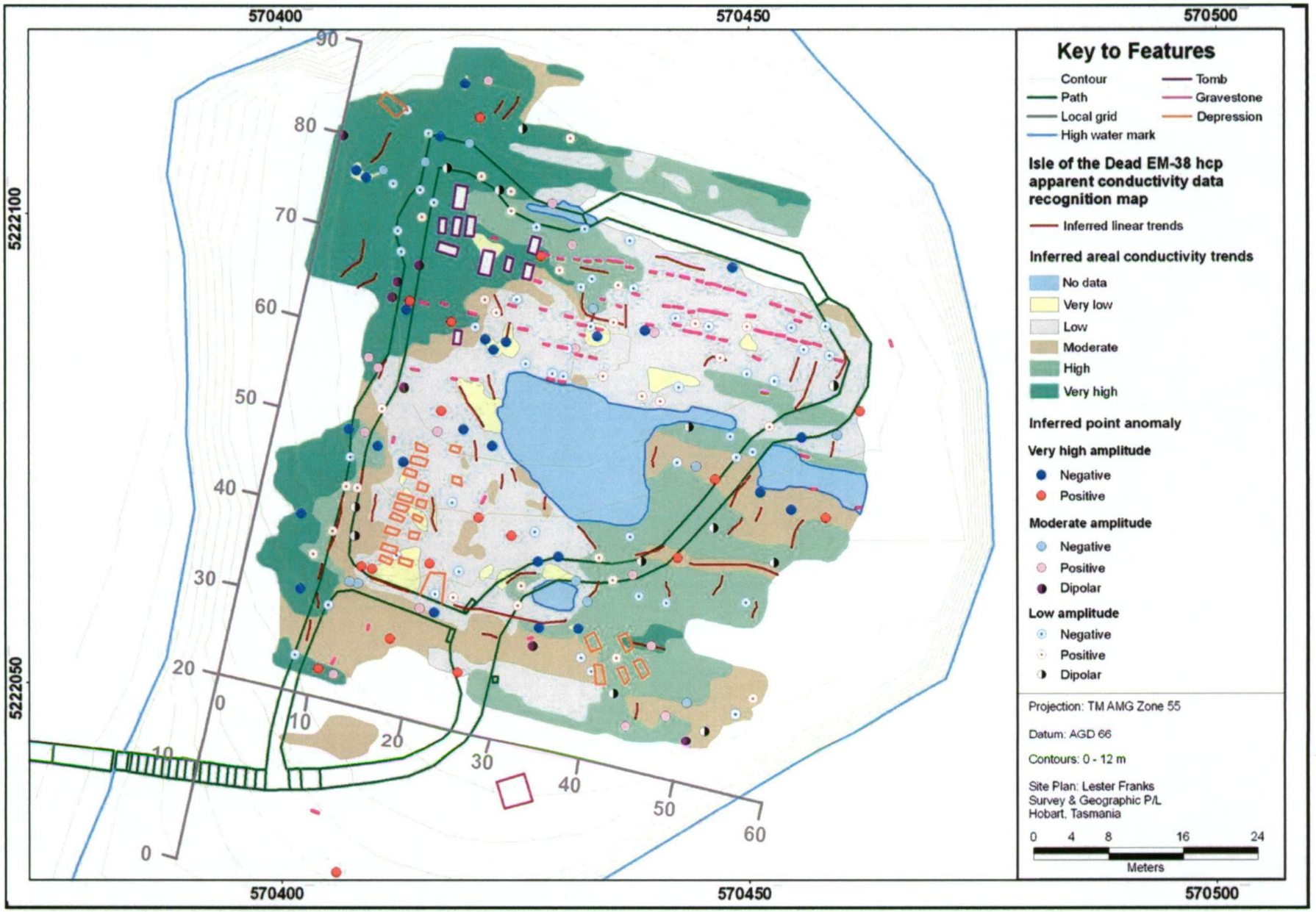

Figure A3: Isle of the Dead EM-38 HCP mode data recognition map showing the lateral variation in apparent conductivity, point anomalies and linear trends.

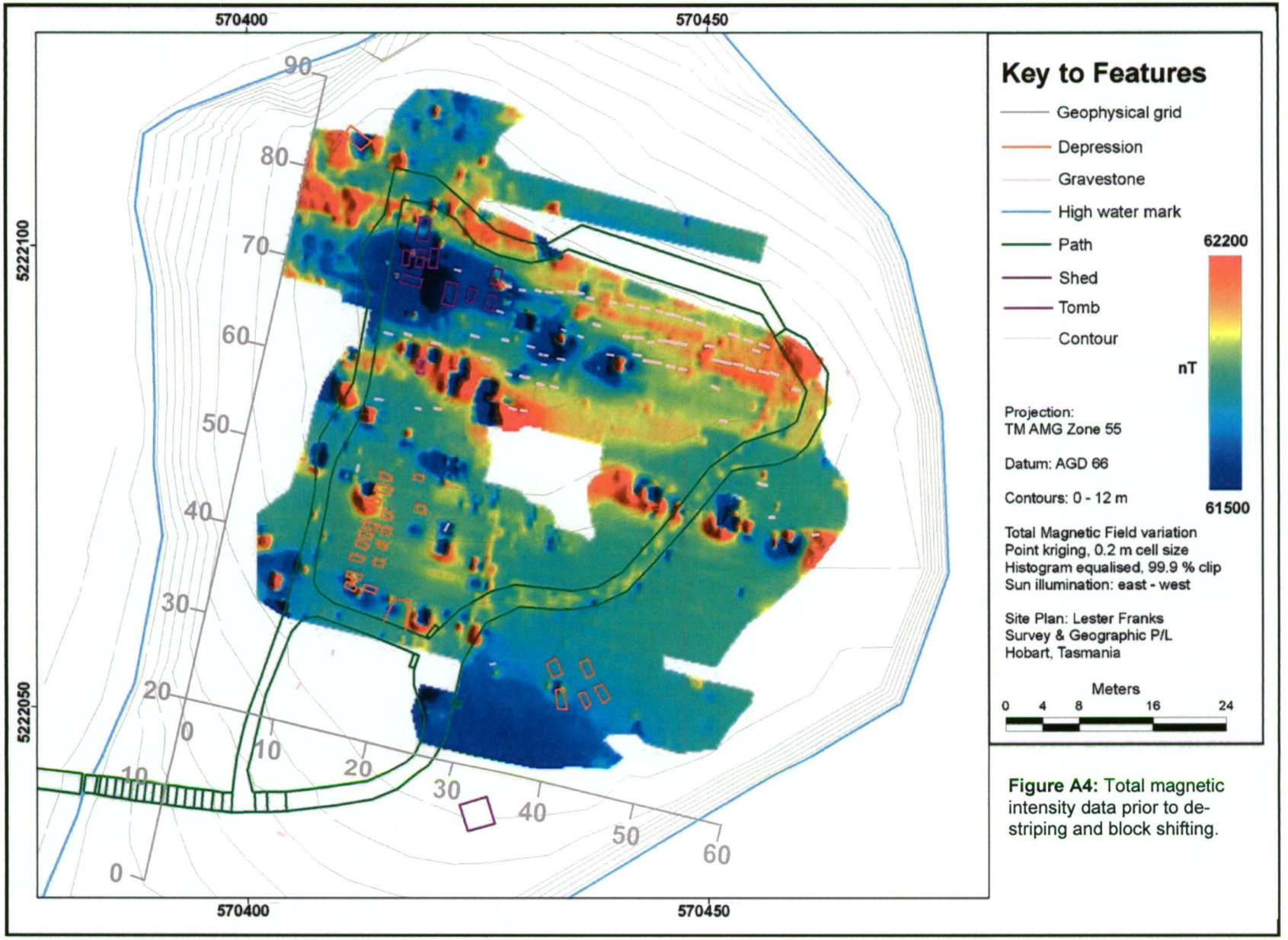

Figure A4: Total magnetic intensity data prior to de-striping and block shifting.

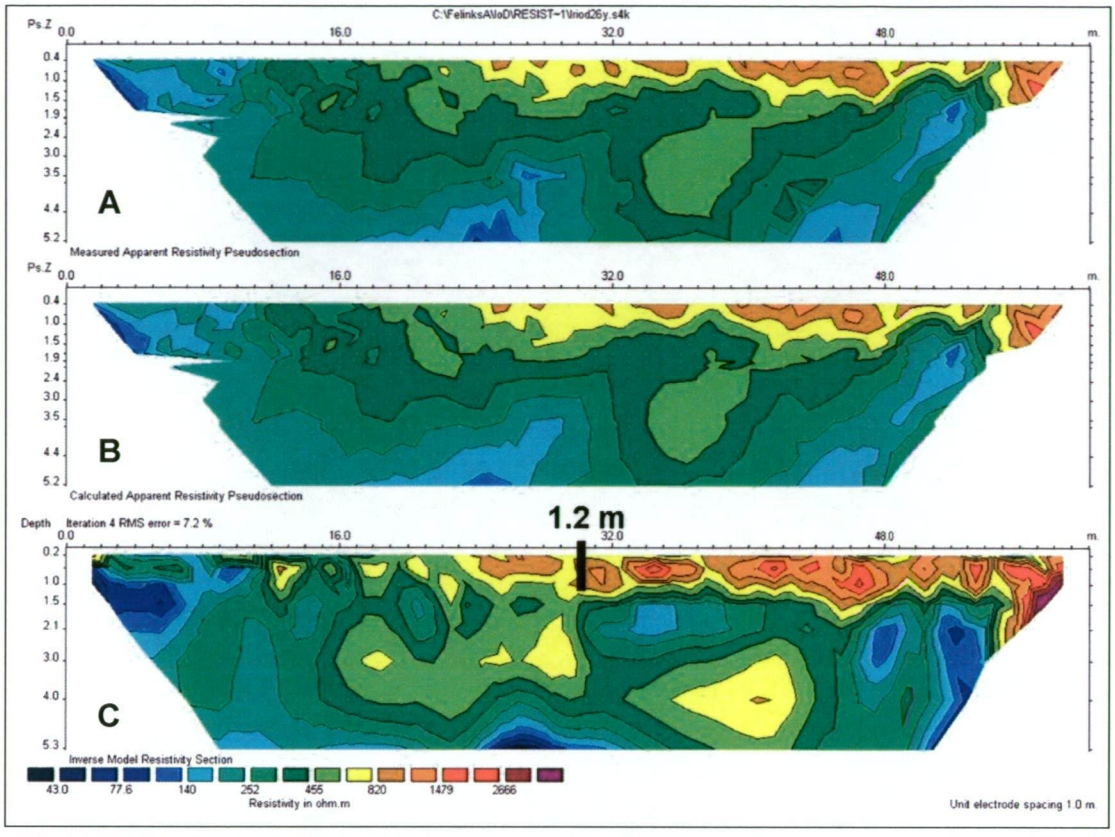

Figure A5: Observed and calculated resistivity pseudosections, and the tomographic model for Line 66y showing resistivity variation to ~5 m and depth to auger refusal.

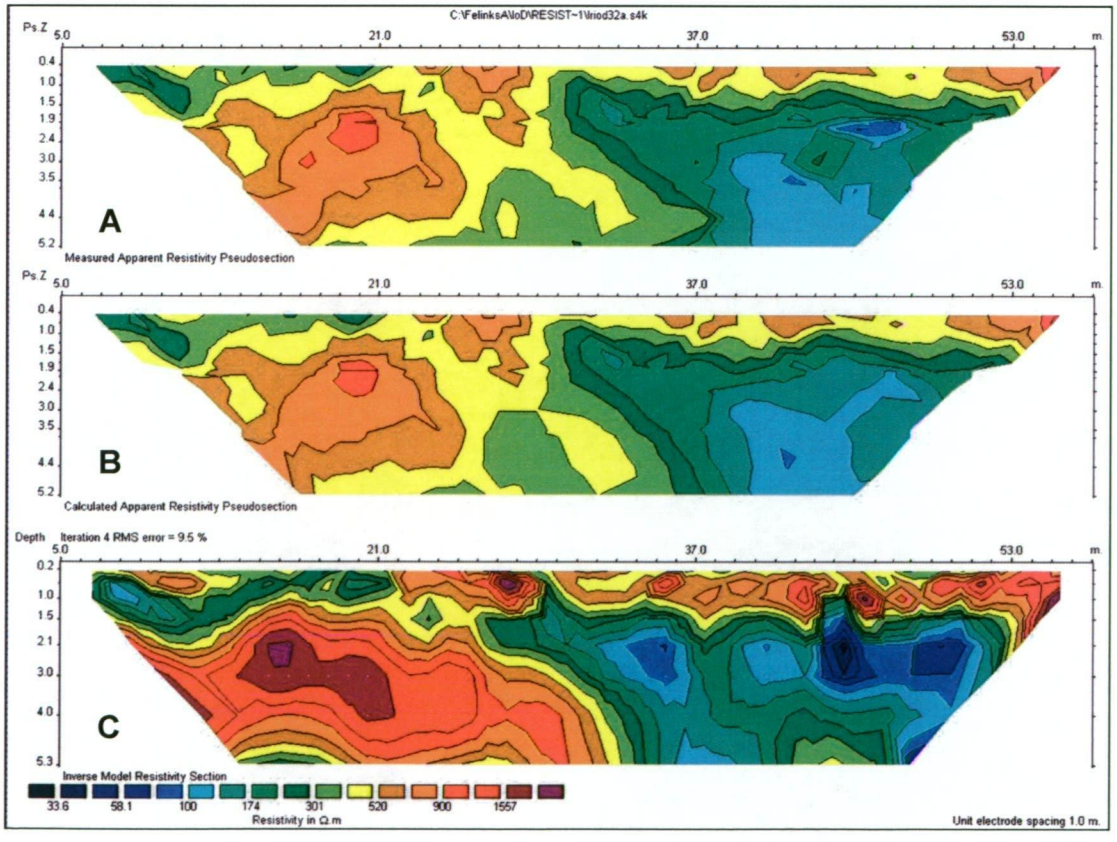

Figure A6: Observed and calculated apparent resistivity pseudosections and tomograph for Line 32y.

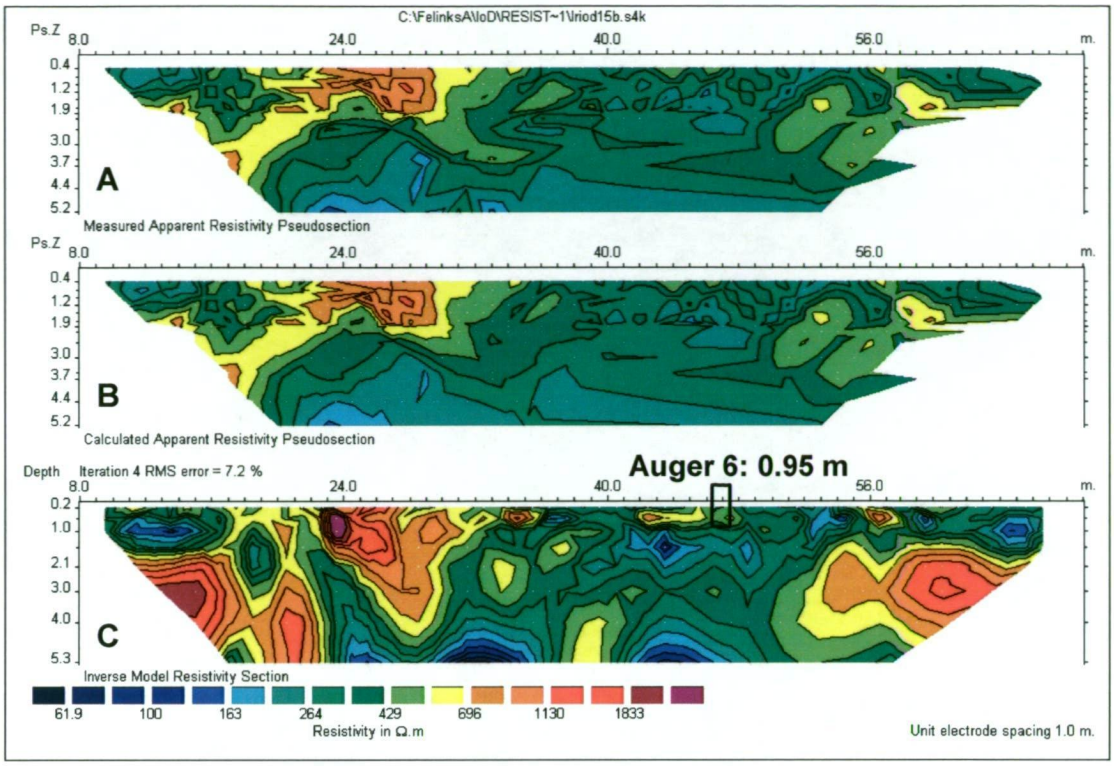

Figure A7: Tomographic resistivity model for Line 15x, showing auger 6 refusal depth.

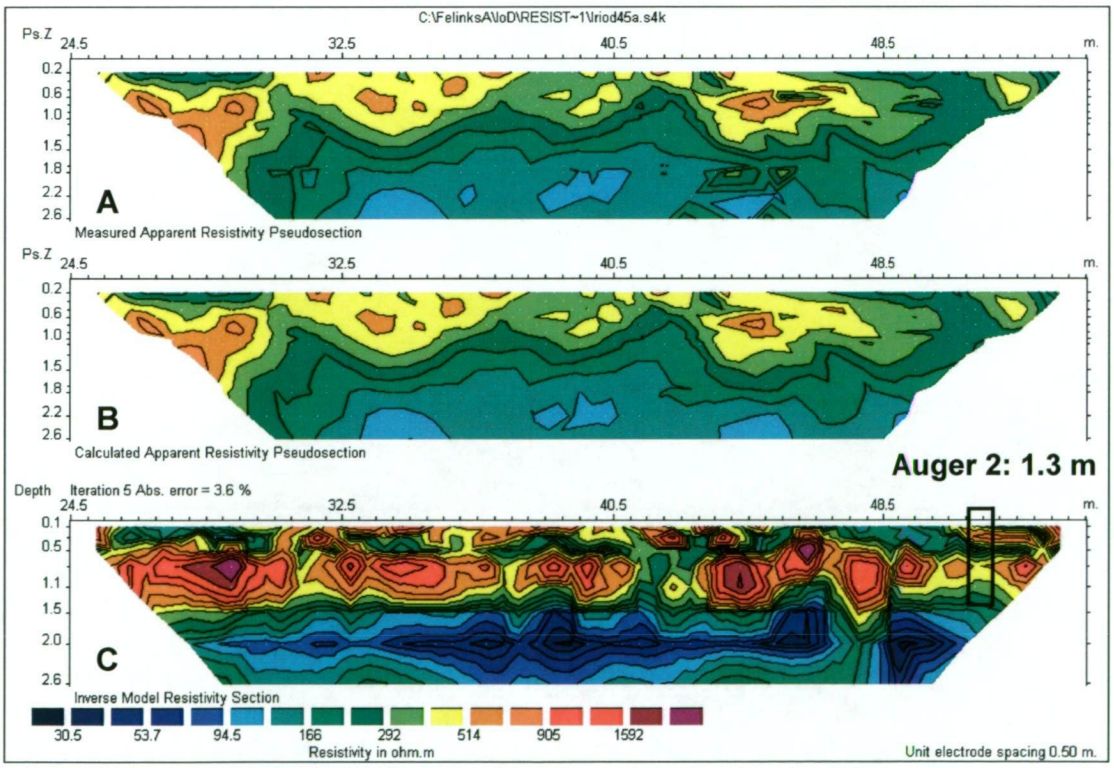

Figure A8: Tomographic resistivity model for Line 45x, showing auger 2 refusal depth.

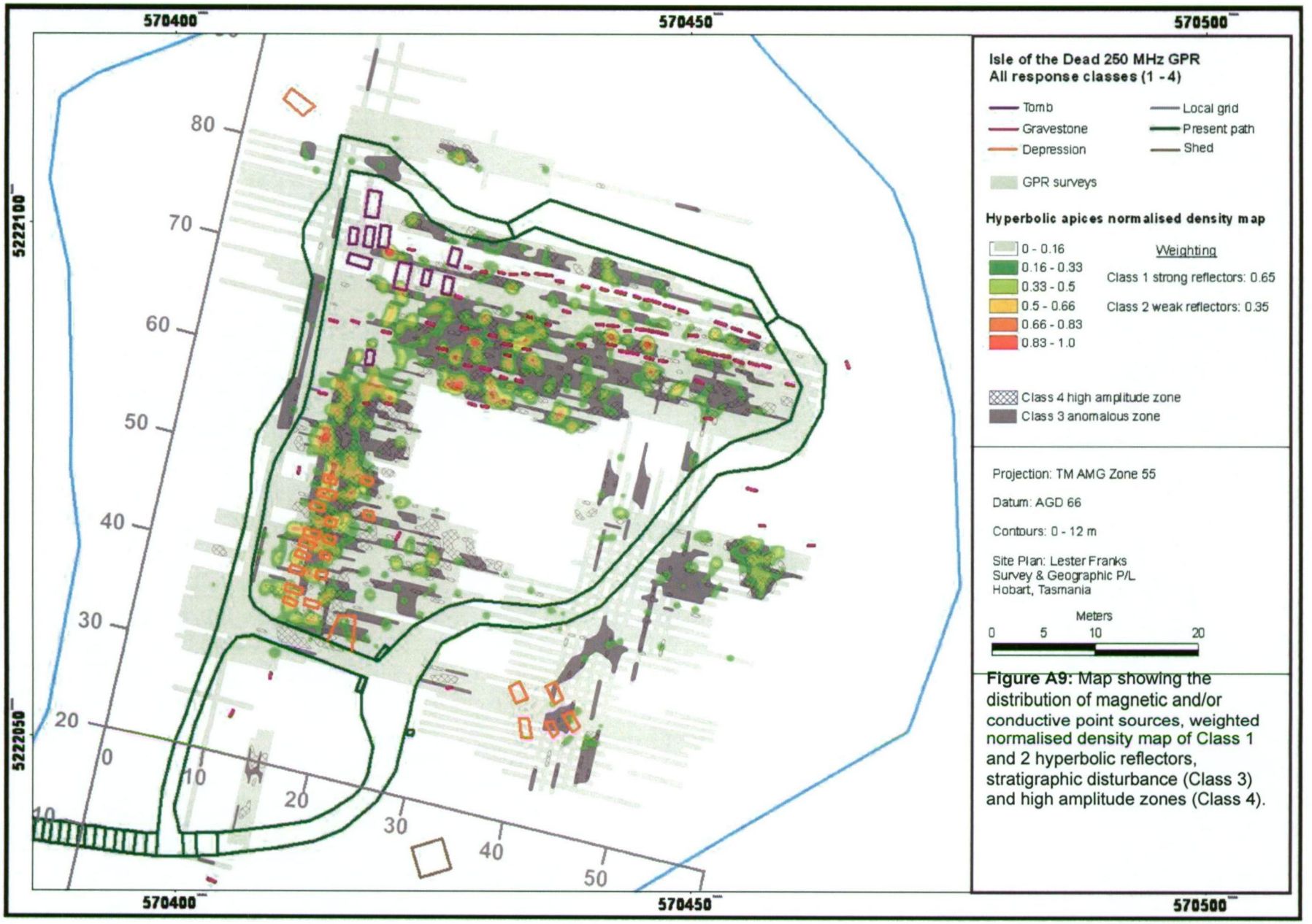

Figure A9: Map showing the distribution of magnetic and/or conductive point sources, weighted normalised density map of Class 1 and 2 hyperbolic reflectors, stratigraphic disturbance (Class 3) and high amplitude zones (Class 4).

Appendix B: Settlement Hill

COMPREHENSIVE INTERPRETATION MAPS

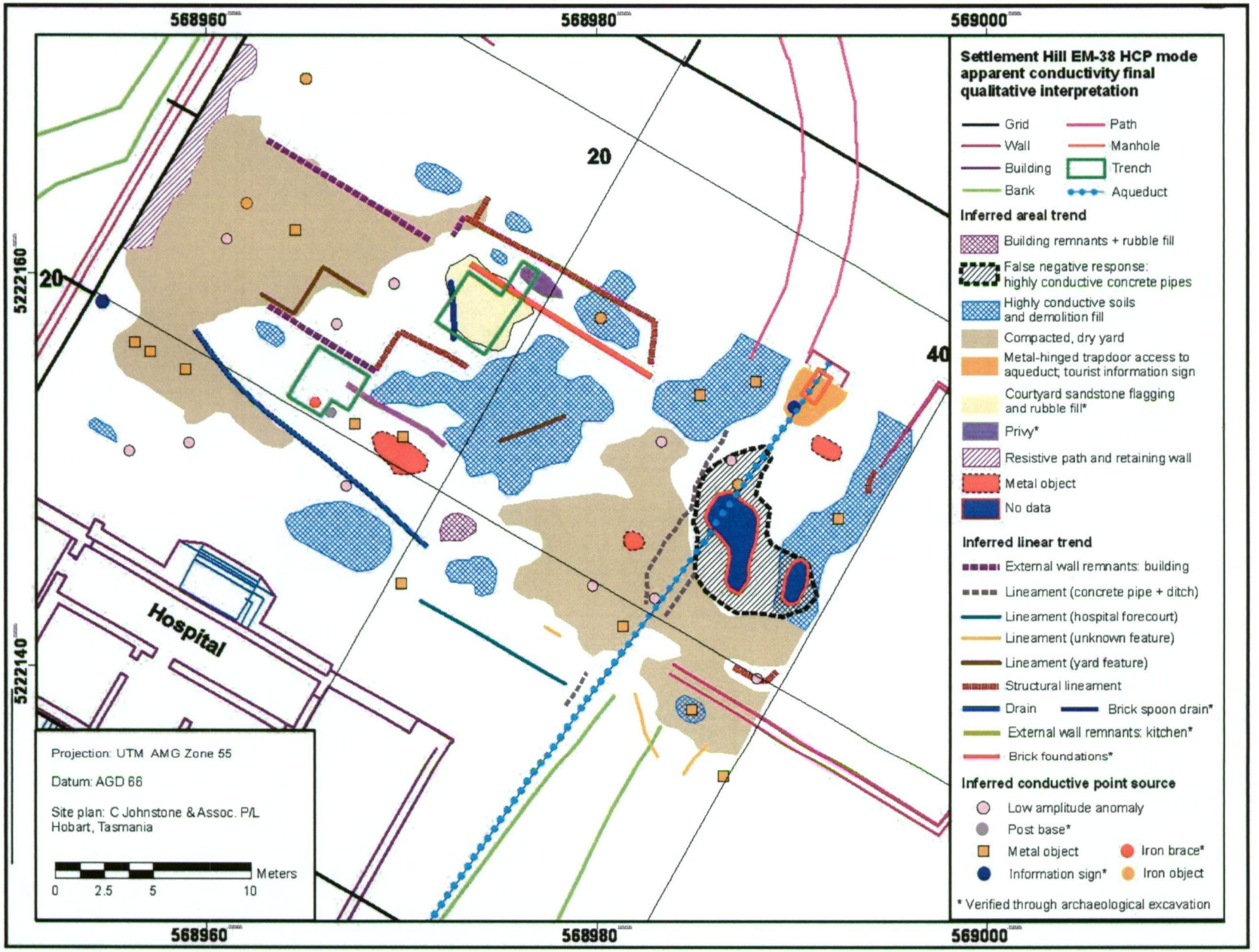

Figure B1: Settlement Hill hospital precinct EM-38 HCP mode apparent conductivity final qualitative interpretation map.

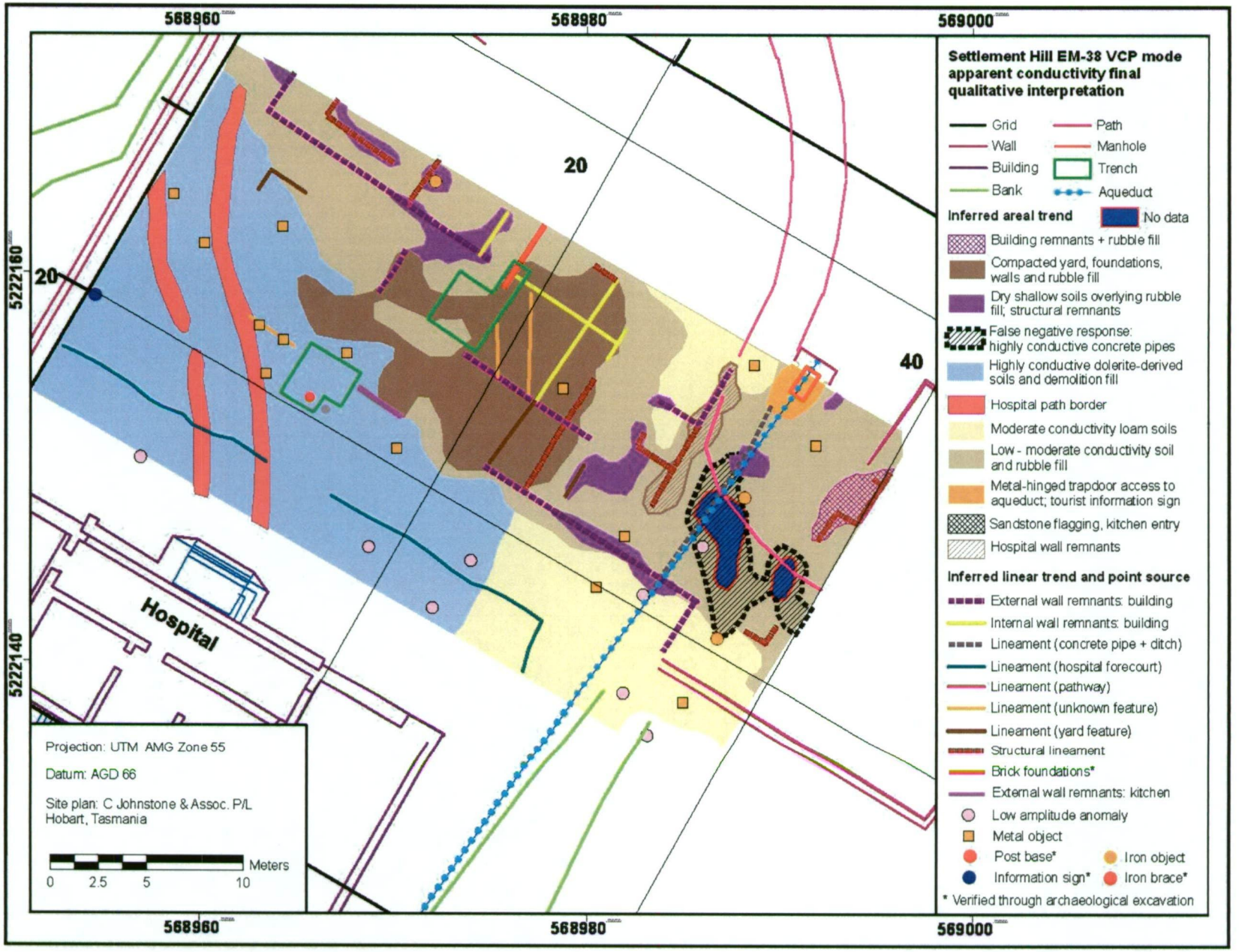

Figure B2: Settlement Hill hospital precinct EM-38 VCP mode apparent conductivity final qualitative interpretation map.

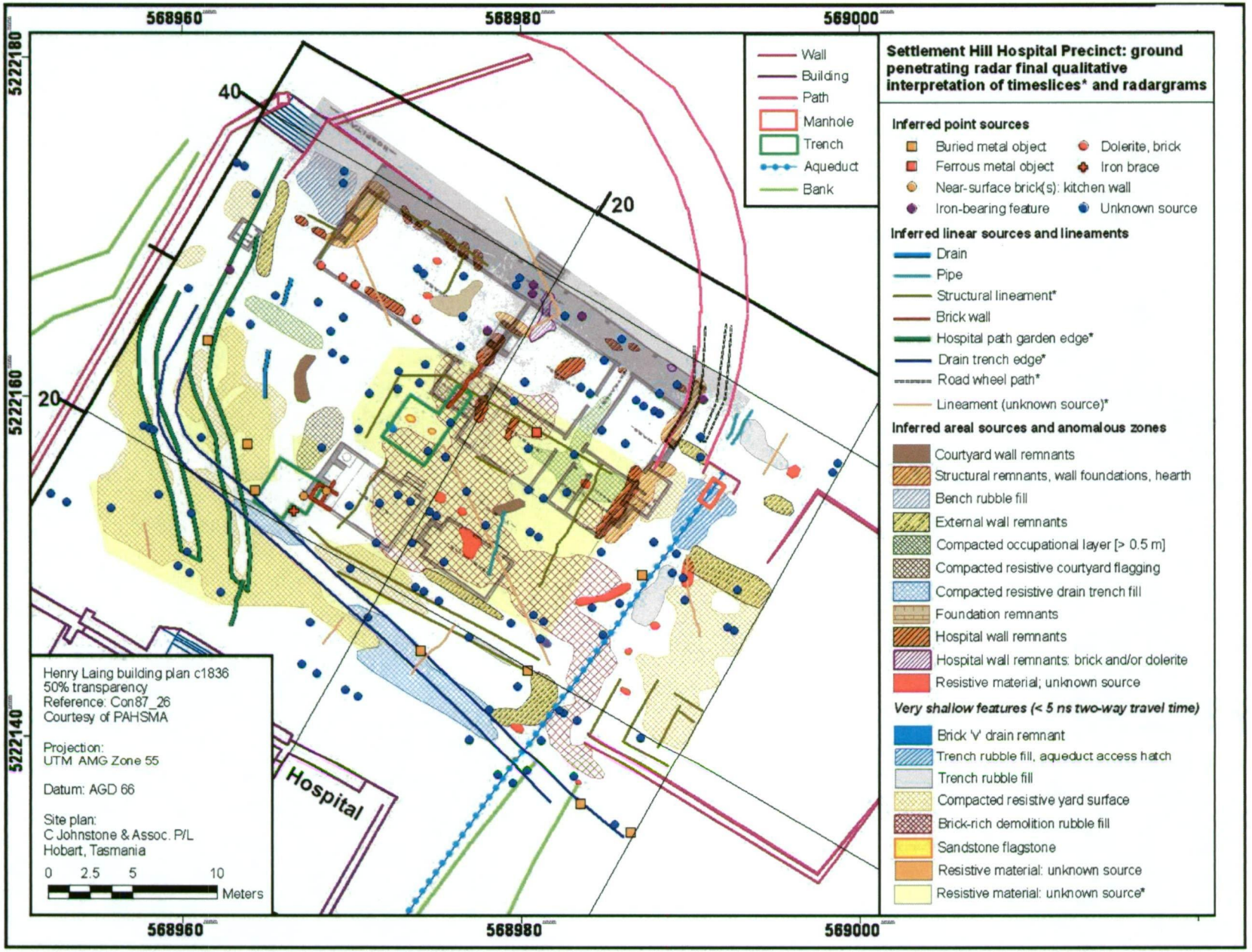

Figure B3: Settlement Hill hospital precinct 500 MHz ground penetrating radar final qualitative interpretation map, derived from timeslice and profile analysis.

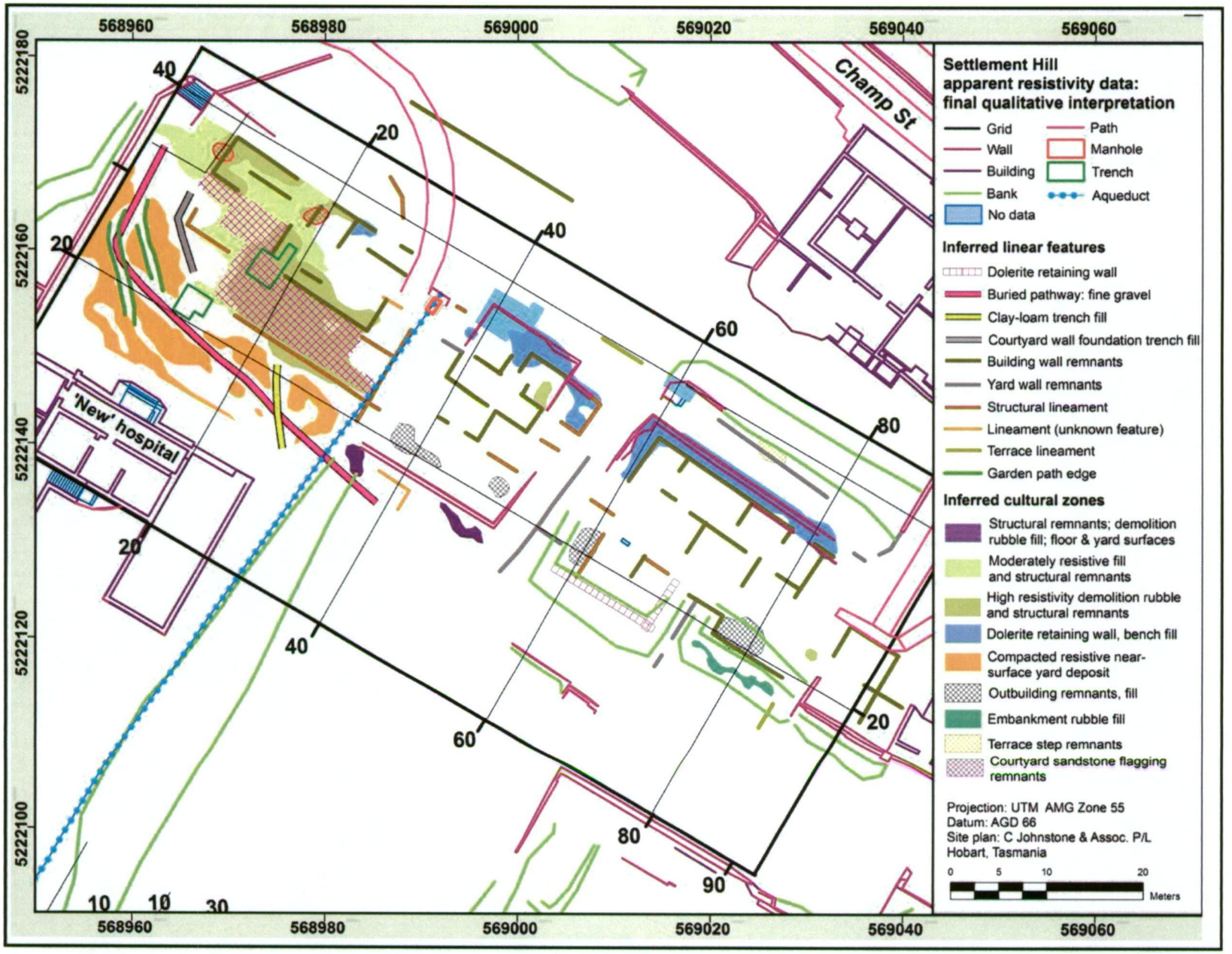

Figure B4: Settlement Hill apparent resistivity final qualitative interpretation map.

Appendix C: Sawpits and Tannery

Geophysical maps by Dorn *et al.* (2002)

Tabulated data collection parameters

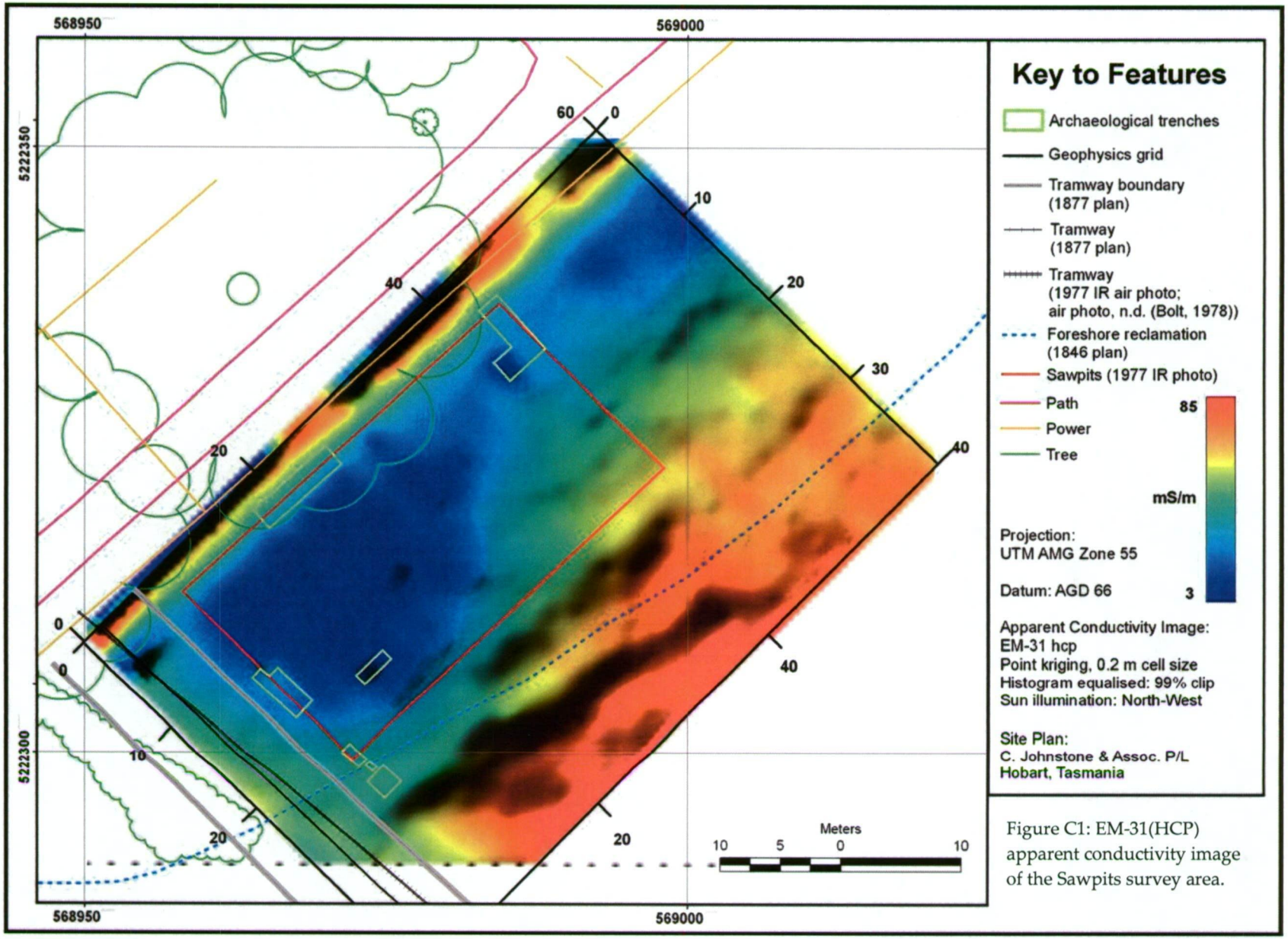

Figure C1: EM-31(HCP) apparent conductivity image of the Sawpits survey area.

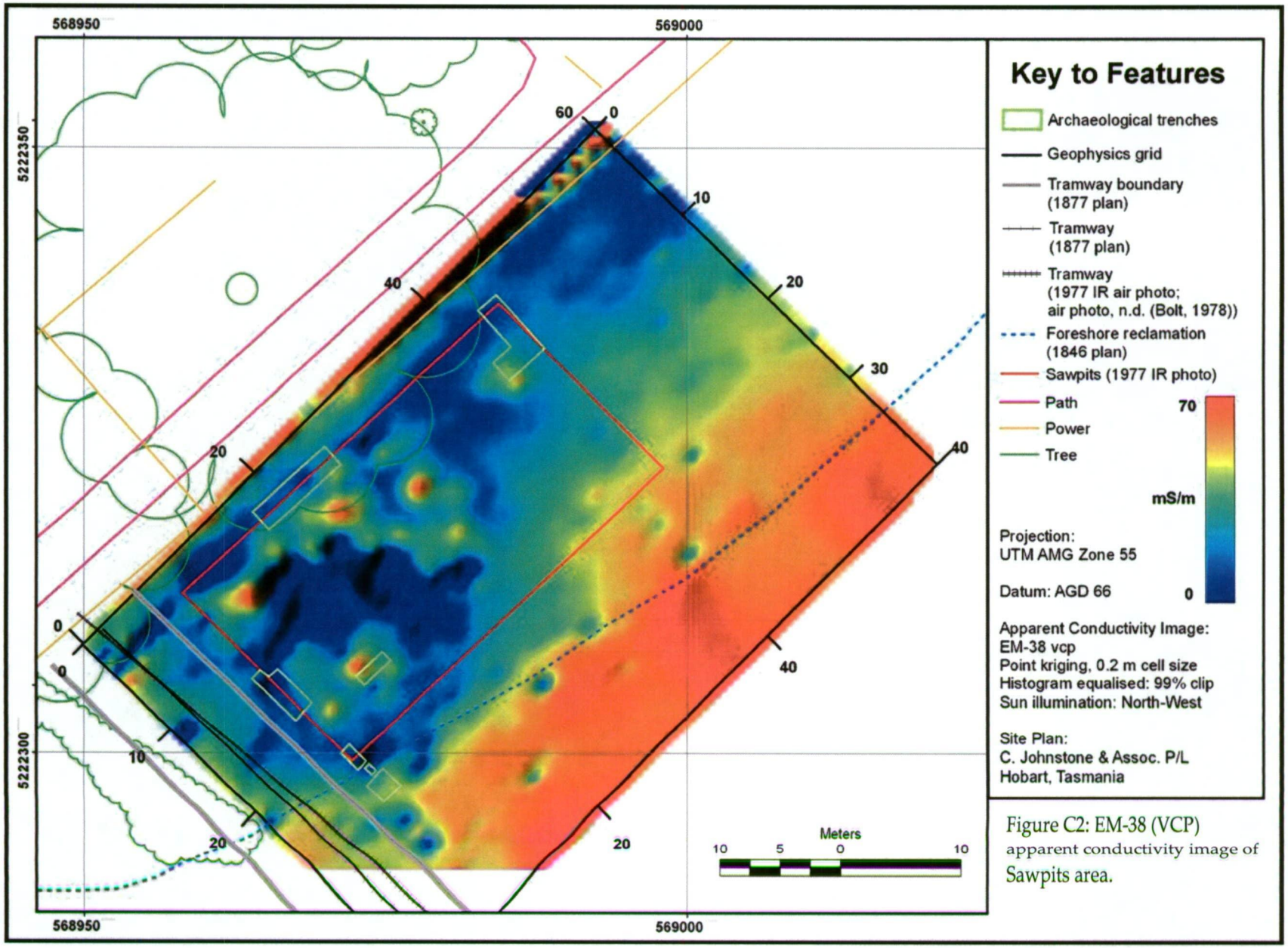

Figure C2: EM-38 (VCP) apparent conductivity image of Sawpits area.

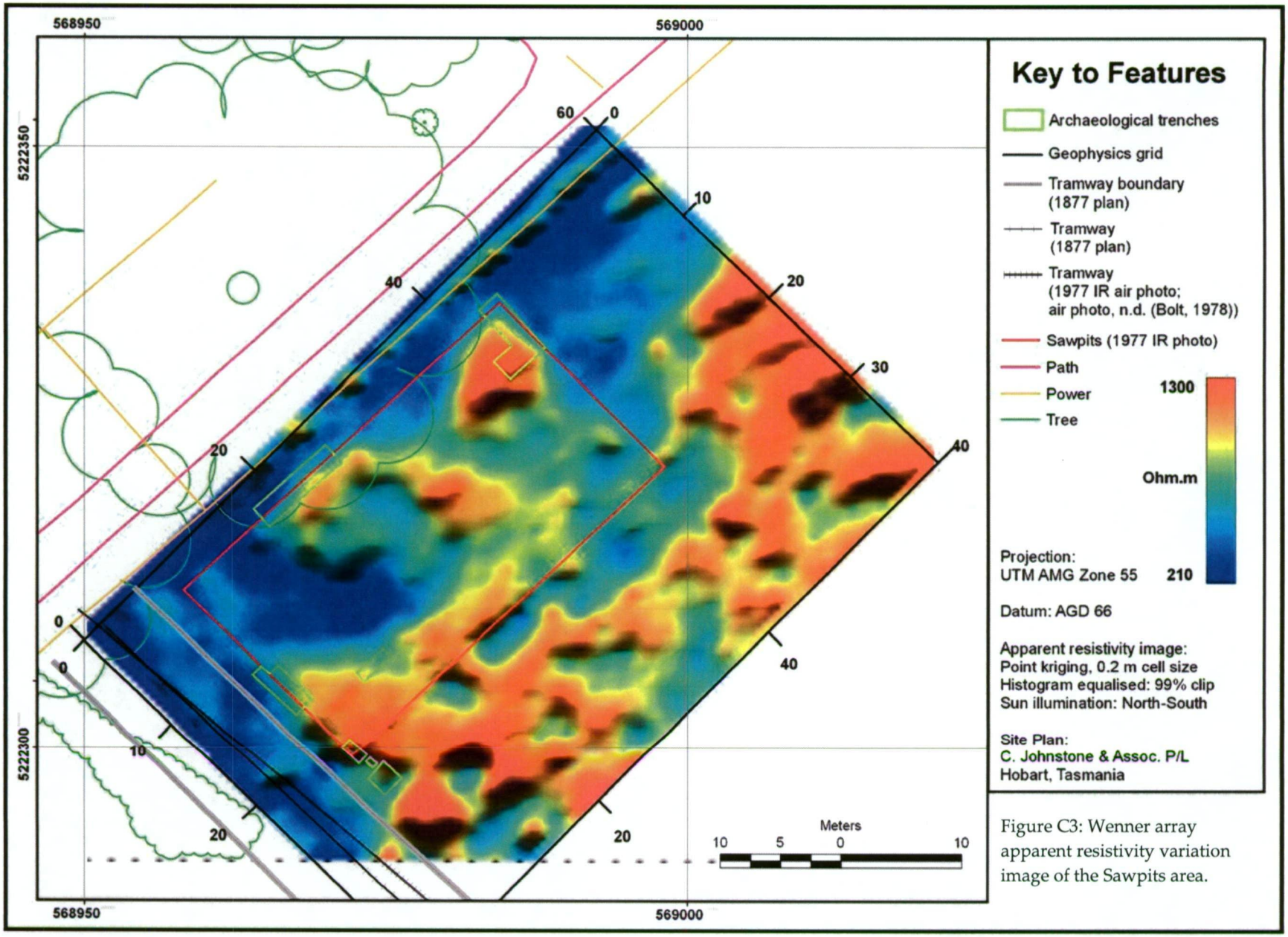

Figure C3: Wenner array apparent resistivity variation image of the Sawpits area.

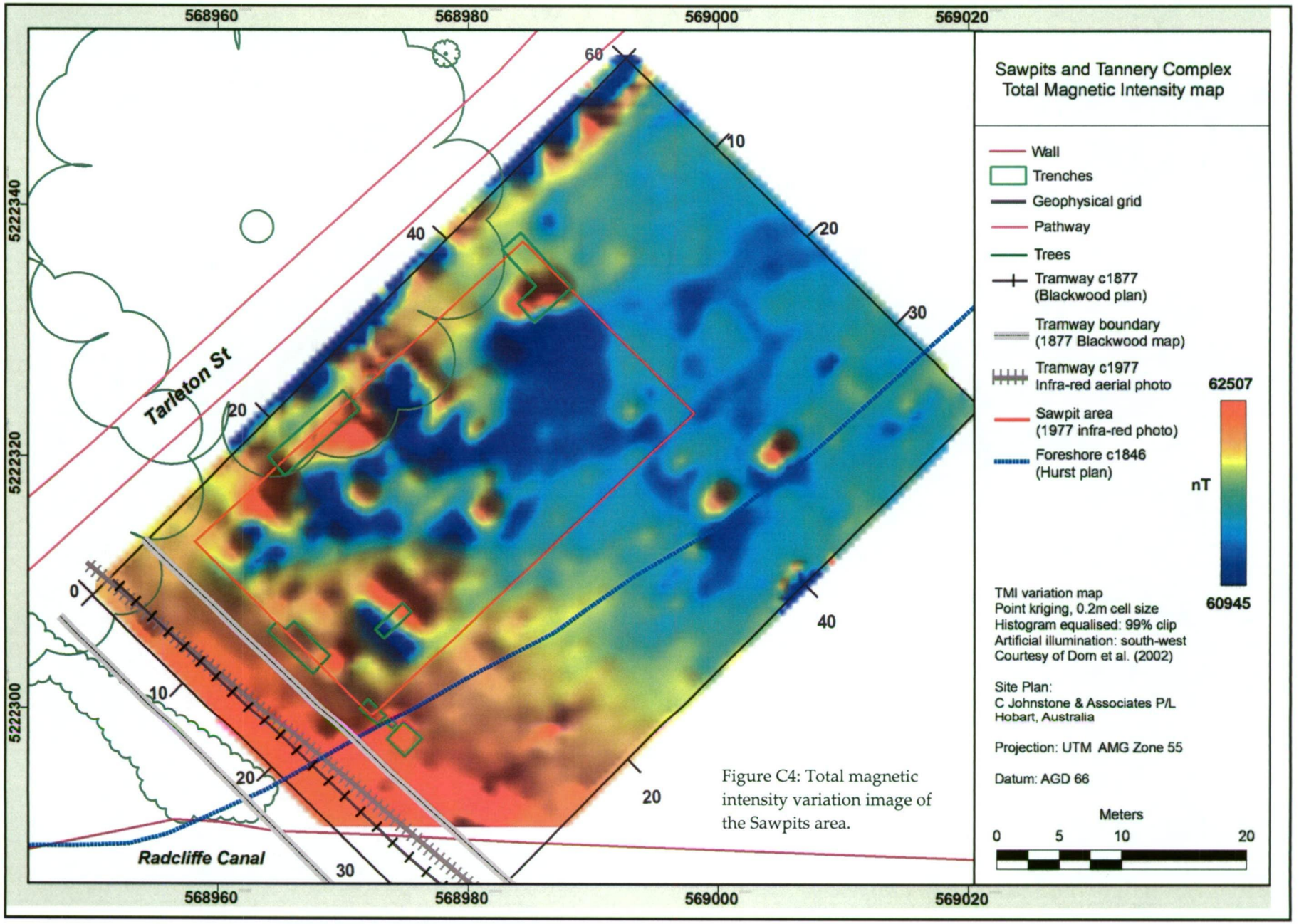

Figure C4: Total magnetic intensity variation image of the Sawpits area.

Survey type	Low frequency electromagnetic induction		
Instrumentation	Geonics EM-38		
Area surveyed	~ 2400 m² (40 x 60 m)		
Method of coverage	Series of parallel transverse lines		
Traverse interval	2.0 m	**Output units**	milliSiemen/m (mS/m)
Station interval	0.5 m	**Tx-Rx separation**	1.0 m
Penetration	1.5 m	**Mode**	Quadrature
Orientation	Vertical co-planar (max. penetration 1.5 m)		
Comments	Profiling conducted with ≤1.0m offset from parallel measuring tape. Calibration at start/end of line to minimize instrumental drift. Removal of metallic objects on surveyor and surface metallic debris on site prior to survey. Digital meter accurate to whole number only. Measurement recording delay time 2 s. Dipole parallel to traverse direction		

Table C1: Frequency domain electro-magnetometry (EM-38) data collection parameters.

Survey type	Low frequency electromagnetic induction		
Instrumentation	Geonics EM-31		
Area surveyed	~ 2400 m² (40 x 60 m)		
Method of coverage	Series of parallel transverse lines		
Traverse interval	2.0 m	**Output units**	milliSiemen/m (mS/m)
Station interval	1.0 m	**Tx-Rx separation**	3.66 m
Penetration	1.5 m	**Mode**	Quadrature
Orientation	Horizontal co-planar (max. penetration 3 m)		
Comments	Profiling conducted with ≤1.0m offset from parallel measuring tape. Calibration at start/end of line to minimize instrumental drift. Removal of metallic objects on surveyor and surface metallic debris on site prior to survey. Digital meter accurate to whole number only. Measurement recording delay time 2 s. Dipole parallel to traverse direction		

Table C2: Frequency domain electro-magnetometry (EM-31) data collection parameters.

Survey type	Magnetic		
Instrumentation	GEM systems GSM-19F Overhauser (fluxgate) magnetometer		
Area surveyed	~ 2400 m² (40 x 60 m)		
Method of coverage	Continuous surveying along transverse gridlines		
Traverse interval	2.0 m	**Sensor height**	0.2 m on trolley
Station interval	0.25 m	**Output units**	Nanotesla (nT)
Sampling rate	0.1 s	**Sensitivity**	0.1 nT
Distance trigger	Hip-chain		
Comments	All lines surveyed east to west. Base: Geometrics G-856 proton precession magnetometer Reading interval 30 s. Removal of metallic objects on surveyor and surface metallic debris on site prior to survey.		

Table C3: Magnetometry data collection parameters.

Survey type	DC resistivity		
Instrumentation	12V Atlas-Copco ABEM Terrameter		
Area surveyed	~ 2400 m² (40 x 60 m)		
Method of coverage	Continuous surveying along transverse gridlines		
Traverse interval	2.0 m	**Array type**	Wenner α
Station interval	0.5 m	**'a' spacing**	0.33 m
Stacking	4	**Output units**	Ohm (Ω)
Electrodes	10 mm stainless steel mounted in wooden frame		
Comments	0.2 mA current typically sufficient to provide non-noisy data		

Table C4: Apparent resistivity data collection parameters.